TESIS DOCTORAL

ÁNGELA MARTÍN-SERRANO ORTIZ

2018

UNIVERSIDAD DE MÁLAGA

TESIS DOCTORAL

ALLERGIC REACTIONS TO ß-LACTAM ANTIBIOTICS: chemical approaches for improving *in vitro* diagnosis

Departamento de Química Orgánica
Doctorado en Química y Tecnologías Químicas. Materiales y Nanotecnología

Facultad de Ciencias. Universidad de Málaga
Málaga, 2018.

Ángela Martín-Serrano Ortiz
Dirigida por:
Dra. Mª José Torres Jaén
Dra. Mª Isabel Montañez Vega

UNIVERSIDAD DE MÁLAGA

UNIVERSIDAD DE MÁLAGA

Facultad de Ciencias

Departamento de Química Orgánica

Programa de doctorado: Química y Tecnologías Químicas. Materiales y Nanotecnología

Tesis doctoral

"Allergic reactions to β-lactam antibiotics: chemical approaches for improving *in vitro* diagnosis"

Ángela Martín-Serrano Ortiz

2018

AUTOR: Ángela Martín-Serrano Ortiz

http://orcid.org/0000-0002-2908-8910

EDITA: Publicaciones y Divulgación Científica. Universidad de Málaga

Doña **María José Torres Jaén**, Doctora en Medicina y Cirugía, Jefa de Servicio y Directora de la Unidad de Gestión Clínica de Alergología del Hospital Regional Universitario de Málaga y Profesora Asociada al Departamento de Medicina de la Universidad de Málaga y Doña **María Isabel Montañez Vega**, Doctora en Química e Investigadora del Instituto de Investigación Biomédica de Málaga (IBIMA) y del Centro Andaluz de Nanomedicina y Biotecnología (BIONAND),

CERTIFICAN:

Que el trabajo que presenta Doña **Ángela Martín-Serrano Ortiz**, con el título **"Allergic reactions to β-lactam antibiotics: chemical approaches for improving *in vitro* diagnosis"** ha sido realizado en el laboratorio de investigación del Hospital Regional Universitario de Málaga-IBIMA y en el Centro Andaluz de Nanomedicina y Biotecnología-BIONAND bajo nuestra DIRECCIÓN y consideramos que tiene el contenido y rigor científico necesario para ser sometido a juicio del tribunal que ha nombrado la Universidad de Málaga para optar al grado de Doctor con Mención Internacional.

Y para que así conste, firmamos el presente certificado en Málaga, a de de 2018.

Fdo. Dra. María José Torres Jaén

Fdo. Dra. María Isabel Montañez Vega

Don **Ezequiel Pérez-Inestrosa de Villatoro**, doctor en Química, Catedrático de Universidad del Departamento de Química Orgánica de la Universidad de Málaga,

CERTIFICA:

Que el trabajo que presenta Doña **Ángela Martín-Serrano Ortiz**, con el título **"Allergic reactions to β-lactam antibiotics: chemical approaches for improving *in vitro* diagnosis"** ha sido realizado en el Laboratorio de Investigación del Hospital Regional Universitario de Málaga-IBIMA y en el Centro Andaluz de Nanomedicina y Biotecnología-BIONAND bajo mi TUTORIZACIÓN y considero que tiene el contenido y rigor científico necesario para ser sometido a juicio del tribunal que ha nombrado la Universidad de Málaga para optar al grado de Doctor con Mención Internacional.

Y para que así conste, firmo el presente certificado en Málaga, a de de 2018.

Fdo. Dr. Ezequiel Pérez-Inestrosa de Villatoro

MINISTERIO DE ECONOMÍA Y COMPETITIVIDAD

Centro de Investigaciones Biológicas
CSIC

La Dra. **Mª Dolores Pérez-Sala Gozalo**, Investigadora Científica del CSIC y responsable del grupo de Modificación Postraduccional de Proteínas del Centro de Investigaciones Biológicas,

CERTIFICA:

Que la estudiante predoctoral Dña. **Ángela Martín-Serrano Ortiz**, adscrita a BIONAND ha realizado una estancia corta en nuestro grupo, del 16 al 25 de Mayo de 2017, en el contexto de la RETIC Aradyal, del ISCIII, para el aprendizaje de técnicas de enriquecimiento en avidina de proteínas haptenizadas por fármacos biotinilados y análisis mediante electroforesis bidimensional.

Y para que así conste firmo la presente en Madrid a 5 de Julio de 2018.

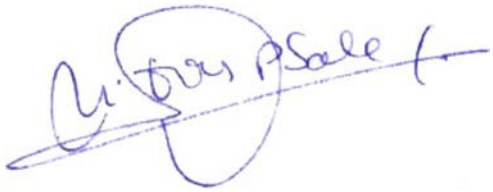

Fdo. Dra. Mª Dolores Pérez-Sala Gonzalo

Stay certificate for Ms. Ángela Martín-Serrano Ortiz

With this letter I confirm that Ms. **Ángela Martín-Serrano Ortiz** did a stay at the Department of Fibre and Polymer Technology, KTH Royal Institute of Technology, Stockholm, Sweden between August 1st and October 31st 2017.

During this period, Ángela worked on the project part of her PhD "Synthesis of fluorescent dendrons for secondary antibodies labeling and their application in detection signal amplification in microarray platforms for diagnosing allergy to drugs" and was guided by Prof. **Michael Malkoch** and PhD student Patrik Stenström.

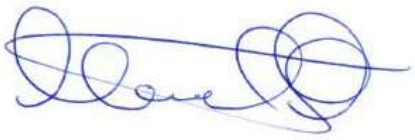

Professor Michael Malkoch

Yo, **Ángela Martín-Serrano Ortiz**, declaro que soy autora del presente trabajo de investigación cuyo título es **"Allergic reactions to β-lactam antibiotics: chemical approaches for improving *in vitro* diagnosis"** y que ha sido realizado en el Laboratorio de Investigación del Hospital Regional Universitario de Málaga-IBIMA y en el Centro Andaluz de Nanomedicina y Biotecnología-BIONAND bajo la codirección de las Dras. **María Isabel Montañez Vega** y **María José Torres Jaén**, y la tutela del Dr. **Ezequiel Pérez-Inestrosa de Villatoro,** y que he realizado una estancia corta en el grupo de Modificación Postraduccional de Proteínas del Centro de Investigaciones Biológicas (CIB-CSIC) de Madrid y otra de tres meses en el Royal Institute of Technology (KTH) de Estocolmo, Suecia, permitiéndome esta última optar a la Mención Internacional del Título de Doctor.

Y para que así conste, firmo en Málaga, a de de 2018.

Fdo. Ángela Martín-Serrano Ortiz

The results obtained with this work leaded to the following scientific production and awards:

Publications:

1. **Martín-Serrano Ortiz, A.;** Stenström, P.; Mesa-Antunez, P.; Andrén, O.C.J.; Torres, M.J.; Montañez, M.I.; Michael Malkoch. (2018) Design of multivalent fluorescent dendritic probes for site-specific labeling of biomolecules, *Journal of Polymer Science Part A: Polymer Chemistry.* **56**(15), 1609-1616.

2. Molina, N.; **Martín-Serrano, A**.; Fernandez, T.; Tesfaye, A.; Najera, F.; Torres, M.; Mayorga, C.; Vida, Y.; Montañez, M.I.; Perez-Inestrosa, E. (2018) Dendrimeric Antigens for Drug Allergy Diagnosis: A New Approach for Basophil Activation Tests, *Molecules.* **23**(5), 997.

3. Montañez, M.I.; Mayorga, C.; Bogas, G.; Barrionuevo, E.; Fernandez-Santamaria, R.; **Martín-Serrano, A.;** Laguna, J.J.; Torres, M.J.;, Fernandez, T.D.; Doña, I. (2017) Epidemiology, Mechanisms, and Diagnosis of Drug-Induced Anaphylaxis, *Frontiers in Immunology.* **8**, 614.

4. **Martín-Serrano, A**.; Barbero, N.; Agundez, J. A.; Vida, Y.; Perez-Inestrosa, E.; Montañez, M.I. (2016) New Advances in the Study of IgE Drug Recognition, *Current Pharmaceutical Design.* **22**(45), 1-14.

5. Ariza, A.; Mayorga, C.; Salas, M.; Doña, I.; **Martín-Serrano, A.;** Pérez-Inestrosa, E.; Pérez-Sala, D.; Guzmán, A.E.; Montañez, M.I.; Torres, M.J. (2016) The influence of the carrier molecule on amoxicillin recognition by specific IgE in patients with immediate hypersensitivity reactions to betalactams, *Scientific Reports.* **6**, 35113.

6. Ariza, A.; Mayorga, C.; Fernández, T.D.; Barbero, N.; **Martín-Serrano, A.**; Pérez-Sala, D.; Sánchez-Gómez, F.J.; Blanca, M.; Torres, M.J.; Montañez, M.I. (2015) Hypersensitivity Reactions to ß-Lactams: Relevance of Hapten-Protein Conjugates, *Journal of Investigational Allergology and Clinical Immunology.* **25**(1), 12-25.

Patent:

P201731240 (October 23rd 2017). Nuevos compuestos tipo pirazolona para el diagnóstico de alergias a antibióticos betalactámicos *(New pyrazolone-kind compounds for diagnosing allergy to betalactam antibiotics).* Montañez, M.I.; Mayorga, C.; **Martín-Serrano, A.**; Doña, I.; Torres M.J.; Pérez-Inestrosa, E.

Communications to conferences:

- **Martín-Serrano, A**.; Mayorga, C.; Barrionuevo, E.; Pérez-Inestrosa, E.; Torres M.J.; Montañez, M.I. New Potential Synthetic Antigenic Determinants for α-Amino-Cephalosporins: design, synthesis and immunological evaluation. Meeting of the European-Academy-of-Allergy-and-Clinical-Immunology (EAACI). 2018 May 26th-30th. Munich, Germany. ***Allergy* 2018 73(S105). Abstract 0590**. Poster Discussion Session. **Abstract Prize.**

- **Martín-Serrano, A.**; Barbero, N.; González-Morena, J.M.; Sánchez-Gómez, F.J.; Fernández, T.D.; Rodríguez-Nogales, A.; Pérez-Inestrosa, E.; Pérez-Sala, D.; Mayorga, C.; Ariza, A.; Torres, M.J.; Montañez, M.I. Study Of Protein Targets For Haptenation By Biotinylated Clavulanic Acid: Usefulness In Studies On Allergy Todwars Betalactams. Drug Hypersensitivity Meeting (DHM). 2018 April 19th-21st. Amsterdam, The Netherlands. **Published in *Clinical and Translational Allergy* 2018 8(Suppl 3):P88.**

- Fernandez, T.D.; Montañez, M.I.; Barbero, N.; **Martín-Serrano, A.**; Bogas, G.; Ariza, A.; Fernández-Santamaría, R.; Rodriguez-Nogales, A.; Mayorga, C.; Pérez-Inestrosa, E.; Torres, M.J. Improving the Diagnosis of Immediate Hypersensitivity to Clavulanic Acid Using Synthetic Antigenic Determinants for Basophil Activation. Drug Hypersensitivity Meeting (DHM). 2018 April 19th-21st. Amsterdam, The Netherlands. **Published in *Clinical and Translational Allergy* 2018 8(Suppl 3):P107.**

- **Martín-Serrano, A.**; Mayorga, C.; Barrionuevo, E.; Rodríguez-Nogales, A.; Pérez-Inestrosa, E.; Torres, M.J.; Montañez, M.I. Study of Specific IgE Recognition of New Potential Synthetic Antigenic Determinants for α-Amino-Cephalosporins. American Academy of Allergy, Asthma & Immunology (AAAAI) annual meeting. 2018 March 2nd-6th. Orlando (Florida), U.S.A. **Published in *Journal of Allergy and Clinical Immunology* 2018 141(2) AB34. Abstract 110.**

- Barrionuevo, E.; Pérez, N.; Gomez, F.; Salas, M.; Guerrero, M.A.; Ruiz, D.; **Martín-Serrano, A.**; Torres, M.J. Descriptive Analysis of Diagnostic Methods In Betalactam Hypersensitivity in our Allergy Unit. American Academy of Allergy, Asthma & Immunology (AAAAI) annual meeting. 2018 March 2nd-6th. Orlando (Florida), U.S.A. **Published in *Journal of Allergy and Clinical Immunology* 2018 141(2) AB42. Abstract 135.**

- **Martín-Serrano, A.**; Stenström, P.; Mesa, P.; Malkoch, M.; Montañez, M.I. Synthesis and Characterization of Fluorescent Dendrimer Structures with Potential Biological Applications. VI Dendrimers Meeting (EDEN 6). 2018 February 22nd-23rd. Seville, Spain.

- **Martín-Serrano, A.**; Barbero, N.; González-Morena, J.; Sánchez-Gómez, F.; Fernández, T.; Sánchez, M.; Pérez-Inestrosa, E.; Pérez-Sala, D.; Cristobalina, M.; Ariza, A.; Torres, M.J.; Montañez, M.I. Biotinylated Clavulanic Acid as a Tool for Identifying Serum Proteins

Target of Haptenation by Clavulanic Acid in the Context of Allergy Studies. Meeting of the European-Academy-of-Allergy-and-Clinical-Immunology (EAACI). 2017 June 17th-21st. Helsinki, Finland. **Published in *Allergy* 2017 72(S103). Abstract 0009.** Oral Abstract Session. **Abstract Prize.**

- Fernandez, T.D.; Montañez, M.I.; Barbero, N.; **Martín-Serrano, A**.; Salas, M.; Bogas, G.; Ariza, A.; Fernández, R.; Guerrero, M.A.; Mayorga, C.; Perez-Inestrosa, E.; Torres, M.J. Basophil Activation Using Synthetic Antigenic Determinants for Diagnosing Immediate Hypersensitivity to Clavulanic Acid. Meeting of the European-Academy-of-Allergy-and-Clinical-Immunology (EAACI). 2017 June 17th-21st. Helsinki, Finland. Published in ***Allergy* 2017 72(S103). Abstract 0142**. Oral Abstract Session. **Abstract Prize**.

- **Martín-Serrano, A.**; Barbero, N.; Ariza, A.; Fernández, T.D.; Pérez-Inestrosa, E.; Salas, M.; Mayorga, C.; Pérez-Sala, D.; Torres, M.J.; Montañez, M.I. Study of Protein Haptenation by Biotinylated Clavulanic Acid: Usefulness in Studies on Allergy Towards Betalactams. American Academy of Allergy, Asthma & Immunology (AAAAI) annual meeting. 2017 March 3rd- 6th. Atlanta (Georgia), U.S.A. **Published in *Journal of Allergy and Clinical Immunology* 2017 139(2) AB46. Abstract 147.**

-Montañez M.I.; Barbero, N.; Fernandez, T.D.; **Martin-Serrano, A**.; Bogas, G.; Ariza, A.; Mayorga, C.; Pérez-Inestrosa, E.; Torres, M.J. Value of synthetic antigenic determinants of clavulanic acid in basophil activation test for evaluating immediate reactions to clavulanic acid. American Academy of Allergy, Asthma & Immunology (AAAAI) annual meeting. 2017 March 3rd- 6th. Atlanta (Georgia), U.S.A. **Published in *Journal of Allergy and Clinical Immunology* 2017 139(2) AB46. Abstract 148.**

- Fernández, T.D.; Salas, M.; Fernández, R.; Montañez, M.I.; **Martín-Serrano, A.**; Barbero, N.; Perez-Inestrosa, E.; Mayorga, C.; Torres, M.J. Basophil Activation Test in Clavulanic Acid Selective Patients. Decrease of IgE Recognition over Time. American Academy of Allergy, Asthma & Immunology (AAAAI) annual meeting. 2017 March 3rd- 6th. Atlanta (Georgia), U.S.A. **Published in *Journal of Allergy and Clinical Immunology* 2017 139(2) AB33. Abstract 109.**

- Ariza, A.; Fernández, T.D.; Mayorga, C.; Salas, M.; Barbero, N.; Montañez, M.I.; **Martín-Serrano, A.**; Fernández, R.; Galindo, L.; Blanca, M.; Torres, M.J. The Administration of the Combination Amoxicillin-Clavulanic Acid can Induce Simultaneous Sensitization to Both Drugs. Report of two clinical cases. Meeting of the European-Academy-of-Allergy-and-Clinical-Immunology (EAACI). 2016 June 11st-15th. Vienna, Austria. Published in ***Allergy* 2016 71(S102). Abstract 762**.

- Ariza, A.; Fernández, T.D.; Mayorga, C.; Salas, M.; Barbero, N.; Montañez, M.I.; **Martín-Serrano, A.**; Fernández, R.; Galindo, L.; Blanca, M.; Torres, M.J. Patients Taking Amoxicillin-Clavulanic Can Become Simultaneously Sensitized to Both Drugs. American

Academy of Allergy, Asthma & Immunology (AAAAI) annual meeting. 2016 March 4rd-7th. Los Angeles (California). **Published in *Journal of Allergy and Clinical Immunology* 2016 137(2) AB43. Abstract 137.**

- **Martín-Serrano, A.** Approach for Studying the Antigenic Determinants of Cephalosporins. I Summer School organized by Research Network for Adverse Reactions to Allergens and Drugs (RIRAAF). 2015 October 1st-2nd. Málaga, Spain.

- **Martín-Serrano, A.**; Ariza, A.; Mayorga, C.; Fernández, T.D.; Montañez, M.I.; Torres, M.J. Synthesis and Characterization of Potential Antigenic Determinants of α-Aminocehalosporins. VII Organic Chemistry Mediterranean Meeting (REQOMED). 2015 June 10th-12th. Málaga, Spain.

Awards:

- **Abstract Prize** for the piece of work entitled "New Potential Synthetic Antigenic Determinants for a-Amino-Cephalosporins: design, synthesis and immunological evaluation", presented at a Poster Discussion Session during the **EAACI 2018** congress held in Munich, Germany.

- Awarded with a **FEBS Summer Fellowship** in 2017 to work in the project "Synthesis of fluorescent dendrons for secondary antibodies labeling and their application in detection signal amplification in microarray platforms for diagnosing allergy to drugs" in collaboration with the Royal Institute of Technology (KTH) in Stockholm, Sweden.

- Member of the team awarded with the **I Unicaja Award to innovation in biomedicine and health** (Unicaja-FIMABIS, 2017) to work in the project *"Desarrollo de un microarray con conjugados betalactámico-proteína y betalactámico-nanoestructura para el diagnóstico de alergia a antibióticos"*.

- **Abstract Prize** for the piece of work entitled "Biotinylated Clavulanic Acid as a Tool for Identifying Serum Proteins Target of Haptenation by Clavulanic Acid in the Context of Allergy Studies", presented at an Oral Abstract Session during the **EAACI 2017** congress held in Finland, Helsinki.

- Co-author of the piece of work entitled "Basophil Activation Using Synthetic Antigenic Determinants for Diagnosing Immediate Hypersensitivity to Clavulanic Acid", presented at an Oral Abstract Session and awarded with an **Abstract Prize** during the **EAACI 2017** congress held in Finland, Helsinki.

Scientific contributions not included in this thesis:

Publications:

1. Porret, E.; Sancey, L.; **Martín-Serrano, A.**; Montañez, M.I.; Seeman, R.; Yahia-Ammar, A.; Okuno, H.; Gomez, F.; Ariza, A.; Hildebrandt, N.; Fleury, J.-B.; Coll, J.L.; Le Guével, X. (2017) Hydrophobicity of Gold Nanoclusters Influences Their Interactions with Biological Barriers, *Chemistry of Materials.* **29**(17), 7497-7506.

2. Fernández, T.D.; Ariza, A.; Palomares, F.; Montañez, M.I.; Salas, M.; **Martín-Serrano, A.**; Fernández, R.; Ruiz, A.J.; Blanca, M.; Mayorga, C.; Torres, M.J. (2016) Hypersensitivity to fluoroquinolones: The expression of basophil activation markers depends on the clinical entity and the culprit fluoroquinolone, *Medicine.* **95**(23), e3679.

Communications to conferences:

- Montañez M.I.; Mayorga C.; Nájera F.; Ariza A.; Fernández T.D.; Salas, M.; **Martín-Serrano, A.**; Blanca, M.; Pérez-Inestrosa, E. Dendrimeric Antigens for Studying the Influence of Penicillin Determinants Orientation on IgE Recognition. 7th Drug Hypersensitivity Meeting (DHM, EAACI). 2016 April 21st-23rd. Málaga, Spain. Published in ***Clinical and Translational Allergy 2016, 6 (Suppl 3):P185*.**

- Ariza, A.; Mayorga, C.; Montañez, M.I.; Salas, M.; Doña, I.; **Martín-Serrano, A.**; Pérez-Inestrosa, E.; Pérez-Sala, D.; Blanca, M.; Guzmán, A.E.; Torres, M.J. Different Patterns of Recognition of Structures Derived from Amoxicillin by IgE Antibodies from Patients with Immediate Hypersensitivity Reactions to Betalactams. 7th Drug Hypersensitivity Meeting (DHM, EAACI). 2016 April 21st-23rd. Málaga, Spain. **Published in *Clinical and Translational Allergy 2016, 6 (Suppl 3):P188*.**

- Montañez; M.I.; Mayorga, C.; Najera, F.; Ariza, A.; Fernández, T.D.; Salas, M.; **Martín-Serrano, A.**; Blanca, M.; Pérez-Inestrosa, E.; Torres, M.J. Study of penicillin epitopes conformation/disposition in carrier dendrimer molecules vs sIgE molecular recognition relationships. Meeting of the European-Academy-of-Allergy-and-Clinical-Immunology (EAACI). 2015 June 6th-10th. Barcelona, Spain. Published in ***Allergy 70(S101)*. Abstract 38**.

The present study has been supported by:

-**ISCIII of MINECO; grants cofunded by European Regional Development Fund (ERDF):**

PI12/02529: **"**Identificación y caracterización inmunológica de conjugados betalactámicos con proteínas y nanoestructuras para su aplicación al diagnóstico *in vitro* de reacciones alérgicas IgE". Principal investigator: María José Torres Jaén.

PI15/01206: "Estudio de biomarcadores y factores de riesgo relacionados con el desarrollo de una respuesta alérgica diferencial frente a amoxicilina o clavulánico". Principal investigator: María José Torres Jaén.

CP15/00103: "Desarrollo de conjugados de antibióticos con nanoestructuras o proteínas y aplicación al diagnóstico *in vitro* de alergia a antibióticos". Principal investigator: María Isabel Montañez Vega.

-**Andalusian Regional Ministry Health:**

PI-0699-2011: "Desarrollo de materiales nanoestructurados dendriméricos con aplicaciones potenciales en el diagnóstico de alergia a fármacos: inmunoensayos y test de activación celular". Principal investigator: Adriana Ariza Veguillas.

PI-0352-2012: "Papel de los linfocitos Th1/Th17 y el eje Galectin-9-Tim-3 en la regulación de la hipersensibilidad no inmediata a fármacos con afección cutánea". Principal investigator: Tahía Diana Fernández Duarte.

PI-0179-2014: "Desarrollo de un microarray con aductos fármaco-proteína/nanoestructura para el diagnóstico de alergia a antibióticos". Principal investigator: María Isabel Montañez Vega.

PI-0241-2016: "Desarrollo de métodos *in vitro* para el diagnóstico de alergia al ácido clavulánico: identificación de los determinantes antigénicos implicados en la respuesta inmunológica". Principal investigator: Tahía Diana Fernández Duarte.

PI-0250/2016: "Desarrollo de nuevos nanobiosensores para el diagnóstico de reacciones adversas a medicamentos". Principal investigator: Ezequiel Pérez-Inestrosa Villatoro.

-**RETICS RIRAAF RD12/0013/0001.**

-**RETICS ARADyAL RD16/0006/0001.**

-**Merck-Serono Research Grant from Fundacion Salud 2000.**

- **I Unicaja Award to innovation in biomedicine and health by Unicaja-FIMABIS:**

PUNI-017-2016. "Desarrollo de un microarray con conjugados betalactámico-proteína y betalactámico-nanoestructura para el diagnóstico de alergia a antibióticos". Principal investigator: María Isabel Montañez Vega.

- **FEBS Summer Fellowship 2017.**

-PS13/12 FIMABIS-ROCHE. Estudio de reacciones de hipersensibilidad por intolerancia cruzada a antiinflamatorios no esteroideos con afectación cutánea: relación fenotipo-genotipo. Principal investgator: Miguel Blanca Gómez.

-RD07/0064/0000: Red de Investigación de Reacciones Adversas a Alérgenos y a Fármacos (RIRAAF).

AGRADECIMIENTOS

Desde mi primer contacto con la investigación en el último año de Licenciatura, he perseguido la oportunidad de hacer un doctorado puesto que me entusiasmaba la idea de aplicar toda esa teoría estudiada en la carrera para desarrollar métodos que permitiesen mejorar la calidad de vida de las personas. Ahora, llegado el momento de presentar mi tesis doctoral, debo reconocer que estoy muy contenta con el hecho de haber estado trabajando en un tema multidisciplinar, que me ha brindado la oportunidad de conocer algunas de las numerosas y prometedoras contribuciones de la química orgánica en el ámbito de la salud y de complementar mi formación química para adquirir un perfil más biológico. Durante este trayecto de cinco años, muchas son las personas que me han acompañado, apoyado y motivado, y por ello les doy gracias.

En primer lugar, agradecer a la Dra. María Isabel Montañez y a la Dra. Mª José Torres la confiada depositada en mí para el desarrollo de este trabajo, y su apoyo.

Continuar dando las gracias al Dr. Ezequiel Pérez-Inestrosa y a todo su grupo de investigación. En especial, gracias a la Dra. Nekane Barbero por toda su dedicación a la obtención de algunas de las estructuras utilizadas en este trabajo. También a Nekane, junto a Noemi, Pablo y Anjara, por toda su ayuda en el día a día del laboratorio y por ayudarme a disfrutar de mi tiempo en Málaga.

No olvidar agradecer a otros compañeros de BIONAND como Rebeca, Dani, John y Xavier por los momentos compartidos investigando la geografía y costumbres andaluzas. Gracias a Patri por su ilusión y ganas de aprender, trabajar y ayudar.

A todos mis compañeros del grupo de Alergia: Raquel, Ana, Miguel, Mª José, Mª Carmen, Francis, Natalia, Tahía, Alba, Jose, Jimmy… Gracias a Rubén por todo el trabajo realizado con los BAT y por estar siempre dispuesto a ayudar. Mil gracias a Adri por ser mi mentora en el Hospital Civil y estar siempre dispuesta a ayudarme y resolver mis dudas.

A todos los compañeros de otros grupos del Hospital Civil que, de algún modo u otro han estado ahí. En especial, gracias a Rosa, Pablo y Antonio. También a Pepe, por contribuir con su experiencia en el laboratorio y tener siempre consejos y respuesta para solucionar los contratiempos que pudiesen surgir en los inmunoensayos.

Agradecerle a la Dra. Pérez-Sala y a su grupo de investigación del Centro de Investigaciones Biológicas por la colaboración en la detección de la modificación de proteínas séricas por fármacos biotinilados y por acogerme en su laboratorio para el aprendizaje de técnicas de enriquecimiento de proteínas haptenizadas y análisis mediante electroforesis bidimensional. Gracias al Dr. Francisco José Sánchez por su tiempo y resolver mis dudas durante la estancia.

To Professor Michael Malkoch and his research group at Royal Institute of Technology, for the collaboration in the design of fluorescent dendrons for antibody labeling and his help to publish the results obtained as outcome of my three-month stay at his laboratory.

To the FEBS for granting me with a Summer Fellowship for my stay. To Patrik, Oliver, Pablo and Matthiew for your tips in the lab. To Ilona, María, Ana and Lorenzo for making me enjoy the city of Stockholm, and to Andrea and Nicola for treating me as one of the family and making me feel like at home. Tack så mycket.

Al personal del Laboratorio de Proteómica del Hospital Vall d´Hebron y del Centro Nacional de Biotecnología por su ayuda en la identificación de los sitios de unión. Al personal de Servicio Central de Apoyo a la Investigación de la Universidad de Málaga encargado de los análisis de MALDI-TOF de los conjugados proteína-fármaco, y las medidas de absorbancia y fluorescencia de los dendrones fluorescentes y el anticuerpo marcado. A la Unidad de Proteómica de la Universidad Complutense de Madrid por el análisis de huella peptídica.

Al personal médico y de enfermería encargado de la evaluación, diagnóstico y obtención de muestras biológicas de los pacientes incluidos en los diferentes estudios, así como a aquellas personas que han participado como pacientes y controles.

No se me puede olvidar mi prima Natalia, por ayudarme a darle el formato final a esta memoria.

A Chiqui, por los “speaking” dentro y fuera de la Escuela de Idiomas. A Lydia, Asier y Lidia, por los buenos momentos y por cuidarme y animarme en la etapa final, la más complicada de este camino.

A Vicente, por este último año, por tratarme como a una reina, respetar como soy, preocuparse por mí, mostrarme su apoyo, y demostrar estar ahí no sólo para lo bueno.

A mi amiga de toda la vida, Inma, y a una un poco más reciente, Alicia, por seguir brindándome su amistad y por poder seguir contando con ellas después de tantos años, a pesar de la distancia y las diferentes circunstancias de cada una.

Por último, el agradecimiento más importante va dirigido a mi familia: mis padres, hermanos, tíos y abuelos. Por su cariño y su apoyo, por preocuparse por mí y cuidarme desde la distancia, por recibirme con los brazos abiertos siempre que vuelvo a casa, por hacerme sentir que siempre puedo contar con ellos. Gracias a mi madre por poder con todo y por ayudarme a levantarme en los momentos más bajos. A mi abuelo Reyes, una persona muy especial para mí, al que estoy segura le hubiese gustado estar presente en este nuevo logro de su nieta mayor, y que me ha dejado el legado de ser siempre fuerte y valiente.

A mis padres

A mis hermanos

A mi abuelo Reyes

TABLE OF CONTENTS

List of Abbreviations 33
GENERAL INTRODUCTION 39
1. Definition and Classification of Adverse Drug Reactions 41
2. Definition and Classification of Drug Hypersensitivity Reactions 41
2.1. Immunological Classification of Allergic Reactions 42
2.2. Clinical Classification of Allergic Reactions 42
3. Epidemiology and Prevalence of Allergic Reactions to Drugs 44
4. Mechanisms of Allergic Reactions to Drugs 44
4.1. Hapten hypothesis 45
4.2. Danger hypothesis 46
4.3. Pharmacological Interaction hypothesis 47
5. Immunological Proccess Related with Immediate Allergic Reactions to β-lactam Antibiotics 48
5.1. Immunoglobulin E 48
5.2. β-lactams Chemical Structures 49
5.3. β-lactams Antigenic Determinants 50
5.4. Protein haptenation by BLs 58
5.5. Candidate Carrier proteins for BLs 58
6. Clinical Symptoms and Diagnosis of Immediate Allergic Reactions to BLs 63
6.1. *In vivo* tests 65
6.2. *In vitro* tests 67
6.3. *In vivo versus in vitro* tests 70
6.4. Limitations and future of *in vitro* tests 70
6.5. Nanotechnology for improving *in vitro* tests 72
7. Dendrimeric Structures for Improving *In Vitro* Tests 73
7.1. Generalities of Dendritic Structures 73
7.2. Dendrimers as Synthetic Carriers 76
7.3. Dendrimers as Fluorescent Probes for Detection Signal Amplification 77
8. Bioconjugation Reactions for Antibodies Labeling 78
JUSTIFICATION AND HYPOTHESIS 83
OBJECTIVES 89
RESULTS AND DISCUSSION 93
I. Study of antigenic determinant structures for amino-cephalosporins 95
I.1. Study of α-aminocephalosporins Reactivity Towards Simple Nucleophiles 98
I.2. Synthesis of New Synthetic Antigenic Determinants for α-aminocephalosporins 103
I.3. Immunological Evaluation of Pyrazinone-Like Antigenic Determinants 106

I.3.1. Patient´s selection 106
I.3.2. In Vitro Evaluation of Specific IgE Molecular Recognition by RAST Inhibition 107
II. Elucidation of antigenic determinant structures for CLV 115
II.1. Elucidation of the Chemical Structure of Antigenic Determinants for CLV 118
II.1.1. Nuclear Magnetic Resonance Studies of CLV reactivity 120
II.1.2. Structure-Activity Relationship of Synthetic Determinant Structures 123
II.1.2.1. Cellulose Discs and Nanoparticles Functionalized with CLV Derivatives 123
II.1.2.2. CLV Derivatives in Free Form 127
II.2. Characterization of CLV-Protein Adducts Generated *In Vitro* 136
II.2.1. Mass Spectrometry Characterization 137
II.2.2. Identification of HSA Binding Sites 138
II.3. Development of Approaches for Detection of Serum Proteins Modified by CLV 141
II.3.1. Synthesis of Biotinylated Derivatives of CLV 142
II.3.2. Reactivity of CLV-TEG-B towards simple nucleophiles 145
II.3.3. Comparison of Reactivity between CLV and CLV-TEG-B 148
II.3.4. Study of CLV Biotynilated Derivatives Proteins Haptenation Capacity 150
II.3.5 Mass Spectrometry Characterization of HSA-CLV-B Conjugates 157
II.3.6. Characterization of HSA-CLV-TEG-B Conjugates by LC-MS/MS 158
II.4. Detection and Identification of Serum Proteins Target of Modification by CLV-TEG-B 159
II.4.1. Conjugation of CLV-TEG-B with Human Serum Proteins and Detection of Modification 160
II.4.2. Identification of Serum Proteins Target of Modification by Peptidic Fingerprint 161
III. Antibody labeling for detecting sIgE in drug allergy 163
III.1. Radiolabeling of a High Specific α-human IgG 164
III.1.1. Labeling optimization 165
III.1.2. Labeling of α-human IgE monoclonal antibody with ^{125}I 166
III.1.3. Labeled IgG sensitivity evaluation by Radio Allergo Sorbent Test (RAST) 166
III.2. Multivalent fluorescent dendritic probes for immunoassays signal amplification 168
III.2.1. Design of Fluorescent Dendrons for Site Specific Antibody Labeling with Application in Microarray Systems 169
III.2.2. Synthesis of Fluorescent Dendrons 170
III.2.3. UV-Visible and Fluorescence Spectroscopy Characterization of Dendrons 183
III.2.4. Chemoselective Conjugation of Dendrons to a Model Antibody 184
GENERAL DISCUSSION 191
CONCLUSIONS 197

EXPERIMENTAL 201
1. Identification of β-lactam Antibiotics Antigenic Determinants Recognized by Specific IgE 203
1.1. Scope of the Study 203
1.2. Study of CLV or α-aminocephalosporins Reactivity towards Nucleophilic Species 203
1.3. Synthesis of structures derived from aminocephalosporins 204
1.4. Synthesis of structures derived from CLV 205
1.5. Patients and controls selection 208
1.6. Conjugation of β-lactam antibiotics with different carrier molecules for *in vitro* studies 209
1.7. *In vivo* tests 210
1.8. *In vitro* tests 212
2. Study for identification of carrier proteins 218
2.1. Synthesis of Biotinylated Derivatives of CLV 218
2.2. Human serum proteins *in vitro* modification by CLV 222
2.3. Enrichment of biotynilated fraction 223
2.4. Characterization of modified proteins by SDS-PAGE techniques 224
2.5. Mass spectrometry 227
2.6. Molecular modeling 231
3. Labeling of secondary antibodies 231
3.1. Radioactive labeling 231
3.2. Fluorescent labeling 236
3.2.1. Synthesis of fluorescent dendrons 237
3.2.2. IgG labeling with Cy5 decorated dendrons 250
3.2.3. SDS-PAGE characterization of Cy5 labeled IgG 251
3.2.4. Spectroscopic Characterization of Dendrons and Labeled IgG 252
RESUMEN 253
BIBLIOGRAPHY 289

List of Abbreviations

1D	One dimension
2D	Two dimension
AAAAI	American Academy of Allergy, Asthma & Immunology
AcN	Acetonitrile
AD	Antigenic Determinant
ADR	Adverse Drug Reaction
AMP	Ampicillin
APC	Antigen presenting cell
AX	Amoxicillin
AX-B	Biotinylated AX
AXO	Amoxicilloyl
BAT	Basophil Activation Test
BL	β-lactam antibiotic
Boc	Tert-butyloxycarbonyl
BP	Benzylpenicillin
BPO	Benzylpenicilloyl
BP-OL	BPO-octa-L-lysine
$BuNH_2$	Butylamine
CDR	Complementarity determining regions
CH_2Cl_2	Dichloromethane
CHCA	α-cyano-4-hydroxycinamic acid
$CHCl_3$	Chloroform
CIB	Centro de Investigaciones Biológicas
ClMs	Mesyl Chloride
ClTs	Tosyl Chloride
CLV	Clavulanic Acid
CLV-B	Non water soluble biotinylated CLV
CLV-TEG-B	Water soluble biotinylated CLV
CNB	Centro Nacional de Biotecnología

cpm	Counts per minute
CPO	Cephalosporoyl
CSIC	Centro Superior de Investigaciones Científicas
CuAAC	Copper(I)-catalyzed azide-alkyne cycloaddition
Cy	Cyanine
DABCO	Diazabicyclo[2,2,2]octane
DCE	Dichloroethane
DCTB	Trans-2-[3-(4-tert-butylphenyl)-2-methyl-2-propenylidene]-malononitrile
DeAns	Dendrimeric antigens
DHB	2,5-dihydroxybenzoic acid
DHR	Drug Hypersensitivity Reaction
DMF	Dimetylformamide
DMSO	Dimethyl sulfoxide
dpm	Desintegrations per minute
EAACI	European Academy of Allergy and Clinical Immunology
ECD	Electron capture dissociation
ECL	Enhanced chemiluminiscence
EDTA	Ethylenediaminetetraacetic acid
EGTA	Ethyleneglycoltetraacetic acid
ELISA	Enzyme-linked immunosorbent assay
ENDA	European Network on Drug Allergy
ESI	Electrospray ionization
EtOAc	Ethyl acetate
Fab	Antigen binding region
Fc	Christallizable region
FcεRI	High affinity Cell Surface receptor
FcεRII	Low affinity IgE receptors
FEIA	Fluorescence enzyme immunoassay
HPLC	High-performance liquid chromatography
HRMS	High resolution mass spectrometry

HRP	Horseradish peroxidase
HSA	Human Serum Albumin
^{i}BuCOCl	Isobutyl chloroformiate
IDT	Intradermal test
Ig	Immunoglobulin
IgE	Immunoglubulin type E
IgG	Immunoglubulin type G
IgM	Immunoglubulin type M
IR	Immediate reactions
IU	International units
LC	Liquid Chromatography
LTQ	Linear trap quadrupole
Lys	Lysine residues
m/z	Mass/charge
MALDI-TOF	Matrix-assisted laser desorption/ionization time of flight
MD	Minor determinant
MDM	Minor determinant mixture
MeOH	Methanol
MHC	Major histocompatibility complex
MS	Mass Spectrometry
MW	Molecular weight
NIR	Non-Immediate Reactions
NK	Natural killer
NMM	*N*-methyl morpholine
NMR	Nuclear Magnetic Resonance
NSAID	Non-steroidal anti-inflammatory drugs
PAMAM	Poly(amidoamine)
PBS	Phosphate buffer saline
PI	Pharmacological Interaction
PLL	Poly-L-lysine
PO	Penicilloyl

PPL	Penicilloyl-polylysine
ppm	Parts per million
PS-p-Ts-OH	Polystyrene supported p-toluenesulfonic acid
PVDF	Polyvinylidene fluoride
QTOF	Quadrupole Time of Flight
RAST	Radioallergosorbent test
RIA	Radioimmunoassay
rpm	Revolutions per minute
RT	Room temperature
SAR	Structure-activity relationship
SCAI	Central service for research support (from Spanish "Servicio central de apoyo a la investigación")
SD	Standard deviation
SDS	Sodium dodecyl sulfate
SDS-PAGE	Sodium dodecyl sulfate-polyacrilamide gel electrophoresis
SI	Stimulation index
sIgE	Specific IgE
SPA	Sinapinic acid
SPAAC	Stain promoted azide-alkyne cycloaddition
SPT	Skin prick test
ST	Skin Test
TCR	T cell receptor
TDCR	Triple-to-double coincidence ratio
TEA	Triethylamine
TEG	Tetraethylene glycol
TFA	Trifluoroacetic acid
Th	Helper T cell
THF	Tetrahydrofuran
TMR	Tetramethylrhodamine
UMA	University of Málaga
UV	Ultraviolet

VH	Variable domains in heavy chains
VL	Variable domains in light chains
WHO	World Health Organization
WTM	Wortmannin

GENERAL INTRODUCTION

1. Definition and Classification of Adverse Drug Reactions

An adverse drug reaction (ADR) is defined by the World Health Organization (WHO) as "a response to a medicine which is noxious and unintended, and which occurs at doses normally used in man" (World Health Organization, 1972).

ADRs constitute a serious public health concern since they cause considerable morbidity and mortality [1]. They are responsible for 3-6% of hospital admissions and 10-15% of hospitalized patients [2]. Among different ADRs classifications the most common is the proposed by Rawlins and Thompson in 1991 [3], which divided ADRs into two types:

Type A: they are predictable, dose and pharmacological action dependent, the most common and account for 80% of ADRs. Reactions consequence of overdose or drug toxicity as well as secondary or side effects and interactions with other drugs are included in this group [4].

Type B: they are unpredictable, dose independent and comprise 15-20% of all ADRs. Although reactions of type B are the less common of ADRs, they are extremely important, because they can be cause of serious health risks and even cause death [5]. Type B ADRs can be sub-classified into [4]:

B.1. Drug intolerance: produced by a non-desired effect of the drug at therapeutic or subtherapeutic drug doses.

B.2. Idiosyncratic reactions: anomalous responses without demonstrable immunological response attributable to pharmacokinetic responses associated with genetic factors.

B.3. Pseudoallergic reactions: adverse responses clinically similar to an actual allergic reaction but with no demonstrable immunological base.

B.4. Drug hypersensitivity reactions (DHRs): include reactions mediated by specific and non-specific immunological mechanisms.

There are also some types of infrequent reactions:

Type C: they are time and dose dependent and are related with dose cumulation.

Type D: they are time dependent, also related with dose and its action is only noticed after a latency time.

Type E: they occur after treatment suspension.

2. Definition and Classification of Drug Hypersensitivity Reactions

DHRs, as it was stated before, are Type B ADRs whose mechanism can be mediated by specific immunological mechanisms or non-specific immunological mechanisms [6]. The

former are called allergic reactions and may be antibody-mediated or T-cell dependent. The latter, non-allergic reactions, are more heterogeneous and majority of patients have cross-intolerance to nonsteroidal anti-inflammatory drugs (NSAIDs). In this work, we will focus on allergic reactions to drugs.

Allergic reactions take place when the immune system recognise a drug specifically and, as consequence, an effector response is unchained, fact that leads to a potetial serious damage in the organism. An important charasteristic of these reactions is that a previous exposure to the drug or a molecule chemically related, called sensitization phase, is required to stimulate the immune system. Once sensitized, allergic reactions to drugs are produced on drug re-exposure [7]. They represent 6-10% of all ADR and can be induced by a diverse range chemicals/drugs by means of the production of antibodies, sensitized T cells or both [5].

2.1. Immunological Classification of Allergic Reactions

DHRs have been traditionally classified into four groups by Gell and Coombs according to the trigger effector mechanism [7]. Allergic reactions to drugs can be consequence of any of the cited mechanisms, being types I and IV the most common.

-**Type I** or immediate hypersensitivity reactions, mediated by drug specific IgE (sIgE) antibodies.

-**Type II** or cytolytic or cytotoxic reactions, mediated by drug-specific IgG or IgM antibodies.

-**Type III** or immune complex-mediated reactions, mediated by drug specific IgG or IgM antibodies.

-**Type IV** or delayed hypersensitivity reactions, mediated by drug specific T cells. Due to the fact that T cell mediated reactions present heterogeneity in clinical manifestations and mechanisms involved, a subclassification of Type IV in Type IVa, IVb, IVc and IVd reactions was proposed [8-10], although this classification is not completely accepted in clinical practice since some clinical pictures can fit in some subtypes of Type IV reactions.

2.2. Clinical Classification of Allergic Reactions

DHRs are difficult to catalog according to the immunological mechanism involved so, in daily clinical practice, a classification based on time elapsed between drug administration and first sympthoms is easier and more convenient. Following this principle, they can be included in two groups: immediate and non immediate.

-**Immediate reactions (IR):** usually occur within the first hour after drug administration and are generally IgE-mediated. Typical clinical manifestations are urticaria, angioedema, anaphylaxis, or anaphylactic shock and can be potentially fatal [5]. They correspond with Type I Gell and Coombs immunological classification.

-**Non-immediate reactions (NIR):** they are delayed hypersensitivity reactions, occuring after one hour of drug administration, mediated by drug specific T cells. Maculopapular exanthema is the most frequent reaction [6]. They correspond with Type IV Gell and Coombs immunological classification.

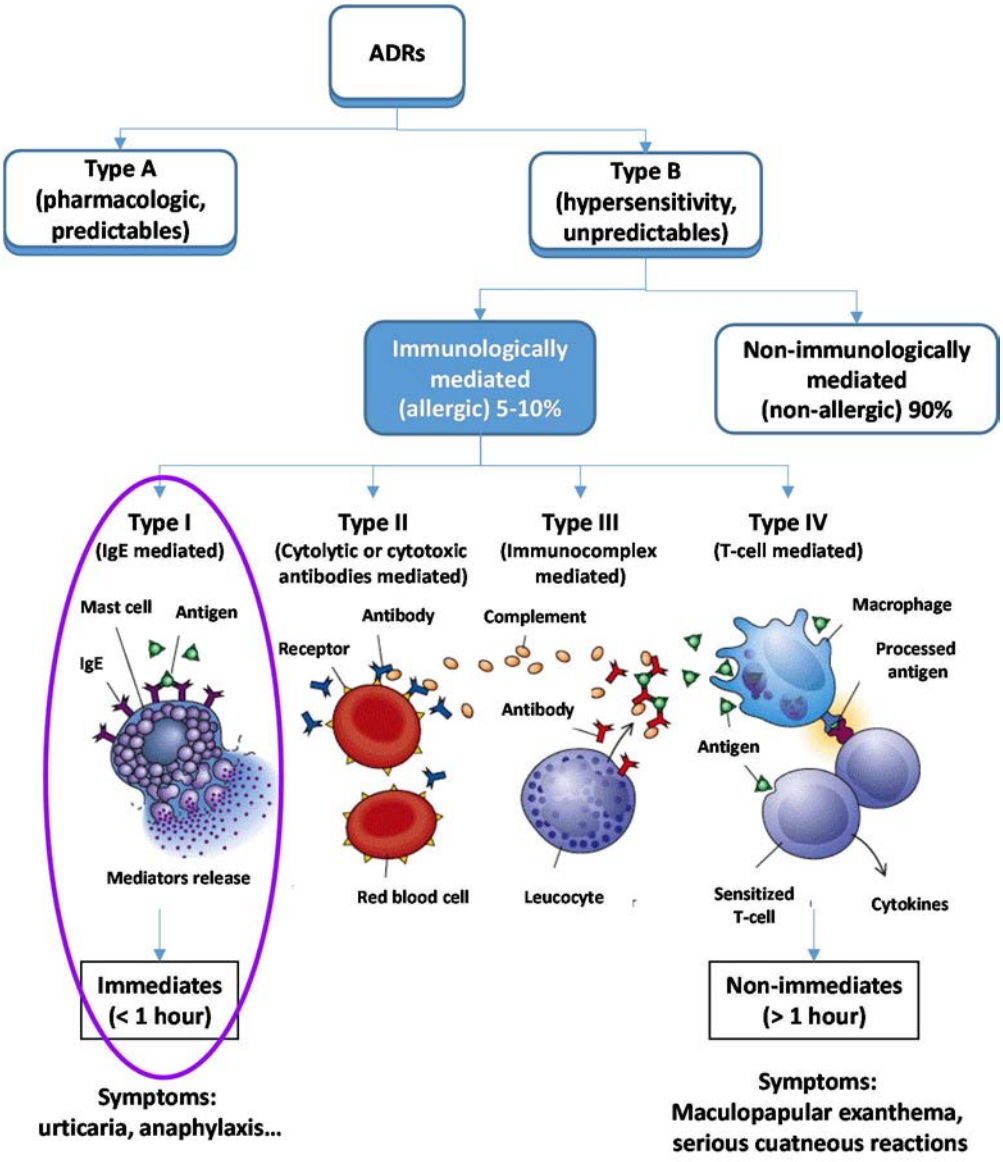

Figure 1. Immunological and clinical classification of DHRs.

3. Epidemiology and Prevalence of Allergic Reactions to Drugs

Currently, actual prevalence of allergic reactions to drugs is unknown [11], and morbidity and mortality data as well as economic costs are subestimated. There are few studies that describe both incidence and prevalence of allergic reactions to drugs in general population, being most of data based on hospitalized patients or emergency services [1], so figures are merely indicative. From these studies is deduced that allergic reactions to drugs represent 6-10% of every ADRs, but this values may change depending on the methods employed for confirming diagnosis [12-14].

In Spain, NSAIDs are the most consumed, followed by betalactam antibiotics (BLs). However, only 10% of hipersensitivity reactions to NSAIDs are associated with a defined immunological mechanism [15], being BLs responsable for most of allergic reactions to drugs mediated by a well-known immunological mechanism, followed by quinolones and other antibiotics [15]. The prevalence and incidence of allergic reactions to BLs in the general population are not well known either [6]. A prevalence of allergic reactions to penicillin ranging from 0.7% to 10% of the population, with anaphylaxis occurring in 0.015% to 0.004% of cases was reported in early studies. The wide range of prevalence rates found in published studies, with overreporting occurring when patients are classified by clinical history only as well as underreporting of mild and severe reactions [6] is due to a considerable proportion of patients with suspected hypersensitivity to BLs showing good tolerance in allergy studies [6].

Frequency of allergic reactions associated with each drug varies over time according to changes in prescription patterns [15]. In the study performed by Doña *et al*. between 2005 and 2010 [15], it was observed that rate of allergic reactions to BLs had the same tendency from 80s, with a progressive decrease of reactions produced by benzylpenicillin (BP) and an increase of reactions produced by amoxicillin (AX). Nowadays, allergy to new cephalosporins are also being reported. Moreover, it is important to highlight an important increase of urticaria and anaphylaxis due to new drugs such as AX-clavulanic acid (CLV) combination, whose consumption has notably grown over the last years, and quinolones [16].

4. Mechanisms of Allergic Reactions to Drugs

Drugs interaction with the immune system can be explained by 3 major working hypotheses: the hapten hypothesis, the danger hypothesis, and, more recently, the pharmacological interaction (PI) hypothesis. Hapten hypothesis explains interaction of the drug with the immune system after drug binding to a carrier molecule, while the

other 2 hypotheses try to explain the interaction without the need for covalent binding to proteins [17].

4.1. Hapten hypothesis

Currently, the most accepted model for explaining the way the immune system recognizes drugs is based on the hapten hypothesis introduced by Landsteiner in 1935 [18]. Haptens are low molecular weight molecules (<1000 Da), chemically reactive and too small to be able to induce an immune response by themselves but they do when covalently bound to a protein, proccess called haptenization [18-20]. Chemically reactive drugs or their metabolites can act as haptens and form covalent adducts with extracellular or intracellular proteins, which are able to induce the production of IgE antibodies or T cells that specifically recognize the adduct. The structure of the adduct that is recognized specifically by the components of the immune system (IgE or T cell) is called the antigenic determinant (AD), or epitope, and usually comprises the drug derivative and part of the carrier protein [5]. According to this hypothesis, antigenic structures must be presented to the immune system as multivalent antigens to lead to a specific immune response and activate immunopathological mechanisms (Figure 2, bottom). Hapten-carrier molecule conjugate can be proccesed and presented by antigen presenting cells (APCs) to lymphocytes for specific antibodies production which can react against AD formed by the hapten and probably by some regions of carrier molecule. The response induced by hapten-carrier molecule conjugates depends on hapten density [21] and its distribution through the carrier molecule [22]. The molecular weight is one of the main characteristics that determine the immune capacity of a molecule [21, 23] but its chemical nature and structural complexity are also important [24].

BLs have been used as models of the hapten hypothesis because of their high reactivity or capacity to bind to proteins through the nucleophilic attack on the β-lactam ring by the amino groups in the protein. However, the identification of the metabolites that act as haptens is difficult for other non-chemically reactive drugs [17].

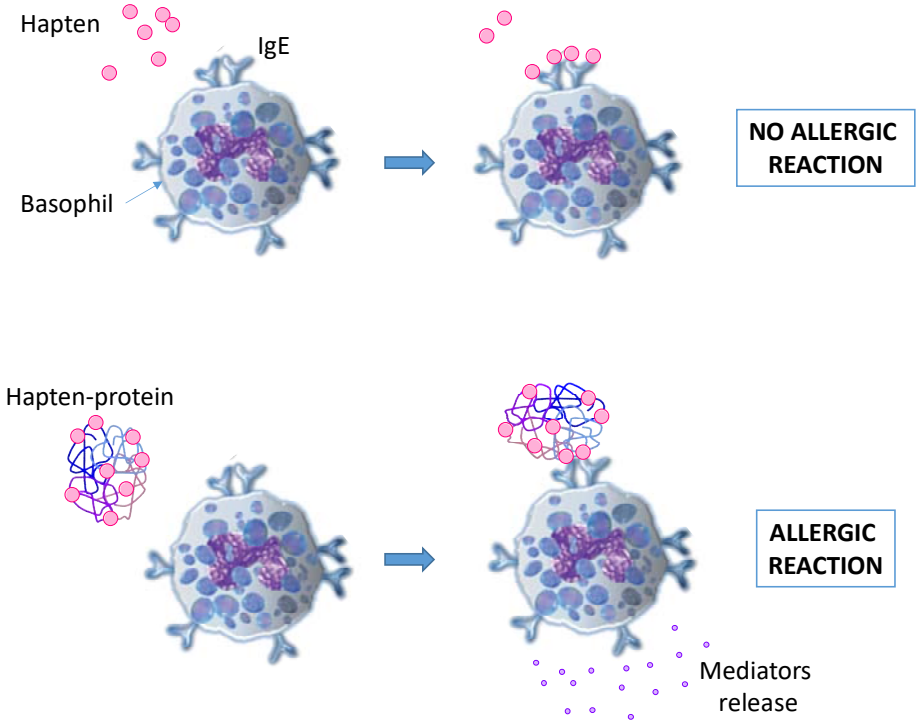

Figure 2. Hapten hypotesis proposed by Landsteiner [18].

4.2. Danger hypothesis

The danger hypothesis (Figure 3) was proposed by Matzinger [25] and is based on the fact that cell damage induces production of danger signals that interact with the immune system, thus activating APCs. The immune system only presents a response against antigens associated with the danger, which in this context can be defined as any element causing stress or cellular death [25]. Two signals are necessary for immunological response induction. The first signal is defined as the signal consequence of the contact between an antigen and its specific receptor (immunoglobulin (Ig) or T cell receptor (TCR)) and the second signal is a set of co-stimulating signals such as concurrent infections, exposure to endotoxins, stimulation by cytokines, metabolic alterations or drug toxicity which were called “danger signals” [26]. The presence or ausence of signal 2 determines whether the consequence is an immune response or a natural immunologic tolerance mechanism [25]. There are some studies that report that “danger signals” increase drug-protein adducts formation [26].

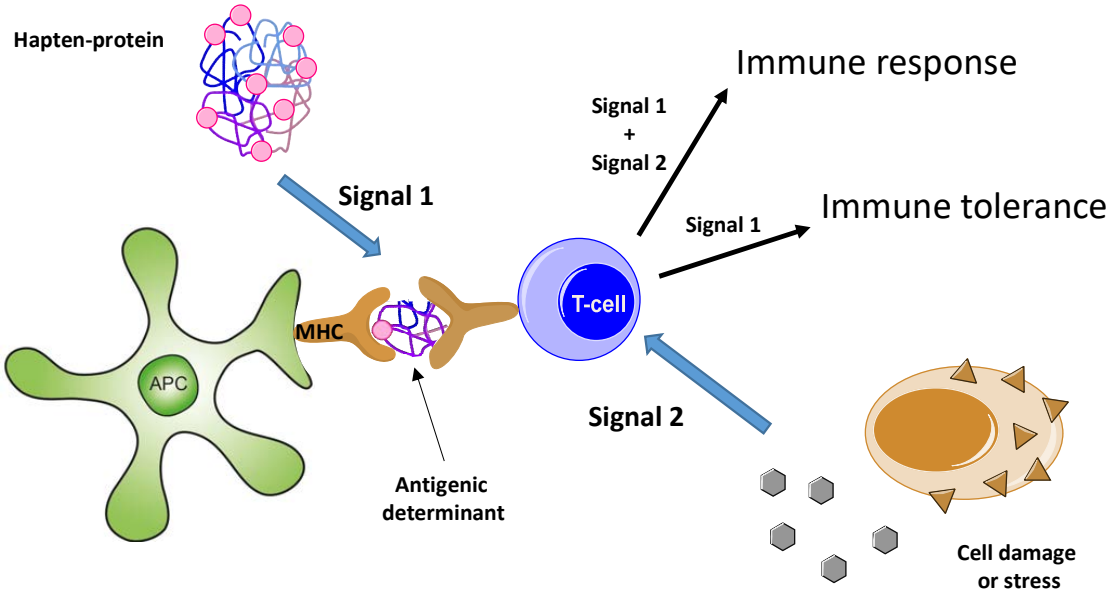

Figure 3. "Danger signal" hypothesis applied to the mechanism described in hapten hypothesis. Adapted from [25, 26].

4.3. Pharmacological Interaction hypothesis

The fact that hapten hypothesis was demostrated only for some drugs leaded, in the last years, to the proposal of a new model in which some drugs would not need covalent binding to macromolecules to induce an allergic response. They could bind directly (without previous drug metabolization) and reversibly to immunological receptors such as major histocompatibility complex (MHC) or TCRs through Van der Waals forces, electrostatic interactions or hydrogen bonds. Thus, cells would be stimulated. This PI model was proposed by Pichler [27] but it has never been confirmed in the case of BLs [17]. It is represented in Figure 4.

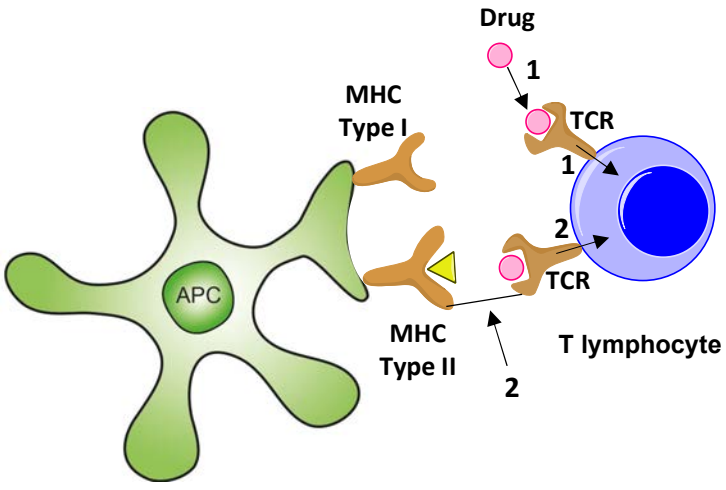

Figure 4. T lymphocytes activation in PI model. Drug binds to some TCRs (1) with enought sensitivity for signal triggering. Drug-TCR interaction is complemented with the interaction with MHC (2). Adapted from [17].

5. Immunological Proccess Related with Immediate Allergic Reactions to β-lactam Antibiotics

IRs to drugs are mediated by sIgE immune mechanisms (Figure 5). In these reactions IgE are produced against a hapten-carrier conjugate during a sensitization phase, these then attach to FcεRI on the surface of mast cells and circulating basophils. During re-exposure, the binding of drug-carrier molecule adducts (multivalent antigen) to at least 2 adjacent IgE molecules induces degranulation of mast cells and basophils, leading to the release of inflammatory mediators, including histamine, leukotrienes, and cytokines, resulting in the allergic symptoms [7, 28]. The drugs most frequently involved in these reactions are BLs, NSAIDs, quinolones and radio contrast media [5].

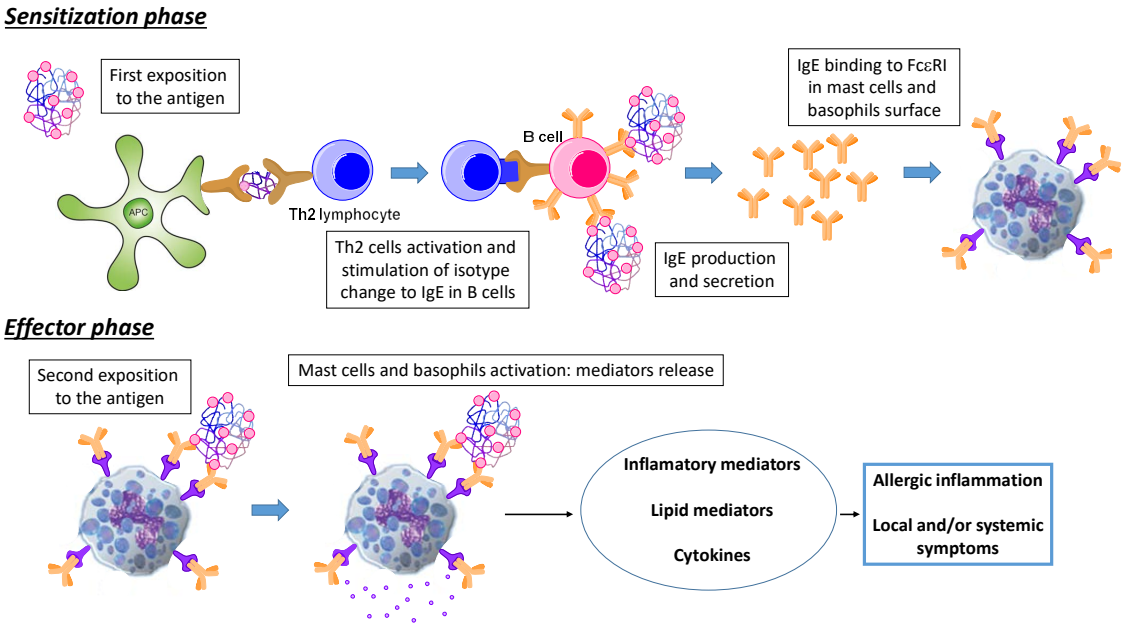

Figure 5. Sequence of events in immediate allergic reactions: sensitization phase and effector phase.

5.1. Immunoglobulin E

IgE was discovered in 1967 by Ishizaka and Johanson [29] and it has been demonstrated its intervention in immediate hypersensitivity reactions as well as in immune response consequence of infections produced by parasites [30-32]. IgE molecular weight is 118-196 kDa [33] and a general structure is depicted in Figure 6. Variable domains in light and heavy chains (V_L and V_H) interact between them to create a globular unit which contains antigen binding site. Complementarity determining regions (CDRs) comprise ten aminoacids which form a surface of contact complementary to the corresponding antigen. The rest of the domain does not take part directly in antigen recognition but it acts as support.

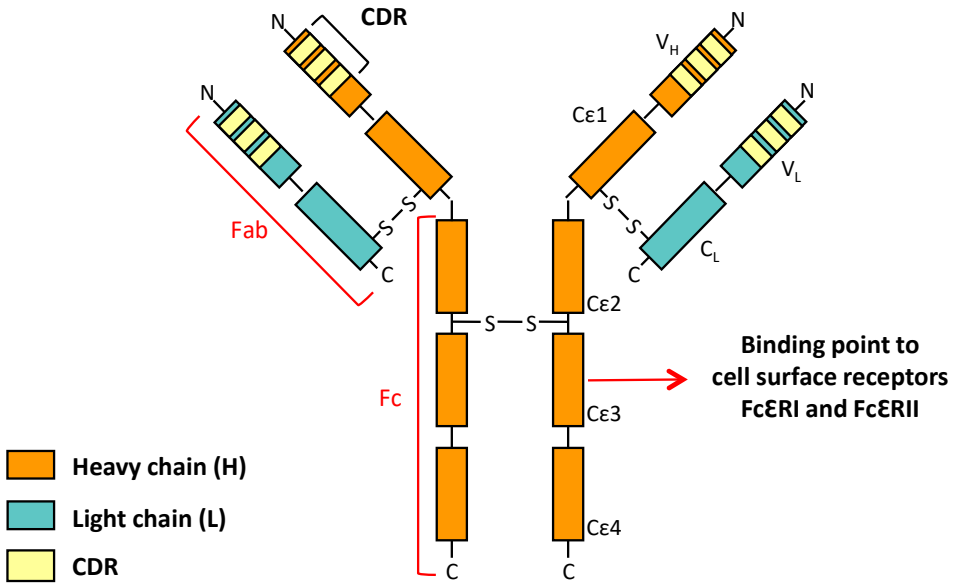

Figure 6. Depiction of IgE general structure with its two functional regions: the (Fab) and the christallizable region (Fc). The former is involved in Ig specificity and the ability to bind to the antigen while Fc mediates effector responses.

IgE molecules are produced mainly by plasmatic cells in linfoid tissues associated with mucous [34]. Most produced IgE binds to high-affinity IgE receptors expressed in mast cells and basophils surface (FcεRI) [34] and the rest binds to FcεRII receptors or circulates free through bloodstream. IgE serum concentration is the lowest among all kind of Igs, which makes necessary the use of high sensitivity techniques for its detection [35]. In spite of IgE low concentration, its action is amplified by numerous factors such as binding to cellular receptors [36].

Total plasma IgE concentration in healthy adults is lower than 20 IU/mL and sIgE is not higher than 0.35 IU/mL [37]. In those people who present an allergic reaction, an amplified production of both non-specific IgE and sIgE against the antigen causing the reaction occurs, reaching IgE levels 1000 times higher than in non-allergic individuals.

5.2. β-lactams Chemical Structures

The basic structure of BLs consists of a four-member β-lactam ring, which provides the antibacterial activity. BLs are classified according to their chemical structure into different groups or classes: penicillins, cephalosporins, monobactams, carbapenems and clavams [38] (Table 1). The core structure of every group, except for monobactams, consists of a bicyclic structure in which the β-lactam ring is fused to another ring: in penicillins this is a five-member sulphur ring (thiazolidine), in cephalosporins a six-member sulfur ring (dihydrothiazine), in carbapenems a five-member ring (dihydropyrrole), and in clavams a five-member oxygen ring (oxazolidine). Every kind of

BL displays different side chains or R substituents. These are linked to either the β-lactam ring (R or R^1), except in the case of clavams, or to the other ring (R^2, R^3) except in the case of penicillins and monobactams. The chemical structures of these side chains vary greatly; however these side chains can be similar or identical between members of different groups of BLs [38].

Table 1. Chemical Structure of BLs [38].

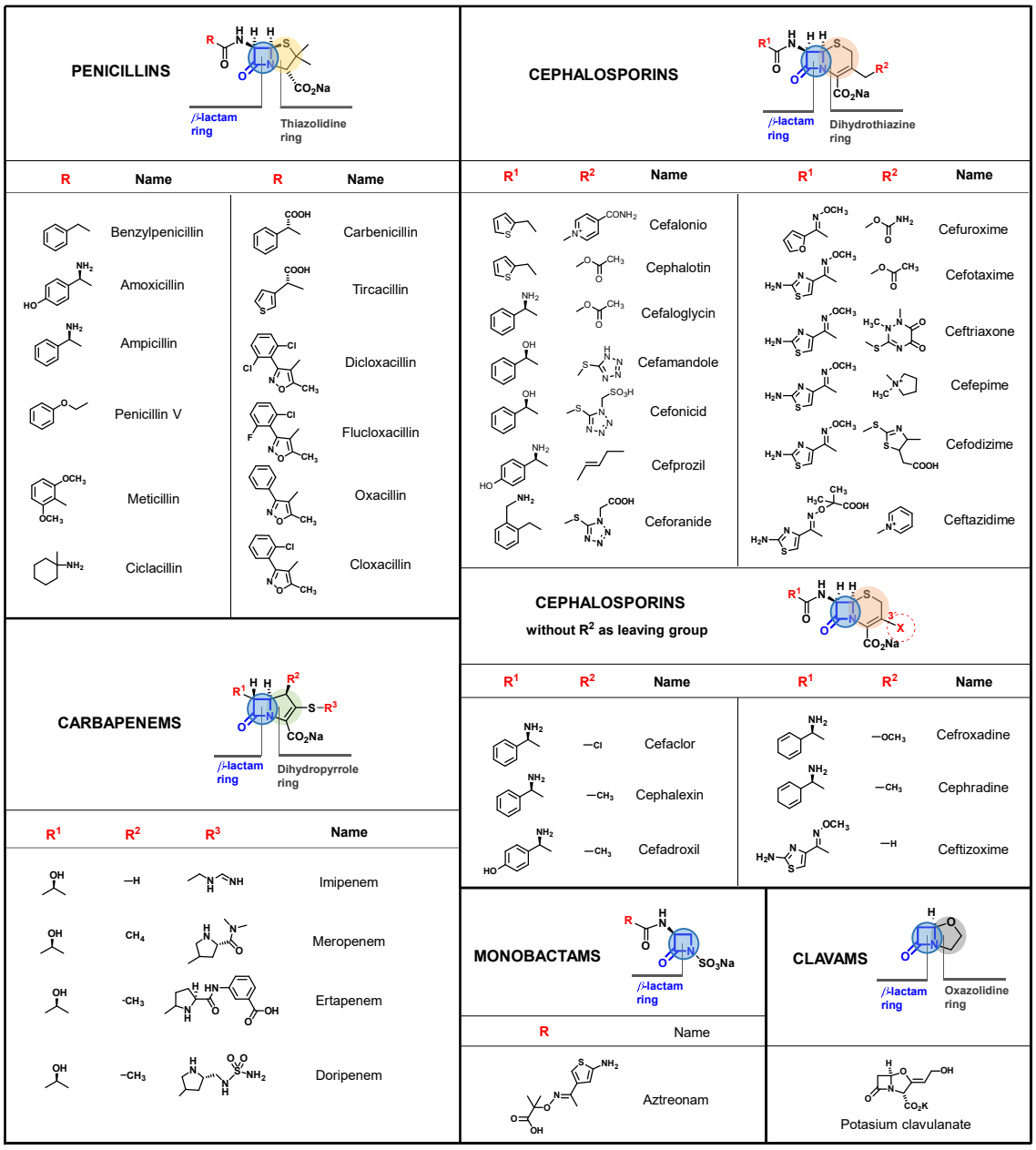

5.3. β-lactams Antigenic Determinants

As stated before, BLs represent a model of the hapten hypothesis because of their high reactivity towards proteins. BLs are small molecules that act as haptens and therefore

are able to induce an immune response only after they covalently bound to exogen or endogen proteins which can be proccessed and recognized by the immune system [18, 39].

It is well established that the immunological behavior of BLs is determined by their intrinsic chemical reactivity without need of a previous metabolic proccess. Due to ring strain, BLs are highly reactive. The electrophilicity of the β-lactam carbonyl group enables binding to protein via nucleophilic attack by the ε-amino groups of their lysine residues (Lys), leading to the opening of the β-lactam ring and the formation of a amide bond to form a drug-protein conjugate [40, 41] (Figure 7). The chemical structure after this conjugation process depends on both the chemical properties of the BL involved, as well as the ring to which the β-lactam is fused, which can further increase tension to the β-lactam ring, leading to the formation of either stable or unstable structures [38, 42, 43]. Haptenization degree of proteins by BLs is hapten concentration dependent [44, 45] and there are studies that infers that binding kinetics vary depending on the nature of proteins, being faster for serum proteins than for cellular proteins [44]. Previously mentioned differences and similarities in the chemical structure of BLs, mainly in the core region and the side chain, among the wide range of BLs, are important for considering the different patterns of immunological recognition in terms of specificity [38].

Identifying the drug metabolites involved in allergic reactions to BLs is important, not only for understanding the underlying immunological mechanisms but also for improving diagnostic tests. To this end, several studies have been performed with different BLs.

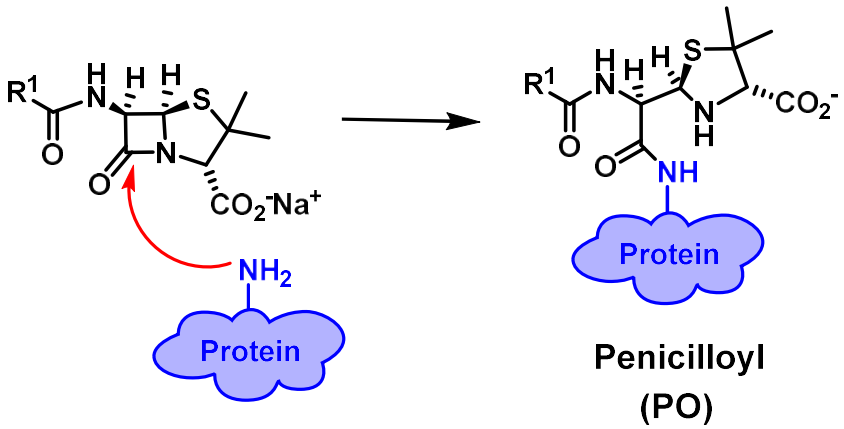

Figure 7. Penicillins conjugation to carrier proteins and the formation of penicilloyl (PO)

-Penicillins

BP was the first hapten studied in detail and it is still considered the reference model for the study of allergy to BLs [40, 46]. The high strain of the β-lactam ring in penicillins makes them highly reactive towards the nucleophilic attack of free amino groups of proteins and haptenization is thus a spontaneous and efficient process. This reactive behavior is common to all penicillins. The conjugate so formed with BP results in the benzylpenicilloyl (BPO) determinant [40, 46] (Figure 8A), whose stability enables the elucidation of its chemical structure by classical characterization techniques [47]. In fact, the BPO group is the major AD of BP, since it represents 95% of the penicillin molecules that become covalently bound to proteins under physiological conditions [46] and is therefore used in its acid form (benzylpenicilloic acid) and amide form (BPO linked to an amine functionalized compound) in diagnostic studies (Figure 8B). The remaining BP has been considered to form other derived structures, classified as minor determinants, including benzylpenicillenic acid, benzylpenicilloic acid, benzylpenilloic acid, benzylpenicillanyl, benzylpenamaldic acid, benzylpenaldate, penicillamine and penicoyl [48] (Figure 8B) although immediate IgE reactions with some of these minor determinants have not been demonstrated in human [49].

With a similar behavior to BP, the major AD of AX is the amoxicilloyl (AXO) amide [50] (Figure 8A), whose chemical stability enabled its characterization by classical spectroscopic techniques [51]. Moreover, AX could form determinants similar to those proposed for BP. For instance, AX might generate a molecule equivalent of penicillenic acid (Figure 8B), which includes a free thiol group that would allow the conjugation with the free thiol cysteine of proteins through disulfide bonds. However, this disulfide-conjugated structure has been neither isolated nor characterized by modern techniques. The difference between AX and BP structures is given by the hydroxyl and amino group present in the AX side chain. This amino group confers reactivity toward electrophiles, such as the carbonyl β-lactam ring, that can lead to different compounds, such as polymers through reaction of the amino group in AX side chain with the β-lactam ring in other AX molecule, or diketopiperazine when the amino group reacts with the β-lactam ring in the same AX molecule, leading to an intramolecular cyclization (Figure 8C). Thus, intermolecular reactions between AX molecules results in dimers [52, 53] and further polymers by cleavage of the β-lactam ring in aqueous solutions. This behaviour is common for aminopenicillins in general [54], and resulting polymers have been considered to be immunogenic [55]. However, further studies are needed since these determinants are not considered when evaluating allergy to aminopenicillins.

The production of monoclonal antibodies against penicillins, employing the drug conjugated to a carrier macromolecule as immunogen, proved that both the nature of the carrier molecule and that of the hapten can influence IgE recognition [56, 57]. The

monoclonal antibodies production has provided information to characterize BP ADs with the identification of three different epitopes (Figure 9): the side chain, the nuclear structure including the thiazolidine ring, and the carbonyl group involved in the conjugation to the carrier protein [58], although these regions can overlap [59]. Similar results have been reported with AX [59] and ampicillin (AMP) [60]. In the case of these aminopenicillins, the majority of the generated monoclonal antibodies recognized an epitope in which the side chain was a major constituent, although with variable contributions from other regions of the molecule.

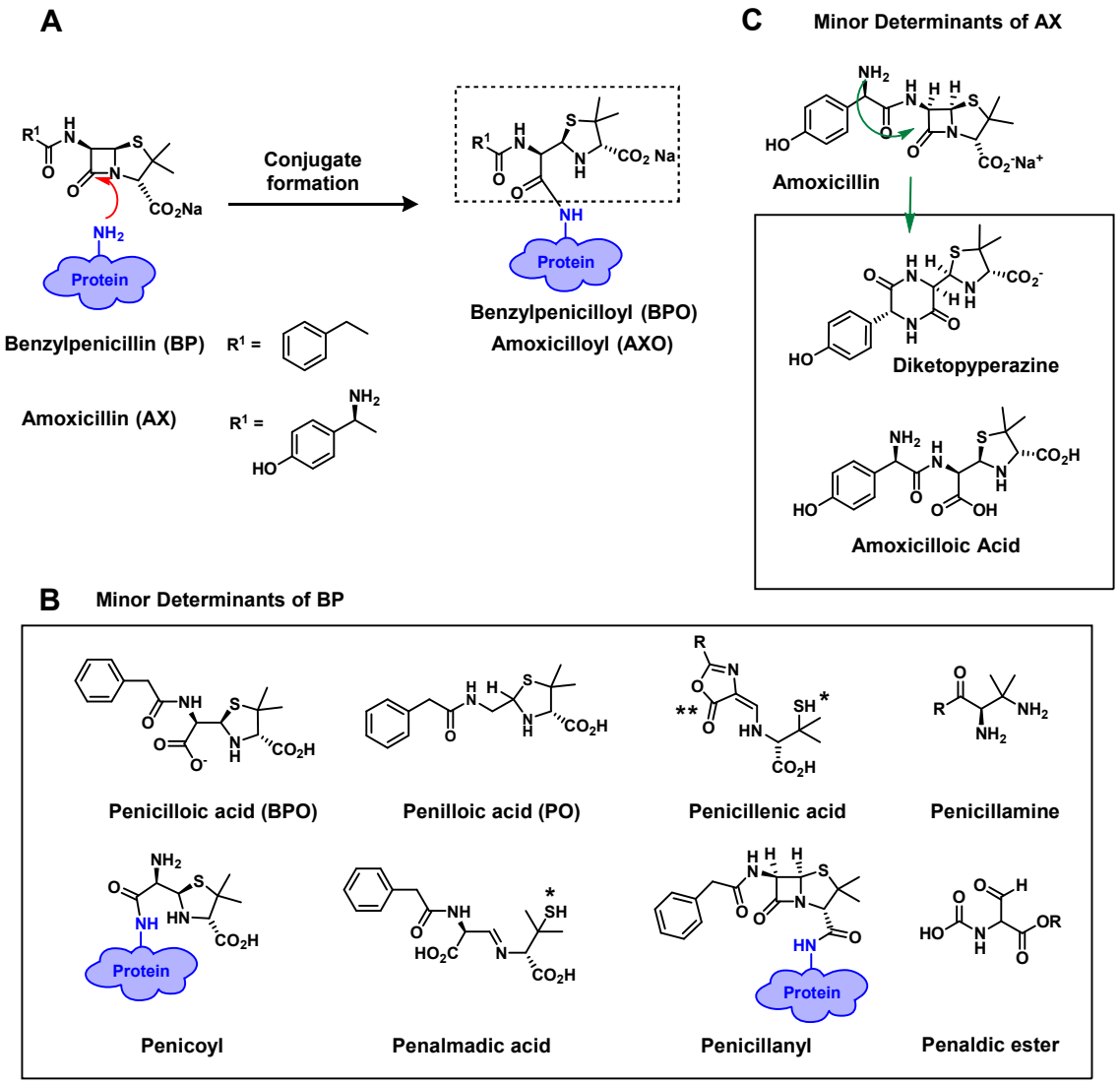

* S-S bond formation with cystein residues of proteins leads to disulfide compounds

* * The formation of diastereoisomeric penicilloyl determinants takes place by means of the nucleophilic attack to the carbonyl moiety

Figure 8. A. BP and AX conjugation to carrier proteins and the formation of their major determinants. B. Described minor determinants for BP. C. Described minor determinants for AX.

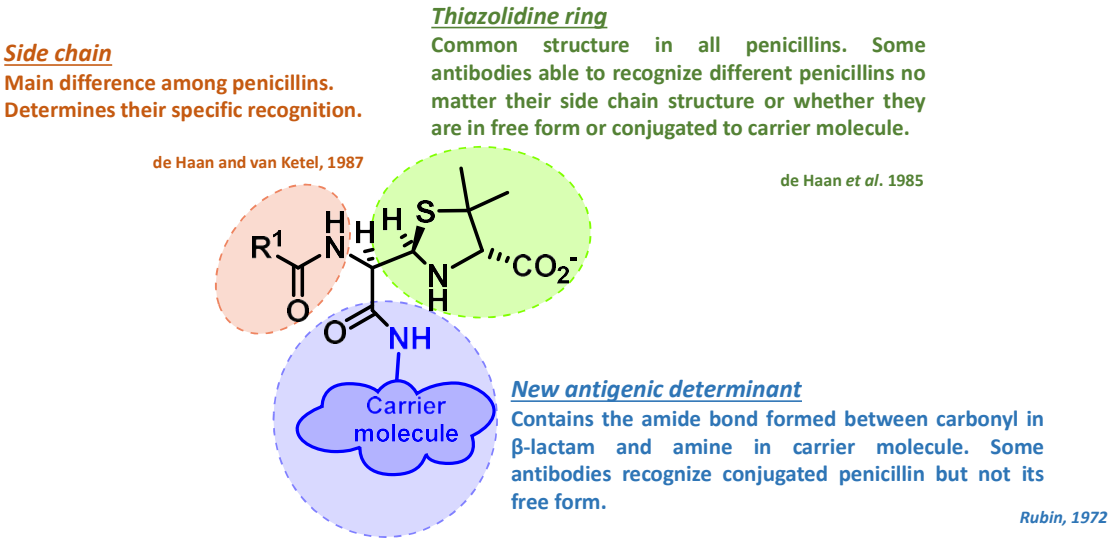

Figure 9. Common ADs for penicillins.

-**Cephalosporins**

Cephalosporins are BLs derived from cephalosporanic acid. After penicillins and quinolones, they are the most used antibacterial agents for infectious illnesses treatment and prophylaxis and, due to variations in BLs prescription patterns, have become one of the main causes of DHRs. The number of publications on allergic reactions to cephalosporins is relevant and growing. However, unlike well-established structures responsible for penicillin allergy, metabolites involved in the immunological response to cephalosporins are still unknown.

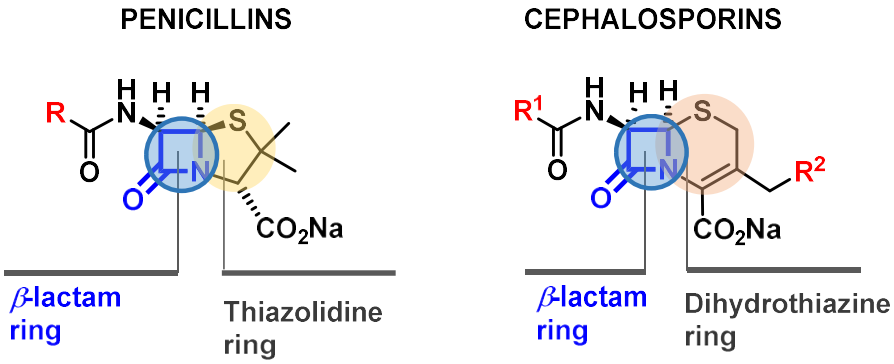

Figure 10. Structural differences between penicillins and cephalosporins.

The main difference between penicillins and cephalosporins is the ring fused to the β-lactam, a five-membered thiazolidine ring in penicillins and a six-membered

dihydrotiazine ring in cephalosporins (Figure 10). These structural differences lead to differences in electrophilic properties of the β-lactam carbonyl and, therefore, in the potential to bind to proteins and form a determinant [42]. The acylation capacity is higher in penicillins compared to cephalosporins, due to the higher tension within the β-lactam fused to the five-membered thiazolidine ring in the former than within the six-membered dihydrotiazine ring in the latter.

In cephalosporins, this lower reactivity of the β-lactam ring slows carrier conjugation. The R^2 chemical structure modulates this reactivity depending on its ability to polarize the electronic binding. The departure of R^2 as a consequence of nucleophilic attack on the β-lactam has been interpreted from both theoretical [65, 66] and experimental [5] evidence, in terms of β-lactam ring opening concerted with the elimination of R^2. Additionally, the non-concerted expulsion of R^2 with the β-lactam ring opening has been described [67, 68] (Figure 11). Kinetic and spectroscopic studies have shown the structure resulting from the β-lactam ring opening: cephalosporoyl (CPO) [67, 68]. Whether the process is concerted or non-concerted, the opening of the β-lactam leads to a clear departure of the good R^2 leaving group generating a very unstable structure which leads to different fragmentation of the dihydrothiazine moiety. These degradation products have not been identified yet, preventing from understanding the mechanisms of cephalosporins immunogenicity [42, 43].

The reaction of cephalosporins with butylamine as a simple nitrogen nucleophile has been chemically studied. Although the identification of the exact chemical structure was not possible, results suggest the CPO conjugate formation and further fragmentation of the dihydrothiazine ring, leading to structures including at least the remaining β-lactam and the R^1 side chain [43, 69]. Also, there is clinical and immunochemical evidence of the R^1 side chain contribution to the sIgE production as well as to cross reactivity responses among different cephalosporins and penicillins. Indeed, some patients have selective reaction to the culprit cephalosporin, others react to some cephalosporins with identical or similar R^1 side chain [70-72] and a third group of patients has cross reactivity with another BLs, specially penicillins, with identical or similar R^1 side chain [64, 71, 73].

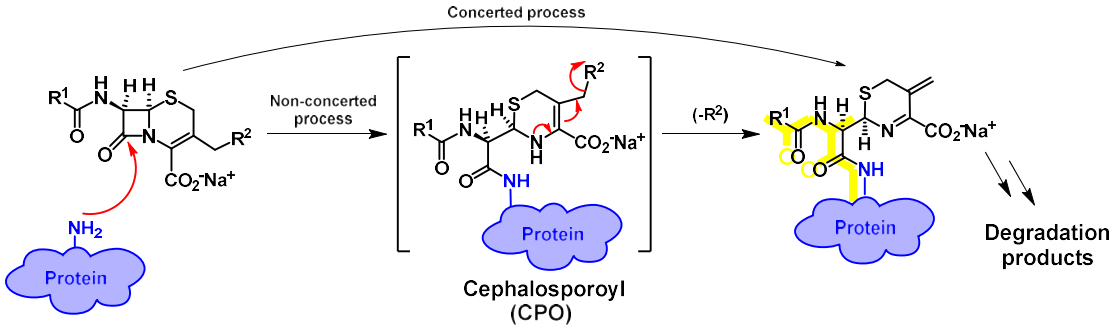

Figure 11. Nucleophilic ring-opening of cephalosporins by proteins and subsequent formation of ADs.

-Carbapenems

Studies on the ADs of carbapenems are scarce. However, conjugation between carbapenems and proteins have been described. These reactions result in a stable structure consisting of the open BL ring bound to the carrier proteins through an amide linkage (Figure 12, top). The specificity of the response to carbapenems is likely to be related to the relatively stable dihydropyrrole ring [74]. A wide range of cross-reactivity between penicillins and carbapenems has been reported in various studies [75, 76]; however, more recent prospective studies have shown no cross-reactivity between penicillin and carbapenem in skin tests (STs) (around 1%) [77, 78].

-Monobactams

Monobactams are the compounds in which the BL ring is not fused to a second heterocycle. The only commercially available monobactam is aztreonam, which has the same side chain as the cephalosporin ceftazidime. The conjugation of aztreonam to protein through amide bond formation might form relatively stable homogeneous ADs (Figure 12, bottom) [74]. The existing three monoclonal antibodies against aztreonam have identified three epitopes: nucleus, side chain and the complete structure of the drug with the carbonyl involved in the conjugation to the carrier protein [79]. Two of these monoclonal antibodies recognize both aztreonam and ceftazidime, highlighting the importance of the side chain as a relevant part of the determinant. The third line monoclonal antibody recognizes the AD which is formed by the conjugation of β-lactam and carrier protein, displaying broad cross-reactivity with several BLs [77].

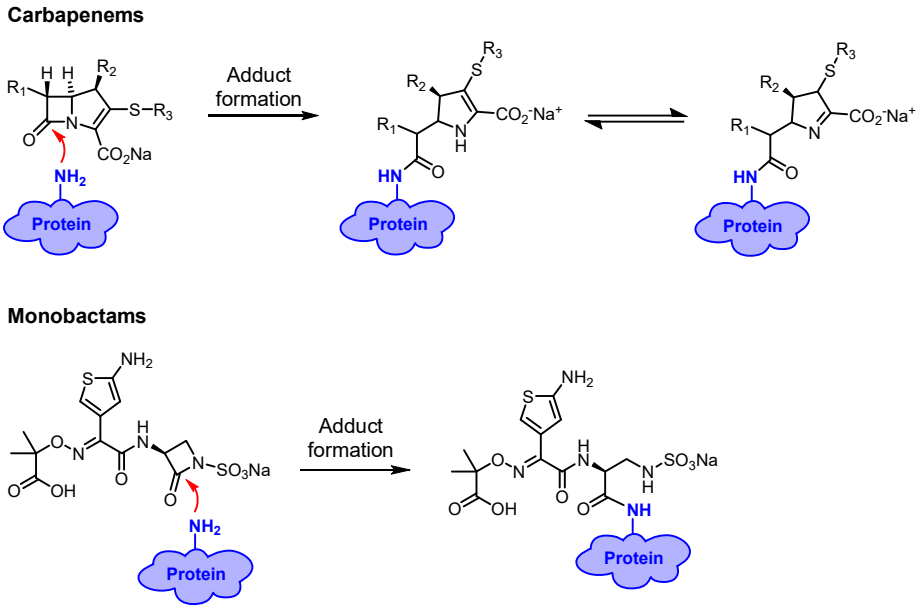

Figure 12. Reactivity of carbapenems (top) and monobactams (bottom) towards nucleophiles.

-Clavams

CLV is the only BL included in this group and is prescribed in combination with AX. The complex chemistry of CLV has made it difficult to advance our knowledge of its ADs; diagnosis is incomplete when an AX-CLV combination is involved in the reaction [80]. The reactivity of CLV can be explained by its strained bicyclic structure (β-lactam ring fused to an oxazolidine ring, which presumably reflects the substitution of an oxygen atom for sulfur), the lack of an acylamino substituent at C-6, and the presence of an exo-p-hydroxyethylidene function at C-2 [81] (Figure 13). These structural differences increase chemical reactivity of the CLV structure. CLV has a more complex chemistry than AX [81-84] in terms of its conjugation process, and relatively little is known about its immunogenicity. Initial studies described a very low intrinsic immunogenicity of CLV, with the formation of small determinants together with other degradation products [74]. According to this study, CLV protein conjugates display very small and heterogeneous epitopes with a very low density in the carrier. Moreover, recent publications out of the context of allergy have described CLV binding to β-lactamases [54, 64, 65, 85] with protein conjugation mechanisms and proposed structures in agreement with those previously described [74].

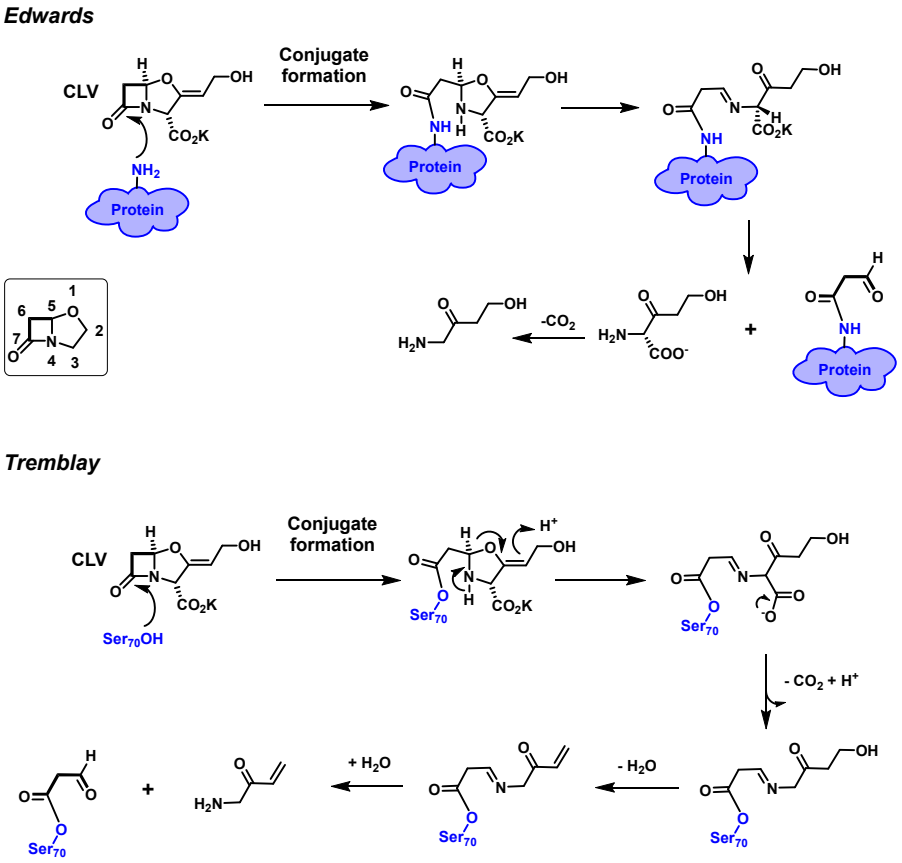

Figure 13. Reactivity of CLV towards nucleophiles. Mechanism proposed by Edwards [74] (top) and Tremblay [85] (bottom).

5.4. Protein haptenation by BLs

The immune response to BLs is determined not only by the chemical structure of the metabolites, but also by the nature of the adduct itself and the characteristics of its uptake, processing, and presentation by APCs [86]. Therefore, studies have been performed to analyze binding of BLs to carrier molecules, as well as the ability of the BL-carrier adducts to activate the immune system and the immunopathogenic relevance of them [17, 63]. It is still not fully known how haptenation occurs *in vivo*, nor do we fully understand the amplification mechanisms that cause an allergic reaction quickly after the drug administration and develop severe clinical manifestations. One of the main limitations of these studies is the difficulty involved in detecting the BL adducts produced after treatment. These studies have succeeded with penicillins due to their straightforward chemistry with proteins and the high stability of the resulting PO anchored structures [5]. However, it has been more difficult to perform when the BL involved in the haptenation process has a more complex chemical behaviour. First studies were performed to characterize the carrier proteins modified *in vitro* by BP, experiments that were performed in alkaline pH aqueous media to enhance the modification of proteins with BP [87], facilitating the detection and characterization of the adducts. New studies have been carried out recently using different conditions and experimental design for characterization of the adducts involved in allergic response to BLs [53, 88, 89]. Ariza *et al*. studied the formation of covalent adducts of low AX concentrations with human serum albumin (HSA) and potentially with other serum proteins in alkaline pH aqueous media [88]. Garzon *et al*. addressed the detection and characterization of the modification of HSA by AX in *ex vivo* samples [89]. Meng *et al*. explored the molecular basis of AX and CLV binding to HSA *in vitro* in neutral pH aqueous media and determined whether similar adducts could be detected in patients [53].

5.5. Candidate Carrier proteins for BLs

- **Human serum albumin as main carrier protein**

HSA is the major protein component of blood plasma. It plays an important role in the regulation of colloidal osmotic pressure and acts as a reservoir and transport protein for endogenous (e.g. fatty acids or bilirubin) and exogenous compounds (e.i. drugs or nutrients) in the blood [90-92]. As far as drugs are concerned, HSA accounts for the majority of binding in serum together with α1-acid-glycoprotein (α-AGP). HSA is a single-chain, non-glycosylated polypeptide that contains 585 amino acids [90, 91] with a molecular weight of 66,500 Da [90, 93]. Most abundant amino acids in albumin are alanine, glutamic acid, leucin and lysine. The high percentage of ionic amino acids (glutamic acid and lysine) confers a relatively high solubility to the protein. Acidic residues are more abundant than basic residues, being -15 the net charge per molecule

at pH 7.0. As far as secondary structure is concerned, HSA is a highly helical molecule. The α-helix content is 67%, while 23% is extended chain and 10% β-turn, as determined by X-ray analysis [91]. HSA contains 35 cysteine (Cys) residues and all of them, except Cys34 that plays a key role in the antioxidant function of HSA, are involved in disulfide bond formation that serves to stabilize HSA [90, 91, 93]. The tertiary structure is a heart-shaped molecule with approximate dimensions of 80 × 80 × 30 Å [90, 91]. Crystallographic data show that HSA contains three structurally similar α-helical domains: I, II and III [90-94], formed by 10 α-helix each, which can be further divided into subdomains A and B, formed by 6 and 4 α-helix respectively [90, 92-94] (Figure 14). Drugs that bind to HSA with high affinities usually interact with one or two specific sites (site I and II) on the protein. X-ray crystallographic data clearly demonstrated the location of sites I and II in subdomains IIA and IIIA, respectively [90, 92, 94]. Both sites are composed of all six helices of subdomains IIA or IIIA and are therefore topologically similar, however, there are significant differences between the two drug pockets [92]. The entrance to site I in subdomain IIA faces subdomain IIIA and this site has an extended binding region owing to the residues from subdomain IIB and IIIA. In contrast, the involvement of other subdomains in the drug binding capacity of site II is relatively modest [90].

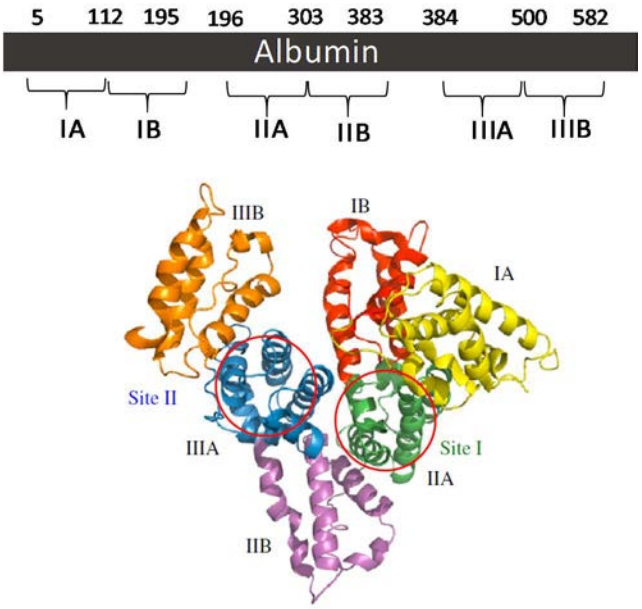

Figure 14. HSA structure showing the organization of the protein in domains and subdomains. Top: Sequence of HSA structure showing the three domains. Bottom: Crystal structure of HSA showing domains (I-III) and subdomains (A and B) as well as the approximate locations of site I and site II. Adapted from Yamasaki *et al*. [90].

HSA structure is affected by variations in the pH conditions due to the high number of acidic and basic residues in its sequence. HSA can suffer some chemical modifications within its lifetime which can affect its antioxidant properties and ligand binding capacity, and furthermore, may confer antigenic properties [95-97]. Some possible modifications are acetylation, cysteinylation, homocysteinylation, nitrosilation, nitration, oxydation, phosphorilation, glutathionylation and glycation.

Based on its extraordinary ligand-binding capacity, HSA has been traditionally considered the main target protein in the haptenation process for penicillins, and most studies have focused on characterization of the PO-HSA adducts. In an early study by Lafaye *et al*. [98], the number of penicillin molecules, which are covalently bound to HSA, was directly proportional to the drug concentration. In fact, the detection of PO groups decreased exponentially over time after interruption of drug treatment, and the half-life of penicilloylated HSA proved to be shorter than or equal to that of non-modified HSA [98]. Some studies have explored the detection and identification of HSA residues modified by BL antibiotics. Early studies by Yvon *et al*. [99, 100] revealed BPO-HSA adducts in serum samples from patients treated with BP or samples generated *in vitro* and in which binding of BPO was observed in 6 of the 59 Lys of HSA (Lys 190, 195, 199, 432, 541, and 545) using separation of trypsinized peptides based on high-performance liquid chromatography (LC) and peptide sequencing by Edman degradation. More recently, the modification of HSA by flucloxacillin [101], piperacillin [102], BP [103, 104], AX [53, 89] and CLV [53] has been characterized using tandem mass spectrometry (MS) coupled to a LC system performed with serum from patients treated with drugs or samples modified *in vitro*. In addition, the degree of HSA modification is dependent on the drug concentration and the incubation time used for the *in vitro* modification [53, 102-104], with BLs showing a binding preference for some HSA-specific residues (Figure 15 and Table 2). Lys residues are the most commonly modified, however, a couple of His residues were found to be modified by CLV [53].

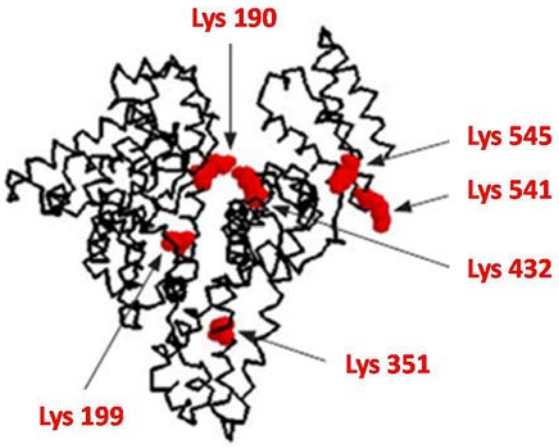

Figure 15. HSA model with the Lys modified by AX, BP, flucloxacillin, and piperacillin identified by MS in several of the studies referenced in the text. Image taken from Ariza *et al*. [17].

Table 2. Identified HSA residues modified by AX, BP, flucloxacillin, piperacillin and CLV.

	AX			BP		Flucoxacillin		Piperacillin			CLV
	[106]	[89]	[53]	[99, 100]	[103]	[104]	[101]	[102]	[107]	[53]	[53]
Lys4						+[a]		+[b]			+[a]
Lys12			+[a]			+[a]		+[b]			
Lys20					+[a,b]						
Lys73						+[a]					
Lys 137			+[a,b]		+[a,b]	+[a]	+[a]	+[b]			+[a]
Lys159					+[a,b]	+[a]					+[a]
Lys162			+[a]				+[a,b]	+[b]			
Lys190	++[a]	++[b]	+[a,b]	+[a]	+[a,b]	+[a]	++[a,b]	+[a,b]	+[a]	+[b]	+[a,b]
Lys195				+[a]	+[a,b]	+[a]	+[a,b]	+[a,b]	+[a]	+[b]	+[a]
Lys199	++[a]		+[a,b]	+[a]	++[a,b]	+[a]	+[a,b]	+[b]	+[a]		+[a,b]
Lys212			+[a]		+[a,b]	+[a]	++[a,b]	+[b]			+[a]
Lys351	+[a]		+[a,b]		+[a,b]	+[a]	+[a,b]	+[b]			+[a]
Lys359						+[a]					
Lys372					+[a]						
Lys414						+[a]					+[a]
Lys432	+[a]		+[a,b]	+[a]	+[a,b]	+[a]	+[a,b]	+[a,b]	+[a]	+[b]	+[a]
Lys436			+[a]		+[a]	+[a]					
Lys444						+[a]					
Lys475			+[a]								
Lys525			+[a,b]		+[a,b]	+[a]	+[b]	+[b]			+[a,b]
Lys541	++[a]		+[a,b]	+[a]	+[a,b]		+[a,b]	+[a,b]	+[a]	+[b]	+[a]
Lys545	+[a]			+[a]	+[a,b]		+[b]	+[b]			
Lys560						+[a]					
His146											+[a]
His338											+[a]

The most reactive residues, which were identified in the shortest times of incubation or with the lowest concentrations of drugs, are shown as ++. [a]Residues identified in HSA-drug adducts generated *in vitro*. [b]Residues identified in HSA purified from serum of patients with drug treatment. His: Histidine residues.

Interestingly, Lys modified residues seem to vary widely between patients in *in vivo* assays, although in the case of flucloxacillin, Lys 190 and Lys 212 appear in 8/8 patients along with other residues that vary from one individual to another [101], and in the case of AX, piperacillin and CLV, Lys 190 is a common modified residue in 4/4 patients studied [53] (Table 2). Furthermore, adducts formed by an AX dimer were seen in the same patients, which is an important observation since AX polymers could possess strong antigenic properties [53]. Lys 190, Lys 195 and Lys 199 are the most frequently modified HSA residues for the various antibiotic studied, being the differences observed in the patterns of *in vitro* modification probably due to structural differences between the BLs or the incubation conditions employed, while the differences observed in samples from patients likely arise from variations in the therapeutic conditions, including dosage and administration route or from the presence of concomitant treatments or pathological conditions [105]. Although the factors that determine which amino acids are modified by BLs are not known, it has been suggested that binding to Lys may be favored by the presence of a serine close to the polypeptide chain or the tertiary configuration of the protein [99, 100]. Molecular modeling studies have suggested in general that the reactivity of Lys is modulated not only by the residue accessibility, but also by the microenvironment around the lysine, which can enhance its intrinsic reactivity and contribute to the binding of AX through a recognition process which can stably constrain AX in a position leading to adduct formation [88].

- **Other seric and cellular carrier proteins:**

Besides HSA, other serum proteins could be involved in the haptenation process and in the induction of an immune response, however, very little is known about their nature or their role in the development of DHRs. In a study by Lafaye and Lapresle [98] based on blood samples from patients treated with BP, BPO groups were detected in a fraction of serum proteins where HSA had been removed, but the modified proteins detected were not identified. In a later study, HSA and transferrin were identified as target proteins for AMP using 2-dimensional electrophoresis and immunological detection with plasma from patients treated with this drug [108]. In a study by our group based on immunological and proteomic methods, we identified serum proteins modified *in vitro* by AX. We observed that transferrin and Ig (light and heavy chains), were modified by AX along with HSA [88, 89]. The fact that other relatively abundant serum proteins did not form detectable adducts under the experimental conditions used, suggests that factors other than plasma protein concentration could determine which serum proteins were targets for BLs.

Most of the attention regarding adduct formation by BLs has been directed towards the characterization of serum proteins, mainly HSA, as a carrier protein for these drugs.

Nevertheless, other possibilities can be considered. Cell surface or intracellular proteins could also play a role in the activation of the immune system [105].

The formation of ADs with cellular proteins has been previously reported by several studies. BP derivatives have the ability to bind to the cellular membranes of macrophages [109, 110] and monocytes [111, 112], and it has been described that the formation of these ADs is slower with cellular proteins than with serum proteins [44]. Moreover, in a study performed in our group, it was showed that confocal fluorescence microscopy with a biotinylated AX analog (AX-B) revealed the presence of intracellular protein adducts and modified proteins in extracts from AX-B treated cell lines (monocytes, B-lymphoma cells, and macrophages) with different patterns, showing that the haptenation process may be cell type-dependent [45].

In a recent study, Sanchez-Gomez *et al*. [113] used a B-lymphocyte cell line to detect, identify and follow the fate of intracellular AX-protein adducts. They observed that in addition to classical pathways in which haptenated serum proteins can be taken up and processed by cells, proteins can be haptenated intracellularly and be secreted either as soluble proteins or in extracellular vesicles. These vesicles can be taken up by other cells and therefore can constitute an additional vehicle for haptenated proteins. They also observed that AX can bind to isolated exosomes. These results expand the array of structures potentially involved in allergic reactions.

6. Clinical Symptoms and Diagnosis of Immediate Allergic Reactions to BLs

Symptoms of immediate allergic reactions may be located in the skin, being the organ most frequently involved (maculopapular, morbilliform, and urticarial rashes) [6], in the respiratory tract (rhinitis, bronchial asthma) or in the digestive tract (vomits, abdominal pain and diarrhea). There also may be generalized or systemic symptoms [6] such as anaphylactic shock (itching, urticaria, hypotension, angioedema and bronchospasm), being even possible patient death.

The allergological work-up often comprises the performance of both a reliable clinical history and different diagnostic tests: *in vivo* methods such as ST and drug provocation test (DPT); and *in vitro* techniques such as immunoassays and celular assays (Figure 16).

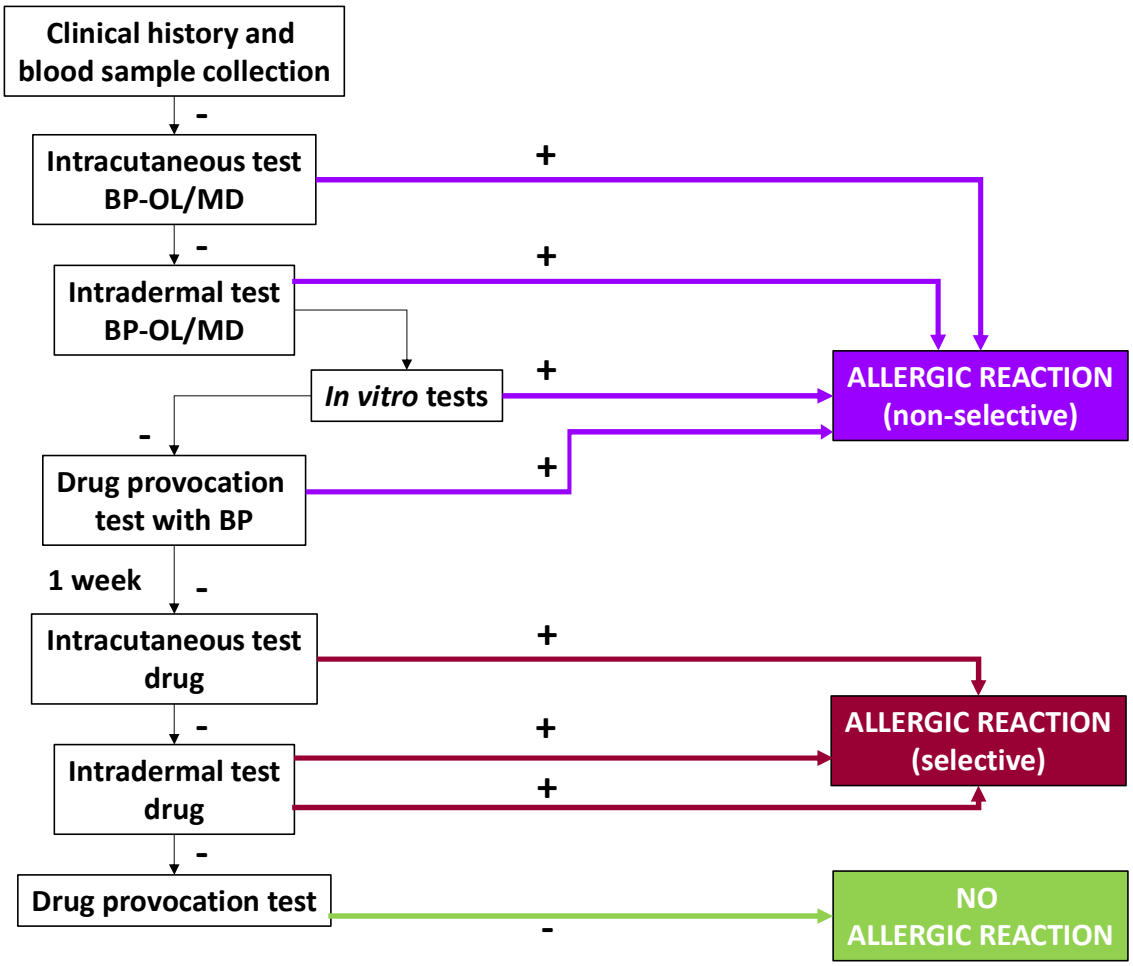

Figure 16. Diagnostic algorithm for evaluation of immediate DHRs to BLs. BP-OL: BPO-octa-L-lysine. MD: Minor determinant (MD): benzylpenilloic acid.

A detailed history is the first and most essential step toward an accurate diagnosis of DHRs. In addition to the clinical history, a careful physical examination can help better classify possible mechanisms underlying the reaction and guide further investigation [114]. Next step for stablishing clinical diagnostics is the testing of tissue mast cells activation by ST, detection and quantification of serum sIgE using different immunoassay methods, use of celular tests for analysis of the percentage of activated basophils after the stimulation with the interest drug [115] and diagnosis confirmation by DPT (Figure 17).

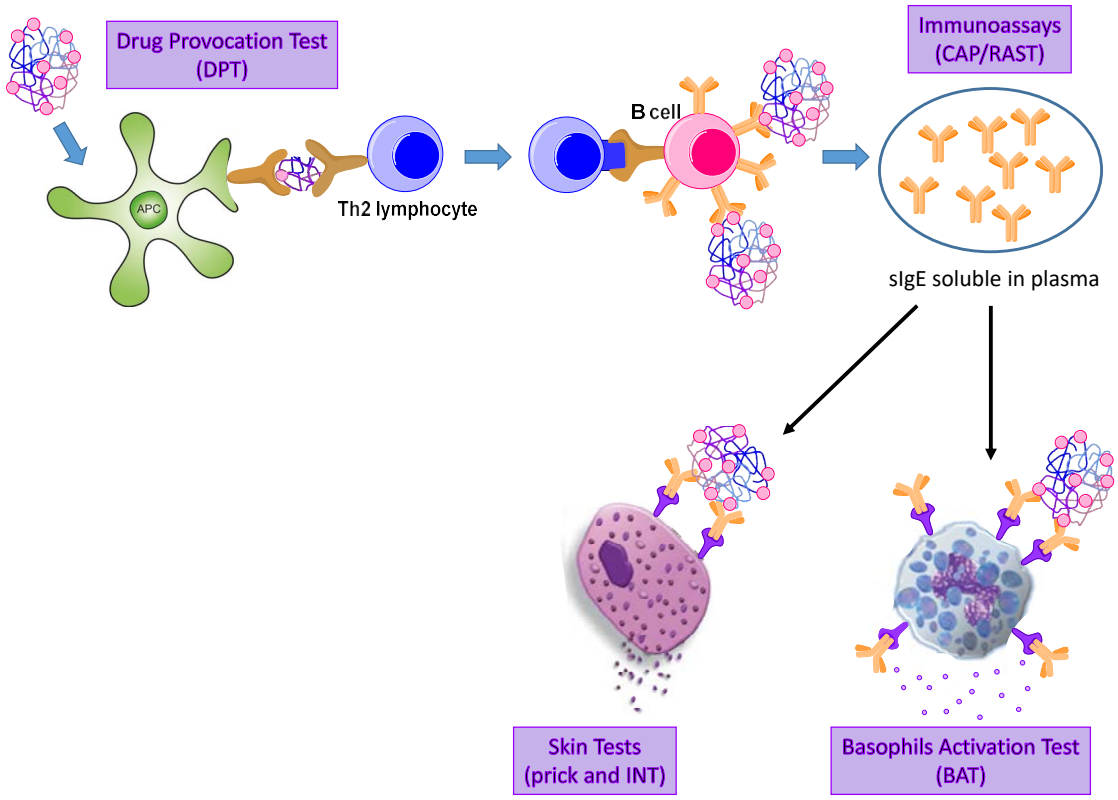

Figure 17. Diagnostic methods for evaluation of DHRs to BLs.

6.1. *In vivo* tests

-Skin test

ST is considered the best validated *in vivo* method for diagnosing IR to BLs. In IRs, STs are usually performed using the skin prick test (SPT), by pricking the skin with an appropriate needle through an allergen solution. If this does not cause a reaction, an intradermal test (IDT) can then be carried out, by the injection of 0.02–0.05 mL of the drug solution, raising a small bleb that is marked initially. Both are usually performed on the volar forearm, although other skin areas can be used [116].

Due to the fact that for many years BP was the most relevant BL involved in immediate allergic reactions [117], classically, the diagnosis has been focused on the use of major and minor determinants of BP [118-122]. The major determinant, the PO-polylysine (PPL), is formed by the conjugation of BP to poly-L-lysine (PLL) [40] (Figure 20). The classic BP reagents used for ST have been penicilloyl-polylysine (PPL) and minor determinant mixture (MDM), originally consisting of BP, benzylpenilloic acid, and benzylpenicilloic acid, although current commercial reagents only include BPO-octa-L-lysine (BP-OL) as major determinant and benzylpenilloic acid as MD [123].

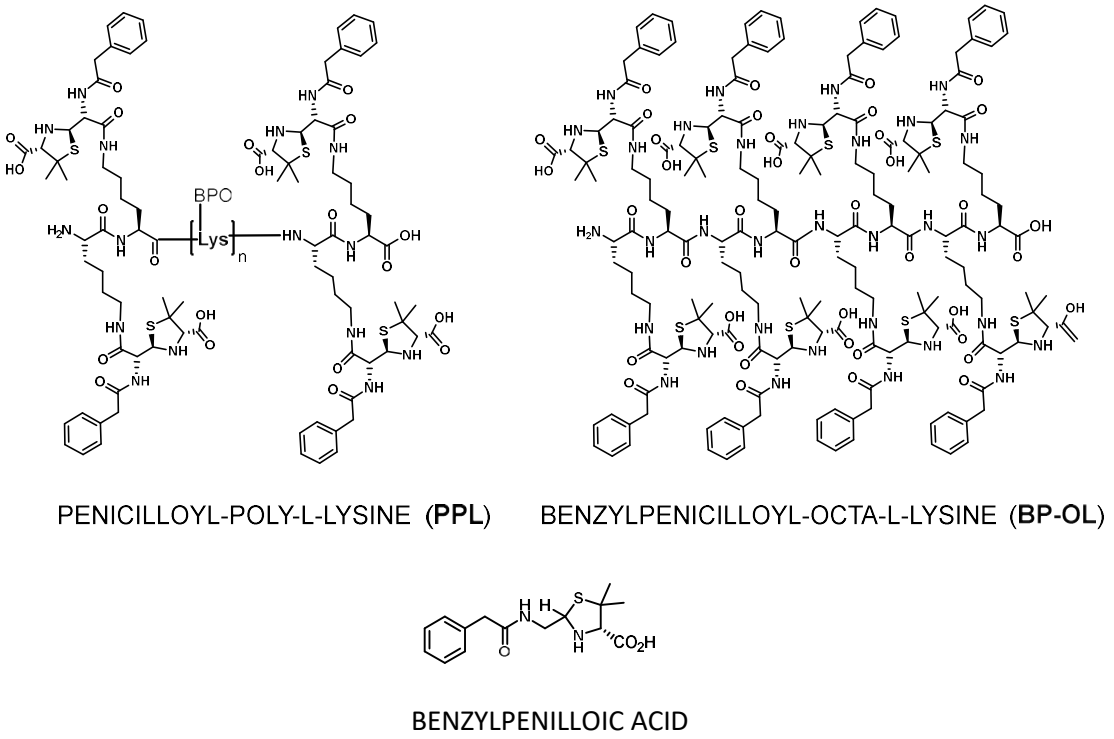

Figure 18. Described major (top) and minor (bottom) determinants for BP used for *in vivo* tests.

The appearance of semisynthetic penicillins with different side chains required the use of other determinants, such as AX, AMP, and various cephalosporins and in the 1990s, the percentage of positive STs with AX or AMP in patients with penicillin allergy ranged from 26% to 47% [116]. In 2001, Torres *et al*. [124] confirmed that BPO was no longer the most relevant hapten in IRs to penicillins and demonstrated that including AX could increase ST positivity to 70%. Inclusion of its minor determinants (diketopiperazine and amoxicilloic acid) did not improve the diagnostic capacity [125]. Following these observations, the European Network on Drug Allergy (ENDA) recomended ST with PPL, MDM and AX [126-128] and in those cases negative to PPL and MDM, BP must be also included. After penicillins, cephalosporins are the BLs that most often induce IgE-mediated reactions and for ST, the culprit cephalosporin diluted in 0.9% NaCl is used [129, 130]. Since the prescription of AX is recently combined with CLV, the description of selective reactions to CLV raised the need to include this drug as a potential culprit in the diagnostic evaluation. Initially, the suspicion of CLV allergy in patients with IR after AX–CLV administration had been classically based on the presence of negative results in both ST and sIgE determination to AX and a positive ST to AX-CLV [131]. However, using AX–CLV, only 18% of CLV IRs could be correctly diagnosed, being this low sensitivity due to the lower concentration of CLV compared to AX in the AX-CLV combination [80]. Attempts to improve the sensitivity of CLV allergy diagnosis by increasing the AX-CLV

concentration produced false-positive results, due to the high concentration of AX [80]. The recent commercialization of CLV for ST has allowed it to be used on its own in the diagnostic work-up [80, 132]. Through its usage, it has been shown that more than 30% of patients with AX–CLV IRs are selective to CLV [80, 132].

-Drug provocation tests

DPT is usually performed in a single-blind procedure in the cases of patients with negative ST and *in vitro* tests in which confirmation of diagnosis is essential [133] and is performed under strict hospital suveillance with access to an emergency room [121, 134]. DPTs consist of the controlled administration of increasing doses of the drug to a patient with a history suggestive of drug allergy. This can be either the suspected culprit, or an alternative structurally or pharmacologically related drug. This procedure is not recommended in patients with a history of life-threatening reactions [114, 116]. However, in those cases in which the drug is considered as potentially useful or mandatory, DPT can be evaluated. Moreover, this diagnostic tool can be used to find alternatives to an implicated drug and assessing tolerance to potentially cross-reactive drugs [116]. DPT is still the gold-standard method for diagnosing IRs to BLs since recent studies showed that more than 30% of patients could be diagnosed accurately only by means of DPT [133].

6.2. *In vitro* tests

The most common *in vitro* tests are based on the detection of sIgE, either in serum (immunoassays) or bound to receptors on the surface of effector cells (basophil activation test, BAT). A detailed review of *in vitro* tests for drug allergic reactions has been done by ENDA/ European Academy of Allergy and Clinical Immunology (EAACI) Drug Allergy Interest Group [28].

-Immunoassays

Immunoassays are the methods employed for sIgE quantification in allergic diseases to BLs. In these assays, quantification relies on the sIgE recognition of a drug(hapten)-carrier complex coupled to a solid phase. For this, the solid phase decorated with the hapten-carrier conjugate is incubated with the patient serum, and then, bound sIgE is detected using α-IgE antibodies labeled with either a radioisotope (radioimmunoassay, RIA), a fluorescent enzyme (fluorescence enzyme immunoassay, FEIA), or a colorimetric enzyme (enzyme-linked immunosorbent assay, ELISA) [28, 56, 114, 134-137], being rarely used.

ImmunoCAP (Thermo-Fisher, Uppsala, Sweden) is the fluoroimmunoassay commercial method most widely used for diagnosing BL allergy [28, 114, 116], which uses a hydrophilic cellulose polymer configured into a small capsule to which the drug-PLL conjugates are covalently bound [114] (Figure 19, right). Fluorescence is induced by an enzimatically labeled α-IgE antibody and proportional to IgE amount in patient´s serum. Detection limits of these methods are 0,01-100 kUA/L (being A sIgE against the drug) with 0,35 KUA/L as cutoff. Values over 0,10 kUA/L are indicative of sensitization.

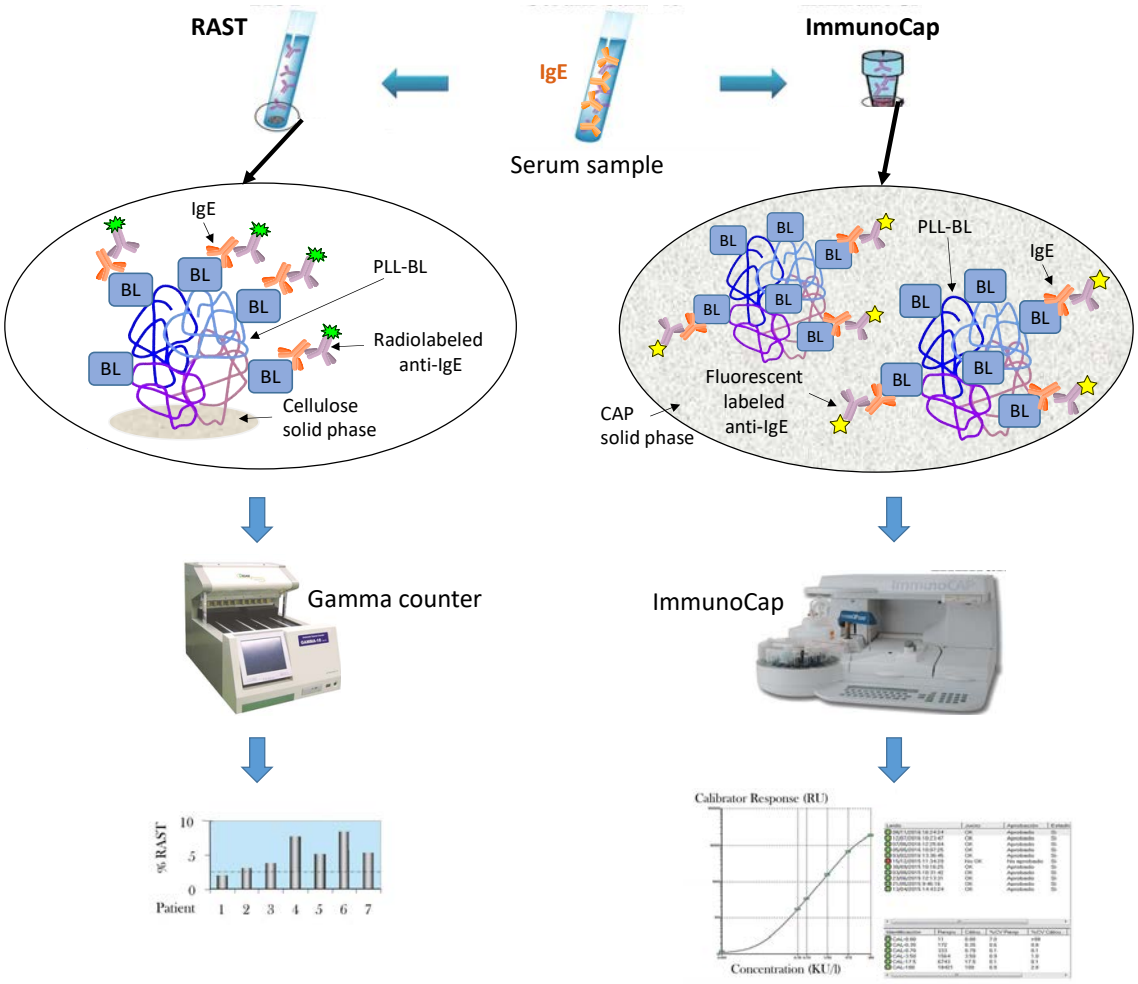

Figure 19. Comparison of RAST (left) and ImmunoCap (right) assays. Adapted from [114].

Radioallergosorbent test (RAST) is a non-commercial RIA used in some laboratories for the detection of allergen-specific antibodies. The solid phase employed for RAST to BLs is cellulose paper disc activated with cyanogen bromide. A carrier molecule haptenized with the drug of interest is covalently coupled to the activated discs. Then, patient sera is incubated with the discs and allergen-specific antibodies recognizing the allergen fixed to the solid phase, and finally, sIgE detection is performed with a secondary α-

human IgE antibody labeled with a radioisotope (^{125}I) Figure 19, left). Advances achieved in these in-house immunoassay designs during last years are very promising [138, 139]. Thus, they have become more quantitative and sensitive although there is a lack of automation.

-Basophil activation test

BAT is based on flow cytometry with different strategies to identify basophils (using α-IgE, CCR3, CRTH2 and/or CD203c) and quantify different activation markers on the basophil surface after the stimulation with the culprit drug or their metabolites [28, 114] (Figure 20). Once basophils have been selected, CD63 and CD203c are the most commonly used activation markers. CD63 is expressed in the membrane of histamine containing vesicles on basophils, mast cells, macrophages, and platelets and is highly displayed on the basophil surface after degranulation. However, CD203c, also upregulated after basophil activation, permits a more specific selection of basophils since it is constitutively expressed exclusively in basophils and mast cells.

BAT sensitivity and specificity values for BLs are 50%-78% and 89%-97%, respectively [114]. It had been observed that BAT sensitivity is higher with haptens which have not been conjugated previously to a carrier molecule [140]. Conversely, in a recent study it has been observed that Poly(amidoamine) (PAMAM) dendrimers conjugated with penicillins are able to induce basophils activation [141].

BAT has received increasing attention for the diagnosis of drug allergy [114, 116] and is recommended for diagnosing BLs as complementary method to other *in vitro* tests. Also, when available, BAT should be performed before *in vivo* tests, including ST, in life-threatening reactions or in high-risk patients [28, 114]. Over the last years, BAT has been included in the allergological workup for AX and CLV selective patients. Torres *et al*. demonstrated that around 30% of reactions in patients taking AX-CLV were CLV selective [80]. In a more recent study, it was observed that BAT sensitivity in the evaluation of CLV-selective patients was 62%, and combining these results with that from ST, the sensitivity increased to 91% [142], which is important because this is the only available *in vitro* test to diagnose CLV-selective patients.

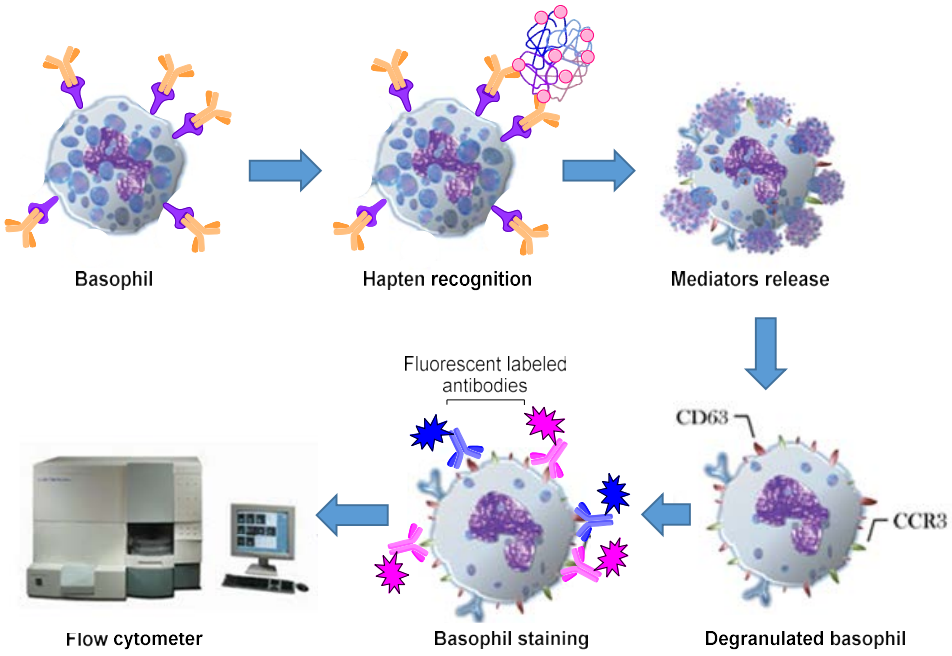

Figure 20. Schematic representation of BAT assays.

6.3. *In vivo versus in vitro* tests

Although the most consensual approach to diagnose BL allergy consists of *in vivo* test since they show higher sensitivity, they can be risky, especially in severe and life-threatening reactions. *In vitro* tests nowadays have shown to be helpful and complementary to *in vivo* tests. They have greatly evolved in recent decades offering numerous advantages in drug allergy diagnosis, such as precise quantitation, absolute safety, controlled conditions, and, for serologic tests, long-term storage of specimens [116].

6.4. Limitations and future of *in vitro* tests

In spite of the above mentioned advantages of *in vitro* tests, their main disadvantage is that they can show low sensitivity due mainly to the low concentration of sIgE in the blood, which is approximately 0.2% of total IgE for BLs allergy [139]. Additionally, in immunoassays other factors such as the drug binding to the solid phase, the carrier forming part of the AD, or the density of haptens in the conjugate can influence in the results [114].

The use of ELISA has been reported for some cephalosporins [143-145] and pyrazolone [146] but optimization of this technique is time consuming since there are a lot of parameters to optimize (conjugate for plates coating and concentration…) for obtaining a suitable sensitivity and specificity, which are difficult to obtain. In case of BLs, ImmunoCAP is only available for several penicillins (BP, penicillin V, AX, and AMP) and

for a cephalosporin (cefaclor). Its sensitivity depends on the BL involved, but is rather low and variable (0%-50%), although specificity is high (83%-100%), and false positives have been described for cases where the hapten is penicillin V (26%) and in patients with high total IgE levels. [114]. Some RIAs have shown higher sensitivity than ImmunoCAP, for example, in-house RAST has shown sensitivity ranging from 43% to 75% and specificity from 68% to 83% for both penicillins and cephalosporins [114]. However, RIA presents the inconvenience of needing specific facilities and trained personnel to manipulate radioactive materials. Thus, other techniques avoiding radioactivity are preferred by many research groups. Moreover, other important drug allergies, such as CLV allergy cannot be diagnosed with this in-house assay, since no successful method has been reported. Several studies have also been carried out to analyze the performance of BAT for BLs allergy, with sensitivity ranging from 50% to 78% and specificity from 89% to 97% [114]. However, although commercially available tests exist, BAT protocols are not standardized between different laboratories in terms of markers, procedures and drug concentrations [28] and its sensitivity should be improved.

Although many *in vitro* tests are available, there is currently no consensus on their diagnostic value in routine clinical care [28]. By one hand, there is a lack of well-controlled studies, most information comes from small studies with few subjects and results are not always confirmed in later studies [28]. On the other hand, they present some disadvantages or technical limitations such as its lower sensitivity (and sometimes specificity) compared with ST. Finally, they are expensive and, in most cases, not refunded by medical insurances; and they require equipment that is not available in all laboratories [116].

As a consequence, it is necessary to validate the currently available *in vitro* tests in a large series of well-characterized patients with DHR and to develop new tests for diagnosis [28].

Regarding future trends, the inclusion of different drug derivatives conjugates at a time in the assessment of sIgE would improve diagnosis accuracy. The variety of antibiotics and their AD structures plus the number of candidate carrier proteins result in a high quantity of potential conjugate combinations. Unfortunately, their inclusion is not possible for current *in vivo* tests and unmanageable for current *in vitro* tests. The only alternative is a microarray platform, which can include many determinants and carriers in the same substrate. The inclusion of a wide library of drug-carrier conjugates on a high-throughput platform together with enhanced and amplified detection methods will greatly improve existing *in vitro* diagnostic tests and could potentially offer the first available *in vitro* diagnostic assays for evaluating BLs allergy. This technology will allow the clinicians to evaluate a wide range of patients with allergy to antibiotics who present different patterns of recognition, and would guarantee a correct diagnosis.

Unfortunately, nowadays there are no microarray platforms for allergy diagnosis and the main reason is the lack of a fluorescent secondary antibody sensitive enough to allow detection of such a low sIgE concentration for these kind of allergies.

6.5. Nanotechnology for improving *in vitro* tests

In contrast with the limited changes in *in vivo* methods, only based on the inclusion of new haptens, major progress has been achieved in last years for *in vitro* tests with more sophisticated assays developed. Current efforts are focused on their sensitivity enhancement to advance in this field.

By one hand, it is necessary to obtain more insight into the chemical structure of the ADs, the nature of the carrier protein, and how they bind [63, 116]. The use of structures similar to that formed *in vivo* may help to mimic *in vitro* the molecular recognition process that actually occurs [5, 43, 116]. Major progress has been made employing materials chemistry and nanotechnology. During last years, the suitability of different nanostructures for improving *in vitro* tests directed to IgE quantification in allergic reactions to drugs has been evaluated [116, 138, 139]. Regarding solid phases, besides the cellulose paper activated with cyanogen bromide, other materials have been investigated such as sepharose beads [130], zeolites [147], and silica particles [148], as well as other activation methods that increase hapten fixation or introduce spacers as linkers, increasing hydrophilicity, flexibility and distance between ADs and surfaces [147]. The high surface area/weight ratio of silica nanoparticles, which permits efficient functionalization and sIgE interaction, makes them the most promising material [116]. For these *in vitro* tests applications, dendrimers are also promising structures [51, 141, 148] that are described in depth in the next section.

On the other hand, the enhancement of immunoassays detection signal, using efficient techniques for site-selective secondary antibodies labeling [149], is also a fine strategy to tackle the issue of low sensitivity in *in vitro* diagnostic of allergy to drugs. Nanostructures such as dendritic probes are of interest in this field due to their capacity of bearing different units of label or reporter molecule [150, 151], which may lead to enhanced signal [150], and a single functionality at focal point for conjugation.

Therefore, much work is still necessary in order to identify the chemical structures involved in the generation of the specific immunogenic epitopes, including candidate protein carriers, and to study their immunogenicity, as well as to successfully enhance detection signal. This will permit us to improve the diagnostic methods currently available and ensure that patients are correctly diagnosed.

Definitely, multidisciplinary studies in the fields of immunology, proteomics, nanotechnology, and chemistry will help to both further understand hypersensitivity

reactions to BLs and improve immunoassays detection signal, and these results would allow to advance in *in vitro* methods [105, 116].

7. Dendrimeric Structures for Improving *In Vitro* Tests

In the previous nanotechnology related point, dendrimers were briefly mentioned as one of the rising nanostructures that have contributed to the advance of the *in vitro* diagnosis of allergy. In fact, major progress in this field using nanotechnology are due to the use of dendrimers as nanostructures able to mimic carrier proteins, with the advantages of simpler structural build-up and the exposure of a greater number of haptens at their surface than conventional carriers. In addition, they are envisioned as promising structures for detection signal amplification through biolabeling. Here, some generalities of dendritic structures that allow to understand the particular characteristics making them promising materials, as well as their usefulness for improving *in vitro* tests for allergy diagnosis are presented.

7.1. Generalities of Dendritic Structures

Definition

Dendrons and dendrimers have been widely studied in recent decades for their potential application in a number of areas [152-155]. Their multivalent nature, narrow polydispersity, unique structural geometry and the possibility of further polymerize or modify their surface with desired functional peripheral groups bring a huge range of applications.

Dendrimers are macromolecules with a highly branched tridimensional structure. The term dendrimer derives from the Greek dendri- (tree-like) and meros (part of) but they have been also referred as arborols or cascade molecules. Branches growing from the core of focal point (red dot in Figure 21) receive the name dendron (grey shaded in Figure 21) and consist of repetitive monomer units that possess new branching points. Each of these branching points allows the incorporation of new repetitive units, thus increasing the generation (G, dotted areas in Figure 21) once all of them have reacted.

The first dendrimeric structure, polypropylenimine (PPI), was synthesized by Vogtle *et al*. in 1978 but due to difficulties in the synthetic approach used, it was only possible the formation of low generation compounds. Newkome *et al*. [156] and Tomalia were able to synthesize well-defined higher generation dendrimers in mids-80 and, since then, over 100 different dendrimer structures have been developed. The most commonly referenced dendrimers along with their inventors and commercial sources are gathered in Figure 22 [153, 157-159].

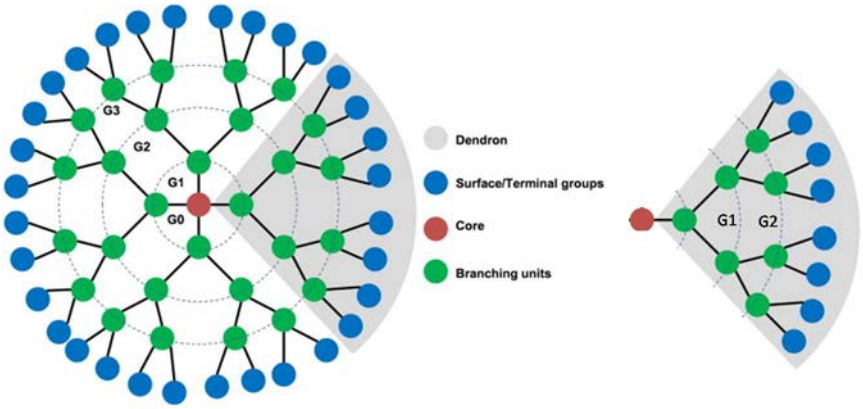

Figure 21. Depiction of general dendrimeric structures: dendrimer (left) and dendron (right).

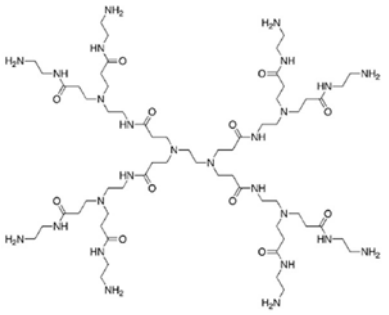

Polyamidoamine (PAMAM)
Invented by: Tomalia
Commercial sources: Dendritech, Sigma Aldrich

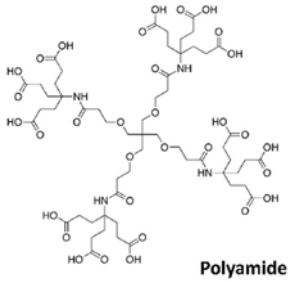

Polyamide
Invented by: Newkome
Commercial sources: Frontier Scientific

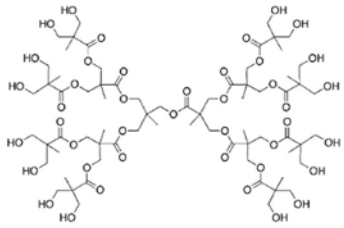

Poly(2,2-bis(hydroxymethyl)propionic acid (bis-MPA)
Invented by: Hult
Commercial sources: Polymer Factory, Perstorp, Sigma Aldrich

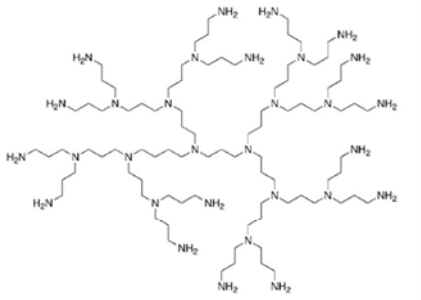

Polypropylenimine (PPI)
Invented by: Vogtle
Commercial sources: DSM, Sigma Aldrich

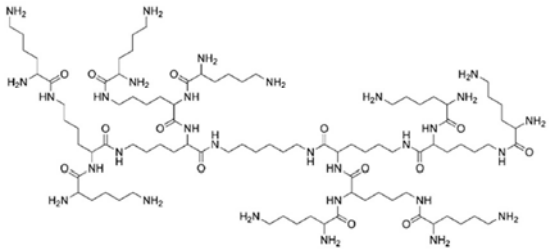

Poly(L-lysine) (PLL)
Invented by: Denkewalter
Commercial sources: Colcom

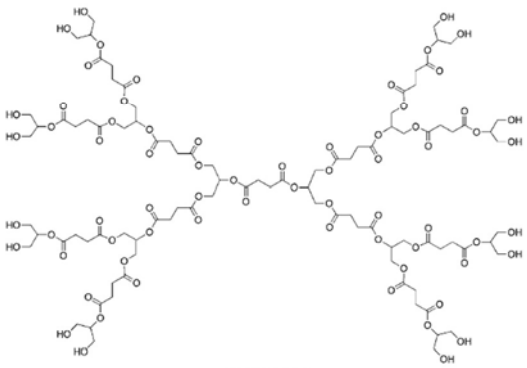

PGLSA-OH
Invented by: Grinstaff

Figure 22. Chemical structures of several commonly used, commercially available dendrimer structures. Adapted from [157].

Synthesis

There are two main methods of synthesizing dendrimers [157, 159, 160] (Figure 23). The first one is the divergent method, which consists of growing the dendron from the core by adding monomer units to branching points in successive steps or generations. The second one is the convergent method, which consists of building a single-branched tree or dendron and after synthesis of individual trees, they are linked to the core structure as single units. The latter method allows the combination of different dendritic starting materials (dendrons) within the same dendrimer structure, also, it is advantageous because only a limited number of active sites are present per reaction, reducing structural defects in the product. The main disadvantage is that its use is limited to small dendrimers due to the fact that steric hindrance avoids the reaction of big dendrons with the core. More recently, introduction of click chemistry in dendrimers synthesis [153, 161] allowed decent yields with little purification steps required. In addition to improving the yields of the divergent strategy using click chemistry techniques, accelerated synthetic strategies have been developed to reduce the number of steps [162]. In this strategy, two different monomer units, AB_2 and CD_2, that have complementary functionalities can react spontaneously without the use of protecting groups or activating agents [159, 163, 164]. Evolution of dendrimer synthesis strategies is shown in Table 3.

Table 3. Evolution of dendrimer synthesis and contributors [158].

Method	Invented or validated by	Year
Divergent synthesis	Tomalia *et al.*	1979-1984
	Newkome *et al.*	1985
	Meijer *et al.*	1993
	Majoral *et al.*	1994
	Hult *et al.*	1993
	Simanek *et al.*	2006
	Tomalia *et al.*	2005
Convergent synthesis	Frechet *et al.*	1989
Self-assembling synthesis	Zimmerman *et al.*	1996
"Lego" chemistry	Maraval *et al.*	2003
Click chemistry	Sharpless *et al.*	2004
	Hult *et al.*	2009
	Calmark *et al.*	2009

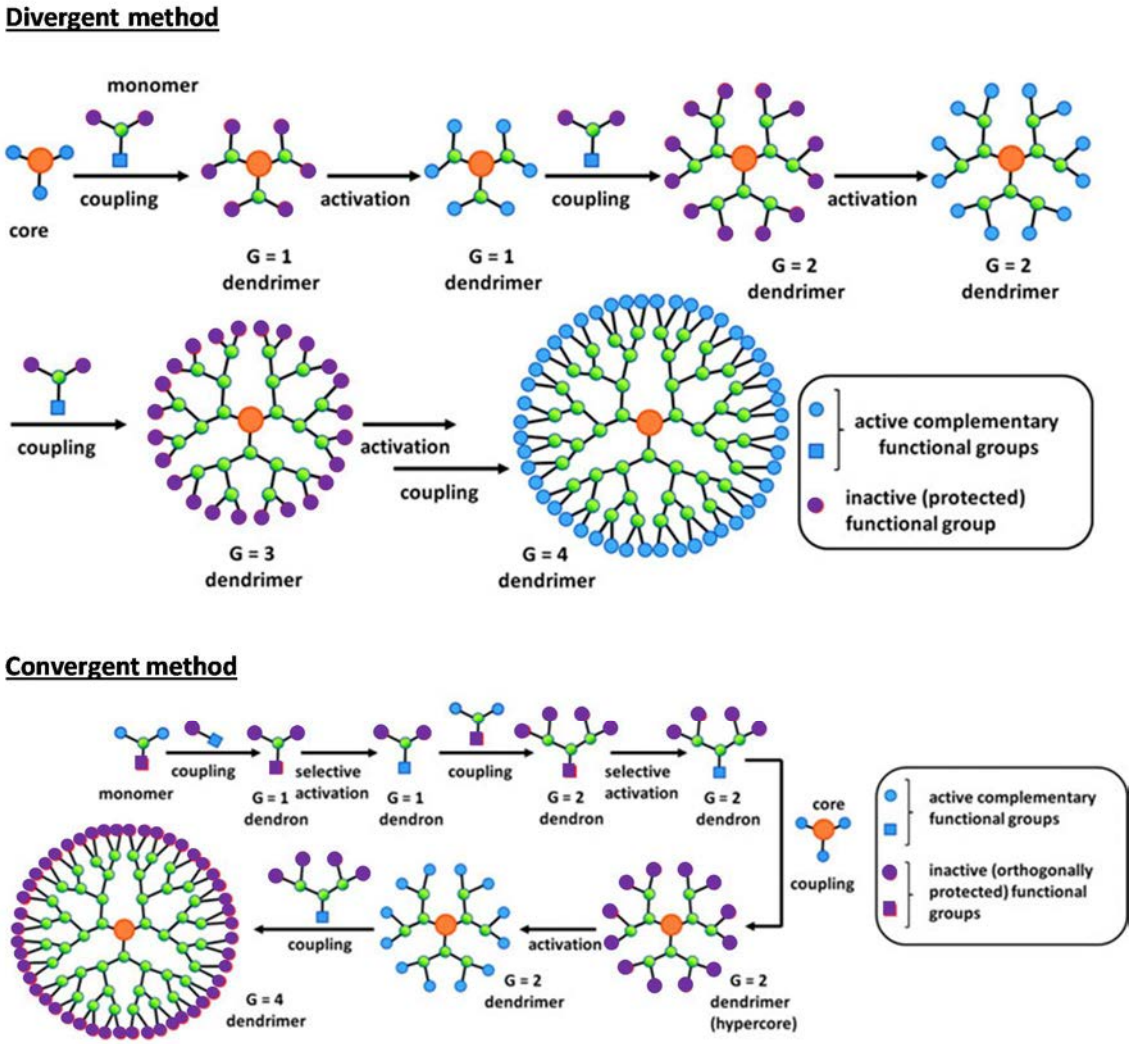

Figure 23. Schematic representation of dendrimer synthetic strategies [159].

7.2. Dendrimers as Synthetic Carriers

Dendrimers have been used as nanostructures able to mimic proteins, and so employed as carriers, enabling the production of conjugates with the advantages of simpler structure, multivalency and the chance to control the number of haptens at their surface compared with conventional carriers [116]. Therefore, they have been used as synthetic carriers, whose multivalence increase the sensitivity and the control structure improves the reproducibility of the assays. The use of dendrimers haptenized with penicillins has permitted the precise definition of the chemical structures recognized by sIgE [148, 165]. Also, their tuneable structures have allowed the inclusion of two different drugs, BP and AX, on the same molecule in a well controlled way leading to bihaptenic structures which enabled the detection of sIgE from selective and cross-reactive patients [51]. Dendrimerized gold nanodisks were employed as a solid phase in a nanoplasmonic sensor device for the evaluation of AX allergic patients, showing a good correlation with

ImmunoCAP. The main advantage of this method is the use of label-free α-IgE and the short analysis time and it represents a potential new assay for the diagnosis of BLs allergy [166]. More recently, AXO and BPO decorated dendrimeric antigens (DeAns) were demonstrated to be able to induce basophils activation in a selective and specific way. This study allowed, for the first time, the performance of BAT with molecules other than the free drug, which enhances the response by way of a better control of the method in terms of reproducibility regarding the immunogen size and density of epitopes. Moreover, potential application to diagnosis are foreseen, in terms of sensitivity of the test [141].

The development of new nanostructure-based immunoassays is envisaged to provide highly sensitive methods, able to detect low concentrations of sIgE. Moreover, they have the potential to enable the testing of a variety of BLs and metabolites in the same assay [116]. However, these methods are currently limited to those drugs whose AD structure is well-known, being necessary structure-activity relationship (SAR) and proteomic studies for those BLs, such as cephalosporins or CLV, whose more complex chemistry has not allowed yet the complete elucidation of the epitope involved in the immune response.

7.3. Dendrimers as Fluorescent Probes for Detection Signal Amplification

Over the last decade, fluorescent labeling of biomolecules has become a powerful tool for bioimaging and diagnostics. In contrast to radioisotopes, fluorescent dyes have the advantage of being of low cost, ease of disposal, and the versatility of multicolor labeling [167]. While promising, there is a major drawback accompanying fluorescent labeling such as inherently low sensitivity [150]. To overcome this issue and expand the applicability of fluorescent probes, it is apparent that dyes with strong fluorescence signal need to be identified, synthesized and conjugated to biomolecules without jeopardizing the biological activity of the final construct.

As a mean to enhance the fluorescence signal, different approaches have been suggested including conjugation of multiple fluorescent dyes to the biomolecules. Unfortunately, an obvious disadvantage of this approach is the high number of involved functionalization sites that may affect the specificity of conjugated biomolecule [150, 168]. A natural strategy to circumvent such concern is the use of orthogonal linkers with the capacity to carry multiple copies of fluorescent dyes as well as a single selective reactive group for site-specific conjugation to the biomolecule. However, a limitation coupled to this approach relates to the high dye content per macromolecule that can reduce fluorescence signal due to various processes such as self-quenching of fluorescence [150, 168-171]. Interestingly, although rare, some studies have described a stronger fluorescence with the inclusion of multiple

fluorescent units [150]. Consequently, the development of a set of intrinsically similar structures, sharing the same functional group for specific conjugation to biomolecules and bearing different concentration of fluorescent units, would provide the appropriate conditions for accurate structure-to-property assessment with emphasis on site-specific labeling and improved fluorescence signals, and dendrimers are suitable for this purpose.

8. Bioconjugation Reactions for Antibodies Labeling

The main goal of most bioconjugation techniques is to use the functional groups on biomolecules to label with another type of biomolecule or link to synthetic probes [160]. Chemoselective bioconjugation (Figure 24) refers to the coupling of two mutually and uniquely reactive functional groups in an aqueous environment, which will react only with each other even among a multitude of potentially reactive functional groups, without side reactions [172, 173].

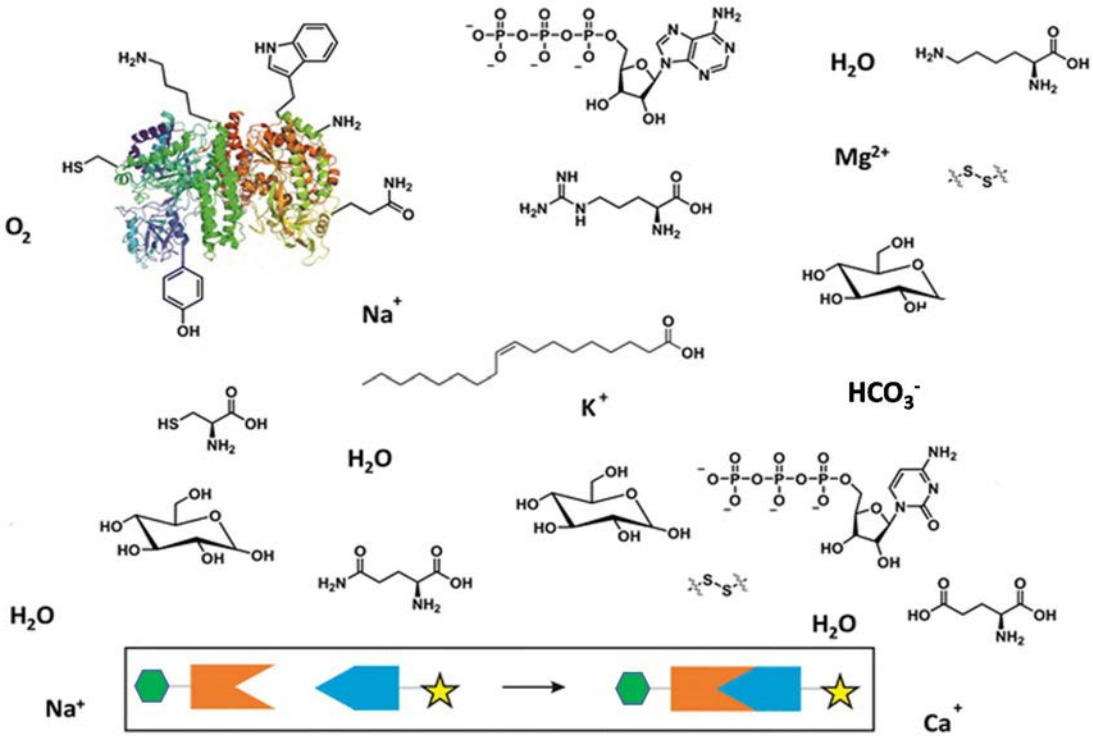

Figure 24. Schematic overview of the vast complexity of functional groups in living systems [174].

The basis of the chemoselective ligation concept is based on the mutually exclusive reactivity of functional groups pairs, which are orthogonal groups. There are quite a few reviews that gather an extent number of chemoselective pairs [160, 172-179], among which, we will focus on the most usual strategies that allow antibody labeling.

The diagnostic relevance of antibodies comprises classical serology (immunoprecipitation, agglutination, complement binding, RIA, ELISA), immunocytochemistry and immunohistochemistry, immunofluorescence (microscopic and flow cytometric), cytotoxicity tests, immunoblots, immunospot assays and immunoabsorption (affinity chromatography) [180]. Ig labeling is the first step for many antibody applications and is mostly based on the following covalent interactions: 1) modification of the lysine amine group, 2) disulfide modifications of the cystein thiol group (Figure 25A), and 3) hydrazone or oxime crosslinking of carbohydrates (Figure 25B).

Regarding the first two above mentioned methods used for labeling antibodies, in spite of using reactives considered to be site specific in their reactions, they often present cross-reactivity with functional groups on biomolecules different than the target ones. For instance, *N*-hydroxysuccinimide (NHS) esters although highly amine-reactive, they also can react with other nucleophilic functional groups present in cysteine, serine, threonine, and tyrosine side chain [160]. Also, although proteins can be site-specifically labeled at their solvent accessible (highly nucleophilic) cysteine residues by thiol-reactive alkylation reagents such as maleimides and iodoacetamides, excess maleimide-based reagents or basic pH values lead to the modification of the amino groups at the side chains of histidine, lysine and terminal α-amino groups [160, 176].

Most of commercially available labeling kits are based on Lys reaction, but this modification makes quantitative control and reproducibility difficult, and antibody specificity can be reduced due to chemical modification of the antigen-binding site. However, the modification of carbohydrate residues located in the antibodies Fc region is specifically oriented, with a well-defined stoichiometry and without affecting the antibody recognition site. 1,2-diols in sialic acids located at the antibody glycan terminus can be easily oxidized to aldehydes in mildly oxidative conditions [181] without losing antibody affinity or causing further oxidative damage, and they can be afterwards functionalized via hydrazone bound with a hydrazide functionalized molecule (Figure III.7B). The fact that immobilisation via an oxidised oligosaccharide moiety present in the Fc region of the antibody is a strategy commonly used for designing immunoassays without assay performance lost [182, 183] proves that antibody binding site is not affected when this kind of linkage is used.

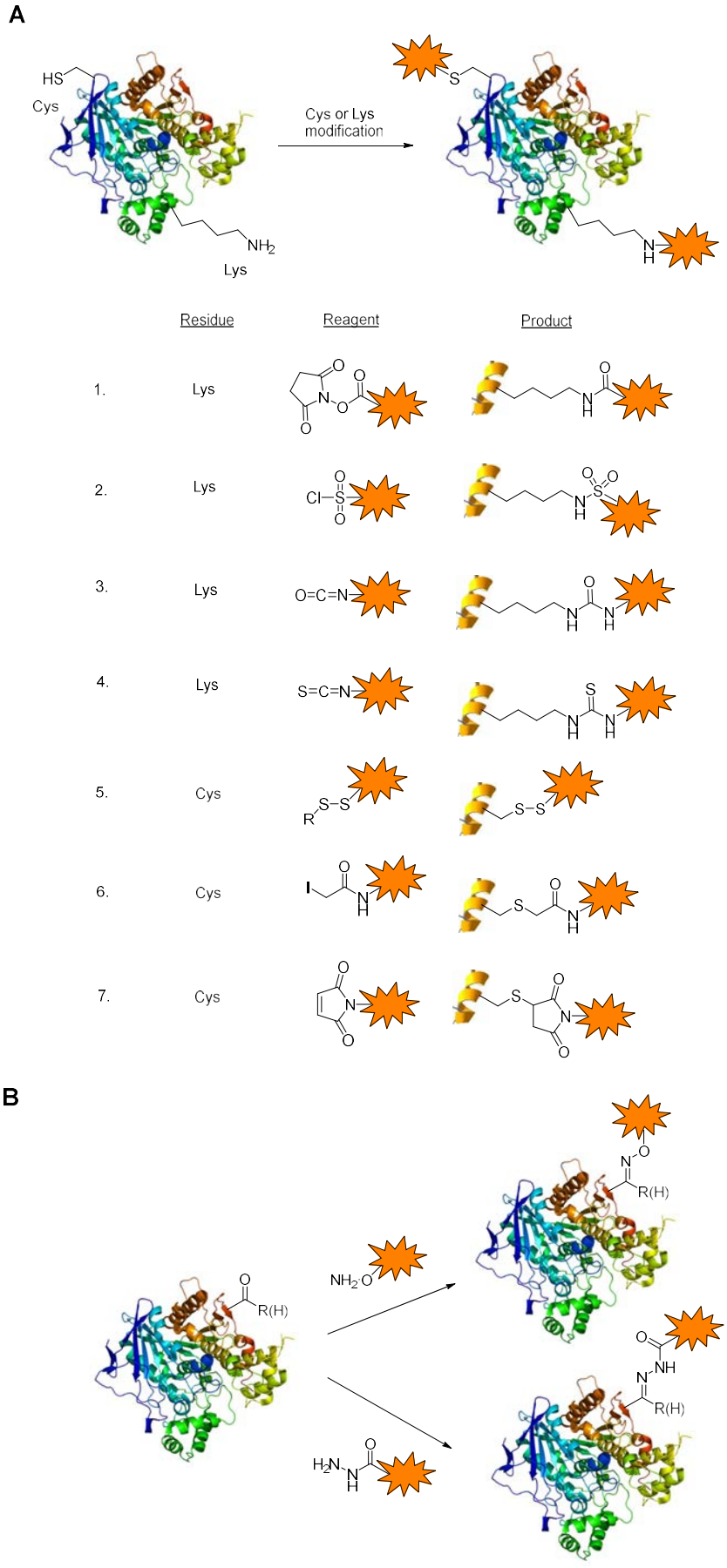

Figure 25. Most common reactions for antibody labeling.

The pairing of a carbonyl group with a hydrazide, thiosemicarbazide or aminooxy moiety is perhaps the most versatile chemoselective ligation strategy in terms of their chemical or metabolic installation into co-reacting species and ability to readily ligate in aqueous media [149]. Over the last few years, bioorthogonal reactions between hydrazide functionalized probes and biomolecules has gained popularity. Examples of hydrazide-functionalized molecules for biomedical and bioimaging applications are dendrons [149], peptide tags [184], and dyes [185, 186]. Conversely, to our knowledge, there are not many commercially available hydrazide or hydrazine based products for targeting biomolecules. One example is the heterobifunctional crosslinker for selectively labeling of antibodies with biotin through aldehyde residues in Fc sugar chains (EZ-Link Biocytin Hydrazide, from Thermo Fisher Scientific).

Another bioorthogonal reaction that last decade has revolutionized the modification of proteins field is Copper(I)-catalyzed azide-alkyne cycloaddition (CuAAC). It was reported independently by Sharpless [187] and Meldal in 2001 and became popular due to the high specificity of azide and alkyne groups towards each other remaining inert chemically to other molecules in live systems, and the stable and inert regioselective 1,4-triazole product formed (Figure 26). Bertozzi´s group introduced in 2004 the strain-promoted azide–alkyne cycloaddition reaction (SPAAC) [188], another strategy for the azide–alkyne cycloaddition without need of Cu-catalysis, in which the ring strain of various cyclooctyne derivatives boost the reaction (Figure III.9B). The number of applications of click chemistry for bioconjugation is growing [189], especially for bioimaging applications [190-195]. Staudinger ligation and the inverse electron demand Diels–Alder cycloaddition are another kind of click chemistry reactions that have also been proven powerful in the hands of chemical biologists, biochemists, and biomedical scientists [191].

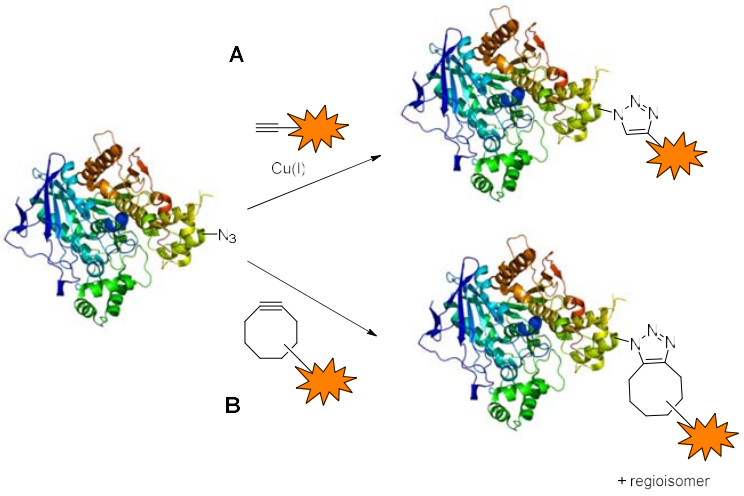

Figure 26. Bioorthogonal (3+2) cycloadditions of azides and alkynes to form triazoles. (A) CuAAC. (B) SPAAC.

JUSTIFICATION AND HYPOTHESIS

DHRs are currently a major public health problem affecting patient health and increasing healthcare costs. They account for 6-10% of all ADRs, and those induced by antibiotics are the most common and best studied. Many pitfalls are related to the adequate diagnosis probably because the immunological mechanism involved has not been fully elucidated. The diagnosis of antibiotic allergy is usually overestimated, and less than 24% and 10% of initial cases are finally confirmed in adults [15] and children [196], respectively.

DHRs are caused by interactions between a drug and the human immune system and result in symptoms ranging from urticaria or angioedema to those more serious such as anaphylaxis or anaphylactic shock, and BLs are the drugs most frequently involved [5, 28]. They are classified according to their chemical structure as penicillins, cephalosporins, monobactams, carbapenems, and clavams. All BLs have a β-lactam ring that is fused to a 5-member or 6-member ring (except in monobactams) and has 1, 2 or 3 side chains (except in clavams). Differences in chemical structure mean that a wide range of BLs are recognized by the immune system, and patients may experience clinical reactions to one BL while tolerating others [17].

The first steps in diagnosis involve a clinical history, which is often unreliable, ST and if negative, a DPT. These methods show major drawbacks depending on the drug, which leads to misdiagnosis. In general, *in vivo* tests are not exempt of risk for the patient, require experienced personnel, and are both time consuming and expensive for the health care systems, in addition ST often show a low sensitivity due to false positive results, and as a consequence, DPT is the only option available. Thus, *in vitro* tests should be the preferred method for diagnosis, however currently available commercial tests do not fulfill the requirements for a reliable diagnosis. The main approach for allergy diagnosis consists of immunoassays, which quantify drug sIgE. In general, immunoassays work through the binding of sIgE present in patient sera to drug-carrier molecule conjugates immobilized onto a solid support. However the sensitivity of these methods is low, false positive results (26%) have been described with some penicillin determinants and in patients with high total IgE levels [197] and there are commercially available (ImmunoCAP-FEIA) for only a few BLs. This situation has led some research groups to produce their own custom-made immunoassays such as RAST, methods showing higher sensitivity (42.9-75%) than ImmunoCAP-FEIA, although still not optimal [114].

The most commonly accepted mechanism for immunological activation by BLs is based on the hapten hypothesis [18]. BLs are low molecular weight substances that cannot cause an immune response on their own but can act as haptens after covalent binding through nucleophilic attack of amino groups in proteins on the β-lactam ring. Thus, the resulting hapten-carrier (drug-protein) conjugate can induce an immune response by

the production of IgE antibodies or T cells. An epitope, or AD, is the part of the drug-protein antigen that is specifically recognized by the immune system, which may involve not only the drug derivative but also part of the carrier protein [17, 115].

The low sensitivity of both skin and *in vitro* tests for BLs allergy diagnosis is probably due to the fact that they are based on drugs or drug conjugates (ADs) which are not optimally recognized by the immune system [17]. Understanding the way in which drugs are metabolized after protein conjugation as well as the nature of the carrier protein and its contribution to the AD is vital in order to make progresses in the diagnosis of clinical allergy [5, 17, 63]. To date, some advances in the identification of the chemical structures of ADs involved in IRs to BLs have been presented relating drug structure, chemical reactivity and immune recognition [5]. ADs have been described for most of BLs [43, 53, 125, 198], although BP is the most widely studied. Also, the influence of the carrier molecule on AX recognition has been recently demostrated [63]. Moreover, formation of BL-protein adducts is selective, as we recently demonstrated for AX, which mainly modifies HSA, transferrin, and Ig heavy and light chains in human serum [88].

In spite of such advances in ADs elucidation, variations in BLs prescription patterns and the introduction of new compounds from this family have modified the ADs that induce the reactions, leading to changes in the patterns of sensitization. From the first description of patients with IRs, the number of cases has progressively increased. Nowadays, allergy to new cephalosporins are also being reported and reactions to CLV have emerged in the last few years and are progressively increasing since the combination AX-CLV is the most highly consumed BL containing medicine worldwide [114]. In fact, IR to CLV are more common than IR to BP in Spain [131]. AX-CLV cross-reactivity has not been reported, probably due to differences in their chemical structures and degradation patterns, which poses a diagnostic challenge. This is an important issue because CLV selective patients can safely take other BLs, including AX [199], increasing therapeutic options and avoiding the use of inappropriate alternative treatments, which are often more expensive and have more potential adverse effects [131]. Unlikely for penicillins, whose haptenic structure is stable and has been isolated and characterized, ADs for cephalosporins and CLV have not been fully characterized yet, although few studies have given relevant information about the potential ADs for cephalosporins [43, 69, 200] and CLV [53]. This has hampered the development of diagnostic tests for these BLs, being immunoCAP-FEIA for cefaclor [114], with low sensitivity, the only *in vitro* test commercially available. For this reason, there is the need for studies focused on the complete elucidation and characterization of ADs for cephalosporins and CLV.

On the other hand, the extremely low abundance of sIgE in serum associated with drug allergy (femtograms or less) also repesents another factor affecting *in vitro* tests

performance. The high sensitivity needed to detect such low IgE levels is difficult to achieve and this is one of the reasons that has avoided the development of microarray platforms for diagnosing drug allergy. In this sense, the use of dendrons as nanostructures for secondary antibody labeling may allow the increase of fluorescent units due to their multivalency. An accurate design of these structures would lead to signal amplification without increasing immunoassay unspecific interactions, reaching an optimal commitement between the number of fluorescent units and fluorescence emission.

Untangling the mechanisms underlying allergy to β-lactam antibiotics for optimization of diagnostic methods require multidisciplinary approaches. To this end, in Chapters I and II of this thesis we shed light on the process involved in allergic response to aminocephalosporins and CLV using synthetic, immunological, proteomic and computational strategies. By one hand, we designed and synthesized structures derived from two aminocephalosporins (cefaclor and cefadroxil) and CLV, and studied their structure-immunological recognition relationships. Also, using a proteomic approach, we identified the AD and the HSA binding sites for CLV from *in vitro* adducted HSA-CLV. Finally, we used a CLV biotinylated derivative as a tool for identifying serum proteins target of modification by CLV. Besides, detection by novel amplification fluorescent measurement approaches are required for addressing the low sensitivity problem of *in vitro* tests, as they are safe, effective and compatible with microarray laser scanners. Thus, chapter III is related to the use of dendrimer molecules for signal amplification in the IgE detection, with the aim of providing high sensitivity and high throughput in diagnosis. For this, secondary antibodies were labeled with fluorescent dendrimers in an innovative fashion.

All results generated from this work could be translated to the improvement of diagnostic methods. This would have a direct impact on clinical practice since it would provide faster and safer diagnostic methods, reducing the cost to public health systems.

OBJECTIVES

The general objective of this thesis is to carry out studies directed to improve current *in vitro* tests for diagnosing immediate allergic reactions to BLs. For this purpose, different approaches were proposed: (i) elucidation of the chemical structure involved in immune system activation and (ii) amplification of immunoassays detection signal.

Cephalosporins and CLV were the BLs object of the studies since their consumption has notably increase during the last years and there is lack of information about their ADs. On the other hand, dendrimeric structures were employed to design new fluorescent probes for signal amplification, making the most of their multivalent architecture.

More specific objectives are the following:

1. Identification of epitopes for α-aminocephalosporins by a synthetic design of hypothetical ADs and their immunological evaluation.

    1.1. Synthesis, purification and characterization of pirazinone-like (cyclized) structures for cefaclor and cefadroxil.

    1.2. SAR study: Recognition of synthesized structures by sIgE in patients allergic to BLs.

2. Elucidation of ADs for CLV using both a synthetic strategy followed by structure-immunological recognition evaluation or proteomic approaches.

    2.1. Synthesis, purification and characterization of structures derived from CLV.

    2.2. SAR study: Recognition of synthesized structures by sIgE in basophil surface from allergic patients selective to CLV.

    2.3. Proteomic analysis of HSA-CLV conjugates generated *in vitro* for elucidation of the AD of CLV and identification of its binding sites in HSA.

3. Use of a biotinylated derivative of CLV as a tool for identification of serum proteins target of modification.

    3.1. Synthesis, purification and characterization of a CLV biotinylated derivative.

    3.2. Nuclear Magnetic Resonance (NMR) comparison of stability and reactivity towards nucleophiles between native CLV and its biotinylated derivative.

    3.3. Assesment of *in vitro* haptenation capacity of the biotinylated derivative using HSA as model.

    3.4. Isolation and identification of serum proteins target of *in vitro* modification by the CLV derivative.

    3.5. Evaluation of the competition between CLV and its biotinylated derivative for protein haptenation *in vitro*.

4. Generation of a series of fluorescent secondary antibodies for amplification of immunoassays detection signal.

4.1. Synthesis, purification and characterization of a set of dendrons with hydazine functionality at focal point and different units of fluorescent moieties at periphery.

4.2. Proof-of-concept site-specific labeling of a model secondary antibody using synthesized fluorescent dendrons as probes and spectroscopic characterization.

RESULTS AND DISCUSSION

I. Study of antigenic determinant structures for amino-cephalosporins

Cephalosporins are BLs that are widely used for infectious illnesses treatment and prophylaxis, and they constitute, after penicillins, the most common cause of ADRs mediated by specific immunological mechanisms [42]. The characterization of their drug determinants [63], the identification of the carrier proteins [63, 201-203] as well as the IgE recognition of the conjugate [204] are crucial for understanding the mechanisms of allergy as well as to implement diagnostic assays.

Although the epitopes for cephalosporins have not been fully elucidated, there is clinical and immunochemical evidence of R^1 side chain contribution to sIgE recognition. Some patients are selective to the culprit cephalosporin, whilst others react to cephalosporins with identical or similar R^1 side chains [9-11], and a third group of patients are cross-reactive to other BLs, especially penicillins, with identical or similar R^1 side chains [10, 12-14]. Structural studies for the identification of the drug epitope linked to the protein for cephalosporins are difficult to perform. It seems that SAR studies have been the only successful approach for investigating the AD of these group of BL antibiotics [42, 43, 69, 70, 205].

Antunez *et al.* [70] prepared a series of monomeric cephalosporin-butylamine conjugates and evaluated their molecular recognition by IgE in patients allergic to different cephalosporins. Although the mixture of different structures formed as result of cephalosporins conjugation to butylamine was difficult to characterize, the presence of the R^1 side chain in most of the formed conjugates is assumed (NMR evidence) [69]. In patients allergic to cephalosporins, selective recognition of R^1 side chain was proved in 67% of cases, with some degree of cross reactivity among cephalosporins with identical or similar R^1 side chain. This study was quite useful to confirm the importance of the side chain in recognition by cephalosporins sIgE, however, it did not provide more information about the epitope or AD specific structure.

Other studies have performed more precise epitope structure elucidation by means of the synthesis and immunological evaluation of well-defined structures as proposed AD for cephalosporins [43, 69, 205] derived from the CPO conjugate. Thus, a series of proposed epitopes were designed (Figure I.1) consisting of the R^1 acyl side chain

condensed to the β-lactam fragment opened by butylamine, chosen as a nucleophile to emulate the ε-amino groups of Lys, and bearing different functionalities or oxidation states at the C-6 of the original cephalosporin (methyl, hydroxymethyl, mercaptomethyl and acetal). Those with hydroxyl or aldehyde functionality showed the strongest immunological recognition [43, 69]. A different pattern, with less recognition of these structures was observed for patients allergic to α-aminocephalosporins, which suggested the existence of other ADs.

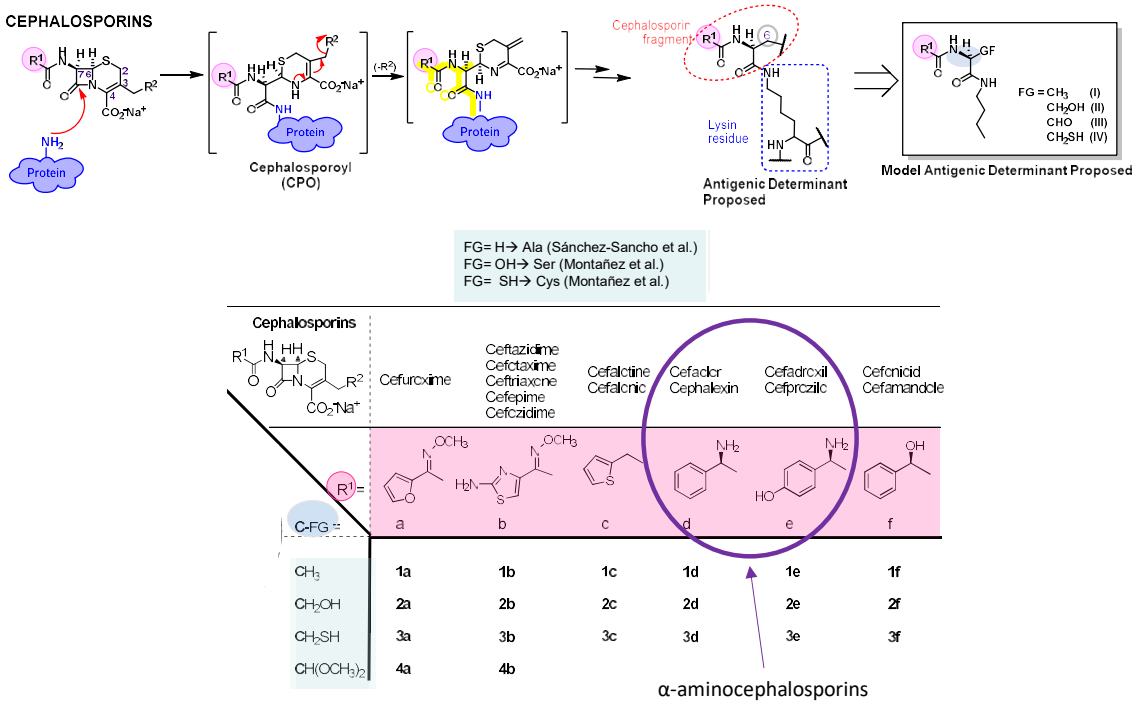

Figure I.1. Top: general degradation hypothesis for cephalosporins. Bottom: structures derived from cephalosporins synthesized and evaluated by Sánchez-Sancho *et al*. [69] and Montañez *et al*. [43].

The nucleophilic group present in R^1 side chain of α-aminocephalosporins allows an additional reactivity. By one hand, autoaminolysis reactions would lead to β-lactam ring intramolecular opening with good leaving group R^2 elimination/leaving to afford diketopyperazine structures similar to the observed for AX [206] (Figure I.2A). The instability of the dihydrothiazine ring compared to the thiazolidine is likely to result in different degradation structures. However, these structures are not conjugated to proteins and, according to hapten hypothesis, would not be involved in allergic reactions [18, 125]. On the other hand, after the protein binding through the nucleophilic attack of lysine amino groups to the β-lactam carbonyl of α-aminocephaloporins, a subsequent intramolecular cyclization would be possible by nucleofilic attack of the amino group in R^1 towards the carbonyl group in the aldehyde proposed to be formed in carbon 6 of

intermediate product [43, 205, 207] to yield, after aromatization, pyrazinone-like degradation products [205, 207, 208] (Figure I.2B).

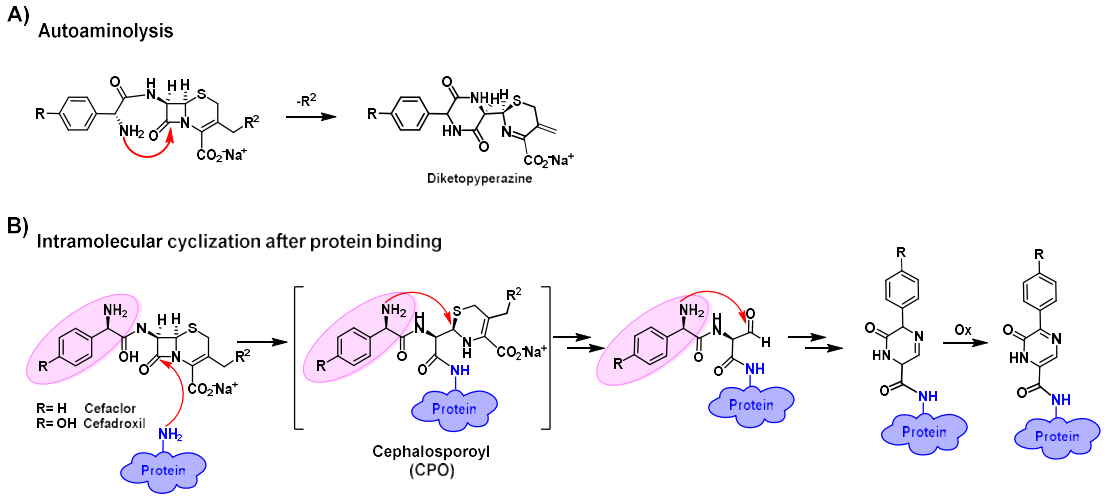

Figure I.2. Additional reactivity for α-aminocephalosporins due to the presence of an amino group in R^1 side chain. A) Autoaminolysis and B) intramolecular cyclization after protein binding.

Venemalm *et al*. [205] isolated this pyrazinone derivatives for cefaclor and cephalexin, although in very low yields, which hampered their immunological evaluation. Consequently, a pyrazinone analog was synthetized and showed specific recognition in cefaclor allergic patients. However, this analog is different to the isolated structure: the carbonyl group of amide linkage with carrier nucleophile, instead of being directly bound to the C-6 of the pyrazine ring (Figure I.3), it is separated by a methylene from the pyrazinone moiety.

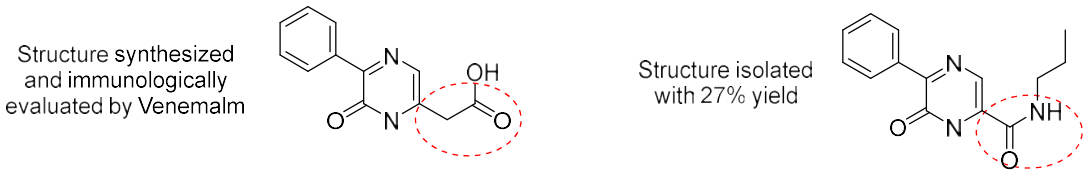

Figure I.3. Left. Synthetic structure for conjugation with carrier molecules and further immunological evaluation.Right. Structure isolated after conjugation of cefaclor and cefalexin with propylamine, with 27% and 10% yield, respectively.

In this chapter, different approaches were carried out to study the chemical structures of the aminocephalosporin ADs formed after protein conjugation able to be recognized by the immune system. One consisted of the NMR monitoring of cefaclor and cefadroxil solutions in presence of a simple nucleophile, butylamine, as emulators of free amino groups from lysine in proteins. In order to better define the structural immunoreactivity

of α-aminocephalosporins, the other approach consisted of the design and synthesis of novel cyclized structures derived from cefaclor and cefadroxil as potential ADs for α-aminocephalosporins. To evaluate the immunological recognition of the well-characterized pyrazinone structures, immunoassays were to be performed with sera from patients allergic to BLs. PhD student carried out both the synthesis of the new ADs of α-aminocephalosporins and their immunological evaluation by RAST inhibition.

I.1. Study of α-aminocephalosporins Reactivity Towards Simple Nucleophiles

Lys amines, Cys thiols, His imidazoles and the amino terminal group are the main nucleophilic sites of HSA potentially able to covalently react with BLs [88, 209], being Lys residues the most reactives [88]. Taking this into account, butylamine and N-acetyl-lysine were used as simple nucleophiles for *in vitro* reactions as a first approach for characterizing protein-BL adducts. NMR studies of this reaction could give valuable information about the structure derived from the remaining BL linked to the nucleophile molecule after conjugation via β-lactam acylation. This resulting structure might be identical or very similar to that formed when the nucleophile is an aminoacid of the protein. Thus, it would help in the structural elucidation of the AD.

Reaction of cefaclor and cefadroxil in presence of butylamine was studied over time by ^{1}H-NMR while incubated at 37˚C. Solutions using nucleophile/BL 1:1 ratio, prepared in deuterated PBS 1X were analyzed.

The following Figures (I.4-I.7) show stability and reactivity NMR studies for cefadroxil and cefaclor. Figure I.4 depicts stability studies for cefadroxil at neutral pH, to be used as control, and it was observed that after 16 hours incubation, β-lactam ring started opening and the dihydrothiazine ring started degrading but there was still starting product. After 40 hours incubation, original structure was degraded and only signals belonging to the side chain were still recognizable. Besides, the new signals appearing in the aromatic region could be related to some pyrazine degradation structures proposed for α-aminocephalosporins [205-207]. Slow β-lactam reactivity for cefadroxil could be attributed to the absence of a good leaving group R^{2}.

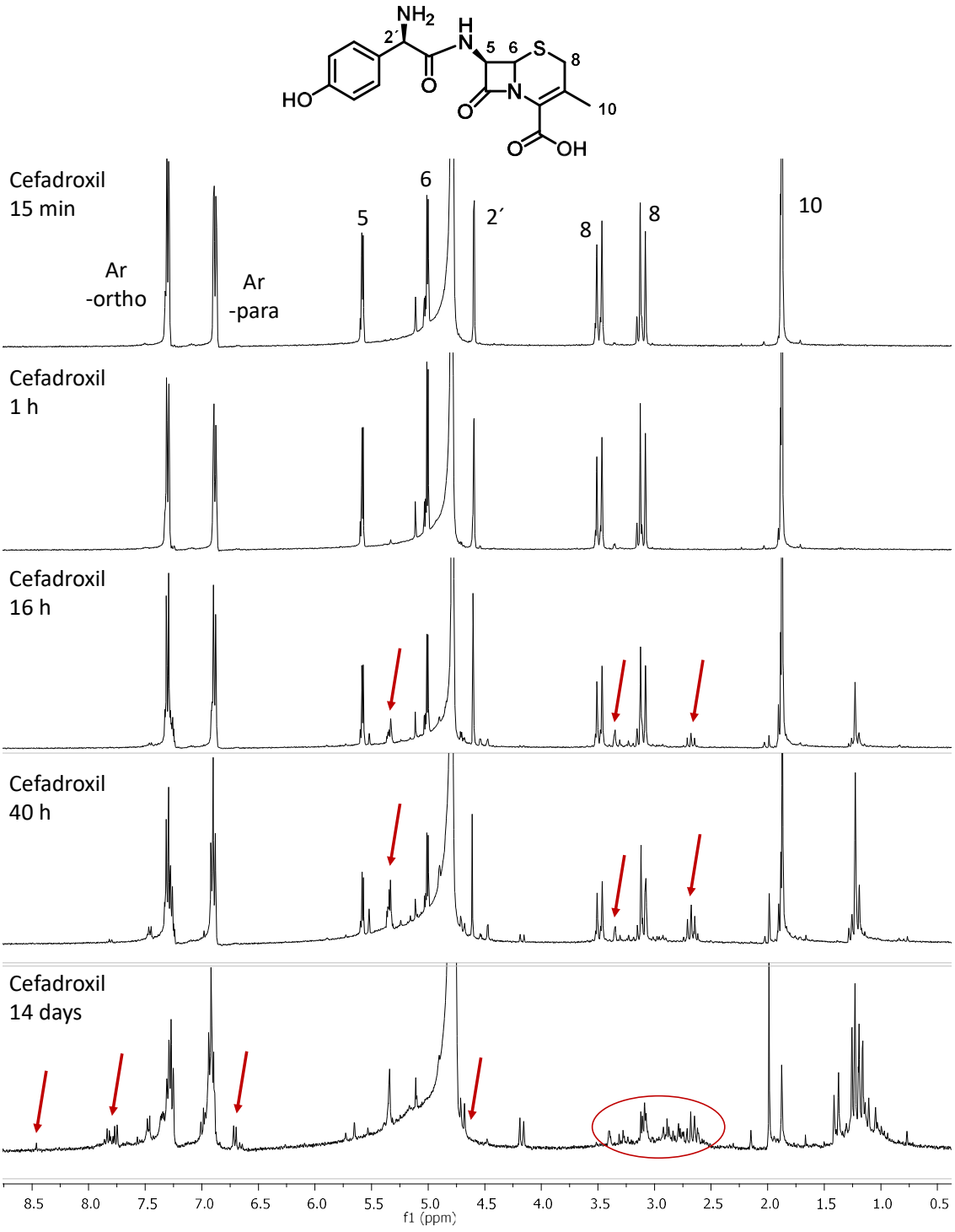

Figure I.4. ^{1}H-NMR spectra of cefadroxil registered in deuterated PBS 1X over time. Pointed with arrows changing signals over time.

Results of cefadroxil reactivity studies with butylamine are presented in Figure I.5. The NMR shows again the opening of the β-lactam, the degradation of the dihydrotiazolidine ring, the presence of the aromatic ring in the side chain and the appearance of new aromatic signals after 14 days of reaction. Compared with control cefadroxil, new signals

appears when reacting with butylamine at 3.0-3.4 ppm but they can be clearly attributed to amide formation.

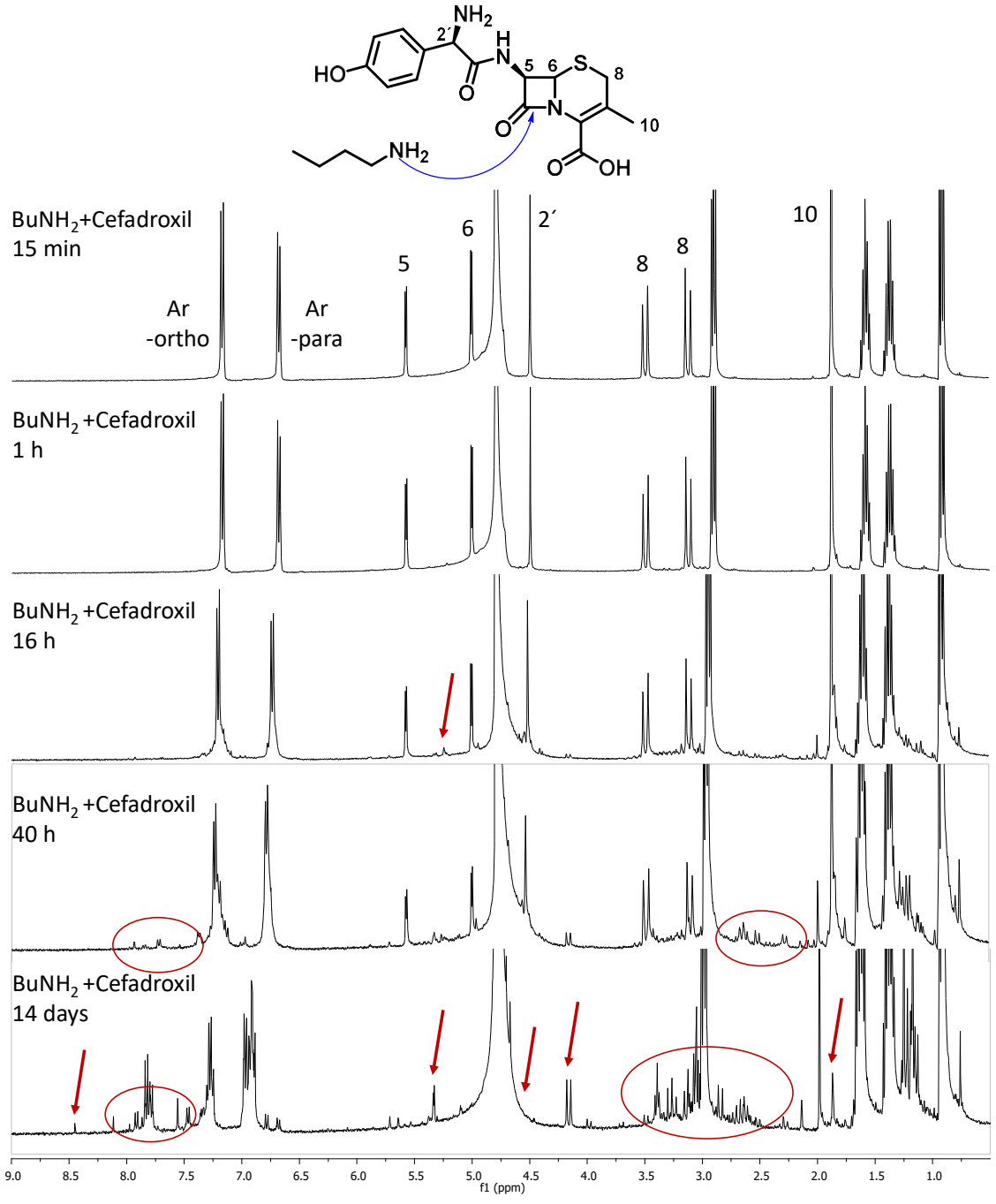

Figure I.5. ^{1}H-NMR study of cefadroxil reactivity with butylamine registered in deuterated PBS 1X. Pointed with arrows and circles changing signals over time.

Stability studies for cefaclor at pH 7.4 were performed and Figure I.6 gathers the results obtained. After 16 hours of incubation, there was evidence of complete degradation of the starting product since signals belonging either to the β-lactam or to the

dihydrothiazine ring were completely gone and only aromatic signals were identifiable. Cefaclor has a chlorine atom, the high electronegative value of which facilitates the opening of the β-lactam ring by induction.

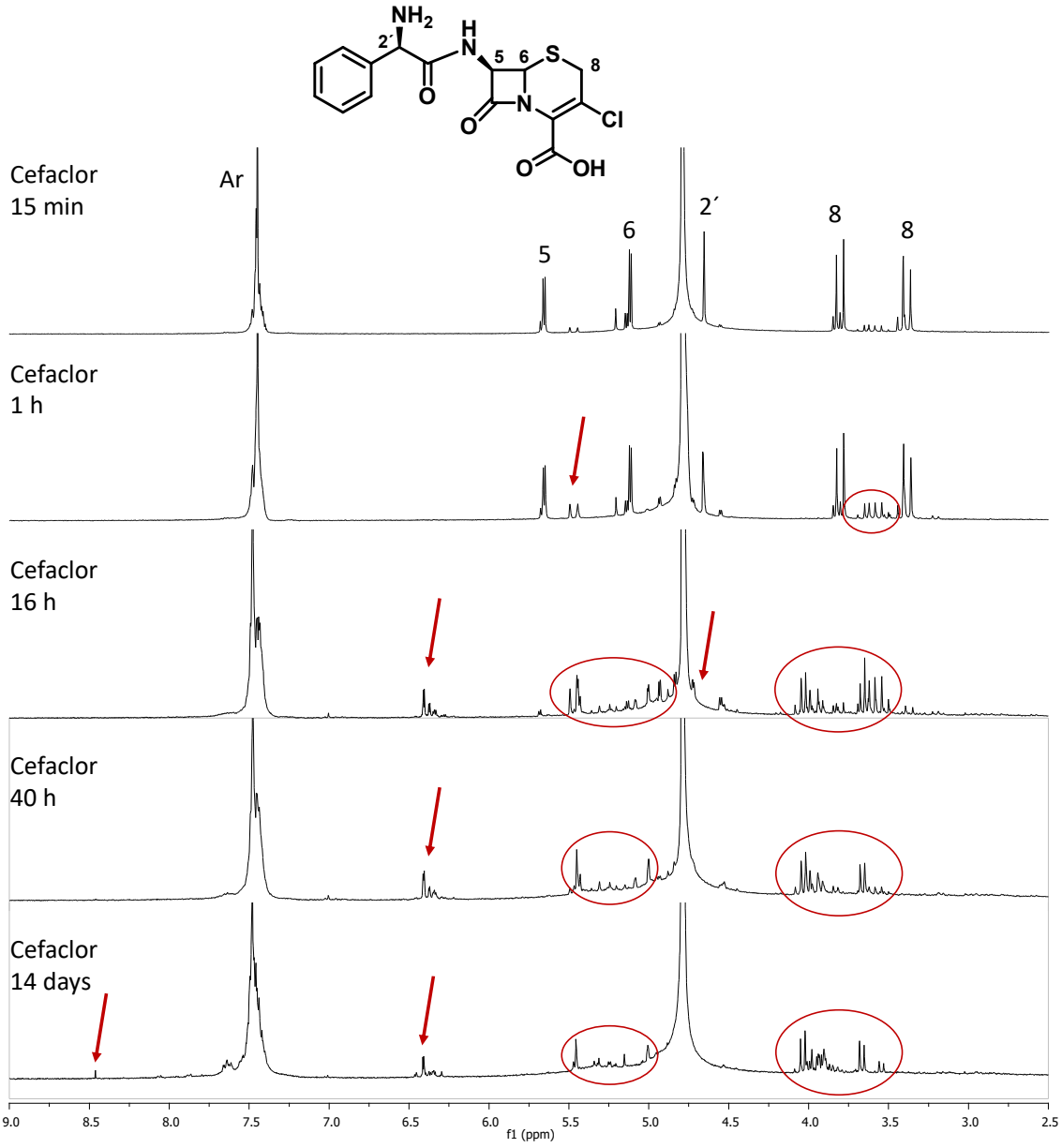

Figure I.6. ^{1}H-NMR spectra of cefaclor registered in deuterated PBS 1X within time. Pointed with arrows and circles changing signals over time.

Reaction with butylamine took place since after 15 minutes incubation, when a signal belonging to amide formation appeared at 3.25 ppm (Figure I.7). The new signals that appeared in the aromatic region after 14 days reaction may be due to the aromatic degradation products for α-aminocephalosporins [205-207].

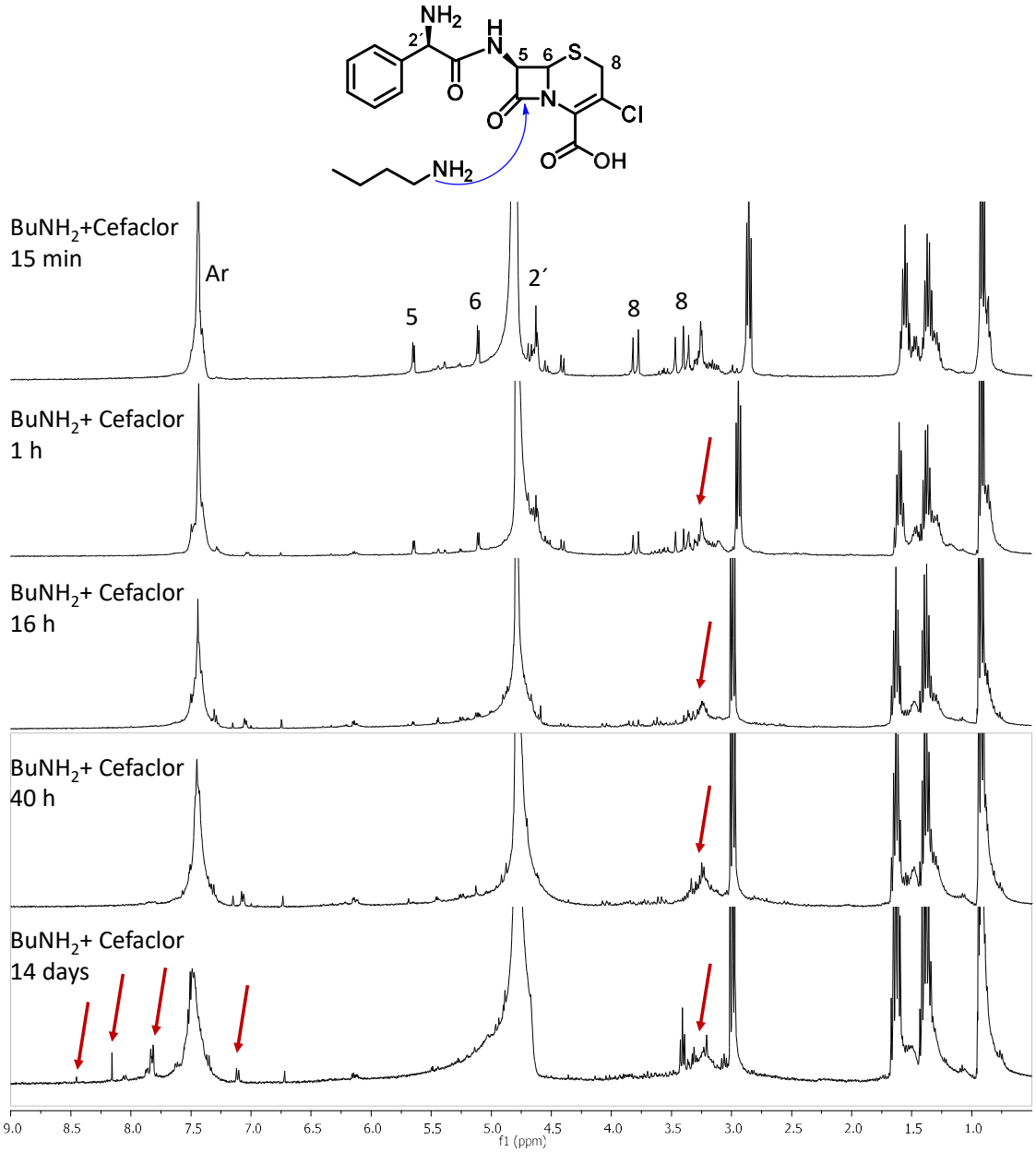

Figure I.7. ^{1}H-NMR study of cefaclor reactivity with butylamine registered in deuterated PBS 1X. Pointed with arrows and circles changing signals over time.

From these results, it was only possible the demonstration of the remaining aromatic side chain of cefaclor and cefadroxil after reaction with nucleophiles, as it was previously inferred [43, 69]. Thus, more sophisticated studies involving SAR evaluation are necessary to fully elucidate the structure of ADs for α-aminocephalosporins.

I.2. Synthesis of New Synthetic Antigenic Determinants for α-aminocephalosporins

IgE recognition evaluation of the exact pyrazinone-like degradation products identified for some α-aminocephalosporins had not been possible so far, due to the low yields in which they were isolated [205], as well as to the lack of a straightforward synthetic methodology that affords them in quantities that allow their evaluation.

We addressed the synthesis of novel cefaclor and cefadroxil target pyrazinone-like derivatives according to the proposed cephalosporins degradation hypothesis, using butylamine as a model nucleophile emulating lysine.

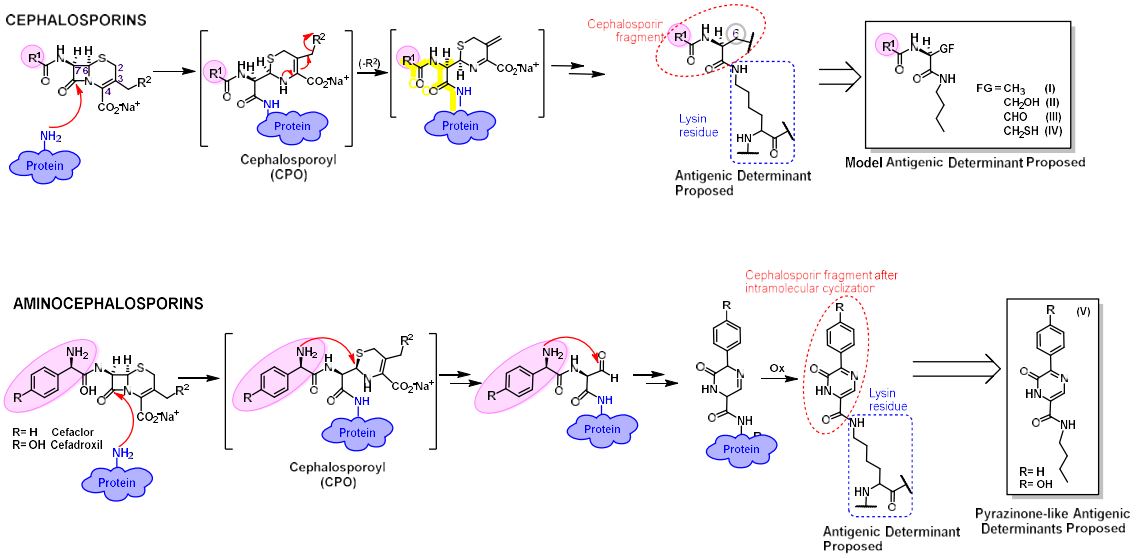

Figure I.8. Degradation hypothesis of cephalosporins (top) and aminocephalosporins (bottom) after β-lactam ring opening by means of nucleophilic attack of amino groups in proteins and consequent AD formation.

Two synthetic methodologies were tried (first approach) for ADs synthesis before we found the successful strategy (second approach, UDC strategy).

First approach (Scheme I.1)**:**

In synthetic methodology I, synthesis was started with Boc-protected serine (*N*-Boc-Ser) and followed by amide coupling with butylamine (residue intended for emulating Lys in proteins) resulting in *N*-Boc-Ser-NHBu [43]. Then, alcohol group was to be activated in order to turn it into a good leaving group. In this step, tosylation did not work, but mesylation did affording *N*-Boc-Ser-NHBu-OMs. Nucleophilic substitution with phenylglycine (Phg) or phenylglycine methyl ester (Phg-COOMe), employing various

conditions such as different solvents or bases, was not successful. Thus, further amino deprotection and condensation could not be carried out to obtain the target structure.

In synthetic methodology II, Boc-protected phenylglycine (*N*-Boc-Phg) was condensated via amide formation with Ser-NHBu to yield *N*-Boc-Phg- Ser-NHBu [43] which hydroxyl group was subsequently mesylated (*N*-Boc-Phg-Ser-NHBu-OMs). However, after deprotection of amino group (Phg-Ser-NHBu-OMs), further intramolecular condensation was not successful. The fact that both approaches failed in the SN2 reaction, could be due to phenyl ring steric hindrance.

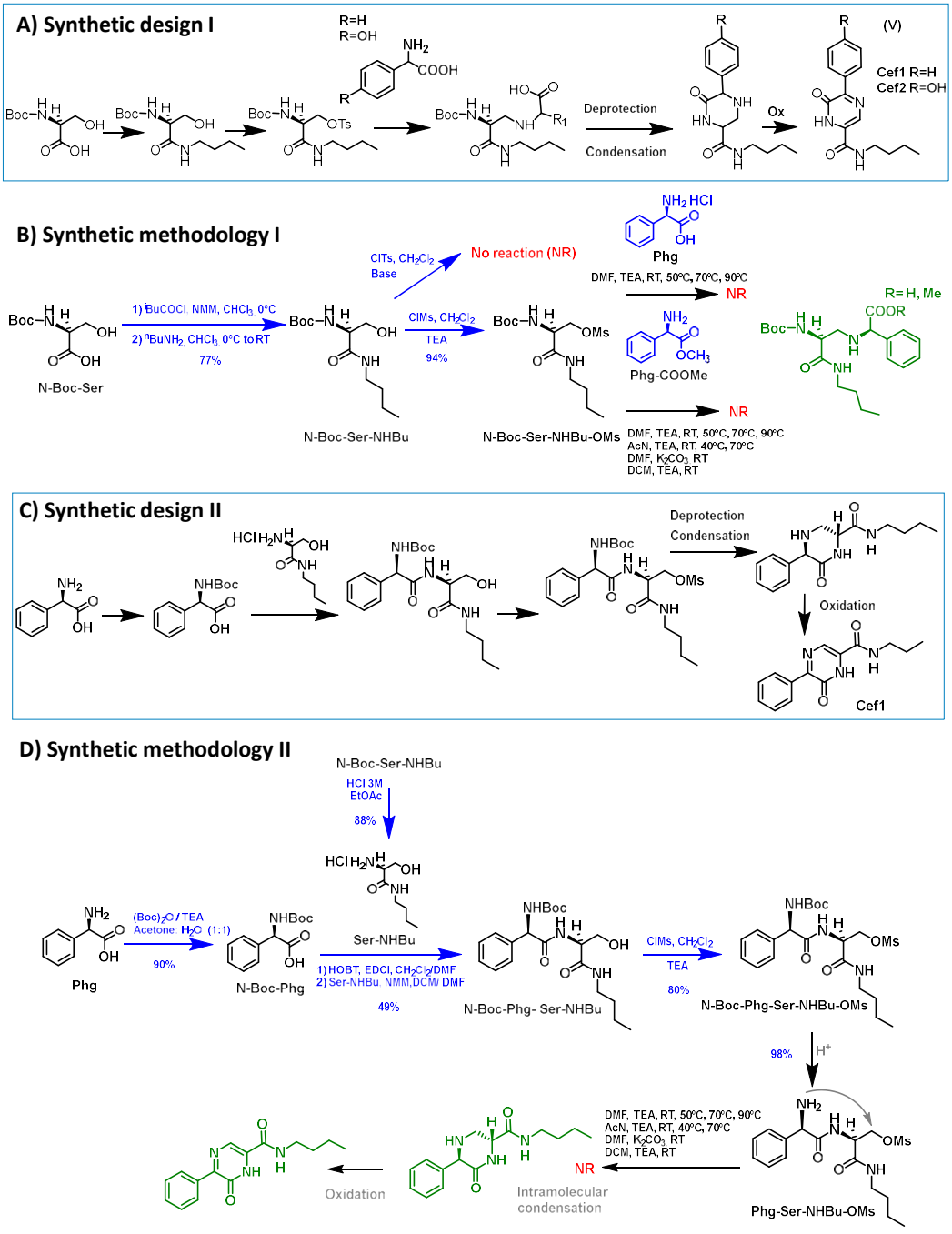

Scheme I.1. First approach tried for aminocephalosporins derivatives synthesis. Details of synthetic designs (A and C) and synthetic methodology (B and D). Molecules in green were not prepared.

Second approach:

The successful synthetic pathway for pyrazin-2(1*H*)-ones followed the Ugi/Deprotect/Cyclize strategy (UDC) [210] (Scheme I.2). First, required structures were assembled by following the one-pot Ugi four-component reaction (U-4CR) in which an isocyanide, an amine, an aldehyde or ketone and a carboxilic acid yielded the Ugi adduct, a bis-amide. More specifically, we selected as starting materials butyl isocyanide, a protected primary amine (2,4-dimethoxybenzylamine) as ammonia substitute, a glyoxal derivative (2,2-dimethoxyacetaldehyde) and a *N*-Boc protected aminoacid (phenylglycine or hydroxyphenylglycine) to produce the Ugi adduct. The subsequent acid-mediated-cleavage of the dimethoxyacetal, 2,4-dimethoxybenzylamine and Boc may result in the amino-functionalized aldehyde intermediate that, after cyclization through intramolecular imine formation and aromatization, directly afforded target pyrazinone **V**, after chromatographic purification, with yields ranging from 25 to 99%. The chemical structures were confirmed by means of 1D and 2D NMR as well as by MS.

This UDC methodology, which finally enabled the versatile synthesis of our target molecules, was based on a convergent strategy previously described for obtaining pyrazin-2-(1*H*)-ones bearing alkyl substituents at positions 3 and 5 of the pyrazine. We adapted the method to prevent substitution at position 5 by using a mono-protected dialdehyde, dimethoxyacetaldehyde, instead of glyoxal derivatives. The diversity at position 3 of the pyrazine is determined by the choice of the starting amino acid, corresponding to the different side chains of α-aminocephalosporins, which means that the corresponding target pyrazinones for both α-aminocephalosporins with different R^1 were obtained by employing the suitable aminoacids. In addition, the method is relatively simple as well as time- and cost-effective since it consists of two synthetic and only one purification steps, compared to other synthetic alternatives involving multi-step chemical procedures [210] and unsuccessful intramolecular cyclization through SN2. The synthesized structures are of interest as potential ADs of α-aminocephalosporins.

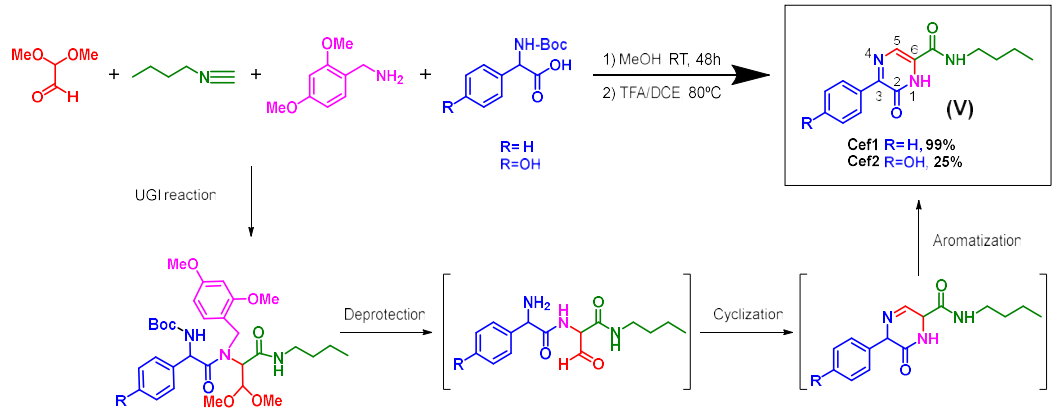

Scheme I.2. Synthesis of pyrazin-2(1H)-ones as ADs for α-aminocephalosporins, by means of UDC strategy.

I.3. Immunological Evaluation of Pyrazinone-Like Antigenic Determinants

I.3.1. Patient´s selection

After clinical evaluation, sera were assayed by RAST using cefaclor, cefadroxil and AX conjugated to PLL in the cellulose solid phase. In order to make sure an accurate evaluation of the synthesized structures, those sera with higher levels of sIgE for the culprit drug (higher than 6.7%) were chosen: eight from patients allergic to cefaclor and nine from patients allergic to AX. Data from the patients included in the study and *in vitro* evaluation of sIgE levels using direct RAST are given in Table I.1.

Table I.1. Classification and clinical characteristics of patients diagnosed with an immediate allergic reaction to cefaclor or AX included in the study. F: female; M: male; AE: angioedema; INT: time interval between reaction and study; (+): positive; (-): negative; ND: non determined; NK: not known. [a]Bold faced values indicate positive RAST results.

Case	Age	Sex	Reaction	Drug involved in the reaction	INT (days)	ST			% RAST		
						AX	Cefaclor	Cefadroxilo	AX-PLL	Cefaclor-PLL	Cefadroxil-PLL
1	38	M	Immediate urticaria	Cefaclor	7	+	+	ND	ND	**33.37**	ND
2	43	F	Immediate urticaria and AE	Cefaclor	NK	+	+	ND	ND	**15.36**	ND
3	37	F	Anaphylactic shock	Cefaclor	240	-	ND	ND	ND	**20.55**	ND
4	56	F	Anaphylaxis	Cefaclor	120	+	+	-	ND	**19.44**	ND
5	13	F	Anaphylactic shock	Cefaclor	450	+	+	ND	ND	**11.17**	ND
6	5	F	Erythema	Cefaclor	30	-	+	ND	ND	**34.56**	ND
7	17	F	Anaphylaixs	Cefaclor	30	-	+	-	ND	**7.69**	ND
8	27	F	Urticaria and AE	Cefaclor	210	-	+	-	ND	**11.67**	ND
9	57	M	Anaphylaxis	AX-CLV	30	+	ND	+	**47.33**	ND	**5.12**
10	26	M	Anaphylaxis	AX	10	+	ND	+	**22.54**	ND	1.90
11	38	F	NK	NK	NK	+	ND	+	**21.52**	ND	3.85
12	60	M	Anaphylactic shock	AX-CLV	NK	+	ND	ND	**26.09**	ND	3.42
13	69	M	Anaphylaxis	AX-CLV	28	+	ND	+	**21.80**	ND	0
14	59	M	Anaphylaxis	AX-CLV	NK	+	ND	ND	**14.68**	ND	**4.83**
15	61	F	Immediate urticaria and AE	AX-CLV	150	-	ND	ND	**7.93**	ND	**5.40**
16	62	M	Immediate urticaria	AX-CLV	NK	ND	ND	ND	**6.77**	ND	**5.15**
17	53	M	Anaphylaxis	AX-CLV	120	+	ND	ND	**6.84**	ND	2.28

I.3.2. *In Vitro* Evaluation of Specific IgE Molecular Recognition by RAST Inhibition

Immunochemical recognition of the new pyrazinone-like structures was evaluated by competitive RAST inhibition. This assay consists of competitive IgE recognition between the solid phase (drug-PLL conjugate attached to cellulose) and the inhibitors (**Cef1**, **Cef2**, **Cef3**, **Cef4** and butylamine monomers for cefaclor and cefadroxil, depicted in Table I.2, at different concentrations in the fluid phase.

Table I.2. Depiction of structures used as inhibitors for RAST inhibition studies.

		Related α-aminocephalosporin	
		Cefaclor	*Cefadroxil*
Type of structure	New pyrazinone-like structures	**Cef1** 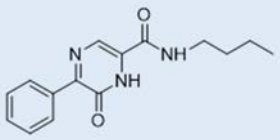	**Cef2** 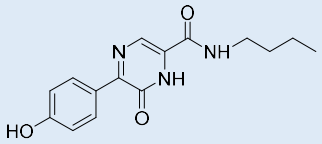
	Previous synthetic determinats	**Cef3** 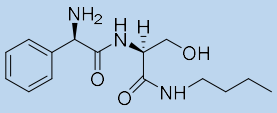	**Cef4** 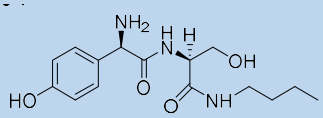
	Butylamine conjugates	**Cef5** 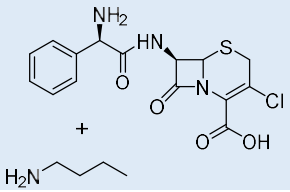	**Cef6** 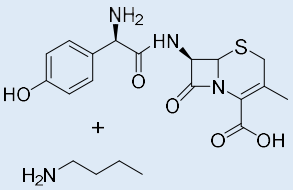

In the previous study of Montañez *et al*. [43] no recognition was obtained for structures **Cef3** and **Cef4**, or related ones includying the same R^1 side chain, no matter the functional group present at C-6, due to the fact that immunological evaluation was performed with sera from patients allergic to cephalosporins bearing a very different R^1 side chain: ceftazidime, cefotaxime or cefuroxime (Figure I.9). However, in our study, immunological evaluation was performed with sera from patients in which the culprit drug (cefaclor or AX) has the same R^1 side chain as the evaluated structures (**Cef1** and **Cef3** or **Cef2** and **Cef4**, respectively).

In spite of being IgE recognition comparison between the two well-defined synthetic structures (**Cef1** vs. **Cef3** and **Cef2** vs. **Cef4**) the main objective, monomeric conjugates of cefaclor and cefadroxil were also included in the study as inhibitors.

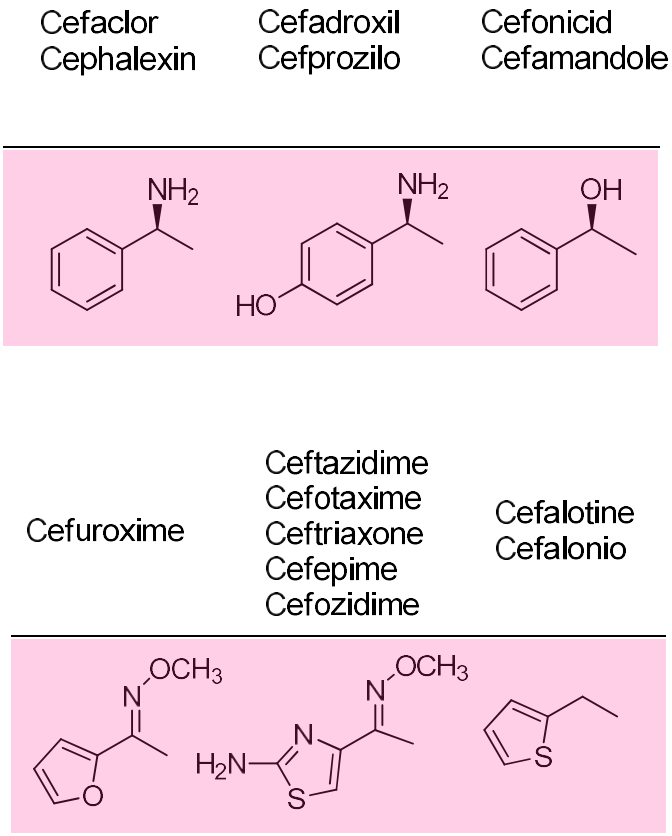

Figure I.9. R^1 side chain for some cephalosporins.

The two structures derived from cefaclor (**Cef1** and **Cef3**) and cefaclor-butylamine conjugate were evaluated in sera from eight patients with allergic reaction to cefaclor (Figure I.10A). In most cases, at the maximum concentration (100 mM) of determinants, a higher percentage of inhibition was obtained for the pyrazinone **Cef1** than for the synthetic determinant **Cef3**, indicating a better recognition of the cyclized structure. In general, inhibition dropped at the minimum concentration (10 mM) of inhibitor. *In vitro* IgE recognition is generally considered positive when the inhibition percentage is higher than 50%. Important differences in the positivity was obtained, since 63% of patients allergic to cefaclor significantly recognized the pyrazinone **Cef1** and 12% of cases recognized the determinant **Cef3**, at the maximum concentration (Figure I.10B). Regarding results obtained for cefaclor-butylamine, IgE recognition is higher than for synthetic structures **Cef1** and **Cef3** only for two cases (5 and 8). This indicates that the sensitivity using the well-defined synthetic structures is higher than using the monomeric conjugates, since the latter may contain many kind of degradation structures possible but in a low concentration each.

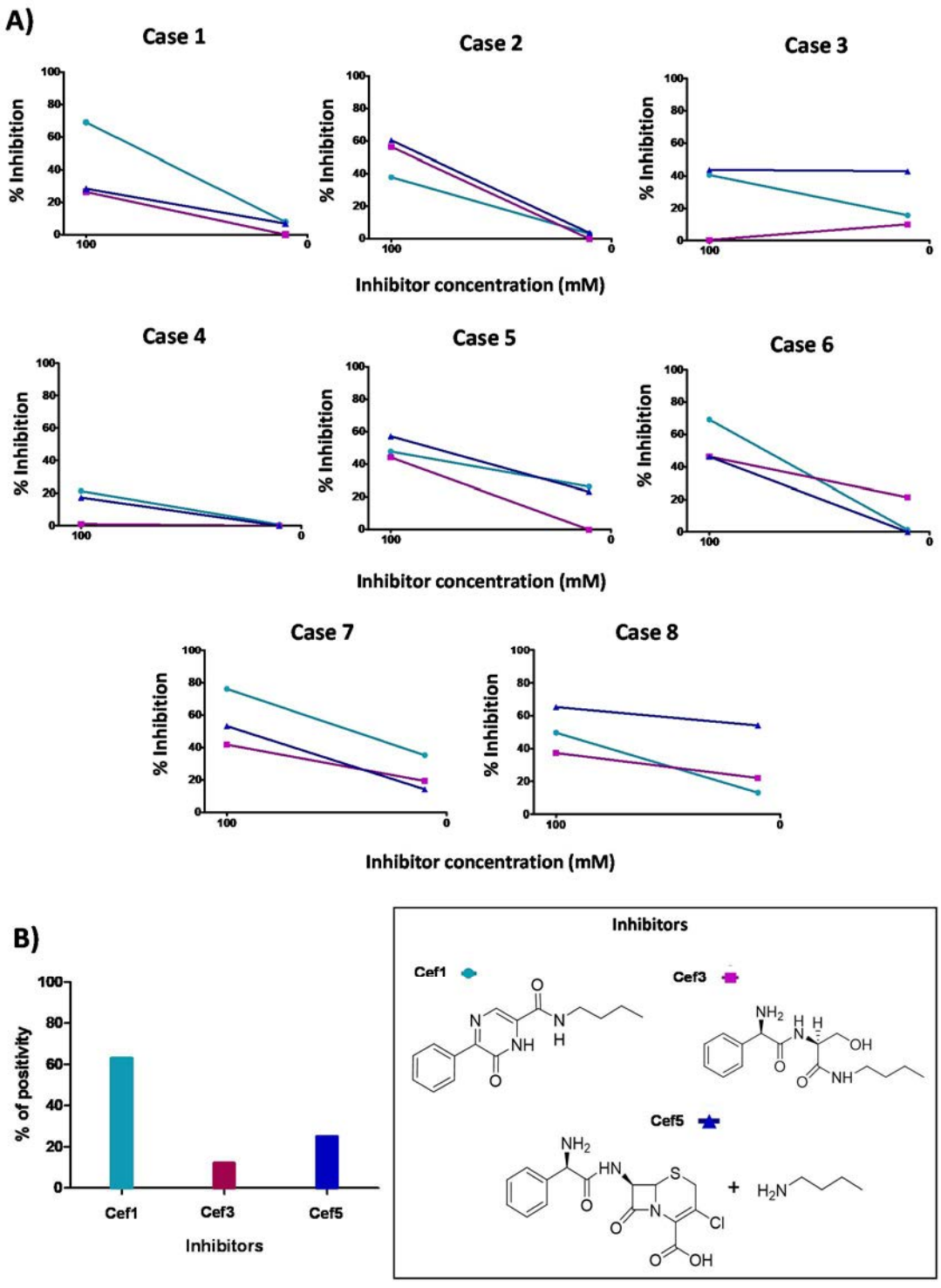

Figure I.10. Immunological evaluation results with cefaclor derivatives. A) RAST inhibition assays performed with sera from 8 patients allergic to cefaclor, using compounds **Cef1**, **Cef3** and cefaclor-butylamine as inhibitors and cellulose discs modified with cefaclor-PLL as the solid phase; B) Comparison of positivity (%RAST inhibition >50%) between **Cef1**, **Cef3** and **Cef5** inhibitors at 100 mM concentration.

Since both AX and cefadroxil contain the same R^1 side chain (Figure I.11), the recognition of cefadroxil proposed epitopes (**Cef2** and **Cef4**) was evaluated in nine patients allergic to AX (Figure I.12) in order to study cross-immunoreactivity with penicillins.

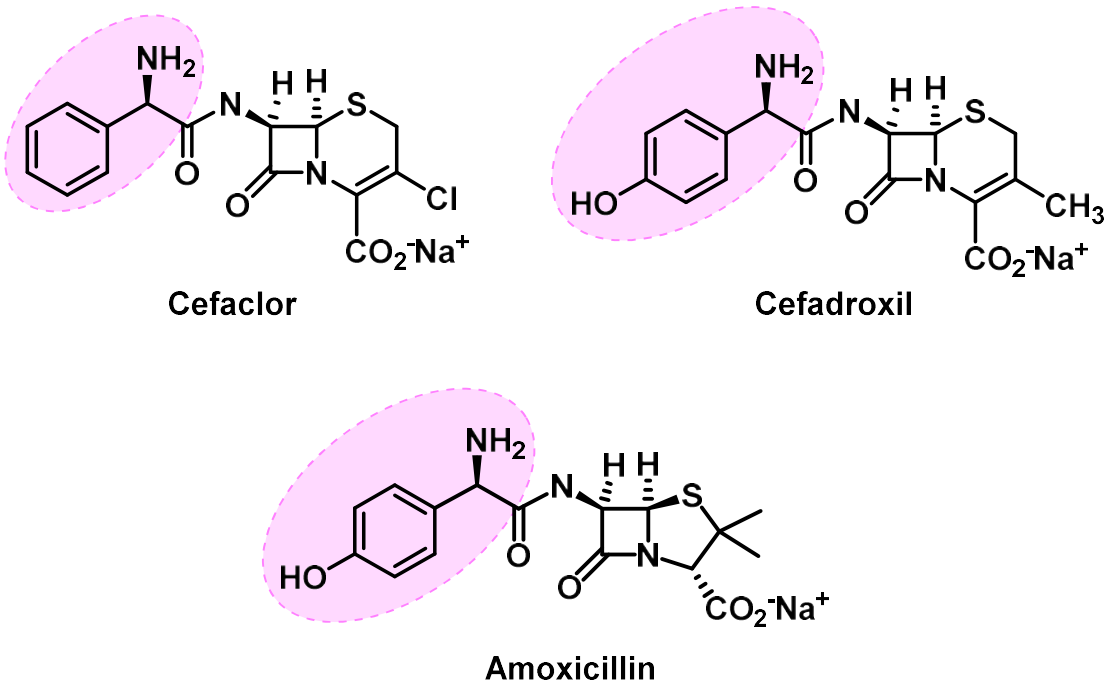

Figure I.11. Comparison of R^1 side chain for aminocephalosporins (cefaclor and cefadroxil) and AX.

Most sera showed similar IgE recognition with both molecules **Cef2** and **Cef4** (Figure I.12A). In fact, similar positive results (% RAST inhibition >50%) between synthetic determinants of cefadroxil (*in vitro* cross-reactivity) was observed in 44% of patients allergic to AX (cases 10, 12, 13 and 17). Also, same values of positivity were obtained with both molecules **Cef2** and **Cef4** (Figure I.12B), with 56% of patients allergic to AX recognizing each synthetic determinant of cefadroxil. Bearing in mind that the culprit is AX, these results can be helpful to get insight into the structure responsible for cefadroxil allergies and study cross-reactivities between penicillins and cephalosporins.

Inhibition results obtained with synthetic structures were in agreement with *in vivo* test results (Table I.1) since there was *in vitro* recognition in all cases of cefadroxil positive ST (cases 9, 10, 11 and 13), either for one of the structures (**Cef2** showed inhibition in case 9 and **Cef4** in case 11) or for both structures **Cef2** and **Cef4** (cases 10 and 13). Furthermore, it is worth to highlight that three out of these four cases presented negative direct RAST results for cefadroxil using cefadroxil-PLL in the solid phase (cases

10, 11 and 13). However the inhibition showed with synthetic determinants, suggests that the cefadroxil-PLL conjugates, anchored to the solid phases for the direct RAST, include other structures different to the ones investigated here. This indicates that structures **Cef2** and **Cef4** would be valuable for improving sensitivity of *in vitro* tests for diagnosing AX/cefadroxil cross-reactivity.

The conjugate cefadroxil-butylamine was better recognized than synthetic structures **Cef2** and **Cef4** for most of cases. As a variety of conjugates may be formed when incubating cefadroxil and butylamine, this is in agreement with the fact that other ADs different from those included in this study could be as well involved in the allergic response.

Previous structure-immunological recognition relationships studies confirmed that besides R^1 side chain structure, the rest of the nuclear structure of cephalosporin is also relevant for optimal molecular recognition, especially for patients with cross-reactivity [43, 69]. The trend observed for patients allergic to cephalosporins that recognized the proposed synthetic epitopes (**I**, **II** and **III**, Figure I.13A) was only found for a minority of patients allergic to aminocephalosporins, indicating a different immunoreactivity pattern, likely due to amino functionality. Our results showed that specificity of IgE antibodies from patients allergic to cefaclor is higher for pyrazinone **Cef1** than for structure **Cef3**, indicating that the cyclized structures better mimic the real AD. Although the enhanced IgE molecular recognition takes place only with those corresponding to the pyrazinone **V** (Figure I.13B), we believe that after conjugation with protein, and subsequent cephalosporyl intermediate formation, molecules with structures **II** and **III** can also be generated.

These findings provide insight into the structure responsible for cefaclor and cefadroxil allergies and cross-reactivity between penicillins and cephalosporins, and these new synthesized structures would be applicable for the diagnosis of allergy to those cephalosporins sharing the same R^1 structure, such as cefprozil (same R^1 than cefadroxil) or cephalexin and cefaloglycin (same R^1 than cefaclor). Further studies involving the attachment of structures **Cef1** and **Cef2** to a solid phase could increase sensitivity by direct immunoassays.

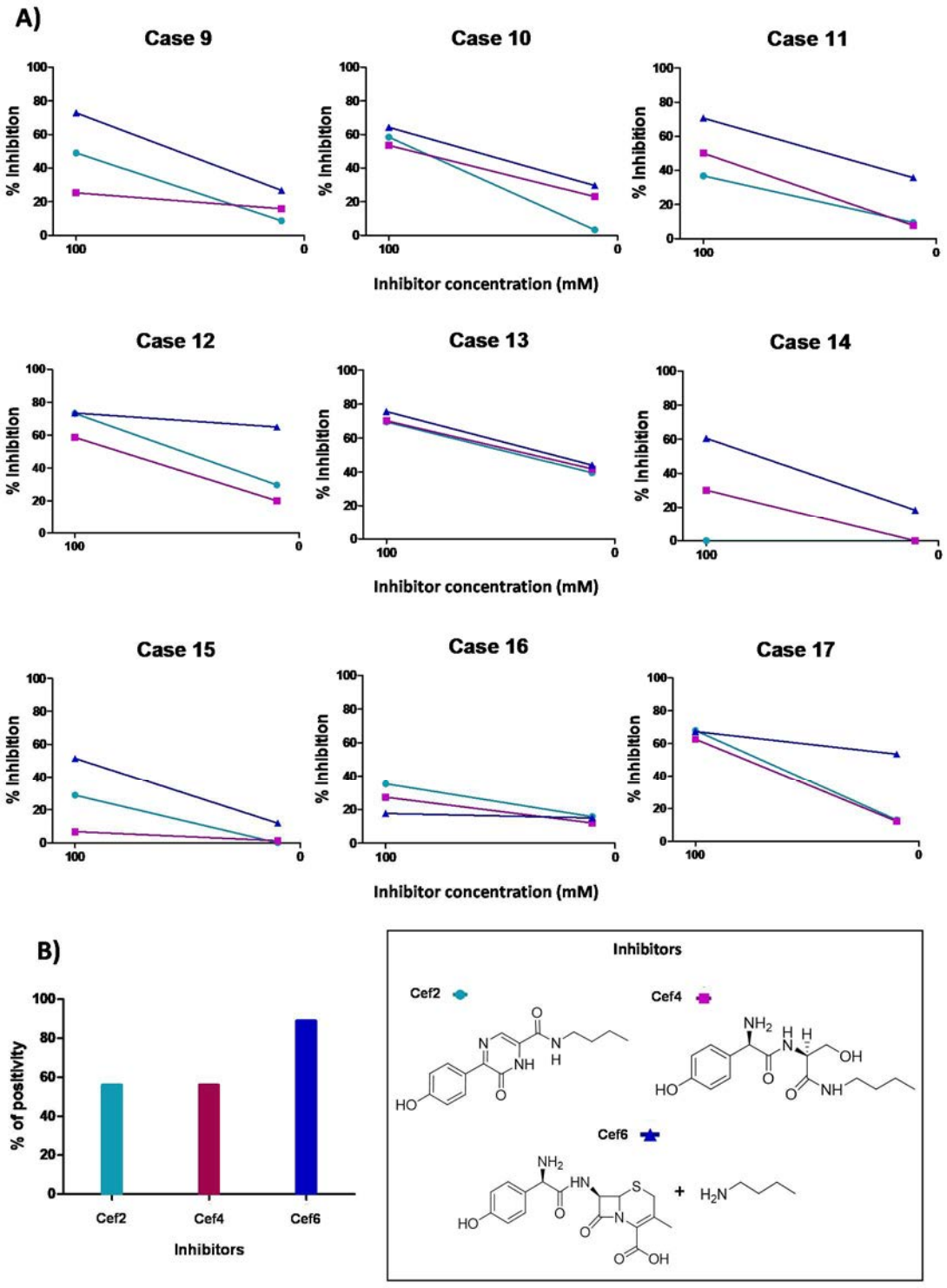

Figure I.12. Immunological evaluation results for cefadroxil derivatives. RAST inhibition assays performed with sera from 9 patients allergic to AX using compounds **Cef2**, **Cef4** and cefadroxil-butylamine as inhibitors and cellulose discs modified with AX-PLL as the solid phase: A) Group of patients cross-reactive with BP; B) Comparison of positivity (%RAST inhibition >50%) between **Cef2**, **Cef4** and **Cef6** inhibitors at 100 mM concentration.

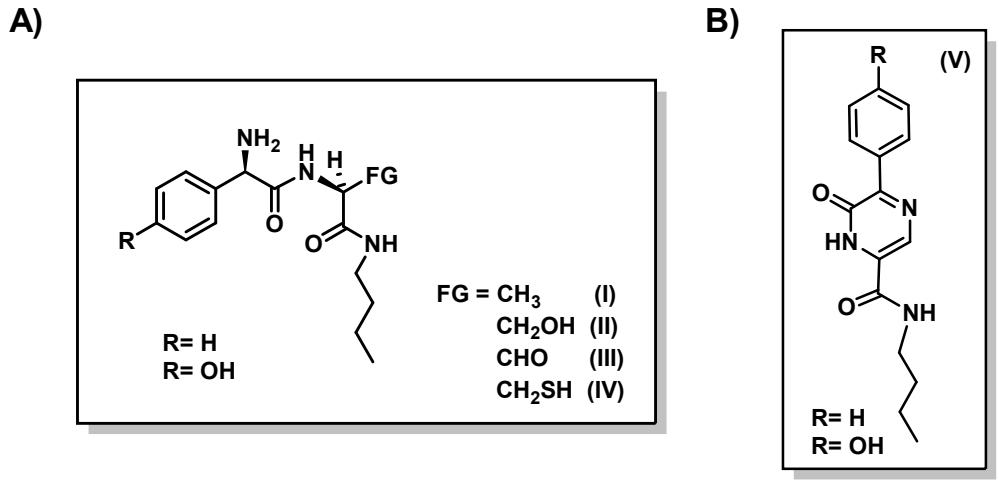

Figure I.13. Structure of A) previously synthesized [43, 69] and B) new proposed pyrazinone-like synthetic ADs of α-aminocephalosporins.

II. Elucidation of antigenic determinant structures for CLV

Immunoassays employed for *in vitro* diagnosis of allergic diseases rely on the sIgE recognition of a drug(hapten)-carrier complex attached to a solid phase. The attachment of the exact AD that induces immune response *in vivo* would assure the immunoassay accuracy for diagnosis and, for this reason, elucidation of the AD involved in the allergic reaction should be the first step to design or implement an *in vitro* test.

As explained in the previous chapter, one approach for ADs elucidation is the synthesis of BL derivatives according to a reactivity or degradation hypothesis, using butylamine as emulator of Lys in proteins, and then evaluate their sIgE recognition by means of RAST inhibition [43, 69]. However, an approach that provides information about the exact structure of the AD, the protein(s) target of modification as well as about binding sites would be more convenient.

Attempts to identify protein targets of reactive electrophilic metabolites have been complicated because of the diversity of structures, the low extent of modification or the unavailability or prohibitively prices of chemicals or antibodies with high specific activity [209]. Thus, identification of novel drug-protein adducts, characterization of their precise chemical nature or identification of specific reactive chemical/metabolite-mediated modification sites within proteins has been extremely challenging. However, recent developments in proteomic and MS ionization methods and instrumentation now make possible the rapid, high-throughput, and sensitive analysis of proteins, which is yielding a great wealth of information on protein adduction by endogenous and exogenous reactive compounds [105, 209, 211-213] integrating work in model systems and in patients [212, 213].

The first step necessary to successfully identify drug−protein adducts is their isolation from complex biological samples or the removal of unbound drug [213]. Isolating individual protein adducts for MS analysis can be achieved using different methods such as affinity chromatography, acrylamide gel electrophoresis (1D or 2D), dialysis or precipitation [213]. Often, it is also necessary sample quantification using, for example, protein spectroscopic assays [213] such as Bradford. Next step is adducts detection,

which can be a complex and challenging issue, especially when they are present in very low concentration.

Radiometric analysis in combination with SDS−PAGE has been the most widely used method for the detection of drug−protein adducts in complex systems. However, the cost and storage/disposal of radioactive material restricts its use in most of the research facilities [213]. Specific antibodies can be used through ELISA and immunoblotting for the detection of drug-protein adducts, and the latter combined with separation methods, such as 1D and 2D sodium dodecyl sulfate-polyacrilamide gel electrophoresis (SDS-PAGE), are quite useful for complex samples as well as highly qualitative and the best methods used that visually display the adducts. However, the lack of specific antibodies for some epitopes and the lack of sensitivity for the detection of drug-protein adducts with a low abundance or with a low level of modification is the major drawback of these techniques [213]. From this follows that sophisticated tools are required to fully characterize drug−protein adducts.

MS is an exceptionally powerful tool used to elucidate structures of both known and unknown adducts [213]. In top-down MS analysis, whole proteins are analyzed into the mass spectrometer where the molecular weight of an intact protein is first identified [213]. On analysis, drug-protein adducts will gain a mass addition, depending on the level of modification, resulting in a mass-shift that would be identifiable on the mass spectra produced. Further fragmentation by tandem MS allows identification of proteins with full sequence coverage (Figure II.1). This strategy is extremely useful for mapping labile drug-protein adducts that may be lost during digestion or cleaved off in MS analysis. High-resolution instruments, such as Quadrupole Time of Flight (QTOF), are needed because of the need to resolve the high molecular weight of intact protein. Matrix-assisted laser desorption/ionization time of flight (MALDI-TOF) MS, “soft” ionization technique, is however a better option for fragile samples that can fragment during initial ionization. The incorporation of novel MS fragmentation techniques such as electron capture dissociation (ECD), has also allowed the identification of modification sites in post translational or chemical modifications. On the other hand, bottom-up MS analysis consists of the injection of peptides from proteins into a mass spectrometer. In this kind of analysis, after sample preparation, proteins are digested using proteolytic enzymes, then, peptides are separated by high performace liquid chromatography (HPLC) and finally analized by MS [213] (Figure II.1).

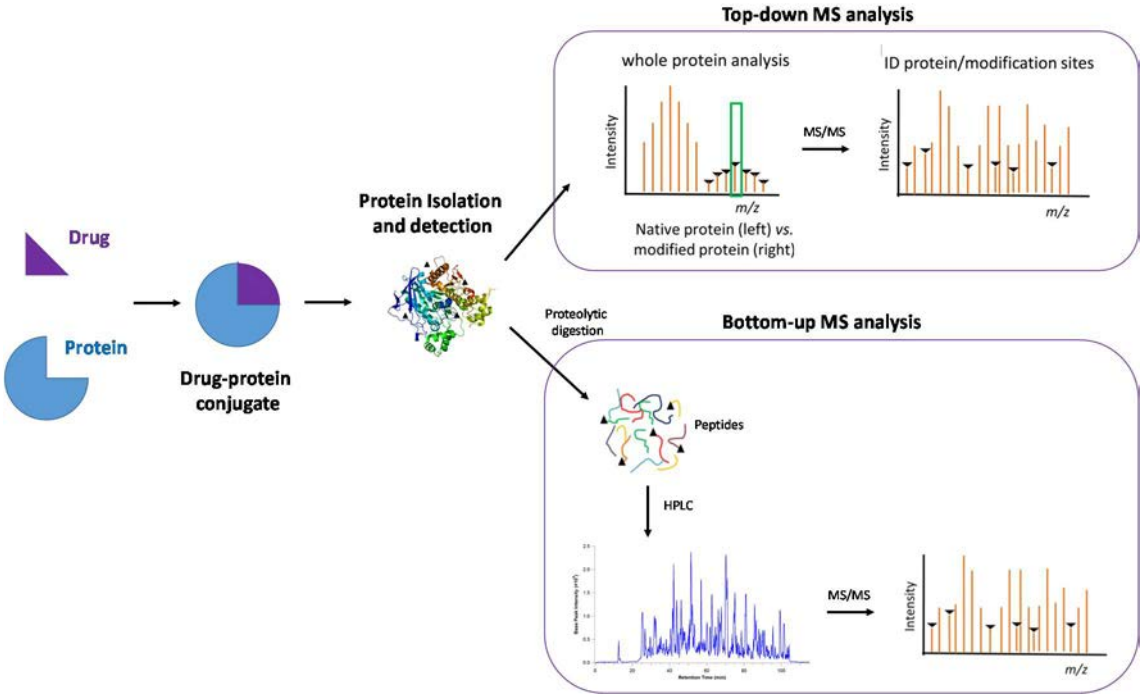

Figure II.1. Representation of drug-protein conjugate analysis. After conjugation, sample of interest must be isolated and detected previous to analysis by MS methods.

Together with proteomic and MS techniques, as well as immunological detection methods, access to the synthetic or purified drug metabolites or labeled derivatives and *in vitro* generation of the drug-protein or metabolite-protein adduct can provide valuable information about the immunogenic structures [45, 214] since, in some cases the adducts formed are not stable and can suffer transformations difficult to predict, giving rise to structures that may be responsible for the hypersensitivity reaction. Therefore, the contributions of chemical synthesis and analytical chemistry to this field are critical. Multiple disciplines should contribute to untangle the complex mechanisms for drug hypersensitivity which are subjected to individual and context factors as well as to factors depending on each drug. Obtained findings may also be useful in the prevention, diagnosis and/or treatment of allergy to drugs.

In this chapter, we used different approaches for identifying CLV derivative structures responsible for immunological recognition by the immune system. First, NMR monitoring of CLV solutions in presence of butylamine as simple nucleophile and emulators of free amino groups from lysine in proteins was performed, in order to study BL conjugation and formed structures. Taking into account that SAR analysis is a strategy successfully employed before for studying the involvement of drug metabolites or derived structures in IgE molecular recognition [215, 216], this was the second approach used. Different structures derived from two possible ADs for CLV, **AD-I** and

AD-II, were synthesized, characterized and their immunological evaluation performed, both anchored to a solid phase (by RAST) and in free form (by BAT), using samples from allergic patients selective to CLV. Moreover, proteomic and MS were employed as third approach. We investigated whether the specifically recognized AD corresponds to the resulting structure of the CLV that remains linked to the protein. Also, we envisaged a strategy that allowed to be a step closer to the identification of serum proteins target of modification by CLV. A biotinylated derivative of CLV was synthesized, and its reactivity with simple nucleophiles as well as its haptenation capacity using HSA as model protein investigated. The use of this biotinylated derivative was demonstrated to be a straightforward tool for identification of serum proteins target of modification. Finally, taking advantage of biotinylation benefits and, in order to gain insight into proteins haptenation by CLV, we prepared and characterized biotinylated derivatives of this BL (**CLV-B** and **CLV-TEG-B**) and evaluated their usefulness for identification of serum proteins target of modification by CLV.

II.1. Elucidation of the Chemical Structure of Antigenic Determinants for CLV

New prescription habits are changing specificity allergic patterns due to the apparition of new ADs [6, 15, 116, 131], fenomena that is nowadays happening in many countries with AX-CLV combination [116]. The ignorance of AD exact structure for CLV leads to an uncomplete diagnosis when this combination is involved in allergic reactions [131].

CLV has increased chemical reactivity and more complex chemistry than AX [81-84] in terms of its conjugation process. Also, a very low intrinsic immunogenicity of CLV, with the formation of small determinants together with other degradation products was described in initial studies [74]. For these reasons, the advance in the elucidation of ADs for CLV and, as consequence, the development of *in vitro* tests for evaluation of allergy to CLV, have been hampered so far.

Protein haptenation by CLV is supposed to occur similarly to other BLs [74, 204]. The reaction of Lys with CLV (Figure II.2) opens the strained β-lactam ring, leading to the formation of acylprotein **1**. However, due to its high instability, the resulting structure rapidly degrades, leading to the formation of multiple fragments: Acylprotein **1** undergoes the subsequent opening of the five-member oxazolidine ring, forming the linear imine **2**. This intermediate **2** may follow different reactivity pathways: a) decarboxylation giving rise to derivative **3**, which like molecule **2**, can break down via the imine bond to yield the protein conjugated to the derived aldehyde [74, 217, 218], which we hypothesize as a possible AD (**AD-I**), and the aminoketone **6** and **7**, respectively, being possible the reaction of **7** with protein amino groups via the ketone

functional group or self-condensation to derive **8**, whose aromatization leads to the pyrazine **9**; b) isomerization of both intermediates **2** and **3** to the imine **5**, which would be hydrolyzed under biological conditions leading to the formation of the protein conjugated to the 3-aminopropanamide, second possible determinant (**AD-II**); and c) isomerization to the corresponding enamine **4**, which apart from decarboxylation, in principle, should not experience further fragmentation.

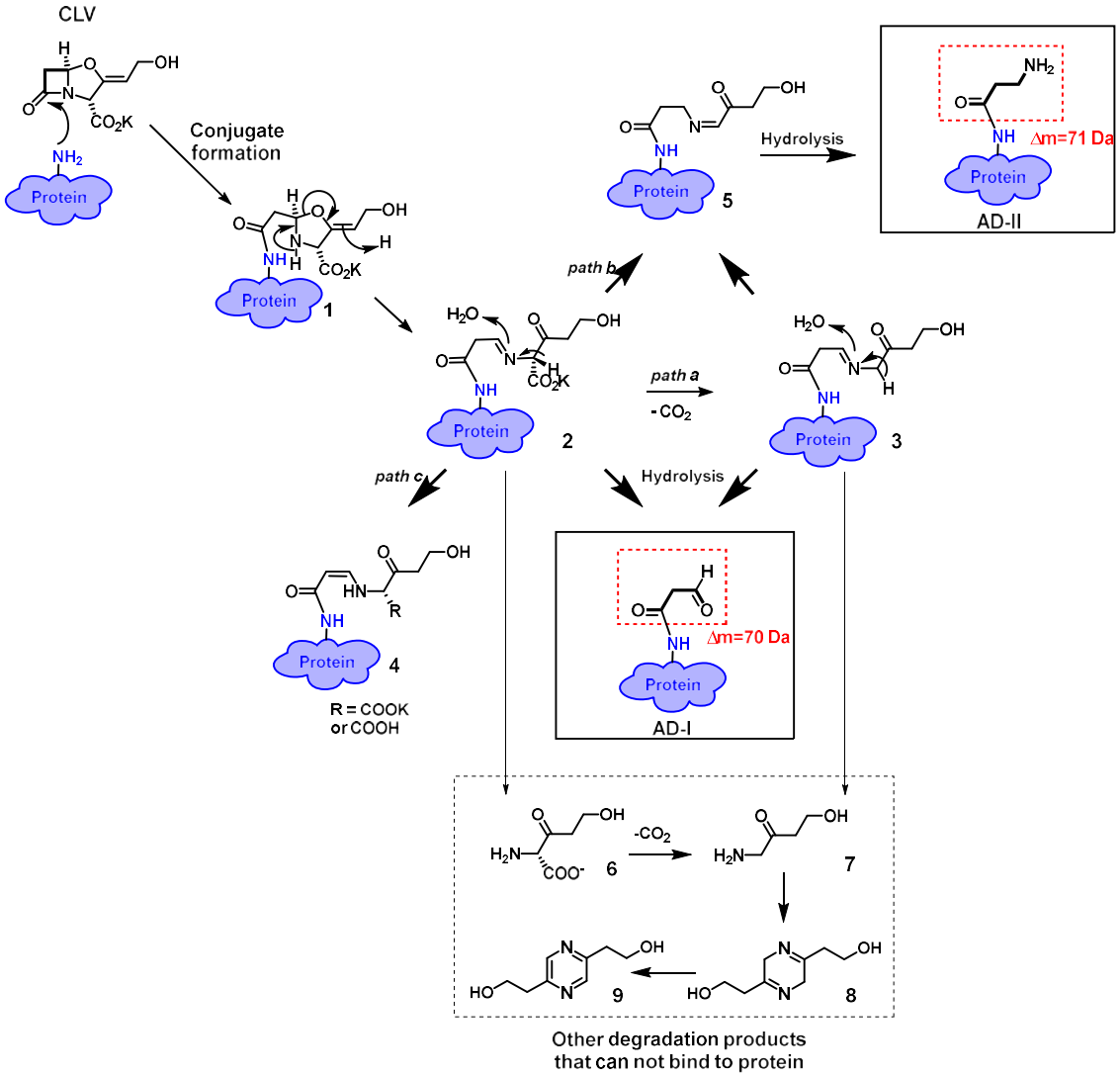

Figure II.2. Proposed reaction mechanism for covalent binding of CLV with protein and different fragmentation pathways leading to different possible ADs.

We proposed two main ADs of CLV, **AD-I** and **AD-II**, which consist of very low molecular weight structures formed by only 3 carbon atoms. Whereas **AD-I** (1,3-dicarbonylic compound) may be fairly reactive towards the nucleophilic attack of amino groups of proteins through its terminal aldehyde functional group, reactivity of **AD-II** appears quite limited. It should be pointed out that the rest of the described intermediates (molecules **1** to **5** of Figure II.2 could also be possible ADs involved in IgE recognition. It

is assumed that different chemical functional groups would influence the molecular recognition and immunogenicity of compounds. However, in-depth studies using defined structures derived from CLV are still needed to elucidate their ADs [131]. This would allow the development of *in vitro* diagnostic tests for allergy to CLV, currently unavailable.

II.1.1. Nuclear Magnetic Resonance Studies of CLV reactivity

Since Lys residues are the most reactive in proteins, butylamine was used as simple nucleophile for *in vitro* reactions as a first approach for studying simple conjugation and optimizing haptenation, that would be further extrapolated to protein adduct formation.

Reaction of CLV in presence of butylamine was studied within time by ^{1}H-NMR while incubated at 37˚C. Solutions nucleophile/BL 1:1 prepared in deuterated PBS 1X for study.

Stability studies for CLV revealed that this clavam rapid degrades at basic pH whereas it is quite stable at neutral pH (Figure II.3). Proton signals from β-lactam ring, labeled as H5 and H6, were used for monitoring the reactivity. They seemed to remain intact after 16 hours incubation, time typically employed for conjugates preparation. However, the broad singlet that appears around 3.8 ppm could be due to degradation. After 40 hours incubation, β-lactam ring remains closed but oxazolidine degradation seems to be more evident (pointed by arrows). CLV stability after almost 5 days is represented in bottom spectrum of Figure II.3. Although degradation of CLV (signals between 3.8-4.0 ppm) seems to be more evident over time, there is still presence of the original drug, which denotes the low kinetic of degradation at neutral pH. Signals at 8.5 and 9.5 ppm could be compatible with pyrazine degradation products reported by Meng *et al*. [53].

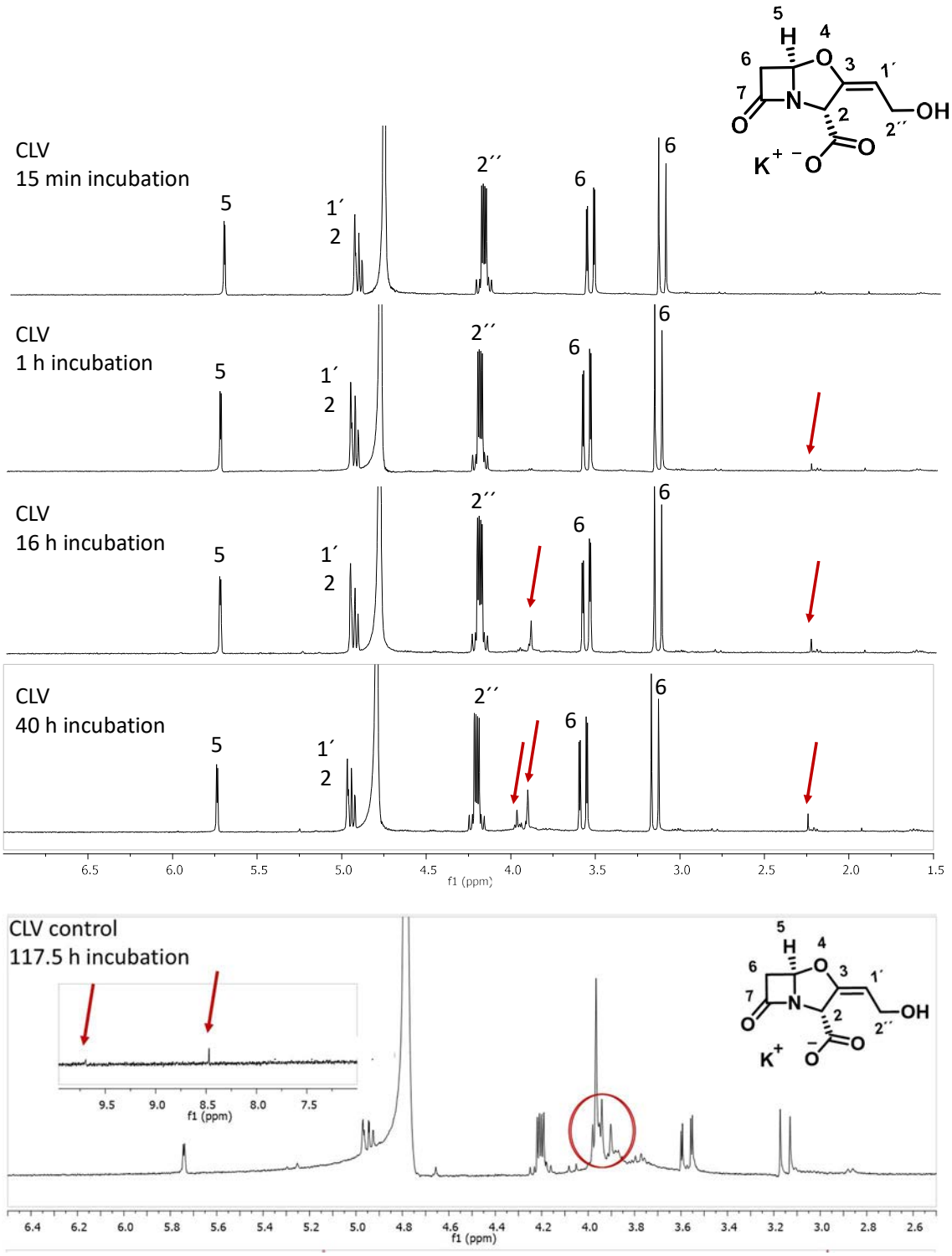

Figure II.3. ^{1}H-NMR spectra of CLV registered in deuterated PBS 1X over time. Pointed with arrows or circle signals changing over time.

The results of CLV reactivity in presence of butylamine (Figure II.4) showed evidence of β-lactam opening, since signals H5 and H6 decreased with time, while a new signal appears at around 3.25 ppm, consistent with an amide bond formation. In addition,

oxazolidine ring also degrades quickly. After 16 hours incubation there is no starting CLV left.

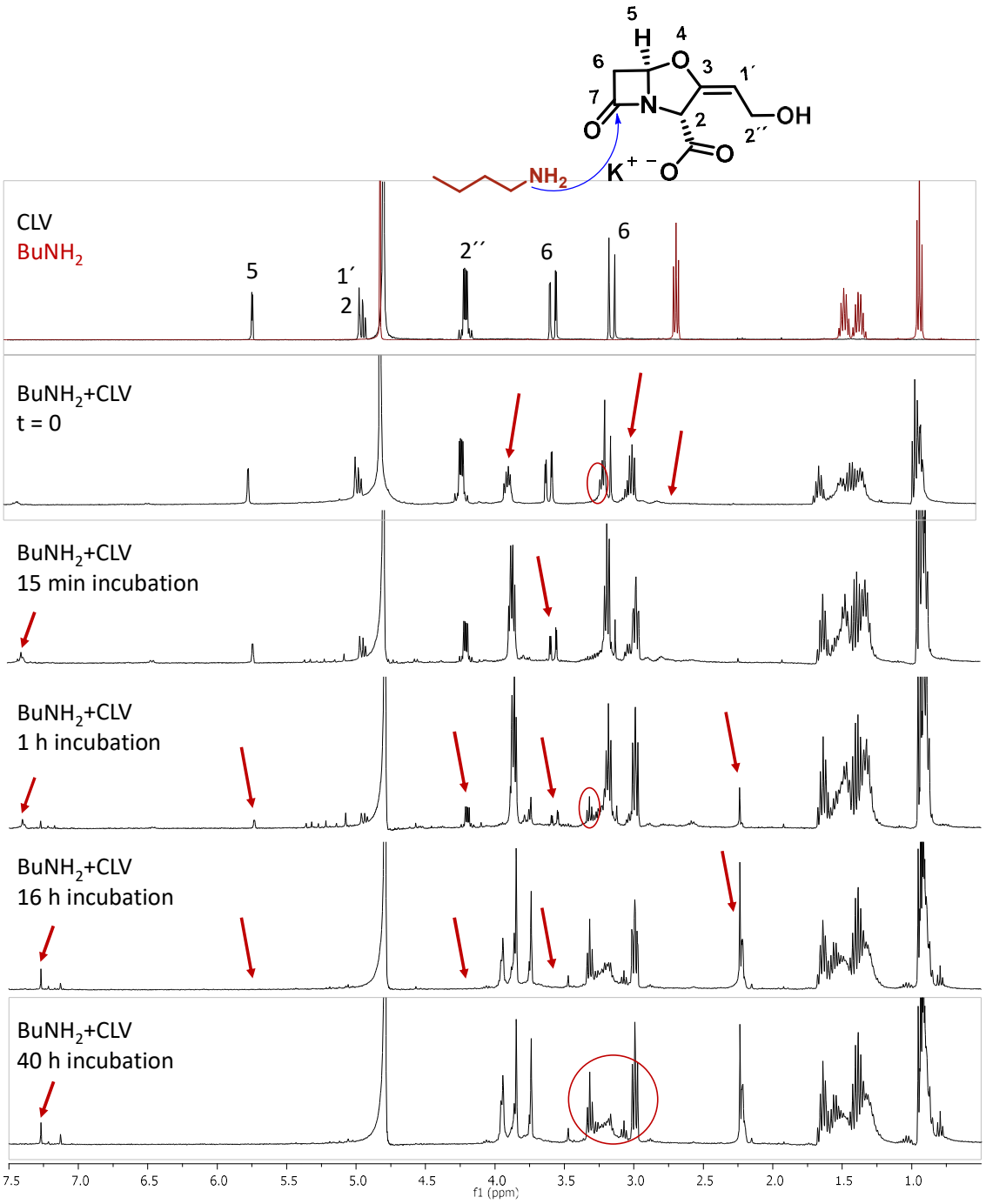

Figure II.4. ^{1}H-NMR study of CLV reactivity with butylamine registered in deuterated PBS 1X. Pointed with arrows or circle signals changing over time.

Here we presented a selection of the most relevant results obtained using physiological conditions or butylamine to study β-lactam ring opening in CLV. From these studies could be deduced that CLV is highly unstable in basic media because of the opening of

the β-lactam. In spite of the fact that these studies did not allow the elucidation of the chemical structure result of CLV reaction with nitrogenous kind nucleophiles, there is clinical evidence of the course of this reaction when the nitrogenous nucleophile is supported in a macromolecule. Then, haptenization of the macromolecule takes place and, as a result, there is conjugation between CLV and the carrier. Obviously, the uncertainty of what is the structure that corresponds to this epitope, and what part of the molecule comprises it still remains.

II.1.2. Structure-Activity Relationship of Synthetic Determinant Structures

II.1.2.1. Cellulose Discs and Nanoparticles Functionalized with CLV Derivatives

The first approach used to evaluate the IgE recognition of **AD-I** and **AD-II** like structures was the use of RAST as immunoassay. For this purpose, it was necessary the coupling to solid surfaces of well defined structures derived from the two ADs proposed as well as CLV complete molecule, using a protein as carrier. These structures were prepared by Dr. Nekane Barbero from Dr. Ezequiel Pérez-Inestrosa research group. Cellulose discs or silica nanoparticles were decorated either with the CLV derivate structures or with whole CLV molecule, with or without spacer between carrier molecule and the β-lactam. Immunological evaluation was performed by RAST by the PhD student in our laboratories using sera from patients selective to CLV and control subjects non-allergic to BLs. All evaluated solid surfaces and results obtained are depicted in (Figures II.5-II.7).

In Figure II.5B and II.5C, it is observed that structures derived from **AD-I** (depicted in purple and blue) were better recognized than discs functionalized with the whole molecule of CLV, and structure derived from **AD-II** (depicted in orange) was the worst recognized. Among **AD-I** derivatives, the structure with deprotected aldehyde was the best recognized. However, there was no difference between patients and controls, obtaining a very similar pattern of recognition in both cases. Therefore, an unspecific IgE recognition was observed with these structures.

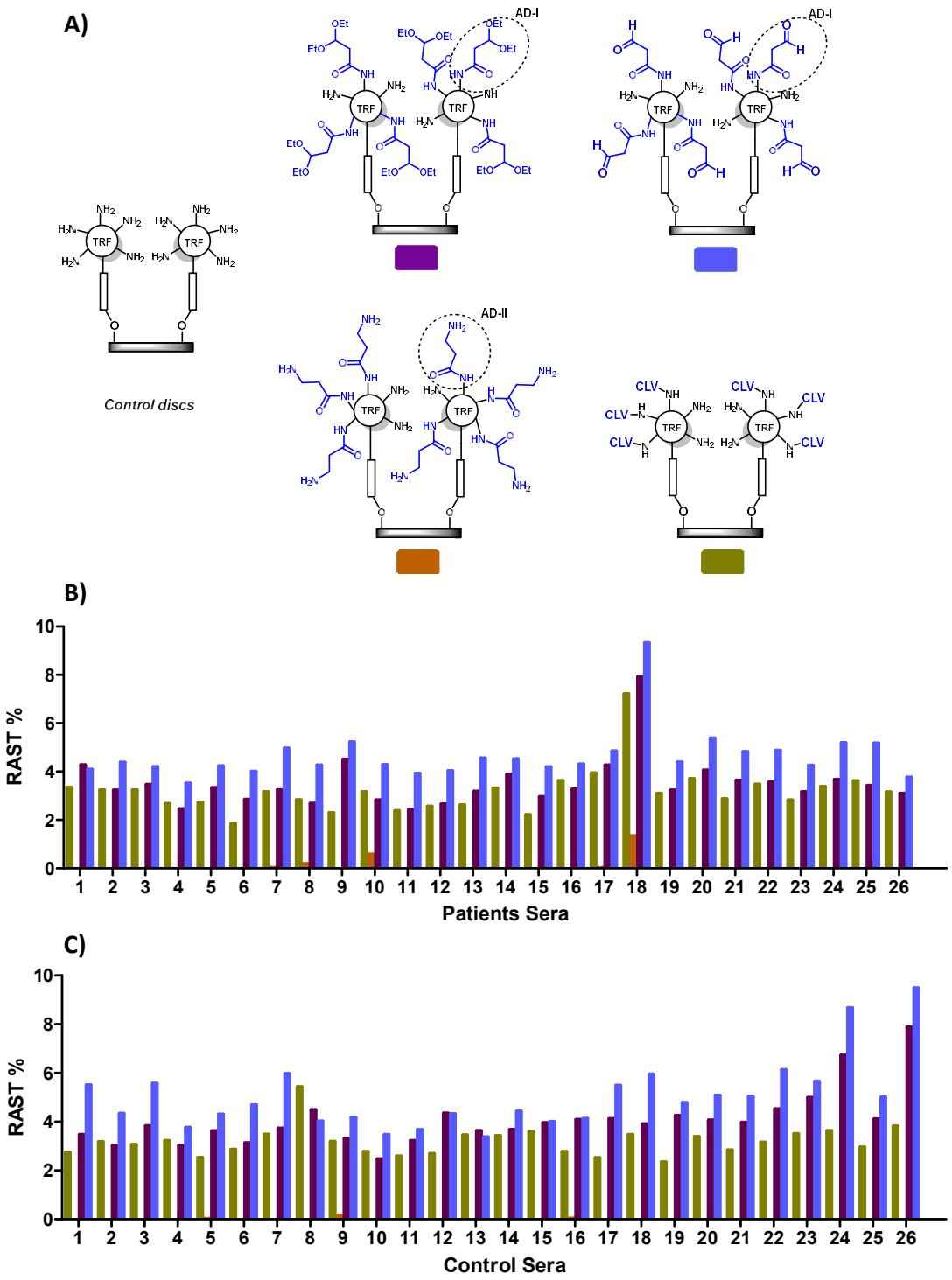

Figure II.5. Evaluation of IgE recognition of structures derived from CLV (**AD-I** and **AD-II**). (A) Structures used for evaluation (**AD-I** and **AD-II**) coupled to transferrin (TRF) and anchored to cellulose discs. (B) RAST results using sera from patients selective to CLV. (C) RAST results using sera from control subjects (non-allergic to BLs).

In previous studies, it was found that the introduction of a spacer molecule improved recognition [147] maybe because of the better flexibility and availability of the potential AD towards IgE. In order to assay the effect of the introduction of a spacer in IgE recognition, we evaluated discs bearing the whole CLV molecule distanced from carrier molecule with a tetraethyleneglycol (TEG) spacer (Figure II.6). This evaluation resulted again in a similar pattern of recognition between patients and controls, although only an isolated patient seemed to recognize selectively both structures. Therefore, an unspecific IgE recognition was observed for these structures as well.

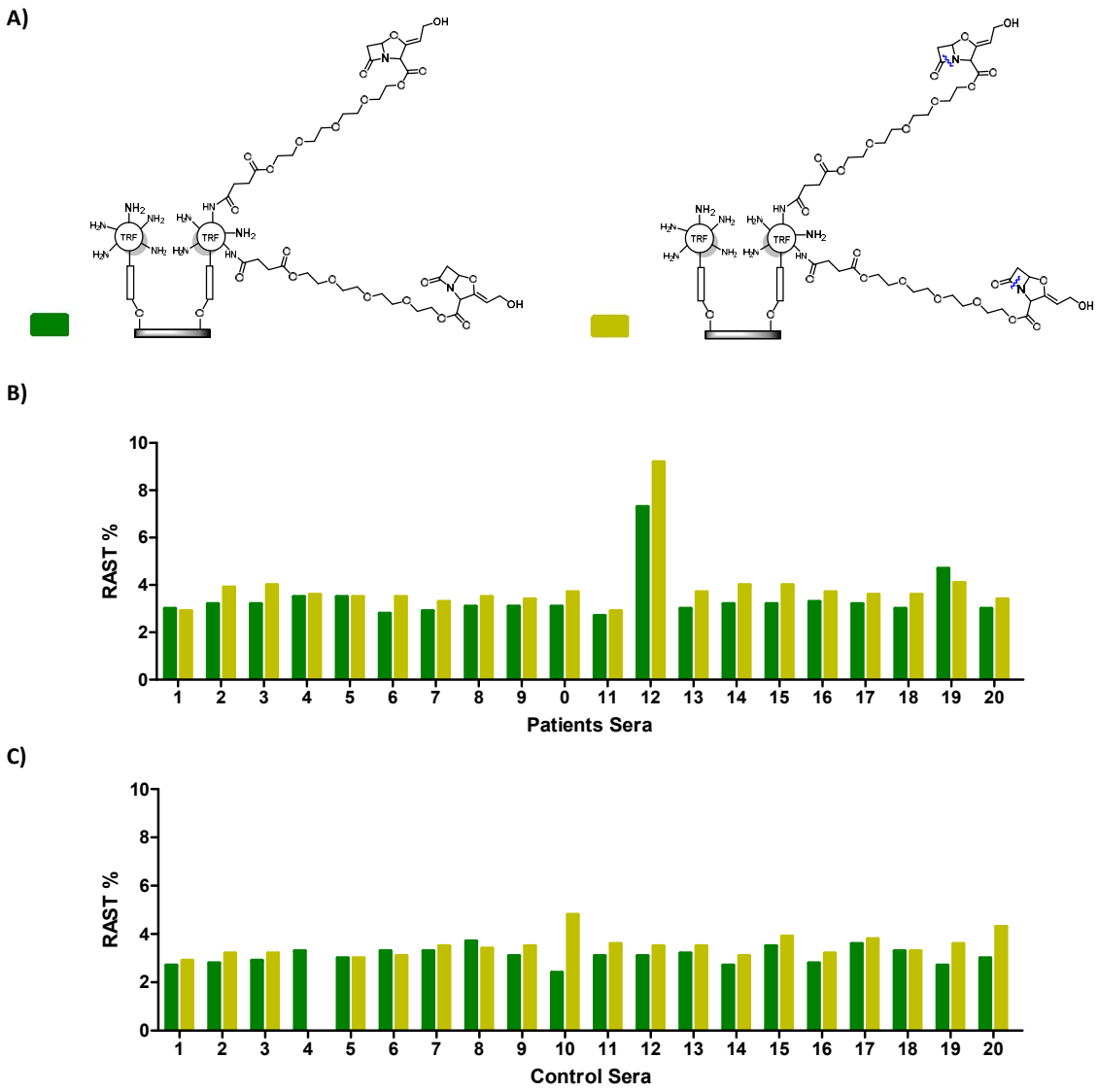

Figure II.6. Evaluation of IgE recognition of CLV. (A) Structures used for evaluation (CLV closed and CLV open) coupled to transferrin (TRF) and anchored to cellulose discs. (B) RAST results using sera from patients selective to CLV. (C) RAST results using sera from control subjects (non-allergic to BLs).

Due to the unsuccessful results obtained after cellulose disc evaluation, we decided to assay CLV derived structures anchored to another kind of solid phase. Silica nanoparticles ($NpSiO_2$) had been used before as solid phase to evaluate ADs of AX [148] so we decided to use them as an alternative solid support for assaying our potential ADs. Results (Figure II.7) showed that IgE recognition of proposed CLV ADs linked to $NpSiO_2$ had a similar pattern of recognition for patients and controls, as observed for cellulose discs. AD derived from **AD-II** seemed to be better recognized than **AD-I** derivative or the whole CLV molecule, however, this recognition would be unspecific.

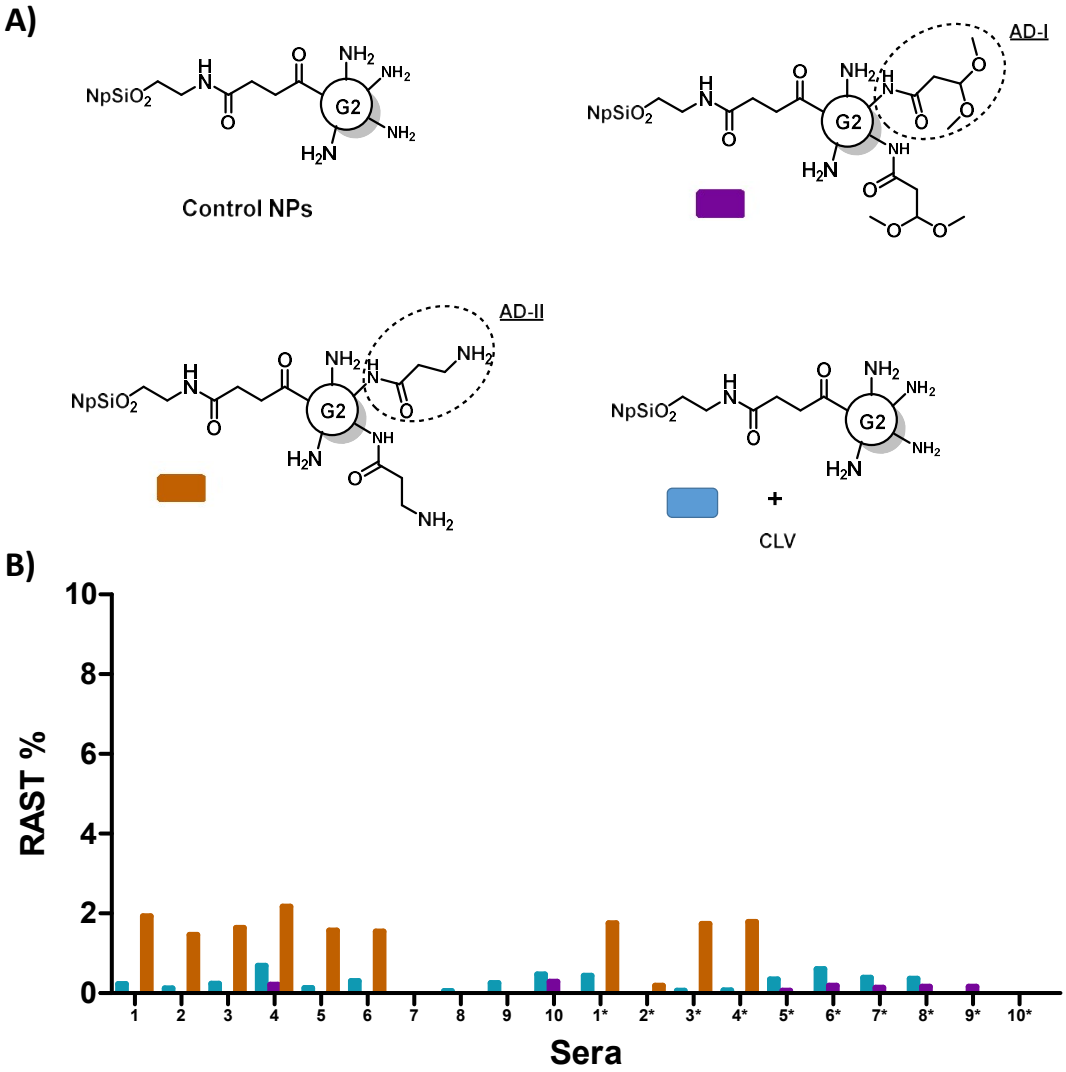

Figure II.7. Evaluation of IgE recognition of structures derived from CLV (**AD-I** and A**D-II**). (A) Structures used for evaluation (**AD-I** and **AD-II**) coupled to G2 PAMAM dendrimer and anchored to silica nanoparticles. (B) RAST results using sera from patients selective to CLV. (C) RAST results using sera from control subjects (non-allergic to BLs). * represent controls, and the rest of sera were from patients.

To sum up, synthetic structures derived from CLV **AD-I** and **AD-II** and the whole CLV molecule (with or without spacer), were anchored to cellulose discs or $NpSiO_2$ and their sIgE recognition evaluated by RAST. The fact that there was no specific recognition for any of the structures, no matter the solid phase to which they were supported, is an evidence of the difficulty of the evaluation of CLV immunogenicity using immunoassays.

II.1.2.2. CLV Derivatives in Free Form

As second approach, six synthetic analogs, whose structure is depicted in Figure II.8, were synthesized for further IgE recognition evaluation by BAT, in order to identify the CLV ADs better recognized by the immune system and gain insight into the exact structure involved in allergic reactions to CLV.

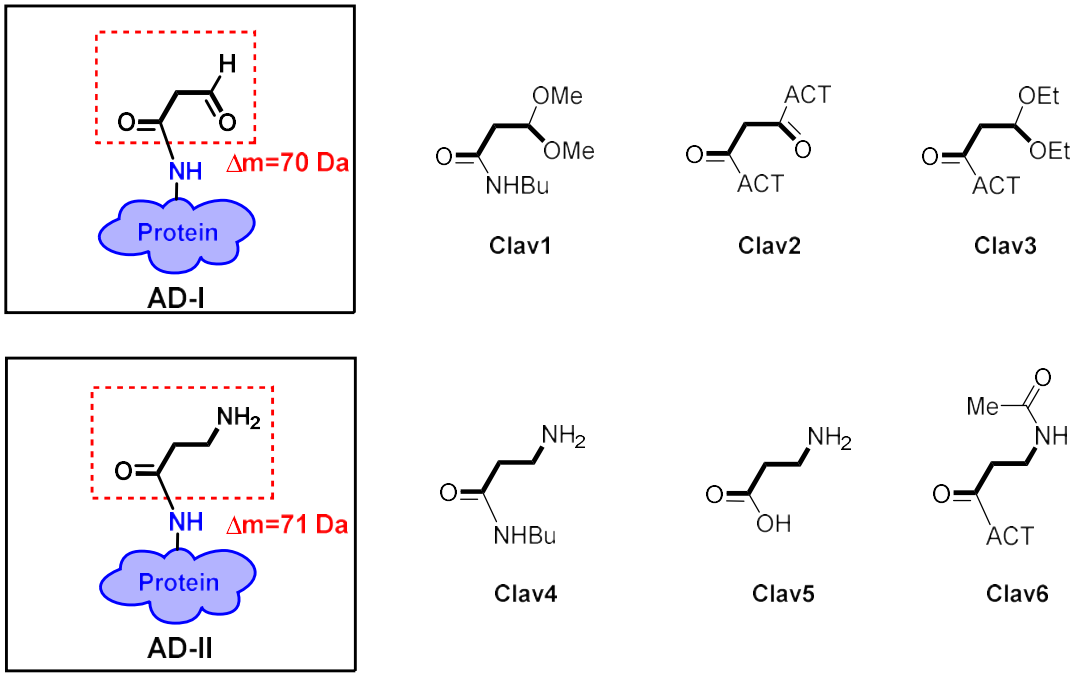

Figure II.8. Synthetic determinants corresponding to **AD-I** (**Clav1**-**Clav3**) and **AD-II** (**Clav4**-**Clav6**).

Synthesis of Antigenic Determinants for CLV

The synthesis was carried out in collaboration with Dr. Nekane Barbero from Dr. Ezequiel Pérez-Inestrosa research group. Three of the proposed ADs, **Clav1**, **Clav2** and **Clav3** were prepared to emulate the **AD-I** structure (*N*-protein, 3-oxopropanamide). In **Clav1**, both carbonyl groups of the molecule are protected, one as an amide and the other as an acetal group, so the expected reactivity is low. However, the carbonyl groups of both **Clav2** and **Clav3** were activated, modified chemically to form the anhydride, to enhance

significant differences (p=0.049). Individual results of BAT expressed as stimulation index (SI), defined as the percentage of activated basophils after allergen stimulation per negative control stimulation, are shown in Table II.2. Concentrations higher than 8 mM were also tested, but they were discarded due to their high cytotoxicity (data not shown). Only the structures that induced basophil activation in patients (CLV, **Clav2** and **Clav3**), at the concentration of 8 mM, were used for further study.

Table II.1. Clinical data and results of *in vivo* test for each allergic patient to CLV. Pat: patient; React: reaction; IDT: intradermal test; MD: minor determinant; DPT: drug provocation test; PV: penicillin V; ND: non-determined.

Pat	Gender	Age (years)	Time drug-react (min)	Time react-study (days)	ST						DPT		
					SPT			IDT					
					BP/MD	AX	CLV	BP/DM	AX	CLV	BP/PV	AX	AX-CLV
P1	F	64	5	1825	-	-	-	-	-	+	ND	ND	ND
P2	F	27	120	180	-	-	-	-	-	+	ND	ND	ND
P3	F	72	15	2190	-	-	-	-	-	+	ND	ND	ND
P4	M	63	15	1095	-	-	+	-	-	ND	ND	-	ND
P5	F	39	30	180	-	-	-	-	-	+	ND	-	ND
P6	F	49	15	1095	-	-	-	-	-	+	ND	-	ND
P7	F	43	5	365	-	-	-	-	-	-	ND	-	+
P8	M	28	30	365	ND	-	ND	ND	-	ND	ND	-	+
P9	F	32	60	730	-	-	-	-	-	+	ND	-	ND
P10	F	40	60	540	-	-	+	-	-	ND	-	-	ND
P11	F	38	30	1095	-	-	+	-	-	ND	-	-	ND
P12	F	50	5	60	-	-	-	-	-	+	ND	-	ND
P13	M	41	15	1095	-	-	-	-	-	-	-	-	+
P14	F	27	15	1460	-	-	-	-	-	+	ND	-	ND
P15	M	38	15	1825	-	-	-	-	-	-	ND	-	+
P16	M	51	30	730	-	-	-	-	-	+	ND	-	ND
P17	M	74	2	40	-	+	+	ND	ND	ND	ND	ND	ND
P18	M	39	5	210	-	-	-	-	-	+	ND	+	ND
P19	M	43	30	730	-	-	+	-	-	ND	ND	-	ND
P20	F	35	15	365	-	-	-	-	-	+	ND	-	ND
P21	F	39	30	2536	-	-	+	-	-	ND	ND	ND	ND
P22	F	43	15	730	-	-	+	-	-	ND	ND	-	ND
P23	M	34	15	1460	-	-	-	-	-	+	ND	ND	ND
P24	F	45	15	640	-	-	+	-	-	ND	ND	-	ND
P25	F	52	UK	UK	-	-	-	-	-	+	ND	ND	ND
P26	F	46	15	120	-	-	-	-	-	+	ND	ND	ND
P27	F	40	30	2920	-	-	+	-	-	ND	ND	ND	ND
P28	M	58	15	1825	-	-	+	-	-	ND	ND	ND	ND
P29	M	63	30	240	-	-	-	-	-	+	ND	ND	ND

their reactivity towards nucleophiles. The main difference is that **Clav3** has one of the carbonyl groups protected as an acetal, decreasing its ability to bind to proteins compared to **Clav2**. For **Clav1** the amide binding with the protein is represented with a butyl amide emulating a side chain of Lys; for **Clav2** and **Clav3** binding is expected to occur with proteins during the cellular assay via the activated carbonyl group. The other three structures, **Clav4**, **Clav5** and **Clav6** were chosen as model analogs of **AD-II** (*N*-protein, 3-aminopropanamide). **Clav4** and **Clav5** are less reactive than **Clav6** because their carbonyl groups have not been activated. The resulting conjugate of **Clav6** would present as an **AD-II** structure but with its amino group protected as an acyl group. For **Clav4**, amide binding with the protein is represented with a butyl amide emulating a side chain of Lys; for **Clav5** and **Clav6** this is expected to occur with proteins during cellular assay via the carboxylic group (**Clav5**) or activated carbonyl group (**Clav6**).

In summary, **AD-I** and **AD-II** consist of small structures (71 Da or 72 Da, respectively) containing only 3 carbon atoms, considered too small to be immunogenic. Some of their corresponding analogs (**Clav2**, **Clav3** and **Clav6**) were designed with greater ability to bind proteins during the cellular assay.

Patient´s Selection

The study involved 29 patients with immediate hypersensitivity reactions to CLV after the intake of AX-CLV. Diagnosis was confirmed by ST or DPT to penicillin, AX or CLV following the European Network for Drug Allergy (ENDA) guidelines [219]. Clinical data and individual results for the allergological work-up are shown in Table II.1. As control group, 25 cases with confirmed tolerance to AX-CLV were selected.

Immunological Evaluation by Basophil Activation Test

IgE recognition of the six different synthetic structures (Figure II.9) derived from **AD-I** and **AD-II** was evaluated by BAT in patients with selective reactions to CLV and tolerant subjects non-allergic to BLs. This evaluation was performed in our research group by Rubén Fernández.

All synthetic analogs of CLV determinants and CLV itself were evaluated in patients and controls. The optimal concentration to study basophil activation with each structure was selected using dose-response curves (Figure II.10). Analyzing the expression of CD63 on basophil surface, the only concentration of CLV that showed significant differences between patients and controls was 8 mM (p=0.042). For the different synthetic analogs, only **Clav2** and **Clav3**, both coming from the **AD-I**, showed significant differences between patients and controls. For **Clav2** the best concentrations were 4 mM (p=0.022) and 8 mM (p=0.008), whereas for **Clav3** only the highest concentration (8 mM) showed

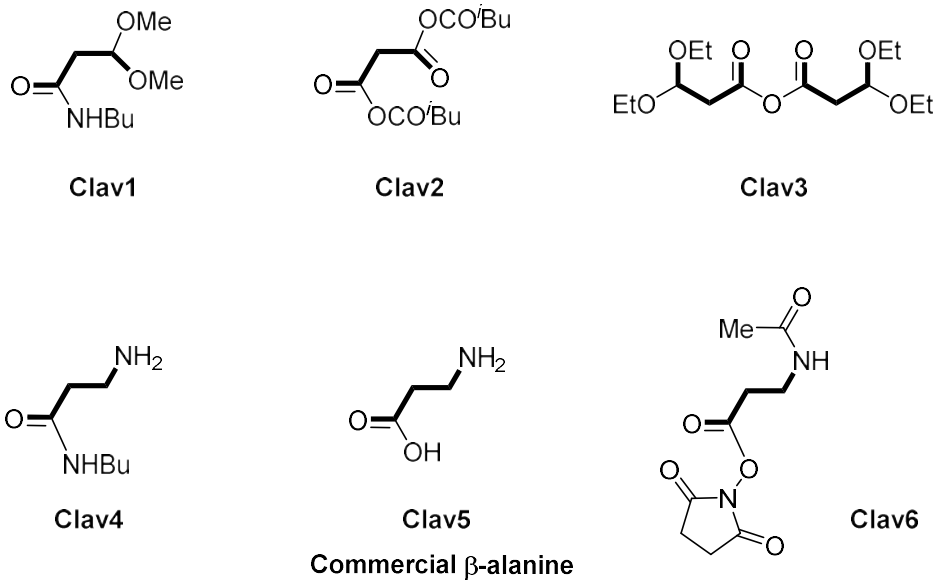

Figure II.9. Detailed structure of the six synthetic ADs derived from CLV.

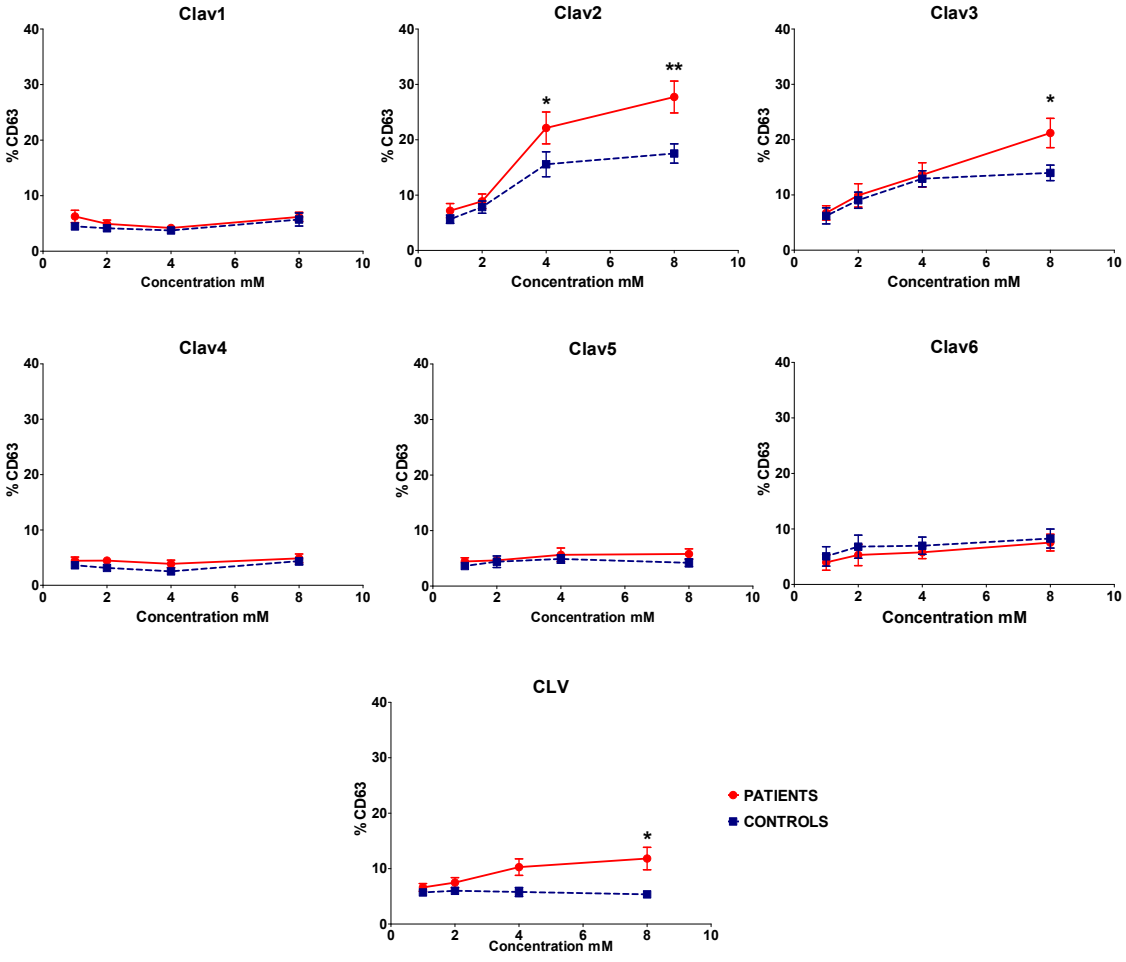

Figure II.10. Dose-response curve for BAT using determinants (**Clav1**-**Clav6**) and CLV.

ROC curves for these structures were performed to select the cut-off to obtain the best sensitivity/specificity balance (Figure II.11A) and this was established at: SI >2 for CLV; and SI >4 for **Clav2** and **Clav3** (Figure II.11B). Based on the chosen cut-off, we observed a positive basophil activation with CLV in 41.4% of patients, with **Clav2** in 58.6% and with **Clav3** in 27.6%. In controls, basophil activation was positive in 12% of cases for all three structures (Figure II.11B).

Finally, to prove that the observed basophil activation was IgE mediated, BAT was performed after incubating cells with wortmannin (WTM), a potent inhibitor of the IgE signaling pathway. In all cases, this treatment significantly reduced the percentage of CD63 expression compared with BAT performed in the absence of WTM ($p<0.001$ for CLV; $p<0.001$ for **Clav2**; $p=0.007$ for **Clav3**) (Figure II.12). Bars show the mean value + standard deviation (SD) of percentage of CD63 on basophil surface obtained for non-inhibited and WTM inhibited basophils in BAT. Results are expressed as the mean + SD of CD63 % in patients (N = 29) and healthy controls (N = 25). Significant differences are indicated in the graph (* $p<0.05$ and ** $p<0.01$).

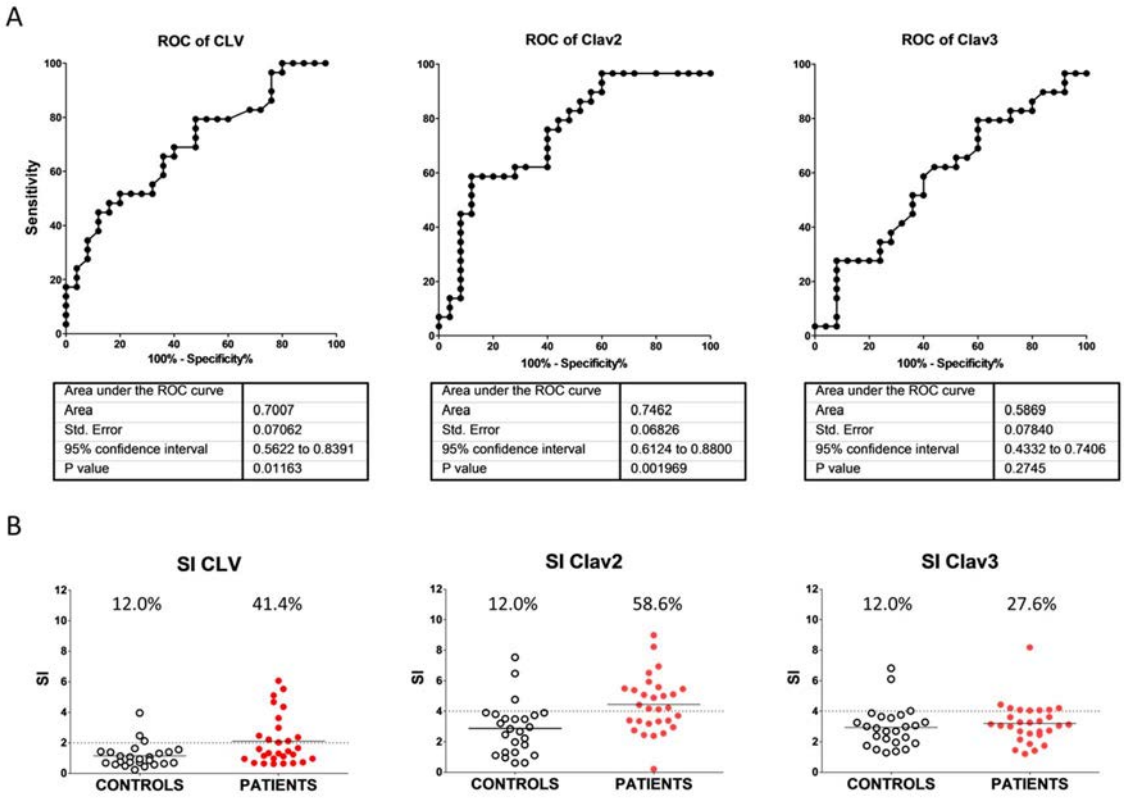

Figure II.11. Determination of BAT cut-off for CLV, **Clav2** and **Clav3** at 8 mM concentration. **A**, ROC curve analysis of each structure. **B**, Dot plots graphs showing individual BAT results expressed as SI of each structure for patients and controls. Positive results for BAT (over cut-off) in allergic patients and controls are represented as percentages.

Table II.2. Results of BAT with CLV and the six synthetic structures at 8 mM, expressed as SI, for each allergic patient to CLV. Positive results are highlighted in bold.

Patient	CLV	Clav1	Clav2	Clav3	Clav4	Clav5	Clav6
P1	0.97	0.92	2.74	1.85	0.31	1.25	0.74
P2	0.68	0.16	2.38	2.67	0.35	0.51	0.65
P3	0.64	0.73	3.38	1.41	0.14	0.34	0.32
P4	1.15	1.07	3.35	3.61	1.08	1.19	0.89
P5	1.32	1.12	2.95	3.05	1.24	0.55	1.00
P6	0.62	0.27	0.21	2.14	0.51	0.24	0.24
P7	0.66	1.25	2.55	1.20	1.07	2.31	0.41
P8	1.44	0.65	3.33	2.53	1.25	0.58	1.12
P9	1.59	1.74	3.18	1.44	0.56	0.79	1.14
P10	**2.98**	0.65	3.39	3.15	0.69	1.27	0.67
P11	**2.11**	0.97	2.44	3.12	1.30	1.20	0.65
P12	**5.52**	1.03	3.70	3.25	0.39	1.08	0.94
P13	1.11	0.59	**5.00**	2.45	0.65	2.51	1.25
P14	0.72	0.51	**5.07**	3.27	0.28	0.63	0.56
P15	0.64	1.87	**4.22**	1.74	0.50	0.37	0.25
P16	1.23	0.43	**8.98**	3.05	0.61	1.00	1.13
P17	**2.02**	1.25	**5.10**	2.68	0.36	1.68	2.22
P18	**2.46**	0.43	**4.88**	3.00	1.25	0.98	1.26
P19	**2.36**	0.98	**5.93**	3.34	0.87	0.54	0.61
P20	**4.35**	0.84	**4.41**	2.72	0.54	0.67	0.92
P21	**3.62**	0.87	**5.49**	3.62	1.07	1.02	0.56
P22	0.95	0.37	**8.22**	**4.43**	0.18	0.53	1.48
P23	0.96	0.56	**4.12**	**4.05**	0.63	1.10	0.99
P24	1.65	1.37	**5.58**	**4.20**	0.77	0.78	1.65
P25	1.30	0.94	**4.16**	**4.09**	0.26	0.56	1.87
P26	**4.67**	1.23	**5.38**	**4.20**	0.25	0.79	1.17
P27	**5.10**	1.25	**6.93**	**4.08**	0.39	1.89	2.14
P28	**2.21**	0.73	**5.45**	**4.06**	0.70	0.53	1.23
P29	**6.06**	0.65	**6.51**	**8.18**	0.98	0.36	0.85

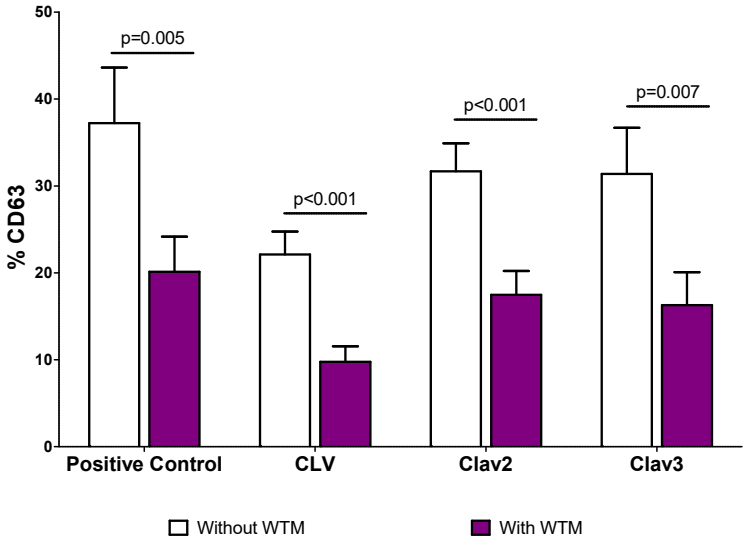

Figure II.12. Results of inhibition of BAT with WTM prior to stimulation with CLV, **Clav2** and **Clav3** or positive control (α-IgE) after optimization of experimental procedures in which it was observed that only IgE mediated pathway was inhibited.

We observed that from those patients with positive BAT to CLV, 75% were also positive to **Clav2** and 33.3% to **Clav3**. More interestingly, from cases with negative BAT to CLV, 47.1% showed positive results with **Clav2** and 23.5% to **Clav3** (Figure II.13A). The percentage of patients showing basophil activation increased significantly to 69.0% when results obtained with CLV and **Clav2** were combined compared with CLV alone (p=0.002), however no improvement was observed when **Clav3** was added (Figure II.13B and Table II.2).

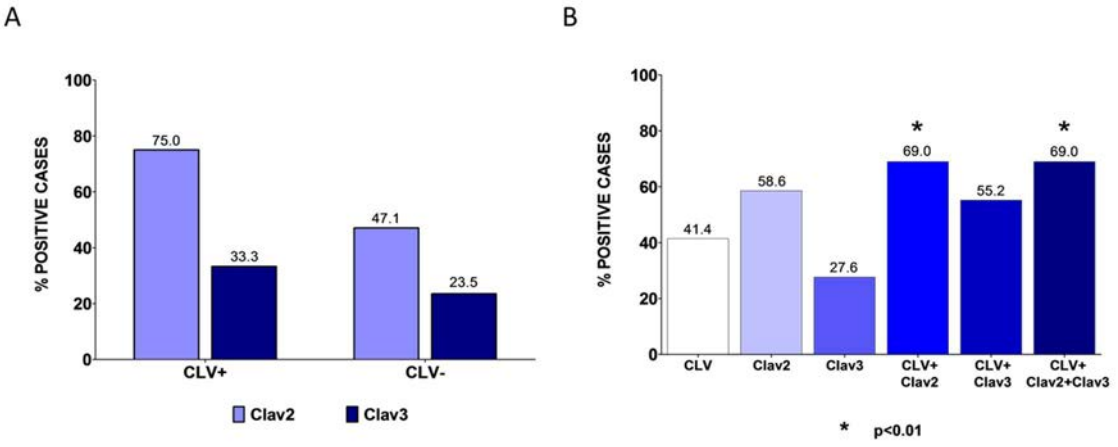

Figure II.13. Positive BAT results in allergic patients. **A**, Comparison of the percentage of positive results of BAT for **Clav2** and **Clav3** in cases with positive or negative BAT to CLV. **B**, Comparison of the percentage of positivity of BAT combining the results with CLV, **Clav2** or **Clav3**. Significant differences are indicated in the graph (* p<0.01).

Herein, the ability to stimulate basophils of synthetic structures designed according our CLV degradation hypothesis was evaluated, finding that only two of them (**Clav2** and **Clav3**) were able to induce activation in allergic patients. Interestingly, both molecules correspond to **AD-I**, suggesting that these synthetic analogs, containing aldehyde functionality, are the ones recognized by IgE bound on the basophil surface.

Clav2 is an analog of **AD-I** modified chemically to form the anhydride of its carboxylic group, to enhance their reactivity towards nucleophiles. In this way, **Clav2** binding is expected to occur with proteins during the cellular assay via the activated carbonyl group. Moreover, the aldehyde group of **AD-I** is represented in **Clav2** as a carboxylic group which may be formed through hydrolysis of the second carboxylic anhydride in the aqueous media, which would lead to a molecule that is more similar to **AD-I** than **Clav3**. Although the oxidation state of **Clav3** is equal to the proposed structure **AD-I**, in contrast to a higher oxidation presented in **Clav2**, **Clav3** may involve a higher steric hindrance through the diethoxyacetal compared to the carboxylic acid group that may be formed in **Clav2**. Thus, in terms of 3D structure, in comparison to **Clav3**, **Clav2** forms a structure more similar to **AD-I**. It is important to highlight that these facts are in agreement with the degree of recognition found (**Clav2** > **Clav3**).

Basophil activation requires the crosslinking of two adjacent IgEs at the cell surface, and this is only possible with the recognition of a structure with a size ranging from 40-100 Å [220]. This explains the fact that in our study only the analogs able to bind proteins can stimulate the basophil. This is in agreement with the hapten hypothesis, which is currently accepted as the mechanism of action for other BLs, such as penicillins [63, 204]. Although **Clav6** can also bind to proteins, their conjugates are not recognized by IgE from CLV allergic patients. This suggests that small differences in the structure can highly influence the immunological recognition. The IgE-mediated mechanism was confirmed by inhibition of the basophil activation with WTM, an inhibitor of phosphoinositide 3-kinase enzymes, which are part of the IgE signaling pathway [221] and have been shown to be a key set of kinases activated by FcεRI receptor cross-linking [222].

We evaluated whether the inclusion of these synthetic analogs can improve the potential of BAT for diagnosing CLV allergic patients. Using the complete molecule of CLV, 41.4% of patients showed a positive BAT, whereas using **Clav2**, this increased to 58.6%. Interestingly, the combination of results obtained with CLV and **Clav2** significantly increased the percentage of patients showing basophil activation to 69.0%, due to a proportion of patients that were activated by only one of the molecules. When CLV is used for the assay, the resulting conjugates can contain different and heterogeneous determinants, including the ones we proposed as main determinants (**AD-I** and **AD-II**) and others (Figure II.2). Thus, the concentration of **AD-I** would be lower

than the one that we used *in vitro* when we included the synthetic analog **Clav2**. This lower density of **AD-I** would affect the recognition in BAT and could explain why some patients that respond to **Clav2** do not respond to CLV. A similar pattern has been observed with metamizole in BAT studies: some patients showing IgE recognition to some of its metabolites did not recognize the parent drug [216]. BAT results showed an increase of positivity from 37% to 62% using metamizole plus metabolites as compared to metamizole alone, demonstrating that these metabolites have an important role in the allergic reaction. All patients that responded to metamizole also responded to any of its metabolites, however in the present study we have found some patients that respond to CLV and not to **Clav2**. These patients may be sensitized to other determinants formed during CLV conjugate fragmentation, which have not been considered in the present study.

Assesment of the haptenation capacity of Clav2 and Clav3

In order to prove the ability to bind proteins (Figure II.14) of the structures that presented BAT positive results (**Clav2** and **Clav3**), we incubated these structures with HSA in PBS 1X for 16 hours at 37˚C using molar ratio HSA/structure 1:10 and, after purification by dialysis resulting conjugates were analyzed by MALDI-TOF MS. PhD student prepared and purified the conjugates, that were analized by at Central Service for Research Support, University of Málaga (SCAI, UMA), and analized the results. The fact that for both conjugates a mass increment was obtained with respect to the mass of control HSA, Δm= 112.3 for HSA-**Clav2** and Δm= 64.5 for HSA-**Clav3**, confirms that both structures derived from CLV (**AD-I**) are able to bind proteins as expected.

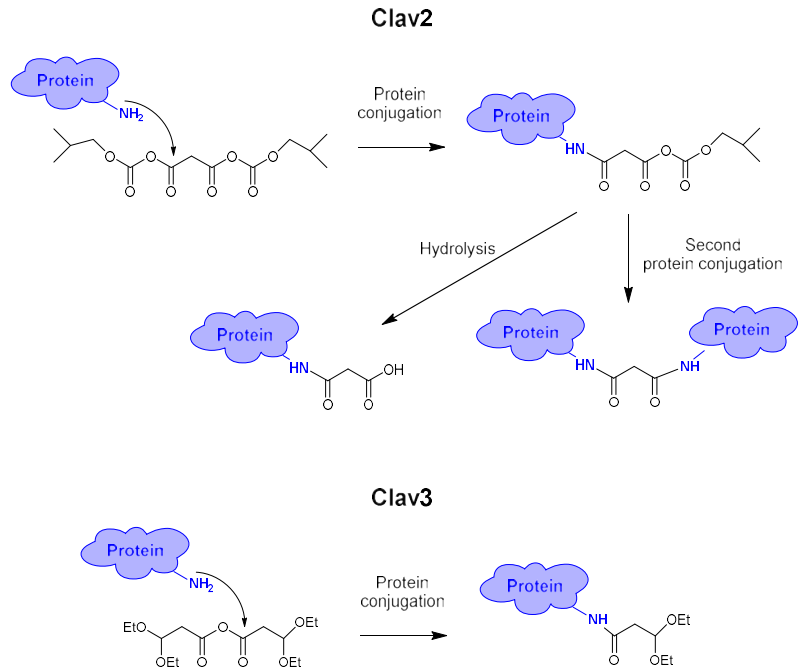

Figure II.14. Clav2 and Clav3 reactivity with proteins.

II.2. Characterization of CLV-Protein Adducts Generated *In Vitro*

As mentioned before, the reactivity of BLs is well known and the formation of hapten-protein conjugates is a key process in BL allergic reactions. The study of these resulting conjugates is really important in terms of understanding the mechanisms involved in the immunological recognition of the BL antibiotics and the fully characterization of these adducts would provide valuable information to improve the diagnosis of drug allergy.

In the last decade, the combination of immunochemical studies with MS techniques have allowed to gain insight not only into the proteins involved [88] but also into the identification of protein binding sites [53, 89, 101-104, 107] and the determination of exact drug moieties forming part of the AD [53]. Among BLs, penicillins conjugation is the most studied: AX [53, 89, 106], BP [103, 104], flucoxacillin [101] and piperacillin [53, 102, 107].

However, in the case of CLV as a hapten, neither the chemical structure of its AD nor the relevance of the proteins involved is known and, to our knowledge, there is only an study directed to study CLV conjugation. Meng *et al*. [53] investigated the haptenation of HSA by AX and CLV in drug-protein adducts generated *in vitro* and in serum samples from drug-induced liver injury (DILI) patients treated with the antibotics. Incubation of HSA with a range of molar ratios of CLV (1:1 to 50:1) was performed and LC-MS/MS analysis of the tryptic digests of HSA-CLV revealed seven types of adducts (Figure II.15), including direct binding of CLV to lysine (Δm=199), subsequent degradation products (Δm=155, 137 and 70), and pyrazine adducts (Δm=222), preferently formed at high concentration of CLV, on lysine and histidine residues.

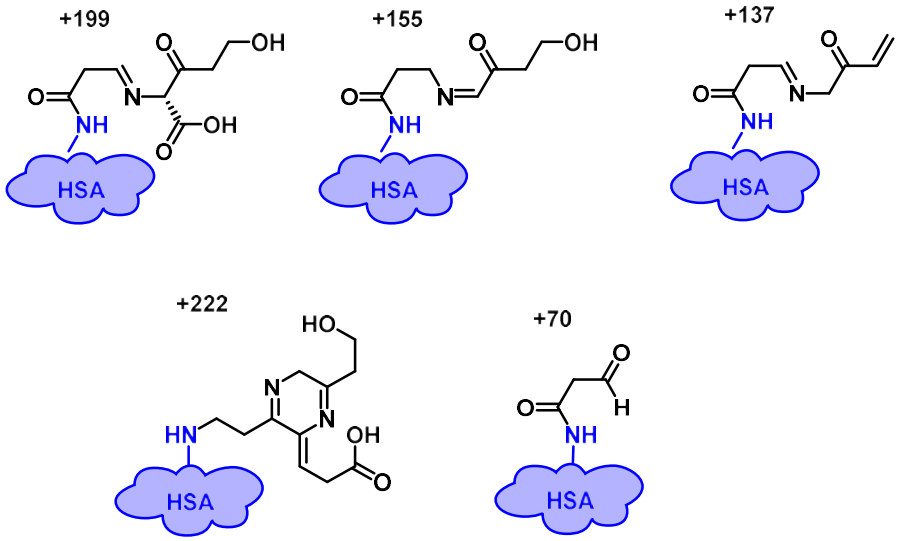

Figure II.15. Representation of CLV residues that were found after HSA incubation with CLV *in vitro* and their mass increments.

The fragment involving Δm=70 seemed to be the most stable. Also, HSA modified by AX-CLV were detected in patients receiving AX-CLV combination. The profile of CLV-modified peptides in patients was less complicated than *in vitro*. Only the Δm=70 adducts were detected, with Lys190 adducts being found in all patients.

With the aim to contribute to the study of CLV haptenation, we propose the use of HSA as a model protein to gain insight into the nature of the relevant determinants formed by CLV. For this, HSA-CLV conjugates were prepared *in vitro* and their detailed characterization performed. To start with, dependence of modification with drug concentration was studied. Besides, studies for identification both HSA nucleophilic residues modified and the exact structure derived from CLV that remains linked to the protein after conjugation were carried out. Results would confirm the structures derived from **AD-I** with positive BAT as the AD involved in allergic reactions to CLV.

II.2.1. Mass Spectrometry Characterization

HSA was incubated with different concentrations of CLV from HSA/CLV molar ratio 1:10 (close to physiological conditions) to a high excess of the drug (1:600). In Figure II.16, each MALDI-TOF MS spectrum shows a peak belonging to monocharged HSA (66846 Da for control HSA) as well as a peak belonging to double charged HSA (33372 Da for control HSA). Conjugates were prepared by the PhD student and analyzed at SCAI, UMA.

[HSA]	[CLV]	HSA:CLV Molar ratio	MALDI-TOF MS	Δ mass
10 mg/mL (0.15 mM)		1 : 0	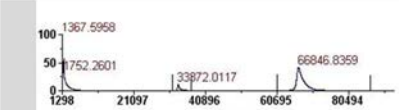	0 (HSA control)
10 mg/mL (0.15 mM)	0.3 mg/mL (1.5 mM)	1 : 10	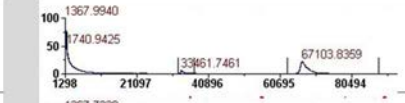	247
10 mg/mL (0.15 mM)	0.7 mg/mL (3 mM)	1 : 20	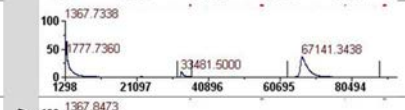	295
10 mg/mL (0.15 mM)	1.4 mg/mL (6 mM)	1 : 40	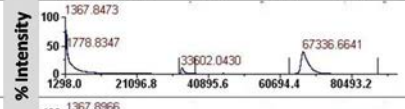	490
10 mg/mL (0.15 mM)	2.9 mg/mL (12 mM)	1 : 80	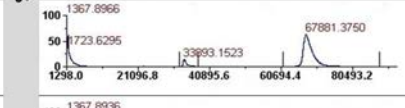	1035
10 mg/mL (0.15 mM)	5.7 mg/mL (24 mM)	1 : 160	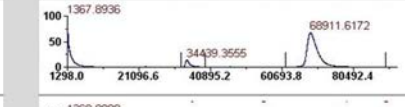	2065
10 mg/mL (0.15 mM)	11.5 mg/mL (48 mM)	1 : 320	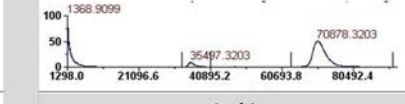	4032

Figure II.16. MALDI-TOF results for different HSA-CLV conjugates.

MALDI-TOF MS results showed that incubation of HSA with increasing concentrations of CLV induced a concentration-dependent increase in the mass of the protein (Figure II.16), from 1:10 up to a 1:320 molar ratio. Saturation of CLV binding to HSA occurs at a 1:320 molar ratio, since conjugates derived from a 1:600 molar ratio showed the same mass increment.

II.2.2. Identification of HSA Binding Sites

a) Characterization of HSA-CLV conjugates by linear trap quadrupole (LTQ) Orbitrap XL

Since HSA modification was observed even in the conjugate derived from a 1:10 molar ratio incubation, we used this for further characterization studies, since it is the closest to therapeutic conditions. Residues modified by CLV were identified by arginine C digestion of native and modified HSA prepared at neutral pH, followed by LC-MS/MS analysis of the resulting peptides. These experiments were carried out in the Proteomic Laboratory at University Hospital Vall d´Hebron Research Institute. We observed that, *in vitro*, CLV binds covalently to the amino groups of Lys in HSA. The resulting conjugates, formed after β-lactam ring opening, show a mass increase of 70 Da, which is consistent with the addition of a fragment of the CLV molecule of 71 Da accompanied by the loss of a hydrogen atom (Figure II.17). This finding is compatible with the haptenation process proposed in Figure II.2. Interestingly, mass increments corresponding to the entire molecule of CLV were not found.

When injecting 1µL of conjugate in the LC-MS/MS analyzer, we observed one peptide (^{473}VTK*CCTESLVNR^{484}, calculated mass: 1421.6625 Da) showing a mass increase of 70 Da on Lys 475. The MS/MS fragmentation pathway was carried out from the $[M+2]^{2+}$ as parent ion at m/z 711.8385 Da (Figure II.17A). In order to increase the coverage and find additional modified peptides, a higher amount of sample was injected (4µL). This led us to observe a new peptide (^{187}DEGKASSAK*QR^{197}, calculated mass: 1245.5949 Da) covalently modified at Lys 195. Figure II.17B shows the MS/MS spectrum for a triply charged ion at m/z 416.2059, corresponding to the peptide HSA 187-197 with the 70 Da mass increment. The peptide sequences were confirmed by the b and y ion series determined by MS/MS. The same peptides were also observed without modification, demonstrating that not all the HSA is modified in those residues at therapeutic dose conditions. It should also be noted that the conditions at which the MS/MS experiments took place, performed in collision induced dissociation (CID) mode, could cause fragmentation due to the unstable nature of this modification, which could be lost during the collision.

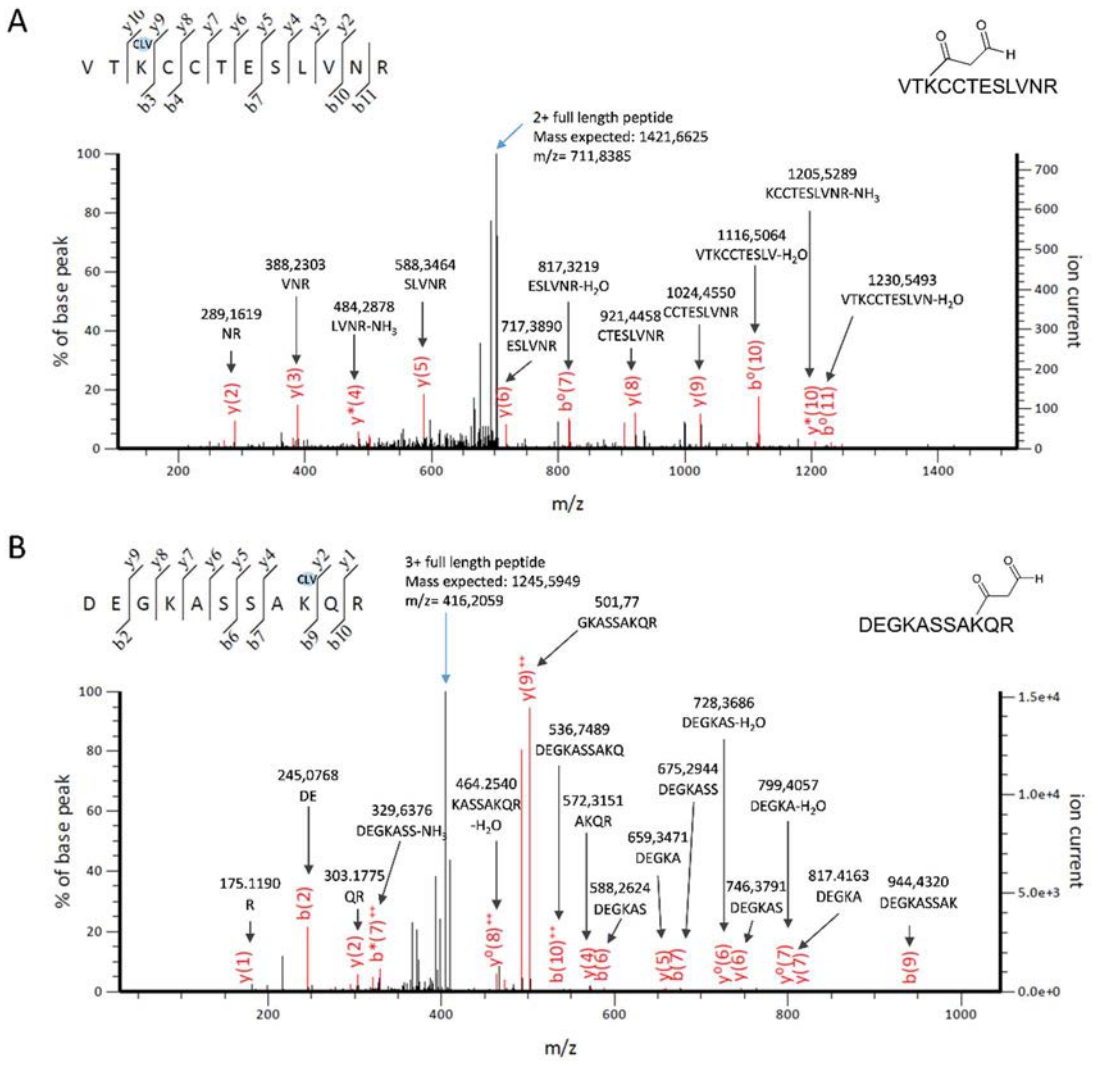

Figure II.17. MS/MS spectra of CLV-HSA derived peptides identified *in vitro* with a mass increment of 70 Da. **A**, Collision-induced dissociation (CID) based MS/MS spectra of the $[M+2H]^{2+}$ precursor ion of the peptide ^{473}VTK(+70)CCTESLVNR^{484} modified at Lys 475. Calculated mass of modified peptide: 1421.6643, experimental mass: 1421.6625 and observed parent ion at *m/z*: 711.8385. **B**, Collision-induced dissociation (CID) based MS/MS spectra of the $[M+3H]^{3+}$ precursor ion of the peptide ^{187}DEGKASSAK(+70)QR^{197} modified at Lys 195. Calculated mass of modified peptide: 1245.5949, experimental mass: 1245.5960 and observed parent ion at *m/z*: 416.2059. Matched b- and y-ions are indicated in the spectra as well as the peptide sequence.

Summing up, we observed that covalent binding of CLV to HSA takes place *in vitro* and that this modification is concentration-dependent, consistent with recent studies [217]. As expected, given the complexity of CLV reactivity, analysis of the CLV-protein conjugates did not allow the detection of mass increments corresponding to the addition of the complete CLV molecule, and only a 70 Da mass increase was observed, which corresponds to an adduct with **AD-I** structure. This result is in agreement with one fragment recently identified in cell culture media and in patients with DILI exposed to AX-CLV [217]. Moreover, these results are also consistent with mechanisms and

structures proposed in other publications out of the context of allergy, describing CLV binding to β-lactamases [82, 223, 224], although through a serine residue rather than a lysine [218].

It is important to highlight that the fact that proteomic results confirmed that HSA was modified with a 70 Da residue is in agreement with the results obtained with BAT, and confirms that the specifically recognized AD derived from **AD-I** forms part of the resulting CLV-protein conjugate.

b) Molecular modeling of HSA residues modified by CLV *in vitro*

In order to obtain further insights into the observed adducted Lys for HSA-CLV (Lys 195 and Lys 475), molecular modeling studies were performed by Dr. Francisco Nájera, from Ezequiel Pérez-Inestrosa Research Group (UMA), exploring the regions surrounding the modified residues. Even though Lys 475 is more basic than Lys 195, the former is more exposed because it is located at the surface of HSA, enabling CLV to get close. Lys 195, although less accessible, is surrounded by other positively charge residues that contribute a reduced basicity [225].

Docking simulations were used to know how the region adjacent to the adducted Lys residues can stabilize an appropriate complex with CLV and contribute to adduct formation. Figure II.18 shows these complexes with the interactions stabilizing CLV in the proximity of Lys 195 or Lys 475. In both complexes, the CLV is visibly close and with the proper orientation to react with the adducted lysines. The nitrogen atom in the Lys reacts with the carbon atom of the carbonyl group of the β-lactam ring. In both cases, the carboxylate group of CLV is involved in a salt bridge (with Arg 218 for Lys 195 and Arg 472 for Lys 475) which plays a key role in the orientation of CLV. In the case of Lys 195, an additional hydrogen bond between the hydroxyl of CLV and His 242 also contributes to stabilizing the complex.

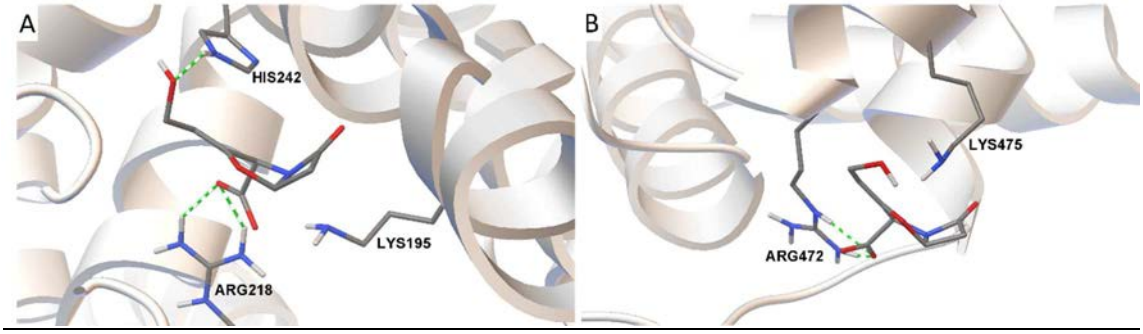

Figure II.18. Docking simulation of the environment of HSA residues adducted by CLV.

Lys 195 has been previously reported to be linked *in vitro* to a bigger CLV-derived structure with a mass equivalent to three **AD-I** moieties [217]. This result can be attributed to the self-condensation of CLV degradation molecules (71 Da) at higher drug concentrations. The same residue has been shown to be modified by BLs, such as BP [226], flucoxacillin [227] and piperacillin [228]. Lys 475 has not been previously reported to be modified by CLV, although it has been identified as target for AX [217].

These modeling studies were able to explain the reactivity of these residues, which is determined by the surrounding environment and residue accessibility.

II.3. Development of Approaches for Detection of Serum Proteins Modified by CLV

As stated before, drug binding to proteins is known to play a key role in the development of drug allergy. Drugs or their metabolites can be labeled to facilitate the detection and enrichment of the adducts in complex samples [105]. The avidin-biotin interaction provides great affinity and sensitivity, and the possibility of coupling modification of proteins by biotinylated compounds with several methods for detection, purification and imaging [45] and that is why the incorporation of a biotin moiety is one of the most used procedures for non-isotopic labeling [229]. Recently, some studies employed biotin as probe for biochemical/pharmacological [230-232] or antigenicity studies [214]. Also, biotin labeling has been combined with proteomic techniques for the identification of potential protein targets for haptenation [45, 113, 233, 234] or modified protein residues [235]. Some of these studies have been performed in our group or with collaborators, using AX-B (Figure II.19) [45, 113]. It was demonstrated that AX and AX-B compete for their binding to proteins, suggesting that they may bind to common sites [45]. Furthermore, the use of AX-B allowed the highly sensitive detection of haptoglobin haptenation although it had not been detected as target of haptenation by AX using immunological procedures [45]. Also, several novel targets for haptenation by AX have been identified in B lymphocytes through the use of AX-B [113].

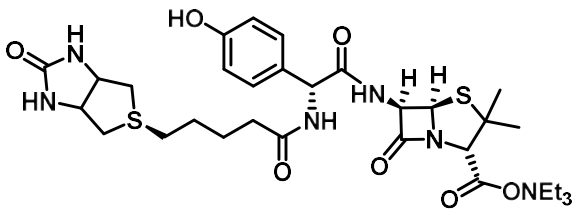

Figure II.19. Structure of AX-B used by Ariza *et al*.

The lack of existence of α-CLV monoclonal antibodies did not allow the immunological evaluation of protein-CLV adducts before and, as a consequence, there are no currently available methods for immunological evaluation of CLV adducts. This fact could make biotinylated derivatives of CLV a really valuable and straightforward tool for studying haptenization and developing methods to identify CLV target proteins. Nevertheless, it should be taken into account that the introduction of a biotin moiety into a parent molecule could result in steric hindrances of its interaction with certain targets, for which it is very important to confirm the results obtained with biotinylated molecules using the parent molecule [45, 105].

II.3.1. Synthesis of Biotinylated Derivatives of CLV

To detect serum proteins that conjugate to CLV, a biotin derivative was chosen as probe, due to its extremely high affinity for streptavidin binding and no impact on the biological activity of its substrate. The synthesis of CLV derivatives was optimized by Dr. Nekane Barbero (Dr. Pérez-Inestrosa research group) and prepared by the PhD student when it was needed for performing the studies.

The functionalization of CLV was carried out in optimal conditions that do not affect the β-lactam ring, its reactive site towards nucleophiles. CLV was successfully labeled with a biotin moiety to its carboxylic group through two different approaches (Schemes II.1 and II.2).

First approach consisted on the direct coupling between CLV and biotin iodide to synthesize **CLV-B** (Scheme II.1). Biotin esterification to form the methyl ester was the first step. Further reduction to alcohol and subsequent tosylation allowed to have a good leaving group which, after substitution by an iodine group, and final reaction with carboxyl in CLV allowed biotinylation of the drug.

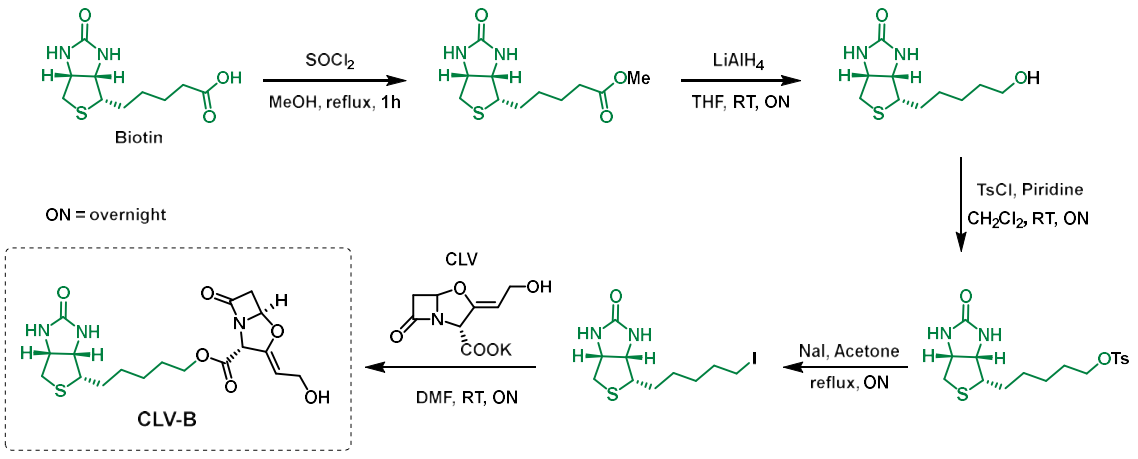

Scheme II.1. Synthesis of biotinylated derivative **CLV-B**

The product was isolated with 73% average yield. Assigned ^{1}H-NMR spectra of pure **CLV-B** is depicted in Figure 20. The resulting compound was not soluble in water and DMSO was used to make it soluble in aqueous media for further protein incubation experiments.

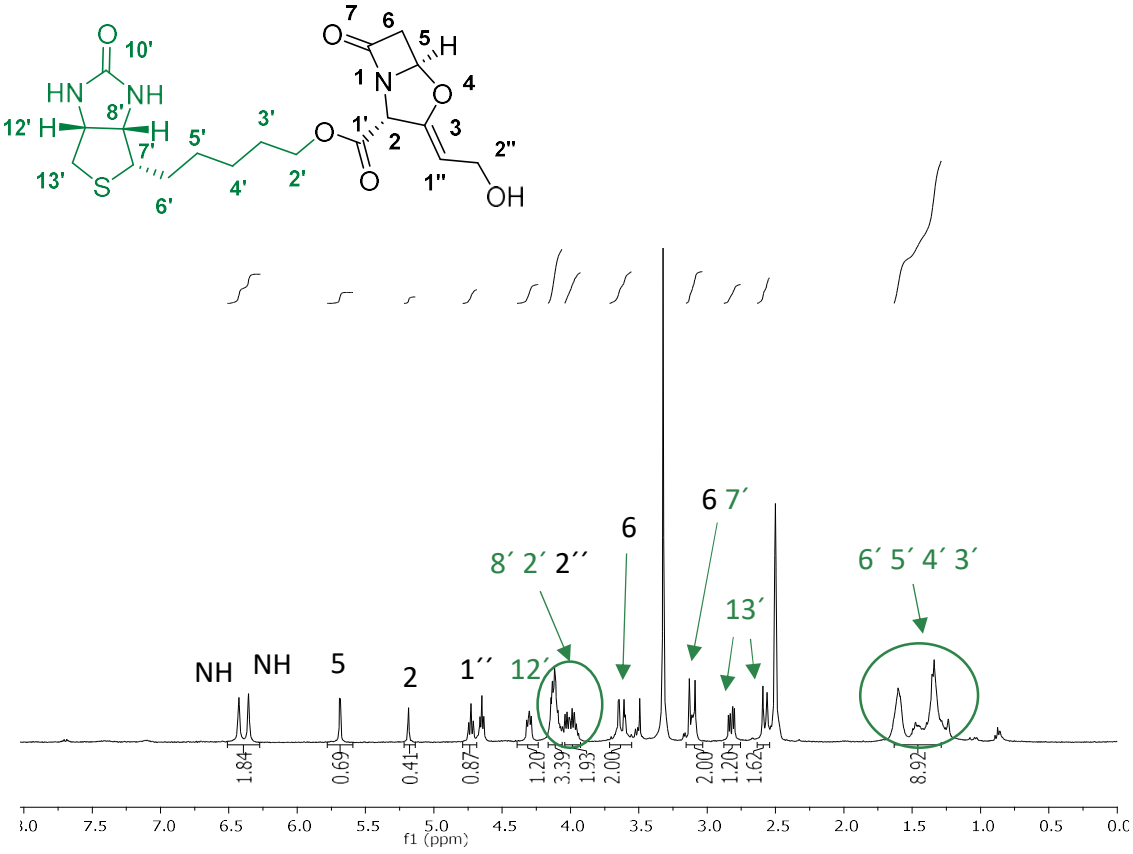

Figure II.20. ^{1}H-NMR (DMSO) of **CLV-B**

Second approach employed an extending TEG linker between CLV and a biotin by means of a two-step synthetic process (Scheme II.2). First, tetraethylenglycol chain was ditosylated and both tosyl groups were substituted by iodine. Selective reaction of commercial biotine with the trioxygenated di-iodide afforded biotine iodide, which was then subjected to reaction with potassium clavulanate leading to the target molecule. These linkers increase the hydrophilicity of the compound, which provides solubility in aqueous media. In addition, the flexibility and length of the spacer make biotin moiety more available to interaction with streptavidin, which may lead to higher detection efficiency.

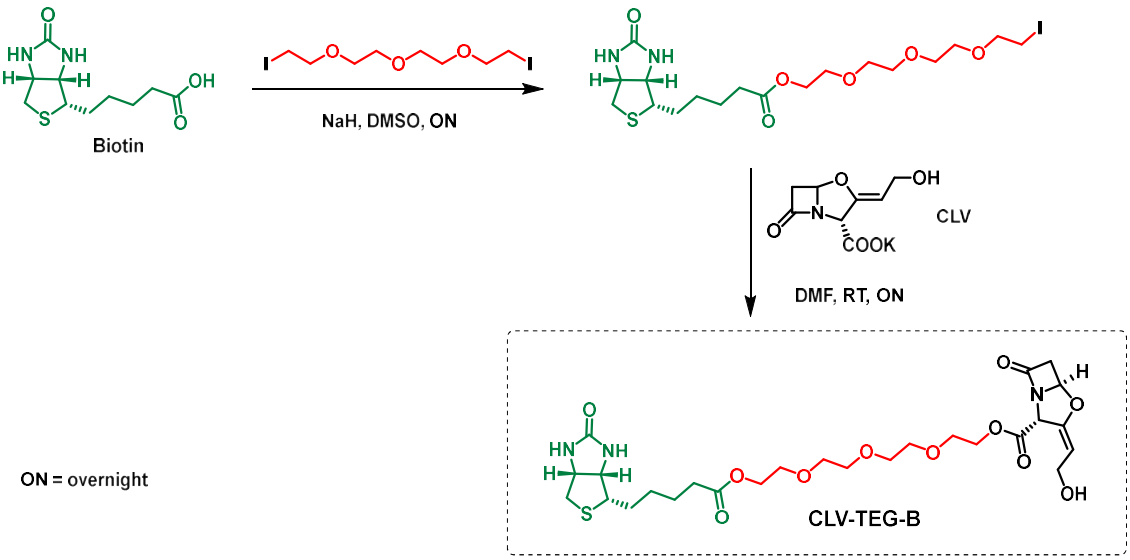

Scheme II.2. Synthesis of biotynilated derivative **CLV-TEG-B**.

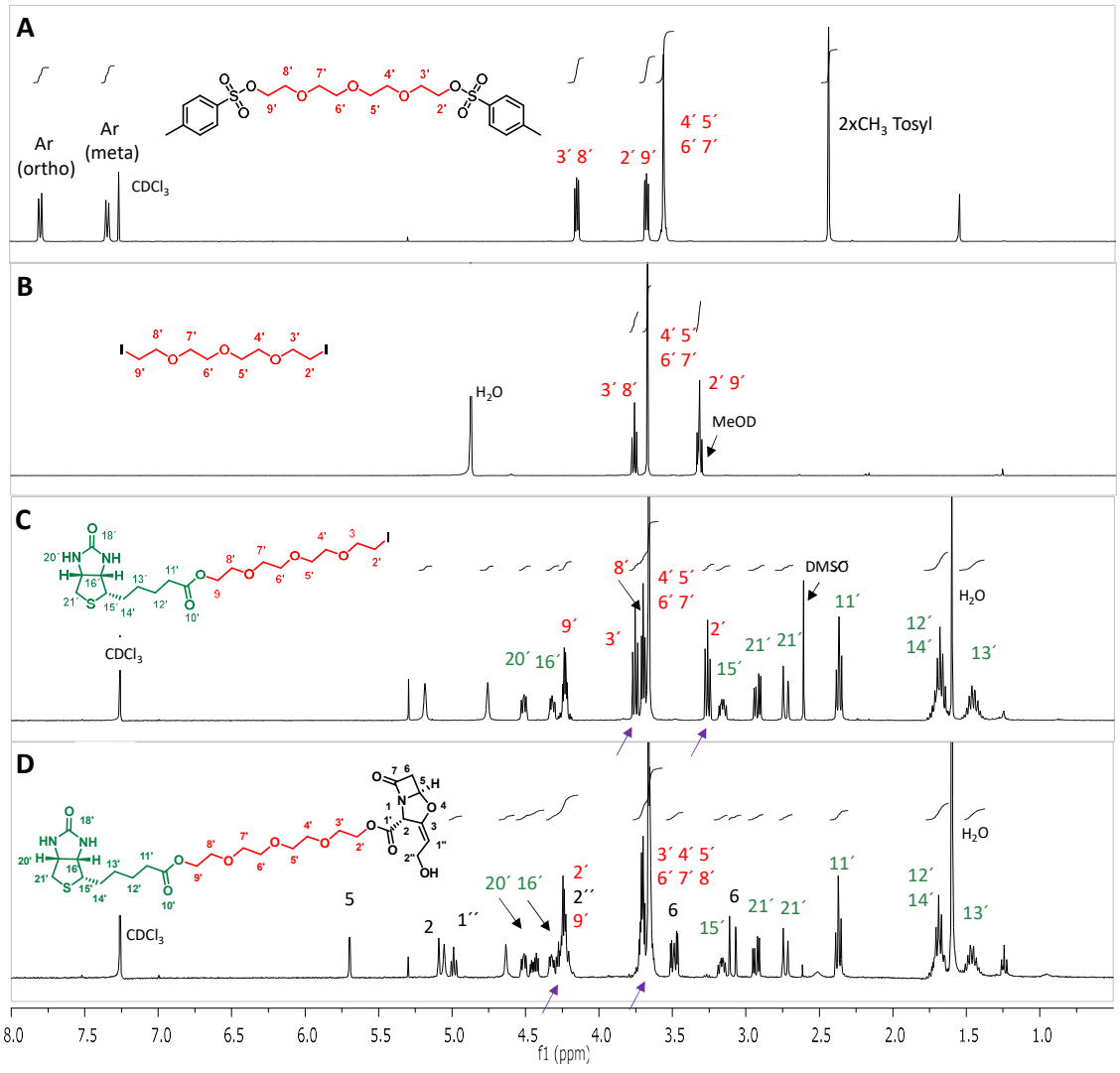

Figure II.21. ^{1}H-NMR monitoring of synthetic steps for preparing CLV-TEG-B.

Reactions were monitored using ^{1}H-NMR (Figure II.21). In Figure II.21B we can notice the disappearance of signals belonging to tosyl groups as well as the shift of the signals adjacent to tosyl groups in A or iodine groups in B. In Figure II.21C, one of the methylene groups near to iodine shifts from 3.25 ppm to 4.25 ppm, which confirms the coupling with biotin. In Figure II.21D, the shift of the methylene near to the iodine in C (2´´) to 4.25 ppm along with the apparition of CLV signals proved the reaction success. The final product **CLV-TEG-B** was isolated with 62% average yield.

Since this second derivative is water soluble and the biotinylated derivative of CLV is aimed to be used in experiments that need to be performed in aqueous media, we will focus on **CLV-TEG-B** further on.

II.3.2. Reactivity of CLV-TEG-B towards simple nucleophiles

Stability studies for **CLV-TEG-B** (Figure II.22) revealed that after 1 hour of incubation 20% of the β-lactam ring was opened and kept on opening over time, with 50% of opened β-lactam at 16 hours and 58% at 40 hours.

The fact that after 16 hours incubation there was still remaining original biotinylated drug, with closed β-lactam ring, is compatible with the use of this time period for conjugates formation. Also after 1 hour, a peak at 2.25 ppm appeared and the oxazolidine ring started to degrade (signal 1´).

The same as we did for cephalosporins in previous chapter and for CLV, the first attempt to understand the reactivity of the biotinylated derivative of CLV was NMR monitoring of its stability and reactivity towards butylamine as simple nucleophile. These studies would allow as well the comparison of chemical behavior between native CLV and its derivative.

Results of **CLV-TEG-B** reactivity studies with butylamine as simple nucleophile are depicted in Figure II.23. After 15 minutes incubation with butylamine, there was no remaining methylene next to the amine in butylamine at 2.6 ppm and a the appearance of a triplet at 3.2 ppm can be due to amide formation. Evidence of β-lactam ring opening is observed as well from 15 minutes of incubation and it was completely consumed after 16 hours (see changes in signals H5 and H6).

From these NMR studies, it is inferred that the β-lactam reactivity toward nucleophiles remains in spite of the modification introduced in the structure of CLV with the incorporation of the biotin moiety. Also, this derivative is stable enough during at least 16 hours (usual incubation time for studying conjugation) in physiological conditions and so, it could be used for further conjugation studies with proteins.

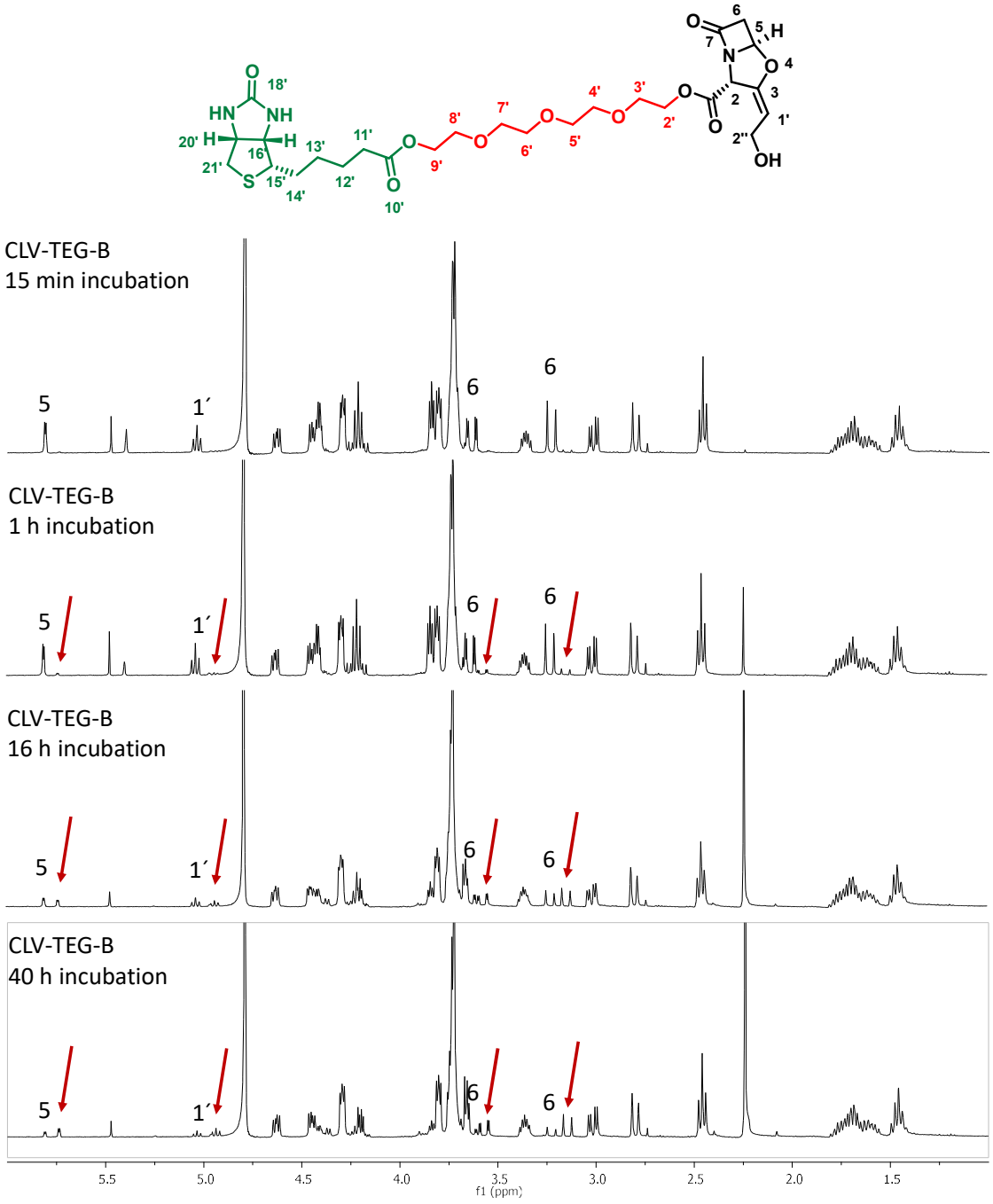

Figure II.22. ^{1}H-NMR spectra of **CLV-TEG-B** registered in deuterated PBS 1X over time.

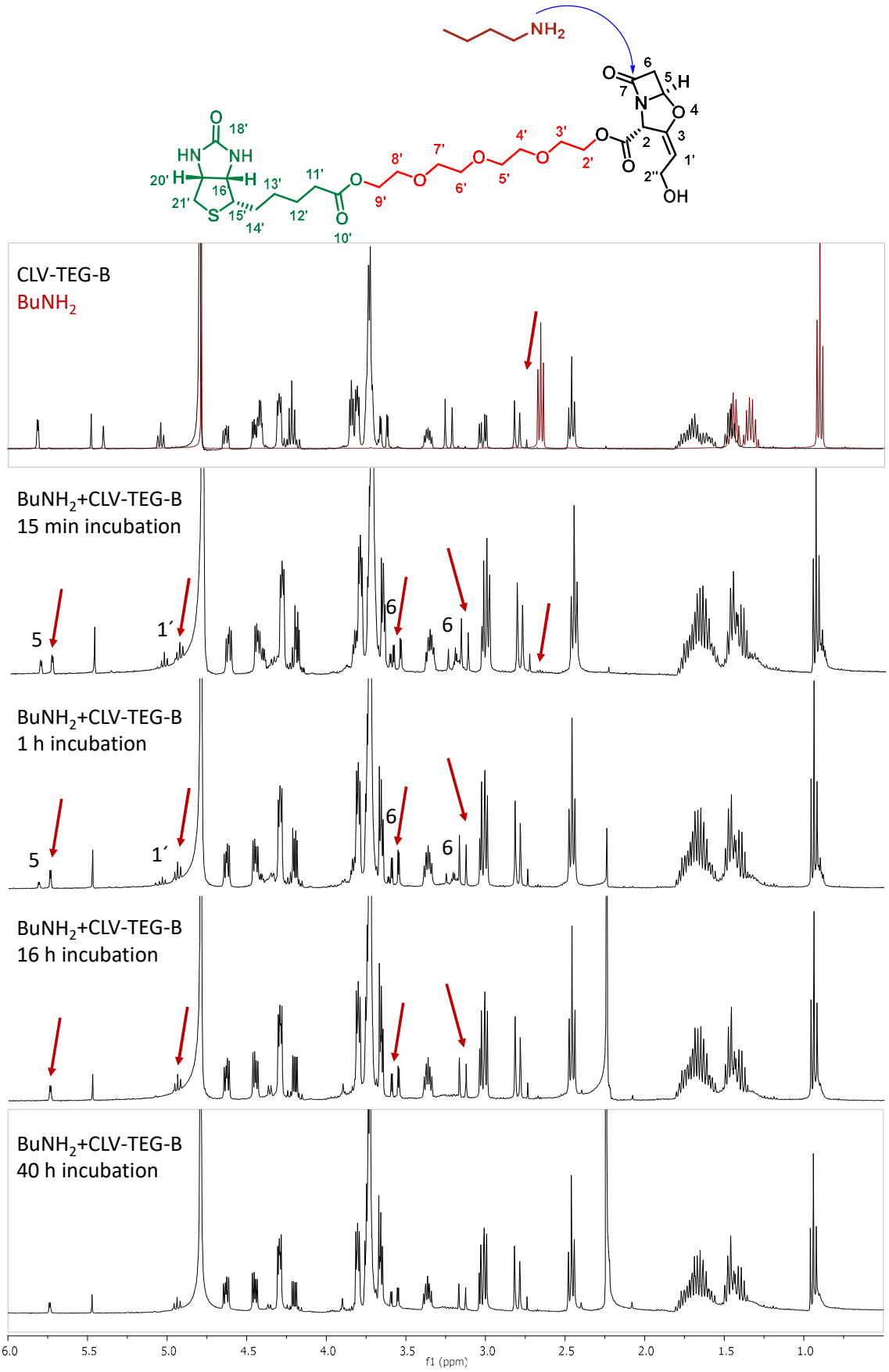

Figure II.23. ^{1}H-NMR study of **CLV-TEG-B** reactivity with butylamine registered in deuterated PBS 1X.

II.3.3. Comparison of Reactivity between CLV and CLV-TEG-B

Figures II.24-II.26 show the comparison of reactivity between CLV and **CLV-TEG-B**. In Figure II.24, in which it can be observed that in physiological conditions, CLV is more stable than **CLV-TEG-B** since β-lactam opening did not take place for the former.

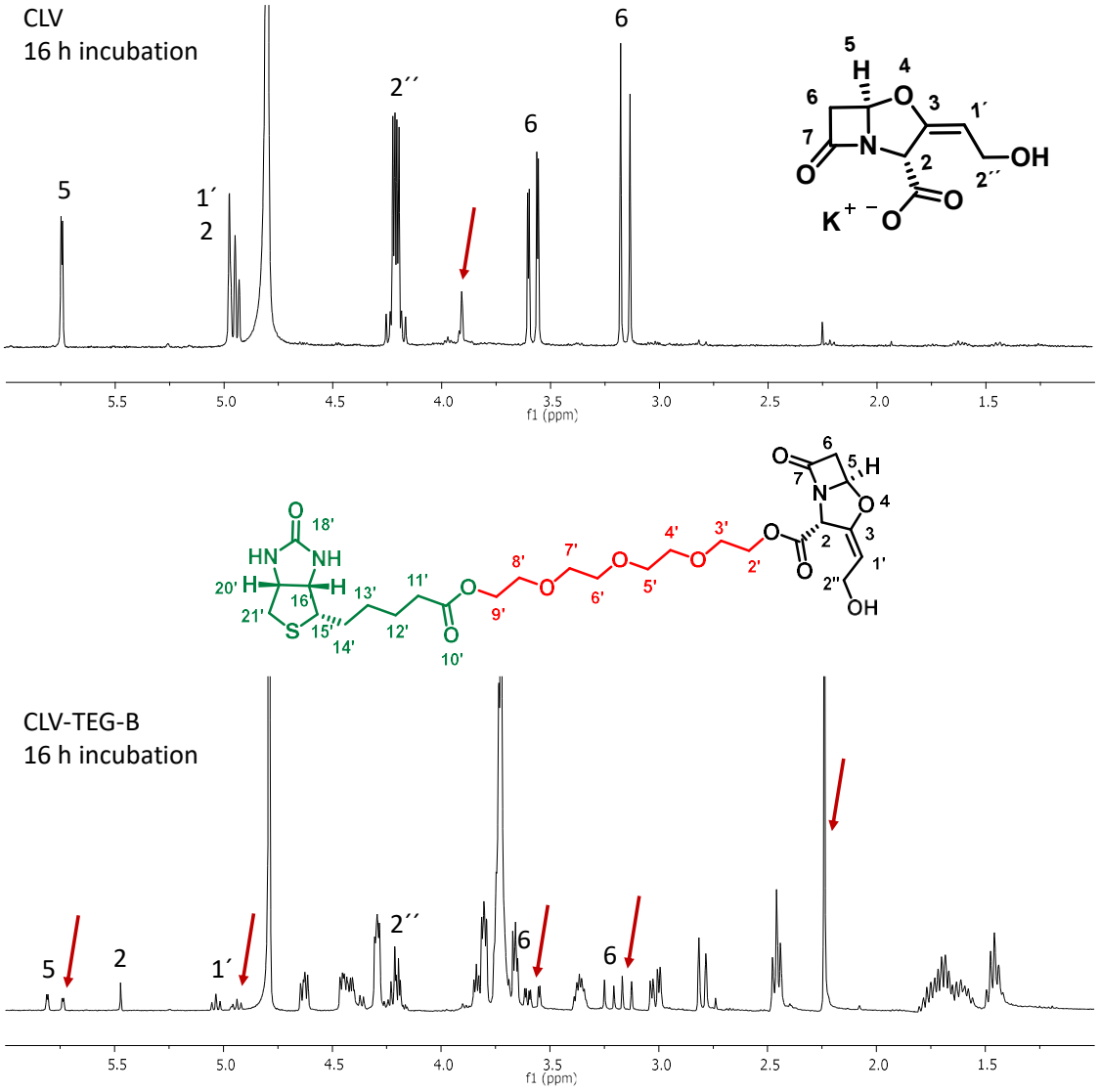

Figure II.24. Stability comparison between CLV (top) and **CLV-TEG-B** (bottom) at the typical incubation time for preparing conjugates. Pointed with arrows changing signals for comparison.

However, in presence of butylamine (Figures II.25 and II.26), CLV degrades quickly with no evidence of amide formation while a signal around 3.2 ppm is evidence of amide formation for **CLV-TEG-B** after 15 min of incubation with butylamine.

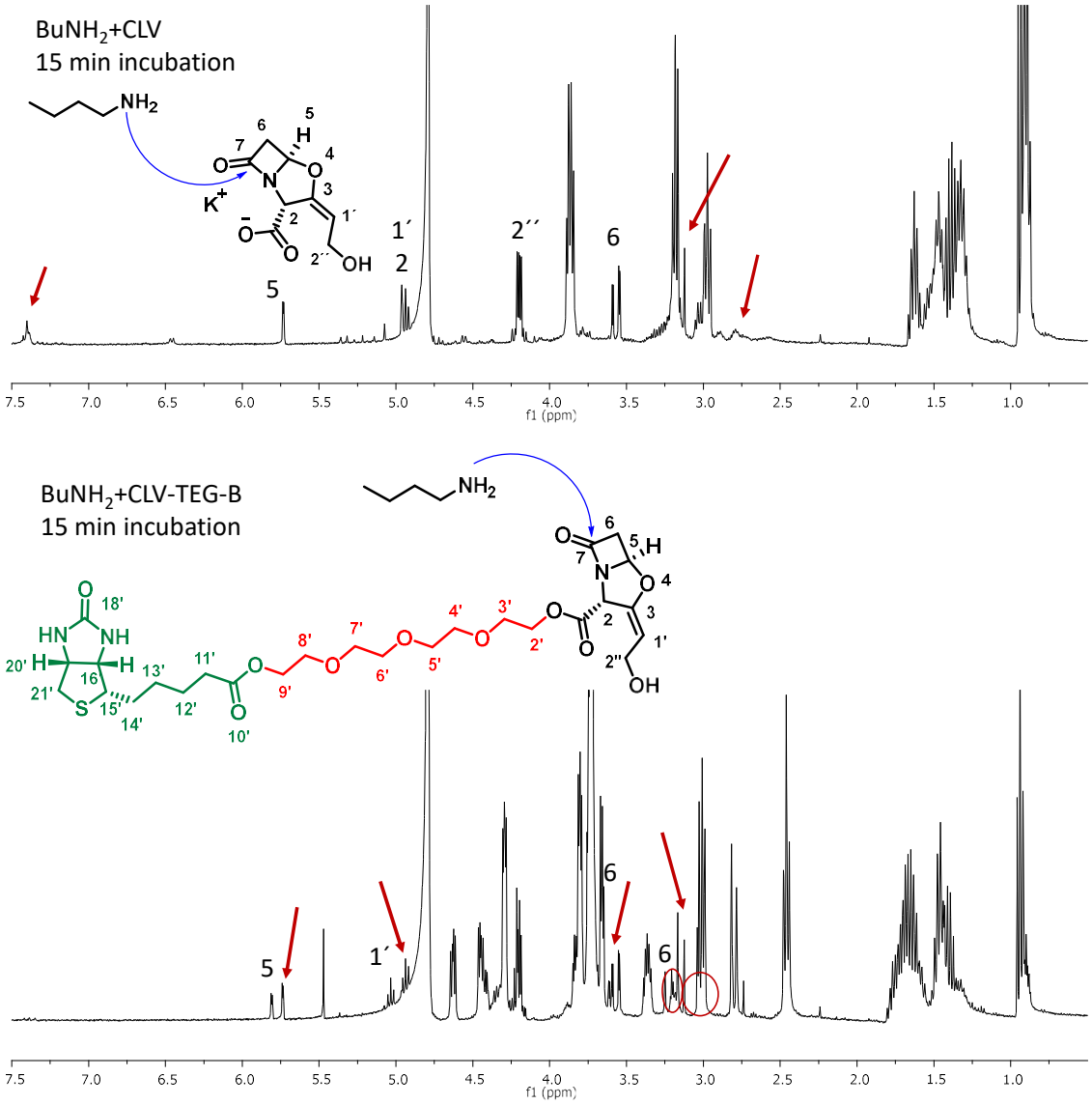

Figure II.25. Reactivity comparison of CLV (top) and **CLV-TEG-B** (bottom) with butylamine after 15 min incubation. Pointed with arrows and circle changing signals for comparison.

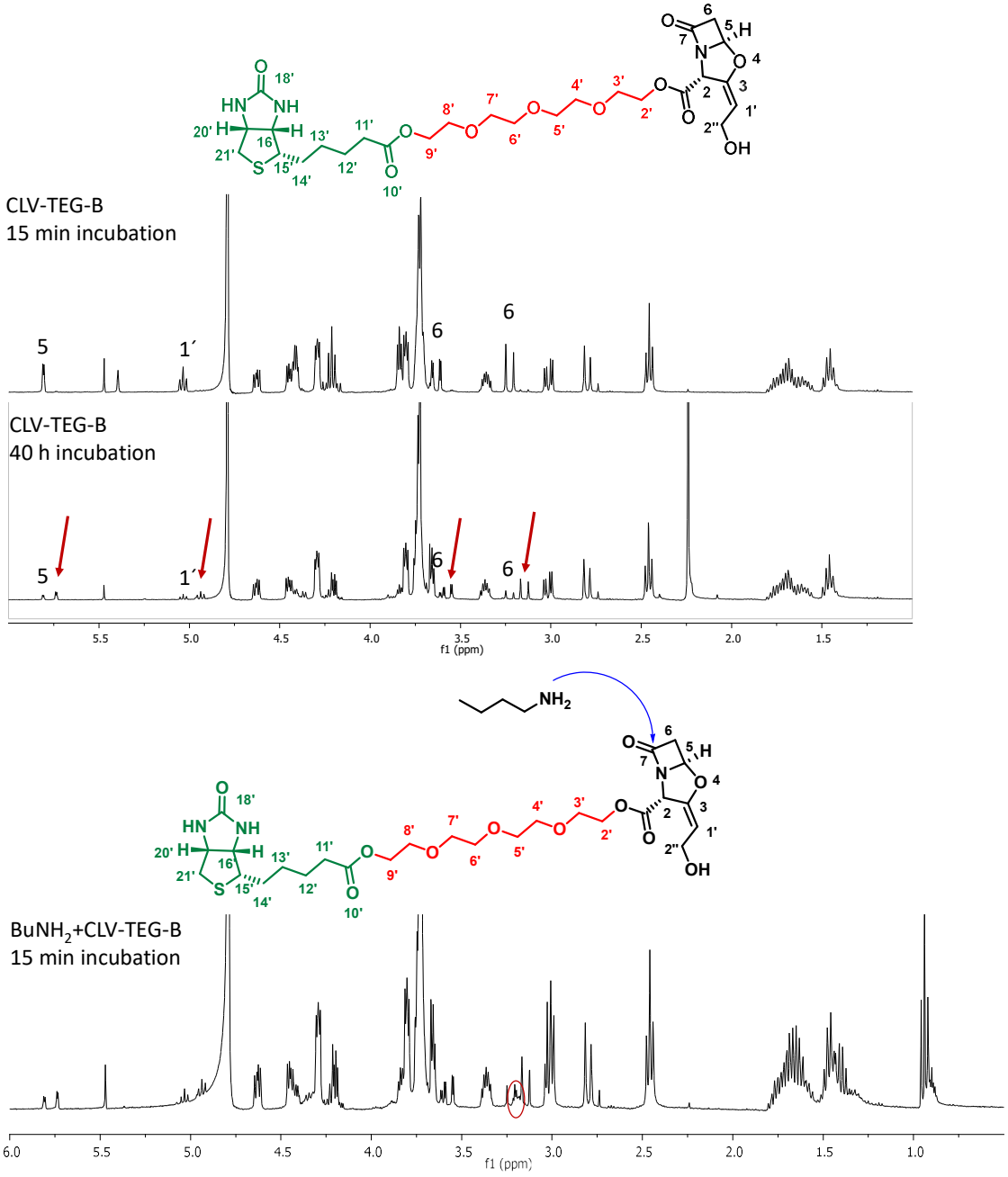

Figure II.26. Evidence of amide formation by nucleophilic attack of butylamine towards the β-lactam ring of CLV. Pointed with arrows and circle changing signals for comparison.

II.3.4. Study of CLV Biotynilated Derivatives Proteins Haptenation Capacity

The chance of using biotinylated derivatives of CLV for the identification of modified serum proteins was studied since biotinylated CLV could be detected by Western blot with a high sensibility using steptavidin conjugated with peroxidase, or by fluorescence microscopy using streptavidin conjugated with a fluorochrome. Furthermore, these CLV derivatives could be useful for complex systems study, such as serum and cellular lysates since modified proteins could be purified with streptavidin columns. However, due to

the modification of the molecule as consequence of the incorporation of the biotin moiety, there is first the need of studying structure-function relationship. For this purpose, conjugation of CLV derivatives with HSA were studied by SDS-PAGE and MALDI-TOF MS. HSA was the protein used as model since in literature it has been inferred that, among serum proteins, it is the main target for protein haptenation [45]. All SDS-PAGE experiments, transferences and detection with enhanced chemiluminiscence (ECL) were carried out by the PhD student and MALDI-TOF MS analysis at SCAI, UMA.

SDS-PAGE Analysis and Detection of HSA-biotynilated CLV Conjugates

a) <u>Study of ability of haptenization of biotinylated derivatives of CLV</u>

After synthesis of the biotynilated derivatives of CLV, the first thing to do was to assay their ability to bind covalently to proteins. HSA prepared in PBS 1X (pH 7.4) was incubated for 16 hours at 37˚C in presence of any of both biotinylated derivatives of CLV prepared in PBS 1X (pH 7.4) at protein/biotinylated CLV ratios from $1{:}3.07{\cdot}10^{-4}$ to 1:600 (final concentration of HSA 0.15 mM and biotinylated CLV from $4{,}61{\cdot}10^{-5}$ to 90 mM). As proof-of-concept, 2 µg aliquots of some of the resulting adducts were subjected to SDS-PAGE electrophoresis, transferred to a polyvinylidene fluoride (PVDF) membrane and detected with streptavidin-horseradish peroxidase (HRP) and ECL (Figure II.27).

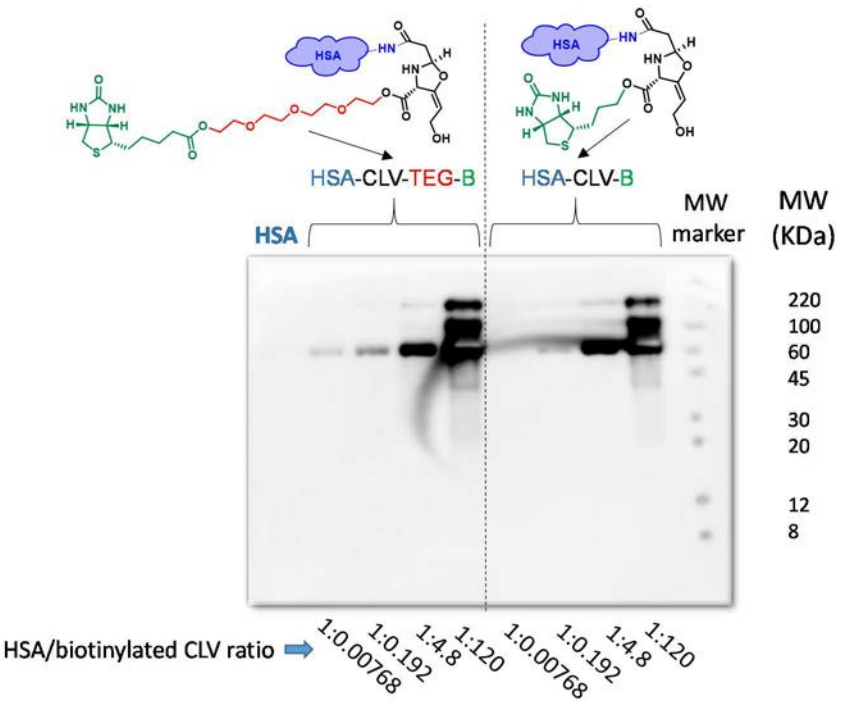

Figure II.27. Detection of HSA modified in presence of different ratios HSA/biotinylated derivatives of CLV.

Results showed that both biotinylated derivatives of CLV bind covalently to HSA and that protein modification was concentration dependent for both cases (using **CLV-B** or **CLV-TEG-B**). Signal obtained after detection is selectively due to HSA conjugation to biotinylated derivatives of CLV, since no signal was detected for control HSA and it was detected even at very low protein/biotinylated ratio (1:0.00768), which confirms the high sensitivity of the method. Also, these results demonstrate that biotin moiety remain linked to CLV after conjugation for both derivatives.

A similar haptenization pattern was obtained for both biotinylated derivatives, so we decided to use **CLV-TEG-B** for further studies since it is completely water soluble and there is no need to use any organic solvent to dissolve it (it was necessary to dissolve **CLV-B** first in DMSO before preparing dilutions using PBS 1X).

b) <u>Dose-response</u>

In order to carry out this assay, 2 µg aliquots of the HSA adducts obtained *in vitro* with protein/**CLV-TEG-B** molar ratios ranging from 1:0.0003072 to 1:24 were subjected to SDS-PAGE electrophoresis, transferred to a PVDF membrane and detected with streptavidin-HRP and following ECL. Higher protein/**CLV-TEG-B** molar ratios (1:600 and 1:120) were not loaded in the gel since for 1:120 conjugates signal reached saturation (Figure II.28).

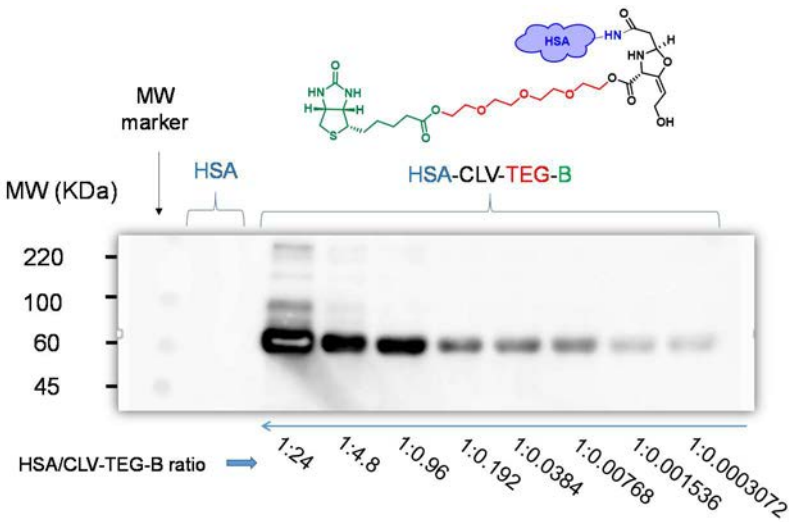

Figure II.28. Detection of HSA modified in presence of different ratios HSA:**CLV-TEG-B.**

These results confirm the usefulness of **CLV-TEG-B** in the detection of HSA adducts with high sensitivity, being detected even the conjugate modified with 1:0.0003072 HSA/**CLV-TEG-B** molar ratio. These properties can be exploited to obtain novel information on the mechanisms of the allergic reactions towards CLV.

c) Degree of biotinylation

Once studied HSA modification dependence with the amount of biotinilated CLV, the extent of incorporation was estimated by comparison with a biotinyated BSA standard (10 mol biotin/mol) [236, 237]. Aliquots of 2 pmol (0.13 µg) of HSA adducts, prepared using different protein/**CLV-TEG-B** molar ratios during incubation (1:1, 1:10 and 1:100) were loaded in a polyacrylamide gel along with different amounts of BSA-B ranging from 0.006 pmol to 0.377 pmol. Proteins were transferred to a PVDF membrane and we confirmed the amount of HSA conjugates transferred by Western blot using an α-human HSA antibody followed by incubation with HRP-conjugated secondary antibody and ECL detection (Figure II.29 top). After, membrane stripping was performed with guanidine hydrochloride to remove previous antibodies used, and the presence of biotinylated species was detected with s treptavidin-HRP and ECL detection (Figure II.29 bottom). The dose-dependent modification of HSA by **CLV-TEG-B** previously observed was confirmed analyzing 1:1, 1:10 and 1:100 HSA/**CLV-TEG-B** conjugates.

Images obtained after detection with streptavidin-HRP for three replicates were analyzed with ImageJ software. The equation obtained after representation of intensity *versus* pmol of BSA-B was used to calculate the amount of biotin in each conjugate taking into account the intensity obtained for each conjugate. Results expressed as pmol biotin/pmol HSA are representative of three assays and resulted to be 0.0935, 0.013, 0.00055 pmol biotin/pmol HSA for HSA-CLV-B 1:100, 1:10 and 1:1, respectively.

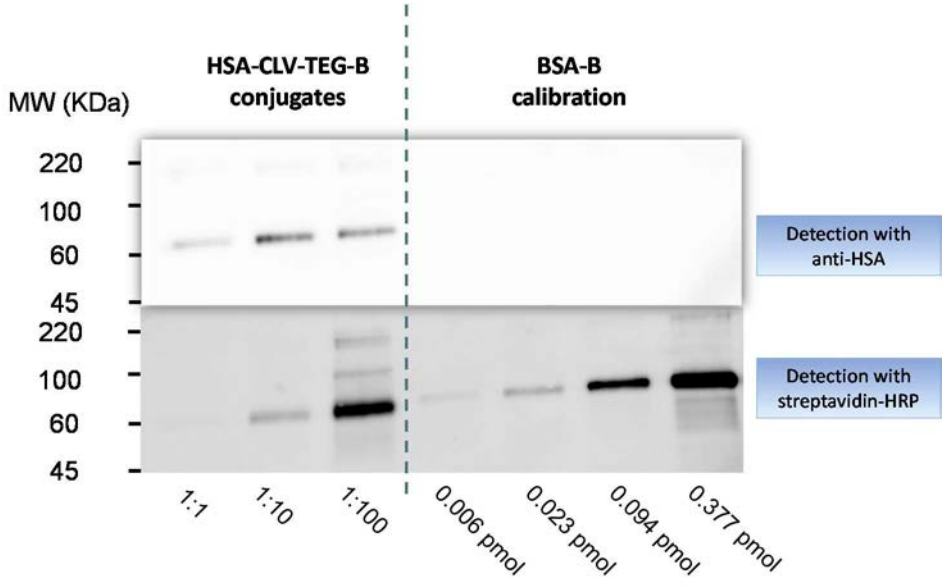

Figure II.29. Detection of HSA (top) and biotin (bottom) by Western blot. Aliquots of HSA-**CLV-TEG-B** (2 pm) (left) and BSA-B standards (right) were analyzed by SAS-PAGE followed by Western bot with α-human-HSA antibody and HRP-conjugated secondary antibody or with streptavidin-HRP followed by ECL detection.

d) Enrichment of HSA-CLV-TEG-B biotinylated fraction by avidin affinity chromatography

It is known that the extent of protein modification is not 100 % and that non-adducted protein can interfere in further analysis of the conjugated protein. Separation of the modified proteins from that which remain unmodified after incubation would improve the chance to characterize the resulting adducts. Thus, the resulting sample of the incubation of HSA with **CLV-TEG-B** at 1:10 protein/ **CLV-TEG-B** was filtered off to remove any excess of unbound **CLV-TEG-B** and then subjected to purification using agarose beads coated with Neutravidin. This purification procedure was learned during a stay of the PhD student in the group of Dr. Dolores Pérez-Sala at CIB, CSIC (Madrid) and replicated by her in our home laboratory. First, the sample was incubated with the beads for two hours at room temperature, time in which biotinylated protein would bind to the beads. Supernatant containing not bound protein was kept. Then, resin was whased with a strong buffer for elimination of unespecifically bound protein and the last washing volume kept for analysis. Finally, biotinylated fraction was released from the resine using a buffer containing SDS and β-mercaptoethanol and denaturalized for analysis. In parallel, control HSA was subjected to affinity purification as well to assay the possibility of unspecific interaction of the protein to the resin. Purification fractions were analyzed by SDS-PAGE, transferred into a PVDF membrane that was incubated with streptavidin-HRP for ECL detection and, after stripping with guanidine chloride, with Ponceau Red (Figure II.30).

As it can be seen in Figure II.30 top, comparing signal obtained for input fraction and eluted fraction from HSA- **CLV-TEG-B** after incubation with streptavidin-HRP, the later showed an enrichment of biotin signal, which means a successful purification of modified protein. Also, for not bound fraction signal is detectable with Ponceau but it is barely detectable with streptavidin-HRP, which confirms that the remaining unmodified protein after incubation was removed from the biotinylated adduct.

The lack of signal for purification carried out with control HSA after incubation with streptavidin-HRP proves that the signal obtained for HSA-**CLV-TEG-B** experiment is due selectively to biotin presence. Besides, the fact that after detection with Ponceau there is signal only for input and not bound fractions means that there is not unspecific binding of HSA to the resin (Figure II.30 bottom). The scale-up of this optimized purification method for purifying HSA-CLV-TEG-B would alow the enrichment of modified proteins in a complex mixture, increasing the chances of detection and identification of binding sites.

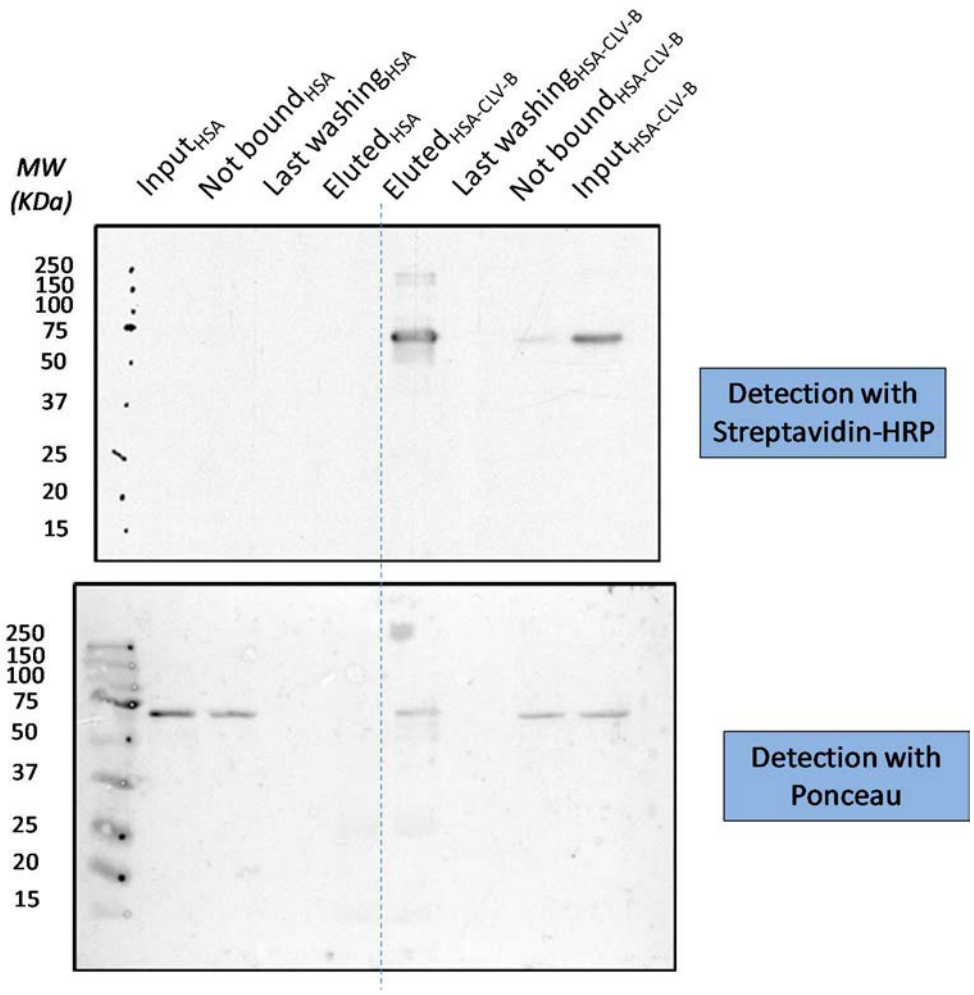

Figure II.30. SDS-PAGE analysis of the fractions obtained by affinity purification with neutravidin beads. Dotted line separates fractions obtained for control HSA on the left or HSA-**CLV-TEG-B** on the right. Top image shows results obtained after membrane incubation with streptavidin-HRP and ECL detection. Bottom image depicts results obtained after membrane incubation with Ponceau for detecting total proteins.

e) <u>CLV-CLV-B competition for protein binding sites</u>

Once probed the capability of **CLV-TEG-B** for HSA haptenization and that the degree of haptenation is dose-dependent, another experiment was designed for studying whether a similar haptenation mechanism is involved with CLV and **CLV-TEG-B**.

In order to compare the binding capacity, competition assays between both drugs were performed. HSA was incubated for 2 h with 80 mM **CLV-TEG-B**, after 16 h preincubation with the indicated concentrations of CLV (Table II.3).

Table II.3. Conjugates prepared for comparison of CLV and CLV-B haptenation ability

	$[HSA]_0$	$[HSA]_f$	$[CLV]_0$	$[CLV]_f$	$[CLV\text{-}TEG\text{-}B]_f$	V_f
CLV 0	20 mg/mL 0,3 mM	10 mg/mL 0,15 mM	0 mg/mL 0 μM	0 mg/mL 0 μM	80 μM	200 μL
CLV 1X			$3{,}80 \cdot 10^{-2}$ mg/mL 160 μM	$1{,}90 \cdot 10^{-2}$ mg/mL 80 μM		
CLV 10X			$3{,}80 \cdot 10^{-1}$ mg/mL 1600 μM	$1{,}90 \cdot 10^{-1}$ mg/mL 800 μM		
CLV 100X			3,80 mg/mL 16000 μM	1,90 mg/mL 8000 μM		

In order to study incorporation of **CLV-TEG-B** in HSA after the preincubation with CLV, aliquots of resulting conjugates were subjected to SDS-PAGE in duplicate. One of the gels was stained with Coomassie in order to check the amount of protein loaded. The second gel was transferred to a PVDF membrane, and assessed by detection with HRP-streptavidin, which allowed to detect the incorporation of **CLV-TEG-B**. Results shown (Figure II.31) are representative of three independent assays with similar results.

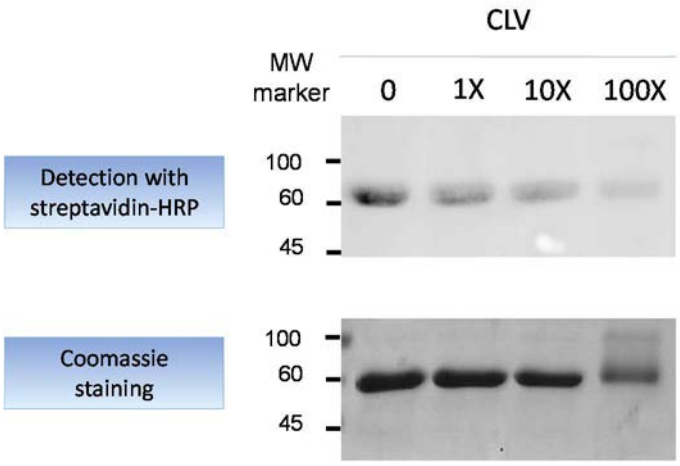

Figure II.31. Competition assay between CLV and **CLV-TEG-B**. Samples were generated by means of preincubation with increasing amounts of CLV and then, the incubation with the same amount of **CLV-TEG-B**. The incorporation to HSA of **CLV-TEG-B** was detected using streptavidin-HRP, while Coomassie staining shows protein load.

Interestingly, preincubation of HSA in the presence of an excess of CLV reduced the formation of adducts containing **CLV-TEG-B**, which means that both compounds compete for their binding to proteins, suggesting that they may bind to common sites.

II.3.5 Mass Spectrometry Characterization of HSA-CLV-B Conjugates

HSA was incubated with 1:1, 1:10 and 1:100 protein/ **CLV-TEG-B** molar ratios. Those concentrations were chosen since we intended to study 1:10 conjugate, close to physiological conditions and also analyzed for HSA-CLV, as well as a lower and a higher concentration of biotinylated derivative. Mass increments obtained after MALDI-TOF MS of conjugates were 35.4, 163.7 and 1658.9 for 1:1, 1:10 and 1:100 conjugates, respectively. With this analysis, we confirmed that HSA haptenization with **CLV-TEG-B** is dependent of the concentration of drug, the same as for haptenation with CLV. This results are in agreement with the SDS-PAGE analysis of these conjugates, in which it was demonstrated as well that the more concentration of **CLV-TEG-B** used during incubation, the more was the extent of biotinylation.

Peptides are more simple systems than a whole protein for studying drug-protein interactions since they have limited nucleophilic sites to react with BLs, so we decided to use an HSA peptide as second approach for studying the interaction between **CLV-TEG-B** and Lys in proteins. $^{182\text{-}195}$HSA peptide (LDELRDEGKASSAK), containing both Lys 190 and Lys 195, was chosen since these residues have been found to be target of modification by some drugs such as abcavir or flucoxacillin (Lys 190) [105], diclofenac (Lys 195) [105] as well as for BLs such as AX and piperacillin [105] or BP and flucoxacillin [17] (both Lys 190 and 195). Taking into account that for peptides modification conformational factor of HSA is lost, we employed more forced conditions for conjugation: peptide/**CLV-TEG-B** molar ratio 1:90, 24 hours incubation at 37˚C. After elimination of the excess of drug by size exclusion chromatography, sample was analyzed by MALDI-TOF-MS. MALDI-TOF spectra (Figure II.41X top) shows a peak belonging to the unmodified peptide 1518.686 Da) and a low peak at 2118.898 Da corresponding to the conjugated peptide. Mass increment found was Δm=600.2 Da.

These results suggest that the extent of conjugation is low since the peak belonging to the adduct formed after conjugation is really low compared with the amount of remaining native peptide. Also, we observed that only one of the two lysines were modified in the conditions used for peptide incubation and mass increment obtained could be a valuable information for further study the modification of the whole HSA with **CLV-TEG-B**.

Taking into account that the relative abundance of the adducts can be considered as a good index of the chemical reactivity of the peptide towards the β-lactam [88], since the amount of unmodified peptide after incubation is high, it can be said that **CLV-TEG-B** is not very reactive towards the peptide. This fact would be in agreement with the difficulty of the identification of the binding residues by **CLV-TEG-B**.

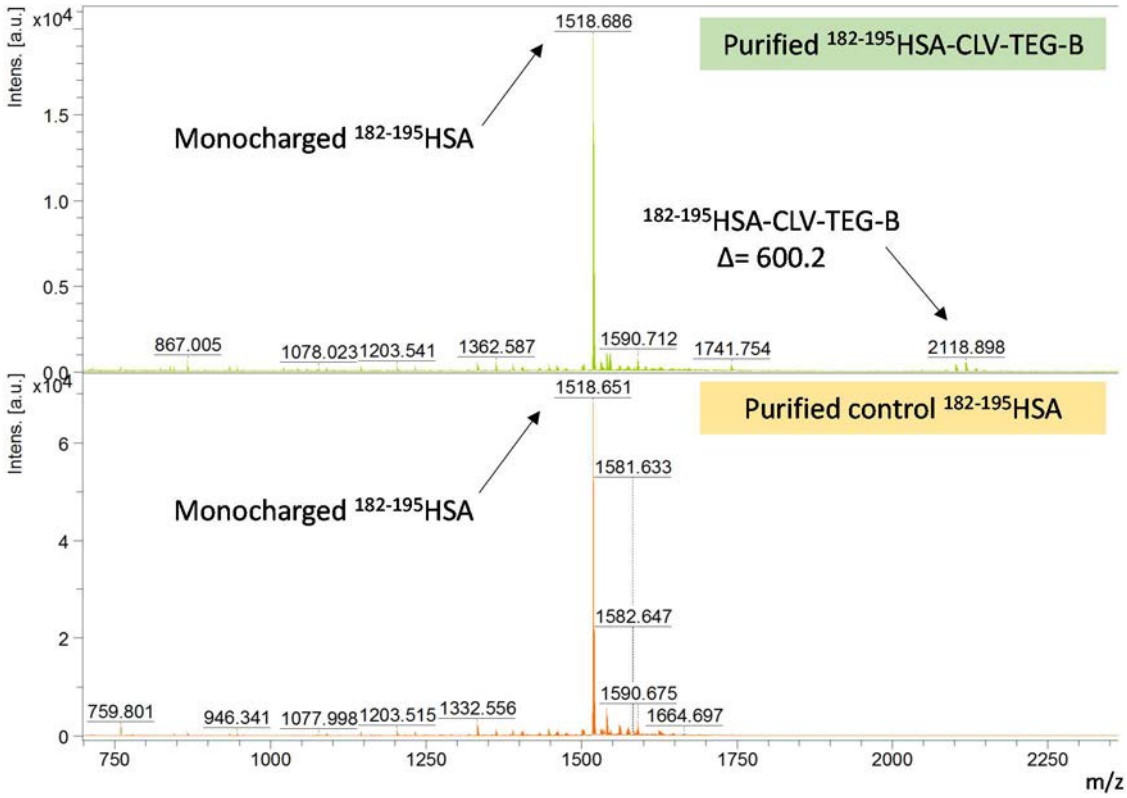

Figure II.32. MALDI-TOF MS spectra of $^{182\text{-}195}$HSA after conjugation with **CLV-TEG-B** (top) and without conjugation (bottom).

II.3.6. Characterization of HSA-CLV-TEG-B Conjugates by LC-MS/MS

In order to compare if HSA residues modified by **CLV-TEG-B** are the same as the modified by CLV, HSA-**CLV-TEG-B** 1:10 conjugate was analyzed by LTQ Orbitrap XL at University Hospital Vall d´Hebron Research Institute Proteomic Laboratory. The analysis was performed for either the conjugate by dialysis filtration after conjugation or for the biotinylated fraction enriched by passing the conjugate through a column packed with Soft Link release Avidin. However, the identification of modified residues was not possible in none of the cases. It could be due to a higher stability of **CLV-TEG-B** compared to CLV, which would difficult ionization in the former case or due to a low degree of modification. Other possibility is that the collision-induced dissociation (CID) method used for fragmentation is too aggressive and fragmentates the expected bound residue preventing the identification of the modified residues because of the search for a wrong mass increment.

We decided to perform the analysis of the conjugate using electron transfer dissociation (ETD) fragmentation mode, which is less aggressive and therefore more suitable for posttranslational modifications identification, either from biological source or chemically induced as in this case, since the structure responsible for the modification is supposed to be preserved. These experiments were carried out at Centro Nacional

de Biotecnología (CNB), Madrid, using a Bruker AmaZon Speed ionic trap for mass fragmentation after sample digestion with trypsin, chemotrypsin and LysC. Both HSA-**CLV-TEG-B** cleaned by dialysis and the conjugate cleaned and further enriched the biotinylated fraction by using an avidin resin were analyzed. Only for the enriched conjugate digested with chemotrypsin, a peptide modified with a mass of 600.22 was found: $^{404\text{-}430}$HSA with the following aminoacid sequence QNALLVRYTKKVPQVSTPTLVEVSRNL.

Table II.4. Information obtained about the modified peptide.

Accession number	Protein name	Score	Molecular weight (Da)	Peptides matched
P02768	HSA	36	3652.96	9

II.4. Detection and Identification of Serum Proteins Target of Modification by CLV-TEG-B

Despite the fact that label-dependent techniques cannot be used to study adduct formation in patients and usually do not provide information on the site of modification and/or structure of the adducts, they are quite useful to visualize adducts and to identify the modified proteins, for instance by peptide mass fingerprinting [105]. This is a big step to gain insight into adducts formation in that cases in which there are no specific antibodies against the drug moiety available (for example CLV) or the adduction takes place in such a low extention that difficults detection using label-free approaches. Furthermore, requirements for adduct detection by label-dependent approaches can be met by most biochemistry laboratories without the need of high specialized equipment and protocols.

Some studies of protein haptenation by BLs were carried out previously in our research group. By assaying serum protein adducts with AX or AX-B by 1D and 2D-electrophoresis and following Western B lot using α-AX antibodies for the AX detection or streptavidin for the biotin detection, it was observed that both compounds bind to the same serum targets (HSA, transferrin and Igs light and heavy chains), with the only difference of a weak binding to haptoglobin, which is undetectable using immunological AX detection, but is visible with AX-B due to the higher sensitivity of this method [45]. Following a similar approach, studies directed to identify serum proteins target of modification by **CLV-TEG-B** were performed. Results would be of great interest since, for the first time, serum proteins that may act as carrier in allergic reactions to CLV would be identified.

II.4.1. Conjugation of CLV-TEG-B with Human Serum Proteins and Detection of Modification

In order to study serum protein haptenation by **CLV-TEG-B**, human sera were incubated in PBS 1X (pH 7.4) with two concentrations of the biotinylated compound. Then, 4 µg aliquots of incubated sera were subjected to SDS-PAGE along with a control serum incubated with PBS 1X, transferred and detected with streptavidin-HRP and ECL (Figure II.33). Some bands were observed for the serum incubated with the highest amount of **CLV-TEG-B** and one band for the serum incubated with a lower concentration. No band was observed in the lane corresponding to the control sera, indicating that signal was specifically detected for biotinylation. Comparison with Coomassie staining revealed that the amount of protein loaded in each lane was the same and thus, intensity change observed for detection with streptavidin-HRP is only due to the modification of samples by **CLV-TEG-B**.

Also, with this experiment, we proved that biotinylated CLV was covalently attached to its target proteins.

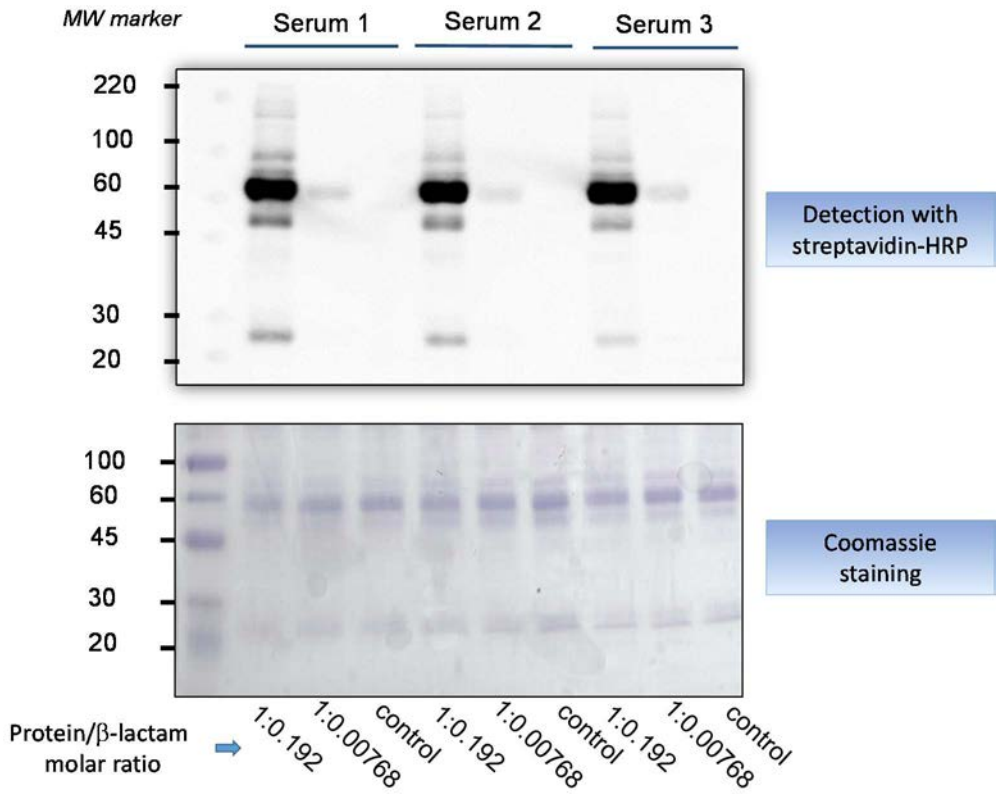

Figure II.33. Detection of biotinylated serum proteins (top) and total protein pattern with Coomassie staining (bottom).

II.4.2. Identification of Serum Proteins Target of Modification by Peptidic Fingerprint

Monodimensional SDS-PAGE allowed us to confirm that besides HSA, other serum proteins were target of haptenation by **CLV-TEG-B** but further studies were necessary for identification of these proteins. 2D-electrophoresis gives more information about samples in which several proteins are present since separation is based in both isoelectric point (first dimension) and molecular weight (second dimension). Thus, sera samples incubated with **CLV-TEG-B** at 1:0.192 total protein/ **CLV-TEG-B** ratio and control serum were analyzed by 2D-electrophoresis, running two gels in parallel. 2D-electrophoresis experiments were performed during the PhD student stay in the group of Dr. Dolores Pérez-Sala in Madrid. One of the gels was transferred and biotinylated proteins detected with streptavidin-HRP. The second gel was used for total proteins detection by Coomassie staining (Figure II.34) and "spots" of interest were excised, digested with trypsin and identified by peptidic fingerprint using MALDI-TOF-TOF MS (Table II.5). This proteomic analysis was performed in the Proteomics Unit of Complutense University of Madrid.

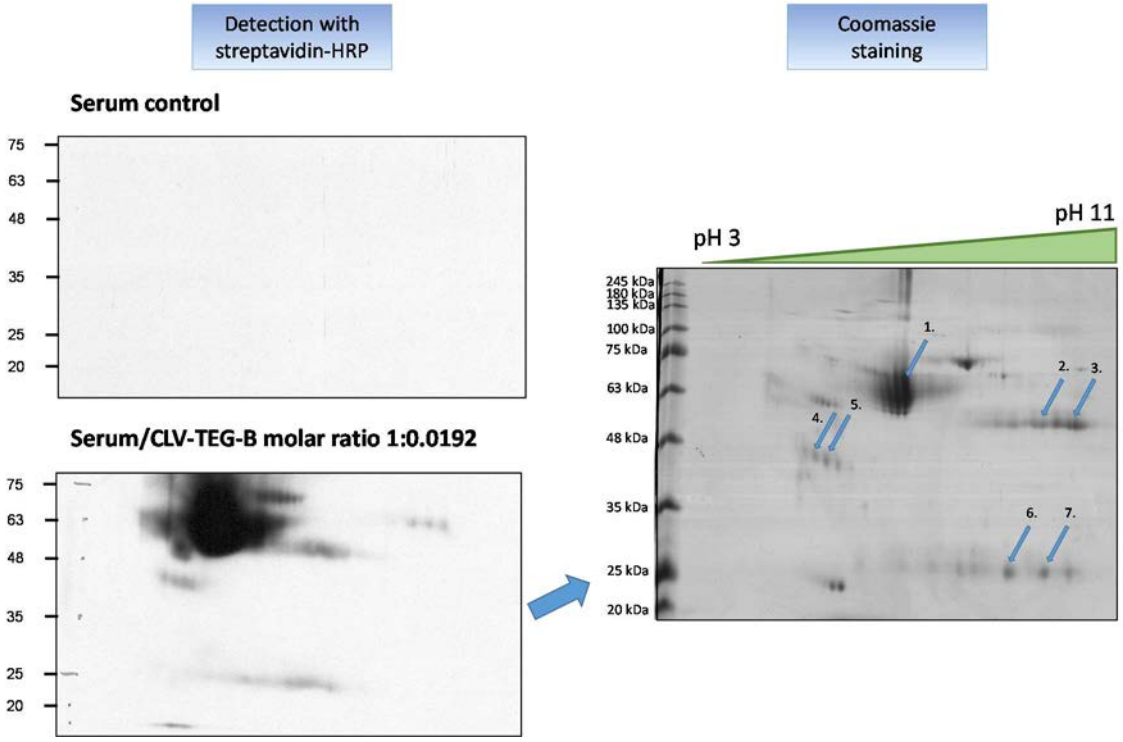

Figure II.34. Detection of adducts of **CLV-TEG-B** and serum proteins and identification of targets.

Serum proteins modified by **CLV-TEG-B** identified in this assay were HSA, haptoglobin and heavy and light chains of inmunoglobulins (Table II.5). The lack of monoclonal antibodies against CLV prevents the immunological evaluation of protein-CLV adducts and, therefore, we could not compare whether the proteins haptenated by CLV are the same as the modified by its biotinylated derivative as Ariza *et al*. did [45, 88]. One of the aspect that should be taken into account is that the presence of the biotin moiety may impose steric impediments for binding to some targets or it may shield part of the molecule [45]. However, we have set up a model that may shed light into the process of protein haptenation by CLV through the use of highly sensitive approaches, such as labeling with biotinylated analogs, which allow the detection of its target serum proteins.

Further structural information on the binding sites on various targets would provide potential ADs to be used in diagnostic procedures and in studies on the mechanisms of CLV induced allergy.

Table II.5. Identification of serum proteins modified by **CLV-TEG-B** by peptidic fingerprint by tryptic digestion and MALDI-TOF MS.

Spot	Accession Number	Protein name	Total score	Limit score	Molecular weight (Da)	pI	Peptides matched	Coverage (%)
1	P02768	HSA	470	56	71317	5.92	43	69
2	P01857	Ig gamma-1 chain C region human	119	56	36596	8.46	13	52
3	P01857	Ig gamma-1 chain C region human	197	56	36596	8.46	18	66
4	P00738	Haptoglobin human	128	56	45861	6.13	18	35
5	P00738	Haptoglobin human	102	56	45861	6.13	16	33
6	P01834	Ig kappa chain C region human	86	56	11773	5.58	7	76
7	P01834	Ig kappa chain C region human	66	56	11773	5.58	6	76

III. Antibody labeling for detecting sIgE in drug allergy

The term "immunoassay" refers to the use of antibodies raised against an analyte of interest with the purpose of detecting the presence of that analyte in a sample. Two important parameters of a reliable immunoassay are specificity and sensitivity, that is to say, the analyte should be selectively detected even in presence of big amount of interfering substances and detectable at the low concentrations required for most applications. Specificity is provided by antibodies raised against the analyte of interest, whereas sensitivity relies on coupling of analyte-antibody binding with a detectable and quantifiable signal [238] (radioactivity, luminescence or enzymatic process).

Sensitive and specific detection of analytes of interest in biological samples is crucial for *in vitro* diagnosis. Biological samples are really complex, containing a huge number of different proteins which makes detection of a specific molecule a special challenge. Also, some proteins, as is the case of sIgE to drugs, are in an extremely low concentration making it difficult to obtain good sensitivity using simple fluorophores [238].

The use of antibodies as detection method requires some way of labeling of the antibody with an easily detectable reporter molecule such as radioisotopes, luminophores or enzymes. First immunoassays used antibodies labeled with radioisotopes and detection using scintillation counters. Although they are high sensitive, problem related with stability and safe disposal of radioisotopes leaded to the development of alternative detection strategies, being the most important enzyme conjugated antibodies, in which an enzymatic reaction leads to a colored product that can be measured by colorimetry. Amplification is the best advantage of these kind of assays but linear range of colorimetic detection is limited and color development requires additional time, steps and reagents. Fluorophore labeled antibodies allow direct measure of immunocomplex on the surface or in solution but conversely, no amplification occurs, requiring very bright luminescence from the fluorophore or high degrees of labeling [238].

This chapter is dedicated to develop antibody labeling methods for signal detection in *in vitro* tests for drug allergy diagnosis. By one hand, we optimized the radiolabeling of a highly specific α-human IgE for our in-house RAST assays. On the other hand, we designed, synthesized and characterized a series of fluorescent dendron structures bearing multiple fluorescent units and proved their suitability for antibody labeling and fluorescent signal amplification for future use in microarray platforms.

III.1. Radiolabeling of a High Specific α-human IgG

Many of the studies performed in our research group which are focused on drug allergy, rely on the use of in-house RAST immunoassays. This practice has been prevented for the last years due to the withdrawal from the market of α-IgE antibodies radiolabeled with ^{125}I, commercialized by Phadia. Other radiolabeled antibodies from different providers were useful for performing RAST assays to allergens but not to drugs, whose outcome was inespecific results with not enough sensitivity. This is likely due to the low concentration of sIgE associated to drug allergy. We got the α-IgE previously provided by Phadia, a mix of two α-IgE monoclonal antibodies, but unlabeled. That is why we arise the optimization of a method for radiolabeling this mix of specific secondary antibodies, which would be evaluated with different samples for validation and making sure that its use is reliable and reproducible for sIgE detection in drug allergy.

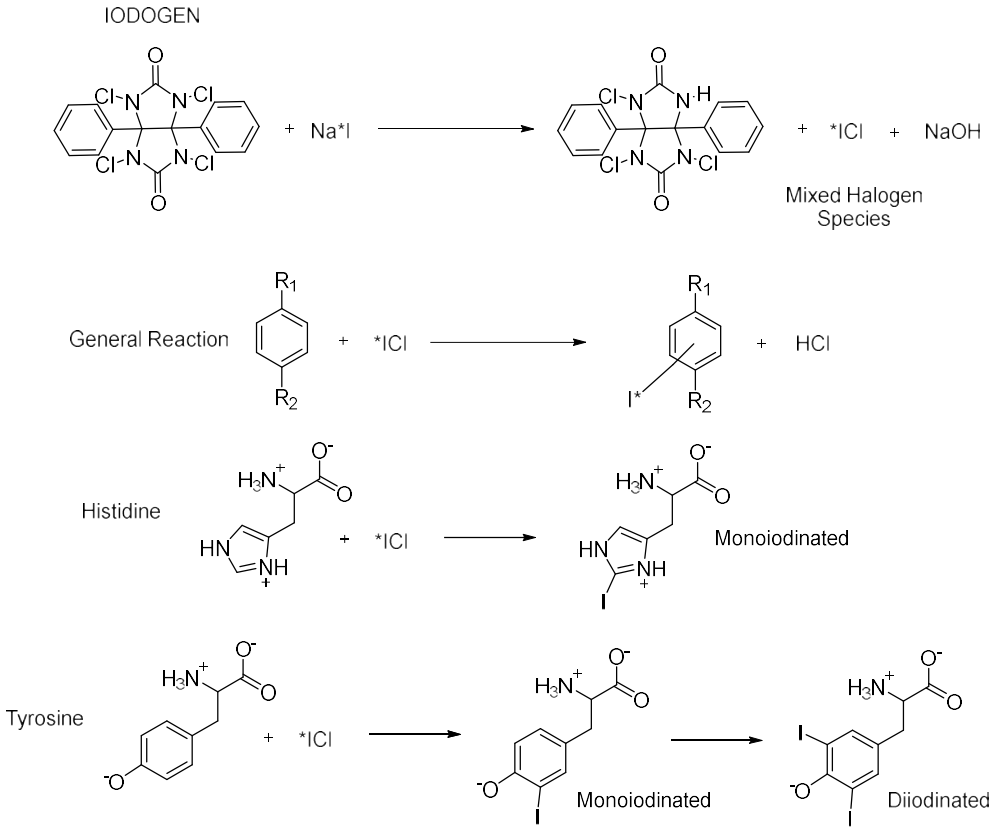

Figure III.1. Oxidation reaction of Iodogen.

Nowadays there are several commercial reagents for general protein radioiodination. We have selected Iodogen, 1, 3, 4, 6- tetrachloro-3α, 6α-diphenylglycouril, an effective and mild oxidizing agent. The advantages of Iodogen over other alternative reagents previously used for radiolabeling such as chloramine T, lactoperoxidase/hydrogen

peroxide and ^{125}I-labeled Bolton-Hunter reagent are that the reaction is rapid, technically simple to perform, and gives reproducibly high levels of incorporations of radioactivity [239] with minimal oxidative damage to the protein [239, 240]. Iodogen is insoluble in aqueous phase so a solution in dichloromethane or chloroform is used to prepare a thin film of material on the walls of the reaction vessel. The reaction of Iodogen with aqueous solution of $Na^+/^{125}I^-$ results in oxidation with generation of the reactive intermediate (I^+/I_3^+), in form of mixed halogen species, that participates in electrophilic attack primarily at tyrosine but also at histidine residues in the protein with minimal oxidative damage to the protein [239]. Oxidative side reactions such as damage to sensitive residues (particularly methionine and tryptophan) is much less using Iodogen [239, 240]. Oxidation reaction of Iodogen is depicted in Figure III.1.

III.1.1. Labeling optimization

Labeling procedures were carried out by the PhD student at SCAI, UMA. In order to optimize the protocol, pre-coated iodination tubes (with Iodogen) were employed to label a commercial α-IgE antibody in aqueous solution. Two different concentrations of ^{125}NaI were used to evaluate the efficacy of the method. After labeling, the protein fractions were purified by size exclusion chromatography, collecting 0.5 mL fractions (Figure III.2).

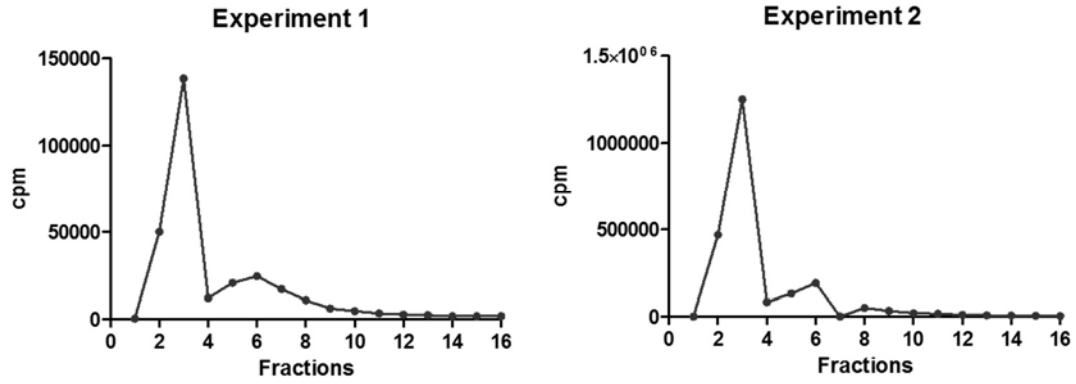

Figure III.2. Elution profile obtained in labeled IgG purification.

Elution profiles allowed to identify fractions 2 and 3 as the ones containing the radiolabeled IgG. Fraction 4 and followings correspond to unreacted NaI^{125}.

Results obtained with different concentration of NaI^{125} are compared in Table III.1, and we can conclude that the more efficient iodination conditions for IgG labeling involved the use of the higher concentration of NaI^{125} (250 μCi).

Table III.1. Labeling results for Experiment 1 and Experiment 2.

	75 µCi	250 µCi
Iodination yield (%)	43.6	54.0
Incorporated activity (µCi)	32.7	135
Specific activity (µCi/µg)	2.18	9.0

III.1.2. Labeling of α-human IgE monoclonal antibody with ^{125}I

Once optimized labeling protocol, the antibody that was to be used in immunoassays was labeled. After size exclusion chromatography, the purification elution profile (Figure III.3) was obtained, indicating that fractions 2 and 3 contained the labeled antibody.

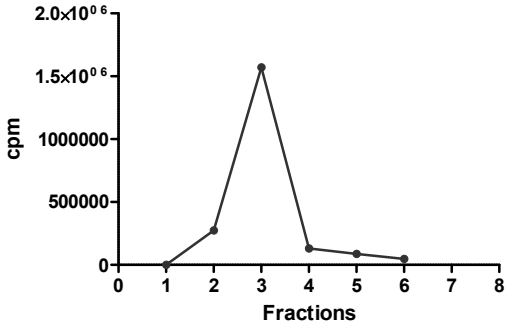

Figure III.3. Elution profile obtained in labeled IgG purification.

After pertinent calculations, we obtained 58.2 % iodination yield, 145.6 µCi incorporated activity and 9.7 µCi/µg specific activity. Both fractions containing labeled antibodies were combined and dissolved in similar buffer conditions to that of previously commercialized by Phadia (1.5% (w/v) BSA in PBS 1X pH 7,4-Tween 0,1%).
Final antibody concentration was 0.15 µg/mL and activity per volume was 1.57 µCi/mL, even higher than the activity per volume of the labeled antibody previously commercialized by Phadia (1.06 µCi/mL).

III.1.3. Labeled IgG sensitivity evaluation by Radio Allergo Sorbent Test (RAST)

PhD student evaluated these labeled antibodies by RAST using sera from well-phenotyped patients and compared the results with other α-IgE antibodies or isotopic labeling procedures.

First, sera from six patients allergic to AX and six tolerant controls (non-allergic to BLs) were included in the study, and RAST results using the same antibody but with different label procedures were compared: the former commercial Phadia antibody, the one

labeled by a company (Chelatec) and the one labeled using our optimized protocol (Figure III.4).

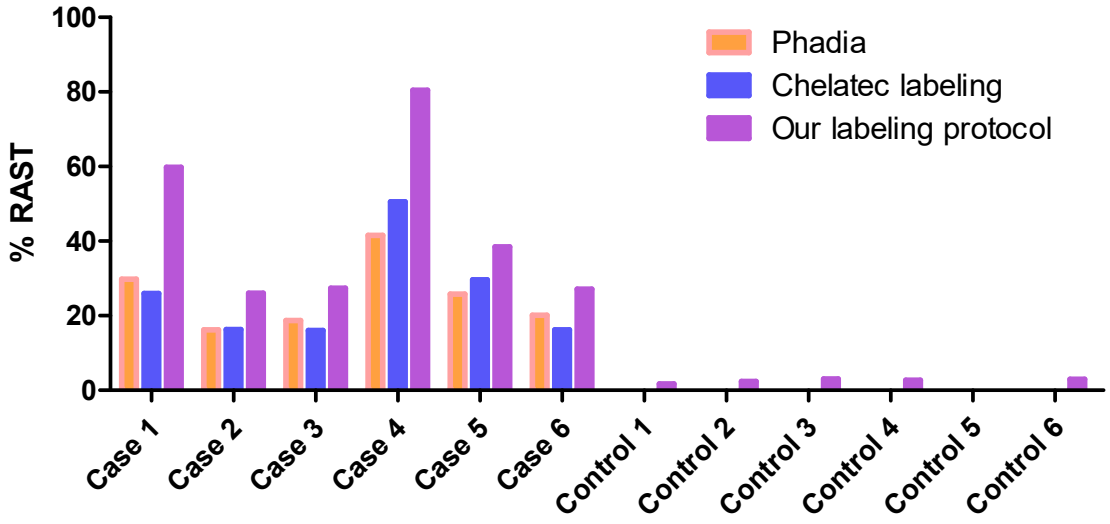

Figure III.4. % RAST results comparison.

Results obtained with the antibody labeled using our optimized procedure show clear positive % of RAST results for all patients allergic to AX, having in mind that % of RAST > 4.8 (the mean +2SD of a negative control group) were considered positive. Moreover, the values of RAST obtained in all AX positive cases with this antibody were higher than those obtained with the other commercial batches (Phadia and Chelatec labeling). From this follows that we got a sensitivity improvement with our labeling conditions. Additionally, RAST results for control individuals were lower than 4.8 % in all cases, indicating that specificity is not affected.

In order to further assay the sensitivity of the labeled antibody, sera from 40 patients allergic to cefaclor were evaluated. These sera had already been assayed by RAST using another batches of Phadia antibody or even using a commercial radiolabeled antibody kindly provided by ALK-Abelló. Results obtained are compared in Figure III.5.

Again, % of RAST results obtained with our antibody labeling are higher than for the rest of batches for most of cases, confirming that the developed procedure is appropriate for the isotopic labeling of antibodies for further detection in immunoassays.

It should be noted that those cases with negative RAST results can be due to other factors intrinsic to the sensitivity of the technique.

As a result, high specific α-human IgE monoclonal antibody labeling with I^{125} was optimized for in-house RAST assays, allowing the performance of immunoassay with a high specificity and improved sensitivity.

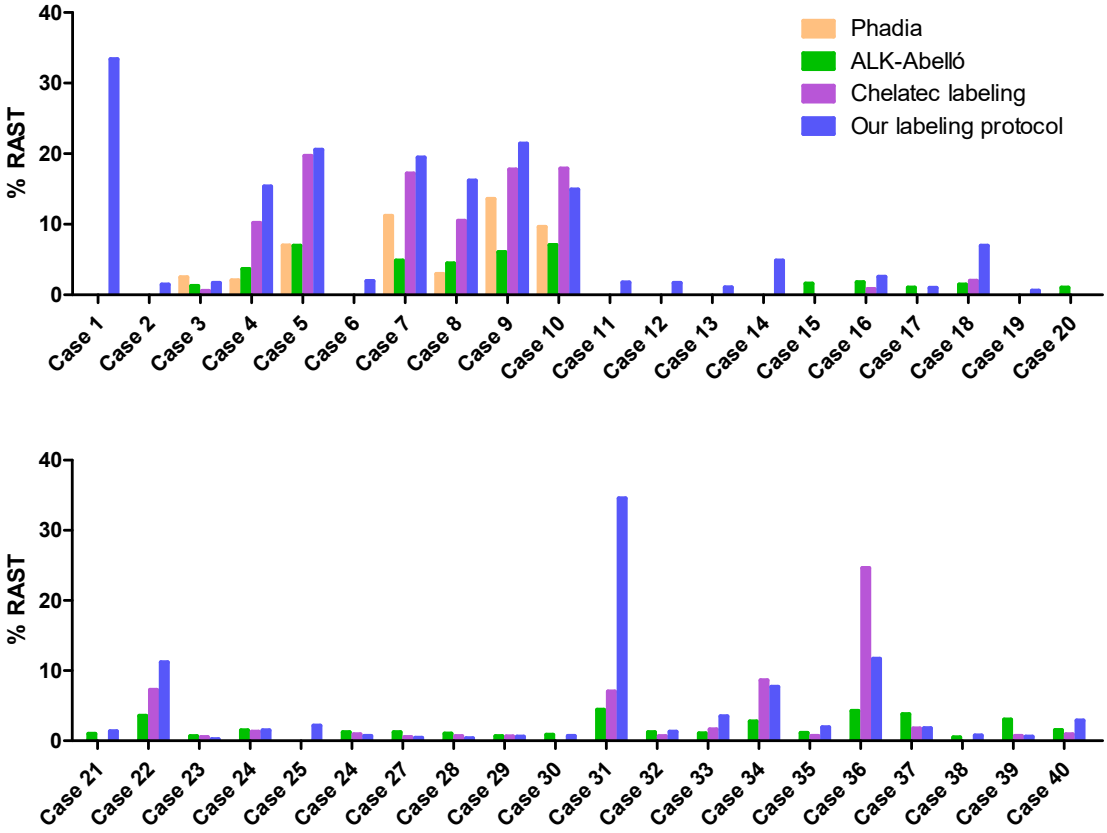

Figure III.5. % RAST results comparison.

III.2. Multivalent fluorescent dendritic probes for immunoassays signal amplification

Dendrons, as highly branched and monodisperse wedge-shaped scaffolds with multiple peripherial end-groups and a single reactive functionality at the focal point, bring the option of orthogonal reactions [151, 241] suited for site-specific labeling of biomolecules [149, 150]. For instance, Wängler *et al.* [150] synthesized a library of PAMAM dendrons being peripherally decorated with various fluorescent dyes and encompassing a single thiol functionality at the focal point. In their work and for most of fluorescently labeled dendrons, the fluorescence signal decreased with increased number of dye units, and only dansylated dendrons met the requirements of enhanced fluorescence signals.

Independent on conjugation chemistry or orthogonal linkers, cyanine-based dyes are one of the most promising Near Infrared (NIR) dyes, ideal for *in vivo* and *in vitro* optical imaging [242]. Among them, Cy5 has been identified as the champion as it can be excited at wavelength above 600 nm *i.e.* where the auto-fluorescence background of live cells is lower by orders of magnitude as compared with the excitation range of TMR (tetramethylrhodamine), Cy3, and Cy3.5 [169]. Moreover, scanners in microarray

systems have the capacity for signal detection of Cy5. Most examples in literature detail the monovalent conjugation of Cy5 probes using simple bifunctional linkers [194, 195, 243-247]. Dendrimers functionalized with Cy5 substituents, either at periphery [192, 248, 249] or at focal point [241, 249, 250], have also been reported on as monodisperse scaffolds, including popular PAMAM [248] or 2,2-bis(methylol)propionic acid (bis-MPA) [250] architecture among others. The bioconjugation of Cy5 *via* covalent linkages to the target molecule often involves click chemistries [192, 194, 195, 246] although 1, 2-addition reaction [243], or reaction with amines through NHS chemistry [247] have also been described. Of note is the use of hydrazide [244] or hydrazine [245] monovalent Cy5 probes, since they react selectively with carbohydrate on the Fc region of antibodies, with a well-defined stoichiometry of conjugation, without affecting the binding site of the biomolecule.

III.2.1. Design of Fluorescent Dendrons for Site Specific Antibody Labeling with Application in Microarray Systems

From the great number of dendritic scaffolds available, orthogonally functionalized dendrons based on bis-MPA belong to the most desirable scaffolds for biomedical applications. This is mainly due to their biodegradable and biocompatible profile, facile synthesis, proven flawless nature as well as the large and exact number of functional groups with orthogonal features [251].

Herein, we propose the synthesis of a set of novel probes displaying mono or multivalent hydrazine/dye functionalities. The multivalent features capitalizes on dendrons based on bis-MPA as sophisticated orthogonal linkers with amplifying capacity, Figure III.6.

To explore bis-MPA based frameworks as versatile fluorescent amplifiers for enhanced detection of biomolecules we sought out a novel synthetic scheme. The dendrons targeted should display (i) a single hydrazine functionality in the focal point, for chemoselective reaction with carbonyl from aldehydes present on the biomolecules; (ii) TEG extender that provides spacious distance between the hydrazine group and the main dendritic skeleton to avoid steric hindrance during bioconjugation and promote solubility in aqueous media; and (iii) multiple fluorescent Cy5 moieties at the periphery, for signal amplification.

For the introduction of fluorescence to the orthogonally functionalized probes, Sulfo-Cyanine 5 azide (sulfo-Cy5-azide) was chosen. This due to its (i) excitation maximum at 646 nm, which makes it suitable for microarray scanner systems; (ii) azide functionality that allows for coupling to alkyne decorated dendrons via CuAAC and (iii) additional sulfo-groups that facilitate water solubility and decrease aggregation of dye molecules in heavily labeled conjugates [252].

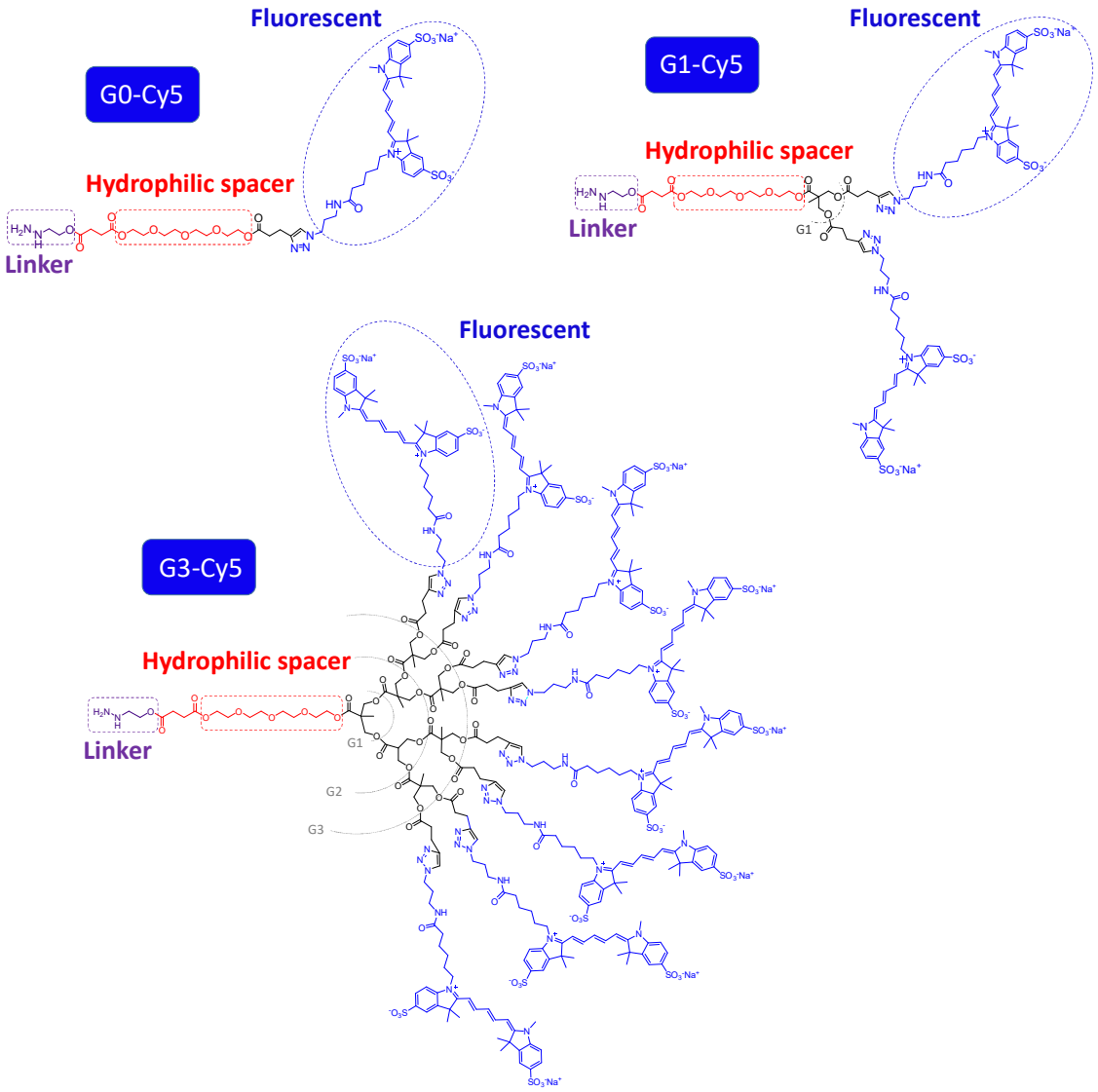

Figure III.6. Mono and multivalent hydrazine/dyes probes consisting of hydrazine functionalization as linking group, a hydrophilic TEG spacer and one or multiple units of fluorescent.

III.2.2. Synthesis of Fluorescent Dendrons

A set of fluorescent dendrons (**G0-Cy5**, **G1-Cy5** and **G3-Cy5**) were synthesized prior to their bioconjugation to Ig as a model biomolecule (Figure III.6). The synthesis as well as NMR and MALDI characterization of fluorescent dendrons were carried out by the PhD student during a stay at Royal Institute of Technology (KTH) in Stockholm, Sweden, funded by a FEBS Summer Fellowship.

Initially, the precursors were constructed to exhibit the appropriate orthogonal functionalities: protected hydrazine in the focal point and alkyne groups in the periphery, for further dye functionalization via click chemistry. A more in-depth description of the synthetic strategy is shown in Scheme III.1.

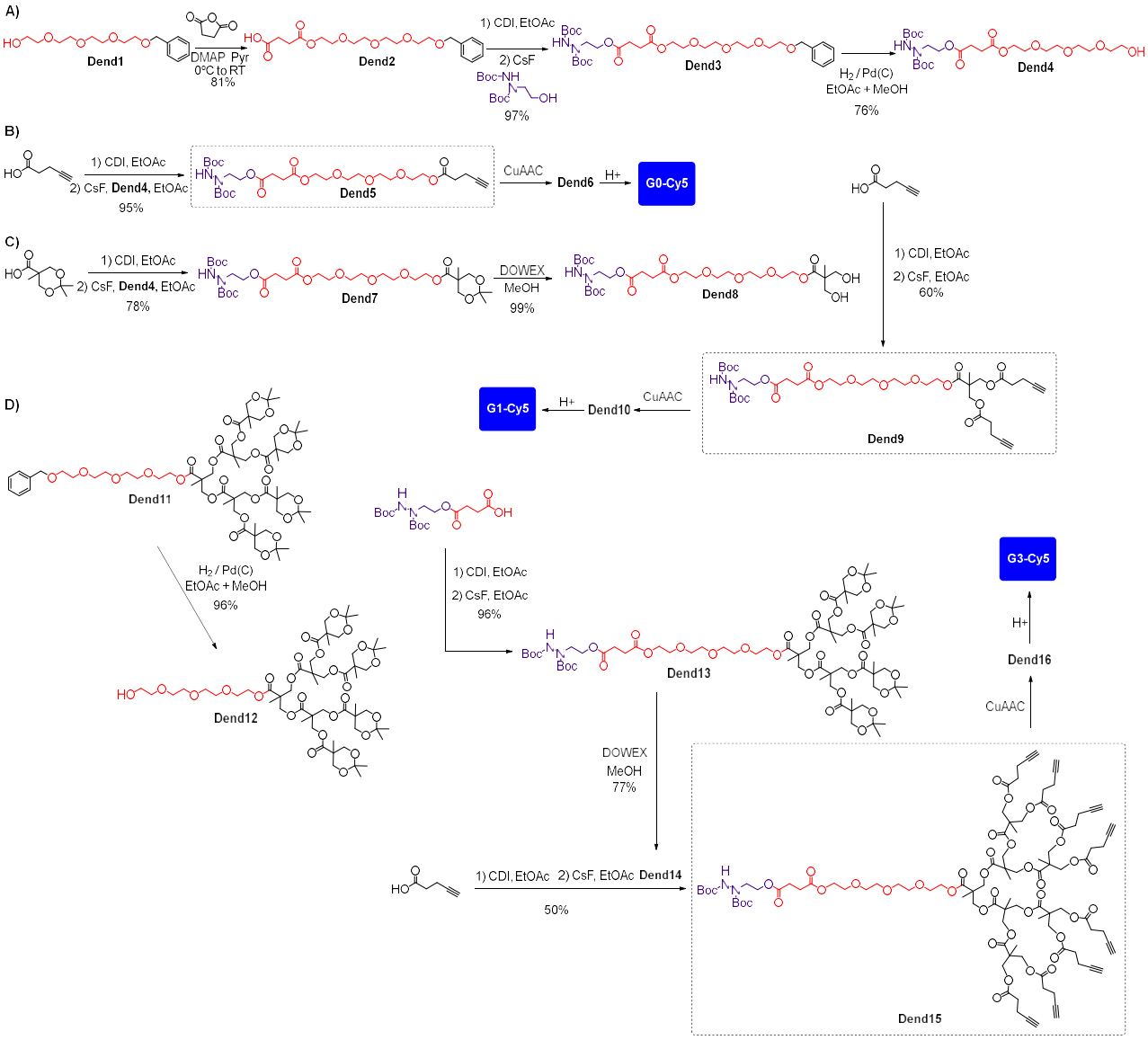

Scheme III.1. Synthesis of fluorescent dendrimers. A) Spacer synthesis based on derivatization of a TEG chain with a diboc-protected hydrazine containing molecule. B) Synthesis of **G0-Cy5** bearing one fluorescent moiety. C) Synthesis of dendron **G1-Cy5** bearing two fluorescent moieties. D) Synthesis of dendron **G3-Cy5** bearing eight fluorescent moieties.

First, Boc- hydrazine-TEG-OH **Dend4** was synthesized in four consecutive reaction steps (Scheme III.1A). The synthesis was initiated by the derivatization of TEG as benzyl protected TEG (**Dend1**) [151]. Then after, a succinic moiety was incorporated to yield the carboxylic acid functional **Dend2** that facilitated covalent coupling of amino-protected diboc-2-hydroxyethylhydrazine, *via* fluoride promoted esterification (FPE) chemistry [253] resulting in **Dend3**. The benzyl group was deprotected using catalytic hydrogenation resulting in the Boc-hydrazine-TEG-OH **Dend4** with an average yield of 85%.

Figure III.7 shows ^{1}H-NMR evidence of the condensation of **diboc-hydrazine** and **Dend2**, since the methylene next to the hydroxyl group in **diboc-hydrazine** was displaced from 3.63 ppm to 4.30-4.21 ppm in **Dend3** due to the esterification that took place. Also, aromatic signals at 7.35-7.32 in **Dend3** disappeared in benzyl deprotection product (**Dend4**). Figure III.8 shows MALDI-TOF characterization.

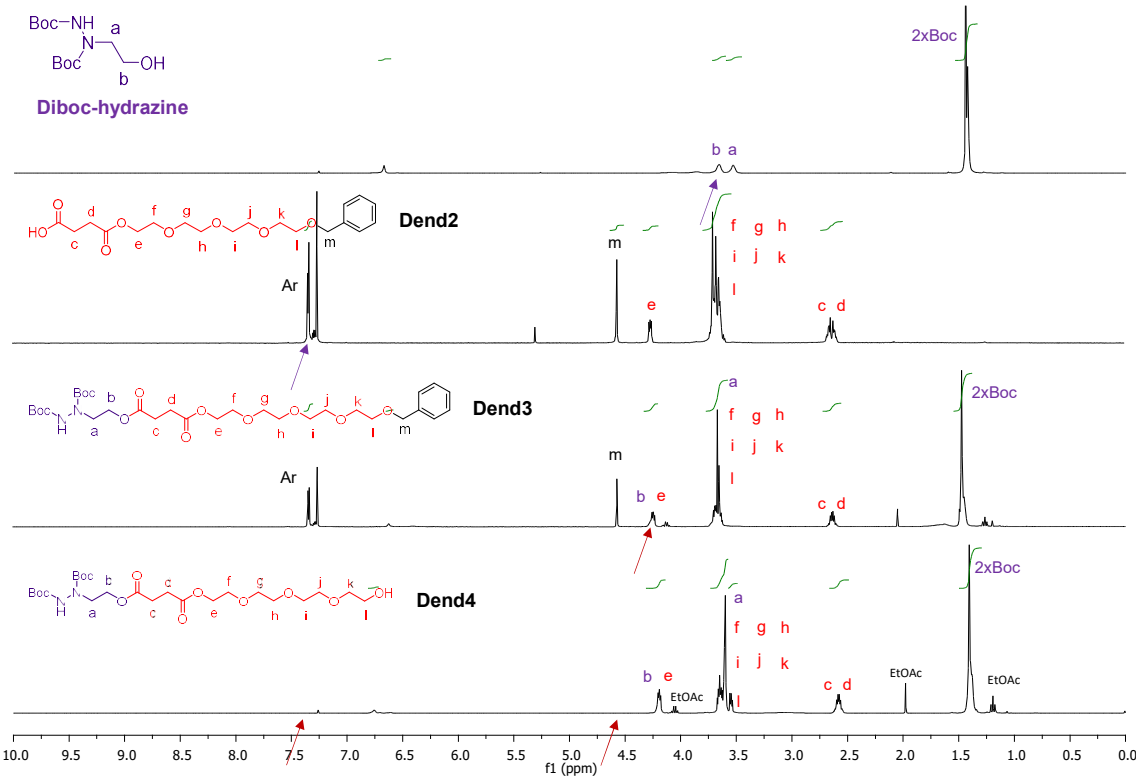

Figure III.7. ^{1}H-NMR monitoring of reactions necessary for obtaining the TEG derived spacer **Dend4.**

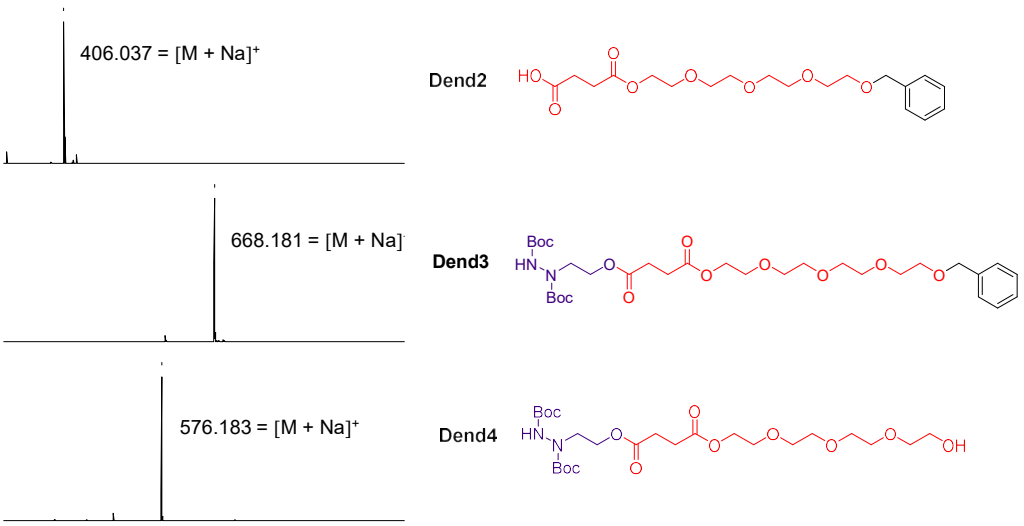

Figure III.8. MALDI-TOF characterization of **Dend2**- **Dend4**.

To generate the mono and multivalent hydrazine/dye probes, **Dend4** was used as a precursor. In one end, the 4-pentynoic acid was covalently attached *via* FPE chemistry which yielded **Dend5** in a quantitative yield. This represents the G0 dendron with protected hydrazine and bearing one alkyne group, ready for click functionalization (Scheme III.1B).

^{1}H-NMR spectra in Figure III.9, provide evidence of the condensation of **Dend4** and 4-pentinoic acid, since the methylene next to the hydroxyl group in **Dend4** is displaced from 3.57-3.52 ppm to 4.26-4.18 ppm in **Dend5** due to esterification and 4-pentinoic acid methylene signals appeared at 2.56-2.52 and 2.50-2.44 ppm and methyne triplet at 1.95 ppm. Figure III.10 shows MALDI-TOF characterization.

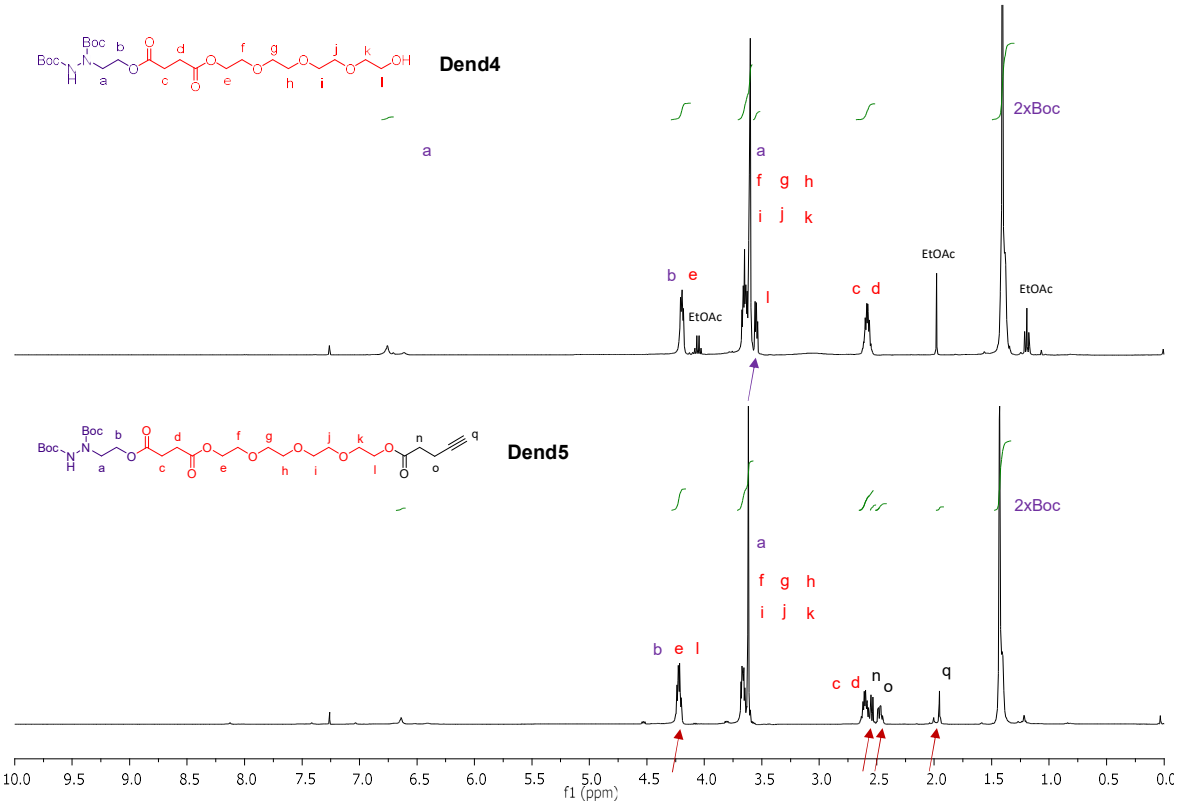

Figure III.9. ^{1}H-NMR monitoring of reaction to obtain **Dend5** starting from **Dend4**.

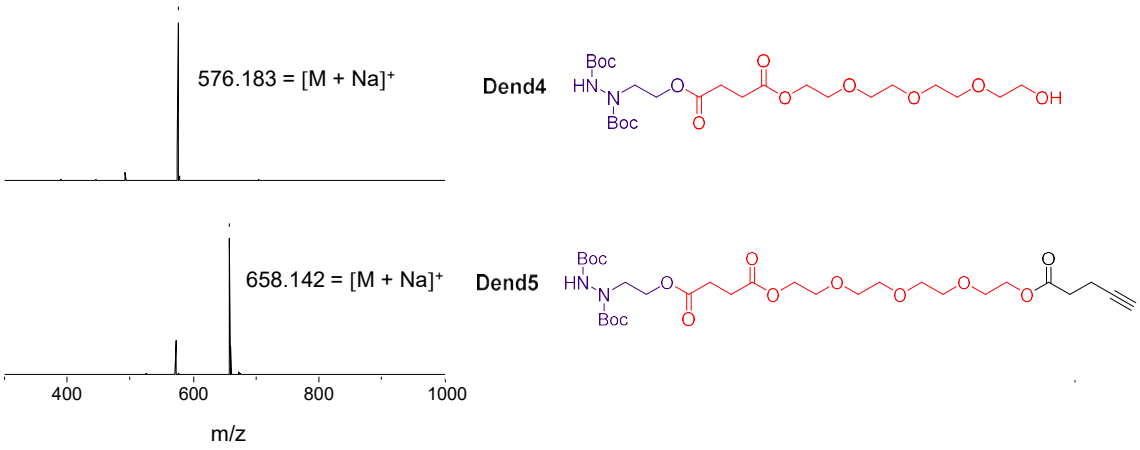

Figure III.10. MALDI-TOF characterization of **Dend4**- **Dend5**.

In the other end, the use of growth/activation divergent growth approach resulted in dendron G1 (**Dend9**), displaying two peripheral alkyne groups (Scheme III.1C). In contrast to the G1 (**Dend9**), the G3 (**Dend15**), with eight peripheral alkyne groups, was synthesized as previously reported [151] prior to the deprotection by palladium-catalyzed hydrogenation, introduction of succinic modified diboc-2-hydroxyethylhydrazine and finally the functionalization with peripheral alkynes (Scheme III.1D). In both cases, the dendritic frameworks were isolated in an average yield of 80% (Scheme III.1C-D). The synthesis of the three alkyne decorated molecules (**Dend5**, **Dend9** and **Dend15**) and their intermediates were monitored by ^{1}H-NMR (Figures III.9, III.11 and III.13) and ^{13}C-NMR as well as by MALDI-TOF MS (Figures III.10, III.12 and III.15).

^{1}H-NMR spectra in Figure III.11 provide evidence of the condensation of **Dend4** and acetonide protected bis-MPA, since the methylene next to the hydroxyl group in **Dend4** is displaced from 3.57-3.52 ppm to 4.32-4.16 ppm in **Dend7** due to esterification, and also, we can see a doublet at 4.22 ppm and a singlet at 1.22 ppm belonging to methylene and methyl groups in bis-MPA, respectively, and two singlet at 1.43 and 1.39 ppm belonging to methyl groups in acetonide protection. We can see in **Dend8** the disappearance of singlets belonging to acetonide methyl groups as the clearest evidence of deprotection and also, methylenes in bis-MPA moiety move to 3.78 ppm. Finally, in compound **Dend9**, due to esterification with 4-pentinoic acid, bis-MPA methylenes move to 4.34-4.22 ppm and alkyne methylene signals appear at 2.58-2.58 and 2.52-2.46 ppm and methyne triplet at 1.98 ppm. Figure III.12. gathers MALDI-TOF characterization of **Dend4**, **Dend7- Dend9**.

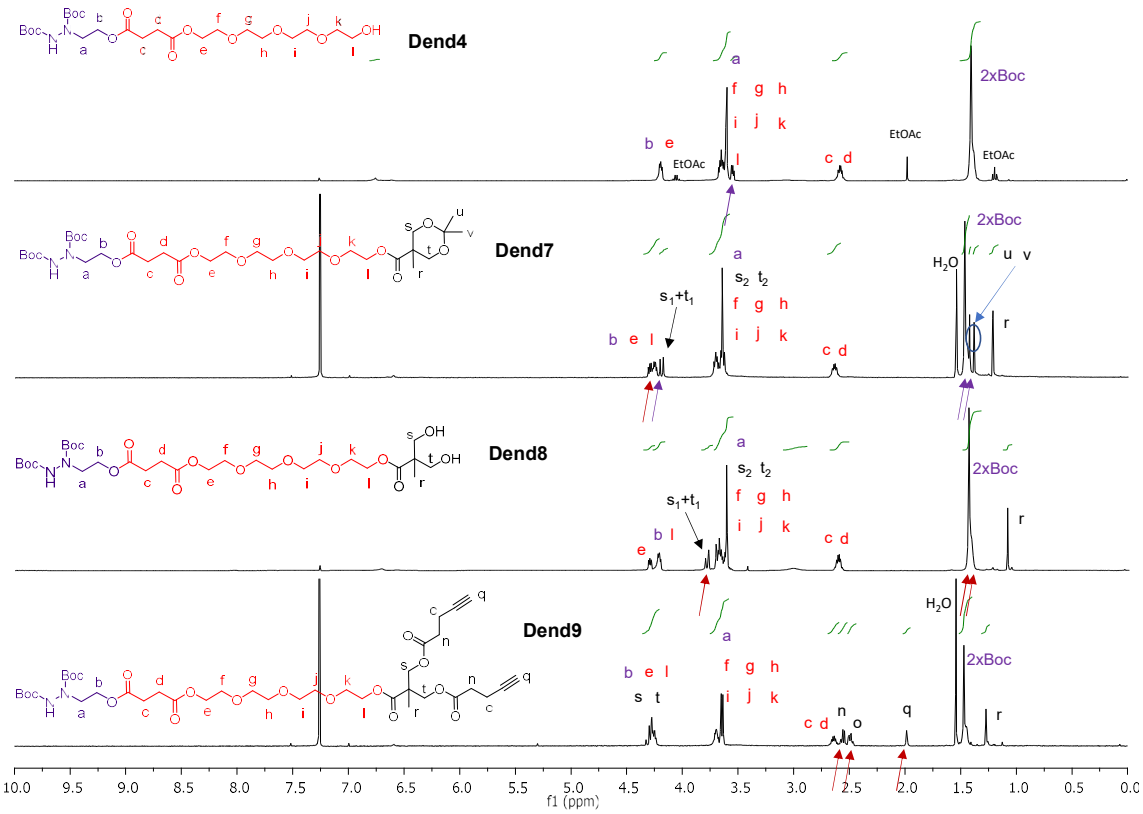

Figure III.11. ^{1}H-NMR monitoring of synthesis of the divalent alkyne decorated dendron **Dend9** from the TEG derived spacer **Dend4.**

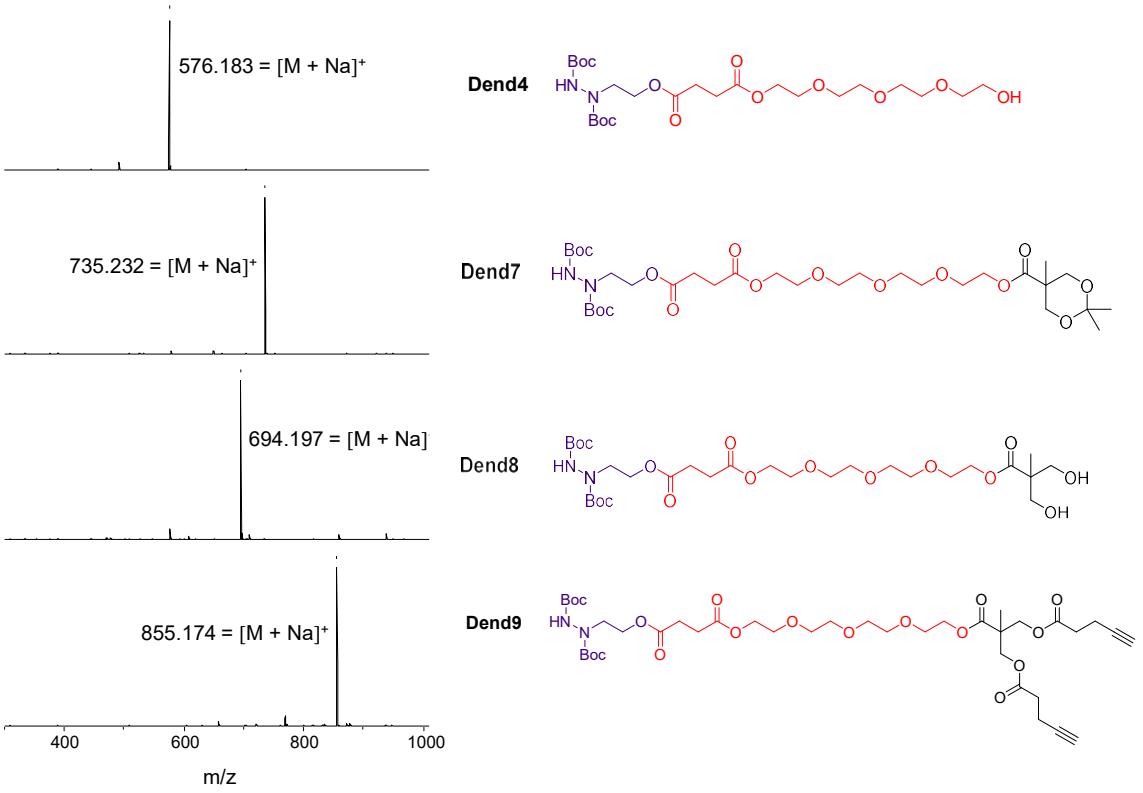

Figure III.12. MALDI-TOF characterization of **Dend4**, **Dend7- Dend9**.

In Figure III.13, the incorporation of **diboc-hydrazine-succinic** moiety to the dendron **Dend12** to afford **Dend13** is proved. The shift of methylene next to the hydroxyl in TEG chain from 3.74-3.18 ppm to 4.36-4.23 ppm multiplet due to esterification is observed. Also, there is evidence of acetonide deprotection in **Dend14** since singlets at 1.37 and 1.31 ppm belonging to methyl groups in acetonide moiety in **Dend13** disappear. Also, esterification of **Dend14** with 4-pentinoic acid to afford **Dend15** can be confirmed by displacement of signals belonging to methylenes next to the peripheral hydroxyls from 3.79-3.54 ppm to 4.37-4.10 and appearance of new signals from alkyne incorporation as methylenes at 2.58-2.51 and 2.50-2.43 ppm and methyne at 2.00 ppm. Characterization of these molecules was completed with MALDI-TOF (Figures III.14 and III.15).

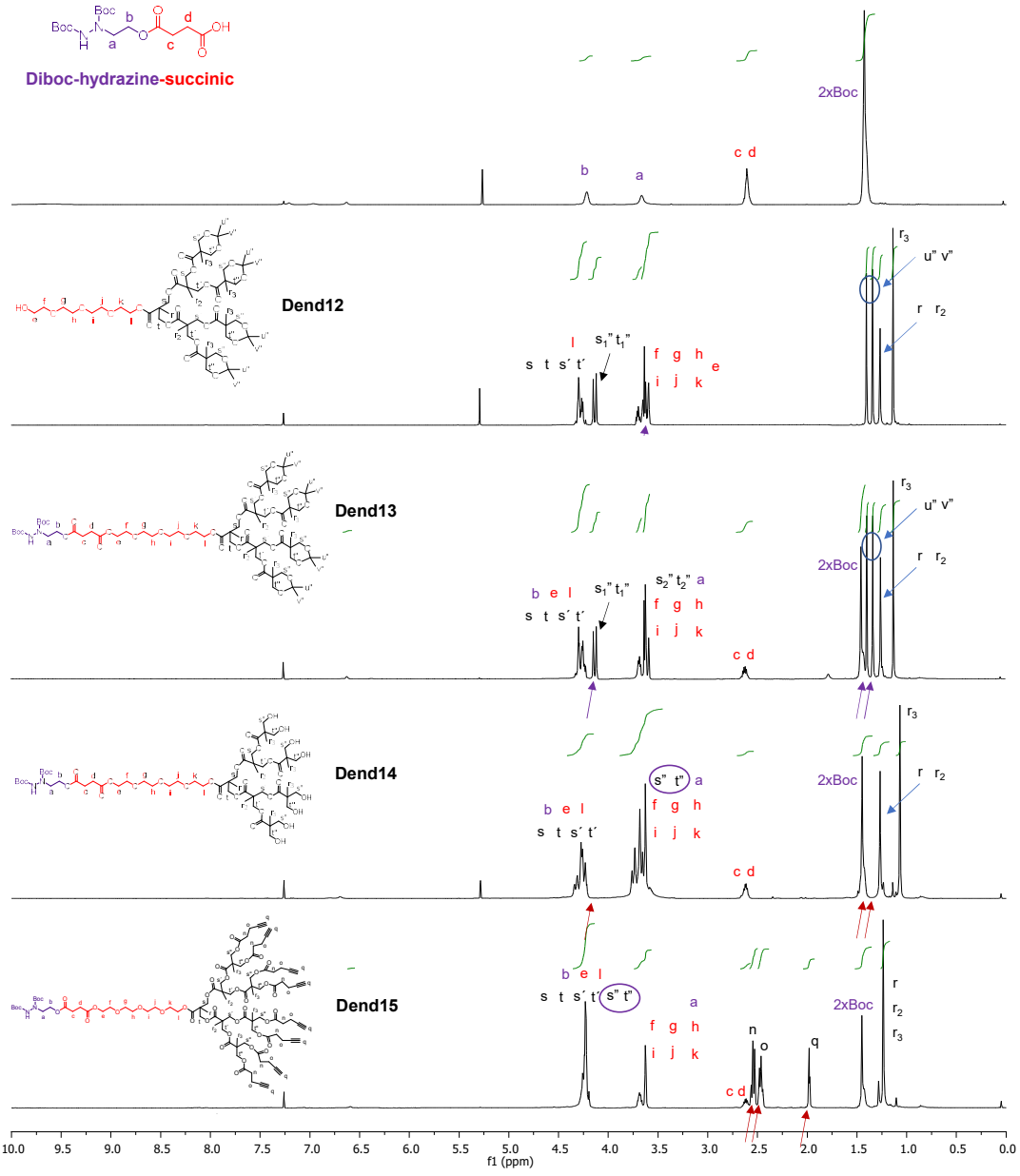

Figure III.13. ^{1}H-NMR monitoring of synthesis of the octavalent alkyne decorated dendron **Dend15**.

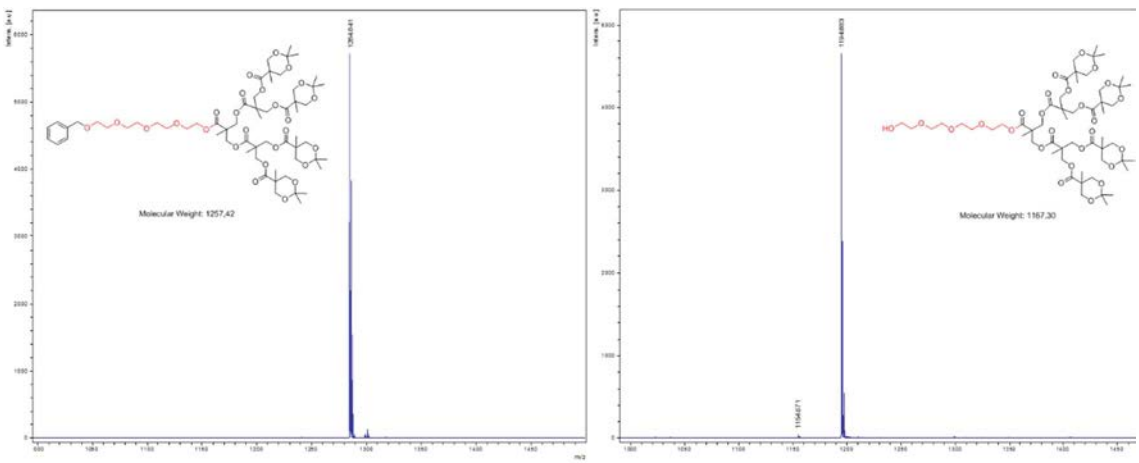

Figure III.14. From left to right, MALDI-TOF MS spectra comparison of **Dend11** and **Dend12**, resulting a mass of 90 Da due to the benzyl deprotection.

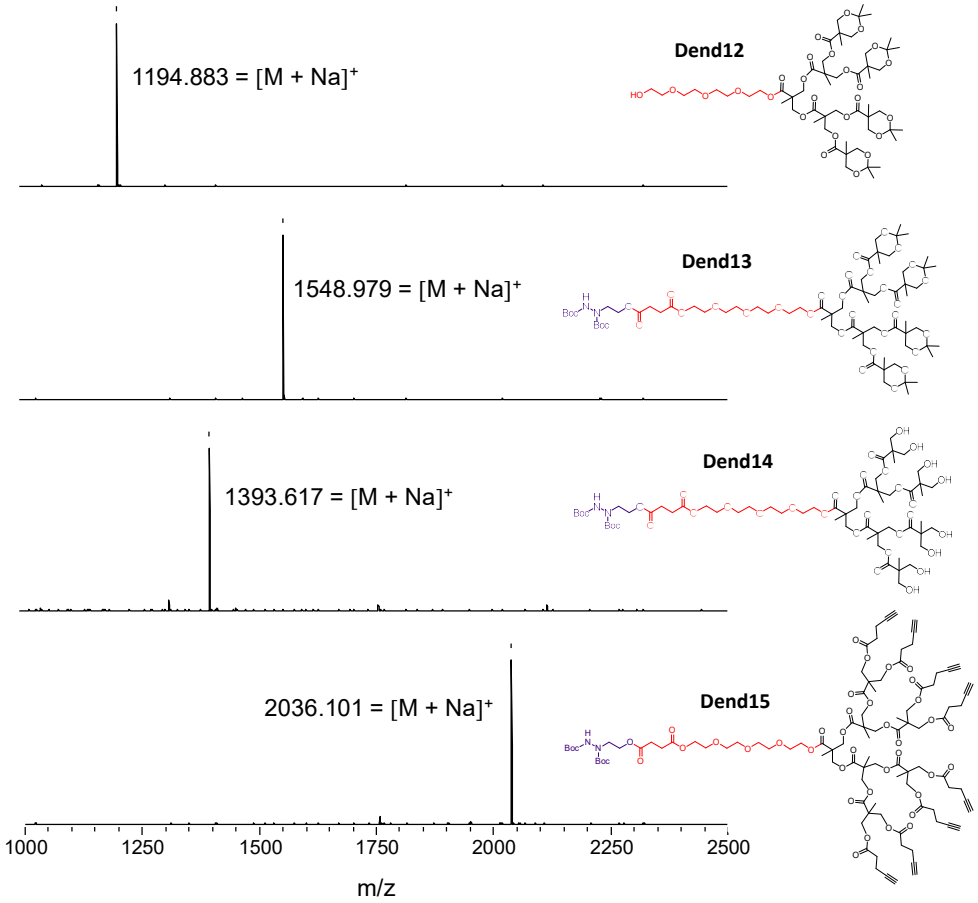

Figure III.15. MALDI-TOF MS characterization of **Dend12- Dend15**.

For the introduction of fluorescent Cy5, the click reaction was optimized for the monovalent molecule **Dend5** (Scheme III.1B). Traditional CuAAC using $CuSO_4$/sodium ascorbate in THF/H_2O (1:1) at 50˚C was first performed. The reaction was monitored by MALDI-TOF MS until completion and the di-Boc-hydrazine monovalent sulfo-Cy5 **Dend6** was isolated in quantitive yields by preparative TLC using EtOAc/MeOH (1:1). Interestingly, the click reaction was found to proceed at much higher rate when performed in DMSO using CuBr/PMDTA as catalyst pair, at room temperature and under argon as inert atmosphere. This is reasoned to be an effect of solubility in which the starting materials were soluble in DMSO in contrast to THF/H_2O mixture. Utilizing the CuAAC with CuBr/PMDTA as catalyst pair and DMSO as solvent were chosen for the synthesis of **Dend10**, a di-Boc-hydrazine TEG core decorated with two sulfo-Cy5 groups (Scheme III.1C). The reaction was complete after overnight stirring and dialyzed against water to obtain **Dend10** as a pure compound with a yield of 88%. For the G3-Cy5 **Dend16** with eight peripheral copies of sulfo-Cy5 (Scheme III.1D), CuAAC in THF/H_2O (1:1) were reaction conditions. To reach completion, the reaction required 48 hours of stirring at elevated temperature (50˚C). After solvents elimination, the crude mixture was dissolved in water and purified by means of sephadex G-25 to exclude excess of dye, affording dendron **Dend16** with 57% yield.

For all probes decorated with sulfo-Cy5, the reactions were considered completed upon the disappearance of alkyne-derived molecules (**Dend5**, **Dend9** and **Dend15**, respectively) in the MALDI-TOF MS and their purity corroborated by NMR (Figures III.16, III.20 and III.21).

For example, Figure III.16 details spectra of **Dend6**, which support the complete consumption of the alkyne group (absence of the signal at 2.25 ppm in sulfo-Cy5 azide, see Figure III.17) along with the formation of triazol ring with specific signal allocated at 7.84 ppm. The click reaction is also exemplified by the shift of signals belonging to methylene groups next to the azide in sulfo-Cy5-azide from 1.44 and 1.79 ppm to 4.39 and 2.75 ppm in **Dend6**, and signal displacement of methylene group directly bounded to alkyne from 2.47 ppm in **Dend5**, to 3.02 ppm in **Dend6** (Figures III.16 and III.18). MALDI-TOF spectra also confirmed the structure of **Dend6** (Figure III.19).

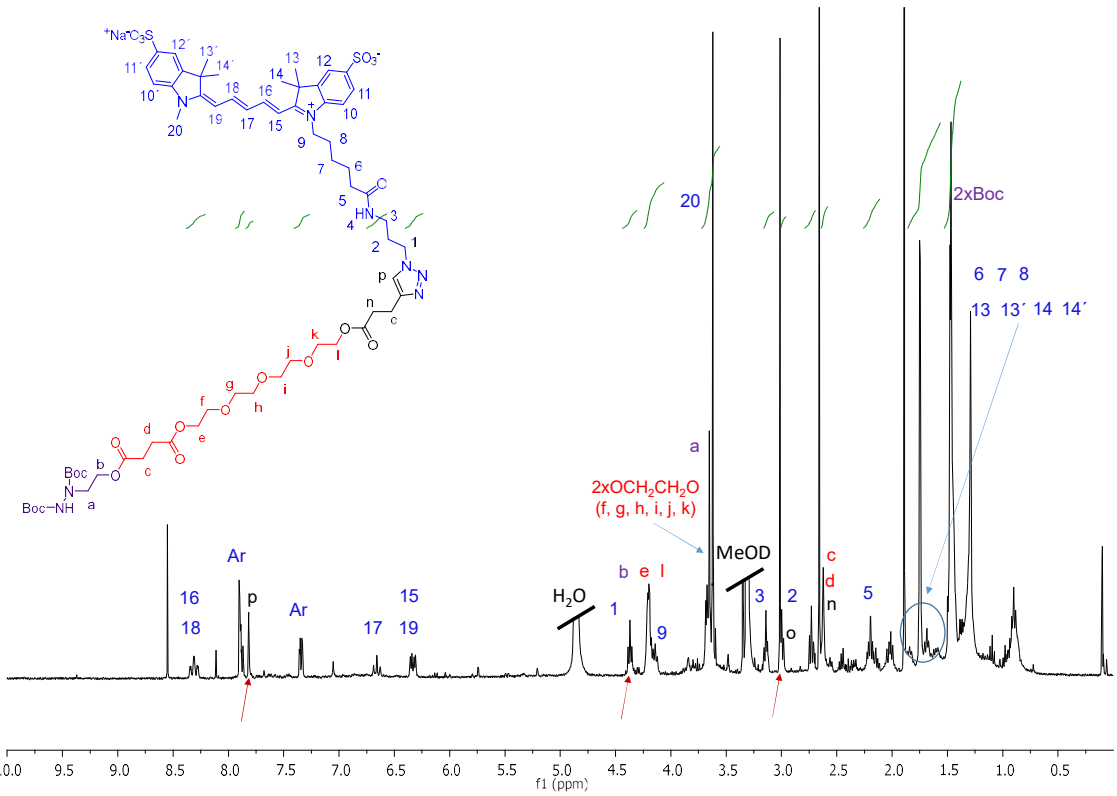

Figure III.16. ^{1}H-RMN spectra of **Dend6**.

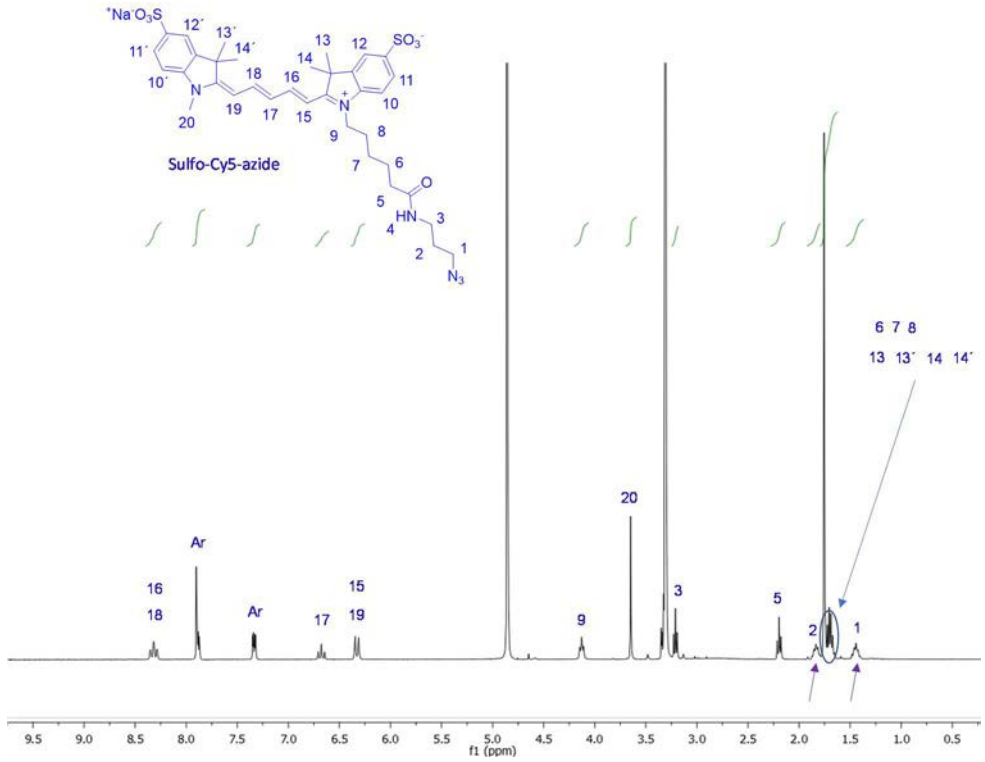

Figure III.17. ^{1}H-RMN spectra of sulfo-Cy5-azide.

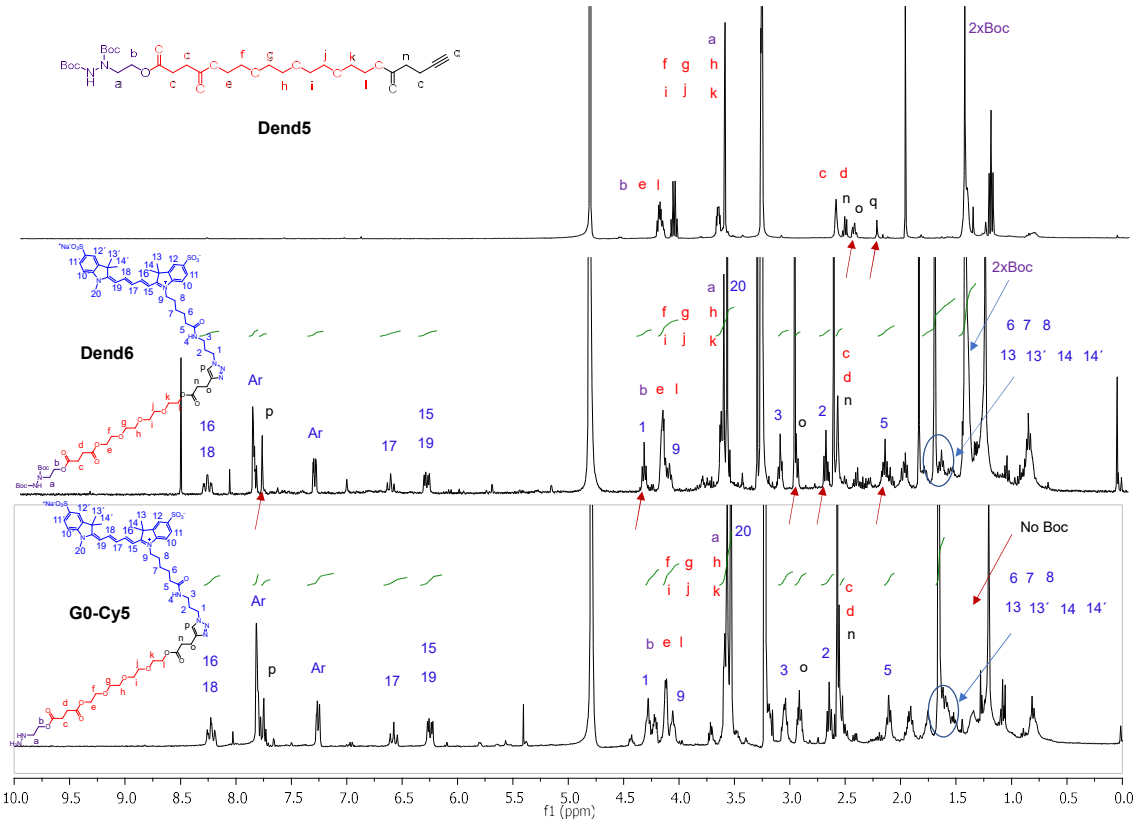

Figure III.18. Monitoring of fluorescent functionalization of the monovalent alkyne decorated molecule **Dend5** to form **Dend6** and following deprotection to yield **G0-Cy5**.

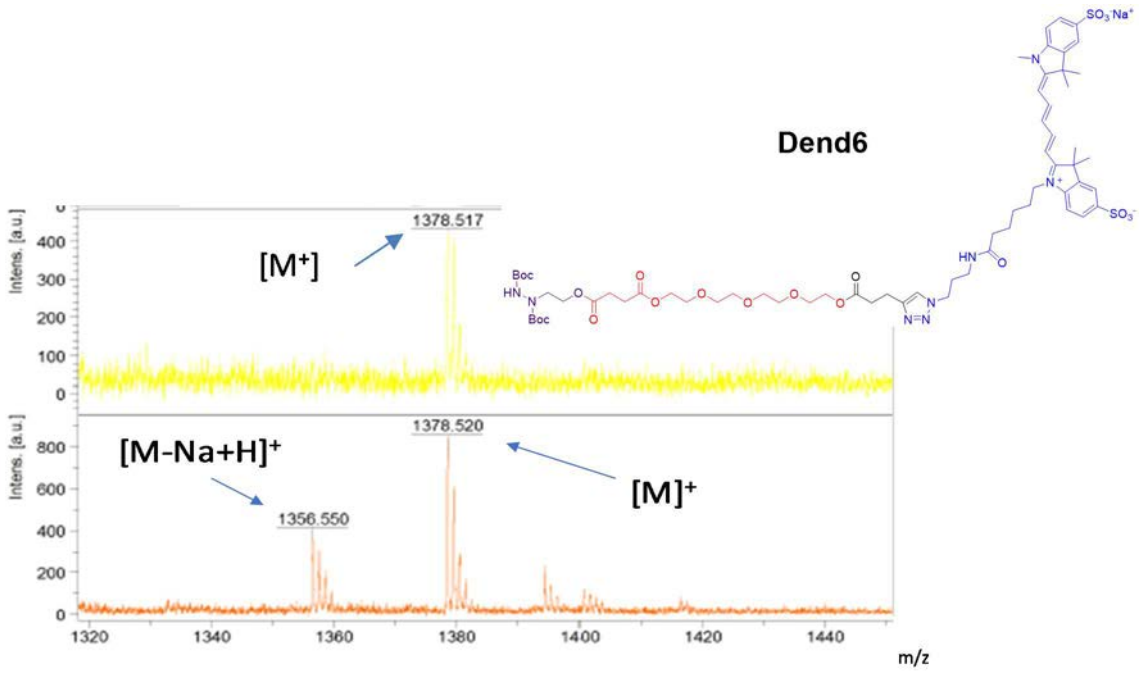

Figure III.19. MALDI-TOF spectra of monovalent Cy5 decorated dendron **Dend6**. Top spectrum was registered using (top) α-cyano-4-hydroxycinamic acid (CHCA) or (bottom) sinapinic acid (SPA) as matrix.

In Figure III.20, ^{1}H-NMR evidence of triazol ring formation in **Dend10** can be observed by displacement of methylene groups close to the azide in free dye, as described for compound **Dend6**. Also, methylene group next to the alkynes in compound **Dend9** are displaced from 2.52-2.46 ppm to 3.02-2.92 ppm due to triazol ring formation. A signal belonging to the methyne in triazol ring appears at 7.80 ppm.

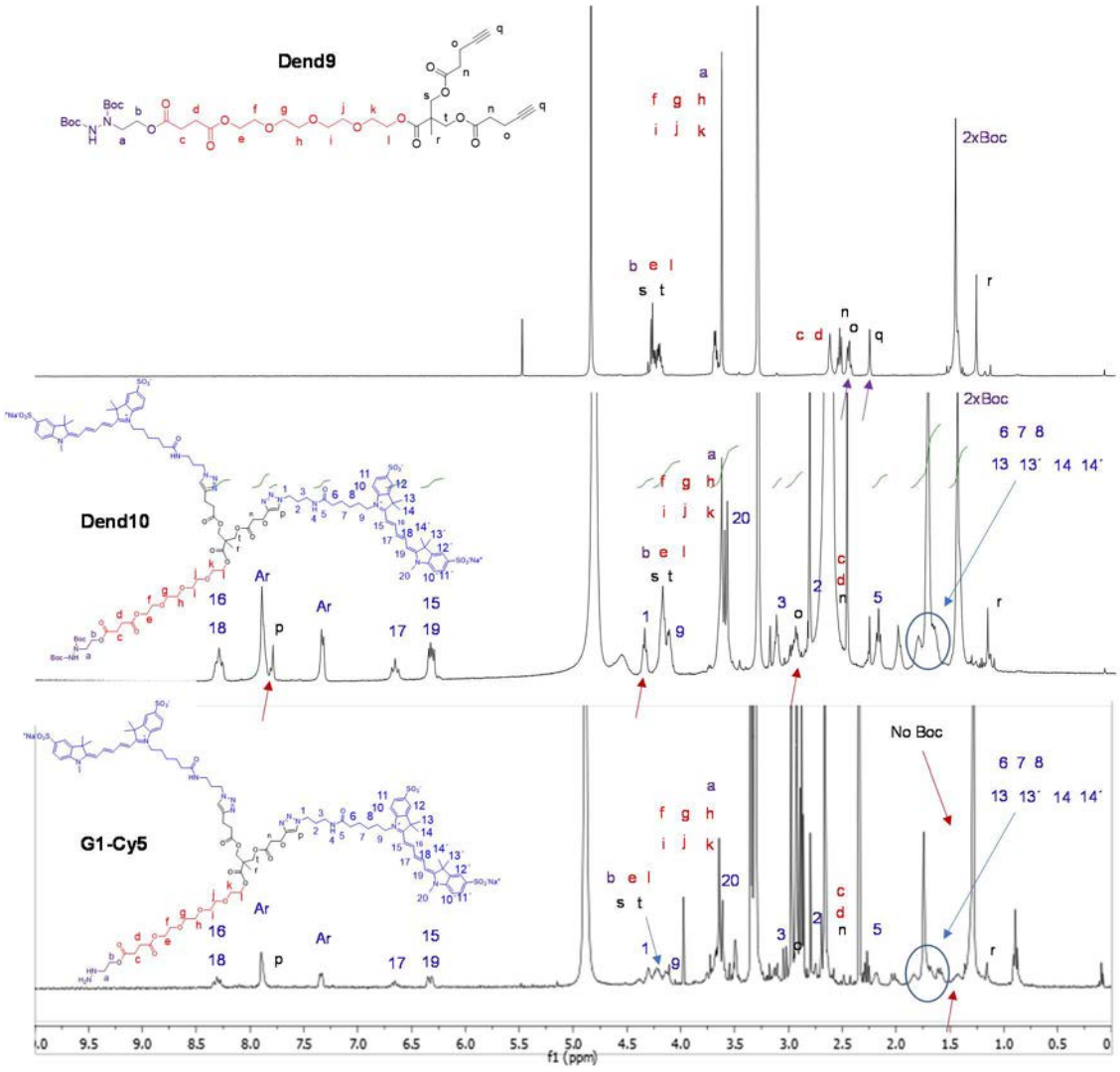

Figure III.20. Monitoring of fluorescent functionalization of the diovalent alkyne decorated linker **Dend9** to form **Dend10** and following deprotection to yield **G1-Cy5.**

In Figure III.21, ^{1}H-NMR evidence of triazol ring formation in **Dend16** can be observed by displacement of methylene groups next to the azide in free dye, as described for **Dend16** and **Dend10**, and appearance of the methyne in triazol ring at 7.99 ppm. Also, methylene group next to the alkyne in compound **Dend15** is displaced from 2.50-2.43 ppm to 3.16-3.05 ppm in compound **Dend16** with disappeareareance of methyne signal.

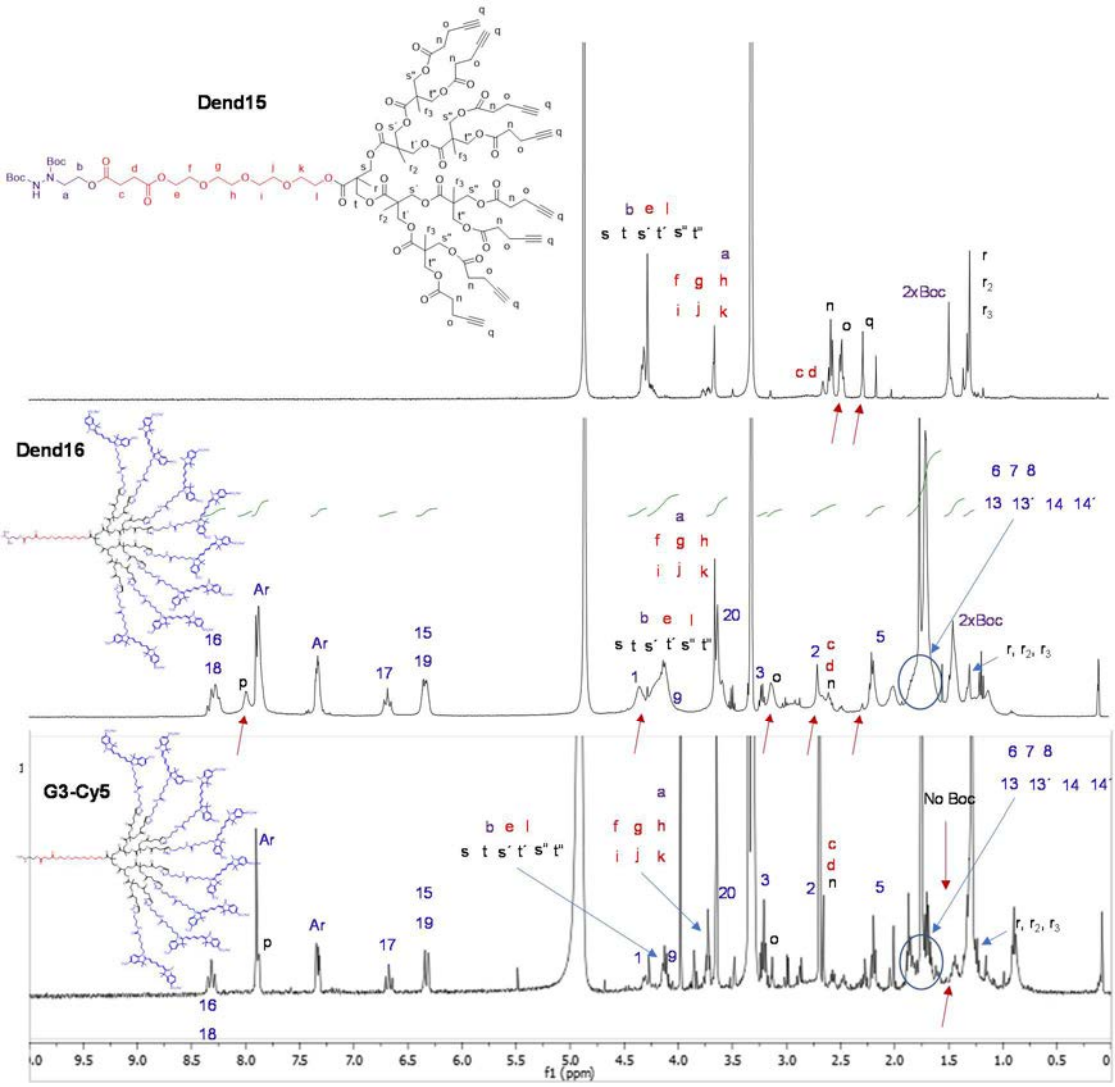

Figure III.21. Monitoring of fluorescent functionalization of the octavalent alkyne decorated linker **Dend15** to form **Dend16** and following deprotection to yield **G3-Cy5.**

The final activation of these probes included the deprotection of the hydrazine groups. For the monovalent sulfo-Cy5 **Dend6** and divalent sulfo-Cy5 **Dend10**, the deprotection was accomplished using TFA/DCM (1:1) at room temperature, affording **G0-Cy5** and **G1-Cy5** in quantitative yields. As can be seen in Figure III.22, the MALDI-TOF MS for the **G0-Cy5** revealed a molecular weight corresponding to expected ionized mass of 1178 $(M)^+$. The deprotection of the octavalent sulfo-Cy5 **Dend16** was carried out in pure TFA. This is due to solubility issues in TFA/DCM (1:1) governed by the higher amount of water soluble dyes at the periphery. The **G3-Cy5** was successfully isolated in a quantitative yield. In all cases, the deprotection of the Boc groups was confirmed by ^{1}H-NMR, looking at the disappearance of Boc signal at 1.40-1.50 ppm (Figures III.18,

III.20 and III.21) and resulted in fluorescently labeled probes **G0-Cy5**, **G1-Cy5** and **G3-Cy5** bearing 1, 2 or 8 dye moieties and a single hydrazine ready for biomolecule labeling (Figure III.6).

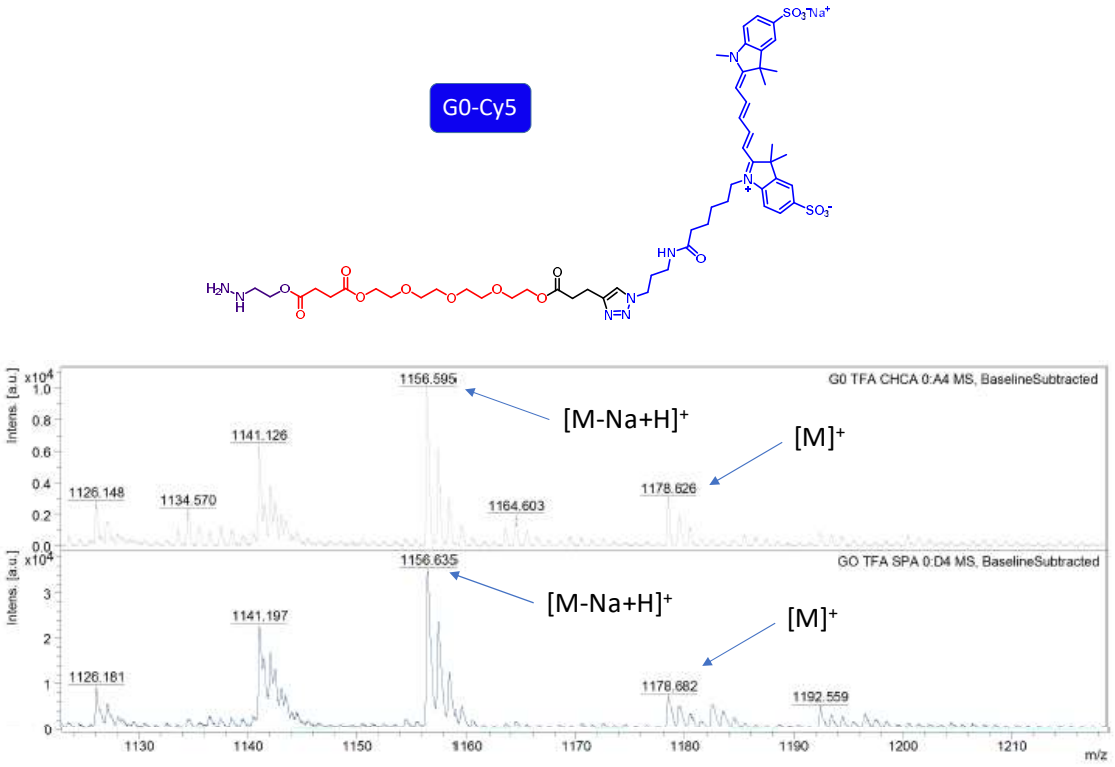

Figure III.22. MALDI-TOF spectra of deprotected monovalent Cy5 decorated dendron **G0-Cy5** using CHCA (top) or SPA (bottom) as matrix.

III.2.3. UV-Visible and Fluorescence Spectroscopy Characterization of Dendrons

Satisfied with the successful synthetic machinery of the probes, their performance was evaluated by UV and fluorescence spectroscopic techniques. This characterization was carried out by José María Montenegro at SCAI, UMA. As shown in Figure III.23A, UV spectra revealed an increase in absorbance at 646 nm along with the number of dyes. The molar extinction coefficient, ε_{646}, was 80342, 154050 and 600459 $M^{-1}\cdot cm^{-1}$ for **G0-Cy5**, **G1-Cy5** and **G3-Cy5**, respectively. ε_{646} ratio obtained for each dendron resulted to be 1/1.9/7.5. These values are in close approximation to the number of fluorescent sulfo-Cy5 units available on each dendron, 1:2:8, confirming the peripheral valence as well as the success of fluorescent decoration. However, besides the band at 646 nm, the presence of a little band at shorter wavelength (600 nm) was observed for **G3-Cy5**, feature that is quite commonly attributed to the presence of aggregates and often results in a decrease in fluorescence.

Concerning the fluorescence of the dendrons, results shown in Figure III.23B, increased number of fluorescent units yields higher fluorescence emission for the dendrons (**G3-Cy5** > **G1-Cy5** > **G0-Cy5**). Quantum yields (ϕ) obtained for **G0-Cy5**, **G1-Cy5** and **G3-Cy5** were noted to 0.33, 0.22 and 0.21, respectively. It should be noted that molecules with high quantum yield and extinction coefficient have the brightest features. To compare the brightness of different fluorophores, the relative brightness of fluorophore is taken by multiplying the extinction coefficient with the quantum yield (ε·ϕ) [254]. Brightness obtained for **G0-Cy5**, **G1-Cy5** and **G3-Cy5** were 26330, 34046 and 128374, respectively. High brightness is required to have a strong fluorescence signal. Although ϕ for **G3-Cy5** is the lowest, it shows the highest brightness. Therefore, the **G1-Cy5** and **G3-Cy5** dendrons decorated with 2 and 8 dye molecules, respectively, met the prerequisites for enhance fluorescence signals compared with the monovalent **G0-Cy5**. These results demonstrate the targeted proof-of-concept, contrary to the reported decrease in fluorescence previously detailed for dendrimers decorated with high number of dyes [150, 170, 171].

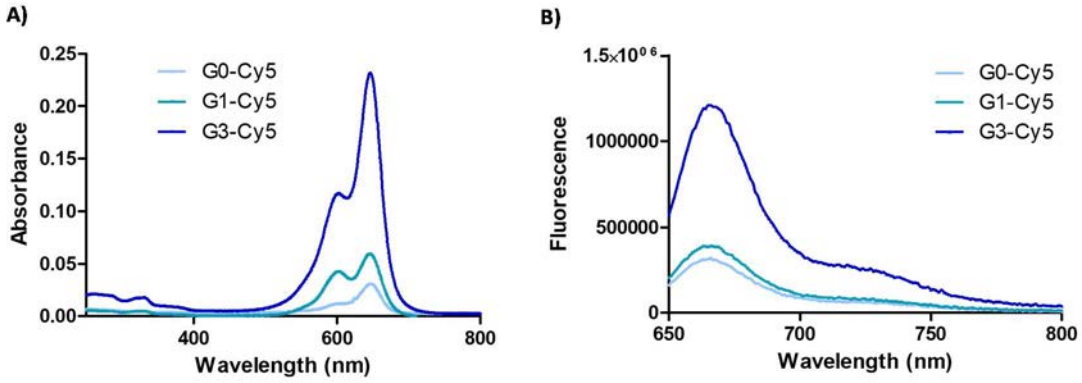

Figure III.23. A) UV-visible spectroscopy of dendrons **G0-Cy5**, **G1-Cy5** and **G3-Cy5**. B) Fluorescence emission of dendrons **G0-Cy5**, **G1-Cy5** and **G3-Cy5**.

III.2.4. Chemoselective Conjugation of Dendrons to a Model Antibody

As the main motivation for the construction of these probes is their applicability in macromolecules labeling for bioimaging or diagnostic, we further demonstrate the conjugation to α-Human IgG Fc as a structural model of antibody. The labeling was performed as well by the PhD student during her stay at KTH. The methodology used for labeling capitalized on site-directed conjugation to the aldehydes of antibody that are generated through the oxidation of 1,2-diols in sialic acids in glycan carbohydrate chains attached to the CH2 domain between the heavy chains in the Fc region [181]. These aldehydes carbonyls were envisaged to selectively react with hydrazine groups

to generate hydrazone linkages without compromising antibody activity, recognition or causing further oxidative damage. The protocol [160] utilized was based on a mild oxidation of polysaccharide chains with $NaIO_4$ and the subsequent conjugation with the set of fluorescent probes **G0-Cy5**, **G1-Cy5** and **G3-Cy5**, Figure III.24. Upon labeling, a purification step using Sephadex-G-25 was necessary to exclude any unconjugated fluorescent probes. Dialysis filtration was also performed as an additional purification step to ensure the exclusion of any remaining dyes. As visualized in Figure III.24, for the purified antibodies a clear shift in blue color intensity can be observed, which reflects the amplification capacity the fluorescent dendrons provides to the final conjugates.

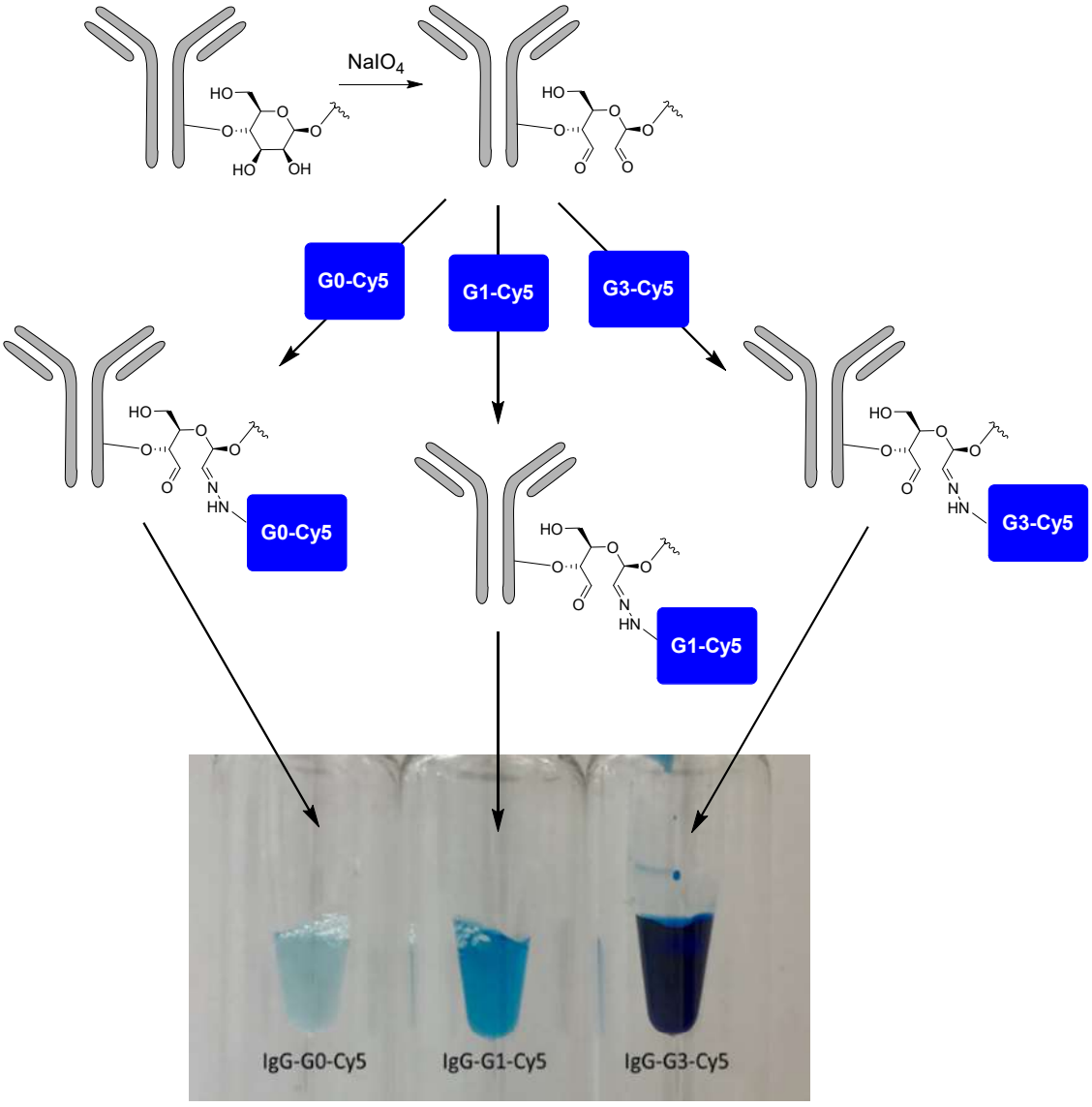

Figure III.24. Antibody labeling scheme. Labeled antibody concentration in the picture was around 8 mg/mL.

SDS-PAGE analysis was performed by the PhD student once back in her home laboratory to confirm covalent attachment of the probes to the antibody (Figure III.25). The use of Commassie staining as a detection technique enabled the semi-quantification of the labeled antibody, by comparison to unlabeled counterparts, and confirmed a similar recovery for all three fluorescently conjugated biomolecules. The fluorescent detection revealed bands for labeled antibodies while the controls were undetectable. This corroborates on successful covalent attachment of the fluorescent probes to the antibody via hydrazone linkages (Figure III.25).

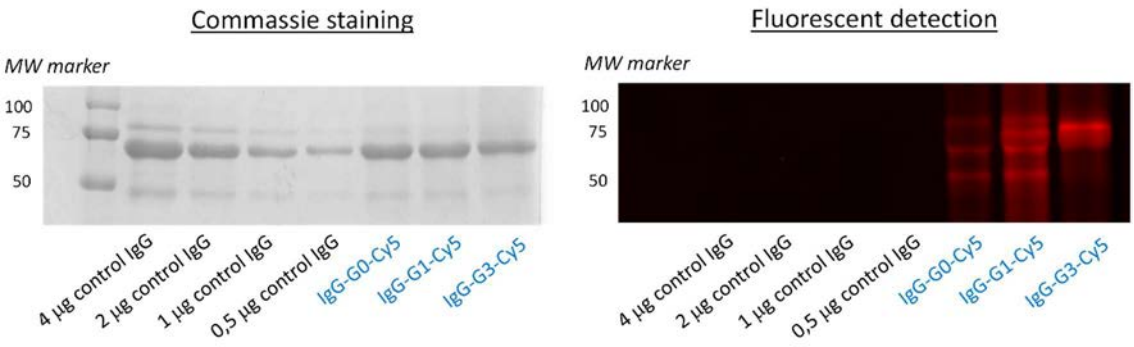

Figure III.25. SDS-PAGE characterization of labeled antibody. A molecular weight marker (lane 1), four decreasing amounts of unlabeled IgG as control (lanes 2-5) and conjugates **IgG-G0-Cy5**, **IgG-G1-Cy5**, **IgG-G3-Cy5** (lanes 6-8) were loaded. Commassie (left) and fluorescent detection (right).

The absorbance for the labeled antibodies, measured by José María Montenegro at SCAI, UMA, registered a band at 646 nm, yielding higher intensity with increasing number of dye units present on the fluorescent probes. ε_{646} values were 49667, 274985 and 2280894 $M^{-1}{\cdot}cm^{-1}$ for **IgG-G0-Cy5, IgG-G1-Cy5** and **IgG-G3-Cy5**, respectively (Figure III.26 top). Interestingly, the spectra for **IgG-G3-Cy5** had a pronounced bimodal shape with a maximum intensity at 600 nm. Such behavior has been previously observed by Gruber *et al.* [169] for IgG labeled with six Cy5 molecules. In their work, it was postulated to be an effect of H aggregates formation, so called H-dimers. This was explained by the tendency of cyanine dyes to aggregate in solution through plane-to-plane stacking (parallel aggregates) or through an end-to-end arrangement (head-to-tail). The transition to the upper state in parallel aggregates leads to a hypsochromic (red) shift and these groups of molecules are called H aggregates [249].

As seen in Figure III.27, the fluorescence properties of labeled antibodies, measured as well at SCAI, UMA, noted the maximum emission for **IgG-G1-Cy5** (ϕ= 0.25, $\varepsilon{\cdot}\phi$= 67891) followed by **IgG-G0-Cy5** (ϕ= 0.41; $\varepsilon{\cdot}\phi$= 20473). The antibody labeled with **G1-Cy5,** compared to the conjugation with **G0-Cy5**, enhanced the fluorescence emission by one degree of magnitude. On the contrary, **IgG-G3-Cy5** was barely fluorescent with an extremely low ϕ value of 0.02. A plausible explanation is that most of the photon are

absorbed and deactivated by means of non-radiative process. The drop in fluorescence of **IgG-G3-Cy5** compared to the neat **G3-Cy5** could be explained by the more restricted environment where the dendron is confined in the IgG, probably hydrophobic, leading to a more rigid conformation and thereof to a higher proximity among Cy5 units. H-dimer formation was previously reported for Cy5, [249, 255] and other dyes [255, 256] as the cause of quenching for cases with a high degree of labeling. To investigate whether the scarce fluorescent properties of **IgG-G3-Cy5** is due to this phenomena, absorbance and fluorescence values with and without Sodium dodecyl sulfate (SDS) were compared [169, 255, 256]. The addition of SDS to **IgG-G3-Cy5** decreased the intensity of the band absorbance at 600 nm and increased that at 646 nm (Figure III.26 bottom) as well as increased the intensity of the band in the fluorescence spectrum (Figure III.27 right). The large reversed anomalous effect could be explained by the partial unfolding of the antibody because of disruption of the tertiary structure due to SDS. In spite of the formation of Cy5 dimers, the quenching of Cy5 fluorescence in the highly Cy5-labeled biomolecule may be due to resonance energy transfer [169]. Similar argument can explain the observed fluorescent band for **IgG-G3-Cy5** after SDS-PAGE, since SDS and β-mercaptoethanol used in denaturalization step may affect protein conformation, being the dendritic structure surrounded by a less restricted environment, which would reduce quenching.

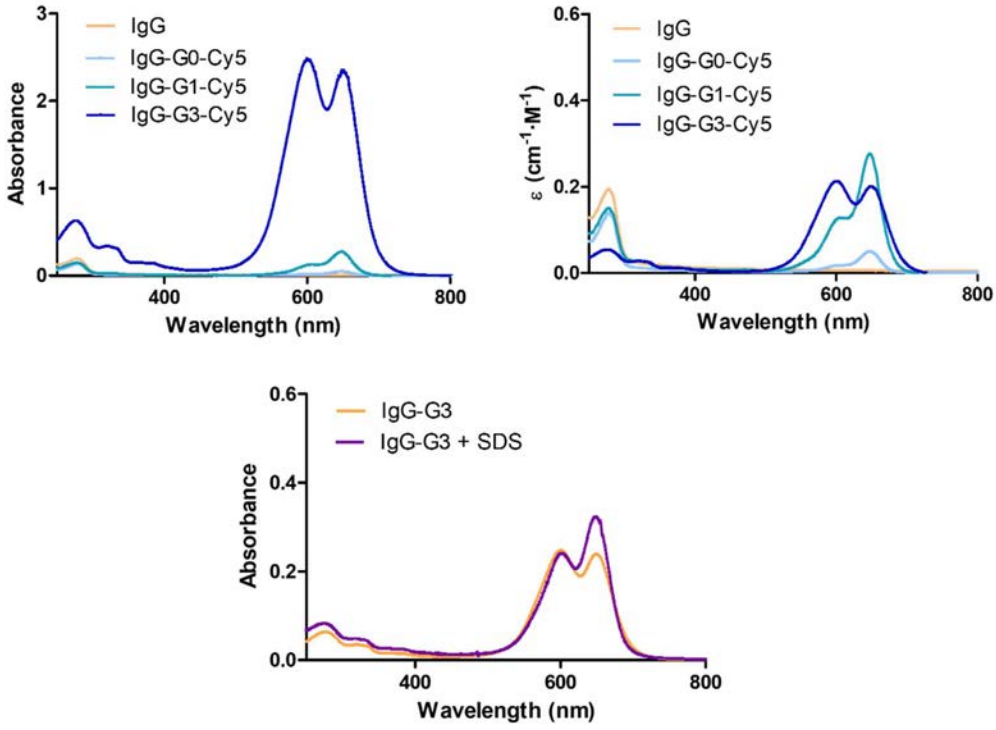

Figure III.26. Absorbance spectra obtained for antibody labeled with the series of synthesized dendrons (**IgG-G0-Cy5**, **IgG-G1-Cy5**, **IgG-G3-Cy5**) (top left). Comparison of the different shape obtained for **IgG-G3-Cy5** (top right). Change in absorbance after 90 min of adding SDS (1%) to **IgG-G3-Cy5** solution (bottom).

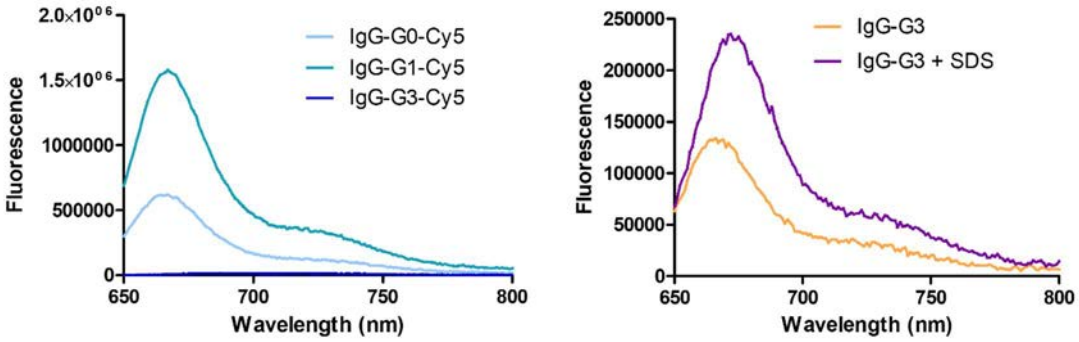

Figure III.27. Fluorescence emission results obtained for labeled IgG (**IgG-G0-Cy5**, **IgG-G1-Cy5**, **IgG-G3-Cy5**) (left) and change in fluorescence 90 min after adding SDS (1%) (right).

Among the three labeling studied, **IgG-G1-Cy5**, functionalized with dendrons bearing two dyes moieties, was found to be the most fluorescent. These findings are in good agreement with previous studies of the monovalent-Cy5/protein ratios in which 2 to 3 Cy5 labels per antibody resulted in optimal fluorescence [169, 257]. However, these studies employed monovalent NHS-activated-dyes as a random-site bioconjugation to present lysines on the biomolecules. In this context, the orthogonality present in hydrazine/click frameworks provides water-soluble probes with site-directed conjugation and detection without jeopardizing the recognition site of the antibody.

Due to the increasing use of fluorescent probes in biomedical applications, the development of novel fluorescent probes that allows for chemoselective labeling of biomolecules is highly desirable. In this context, we herein described the synthetic design of dendritic scaffolds based bis-MPA as a monomer displaying a single protected hydrazine and multiple alkyne functionalities. These scaffolds (**Dend5**, **Dend9** and **Dend15**), with orthogonal features were, for the first time, successfully decorated with the highly desirable bioimaging dye sulfo-Cy5, bearing one, two or eight fluorescent copies along with a single reactive hydrazine. The potential of the multivalent hydrazine/dyes probes, as a conjugation reagent to functionalize biomolecules, was demonstrated on α-Human IgG Fc. The most favorable signal amplification was obtained for Ig labeled with **G1-Cy5** bearing 2 units of sulfo-Cy5. It was found to enhance the fluorescence by one order of magnitude when compared to the monovalent crosslinker **G0-Cy5**. This makes hydrazine functionalized **G1-Cy5** dendron a valuable candidate for macromolecules labeling for applications such as immunoassays signal amplification. In contrast, strong fluorescence quenching was observed for α-Human IgG Fc labeled with **G3-Cy5**.

The results presented in section III.2. gave rise to the following publication in collaboration with the KTH, being first author the PhD student presenting this memory: Design of multivalent fluorescent dendritic probes for site-specific labeling of biomolecules, *Journal of Polymer Science Part A: Polymer Chemistry.* **56**(15), 1609-1616), reference [278].

While not favorable in this study, quenching phenomena observed for **IgG-G3-Cy5** may be suppressed by the conjugation of the probe to biomolecules with less restricted environment. This could facilitate the exploitation of **G3-Cy5** as a strong fluorescent enhancer for bioimaging and diagnostic applications. Finally, the chemistry is not limited to Cy5 and alternative dyes may lead to higher fluorescent emission for biomolecules labeled with dendron utilizing the presented synthetic strategy.

GENERAL DISCUSSION

DHRs are a significant public health problem with important consequences on patient health and healthcare costs. It has been reported that only a low percentage of initial cases suspected of allergy to antibiotics are finally confirmed [15, 196], and BLs are the drugs most frequently involved [5, 28]. *In vivo* tests (ST and DPT) are often the first and only option for diagnosis, however they could be risky for patients. Thus, *in vitro* tests are a more convenient and safer alternative for diagnosis.

Sensitive and specific detection of sIgE is crucial for *in vitro* allergy diagnosis, which is difficult to achieve due to the extremely low concentration present in patients serum [238]. Due to the low sensitivity and the report of some cases of false positives [197] for ImmunoCAP-FEIA, the only commercially available *in vitro* test for allergy diagnosis, currently, most of laboratories rely on the design and use of in-house immunoassays [138, 139], which have become more quantitative and sensitive.

The sensitivity of *in vitro* tests for diagnosing allergy to BLs depends, among other factors, on: (i) the similarity between the structure used in the assay as emulator of the AD formed *in vivo* and the structure actually formed after BL intake, which is related to the mechanisms involved in the allergic process, and (ii) the intensity of the detection signal (radioactivity, enzimatic proccess or fluorescence) at low concentrations of sIgE to drugs. In the work presented, we did our bit to help to the improvement of *in vitro* tests for BLs allergy diagnosis by tackling the both previous mentioned points.

Regarding the mechanism, it is known that the formation of hapten-protein conjugates takes place for BLs. Penicillins have been studied as model BLs [40, 46, 50] and their AD are well defined. Also, some studies allowed the identification of serum target proteins [45, 88, 89], binding sites [53, 89, 101-104] and the influence of the carrier molecule in recognition [63], allowing the advance in the design of *in vitro* tests for AX and BP using synthetic carriers or using novel solid surfaces [51, 148]. Nevertheless, ADs for cephalosporins and CLV are still to be characterized, and only a few studies have been published about the potential ADs for cephalosporins [43, 69, 200] and CLV [53]. It is important to highlight that the elucidation of the mechanism involved in allergy to cephalosporins and CLV has become of great interest, since cases of allergy to these BLs have increased in the last years due to the change in prescription patterns [15].

In this study, we aimed to research, from a chemical approach, the structures recognized by sIgE for cephalosporins and CLV. We designed and synthesized structures derived from these BLs and performed their immunological evaluation using RAST or BAT. Degree of sIgE recognition of new synthetic structures were compared with previous reported structures or the native BL itself. Moreover, a biotinylated derivative of CLV was used as tool for identification of serum proteins target of modification.

There are some works published in which SAR studies were employed for investigating the AD for cephalosporins [42, 43, 69, 70, 205], and it was the strategy we also used.

First, UDC methodology [210] was adapted to synthesize the target pyrazinone-like structures of interest (**Cef1** and **Cef2**) as potential ADs of α-aminocephalosporins. Recognition of these molecules was evaluated by RAST inhibition and compared with the structures derived from cefaclor and cefadroxil reported previously by Montañez *et al.* [43], **Cef3** and **Cef4**, respectively. Results after evaluation of **Cef1** and **Cef3** using sera from patients allergic to cefaclor showed that the pyrazinone **Cef1** was better recognized (63% of patients) than **Cef3** (12% of patients) and so, that the pyrazinone derivatives would be potential ADs for α-aminocephalosporins. Furthermore, evaluation of **Cef2** and **Cef4** using sera from patients allergic to amoxicillin showed similar results for both structures, being these results helpful to get insight into the structure responsible for cefadroxil allergies and study cross-reactivities between penicillins and cephalosporins.

Regarding CLV, the ignorance of its AD exact structure leads to an uncomplete diagnosis when allergic reactions are consequence of the administration of the AX-CLV combination [131]. Protein haptenation by CLV is supposed to occur similarly to other β-lactams [74, 204], but due to its high instability, the resulting structure rapidly degrades, leading to the formation of multiple fragments [74]. Thus, the formation of two main ADs of CLV, **AD-I** and **AD-II**, very low molecular weight structures formed by only 3 carbon atoms, was hypothesized and six structures derived from them synthesized. Basophil activation by these structures was evaluated and only **Clav2** and **Clav3**, both coming from the **AD-I**, an 1,3-dicarbonylic compound, showed significant differences between patients and controls. The hydrolysis of the second carbonyl group of **Clav2** after protein conjugation would lead to a molecule that is more similar to **AD-I** than **Clav3**, which is in agreement with the degree of recognition found (**Clav2** > **Clav3**). The percentage of patients with BAT positive increased significantly to 69.0% when CLV and **Clav2** were combined compared with native CLV, so the use of **Clav 2** in BAT could be used to improve assay sensitivity.

In order to study CLV conjugation with proteins, LC-MS/MS analysis of the tryptic digests of HSA-CLV were performed and only a 70 Da mass increment was observed. It is worth to highlight that this mass is compatible with that of **AD-I**, which is in agreement with BAT results and confirms that the specifically recognized **Clav2** molecule is part of the resulting CLV-protein conjugate. Meng *et al.* previously investigated the haptenation of HSA by CLV and also found the 70 Da mass increment both in conjugates generated *in vitro* and in serum from patients taking AX-CLV [53].

The study of the serum proteins target of modification by CLV could give important information about haptenation process but the lack of a monoclonal antibody makes difficult the identification of these adducts. In recent publications, biotin labeling has been combined with proteomic techniques to identify protein targets of haptenation

[45, 113, 233, 234] or modified protein residues [235]. In our group, it was demonstrated that AX and an biotinylated derivative of AX compete for their binding to proteins studies, which suggests that they may bind to common sites [45]. Using this same approach, we used **CLV-TEG-B** for identification of serum proteins target of modification by CLV and HSA, haptoglobin and heavy and light chains of inmunoglobulins were the proteins isolated.

About immunoassays detection signal, radioactivity is the label for secondary antibodies presenting the highest sensitivity in immunoassays for allergy diagnosis (RAST). However, fluorescent labeling is a desirable alternative that would finish with the special requirements intrinsic to radioactivity handling. The focus of this study was to design fluorescent dendrimers as probes that allow fluorescent signal amplification, without affecting secondary antibody specificity, with the objective of reaching the sensitivity needed for detecting the low levels of IgE associated with allergy to drugs.

Some studies have reported the coupling of fluorescent moieties to different kind of dendrons, such as PAMAM [248] or bis-MPA [250]. However, only in a few cases fluorescent signal increased with dendron generation, that is to say, with the number of fluorescent units. For instance, Wängler *et al.* [150] synthesized a library of increasing generations of PAMAM dendrons decorated in the periphery with different dansyl chloride, 7-nitro-2,1,3-benzoxadiazol-4-yl chloride, coumarin-343, 5(6)-carb-oxyfluorescein pentafluorophenyl ester and sulforhodamine B2 acid fluoride and a single thiol functionality at the focal point. Fluorescent evaluation of the set of dendrons resulted in enhanced fluorescence signal with dye units only for dansylated dendrons. However, dansyl moieties would prevent solubility in water, and bioconjugation through amine groups in the antibody could affect binding site and so, specificity.

We designed and synthesized bis-MPA dendrimers (**G0-Cy5**, **G1-Cy5** and **G3-Cy5**) bearing hydrazine functionality at focal point for site-specific conjugation to biomolecules, a TEG spacer to make sure their solubility in water, and decorated with sulfo-Cy5 fluorescent units [278], molecule also water soluble and compatible with microarray scanners. Their spectroscopic characterization showed an increment of fluorescence with the number of fluorescent units, and they were proved to be suitable for antibody labeling. **IgG-G1-Cy5**, with two fluorescent moieties, showed the highest fluorescence, being an order of magnitude higher than for the antibody labeled with an only fluorescent moiety **IgG-G0-Cy5**. However, **IgG-G3-Cy5**, with eight fluorescent units, was barely fluorescent, effect that has already been described for high degrees of Cy5 labeling [169].

To sum up, results presented in this memory shed light into the mechanism involved in allergy to α-aminocephalosporins and CLV, as well as the possible proteins target of

modification by CLV, and shows the potential of dendrons as fluorescent labels allowing signal amplification. As future applications, the attachment to solid phases of the new pyrazinone-like structures for cefaclor and cefadroxil could improve sensitivity of *in vitro* tests directed to cephalosporins allergy. Furthermore, the elucidation of AD and carrier proteins for CLV, besides to give information about the mechanism involved in allergy and contribute to *in vitro* tests sensitivity, could help to the development of a monoclonal antibody which would allow to provide further information about CLV conjugation with serum proteins. Finally, synthesized fluorescent dendrons with hydrazine functionality could be used not only for labeling antibodies but for labeling other biomolecules bearing oxidizable carbonyl functionality, and they could be functionalized with dyes different from Cy5 for different applications. Added to that, the use of elucidated ADs in *in vitro* tests combined with the use of an antibody labeled with our fluorescent dendrons would be an important breakthrought in drug allergy diagnosis.

CONCLUSIONS

1. From SAR studies of α-aminocephalosporin determinants, through the synthesis of pyrazinone-like structures **V** (**Cef1** and **Cef2**), derived from cefaclor and cefadroxil respectively, and their immunological recognition, it is deduced that these cyclized structures are specifically recognised by sIgE from patients allergic to the corresponding cephalosporin or to penicillins containing the same R^1 side chain.

Structure **Cef1** (pyrazinone) seems to improve sIgE recognition to cefaclor compared with previous synthetic determinant **Cef3**.

New structure **Cef2** (pyrazinone) in combination with previous synthetic determinant **Cef4** resulted to be useful for studying cross-reactive recognition between α-aminocephalosporins and α-aminopenicillins.

2. From the synthesis of well-defined structures derived from CLV, it was concluded that the ability of synthetic determinants of CLV to activate basophils from patients with immediate reactions to this drug is influenced by the chemical structure and their reactivity to proteins. The AD analog of **AD-I** (*N*-protein, 3-oxopropanamide derivative), **Clav2**, can activate basophils in a higher proportion of patients compared to the native drug, CLV, and thus represents a promising structure to improve the sensitivity of *in vitro* diagnosis.

The identified fragment of the CLV structure (of 70 Da mass) that remains linked to the protein (modifying Lys 195 and Lys 475 of HSA), **AD-I**, is in agreement with that synthetic determinant able to activate basophils, confirming SAR results.

3. A water soluble biotinylated derivative of CLV (**CLV-TEG-B**) was designed and synthesized, and showed *in vitro* protein haptenation capacity, which is concentration-dependent.

From the study of serum proteins haptenation by the biotinylated derivative of CLV it is deduced that **CLV-TEG-B** is an useful tool for target proteins identification. In fact, HSA, haptoglobin and heavy and light chains of immunoglobulins were identified as potential serum proteins target of modification by CLV.

4. Three scaffolds (**Dend5**, **Dend9**, and **Dend15**), with orthogonal features, were successfully decorated with the dye sulfo-Cy5, bearing one, two, or eight fluorescent copies along with a single reactive hydrazine (**G0-Cy5**, **G1-Cy5** y **G3-Cy5**). From spectroscopical studies, it is deduced that absorbance and fluorescence values increase with fluorescent units.

From the proof-of-concept consisting of the use of the dendrons **G0-Cy5**, **G1-Cy5** and **G3-Cy5** as fluorescent probes for antibody labeling is deduced that they can be used for site-specific labeling. The potential of the multivalent hydrazine/dyes probes, as a conjugation reagent to functionalize biomolecules, was demonstrated on α-Human IgG Fc.

The most favorable signal amplification was obtained for IgG labeled with **G1-Cy5**, bearing 2 units of sulfo-Cy5. It was found to enhance the fluorescence by one order of magnitude when compared to the monovalent probe **G0-Cy5**. This makes hydrazine functionalized **G1-Cy5** dendron a valuable candidate for macromolecules labeling for applications such as immunoassays signal amplification.

In contrast, strong fluorescence quenching was observed for α-Human IgG Fc labeled with **G3-Cy5**.

EXPERIMENTAL

1. Identification of β-lactam Antibiotics Antigenic Determinants Recognized by Specific IgE

Two studies were carried out for evaluating recognition of new syntetic ADs by sIgE from patients who had suffered from an immediate hypersensitivity reaction due to that BLs:

A. Immunological evaluation of pyrazinone-like potential ADs for aminocephalosporins: cefaclor and cefadroxil.
B. Immunological evaluation of structures derived from CLV.

The studies were conducted according to the Declaration of Helsinki principles and were approved by the Provincial Ethics Committee of Malaga. All subjects included in the study were informed orally and signed the corresponding informed consent.

1.1. Scope of the Study

Experimental work was carried out at Regional University Hospital of Malaga research laboratory, belonging to IBIMA and except for chemical synthesis and molecules characterization, which were performed at BIONAND. Evaluation and selection of patients was performed at Regional University Hospital of Malaga Allergy Unit. Regional University Hospital of Malaga is a third level hospital, the one reference centre for allergy diseases in Malaga province, Melilla and Gibraltar.

1.2. Study of CLV or α-aminocephalosporins Reactivity towards Nucleophilic Species

Stability of different β-lactam was studied in the presence of butylamine. Solutions nucleophile/BL 1:1, at 10 mM concentration for each specie, were prepared. For CLV or derivatives the solvent used was deuterated PBS1X and for the rest of BLs deuterated PBS1X and deuterated CO_3^{2-}/HCO_3^- 1:1 mixture (Table E.1). ^{1}H-RMN was registered after 15 minutes, 1 hour, 16 hours and 40 hours while incubated at 37˚C.

Table E.1. Solutions used for NMR monitoring of cefaclor, cefadroxil and CLV reaction towards butylamine.

	Nucleophile	BL	V_F	C_F
Cefaclor control	---	1.90 mg	0.5 mL	10 mM
Cefadroxil control	---	1.90 mg	0.5 mL	10 mM
CLV control	---	1.26 mg	0.5 mL	10 mM
Butylamine-cefaclor	0.5 µL	1.86 mg	0.5 mL	10 mM
Butylamine-cefadroxil	0.5 µL	1.84 mg	0.5 mL	10 mM
Butylamine-CLV	0.831 µL	2.00 mg	0.5 mL	17 mM

1.3. Synthesis of structures derived from aminocephalosporins

General procedure for pyrazinone synthesis. Ugi/Desprotect/Cyclize (UDC) strategy was employed for synthesizing the desired products [279]. Equimolar amounts of each substrate (butyl isocyanide, 2,5-dimethoxybenzylamine, 2,2-dimethoxyacetaldehyde solution 60% in H_2O and Boc-protected corresponding aminoacid) were left to react in methanol (MeOH) at room temperature until Ugi adduct formation was completed. In order to remove a possible rest of isocyanide, CH_2Cl_2 and polystyrene supported p-toluenesulfonic acid (PS-p-TsOH) were added and submitted to orbital stirring at room temperature for approximately 1,5h. The PS-p-TsOH was filtered off and successively washed with MeOH, AcOEt and CH_2Cl_2 (3 times with 5 mL of each solvent). For deprotection and cyclization, the residue (Ugi adduct) obtained after solvents evaporation was treated with 30% TFA in DCE and heated to 80ºC for 2h. The solution was then treated with saturated solution of $NaHCO_3$ until pH 8 and extracted with EtOAc. Organic phase was dried over $MgSO_4$ and evaporated under reduced pressure to afford a yellow oily residue that was purified by chromatographic methods on silica gel using DCM/MeOH mixtures.

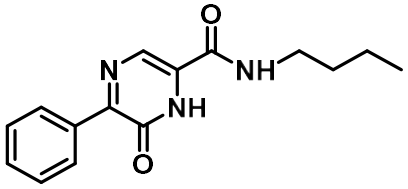

Cefaclor pyrazinone. **N-butyl-6-oxo-5-phenyl-1,6-dihydropyrazine-2-carboxamide (Cef1)**. Synthetized following the general procedure. Corresponding aminoacid is *N*-Boc-phenylglycine. The time needed for Ugi aduct formation was 7 days. For purification, 2% NH_3 had to be added to DCM/MeOH mixtures to allow a good yield. Fair yellow solid, 99% yield. **^{1}H-NMR** (400 MHz, MeOD): δ (ppm) 8.52 (s, 1H; *N*-CH=CCO), 8.19 (m, 2H; Ar-ortho), 7.45 (m, 3H; Ar-meta+para), 3.41 (t, ^3J(H,H) = 7.2 Hz, 2H; -CO*N*H-CH_2-), 1.62 (m, 2H; -CH_2-$C\underline{H}_2$-CH_2-), 1.43 (m, 2H; -CH_2-$C\underline{H}_2$-CH_3), 0.98 (t, ^3J(H,H) = 7.6 Hz, 3H; -CH_2-$C\underline{H}_3$). **^{13}C-NMR** (100 MHz, MeOD): δ (ppm) 164.3, 157.7, 149.8, 136.9, 133.5, 131.0, 130.29, 129.1(x2), 40.41, 32.61, 21.14, 14.08. **ESI MS** calculated for $C_{15}H_{17}N_3O_2$ $(M + H)^+$ 272.1399, found: 272.1393.

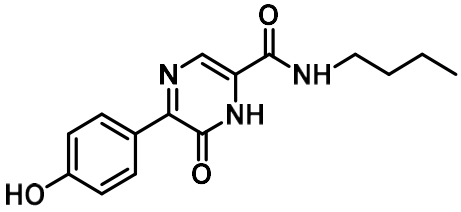

Cefadroxil pyrazinone. **N-butyl-5-(4-hydroxyphenyl)-6-oxo-1,6-dihydropyrazine-2-carboxamide (Cef2)**. Synthetized following the general procedure. Corresponding aminoacid is *N*-Boc-hydroxyphenylglycine. The time need for Ugi aduct formation was 48 hours. Bright(dark) yellow solid, 25% yield. After extraction with EtOAc as stated in the general procedure, the aqueous phase was treated with saturated solution of $NaHCO_3$ until pH 7 and extracted again with EtOAc. Organic phases were combined. **^{1}H-NMR** (400 MHz, MeOD): δ (ppm) 8.39 (s, 1H; *N*-CH=CCO), 8.17 (d, ^3J(H,H) = 9.5 Hz, 2H; Ar-ortho), 6.86 (d, ^3J(H,H) = 9.5 Hz, 2H; Ar-meta), 3.39 (t, 2H; -CO*N*H-CH_2-), 1.60 (m, 2H; -CH_2-CH_2-CH_2-), 1.40 (m, 2H; -CH_2-CH_2-CH_3), 0.97 (t, ^3J(H,H) = 7.6Hz, 3H; -CH_2-CH_3). **^{13}C-NMR** (150 MHz, MeOD): δ (ppm) 164.1, 160.9, 157.1, 150.5, 135.6, 131.7, 130.4, 128.0, 115.9, 40.4, 32.6, 21.1, 14.1. **ESI MS** calculated for $C_{15}H_{17}N_3O_3$ $(M + H)^+$ 288.1348, found: 288.1342.

1.4. Synthesis of structures derived from CLV

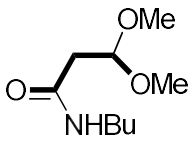

***N*-Butyl-3,3-dimethoxypropanamide (Clav1):** In a Schlenk flask (oven dried and cooled *under nitrogen*), butylamine (3.5 mL, 35 mmol) and commercially available methyl 3,3-dimethoxypropanoate (0.7 mL, 5 mmol) were mixed and stirred at 60°C for four days. The reaction mixture was cooled, diluted with dichloromethane (10 mL) and washed with 10 mL of HCl 2M. The organic layer was dried over anhydrous $MgSO_4$, filtered, and concentrated *in vacuo* to afford quantitatively the target pure compound as a yellow oil (1.05 g). **^{1}H-NMR** (400 MHz, $CDCl_3$): δ 0.89 (3H, t, *J* = 7.3 Hz, CH_3), 1.27-1.36 (2H, m, CH_2), 1.43-1.51 (2H, m, CH_2), 2.55 (2H, d, *J* = 5.3 Hz, $\underline{CH_2}CH$), 3.17-3.26 (2H, m, $\underline{CH_2}NH$), 3.35 (6H, s, 2 x OMe), 4.67 (1H, t, *J* = 5.3 Hz, $\underline{CH}CH_2$), 6.08 (1H, bs, NH); **^{13}C-NMR** (400 MHz, $CDCl_3$): δ 13.8 (CH_3), 20.1 (CH_2), 31.6 (CH_2), 39.2 (CH_2), 41.0 (CH_2), 54.2 (2 x OCH_3), 102.3 (CH), 169.1 (CO). **HRMS** ($C_9H_{19}NO_3$ + Na, 212.1263), found: 212.1258.

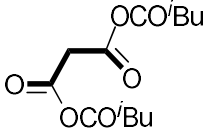

Bis(isobutylcarbonic) malonic anhydride (Clav2): Under nitrogen atmosphere, malonic acid (105 mg, 1.0 mmol) was dissolved in dry CH_2Cl_2 (3 mL) and cooled to 0°C. *N*-Methyl morpholine (0.44 mL, 4 mmol) and isobutylchloroformate (0.26 mL, 2 mmol) were added slowly and the reaction mixture was allowed to stir and reach room temperature for two

hours. The solution was then washed with HCl 1M (5 mL), 1M $NaHCO_3$ aqueous solution (5 mL) and water (5 mL). The organic layer was dried over anhydrous $MgSO_4$, filtered, and concentrated *in vacuo* to afford the target pure compound as a brownish oil (250 mg, 82%). **^{1}H-NMR** (400 MHz, $CDCl_3$): δ 0.92 (12H, d, *J* = 6.7 Hz, 4 x CH_3), 1.89-1.99 (2H, m, 2 x CH), 3.38 (2H, s, $COCH_2CO$), 3.92 (4H, d, *J* = 6.7 Hz, CH_2). **^{13}C-NMR** (400 MHz, $CDCl_3$): δ 19.0 (4 x CH_3), 27.7 (2 x $\underline{C}HCH_2$), 41.7 ($CO\underline{C}H_2CO$), 71.6 (2 x $\underline{C}H_2CH$), 166.7 (4 x CO).

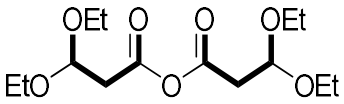

3,3-Diethoxypropanoic anhydride (Clav3): Under nitrogen atmosphere, 3,3-diethoxypropanoic acid (300 mg, 1.85 mmol) was dissolved in dry CH_2Cl_2 (5 mL) and cooled to 0˚C. EDCI (177 mg, 0.92 mmol) was added slowly and the reaction mixture was allowed to stir and reach room temperature overnight. The solution was then washed with water (2 x 5 mL) and the organic layer was dried over anhydrous $MgSO_4$, filtered, and concentrated *in vacuo* to afford the target pure compound as a brownish oil (198 mg, 71%). **^{1}H-NMR** (400 MHz, $CDCl_3$): δ 1.23 (12H, t, *J* = 7.0 Hz, 4 x CH_3), 2.82 (4H, d, *J* =5.8 Hz, 2 x CH_2CO), 3.59 (4H, m, 2 x CH_2), 3.70 (4H, m, 2 x CH_2), 4.97 (2H, t, *J* = 5.8 Hz, 2 x CH); **^{13}C-NMR** (400 MHz, $CDCl_3$): δ 15.3 (4 x CH_3), 41.0 (2 x CH_2CO), 62.5 (4 x $\underline{C}H_2CH_3$), 99.0 (2 x CH), 165.3 (2 x CO); **HRMS** ($C_{14}H_{26}O_7$ + Na, 329.1576), found: 329.1571.

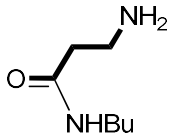

3-Amino-*N*-butylpropanamide (Clav4): Previously prepared ***N*-butyl-3-(1,3-dioxoisoindolin-2-yl)propanamide** (147 mg, 0.53 mmol) and hydrazine hydrate (4 mL) in EtOH (5 mL) were heated at 100˚C for three hours. The solution was then extracted with CH_2Cl_2 (3 x 10 mL), dried over anhydrous $MgSO_4$, filtered, and concentrated *in vacuo* to afford the target pure compound as a white solid (50 mg, 65%). **^{1}H-NMR** (400 MHz, MeOD): δ 0.94 (3H, t, *J* = 7.3 Hz, CH_3), 1.33-1.40 (2H, m), 1.45-1.52 (2H, m), 2.39 (2H, t, *J* = 6.6 Hz), 2.94 (2H, t, *J* = 6.6 Hz), 3.18 (2H, t, *J* = 7.0 Hz); **^{13}C-NMR** (400 MHz, MeOD): δ 14.1 (CH_3), 21.1 (CH_2), 32.5 (CH_2), 37.9 (CH_2), 38.6 (CH_2), 40.0 (CH_2), 173.7 (CO). **HRMS** ($C_7H_{16}N_2O$+H, 145.1335), found: 145.1335.

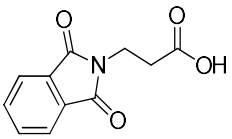

1,3-Dihydro-1,3-dioxo-2H-isoindole-2-propanoic acid: A vigorously stirred solution of β-alanine (1.0 g, 11.23 mmol) and phthalic anhydride (1.0 g, 6.75 mmol) in glacial acetic acid (5 mL) was heated at 120°C overnight. The solution was cooled, diluted with CH_2Cl_2 (10 mL) and washed with water (2 x 15 mL). The organic layer was dried over anhydrous $MgSO_4$, filtered, and concentrated *in vacuo* to afford the target pure compound as a white solid (1.16 g, 78%). Spectral data are in agreement with those reported in the literature [258].

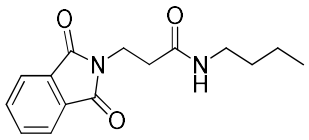

N-Butyl-1,3-dihydro-1,3-dioxo-2H-isoindole-2-propanamide: Under nitrogen atmosphere, previously prepared 1,3-Dihydro-1,3-dioxo-2*H*-isoindole-2-propanoic acid (250 mg, 1.14 mmol) was dissolved in dry CH_2Cl_2 (2 mL) and cooled to 0°C. Then, HOBt (170.1 mg, 1.25 mmol) dissolved in CH_2Cl_2/DMF (2 mL / 1 mL) and EDCI (235 mg, 1.4 mmol) dissolved in CH_2Cl_2 (2 mL) were added. The reaction mixture was allowed to stir and reach room temperature for 2 hours. Then, butylamine (0.1 mL, 1.02 mmol) was added and the reaction mixture was stirred at room temperature overnight. The solution was washed with HCl 1M (10 mL), 1M $NaHCO_3$ aqueous solution (10 mL) and water (10 mL). The organic layer was dried over anhydrous $MgSO_4$, filtered, and concentrated *in vacuo* to afford the target pure compound as a white solid (270 mg, 86%). Spectral data are in agreement with those reported by the commercial firm.

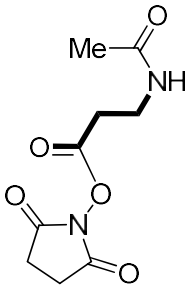

Succinimidyl 3-acetamidopropanoate (Clav 6) [259]: Under nitrogen atmosphere, 3-acetamidopropanoic acid (201 mg, 1.5 mmol) was dissolved in dry CH_2Cl_2 (5 mL) and cooled to 0°C. EDCI (352 mg, 1.8 mmol) and *N*-hydroxysuccinimide (211 mg, 1.8 mmol) were added slowly and the reaction mixture was allowed to stir and reach room temperature overnight. The solution was then washed with water (2 x 5 mL) and the organic layer was dried over anhydrous $MgSO_4$, filtered, and concentrated in vacuo to afford the target pure compound as a colorless oil (175 mg, 50%). **^{1}H-NMR** (400 MHz, $CDCl_3$): δ 1.99 (3H, s, CH_3), 2.81-2.88 (6H, m, 3 x CH_2), 3.63-3.68 (2H, m, CH_2NH), 6.26 (1H, s, NH). **^{13}C-NMR** (400 MHz, $CDCl_3$): δ 22.8 (CH_3), 25.5 (2 x CH_2), 31.4 (CH_2), 34.8 (CH_2), 167.3 (CO), 169.3 (2 x CO), 170.7 (CO). **HRMS** ($C_9H_{12}N_2O_5$+H, 229.0824), found: 229.0812.

1.5. Patients and controls selection

Selection and evaluation of patients was carried out by medical doctors belonging to Allergy Unit at IBIMA-Regional University Hospital of Malaga.

Samples from patients were processed following current procedures and frozen immediately after their reception by the Málaga Regional Hospital Biobank, Andalusian Public Health System Biobank. The studies were conducted according to the Declaration of Helsinki principles and were approved by the Provincial Ethics Committee of Malaga. All subjects included in the studies were informed orally and signed the corresponding informed consent.

A. Immunological evaluation of synthetic ADs of aminocephalosporins.

Patients with a clinical history of immediate allergy to BLs, with a positive *in vivo* test (ST or drug provocation test) and/or *in vitro* detection of sIgE antibodies, following European Network of Drug Allergy (ENDA) guidelines [219] were diagnosed as allergic to BLs. Those with severe reactions, for which drug provocation tests are not recommended, were diagnosed based on positive RAST results and/or the suggestive clinical history. Depending on their response to drugs, patients were further classified into three groups: cefaclor reactors, which included patients with a positive ST for cefaclor; selective AX reactors, which included patients with a positive ST for AX, a negative ST for determinants of BP ((BP-OL or MD) and tolerance to BP in a drug provocation test; and cross-reactors, which included patients with a positive ST for both determinants of BP (BP-OL or MD) and AX.

Of the patients with a confirmed diagnosis of an immediate reaction to cefaclor, we selected eight cases that showed high levels (greater than 7%) of sIgE antibodies to the cephalosporin involved in the reaction measured by direct RAST.

Of the patients with a confirmed diagnosis of an immediate reaction to AX, we selected those that showed high levels (greater than 6.7%) of sIgE antibodies to the AX.

B. Immunological evaluation of synthetic ADs of CLV.

Patients selective to CLV were chosen for the study by following the evaluation workup represented in Figure E.1 [142]. Diagnosis was confirmed by ST or drug provocation test (DPT) to penicillin, AX or CLV following the European Network for Drug Allergy (ENDA) guidelines [219]. As control group, cases with confirmed tolerance to AX-CLV and negative ST to major (BP-OL) and MD of BP, and to AX and CLV were chosen.

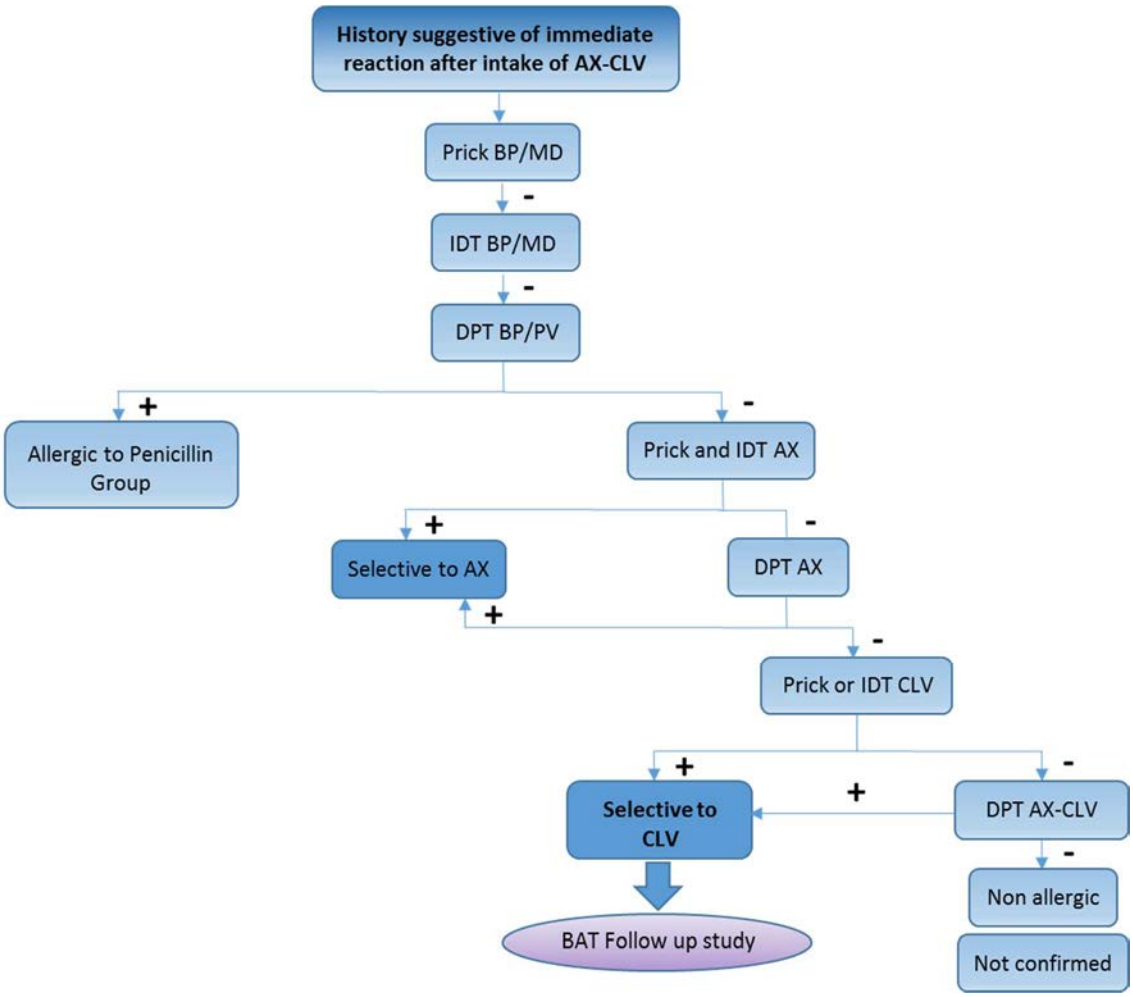

Figure E.1. Flow chart of the allergologic workup for patients classification.

1.6. Conjugation of β-lactam antibiotics with different carrier molecules for *in vitro* studies

Monomeric conjugates of cephalosporins with butylamine for RAST inhibition assays

Monomeric conjugates for cefaclor and cefadroxil with butylamine were prepared dissolving the corresponding cephalosporin in an excess of butylamine and then adding milliQ water. The mixture was left to react at room temperature for 48 hours and was kept in a desiccator until the conjugate was completely dry.

General procedure for preparation of β-lactam conjugates with different carrier molecules

Conjugates were prepared dissolving the carrier protein at 20 mg/mL in PBS 1X (pH 7.4) and incubating it with an equivalent volume of the corresponding β-lactam dissolved in

CO_3^{2-}/HCO_3^- 50 mM (pH 10.2), except for CLV, that was dissolved in PBS 1X (pH 7.4), in order to have the desired protein/BL molar ratio. Resulting solution was incubated at 37˚C for 16-18 hours. BL amount not bound to the protein after conjugation was removed by dialysis filtration using Amicon filters (Merck-Millipore). Several washing steps were performed with milliQ water and resulting filtrates were freeze dried, dissolved in D_2O and analyzed by ^{1}H-NMR. Conjugates were considered completely clean when NMR revealed the absence of drug in the filtrate. Once clean, conjugates were freeze dried and kept at -20˚C until use. An aliquote of each conjugate was analyzed by MALDI-TOF MS to confirm conjugation.

Conjugates with synthetic structures derived from CLV

HSA conjugates with Clav2 or Clav3 were prepared following the general procedure. Protein/CLV-derivated-structure molar ratio employed was 1:10.

1.7. *In vivo* tests

Skin test

ST was performed by prick, and if negative followed by IDT as recommended [219]. For ST procedure, target hapten solutions were freshly prepared daily in saline and histamine (ALK Abelló) and saline solution (Serra Pamies) were used as positive and negative controls, respectively. For prick or intracutaneous test, a drop of hapten solution is deposited in the forearm and then, skin under is scratched with a lancet. If result is negative, intradermal test was performed, in which 20-50 µL of hapten solution is injected under the skin forming a papule whose initial diameter is measured. In those cases with a history of severe anaphylaxis test was performed with increasing concentrations until the maximum was reached, as described [219]. In the SPT, a wheal larger than 3 mm along with erythema and no whealing for the control saline after 30 minutes was considered positive [260]. In the IDT, the wheal area was measured initially and 20 min after testing and a diameter increase bigger than 3 mm was considered positive [260].

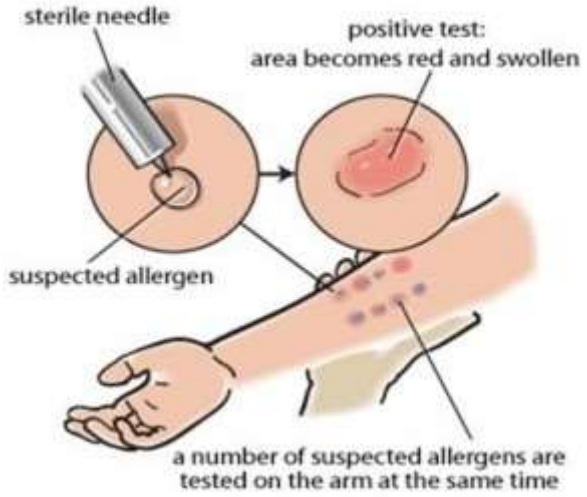

Figure E.2. Representation of ST procedure.

The ADs and maximum concentrations used for prick tests were as follows: BP-OL 0.04 mg/mL (with a molar concentration of the BPO moiety of $8.64x10^5$ mol), MD 0.5 mg/mL (with a molar concentration of sodium benzylpenilloate of $1.5x10^3$ mol), AX 20 mg/ml and CLV 20 mg/ml (all from DIATER Laboratories, Madrid, Spain).

Drug provocation test

Single-blind placebo controlled DPT consists on administration of drug increasing doses at regular time intervals of 30-60 minutes until therapeutical dose is reached, under strict medical surveillance[219, 261]

A. Immunological evaluation of pyrazinone-like potential ADs for aminocephalosporins.

When *in vitro* tests and ST s for cephalosporins were negative, DPT is performed using a cephalosporin with different side chain to that in the culprit drug in case of serious reactions. In cases of mild reaction, DPT with the culprit cephalosorin was performed in two days course, reaching a quarter of the therapeutic dose the first day and the whole dose the second.

B. Immunological evaluation of structures derived from CLV.

To confirm selective reactions, a single-blind, placebo controlled DPT was performed using BP and AX. In brief, in subjects with negative ST to BP-OL and MD, DPT with BP was performed by parenteral route with increasing doses until reaching the cumulative dose (10^6 IU) and this was followed by a 2 days therapeutic course of PV of 500 mg/8-hours. If DPT with BP and PV was negative and ST was negative to AX, a DPT with AX

was performed using incremental doses with 30-min time intervals until reaching a 500 mg cumulative dose and this was followed by a 2-day therapeutic course of AX 500 mg/8-hours. If good tolerance to AX was demonstrated and the ST result with CLV was negative, a DPT with AX-CLV was performed following the same procedure described earlier for DPT with AX.

1.8. *In vitro* tests

Sample collection

Nursing staff of different hospitals Allergy Units (Malaga and Italia) extracted 10 mL of peripheral blood in gels filled with gel (Vacuette, Greiner bio-one) and of 10-20 mL in lytic heparin tubes (Vacuette, Greiner bio-one). Tubes with gel were used for serum extraction by 4000 rpm centrifugation for 5 minutes and serum obtained was kept at -20˚C until use. Blood extracted in lytic heparin tubes was used for cellular tests which were performed up to 24 hours after extraction at the latest.

Radio Allergo Sorbent Test

SIgE levels in patient´s serum were quantified by RAST following the protocol previously described in our research group [262]. Cellulose discs (nº 54, Whatman International Ltd) were used as solid phase. They were activated by cyanogen bromide (Sigma-Aldrich), reacted with PLL (Sigma-Aldrich) as carrier molecule and then, ethanolamine or BSA were used for blocking remaining activated groups in cellulose discs (Figure E.3). Finally, discs were conjugated with AX (Glaxo Smithkline), BP (Normon), cefaclor (Sigma-Aldrich) or cefadroxil (Sigma-Aldrich) as previously described [56, 263]. Control discs containing PLL and blocked but without conjugation to drug were also prepared. Discs and silica nanoparticles (NPs) bearing different structures derived from CLV with transferrin or G2 PAMAM dendrimer as carrier molecules were prepared by Dr. Nekane Barbero. In this case, control discs or NPs beared carrier molecule in their surface without further conjugation with drug.

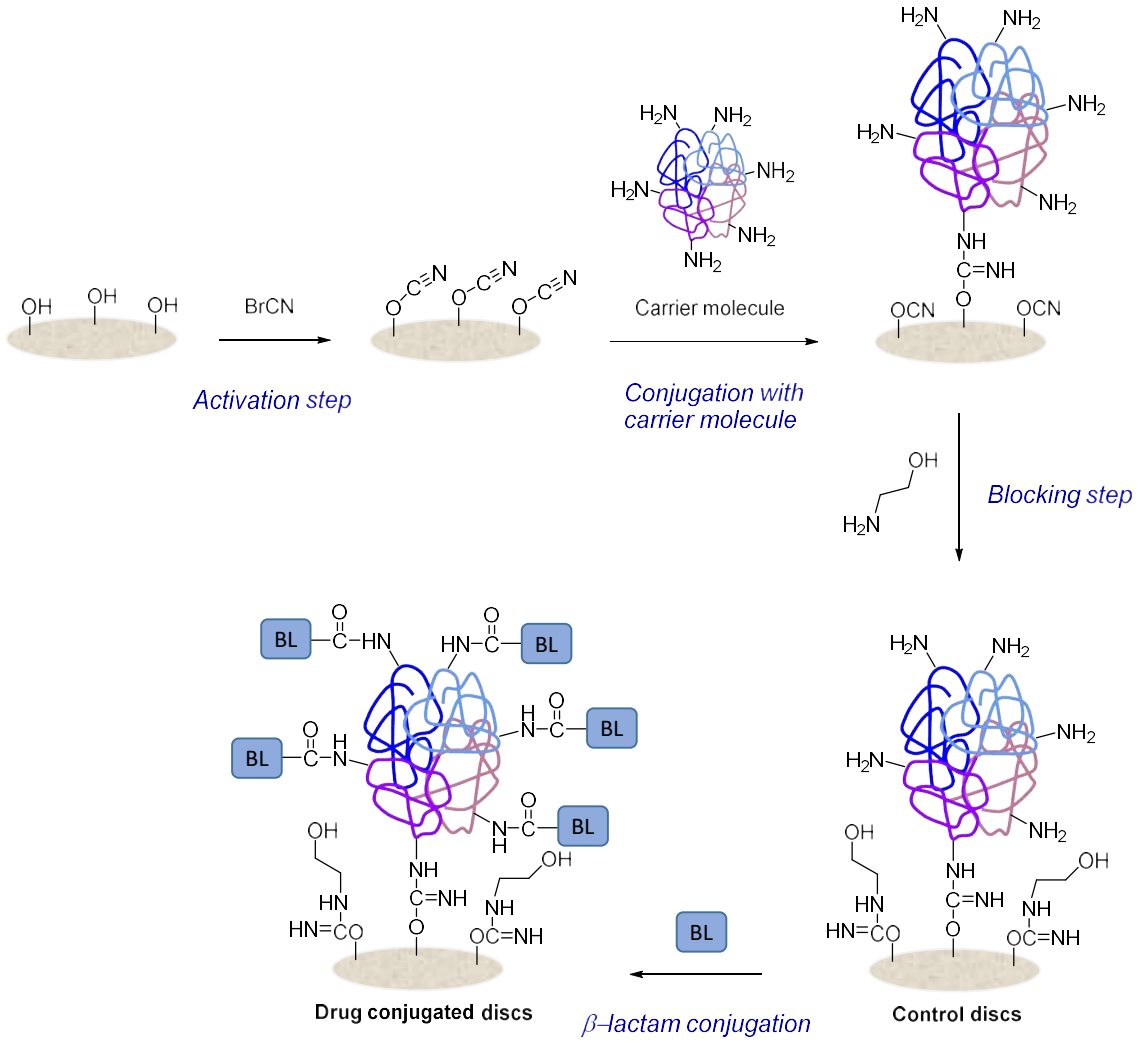

Figure E.3. Scheme of cellulose discs activation and conjugation with BLs.

Protocol used for RAST (Figure E.4) assays was the previously described by Wide *et al.* [264]. First, 30 µL of serum were incubated in duplicate with both drug conjugated and control discs for 3 hours at room temperature. After incubation, 3 washing steps with PBS1X-0.05% Tween 20 (v/v) were done and then, 25 µL of ^{125}I labeled α-human IgE (labeled by Chalatec or using our optimized protocol) added and incubated with samples for 16 hours. After incubation, 3 washing steps with PBS1X-0.05% Tween 20 (v/v) were done and counts per minute measured in a gamma counter (Cobra II Auto Gamma Counting System, Perkin-Elmer Packard). Counts per minute of 25 µL of I^{125} labeled α-human IgE were measured in duplicate as a reference maximum value. For NPs, described protocol was adapted being the only change the need of using centrifugation in washing steps.

Results were expressed as counts per minute obtained for drug conjugated discs minus counts per minute obtained for control discs, expressed as a counts per minute

percentage with respect to the maximum value (Equation E.1). Results were considered positive if calculated percentage was higher than mean + 2SD of results obtained for negative control sera group.

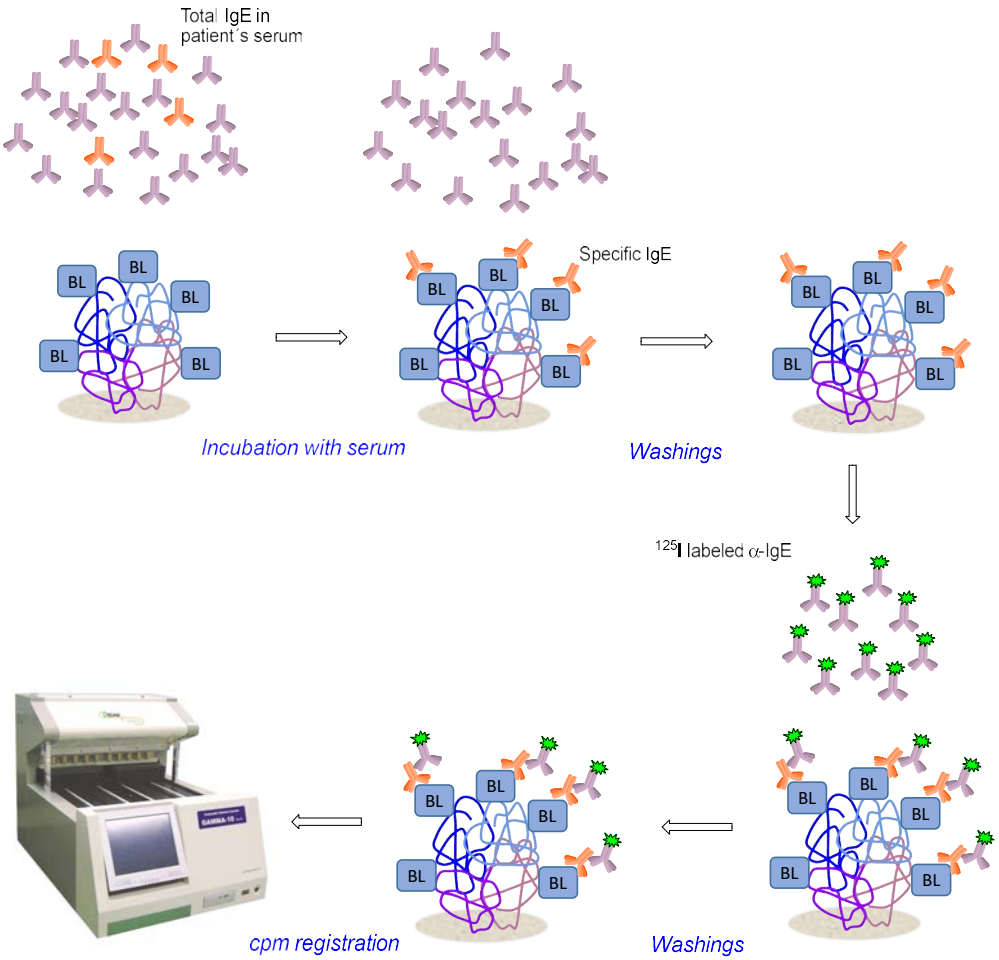

Figure E.4. Representation of RAST procedure.

$$RAST\% = \frac{cpm_{carrier\text{-}BL} - cpm_{control}}{cpm_{maximum}} x100$$

Equation E.1.

RAST inhibition

RAST inhibition assays were performed following previously described procedures [56, 262, 265]. Only sera with RAST % higher than 7% were inhibited and synthetic ADs and monomeric conjugates at two concentrations (10 and 100 mM) were used as inhibitors.

First, 30 µL of serum were incubated in duplicate with 15 µL of inhibitor for 3 hours at room temperature. As control, each serum was as well incubated in duplicate without inhibitor, with 15 µL of PBS1X. Then, solid phase (cellulose discs conjugated with cefaclor or AX) was added to each tube and were incubated for 3 hours. This incubation was followed by three washing steps with PBS1X-0.05% Tween 20 (v/v), after which, 25 µL of ^{125}I labeled α-human IgE were added and incubated for 16 hours. Again, incubation was followed by three washing steps with PBS1X-0.05% Tween 20 (v/v) and, finally, counts per minute were registered using a gamma counter (Figure E.5). Counts per minute of 25 µL of I^{125} labeled α-human IgE were also measured in duplicate as a reference maximum value.

Results were expressed as inhibition percentage of counts per minute obtained with inhibitors with respect to the control sample incubated with PBS1X (Equation E.2). Inhibition capacity was compared among structures used as inhibitors taking into account whether their inhibition percentage was higher than 50% at 100 mM.

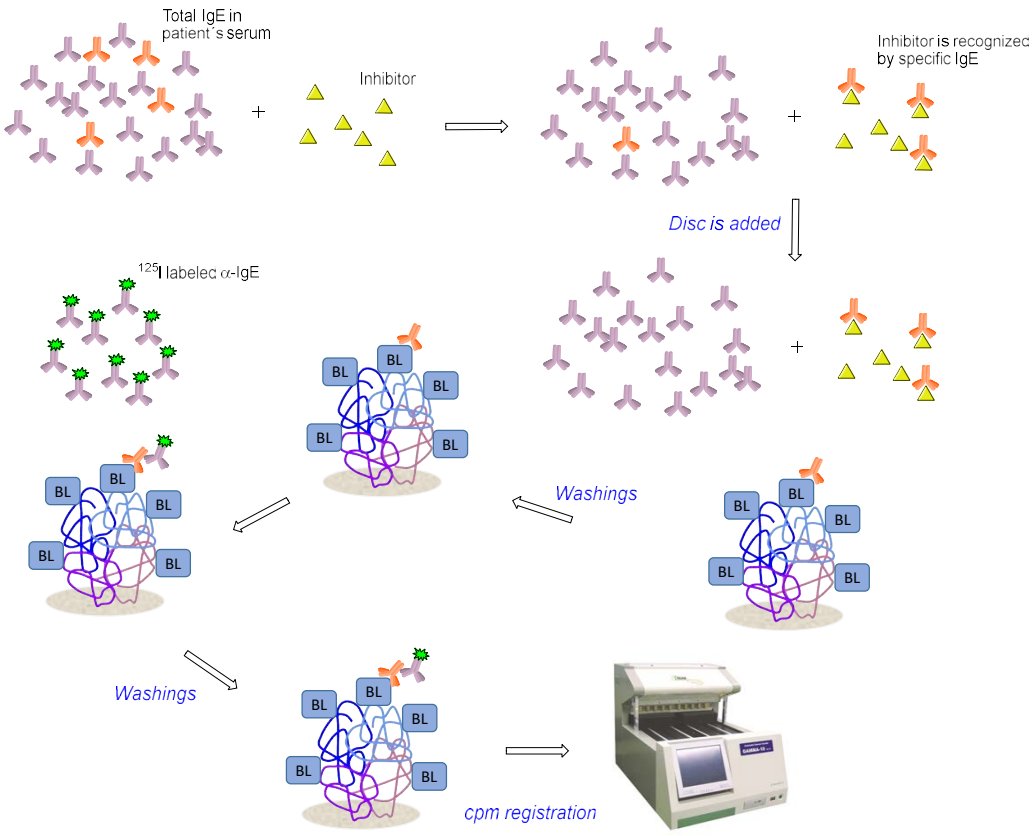

Figure E.5. Representation of RAST inhibition procedure.

$$Inhibition\% = \frac{RAST_{control}\% - RAST_{with\_inhibitor}\%}{RAST_{control}\%} x100$$

Equation E.2.

Basophil activation test

BAT was carried out following a four-step protocol adapted from the previously described [140] with CLV (Sigma Aldrich, Saint Louis, USA) and different synthetized structures (**Clav1** to **Clav6**) at different concentrations: 8, 4, 2 and 1 mM. Optimal concentrations for haptens were chosen on the basis of dose-response curves and cytotoxicity studies in order to avoid cytotoxic and non-sensitive concentrations.

1.Degranulation. 100 µL of heparinized whole blood was aliquoted per tube and 20 µL of stimulation buffer (0.78% NaCl, 0.037% KCl, 0.078% $CaCl_2$, 0.033% $MgCl_2$, 0.1% HSA, 1 M HEPES and 10 µg/ml IL-3) and 1 µL CCR3-APC (Biolegend) were added and incubated for 10 min at 37˚C in a water bath. Then, 100 µL of the washing solution was added to the negative control tube, 100 µL of α-human IgE (Dako, Santa Clara, CA, USA) to the positive control tube and 100 µL of different concentrations of haptens to the different samples. The samples were incubated for 30 min at 37˚C swinging in a water bath. The degranulation was stopped by incubating the samples on ice for 5 min.

2.Labeling. Cells were stained with monoclonal antibodies. 1 µL of α-CD63-FITC and 1 µL of CD203c-PE (Biolegend) were added to each tube and incubated for 20 min at 4˚C in the dark.

3.Lysis. Red blood cells were lysated and the rest of cells fixated by adding 2 mL of pre-warmed lysing solution (BD FACS Lysing solution, BD Biosciences) was added and incubated for 5 min at room temperature. Then, samples were centrifuged for 5 min at 1500 rpm and supernatant was discarded.

4.Washing. Samples were washed with 3mL PBS1X-0.05% Tween 20 (v/v) and centrifuged for 5 min at 1500 rpm, discarding the supernatant.

Cells were analyzed in a flow cytometer FACSCalibur flow cytometer (Becton-Dickinson Bioscience, San Jose, CA) by acquiring at least 500-1000 basophils per sample, selected as $CCR3^+CD203c^+$ cells (Figure E.7) and results were analized with FlowJo® software (Tree Star, Inc. USA) Activation was expressed as SI, calculated as the ratio between the percentage of activated basophils ($CD63^+$ cells) in samples stimulated with the different haptens and the negative control. Results were considered as positive when the SI) was ≤2 to at least one of the cocentrations mentioned above. The percentage of spontaneously activated basophils was required to be equal to or greater than 5% to

calculate the SI, as previously described [266]. ROC curves for evaluated haptens were performed to select the cut-off to obtain the best sensitivity/specificity balance.

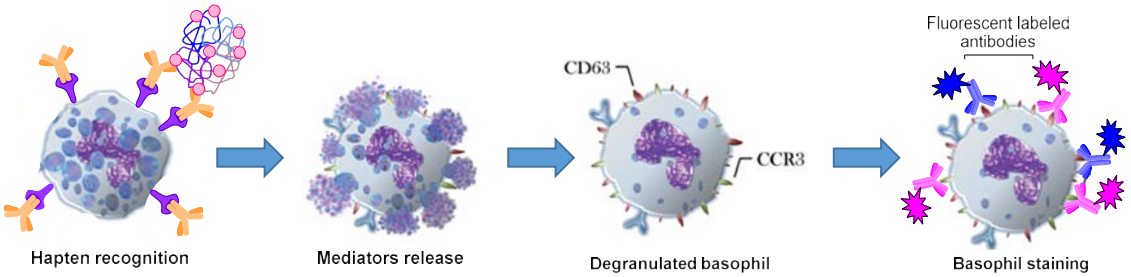

Figura E.6. Representation of steps involved in basophils activation.

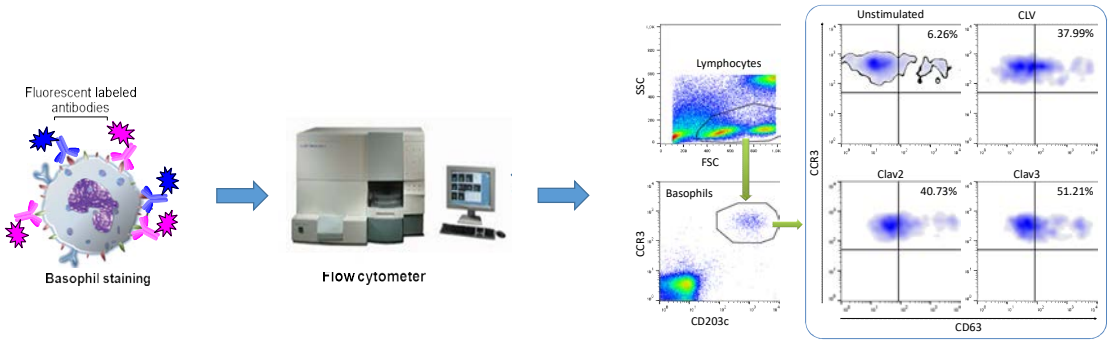

Figure E.7. Analysis of fluorescent labeled basophils and following cytometry dot plots showing basophils selection strategy and a representative example of positives results for tree different haptens.

BAT inhibition with Wortmannin

WTM acts as a specific inhibitor of phosphatidylinositol 3-kinase (PI3-K), which has been shown to be one of the important kinases activated by FcεRI receptor cross-linking involved in IgE-mediated stimulation of human basophils.[221]

To confirm that basophil activation was IgE mediated, we analyzed the WTM inhibitory effect at 1 µM [221]. This was used with the positive control (α-IgE) and the different haptens and synthetized structures at the same concentrations described previously. Protocol was the same as for BAT, but after peripheral blood sample incubation with stimulation buffer, 2.5 µL of 50 µM WTM were added and samples incubated swinging for 5 minutes at 37˚C. Then, 100 µL of hapten, washing buffer as negative control or α-IgE as positive control were added and protocol described in previous point was

followed.

1.9. Statistics for Basophil Activation Test

Continuous variable results were expressed as mean ± standard statistical error. Comparisons of quantitative variables without a normal distribution were done by the Mann-Whitney test for two variables and Kruskall-Wallis test for cases with more than two independent variables. Comparisons of qualitative variables were done by means of the χ^2 test. All reported P-values represent two-tailed tests, with values ≤ 0.05 considered statistically significant.

2. Study for identification of carrier proteins

2.1. Synthesis of Biotinylated Derivatives of CLV

Synthesis of CLV-B

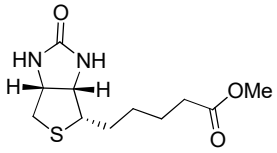

Methyl biotinate: Reported procedure was followed [267]. Thionyl chloride (45 μL) was added slowly to a suspension of biotin (50 mg, 0.204 mmol) in methanol (1.2 mL) and the mixture was stirred at ambient temperature for one hour. The reaction mixture was concentrated *in vacuo* to give quantitatively the methyl ester as a white solid (52 mg). Spectral data are in agreement with those reported in the literature [268].

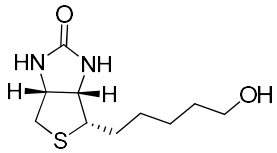

Biotinol: Reported procedure was followed [267]. To a suspension of methyl biotinate (52 mg, 0.204 mmol) in dry THF (2 mL) was added carefully $LiAlH_4$ (31 mg, 0.816 mmol) and stirred at room temperature overnight. The reaction mixture was quenched with MeOH (1 mL) and water (1 mL). $MgSO_4$ was added to the mixture and it was stirred for additional twenty minutes. Then, the reaction mixture was concentrated *in vacuo*, filtered and washed with 1:4 MeOH/CH_2Cl_2 (10 mL). The filtrate was concentrated *in*

vacuo to give quantitatively the target product as a white solid (47 mg). Spectral data are in agreement with those reported in the literature [269].

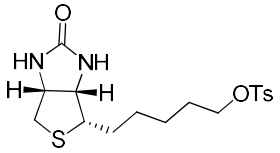

Biotin tosylate: Reported procedure was followed [267]. Tosyl chloride (47 mg, 0.245 mmol) was added to a suspension of biotinol (47 mg, 0.204) in dry pyridine (1.0 mL) in an ice bath. The reaction mixture was stirred at zero degrees for one hour and at ambient temperature overnight. Then, it was diluted with CH_2Cl_2 (5 mL) and washed with aqueous HCl 1M (5 mL), aqueous saturated $NaHCO_3$ (5 mL), water (5 mL) and brine (5 mL). The organic layer was dried over anhydrous $MgSO_4$, filtered, concentrated *in vacuo* and purified by flash chromatography eluting with 5% methanol in CH_2Cl_2 to give a white solid (29%). Spectral data are in agreement with those reported in the literature [270].

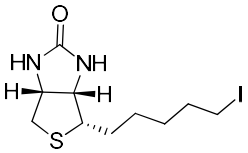

Biotin iodide: Reported procedure was followed [271]. Biotin tosylate (75 mg, 0.196 mmol) and NaI (60 mg, 0.391 mmol) were stirred at reflux in acetone (10 mL) for 24 h. The solvent was removed under reduced pressure and the residue was dissolved in CH_2Cl_2 and the organic layer was successively washed with aqueous saturated sodium thiosulfate (10 mL) and water, dried over anhydrous Mg_2SO_4, and concentrated under vacuum. Purification of the crude material by flash chromatography eluting with 5% MeOH in CH_2Cl_2 gave the target compound as a white solid (52 mg, 78%). Spectral data are in agreement with those reported in the literature [271].

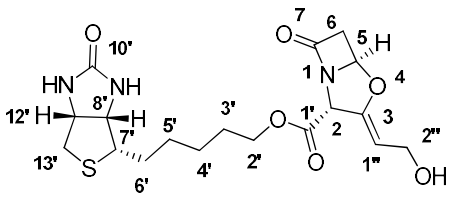

2-Biotin clavulanate (CLV-B): Reported procedure was followed [272]. Commercially available potassium clavulanate (44 mg, 0.173 mmol) and previously synthesized biotin iodide (49 mg, 0.144 mmol) under nitrogen atmosphere were stirred in dry DMF (2 mL)

at ambient temperature overnight. The solvent was removed under vacuum and the crude was purified by flash chromatography eluting with 5% methanol in CH_2Cl_2 to give the target compound as a white solid (35 mg, 60%).

^{1}H-NMR (400 MHz, DMSO-d_6): δ 6.43 (1H, s, NH), 6.36 (1H, s, NH), 5.69 (1H, d, *J* = 2.7 Hz, H_5), 5.18 (1H, s, H_2), 4.73 (1H, t, *J* = 6.8 Hz, H_1''), 4.30 (1H, t, *J* = 7.3 Hz, H_{12}'), 4.14-3.94 (5H, m, H_8'+ H_2' + H_2''), 3.62 (1H, dd, *J* = 16.8, 2.7 Hz, H_6, diastereotopic protons), 3.13-3.09 (2H, m, H_6 + H_7'), 2.82 (1H, dd, *J* = 12.5, 5.1 Hz, H_{13}', diastereotopic protons), 2.58 (1H, d, *J* = 12.5 Hz, H_{13}'), 1.60-1.23 (8H, m, H_6' + H_5' + H_4' + H_3'); **^{13}C-NMR** (400 MHz, DMSO-d_6): δ 175.5 (C7), 167.2 (C1'), 162.7 (C10'), 150.4 (C3), 101.2 (C1'), 87.5 (C5), 65.5 (C2'), 61.0 (C8'), 69.9 (C2), 59.2 (C12'), 55.5 (C2''), 55.4 (C7'), 46.0 (C6), 28.14, 28.11, 27.7 (C5', C4', C3'), 25.2 (C6'). C13' signal coincides with DMSO-d6 solvent signal (see HSQC). **HRMS** ($C_{18}H_{25}N_3O_6S$-H, 410.1385), found: 410.1385.

Synthesis of CLV-TEG-B

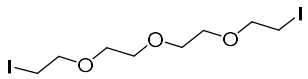

1-iodo-2-(2-(2-(2-iodoethoxy)ethoxy)ethoxy)ethane was prepared as follows: Tetraethylenglycol was first tosylated and this ditosylate was then subjected to reaction with NaI in acetone at reflux for 24h. Both reactions proceeded smoothly and quantitatively. Spectral data are in agreement with those reported by commercial firms.

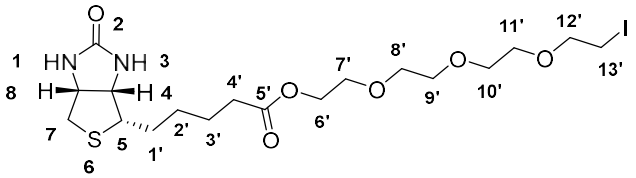

2-(2-(2-(2-Iodoethoxy)ethoxy)ethoxy)ethyl biotinate: Reported procedure was followed [230]. DMSO (5 mL) was added into a 25-mL Schlenk containing Biotin (244 mg, 1.0 mmol) under nitrogen atmosphere at room temperature. Then, NaH (44 mg, 1.1 mmol, 60% dispersion in mineral oil) was added under N_2 atmosphere and the reaction mixture was allowed to stir for 10 minutes. Then, previously prepared **1-iodo-2-(2-(2-(2-iodoethoxy)ethoxy)ethoxy)ethane** (555 mg, 1.4 mmol) in DMSO (2 mL) was added to the reaction and the mixture was stirred at room temperature overnight. Then, saturated aqueous NH_4Cl was added. Subsequently, it was extracted with EtOAc (3 x 10 mL) and the combined organic phases were dried over anhydrous $MgSO_4$, filtered and

concentrated *in vacuo*. The crude was purified by flash chromatography eluting with 5% methanol in CH_2Cl_2 to give the target compound as a white solid (184 mg, 35%).

^{1}H-NMR (400 MHz, $CDCl_3$): δ 6.29 (1H, s, NH), 5.83 (1H, s, NH), 4.38-4.35 (1H, m, H_8), 4.18-4.15 (1H, m, H_4), 4.10-4.07 (2H, m, H_6'), 3.62 (2H, t, *J* = 6.7 Hz, H_{12}'), 3.57 (2H, t, *J* = 4.9 Hz, H_7'), 3.53 (s, 8H, H_8', H_9', H_{10}', H_{11}', H_{12}'), 3.13 (2H, t, *J* = 7.0 Hz, H_{13}'), 3.04-2.99 (1H, m, H_5), 2.76 (1H, dd, *J* = 12.8, 5.0 Hz, H_7, diastereotopic protons), 2.61 (1H, d, *J* = 12.7 Hz, H_7), 2.24 (2H, t, *J* = 7.6 Hz, H_4'), 1.64-1.48 (4H, m, H_1', H_3'), 1.36-1.27 (2H, m, H_2'). **^{13}C-NMR** (400 MHz, $CDCl_3$): δ 173.6 (C5'), 164.0 (C2), 71.8, 70.5, 70.46, 70.40, 70.07, 69.04 (C7', C8', C9', C10', C11', C12'), 63.3 (C6'), 61.8 (C8), 60.0 (C4), 55.5 (C5), 40.4 (C7),33.7 (C4'), 28.26, 28.11 (C2', C3'), 24.6 (C1'), 3.1 (C13'). **HRMS** ($C_{18}H_{31}IN_2O_6S$+H, 531.1020), found: 531.1015.

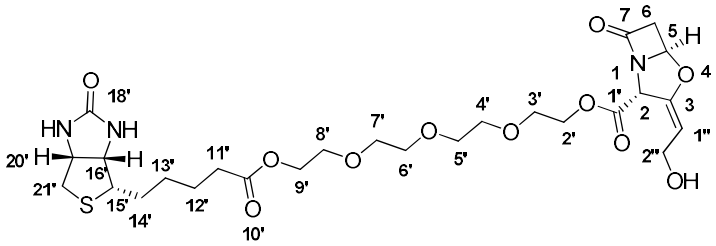

2-Tetraoxadodecane-biotin clavulanate (CLV-TEG-B): Reported procedure was followed [272]. Commercially available potassium clavulanate (53 mg, 0.223 mmol) and previously synthesized 2-(2-(2-(2-Iodoethoxy)ethoxy)ethoxy)ethyl biotinate (130 mg, 0.246 mmol) under nitrogen atmosphere were stirred in dry DMF (2 mL) at ambient temperature overnight. The solvent was removed under vacuum and the crude was purified by flash chromatography eluting with 5% methanol in CH_2Cl_2 to give the target compound as a colorless oil (20.0 mg, 15%).

^{1}H-NMR (400 MHz, $CDCl_3$): δ 5.90 (1H, s, NH), 5.68 (1H, d, *J* = 2.3 Hz, H_5), 5.35 (1H, s, NH), 5.05 (1H, d, *J* = 1.1 Hz, H_2), 4.97 (1H, dt, *J* = 6.9, 1.3 Hz, H_1''), 4.51-4.47 (1H, m, H_{16}'), 4.31-4.19 (7H, m, H_{20}', H_2', H_2'', H_9'), 3.71-3.58 (12H, m, H_3', H_4', H_5', H_6', H_7', H_8'), 3.48 (1H, dd, *J* = 16.7, 2.8 Hz, H_6, diastereotopic protons), 3.16-3.11 (1H, m, H_{15}'), 3.08 (1H, d, *J* = 16.7 Hz, H_6), 2.89 (1H, dd, *J* = 12.8, 5.0 Hz, H_{21}', diastereotopic protons), 2.74 (1H, d, *J* = 12.8 Hz, H_{21}'), 2.36 (2H, t, *J* = 7.3 Hz, H_{11}'), 1.74-1.63 (4H, m, H_{12}', H_{14}'), 1.48-1.39 (2H, m, H_{13}'). **^{13}C-NMR** (400 MHz, $CDCl_3$): δ 174.8, 173.8, 167.3, 163.7 (C=O), 152.0 (C3), 101.0 (C1''), 87.9 (C5), 70.8, 70.6, 70.4, 69.3, 69.8 (oxygenated chain), 63.51, 63.49 (C2', C9'), 62.0 (C20'), 61.7 (oxygenated chain), 60.5, 60.2 (C2, C16'), 57.2 (C2''), 55.6 (C15'), 46.5 (C6), 40.6(C21'), 33.9 (C11'), 28.4, 28.3 (C12', C13'), 24.8 (C14'). **HRMS** ($C_{26}H_{40}N_3O_{11}S$+H, 602.2378), found: 602.2378.

2.2. Human serum proteins *in vitro* modification by CLV

HSA *in vitro* modification by CLV

Some solutions were prepared with different concentrations of CLV in PBS1X (pH 7.4). These solutions were incubated with an equivalent volume of HSA 20 mg/mL prepared in PBS1X (pH 7.4) for 16 hours at 37˚C. HSA final concentration was 10 mg/mL (0.15 mM) in every case and CLV final concentrations were from 0.36 to 11.52 mg/mL (1.5 to 48 mM) to include molar ratio protein/drug from 1:10 to 1:320. In order to eliminate unbound β-lactam after conjugation, Amicon Filters (Merck Millipore) were used. Several washing steps were performed with milliQ water and filtrates were collected, freeze-dried and analyzed by ^{1}H-NMR. Conjugates were considered clean when NMR evidence of no drug left in filtrates.

HSA *in vitro* modification by CLV-B and CLV-TEG-B

Solutions of each biotynilated derivative, **CLV-B** and **CLV-TEG-B**, were prepared at 180 mM in DMSO and PBS1X (pH 7.4), respectively. Nine decreasing fivefold dilutions of each solution were prepared in PBS1X (pH 7.4) and these solutions were incubated for 16 hours at 37˚C with an equivalent volume of HSA 20 mg/mL prepared in PBS1X (pH 7.4). HSA final concentration was 10 mg/mL (0,15 mM) in every case and final concentrations of CLV biotynilated derivatives were from 1:600 to 1:3,1·10^{-4} molar ratio protein/drug.

Also, HSA-**CLV-TEG-B** conjugates were prepared at 1:1, 1:10 and 1:100 protein/drug molar ratio. They were purified by dialysis filtration using Amicon filters (Merck-Millipore).

Resulting conjugates were analyzed by monodimensional SDS-PAGE followed by modification detection with streptavidin-HRP and ECL and/or MALDI-TOF MS.

In vitro modification of a HSA peptide by CLV-TEG-B

CLV-TEG-B was dissolved in PBS1X (pH 7.4) at 0.30 mM [88] and incubated with an equivalent volume of 27 mM $^{182\text{-}195}$HSA peptide (MW = 1518.68 Da) in PBS1X (pH 7.4) for 24 hours at 37˚C. Final peptide/ **CLV-TEG-B** ratio was 1:90. Resulting conjugate was purified using PD G-10 Desalting Columns (GE Healthcare) and analyzed by MALDI-TOF MS.

Human serum *in vitro* modification by CLV-TEG-B

Total amount of protein in tree human sera obtained from healthy donors was quantified by Bradford. **CLV-TEG-B** was dissolved in PBS1X (pH 7.4) to get the needed concentration and was incubated with an equivalent volume of serum for 16 hours at 37˚C. Conditions chosen for incubation were total protein/**CLV-TEG-B** ratios 1:0.192 and 1:0.00768 since a good signal was obtained in these conditions, without saturation. Resulting conjugates were analyzed by monodimensional SDS-PAGE as well as by 2D-electrophoresis followed by modification detection with streptavidin-HRP and ECL and proteins identification by MS (peptidic fingerprint).

2.3. Enrichment of biotynilated fraction

- Soft Link release Avidin, Promega

HSA-**CLV-TEG-B** 1:10 was purified with SoftLink Soft Release Avidin Resin (Promega) following manufacturer´s instructions.

-Pull-down

First, NeutrAvidin-Agarose resin (Thermo Scientific) was equilibrated. 200 µL of resin slurry (corresponding to 100 µL of settled resin) were washed 5 times with mild homogenization buffer (50 mM Tris-HCl pH 7.4, 1 mM EDTA, 1 mM EGTA, 0.2% NP-40 and 0.1% SDS). Each washing step consisting on stirring for some seconds, centrifuging at 500 g and 4˚C for 1 minute and discarding the supernatant. 100 µL of mild hogenization buffer were added to the resulting 100 µL of dried beads in order to have a 1:1 (v/v) resin slurry.

Purification of an HSA-**CLV-TEG-B** 1:10 and control HSA aliquots were carried out in parallel.

Sample was diluted with mild homogenization buffer to 0.4 µg/µL (input) and 50 µL (20 µg) were added to 50 µL resin slurry (25 µL dried resin) and volume completed up to 200 µL with mild homogenization buffer. Samples were incubated stirring for two hours at room temperature. Then, samples were centrifuged at 500 g and 4˚C for 1 minute and supernatant volume recovered and kept (not bound). Resin was washed four times with 500 µL strong buffer (50 mM Tris-HCl pH 7.4, 1 mM EDTA, 1 mM EGTA, 1% NP-40 and 0.5% SDS) stirring for some seconds, centrifuging at 500 g and 4˚C for 1 minute and discarding the supernatant. A fifth washing was made with 200 µL strong buffer and, after centrifugation, supernatant volume recovered and kept (last washing).

In order to release biotynilated protein from the resin, 100 µL of sample buffer 1X (1/5 dilution of 1g SDS, 5 mL glycerol, 4 mL 1 M Tris-HCl pH 6.8, 2.5 mL β-mercaptoethanol and bromophenol blue) were added over the dried resin, the slurry was stirred for some minutes at room temperature and then, heated at 95˚C for 5 minutes. After a "short spin" supernatant was recovered and kept (elution) and dried resin was discarded.

2 µg of samples and a molecular weight marker were loaded in a SDS-polyacrylamide gel (10%, 1.5 mm) in a final volume of 50 µL (sample volume completed up to 40 µL with mild homogenizing buffer and 10 µL sample buffer 5X) as follows:

$Input_{HSA}$/Not $bound_{HSA}$/Last $washing_{HSA}$/$Eluted_{HSA}$//$Eluted_{HSA\text{-}CLV\text{-}B}$/Last $washing_{HSA\text{-}CLV\text{-}B}$/Not $bound_{HSA\text{-}CLV\text{-}B}$/$Input_{HSA\text{-}CLV\text{-}B}$

2.4. Characterization of modified proteins by SDS-PAGE techniques

Monodimensional SDS-PAGE characterization of proteins conjugated with CLV biotynilated derivatives general procedure

After conjugation, HSA or human sera modified *in vitro* by CLV derivatives were denaturalized by adding Laemmli buffer and heating at 96˚C for 5 minutes. Eppendorf tubes containing denaturalized samples were centrifuged for some seconds (were given a short spin) and quickly cold in ice bath to avoid renaturalization. 2-4 µg of protein from each sample were loaded in 12% SDS-polyacrilamide gel and electrophoresis system was connected to a power supply with a 80 V current until samples pass through stacking gel and 120 V for separation since samples reached running (resolving) gel.

Once finished electrophoresis, proteins were transferred to a PVDF membrane (Trans-Blot Turbo Mini PVDF Transfer Packs, Bio-Rad) using Trans-Blot Turbo Transfer System from Bio-Rad following manufacturer´s indications. Membranes were blocked for 1 hour at room temperature with 1X blocking solution in H_2O milliQ (prepared from 10X Blocking Buffer, SIGMA) and washed three times for 10 minutes with PBS-Tween 20 0,05% (v/v). Then, membranes were incubated with streptavidin-horseradish peroxidase (HRP) conjugate (Amersham, GE Biosciences) dilution 1/1000 in 1% BSA (w/v) in PBS-Tween20 0.05% (v/v) and washed three times for 10 minutes with PBS-Tween 20 0,05% (v/v). Chemiluminiscence was used for detection (Clarity Western ECL Substrate, Bio-Rad) and images were analyzed using ImageQuant LAS4000, GE Healthcare.

Identification of modified serum proteins by 2D-electrophoresis

For two-dimensional electrophoresis, aliquots of control and **CLV-TEG-B**-treated human serum, with protein/drug ratio 1:0,192, containing 20 µg of protein were precipitated with cold acetone stirring overnight at 4˚C. Then, acetone was decanted and the pellet

completely dried using a Speedvac system. The dried pellet was resuspended in 278.4 µL of IEF simple buffer (4% CHAPS, 2 M thiourea, 7 M urea, 100 mM DTT) and 1.5 µL of Bio-lyte ampholytes pH range 3-10 and 2 µL of bromophenol blue added.

Sample was then divided in two aliquots and loaded on two ReadyStrip IPG Strips (pH 3–10 lineal, 7 cm, Bio-Rad) placed in a Protean IEF cell (Bio-Rad) and rehydrated for 12 hours at 50 V and 20˚C, 50 µA per strip before six steps isoelectrofocusing: 1) 250 V for 1 hour; 2) 500 V for 1 hour; 3) 1000 V for 1 hour; 4) 2000 V for 1 hour; 5) 8000 V for 1 hour and 6) 8000 V for 1 hour. After isoelectrofocusing, strips were washed with milliQ water and equilibrated in two fifteen-minute steps stirring at room temperature in the dark with equilibration buffer (6 M urea, 2% SDS, 0.375 M Tris-HCl pH 8.8, 20% glycerol and bromophenol blue) containing 130 mM DTT for first step and 135 M iodoacetamide for second step.

Equilibrated strips were loaded in duplicate in SDS-polyacrilamide gels (10%, 1.5 mm) using 0,5% agarose to fix them to the gels, which were run in duplicate. One of them was stained with SYPRO Ruby (Bio-Rad) for total protein pattern and the other one transferred to a PVDF membrane to detect proteins modified by **CLV-TEG-B** with streptavidin-HRP and chemiluminiscent detection (Clarity Western ECL Substrate, Bio-Rad).

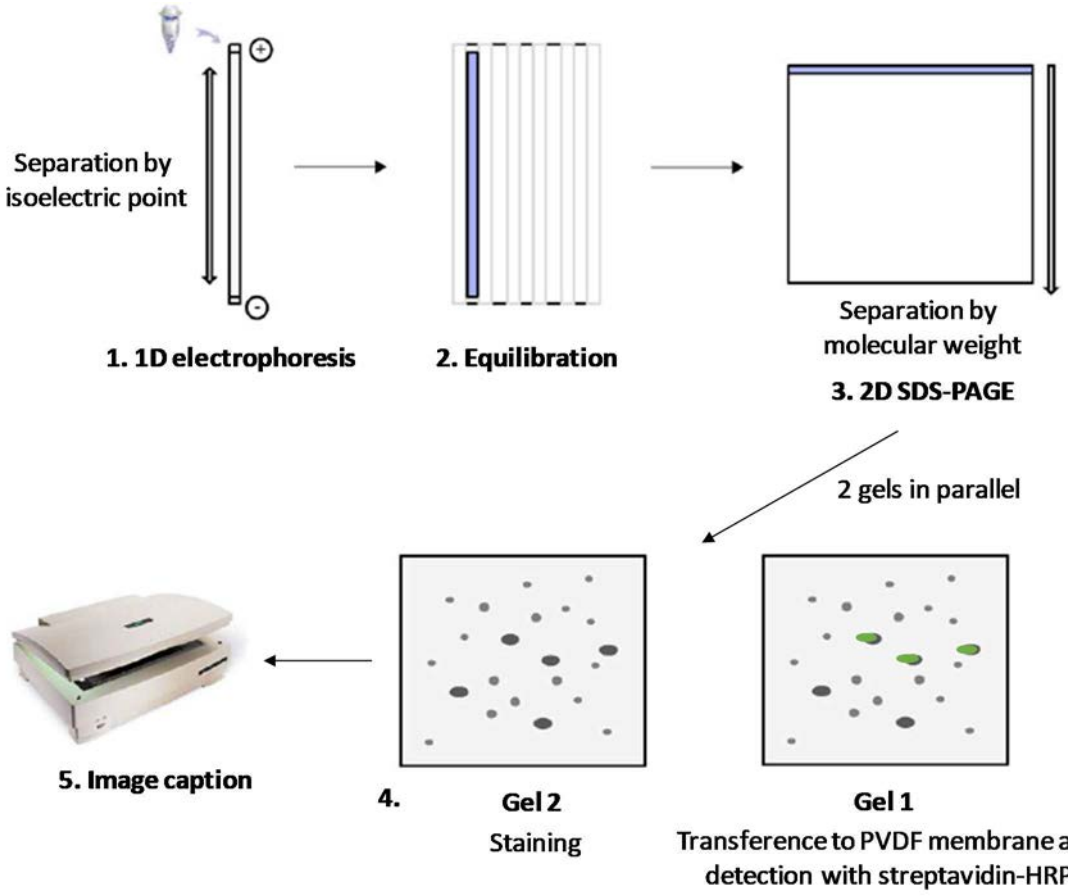

Figure E.8. Representation of 2D SDS-PAGE procedure. Adapted from Laborde *et al.* [273]

Determination of the Extent of Biotinylation in HSA conjugates

Estimation of the incorporation of CLV-B in HSA conjugates (1:1, 1:10 and 1:100) was made by comparison with a biotinylated BSA standard (Pierce). A known amount of conjugates (2 pmol) and six increasing amounts of biotinylated BSA (from 0.006 to 6 pmol) were subjected to SDS-PAGE and transferred to a PVDF membrane following the general procedure.

First of all, HSA conjugates correct load was checked. Membranes were blocked for 1 hour at room temperature with 1X blocking solution in H_2O milliQ (10X Blocking Buffer, SIGMA) and washed three times for 10 minutes with PBS-Tween 20 0,05% (v/v). After that, membranes were incubated with 1 µg/mL α-HSA primary antibody (ALB(F-10):sc-271605, Santa Cruz Biotechnology) in 1% BSA (w/v) in PBS-Tween20 0,05% (v/v), washed three times for 10 minutes with PBS-Tween 20 0,05% (v/v) and incubated with 1/2000 dilution polyclonal rabbit α-mouse IgG conjugated with HRP (P0260, DAKO) in 1% BSA (w/v) in PBS-Tween20 0,05% (v/v) and finally washed three times for 10 minutes with PBS-Tween 20 0,05% (v/v) and detected by chemiluminiscence (Clarity Western ECL Substrate, Bio-Rad) and images were analyzed using ImageQuant LAS4000, GE Healthcare.

For detection of biotinylation, stripping of the membranes was necessary. Membranes were washed three times for 5 minutes with milliQ water and incubated with HCl guanidine 8M for 15 min at room temperature. After three five-minute washings with milliQ water, membranes were incubated with streptavidin-HRP (Amersham, GE Biosciences) dilution 1/1000 in 1% BSA (w/v) in PBS-Tween20 0,05% (v/v) and washed three times for 10 minutes with PBS-Tween 20 0,05% (v/v). Chemiluminiscence was used for detection (Clarity Western ECL Substrate, Bio-Rad) and images were analyzed using ImageQuant LAS4000, GE Healthcare.

We analyzed images obtained with ImageJ software (National Institutes of Health) for three replicates and expressed the results as pmol biotin/pmol HSA.

Competition between CLV and CLV-TEG-B for HSA modification

A solution of HSA 20 mg/mL and solutions of CLV 160, 1600, 16000, 24000, 48000, 96000, 160000 and 192000 µM were prepared in PBS 1X pH 7.4. HSA was preincubated overnight at 37˚C with equivalent volumes of the indicated increasing concentrations of CLV, and only with PBS 1X pH 7.4 as control. The final concentration of HSA was 10 mg/mL in every case and the final concentration of CLV was 80, 800, 8000, 12000, 24000, 48000, 80000 and 96000 µM, respectively.

After preincubation, **CLV-TEG-B** was added to each conjugate to have a final concentration of 80 µM. They were incubated for 2 hours at 37˚C.

CLV molar excess in conjugates with respect to **CLV-TEG-B** was: 0X, 1X, 10X, 100X, 150X, 300X, 600X, 1000X and 1200X (Table E.2).

Table E.2. CLV and **CLV-TEG-B** concentrations used for comprtitions experiments.

	$[HSA]_0$	$[HSA]_f$	$[CLV]_0$	$[CLV]_f$	$[CLV\text{-}TEG\text{-}B]_f$	V_f
CLV 0	20 mg/mL 0,3 mM	10 mg/mL 0,15 mM	0 mg/mL 0 µM	0 mg/mL 0 µM	80 µM	200 µL
CLV 1X			$3{,}80\cdot10^{-2}$ mg/mL 160 µM	$1{,}90\cdot10^{-2}$ mg/mL 80 µM		
CLV 10X			$3{,}80\cdot10^{-1}$ mg/mL 1600 µM	$1{,}90\cdot10^{-1}$ mg/mL 800 µM		
CLV 100X			3,80 mg/mL 16000 µM	1,90 mg/mL 8000 µM		
CLV 150X			5,69 mg/mL 24000 µM	2,85 mg/mL 12000		
CLV 300X			11,39 mg/mL 48000 µM	5,69 mg/mL 24000 µM		
CLV 600X			22,78 mg/mL 96000 µM	11,40 mg/mL 48000 µM		
CLV 1000X			37,96 mg/mL 160000 µM	19,00 mg/mL 80000 µM		
CLV 1200X			45,55 mg/mL 192000 µM	22,80 mg/mL 96000 µM		

SDS-PAGE of 2 µg aliquots from the incubation was carried out. After transfer to a PVDF membrane, incorporation of CLV-B was assessed by detection with HRP-streptavidin followed by ECL.

2.5. Mass spectrometry

MALDI-TOF of protein conjugates

The MALDI-TOF mass spectra of complete protein were acquired at SCAI, UMA, Proteomic Unit, using a MALDI TOF TOF Bruker UtraFlextreme and were recorded by dissolving conjugates in milliQ water containing 0.1% trifluoroacetic acid (TFA) and using sinapinic acid (SPA) or α-cyano-4-hydroxycinamic acid (CHCA) as the matrix for proteins or peptides, respectively.

Binding sites identification

These experiments were carried out at University Hospital Vall d´Hebron Research Institute Proteomic Laboratory.

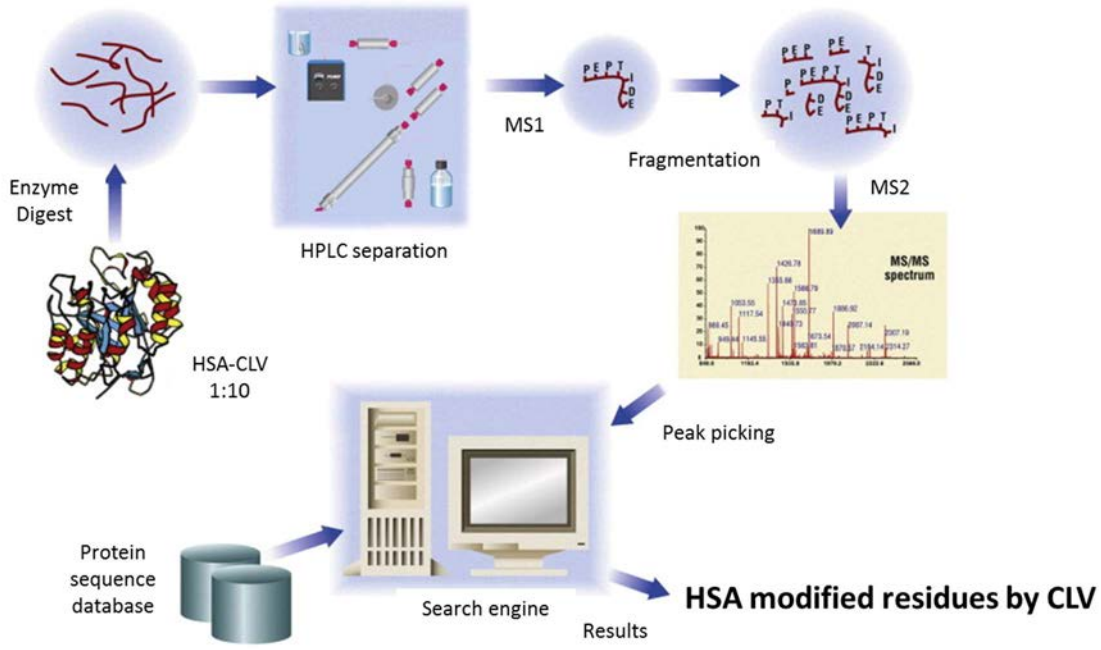

Figure E.9. Scheme of experimental procedure used for binding sites identification.

- Liquid chromatography-Mass spectrometric analysis (Orbitrap):

Control HSA as well as HSA modified with ten molar excess of CLV (HSA-CLV 1:10), were digested with Arg-C, Trypsin and chymotrypsin, and then analyzed on an LTQ Velos-Orbitrap mass spectrometer (Thermo Fisher Scientific, Bremen, Germany), coupled to a nano-HPLC system (Proxeon, Denmark) and an Impact HD high resolution Q-TOF spectrometer (Bruker, Bremen), coupled to a nano-HPLC system (Proxeon, Denmark). Peptide mixtures were initially concentrated on a 100 µm ID, 2cm Proxeon nanotrapping column packed with Reprosil C18, 5 mm particle size (Proxeon, Denmark), and subsequently separated on the analytical nano reverse phase column, as indicated below.

- Orbitrap analysis: an EASY-column, 75 mm ID, 10 cm long and packed with Reprosil, 3 µm particle size (Proxeon, Denmark) was used as analytical column. An acetonitrile gradient (5-35% ACN/0.1% formic acid in water, in 22 min, flow rate ca. 300 nL/min) was used to elute the peptides through a stainless steel nano-bore emitter (Proxeon, Denmark) onto the nanospray ionization source of the LTQ Velos-Orbitrap mass spectrometer. MS/MS fragmentation (200 ms, 100–2800 m/z) of twenty of the most intense ions when their intensity exceeded a minimum threshold of 1000 counts was carried out, as detected from a 500 ms MS survey scan (300–1500 m/z), using a dynamic exclusion time of 20 sec for precursor selection and excluding single-charged ions.

- Impact QTOF analysis: a 75 µm ID, 15 cm Acclaim PepMap column (Dionex) was used for separation. Chromatography was run using a 0.1% formic acid-acetonitrile gradient (5-35% in 22 min; flow rate 300 nL/min). The column was coupled to the mass spectrometer inlet through a Captive Spray (Bruker) ionization source. MS acquisition was set to cycles of MS (1Hz), followed by MS/MS (0.5-2Hz) of the 8 most intense precursor ions with an intensity threshold for fragmentation of 5000 counts and using a dynamic exclusion time of 0.5 min and exclusion of single charged ions. All spectra were acquired in the range 100-2200 Da. LC-MS/MS data was analyzed using the Data Analysis 4.2 software (Bruker).

- Peptide identification: Proteins were identified using Mascot (Matrix Science, London UK) to search against the sequence of isoform 1 of HSA; ALBU_HUMAN. MS/MS spectra were searched with a precursor mass tolerance of 10 ppm, fragment tolerance of 0.7 Da (Orbitrap) or 0.05 Da (Impact), and the corresponding enzyme specificity. Cysteine carbamidomethylation was set as fixed modification and methionine oxidation, as well as the CLV modifications, were set as variable modifications. The specificity for the CLV fragment modifications was defined in Cys, Hys and Lys as well as in the protein N-terminal.

Peptidic fingerprint

This proteomic analysis or identification of serum poteins modified by **CLV-TEG-B** was performed in the Proteomics Unit of Complutense University of Madrid that belongs to ProteoRed, PRB2-ISCIII, supported by grant PT13/0001.

First step was 2D-electrophoresis of samples. The spots of interest were then manually excised from gels. Proteins selected for analysis were in-gel reduced, alkylated and digested with trypsin according to Sechi *et al*. Briefly, the samples were reduced with 10 mM dithioerytritol in 25 mM ammonium bicarbonate for 30 min at 56˚C and subsequently alkylated with 25 mM iodoacetamide in 25 mM ammonium bicarbonate for 15 min in the dark. Finally, samples were digested with 12.5 ng/µl sequencing grade trypsin (Roche Molecular Biochemicals) in 25 mM ammonium bicarbonate (pH 8.5) overnight at 37˚C.

After digestion, the supernatant was collected and 1µl was spotted onto a MALDI target plate and allowed to air-dry at room temperature. Then, 0.6 µl of a 3 mg/ml of α-cyano-4-hydroxy-cinnamic acid matrix (Sigma) in 50% acetonitrile were added to the dried peptide digest spots and allowed again to air-dry at room temperature.

MALDI-TOF MS analyses were performed in a 4800 Plus Proteomics Analyzer MALDI-TOF/TOF mass spectrometer (Applied Biosystems, MDS Sciex, Toronto, Canada). The MALDI-TOF/TOF operated in positive reflector mode with an accelerating voltage of

20000 V. All mass spectra were calibrated internally using peptides from the auto digestion of trypsin.

For protein identification SwissProt 20170116 (553231 sequences; 197953409 residues) with taxonomy restriction to human was searched using MASCOT 2.3 (www.matrixscience.com) through the software Global Protein Server v 3.6 (ABSciex). Search parameters were:

-Carbamidomethyl Cystein as fixed modification and oxidized methionine as variable modification

-Peptide mass tolerance, 50 ppm (PMF)

-1 missed trypsin cleavage site

In all protein identification, the probability scores were greater than the score fixed by mascot as significant with a p-value minor than 0.05.

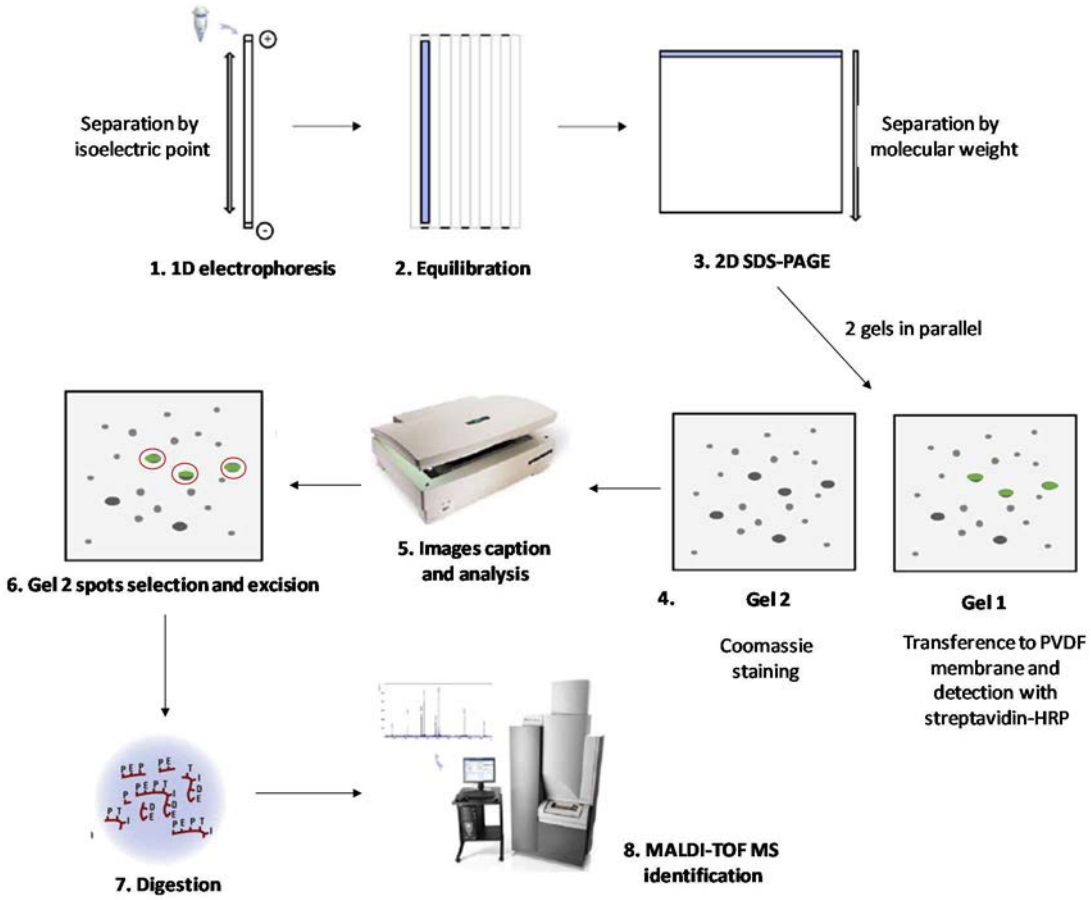

Figure E.10. Schamatic representation of procedure for proteins identification by peptidic fingerprint. Adapted from Laborde *et al.* [273].

2.6. Molecular modeling

In order to obtain further insights into the observed adducted Lys, molecular modeling studies were performed, exploring the regions surrounding the modified residues.

The crystal structures of HSA and CLV, considered in its carboxylate form (CLV), were obtained from RCSB Protein Data Bank (PDB ID: 1AO6 and PDB ID: J01) [274]. The relaxation of the chain-A from HSA was performed with AMBER 12 MD software package [275] and the parm99 force field, using a full atomistic simulation. To preserve the charge neutrality, an appropriate number of chloride counterions were added. Then, the protein was solvated in a truncated octahedral cell, with a minimum of 10 Å solvation shell around the structure, and the TIP3P water model [276]. To retain the experimental folding, the solvated structure was minimized keeping fixed the backbone atoms during the initial cycle of conjugated gradient minimization. The optimized structure obtained was used in the docking analysis.

For each recognized site of addition, a docking search was performed using the AutoDock 4.2 software [277] and a 14 Å sphere around the adducted lysines (in their neutral form) was considered. CLV was docked into this grid with the Lamarckian algorithm and the ligand flexible bonds were left free to rotate. The genetic-based algorithm generated 100 poses and the other parameters were left at default settings. The obtained complexes were ranked considering both the docking scores and the distance between the lysine's amino group and the CLV β-lactam carbonyl group.

3. Labeling of secondary antibodies

3.1. Radioactive labeling

Labeling optimization

α-Human IgG Fc clone SG-11 (ICN Biomedicals Inc) was diluted at 1 mg/mL with PBS 1X. An aliquot of 15 µL (15 µg) was separated from the stock solution and volume completed up to 45 µL with PBS 1X. Previous mixture was added to the bottom of a Pierce Pre-Coated Iodination Tube (Thermo Fisher Scientific) and, immediately after, NaI^{125} (NEZ033A001MC, Perkin Elmer) of 103, 23 mCi/mL concentration and 17 Ci/mg specific activity incorporated to the reaction. Two experiments were carried out in parallel with different amount of NaI^{125}. In Experiment 1, 0.7 µL (75 µCi) of NaI^{125} were added, and in Experiment 2, 2.4 µL (250 µCi). The following steps were the same for each of them.

Antibody solution and NaI^{125} in iodinating tubes were left to react at room temperature for 15 minutes, moving softly the mixture for 10 seconds every minute. After this time, the mixture was taken out of the iodination tube and the volume completed with PBS1X

up to 500 µL to stop the reaction (stop solution). We kept 5 µL to measure the maximum as reference for calculations.

For antibody purification, a sephadex PD Minitrap G-25 (GE Healthcare Life Sciences) column was used. First, top and bottom caps were removed and column storage solution discarded. Then, column was equilibrated with 8 mL of PBS 1X, discarding the flow-through. When all equilibration buffer had entered completely the packed bed, the 500 µL of stop solution were immediately loaded in the column. The sample was allowed to enter the packed bed completely and the flow-through collected as fraction number one. Then, PBS 1X was added and 15 more 0.5 mL fractions were collected in 15 eppendorfs (separately).

As many measurement solutions as fractions collected were prepared adding 5 µL of the fraction to 4 mL of scintilliating liquid. Maximum solutions were prepared the same way. Radioactivity was measured using a HIDEX 300 SL gamma counter for identification of fractions containing radiolabeled IgG for both Experiment 1 and Experiment 2.

Radioactivity values obtained for fractions and maximums by measurement in gamma counter are collected in Table E.3.

Table E.3. Radioactivity results for fractions collected during purification step in optimization experiments. Cpm: counts per minute; dpm: desintegrations per minute; TDCR: Triple-to-double coincidence ratio. *Values of 1/2 dilution since direct measurement leaded to detector saturation.

	75 µCi			250 µCi		
	cpm	**dpm**	**TDCR**	**cpm**	**dpm**	**TDCR**
Maximum	432515	627685	0,689	1590000*	2280000*	0,696*
Fraction 1	419	12594	0,033	747	23301	0,032
Fraction 2	50097	79930	0,626	468582	737185	0,653
Fraction 3	138510	218914	0,632	1250000	1960000	0,639
Fraction 4	12062	19497	0,618	83203	128487	0,647
Fraction 5	20637	32473	0,635	131147	199934	0,655
Fraction 6	24623	38486	0,639	190406	289038	0,658
Fraction 7	17239	27132	0,635	400	7653	0,052
Fraction 8	10784	17178	0,627	50562	77511	0,652
Fraction 9	6133	10378	0,59	33249	51693	0,643
Fraction 10	4672	8059	0,579	21014	32966	0,637
Fraction 11	3394	6203	0,547	16641	25974	0,64
Fraction 12	2689	5301	0,507	11116	17412	0,638
Fraction 13	2424	4819	0,503	8342	12838	0,649
Fraction 14	1809	3623	0,499	6961	11166	0,623
Fraction 15	1809	4089	0,442	5251	8513	0,616
Fraction 16	1873	4410	0,424	4491	7156	0,627

Antibody containing fractions were combined and iodination yield, incorporated activity and specific activity calculated as follows for each experiment.

$$\text{Iodination yield (\%)} = \frac{\text{Labeled IgG counts}}{\text{Total counts}} \cdot 100$$

$$\text{Incorporated activity (µCi)} = \frac{\text{Iodination yield (\%)} \cdot \text{ I125 initial activity}}{100}$$

I^{125} initial activity = 75 or 250 µCi added in Experiment 1 and Experiment 2, respectively

$$\text{Specific activity (µCi/µg)} = \frac{\text{Incorporated activity (µCi)}}{\text{Labeled IgG mass}}$$

Labeling of α-human IgE monoclonal antibody with I^{125}

Once optimized the amount of NaI^{125} that leaded to a better specific activity, we labeled a high specific mix of α-human IgE monoclonal antibodies kindly provided by Phadia. Protocol described for optimization was used, employing 2.4 µL (250 µCi) of NaI^{125} (optimization Experiment 2 conditions). Iodination yield, incorporated activity and specific activity were calculated for combination of fractions 2 and 3 (Table E.4) using equations in previous point.

Table E.4. Radioactivity results for fractions collected during purification step. In bold, fractions containing labeled antibody. *Values of 1/2 dilution since direct measurement leaded to detector saturation.

	cpm	dpm	TDCR
Maximum	1350000*	1860000*	0,728*
Fraction 1	842	37395	0,022
Fraction 2	**274745**	378274	0,726
Fraction 3	**1570000**	2150000	0,73
Fraction 4	130447	182347	0,715
Fraction 5	87764	120273	0,729
Fraction 6	48081	75982	0,632

Complete recovery was considered, thus having 15 µg of protein in 1 mL (combination of two 0.5 mL fractions). Finally, a hundred-fold dilution of the I^{125} labeled antibody was prepared in 1.5% (w/v) BSA in PBS 1X pH 7.4-Tween 0,1% so we have it in similar conditions to the old Phadia commercial antibody (0.15 µg/mL antibody concentration, 1.065 µCi/mL activity per volume, 7.1 mCi/mg specific activity).

Labeled IgG sensitivity evaluation by Radio Allergo Sorbent Test (RAST)

Radiolabeled α-human IgE was subjected to immunological validation by RAST. Success in labeling was proved by comparison of RAST % results obtained with data acquired previously using other batches or kind of antibody used (Tables E.5 and E.6).

Table E.5. % RAST results obtained for AX positive patients, using different I^{125} labeled antibodies. Solid phase used in RAST assays was AX-PLL.

	% RAST Phadia	% RAST Chelatec labeling	% RAST Our labeling protocol
Case 1	29,80	25,96	59,78
Case 2	16,22	16,31	26,07
Case 3	18,74	16,00	27,41
Case 4	41,52	50,51	80,49
Case 5	25,79	29,62	38,43
Case 6	20,14	16,17	27,11
Control 1	-	-	1,72
Control 2	-	-	2,34
Control 3	-	-	3,04
Control 4	-	-	2,71
Control 5	-	-	0
Control 6	-	-	2,95

Table E.6. % RAST results obtained for patients presenting allergic reactions to cefaclor, using different I^{125} labeled antibodies. Solid phase used in RAST assays was cefaclor-PLL. (-): not determined.

	% RAST Phadia	% RAST ALK-Abelló	% RAST Chelatec labeling	% RAST Our labeling protocol
Case 1	-	-	-	33,37
Case 2	-	-	-	1,45
Case 3	2,48	1,25	0,56	1,67
Case 4	2,06	3,65	10,20	15,36
Case 5	6,99	6,95	19,69	20,55
Case 6	-	-	-	1,96
Case 7	11,17	4,84	17,19	19,44
Case 8	2,94	4,45	10,49	16,18
Case 9	13,59	6,06	17,76	21,43
Case 10	9,62	7,04	17,89	14,92
Case 11	-	-	-	1,74
Case 12	-	-	-	1,68
Case 13	-	-	-	1,04
Case 14	-	-	-	4,86
Case 15	-	1,59	0,00	0,00
Case 16	-	1,80	0,83	2,54
Case 17	-	1,03	0,00	0,97
Case 18	-	1,44	1,98	6,96
Case 19	-	-	-	0,59
Case 20	-	1,02	0,00	0,00
Case 21	-	0,99	0,00	1,34
Case 22	-	3,54	7,24	11,17
Case 23	-	0,66	0,52	0,21
Case 24	-	1,49	1,28	1,47
Case 25	-	-	-	2,14
Case 26	-	1,22	0,91	0,69
Case 27	-	1,20	0,51	0,41
Case 28	-	1,00	0,66	0,36
Case 29	-	0,64	0,62	0,57
Case 30	-	0,85	0,00	0,68
Case 31	-	4,43	7,02	34,56
Case 32	-	1,21	0,64	1,28
Case 33	-	1,04	1,60	3,48
Case 34	-	2,75	8,62	7,69
Case 35	-	1,12	0,67	1,91
Case 36	-	4,25	24,63	11,67
Case 37	-	3,78	1,75	1,79
Case 38	-	0,49	0,00	0,74
Case 39	-	3,02	0,69	0,58
Case 40	-	1,51	0,93	2,89

3.2. Fluorescent labeling

Materials

All chemicals were purchased from Sigma Aldrich (St. Louis, MO, USA), Merck (Hohenbrunn, Germany), VWR (Fontenay-sous-Bois, France) and Lumiprobe (Hunt Valley, Maryland USA) and used as received unless otherwise stated.

Nomenclature

Dendrons are abbreviated as "Focal functionality"-"Spacer"-"Generation"-"Peripheral functionality". For example, a third generation dendron with a benzylidene protected TEG spacer and an acetonide protected periphery is denoted as Bz-TEG-G3-Acetonide, and the same generation dendron, but with hydrazine functionalization at the focal point and Cy5 decorated in the periphery is named hydrazine-succinic-TEG-G3-Cy5.

MALDI-TOF

MALDI-TOF spectra were obtained using an UltraFlex MALDI-TOF with SCOUT-MTP Ion Source (Bruker Daltonics, Bremen, Germany) equipped with a nitrogen laser (337 nm), a gridless ion source and a reflector. The instrument was calibrated using SpheriCal™ calibrants. Samples were prepared by mixing 5 µL of 1 mg/mL analyte in EtOAc or MeOH with 5 µL of a 1 mg/mL counter-ion solution of sodium trifluoroacetate (NaTFA) in tetrahydrofuran (THF) and 20 µL of a matrix solution of 10 mg/mL in THF and applying 1 µL this mixture to a stainless steel sample plate using the dried droplet method. The matrix used depended on the sample polarity and was either trans-2-[3-(4-tert-butylphenyl)-2-methyl-2-propenylidene]-malononitrile (DCTB) or 2,5-dihydroxybenzoic acid (DHB). The obtained spectra were analyzed with FlexAnaysis version 2.2 from Bruker Daltonics.

^{1}H- and ^{13}C-NMR

^{1}H-NMR (400 MHz) and ^{13}C-NMR (101 MHz) were acquired using a Bruker Avance instrument (Bruker Biospin, Rheinstetten, Germany). The spectra were processed and analyzed with Mestre Nova version 9.0.0-12821 from Mestrelab Research (Santiago de Compostela, Spain).

3.2.1. Synthesis of fluorescent dendrons

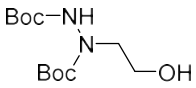

Diboc-hydrazine. Boc_2O (8.046 g, 36.9 mmol, 2.5 eq.) was dissolved in 5 mL of dichloromethane (DCM) in an ice bath and 2-hydroxyethylhydrazine (1.123 g (1 mL), 14.76 mmol, 1 eq.) was added dropwise. The mixture was left to reach room temperature and stirred overnight. After elimination of the solvent by rotoevaporation, the crude was purified by silica chromatography using heptane/EtOAc mixtures to afford the product (4.078 g, 9.51 mmol, 65%) as a white solid. **^{1}H-NMR** (400 MHz, $CDCl_3$) δ (ppm) 6.67 (1H, s), 3.63 (s, 2H, CH_2OH b), 3.53 (s, 2H, NCH_2CH_2 a), 1.46-1.40 (broad s, 18H, 6xCH_3 Boc). **^{13}C-NMR** (100 MHz, $CDCl_3$) δ (ppm) 157.2, 155.4, 82.1, 81.7, 59.5, 54.0, 52.8, 28.2.

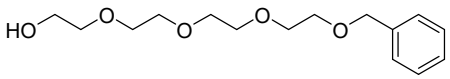

TEG-Bz, (Dend1). Synthesized as previously reported.[151]

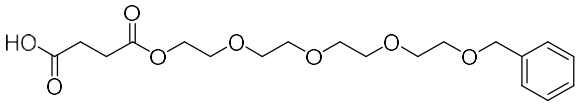

Succinic-TEG-Bz, (Dend2). Monobenzylated tetraethylene glycol (TEG-Bz) (300 mg, 1.06 mmol, 1eq.), pyridine (62.9 mg (64 μL), 0,795 mmol, 0.75 eq.) and 4-(Dimethylamino)pyridine (DMAP) (25.9 mg, 0.212 mmol, 0.2 eq.) were dissolved in 10 mL of DCM in an ice bath and succinic anhydride (127.5 mg, 1.27 mmol, 1.2 eq.) was added slowly. The mixture was left to reach room temperature and stirred overnight. Once there was no Bz-TEG left (^{1}H-NMR evidence), water was added for quenching of remaining succinic anhydride (^{1}H-NMR evidence) and the reaction was washed with $NaHSO_4$ 10% and deionized water, dried over $MgSO_4$, filtered and rotoevaporated to afford the product (328 mg, 0.853 mmol, 81%) as a colorless syrup. **^{1}H-NMR** (400 MHz, $CDCl_3$) δ (ppm) 7.35-7.32 (m, 5H, C_6H_5-CH_2 Ar), 4.57 (s, 2H, C_6H_5-CH_2 m), 4.28-4.26 (m, 2H, CH_2OCO e), 3.73-3.59 (m, 14H, OCH_2CH_2OCO f + 2xOCH_2CH_2O g,h,i,j + C_6H_5-$CH_2OCH_2CH_2O$ k + C_6H_5-CH_2OCH_2 l), 2.68-2.58 (m, 4H, $OCOCH_2CH_2COOH$ c+d). **^{13}C-NMR** (100 MHz, $CDCl_3$) δ (ppm) 175.7, 172.1, 138.1, 128.2, 127.7, 127.5, 73.1, 72.4, 70.5, 70.4, 70.2, 69.3, 68.9, 63.7, 61.4, 29.0, 28.8. **MALDI**: m/z calc. 384.18 Da. Found $[M + Na]^+$ 406.04 Da.

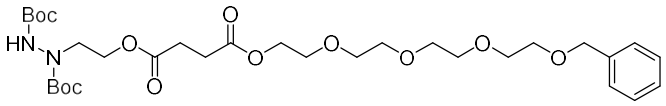

Diboc-hydrazine-succinic-TEG-Bz, (Dend3). Succinic-TEG-Bz (**2**) (248 mg, 0.646 mmol, 1.5 eq.) was dissolved in EtOAc to a 1M concentration and CDI (104.65 mg, 0.646 mmol, 1.5 eq.) was added and stirred at 50˚C about 1 hour. Once imidazolide-activated acid formation finished (^{1}H-NMR evidence), **diboc-hydrazine** (135 mg, 0.50 mmol, 1 eq.) and catalytic amount of CsF were added and left to react overnight. Water was added to quench activated acid (^{1}H-NMR evidence) and then, the reaction mixture was washed with $NaHSO_4$ 10% and $NaHCO_3$ 10%, dried over $MgSO_4$, filtered and rotoevaporated to afford the product (313 mg, 0.487 mmol, 97%) as a colorless syrup. **^{1}H-NMR** (400 MHz, $CDCl_3$) δ (ppm) 7.35-7.32 (m, 5H, $C_6\underline{H_5}$-CH_2 Ar), 6.62 (s, H, NH-Boc), 4.56 (s, 2H, C_6H_5-$C\underline{H_2}$ m), 4.30-4.21 (m, 4H, 2xCH_2OCO b+e), 3.70-3.60 (m, 16H, N$C\underline{H_2}CH_2$ a + O$C\underline{H_2}CH_2$OCO f + 2xO$C\underline{H_2}C\underline{H_2}$O g,h,i,j + C_6H_5-$CH_2OCH_2C\underline{H_2}$O k + C_6H_5-$CH_2OC\underline{H_2}$ l), 2.68-2.58 (m, 4H, OCO$C\underline{H_2}C\underline{H_2}COOCH_2$ c+d), 1.50-1.42 (broad s, 18H, 6xCH_3 Boc). **MALDI**: m/z calc. 642.34 Da. Found $[M + Na]^+$ 668.17 Da.

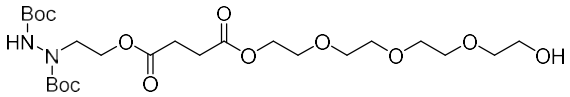

Diboc-hydrazine-succinic-TEG-OH, (Dend4). In a round bottom flask, Diboc-hydrazine-succinic-TEG-Bz (**3**) (313 mg, 0.487 mmol, 1 eq.) was dissolved in a mixture of 20 mL of DCM and 2 mL of MeOH and palladium on carbon (10 wt % loaded, 15.7 mg, 5 wt %) was suspended in the mixture. The flask was evacuated and hydrogen gas was introduced. The reaction was carried out for one hour under heavy stirring (complete deprotection confirmed with MALDI), the palladium on carbon was filtered off and the solvent was rotoevaporated, affording the product (209 mg, 0.378 mmol, 76%) as a colorless syrup. **^{1}H-NMR** (400 MHz, $CDCl_3$) δ (ppm) 6.67 (s, H, NH-Boc), 4.23-4.17 (m, 4H, 2xCH_2OCO b+e), 3.68-3.58 (m, 16H, N$C\underline{H_2}CH_2$ a + O$C\underline{H_2}CH_2$OCO f + 2xO$C\underline{H_2}C\underline{H_2}$O g,h,i,j + HO$CH_2C\underline{H_2}$O k), 3.57-3.52 (m, 2H, CH_2OH l), 2.62-2.54 (m, 4H, OCO$C\underline{H_2}C\underline{H_2}COOCH_2$ c+d), 1.44-1.32 (broad s, 18H, 6xCH_3 Boc). **^{13}C-NMR** (100 MHz, $CDCl_3$) δ (ppm) 172.3, 155.0, 81.2, 72.6, 70.6, 70.3, 69.0, 63.9, 61.5, 48.2, 29.1, 28.2. **MALDI**: m/z calc. 552.29 Da. Found $[M + Na]^+$ 576.18 Da.

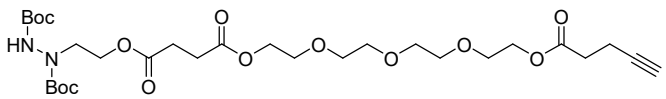

Diboc-hydrazine-succinic-TEG-G0-Alkyne, (Dend5). 4-pentinoic acid (22.9 mg, 0.233 mmol, 1.5 eq.) was dissolved in EtOAc to a 1M concentration and CDI (37.7 mg, 0.233

mmol, 1.5 eq.) was added and stirred at 50˚C about 1 hour. Once imidazolide-activated acid formation finished (^{1}H-NMR evidence), Diboc-hydrazine-succinic-TEG-OH (**Dend4**) (85.65 mg, 0.155 mmol, 1 eq.) and catalytic amount of CsF were added and left to react overnight. Water was added to quench activated acid (^{1}H-NMR evidence) and then, the reaction mixture was washed with $NaHSO_4$ 10% and $NaHCO_3$ 10%, dried over $MgSO_4$, filtered and rotoevaporated to afford the product (93 mg, 0.147 mmol, 95%) as a colorless syrup. **^{1}H-NMR** (400 MHz, $CDCl_3$) δ (ppm) 6.64 (s, 1H, NH-Boc), 4.26-4.18 (m, 6H, 3xCH_2OCO b+e+l), 3.70-3.60 (m, 14H, NC$H_2$$CH_2$ a + OC$H_2$$CH_2$OCO f + 2xOC$H_2CH_2$O g,h,i,j + COOC$H_2CH_2$O k), 2.65-2.57 (m, 4H, OCOCH_2CH_2COOCH_2 c+d), 2.56-2.52 (m, 2H, CHCCH_2CH_2COO n), 2.50-2.44 (m, 2H, CHCCH_2 o), 1.95 (t *J*=2.6Hz, 1H, CCH q), 1.47-1.37 (broad s, 18H, 6xCH_3 Boc). **^{13}C-NMR** (100 MHz, $CDCl_3$) δ (ppm) 172.4, 171.8, 155.0, 82.5, 81.3, 70.7, 69.2, 69.1, 63.9, 61.6, 48.3, 33.3, 29.1, 28.1, 14.4. **MALDI**: m/z calc. 632.32 Da. Found $[M + Na]^+$ 658.14 Da.

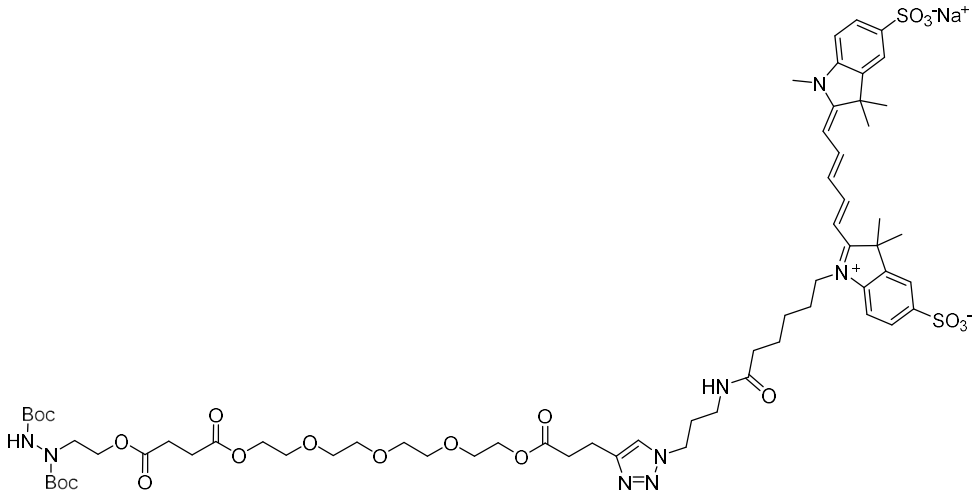

Diboc-hydrazine-succinic-TEG-G0-Cy5, (Dend6).

Procedure 1; Alkyne-TEG-succinic-diboc-hydrazine (**Dend5**) (16 mg, 0.0253 mmol, 1 eq.) and sulfo-Cy5-azide (Lumiprobe) (20.77 mg, 0.0278 mmol, 1.1 eq.) were dissolved in 100 μL THF/H_2O 1:1 and Na ascorbate (1.614 mg, 0.01012 mmol, 0,4 eq.) and $CuSO_4$ (1.002 mg, 0.00506 mmol, 0.2 eq.) were added. The mixture is left to react overnight at 50° protected from light. Once there was no alkyne left (MALDI evidence), solvents were eliminated and the product **Dend10** was isolated by preparative TLC using EtOAc:MeOH 1:1 (35 mg, 0.0253 mmol, quantitative yield) as a brilliant blue solid.

Procedure 2; Alkyne-TEG-succinic-diboc-hydrazine (**Dend5**) (10 mg, 0.0158 mmol, 1 eq.) and sulfo-Cy5-azide (Lumiprobe) (14.16 mg, 0.0190 mmol, 1.2 eq.) were dissolved in 500 μL DMSO and PMDTA (5.48 mg (6.6 μL), 0.0316 mmol, 2 eq.) was added. Immediately, after three cycles of freeze/pump thaw, CuBr (4.53 mg, 0.0316 mmol, 2 eq.) was added and the mixture was left to react overnight under Ar atmosphere at room temperature.

The product **Dend10** was isolated by preparative TLC using EtOAc:MeOH 1:1 (38 mg, 0.0275 mmol, quantitative yield) as a brilliant blue solid.

^{1}H-NMR (400 MHz, MeOD) δ (ppm) 8.38-8.28 (t *J*= 11.7 Hz, 2H, CHC<u>H</u>CHC<u>H</u>CH 16+18) 7.93-7.88 (m, 3H, Ar), 7.84 (s, 1H, C=CHN p), 7.36 (dd J_1= 8.6Hz, J_2= 2.4 Hz, 2H, Ar), 6.68 (t *J*= 12.5 Hz, 2H, CHCHC<u>H</u>CHCH 17), 6.35 (dd J_1=13.6, J_2=5.7 Hz, 2H, C<u>H</u>CHCHCHC<u>H</u> 19+15), 4.42-4.36 (t J=6.8 Hz, 2H, CH_2NN 1), 4.28-4.12 (m, 8H, 3xCH_2OCO b+e+l + CH_2N^+ 9), 3.72-3.62 (m, 17H, N-CH_3 20 + NC<u>H_2</u>CH_2 a + OC<u>H_2</u>CH_2OCO f + 2xOC<u>H_2</u>C<u>H_2</u>O g,h,i,j + $COOCH_2$C<u>H_2</u>O k), 3.17-3.11 (m, 2H, CH_2NHCO 3), 3.02 (t *J*=7.3 Hz, 2H, CH_2C=CN o), 2.75 (t *J*=7.3 Hz , 2H, C<u>H_2</u>CH_2NN 2), 2.68-2.62 (m, 6H, OCOC<u>H_2</u>C<u>H_2</u>$COOCH_2$ c+d, NCCH_2C<u>H_2</u>COO n), 2.26-2.12 (m, 2H, C<u>H_2</u>CONH 5), 1.79-1.75 (m, 18H, N^+CH_2(C<u>H_2</u>)$_3$$CH_2$CONH 6,7,8 + 4x$CH_3$ 13+13´+14+14´), 1.50-1.40 (broad s, 18H, 6xCH_3 Boc). **MALDI**: m/z calc. 1378.57 Da. Found $[M]^+$ 1378.520 Da; $[M–Na+H]^+$ 1356.550 Da.

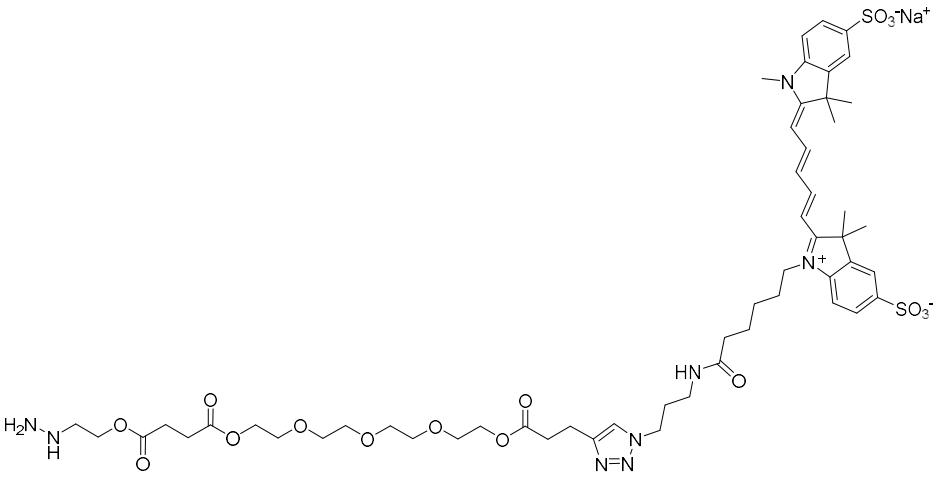

G0-Cy5. Boc protected G0-Cy5 was dissolved in TFA/DCM (1:1) and left to react for 2h at room temperature. TFA was eliminated by rotoevaporation to afford deprotected product (see Figure S4 for ^{1}H-NMR evidence) as TFA salt as a blue solid. **^{1}H-NMR** (400 MHz, MeOD) δ (ppm) 8.38-8.28 (t *J*= 11.7 Hz, 2H, CHC<u>H</u>CHC<u>H</u>CH 16+18) 7.93-7.88 (m, 3H, Ar), 7.85 (s, 1H, C=CHN p), 7.36 (dd J_1= 8.6Hz, J_2= 2.4 Hz, 2H, Ar), 6.68 (t *J*= 12.5 Hz, 2H, CHCHC<u>H</u>CHCH 17), 6.35 (dd J_1=13.6, J_2=5.7 Hz, 2H, C<u>H</u>CHCHCHC<u>H</u> 19+15), 4.42-4.36 (t J=6.8 Hz, 2H, CH_2NN 1), 4.28-4.12 (m, 8H, 3xCH_2OCO b+e+l + CH_2N^+ 9), 3.72-3.62 (m, 17H, N-CH_3 20 + NC<u>H_2</u>CH_2 a + OC<u>H_2</u>CH_2OCO f + 2xOC<u>H_2</u>C<u>H_2</u>O g,h,i,j + $COOCH_2$C<u>H_2</u>O k), 3.17-3.11 (m, 2H, CH_2NHCO 3), 3.02 (t *J*=7.3 Hz, 2H, CH_2C=CN o), 2.75 (t *J*=7.3 Hz , 2H, C<u>H_2</u>CH_2NN 2), 2.68-2.62 (m, 6H, OCOC<u>H_2</u>C<u>H_2</u>$COOCH_2$ c+d, NCCH_2C<u>H_2</u>COO n), 2.26-2.12 (m, 2H, C<u>H_2</u>CONH 5), 1.79-1.75 (m, 18H, N^+CH_2(C<u>H_2</u>)$_3$$CH_2$CONH 6,7,8 + 4x$CH_3$ 13+13´+14+14´). **MALDI**: m/z calc. 1178.46 Da. Found $[M]^+$ 1178.626 Da; $[M–Na+H]^+$ 1156.595.

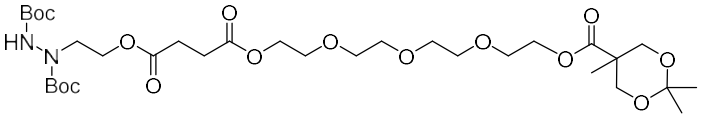

Diboc-hydrazine-succinic-TEG-G1-Acetonide, (Dend7). Acetonide protected bis-MPA (52.74 mg, 0.303 mmol, 1.5 eq.) was dissolved in EtOAc to a 1M concentration and CDI (49.1 mg, 0.303 mmol, 1.5 eq.) was added and stirred at 50˚C about 1 hour. Once imidazolide-activated acid formation finished (^{1}H-NMR evidence), Diboc-hydrazine-succinic-TEG-OH (**Dend4**) (111.63 mg, 0.202 mmol, 1 eq.) and catalytic amount of CsF were added and left to react overnight. Water was added to quench activated acid (^{1}H-NMR evidence) and then, the reaction mixture was washed with $NaHSO_4$ 10% and $NaHCO_3$ 10%, dried over $MgSO_4$, filtered and rotoevaporated to afford the product (111 mg, 0.157 mmol, 78%) as a colorless syrup. **^{1}H-NMR** (400 MHz, $CDCl_3$) d (ppm) 4.35-4.25 (m, 6H, 3xCH_2OCO b+e+l), 4.22 (d J= 11.8 Hz, 2xC<u>H</u>H´O s_1+t_1), 3.75-3.59 (m, 16H, NC<u>H</u>$_2$CH$_2$ a + OC<u>H</u>$_2$CH$_2$OCO f + 2xOC<u>H</u>$_2$C<u>H</u>$_2$O g,h,i,j + COOCH$_2$C<u>H</u>$_2$O k + 2xCH<u>H</u>´O s_2+t_2), 2.69-2.59 (m, 4H, OCOC<u>H</u>$_2$C<u>H</u>$_2$COOCH$_2$ c+d), 1.48-1.44 broad s, 18H, 2xBoc), 1.43 (s, 3H, OCC<u>H</u>$_3$ u), 1.39 (s, 3H, OCC<u>H</u>$_3$´ v), 1.22 (s, 3H, OCH$_2$CC<u>H</u>$_3$ r). **^{13}C-NMR** (100 MHz, $CDCl_3$) d (ppm) 174.0, 172.2, 154.9, 97.9, 81.1, 72.4, 70.5, 70.4, 70.2, 68.9, 65.8, 63.8, 61.6, 61.4, 48.1, 41.7, 28.9, 28.1, 24.1, 23.0, 18.6. **MALDI**: m/z calc. 708.37 Da. Found $[M + Na]^+$ 735.23 Da.

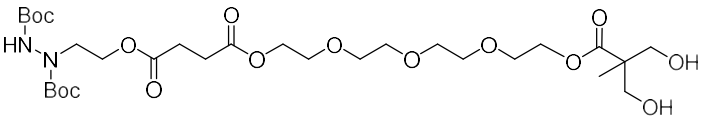

Diboc-hydrazine-succinic-TEG-G1-OH, (Dend8). Diboc-hydrazine-succinic-TEG-G1-Acetonide (**7**) (106 mg, 0.149 mmol, 1 eq.) was dissolved in 500 µL of MeOH and DOWEX (26.5 mg, 25% wt) was added and stirred at room temperature for 2 hours. When complete deprotection was confirmed with MALDI, the solution was filtered off to remove DOWEX and the solvent was rotoevaporated, affording the product (100.5 mg, 0.150 mmol, quantitative yield) as a colorless syrup. **^{1}H-NMR** (400 MHz, $CDCl_3$) δ (ppm) 4.32-4.28 (m, 2H, C<u>H</u>$_2$OCO(CH$_2$)$_2$COO e), 4.25-4.19 (m, 4H, C<u>H</u>$_2$OCOCCH$_3$ b + OCH$_2$C<u>H</u>$_2$OCOCCH$_3$ l), 3.78 (d *J*= 11.3 Hz, 2H, 2xC<u>H</u>H´OH s_1+t_1), 3.72-2.52 (m, 16H, NC<u>H</u>$_2$CH$_2$ a + OC<u>H</u>$_2$CH$_2$OCO f + 2xOC<u>H</u>$_2$C<u>H</u>$_2$O g,h,i,j + COOCH$_2$C<u>H</u>$_2$O k + 2xCH<u>H</u>´OH s_2+t_2), 2.65-2.55 (m, 4H, OCOC<u>H</u>$_2$C<u>H</u>$_2$COOCH$_2$ c+d), 1.46-1.38 (broad s, 18H, 2xBoc), 1.07 (s, 3H, CH$_2$CC<u>H</u>$_3$ r). **^{13}C-NMR** (100 MHz, $CDCl_3$) δ (ppm) 175.7, 172.4, 155.1, 81.3, 72.6, 70.6, 70.5, 70.4, 69.1, 68.8, 67.4, 63.9, 63.4, 61.7, 61.6, 49.8, 48.3, 29.1, 28.3, 17.2. **MALDI**: m/z calc. 668.34 Da. Found $[M + Na]^+$ 694.19 Da.

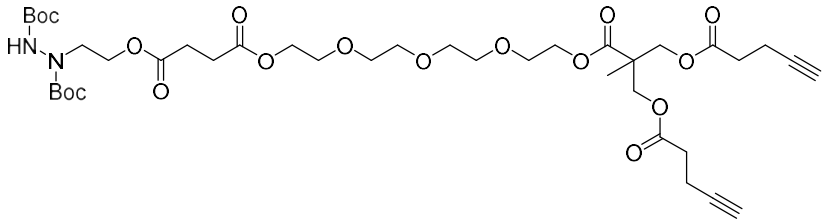

Diboc-hydrazine-succinic-TEG-G1-Alkyne, (Dend9). 4-pentinoic acid (78.83 mg, 0.803 mmol, 3.0 eq.) was dissolved in EtOAc to a 1M concentration and CDI (130.2 mg, 0.803 mmol, 3.0 eq.) was added and stirred at 50˚C about 1 hour. Once imidazolide-activated acid formation finished (^{1}H-NMR evidence), Diboc-hydrazine-succinic-TEG-G1-OH (180 mg, 0.269 mmol, 1 eq.) and catalytic amount of CsF were added and left to react overnight. Water was added to quench activated acid (^{1}H-NMR evidence) and then, the reaction mixture was washed with $NaHSO_4$ 10% and $NaHCO_3$ 10%, dried over $MgSO_4$, filtered and rotoevaporated to afford the product (134 mg, 0.162 mmol, 60%) as a colorless syrup. **^{1}H-NMR** (400 MHz, $CDCl_3$) δ (ppm) 4.34-4.22 (m, 10H, 5xCH_2OCO b+e+l+s+t), 3.74-3.62 (m, 14H, NCH_2CH_2 a + OCH_2CH_2OCO f + 2xOCH_2CH_2O g,h,i,j + COOCH_2CH_2O k), 2.68-2.60 (m, 4H, OCOCH_2CH_2COOCH_2 c+d), 2.58-2.52 (m, 4H, 2xCHCCH_2CH_2COO n), 2.52-2.46 (m, 4H, 2xCHCCH_2 o), 1.98 (t *J*= 2.5Hz , 2H, 2xCCH q), 1.50-1.42 (broad s, 18H, 2xBoc), 1.27 (s, 3H, CH_2CCH_3 r). **^{13}C-NMR** (100 MHz, $CDCl_3$) δ (ppm) 172.4, 172.2, 171.6, 171.0, 157.9, 82.2, 81.0, 70.5, 70.4, 69.3, 69.1, 68.9, 68.7, 65.3, 64.1, 63.7, 61.4, 49.4, 48.1, 46.2, 33.1, 28.9, 28.1, 17.7, 14.2. **MALDI**: m/z calc. 828.39 Da. Found $[M + Na]^+$ 855.28 Da.

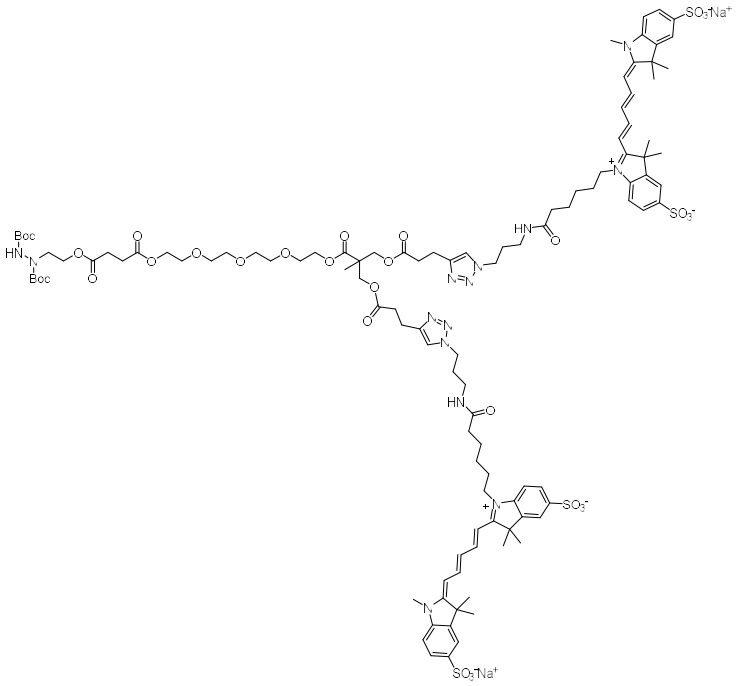

Diboc-hydrazine-succinic-TEG-G1-Cy5, (Dend10). Diboc-hydrazine-succinic-TEG-G1-Alkyne (**9**) (14 mg, 0.0170 mmol, 1 eq.) and sulfo-Cy5-azide (Lumiprobe) (26.9 mg, 0.0360 mmol, 2.1 eq.) were dissolved in 500 μL DMSO and PMDTA (11.74 mg (14.1 μL), 0.064 mmol, 4 eq.) was added. Immediately, after three cycles of freeze/pump thaw, CuBr (5.76 mg, 0.064 mmol, 4 eq.) was added and the mixture was left to react overnight under Ar atmosphere at room temperature. Presence of triazol ring was confirmed by ^{1}H-NMR (MeOD) of reaction crude. 1KDa dialysis membrane was used to get rid of sulfo-Cy5-azide excess and DMSO, affording the product (35 mg, 0.0149 mmol, 88%) as a brilliant blue solid. **^{1}H-NMR** (400 MHz, MeOD) δ (ppm) 8.38-8.28 (t *J*= 13.6 Hz, 4H, CHC<u>H</u>CHC<u>H</u>CH 16+18), 8.00-7.84 (m, 6H, Ar), 7.80 (s, 2H, C=CHN p), 7.40-7.30 (m, 4H, Ar), 6.67 (t *J*= 12.8 Hz, 4H, CHCHC<u>H</u>CHCH 17), 6.40-6.28 (m, 4H, C<u>H</u>CHCHCHC<u>H</u> 19+15), 4.40-4.30 (m, 4H, CH_2NN 1), 4.27-4.07 (m, 10H, 3xCH_2OCO b+e+l + CH_2N^+ 9), 3.75-3.55 (m, 17H, N-CH_3 20 + NC<u>H</u>$_2$C<u>H</u>$_2$ a + OC<u>H</u>$_2$C<u>H</u>$_2$OCO f + 2xOC<u>H</u>$_2$C<u>H</u>$_2$O g,h,i,j + COOC<u>H</u>$_2$C<u>H</u>$_2$O k), 3.18-3.10 (m, 4H, CH_2NHCO 3), 3.02-2.92 (m, 4H, CH_2C=CN o), (C<u>H</u>$_2$C<u>H</u>$_2$NN 2), (OCOC<u>H</u>$_2$C<u>H</u>$_2$COOC<u>H</u>$_2$ c+d, NCC<u>H</u>$_2$C<u>H</u>$_2$COO n), 2.25-2.15 (t *J*=6.8 Hz, 4H, C<u>H</u>$_2$CONH 5), 1.78-1.70 (m, 36H, N^+CH_2(C<u>H</u>$_2$)$_3$$CH_2$CONH 6,7,8 + 4x$CH_3$ 13+13´+14+14´), 1.50-1.40 (m, 18H, 6xCH_3 Boc), 1.18 (s, 3H, CH_3 bis-MPA r).

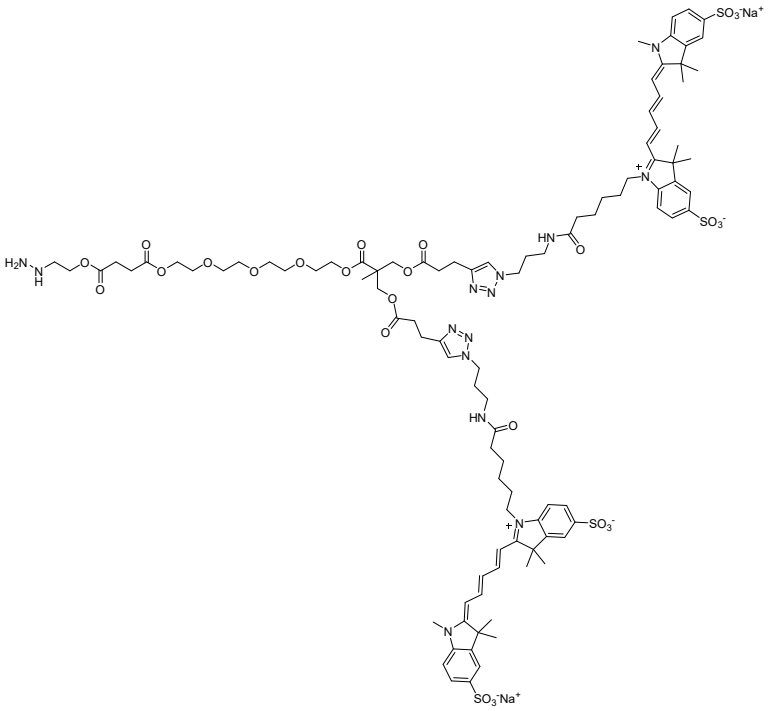

G1-Cy5. Boc protected G1-Cy5 was dissolved in TFA/DCM (1:1) and left to react for 2h at room temperature. TFA was eliminated by rotoevaporation to afford deprotected product (see Figure S6 for ^{1}H-NMR evidence) as TFA salt as a blue solid. **^{1}H-NMR** (400 MHz, MeOD) δ (ppm) 8.38-8.28 (t *J*= 13.6 Hz, 4H, CHC<u>H</u>CHC<u>H</u>CH 16+18), 8.00-7.84 (m, 8H, Ar + C=CHN p), 7.40-7.30 (m, 4H, Ar), 6.67 (t *J*= 12.8 Hz, 4H, CHCHC<u>H</u>CHCH 17), 6.40-

6.28 (m, 4H, CHCHCHCHCH 19+15), 4.40-4.30 (m, 4H, CH_2NN 1), 4.27-4.07 (m, 10H, 3xCH_2OCO b+e+l + CH_2N^+ 9), 3.75-3.55 (m, 17H, N-CH_3 20 + NCH_2CH_2 a + OCH_2CH_2OCO f + 2xOCH_2CH_2O g,h,i,j + $COOCH_2CH_2O$ k), 3.18-3.10 (m, 4H, CH_2NHCO 3), 3.02-2.92 (m, 4H, $CH_2C{=}CN$ o), (CH_2CH_2NN 2), ($OCOCH_2CH_2COOCH_2$ c+d, $NCCH_2CH_2COO$ n), 2.25-2.15 (t *J*=6.8 Hz, 4H, CH_2CONH 5), 1.78-1.70 (m, 36H, $N^+CH_2(CH_2)_3CH_2CONH$ 6,7,8 + 4xCH_3 13+13´+14+14´), 1.18 (s, 3H, CH_3 bis-MPA r).

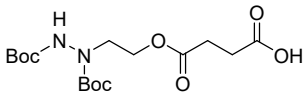

Diboc-hydrazine-succinic. **Diboc-hydrazine** (2.543 g, 9.203 mmol, 1 eq.), pyridine (545,95 mg (556 µL), 6.902 mmol, 0.75 eq) and 4-(Dimethylamino)pyridine (DMAP) (672 mg, 5.523 mmol, 0.6 eq.) were dissolved in 70 mL of DCM in an ice bath and succinic anhydride (1.101 g, 11.044 mmol, 1.2 eq.) was added slowly. The mixture was left to reach room temperature and stirred until no diboc-hydrazine was left (TLC evidence). Then, water was added for quenching of remaining succinic anhydride (^{1}H-NMR evidence) and the reaction was washed with $NaHSO_4$ 10% and Brine, dried over $MgSO_4$, filtered and rotoevaporated to afford the product (3.179 g, 8.445 mmol, 92%) as a white solid. **^{1}H-NMR** (400 MHz, $CDCl_3$) δ (ppm) 4.21 (s, 2H, CH_2OCO b), 3.66 (s, 2H, NCH_2CH_2 a), 2.65-2.55 (m, 4H, $OCOCH_2CH_2COOH$ c+d), 1.50-1.35 (broad s, 18H, 6xCH_3 Boc). **^{13}C-NMR** (100 MHz, $CDCl_3$) δ (ppm) 176.9, 176.6, 172.5, 155.4, 82.2, 81.5, 61.9, 61.6, 53.5, 49.4, 48.1, 29.0, 28.2.

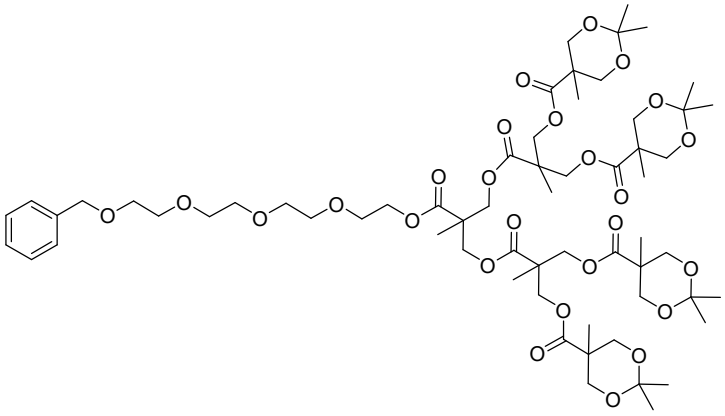

Bz-TEG-G3-acetonide, (Dend11). Synthesized as previously reported [151].

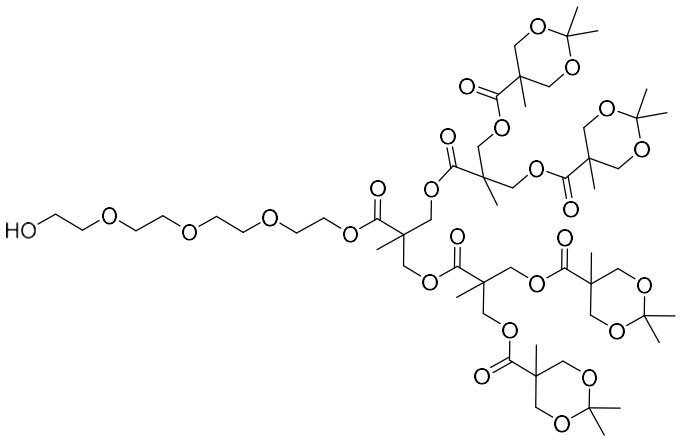

HO-TEG-G3-acetonide, (Dend12). Bz-TEG-G3-acetonide (**11**) (253 mg, 0.201 mmol, 1eq.), was dissolved in 20 mL of EtOAc, palladium on carbon (10 wt % loaded, 25 mg, 10 wt %) was suspended and 3 mL of DCM added. The flask was evacuated and hydrogen gas was introduced. The reaction was carried out for 35 minutes under heavy stirring (complete deprotection confirmed with MALDI), the palladium on carbon was filtered off and the solvent was rotoevaporated, affording the product (225 mg, 0.192 mmol, 96%) as a colorless syrup. **^{1}H-NMR** (400 MHz, $CDCl_3$) δ (ppm) 4.33-4.25 (m, 14H, $OCH_2C\underline{H_2}OCO$ l, 6xCH_2O (G1+G2) s+t+2xs´+2xt´), 4.18-4.11 (d J=12Hz, 8H, 2x(4x$C\underline{H}H´O$) (G3) $4xs_1$" + $4xt_1$"), 3.74-3.18 (m, 22H, $C\underline{H_2}OH$ e + $OC\underline{H_2}CH_2OH$ f + 2x$OC\underline{H_2}C\underline{H_2}O$ g,h,i,j + $OC\underline{H_2}CH_2OCO$ k + 2x(4x$CH\underline{H´}O$) (G3) $4xs_2$" + $4xt_2$"), 1.41 (s, 12H, 4x$OCCH_3$ u"), 1.35 (s, 12H, 4x$OCCH_3$ v"), 1.28 (s, 9H, 3x$COCCH_3$ (G1+G2) r+2xr_2), 1.15 (s, 12H, 4x$COCCH_3$ (G3) r_3). **^{13}C-NMR** (100 MHz, $CDCl_3$) δ (ppm) 173.6, 172.2, 172.0, 98.2, 72.6, 70.7, 70.6, 70.5, 70.4, 68.9, 66.1, 66.0, 65.0, 64.5, 61.8, 47.0, 46.7, 42.1, 25.3, 22.2, 18.6, 17.8, 17.7. **MALDI**: m/z calc. 1166.57 Da. Found $[M + Na]^+$ 1194.88 Da.

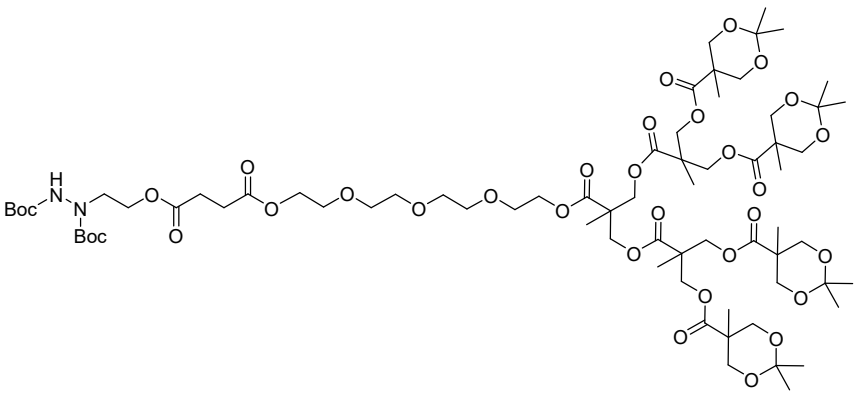

Diboc-hydrazine-succinic-TEG-G3-acetonide, (Dend13). Diboc-hydrazine-succinic (114.15 mg, 0.303 mmol, 1.5 eq.) was dissolved in EtOAc to a 1M concentration and CDI (49.1 mg, 0.303 mmol, 1.5 eq.) was added and stirred at 50˚C about 1 hour. Once imidazolide-activated acid formation finished (^{1}H-NMR evidence), OH-TEG-G3-acetonide (**Dend12**) (236 mg, 0.202 mmol, 1 eq.) and catalytic amount of CsF were

added and left to react overnight. Water was added to quench activated acid (^{1}H-NMR evidence) and then, the reaction mixture was washed with $NaHSO_4$ 10% and $NaHCO_3$ 10%, dried over $MgSO_4$, filtered and rotoevaporated to afford the product (300 mg, 0.197 mmol, 97%) as a colorless syrup. **^{1}H-NMR** (400 MHz, $CDCl_3$) δ (ppm) 6.65 (s, 1H, NH), 4.36-4.23 (m, 18H, 3xCH_2OCO b+e+l + 6xCH_2O (G1+G2) s+t+2xs´+2xt´), 4.18-4.12 (d J=12Hz, 8H, 2x(4xCHH´O) (G3) 4xs_1" + 4xt_1"), 3.74-3.58 (m, 22H, NCH_2CH_2 a + OCH_2CH_2OCO f + 2xOCH_2CH_2O g,h,i,j + OCH_2CH_2OCO k + 2x(4xCHH´O) (G3) 4xs_2" + 4xt_2"), 2.70-2.60 (m, 4H, OCOCH_2CH_2COOH c+d), 1.50-1.44 (broad s, 18H, 2xBoc), 1.37 (s, 12H, 4x$OCCH_3$ u"), 1.31 (s, 12H, 4x$OCCH_3$ v"), 1.26 (s, 9H, 3x$COCCH_3$ (G1+G2) r+2xr_2), 1.15 (s, 12H, 4x$COCCH_3$ (G3) r_3). **^{13}C-NMR** (100 MHz, $CDCl_3$) δ (ppm) 173.6, 172.4, 172.2, 172.0, 98.2, 70.7, 70.7, 70.6, 70.5, 69.2, 68.9, 66.1, 66.0, 65.9, 65.0, 64.5, 64.0, 61.7, 47.0, 46.7, 12.2, 29.1, 28.3, 25.3, 22.2, 18.6, 17.8, 17.7. **MALDI**: m/z calc. 1556.81 Da. Found $[M + Na]^+$ 1548.97 Da.

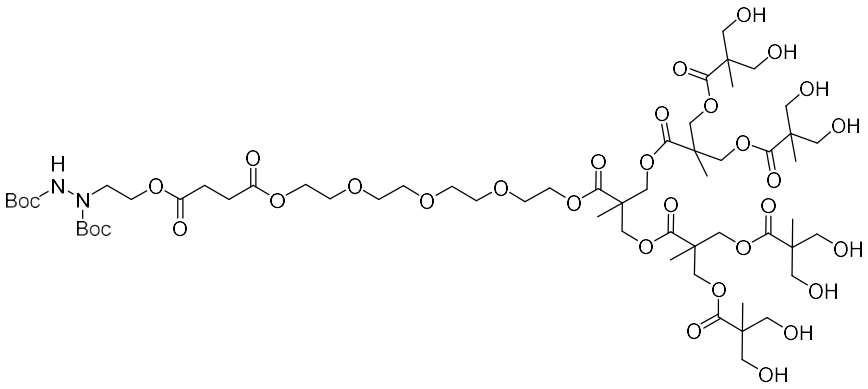

Diboc-hydrazine-succinic-TEG-G3-OH, (Dend14). Diboc-hydrazine-succinic-TEG-G3-acetonide (**13**) (60 mg, 0.039 mmol, 1 eq.) was dissolved in 15 mL of MeOH and DOWEX (15mg, 25% wt) was added and stirred at room temperature and after 2 hours, DOWEX was filtered off and an aliquot was assayed by MALDI (x6). When complete deprotection was confirmed with MALDI, the solution was filtered off to remove DOWEX and the solvent was rotoevaporated, affording the product (41 mg, 0.030 mmol, 77%) as a yellowish syrup. **^{1}H-NMR** (400 MHz, $CDCl_3$) δ (ppm) 6.65 (s, 1H, NH), 4.37-4.18 (m, 18H, 3xCH_2OCO b+e+l + 6xCH_2O (G1+G2) s+t+s´+t´), 3.79-3.54 (m, 30H, NCH_2CH_2 a + OCH_2CH_2OCO f + 2xOCH_2CH_2O g,h,i,j + OCH_2CH_2OCO k + 8xCH_2OH 4xs" + 4xt") 2.68-2.56 (m, 4H, OCOCH_2CH_2COOH c+d), 1.50-1.40 (broad s, 18H, 2xBoc), 1.25 (s, 9H, 3x$COCCH_3$ (G1+G2) r+2xr_2), 1.07 (s, 12H, 4x$COCCH_3$ (G3) r_3). **MALDI**: m/z calc. 1366.98 Da. Found $[M + Na]^+$ 1393.61 Da.

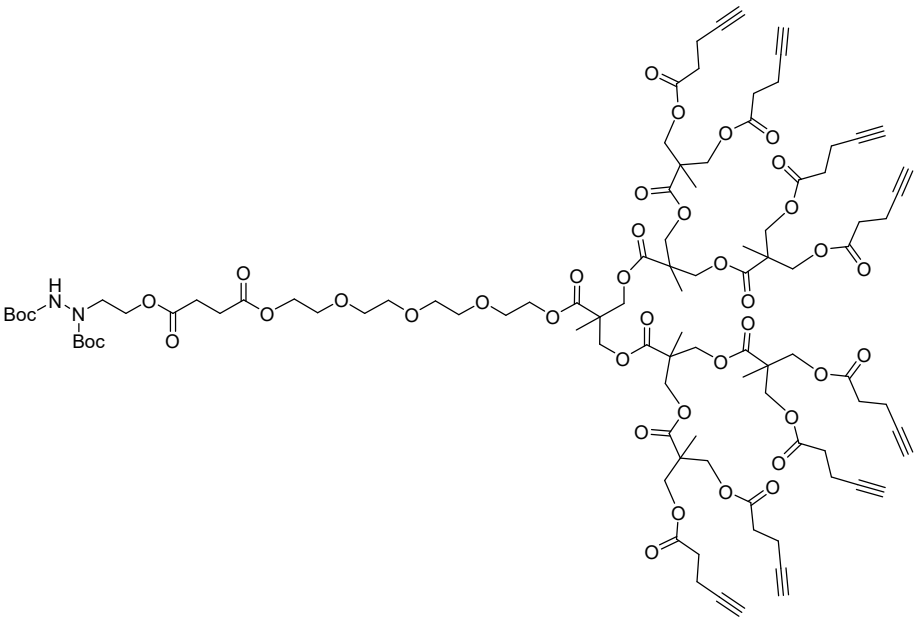

Diboc-hydrazine-succinic-TEG-G3-Alkyne, (Dend15). 4-pentinoic acid (35.32 mg, 0.36 mmol, 12.0 eq.) was dissolved in EtOAc to a 1M concentration and CDI (58.32 mg, 0.36 mmol, 12.0 eq.) was added and stirred at 50˚C about 1 hour. Once imidazolide-activated acid formation finished (^{1}H-NMR evidence), diboc-hydrazine-succinic-TEG-G3-OH (**Dend14**) (41 mg, 0.030 mmol, 1 eq.) and catalytic amount of CsF were added and left to react overnight. Water was added to quench activated acid (^{1}H-NMR evidence) and then, the reaction mixture was washed with $NaHSO_4$ 10% and $NaHCO_3$ 10%, dried over $MgSO_4$, filtered and rotoevaporated to afford the product (30 mg, 0.015 mmol, 50%) as a brownish syrup. **^{1}H-NMR** (400 MHz, $CDCl_3$) δ (ppm) 6.59 (s, 1H, NH), 4.37-4.10 (m, 34H, 3xCH_2OCO b+e+l + 14xCH_2O (G1+G2+G3) s+t+2xs´+2xt´+4xs"+4xt"), 3.80-3.50 (m, 14H, NC$\underline{H_2}CH_2$ a + OC$\underline{H_2}CH_2$OCO f + 2xOC$\underline{H_2}C\underline{H_2}$O g,h,i,j + OC$\underline{H_2}CH_2$OCO k), 2.66-2.58 (m, 4H, OCOC$\underline{H_2}C\underline{H_2}$COOH c+d), 2.58-2.51 (m, 16H, 8xCHCC$H_2C\underline{H_2}$COO n), 2.50-2.43 (m, 16H, 8xCHCC$\underline{H_2}$ o), 2.00 (t *J*= 2.5Hz, 8H, 8xCCH q), 1.52-1.36 (broad s, 18H, 2xBoc), 1.24 (s, 21H, 7x$COCCH_3$ (G1+G2+G3) r+2xr_2+4xr_3). **^{13}C-NMR** (100 MHz, $CDCl_3$) δ (ppm) 172.4, 172.0, 171.5, 171.2, 82.4, 70.7, 70.6, 70.6, 70.5, 69.4, 69.1, 68.9, 66.2, 65.4, 64.5, 46.8, 46.7, 46.5, 33.2, 29.8, 29.1, 28.3, 17.9, 17.7, 14.4. **MALDI**: m/z calc. 2004.89 Da. Found $[M + Na]^+$ 2036.10 Da.

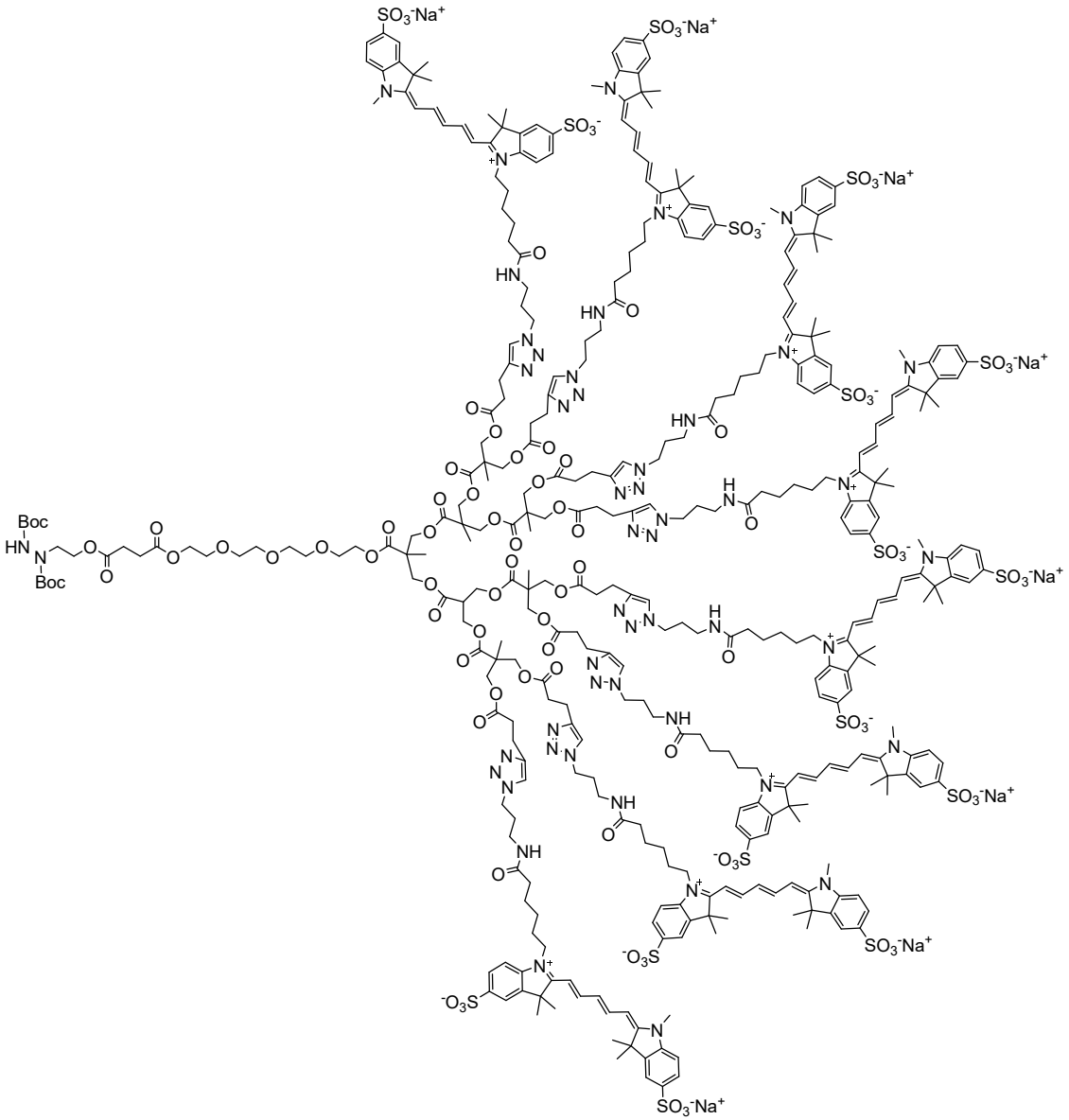

Diboc-hydrazine-succinic-TEG-G3-Cy5, (Dend16). Diboc-hydrazine-succinic-TEG-G3-Alkyne (**15**) (7 mg, 0.00349 mmol, 1 eq.) was dissolved in 150 µL THF and sulfo-Cy5-azide (Lumiprobe) (25 mg, 0.0335 mmol, 9.6 eq.) in 150 µL H_2O and Na ascorbate (2.67 mg, 0.0167 mmol, 4,8 eq.) and $CuSO_4$ (1.659 mg, 0.00837 mmol, 2.4 eq.) were added. Some drops of DMF were added as well to solubilize better the reagents. The mixture is left to react for two nights at 50° protected from light. The solvents were eliminated and the crude dissolved in 500 µL H_2O and purified by sephadex using PD Minitrap G-25 columns (GE Healthcare) to afford after freeze-drying the product (16 mg, 0.002 mmol, 57%) as a brilliant blue solid. **^{1}H-NMR** (400 MHz, MeOD) δ (ppm) 8.37-8.19 (m, 16H, CHC<u>H</u>CHC<u>H</u>CH 16+18), 7.99 (s, 8H, C=CHN p), 7.91-7.81 (m, 24H, Ar), 7.37-7.28 (m, 16H, Ar), 6.68 (t *J*= 12.4 Hz, 16H, CHCHC<u>H</u>CHCH 17), 6.85-6.25 (m, 16H, C<u>H</u>CHCHCHC<u>H</u> 19+15), 4.42-4.27 (m, 16H, CH_2NN 1), 4.27-4.00 (m, 10H, 3xCH_2OCO b+e+l, 14xCH_2O (G1+G2+G3) s+t+2xs´+2xt´+4xs"+4xt, CH_2N^+ 9), 3.68-3.52 (m, 38H, N-CH_3 20 + NC<u>H</u>$_2$$CH_2$ a + OC<u>H</u>$_2$$CH_2$OCO f + 2xOC<u>H</u>$_2$C<u>H</u>$_2$O g,h,i,j + COOC$H_2$C<u>H</u>$_2$O k), 3.25-3.17 (m, 16H, CH_2NHCO 3),

3.16-3.05 (m, 16H, CH_2C=CN o), 2.70 (m, 16H, $C\underline{H}_2CH_2NN$ 2), 2.64-2.54 (m, 20H, $OCOC\underline{H}_2C\underline{H}_2COOCH_2$ c+d, $NCCH_2C\underline{H}_2COO$ n), 2.25-2.10 (m *J*=6.8 Hz, 16H, $C\underline{H}_2CONH$ 5), 1.91-1.57 (m, 36H, $N^+CH_2(C\underline{H}_2)_3CH_2CONH$ 6,7,8 + 4xCH_3 13+13´+14+14´), 1.48-1.38 (broad s, 18H, 6xCH_3 Boc), 1.29 (s, 21H, 7xCH_3 bis-MPA (G1+G2+G3) r, r_2, r_3)

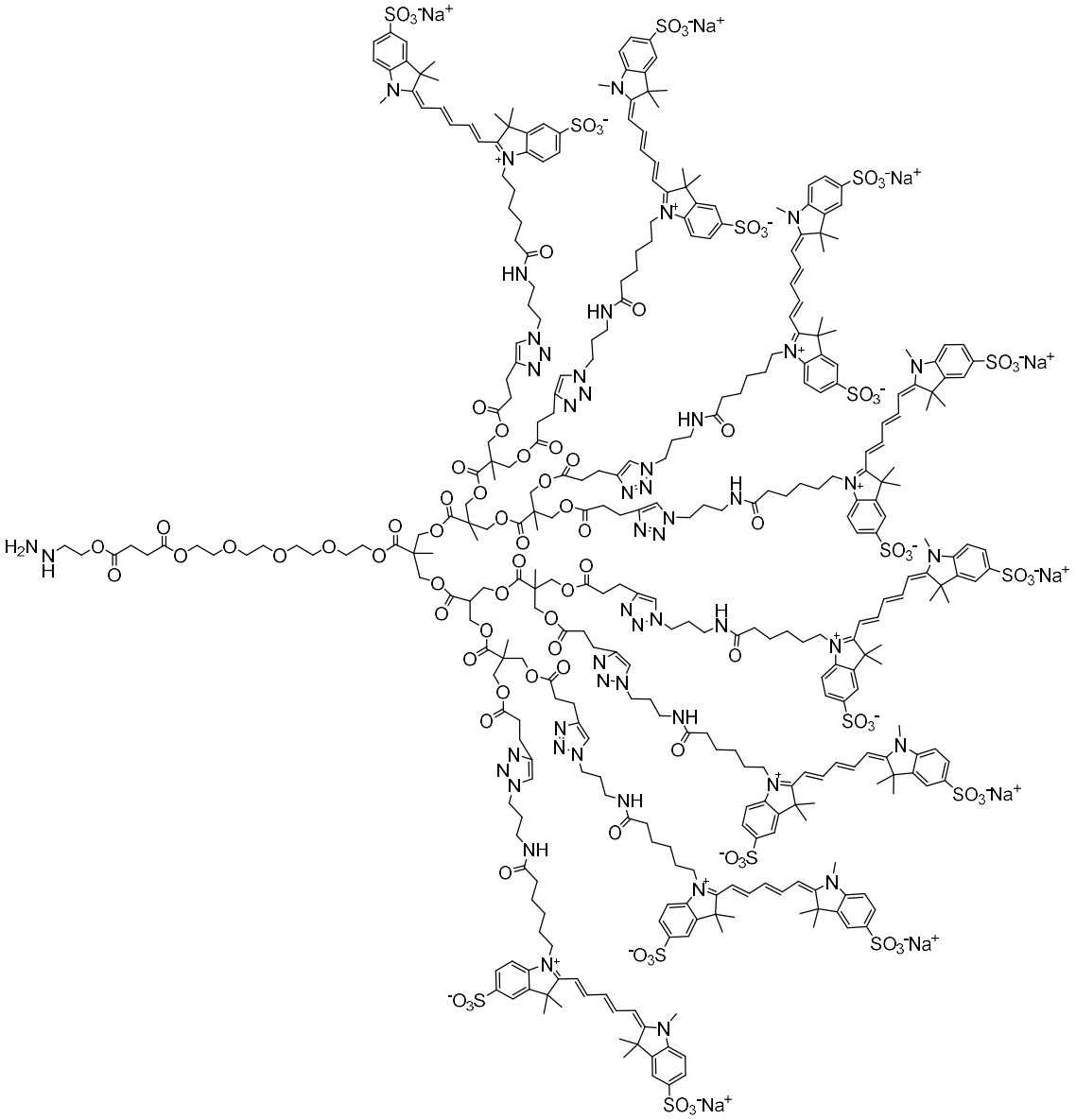

G3-Cy5. Boc protected G3-Cy5 was dissolved in pure TFA and left to react for 20 min at room temperature. The acid was eliminated by rotoevaporation to afford the deprotected product (see Figure S9 for ^{1}H-NMR evidence) as TFA salt as a blue solid. **^{1}H-NMR** (400 MHz, MeOD) δ (ppm) 8.37-8.19 (m, 16H, CHC$\underline{H}$CHC$\underline{H}$CH 16+18), 7.91-7.81 (m, 24H, Ar), 7.80 (s, 8H, C=CHN p), 7.37-7.28 (m, 16H, Ar), 6.68 (t *J*= 12.4 Hz, 16H, CHCHC$\underline{H}$CHCH 17), 6.85-6.25 (m, 16H, C$\underline{H}$CHCHCHC$\underline{H}$ 19+15), 4.42-4.27 (m, 16H, CH_2NN 1), 4.27-4.00 (m, 10H, 3xCH_2OCO b+e+l, 14xCH_2O (G1+G2+G3) s+t+2xs´+2xt´+4xs"+4xt, CH_2N^+ 9), 3.68-3.52 (m, 38H, N-CH_3 20 + $NC\underline{H}_2CH_2$ a + $OC\underline{H}_2CH_2OCO$ f + 2x$OC\underline{H}_2C\underline{H}_2O$

g,h,i,j + $COOCH_2C\underline{H_2}O$ k), 3.25-3.17 (m, 16H, CH_2NHCO 3), 3.16-3.05 (m, 16H, $CH_2C{=}CN$ o), 2.70 (m, 16H, $C\underline{H_2}CH_2NN$ 2), 2.64-2.54 (m, 20H, $OCOC\underline{H_2}C\underline{H_2}COOCH_2$ c+d, $NCCH_2C\underline{H_2}COO$ n), 2.25-2.10 (m *J*=6.8 Hz, 16H, $C\underline{H_2}CONH$ 5), 1.91-1.57 (m, 36H, $N^+CH_2(C\underline{H_2})_3CH_2CONH$ 6,7,8 + 4xCH_3 13+13´+14+14´), 1.29 (s, 21H, 7xCH_3 bis-MPA (G1+G2+G3) r, r_2, r_3).

3.2.2. IgG labeling with Cy5 decorated dendrons

The protocol used for IgG labeling was the one registered in Bioconjugate techniques [160]. The two steps necessary are described in the two following points.

Activation of antibodies with sodium periodate ($NaIO_3$)

IgG chosen for labeling procedure optimization was α-Human IgG Fc clone SG-11 (ICN Biomedicals Inc). Protein main concentration was determined by Bradford.

IgG (20 mg/mL, 4 mg, 1 eq., $2.67.10^{-5}$ mol) was dissolved at a concentration of 10 mg/mL in 0.01 M Na_3PO_4, 0.15 M NaCl, pH 7.2 and 40 µL (100 µL per mL of IgG) of freshly prepared 0.1 M $NaIO_3$ were added. After homogenization, the mixture was left to react in the dark for 20 min in a swinging tray. Then, 1 mg of Na_2SO_3 was added to quench remaining $NaIO_3$ and left to react in the dark for 30 min in a swinging tray. Meanwhile, a PD MiniTrap G-25 sephadex desalting column (GE Healthcare) was equilibrated with 8 mL of chromatography buffer (Na_3PO_4 0.1M, NaCl 0.15 M, pH 7.2).

After quenching, the reaction mixture was completed to 500 µL with chromatography buffer (Na_3PO_4 0.1M, NaCl 0.15 M, pH 7.2) and introduced in the desalting column once the buffer used for equilibration entered the packed bed completely. The 500 µL that come out of the column after adding sample volume were discarded and then, 1 mL of chromatography buffer was added and the flow through collected. After removing $NaIO_3$ excess by desalting step, IgG concentration was 4 mg/mL.

Amicon ultra 0.5 mL 30K centrifugal filters (Merck Millipore) were used to reduce volume to 400 µL for having a final antibody concentration of 10 mg/mL. The oxidized antibody was used immediately.

Conjugation of periodate-oxidized antibodies with Cy5 decorated dendrons

This is the general procedure for labeling, used for the conjugation of each of three dendrons. Two to ten milligrams of the hydrazine containing molecule were weighted and dissolved in the amount of milliQ water necessary so that in 25 µL we have the amount corresponding to a 15-fold molar excess ($4.24{\cdot}10^{-4}$ mol) over the amount of antibody present. The fluorescent probe solution was added to the 400 µL of oxidized

antibody in chromatography buffer and left to react in the dark for 2 hours in a swinging tray.

All following steps were carried out in a fume hood. In order to stabilize the hydrazine bond formed, 4 µL of 5 M $NaBH_3CN$ in 1M NaOH (10 µL per mL of conjugation solution) were added and left to react for 30 minutes in the dark in a swinging tray. Unreacted aldehyde sites were blocked by addition of 20 µL of ethanolamine 1M pH 9.6 (50 µL per mL of conjugation solution), 30 min reaction in the dark. Purification from excess of reactants was made in case of **IgG-G0-Cy5** and **IgG-G1-Cy5** by gel filtration, using a PD MiniTrap G-25 sephadex desalting column (GE Healthcare) as described in purification step after oxidation, using this time 0.01 M Na_3PO_4, 0.15 M NaCl, pH 7.0 as chromatography buffer (chromatography buffer after labeling). Amicon ultra 0.5 mL 30K centrifugal filters (Merck Millipore) was used for **IgG-G3-Cy5** purification.

In order to make sure that no excess of the fluorescent probe was still remaining, we further filtrated the conjugated antibody with Amicon ultra 4 mL 30K centrifugal filters (Merck Millipore) and washed it with milliQ water as many times as necessary to get a crystal clear filtrate.

After filtration, we completed each labeled IgG volume up to a 1 mL with 0.01 M Na_3PO_4, 0.15 M NaCl, pH 7.0 (chromatography buffer after labeling) and considered complete recovery after all labeling and purification steps.

3.2.3. SDS-PAGE characterization of Cy5 labeled IgG

After conjugation, control IgG and Cy5 labeled IgG samples were denaturalized by adding Laemmli buffer and heating at 96˚C for 5 minutes. Eppendorf tubes containing denaturalized samples were centrifuged for some seconds (were given a short spin) and quickly cool down in ice bath to avoid renaturalization. Four decreasing amounts of control IgG (4, 2, 1, 0.5 µg), 4 µg of each of three IgG-Cy5 samples and a molecular weight marker (Precision Plus Protein Standards Dual color, Bio-Rad) were loaded in 12% SDS-polyacrilamide gel and electrophoresis system was connected to a power supply with a 80 V current until samples pass through stacking gel and 120 V since samples reached running gel.

Once electrophoresis finished, gels were analyzed with Molecular Imager Pharos FX and, after fluorescence registration, stained with Coomassie and digitalized with ChemiDoc Imaging Systems (Bio-Rad).

3.2.4. Spectroscopic Characterization of Dendrons and Labeled IgG

Boc-deprotected dendrons **G0-Cy5**, **G1-Cy5** and **G3-Cy5** were dissolved in in 0.01 M Na_3PO_4, 0.15 M NaCl, pH 7.0 (chromatography buffer after labeling) at $3.8 \cdot 10^{-7}$ M and solutions of control IgG and labeled IgG (**IgG-G0-Cy5**, **IgG-G1-Cy5** and **IgG-G3-Cy5**) were prepared using the same solvent at 10^{-6} M. Absorbance was measured in an Agilent 8453 UV-Visible Spectroscopy System and fluorescence in an Edinburgh Instruments FLS 920 fluorimeter. Data were processed with GraphPad Prism 5.01 (GraphPad Software, Inc., California).

For cited solvent, knowing the solutions concentration we calculated the molar extinction coefficient, ε, from absorbance obtained at absorption maximum wavelength (646 nm) by using Lambert Beer Law ($A = \varepsilon \cdot b \cdot c$). Qantum yield (ϕ) was calculated as described in [280] using sulfo-Cy5 as standard dye, and relative brightness ($\varepsilon \cdot \phi$) [254] was also calculated. The quenching-dequenching characteristics of **IgG-G3-Cy5** were studied by adding to the conjugates 1% SDS to disassociate any molecular interaction between fluorophores.

RESUMEN

INTRODUCCIÓN

Según la Organización Mundial de la Salud (OMS), las reacciones adversas a fármacos se definen como "todas aquellas respuestas nocivas y no intencionadas, o cualquier otro efecto perjudicial no deseado que ocurre tras la administración de una dosis habitualmente utilizada del fármaco en la especie humana para la profilaxis, diagnóstico y tratamiento de una enfermedad o para la modificación de una función biológica". Las reacciones de hipersensibilidad a fármacos pertenecen al grupo B de las reacciones alérgicas a fármacos y se definen como los efectos adversos de las formulaciones farmacéuticas (incluyendo el principio activo y los excipientes) que clínicamente recuerdan una alergia. En función del mecanismo implicado se clasifican en dos grupos. Las reacciones alérgicas están mediadas por mecanismos inmunológicos específicos y las no alérgicas por mecanismos no inmunológicos (Figura R.1). Las reacciones alérgicas representan entre el 5-10% de las reacciones tipo B.

A su vez las reacciones alérgicas a antibióticos betalactámicos pueden clasificarse en función del mecanismo inmunológico implicado (Gell y Coombs) o del tiempo transcurrido desde la toma del fármaco hasta que aparece la reacción.

Las reacciones inmediatas a antibióticos betalactámicos, mediadas por anticuerpos IgE, constituyen el objeto de estudio de esta tesis doctoral.

Todas las reacciones adversas a fármacos con base inmunológica requieren un período de previo sensibilización tras la primera exposición al antígeno, en el que se producen anticuerpos IgE específicos implicados en el desarrollo de una respuesta alérgica después de una nueva exposición a dicho antígeno (Figura R.2).

El modelo actual más aceptado por la comunidad científica para explicar el modo en el que el sistema inmune reconoce a los fármacos está basado en la hipótesis del hapteno formulada por Landsteiner en 1935 (Figura R.3). Un hapteno es una especie de bajo peso molecular (< 1000 Da), químicamente reactiva y demasiado pequeña para inducir una respuesta inmunológica por sí misma, pero que sí alcanza el tamaño suficiente para inducirla cuando se une covalentemente a macromoléculas, proceso que se denomina haptenización.

Según esta hipótesis, después de la unión covalente del hapteno a una macromolécula, el conjugado hapteno-molécula portadora puede ser procesado y presentado por las células presentadoras de antígenos a los linfocitos para la producción de anticuerpos específicos que pueden reaccionar contra el determinante antigénico, formado por el hapteno y posiblemente por algunas regiones de la molécula portadora.

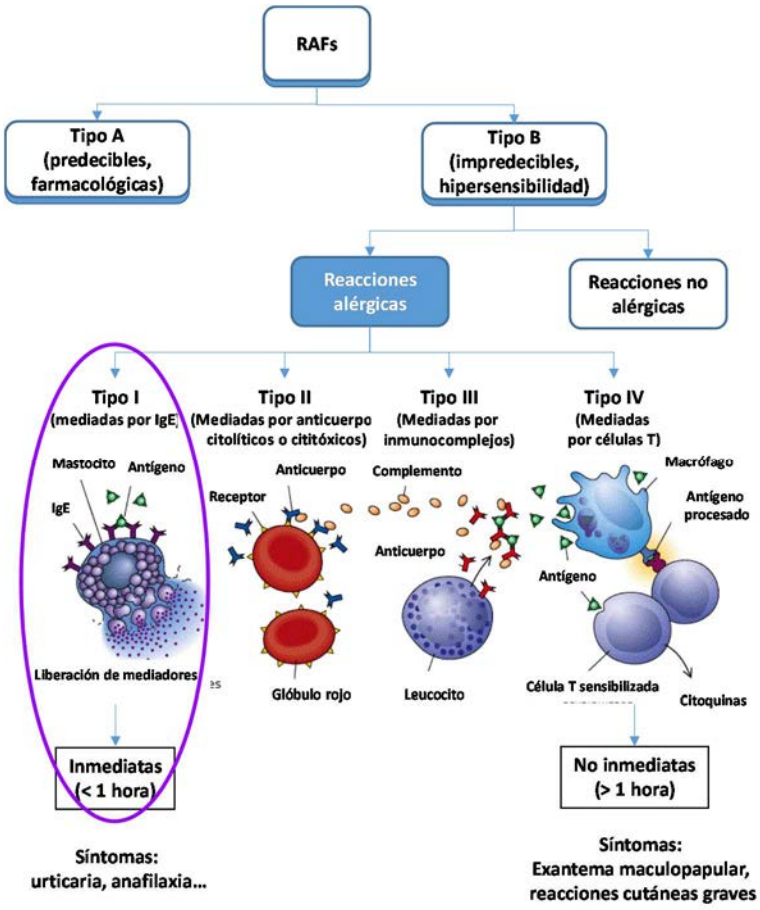

Figura R.1. Clasificación inmunológica y clínica de las reacciones alérgicas a fármacos con base inmunológica. RAF: Reacciones adversas a fármacos.

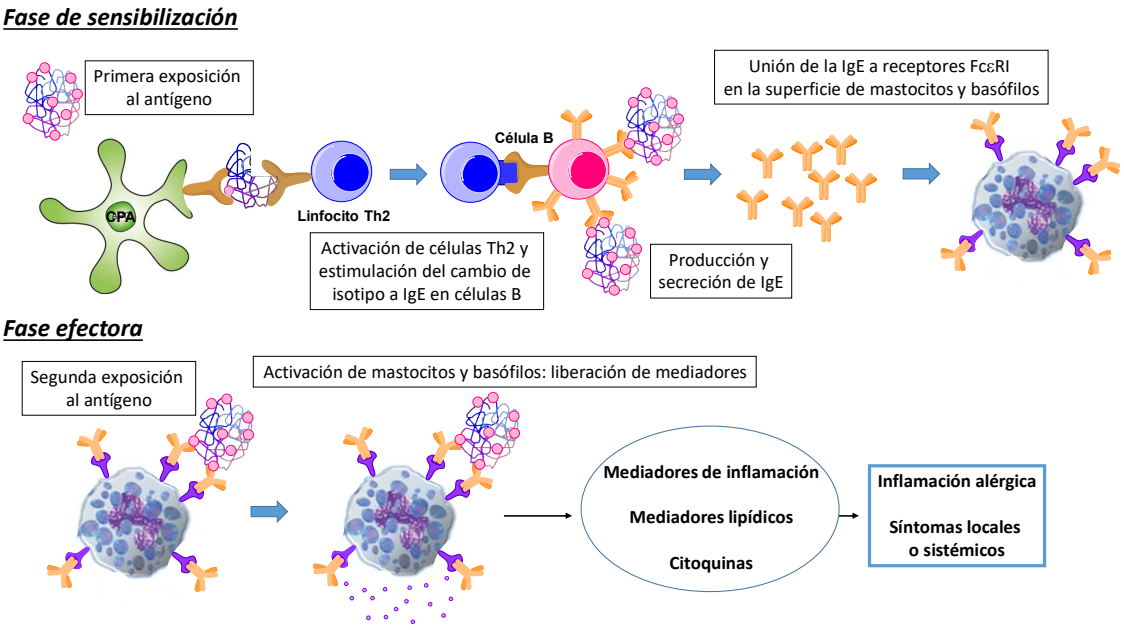

Figura R.2. Secuencia de acontecimientos de las reacciones alérgicas inmediatas: fase de sensibilización y desarrollo de la respuesta alérgica inmediata. CPA: célula presentadora de antígenos. FcεRI: receptor celular de alta afinidad.

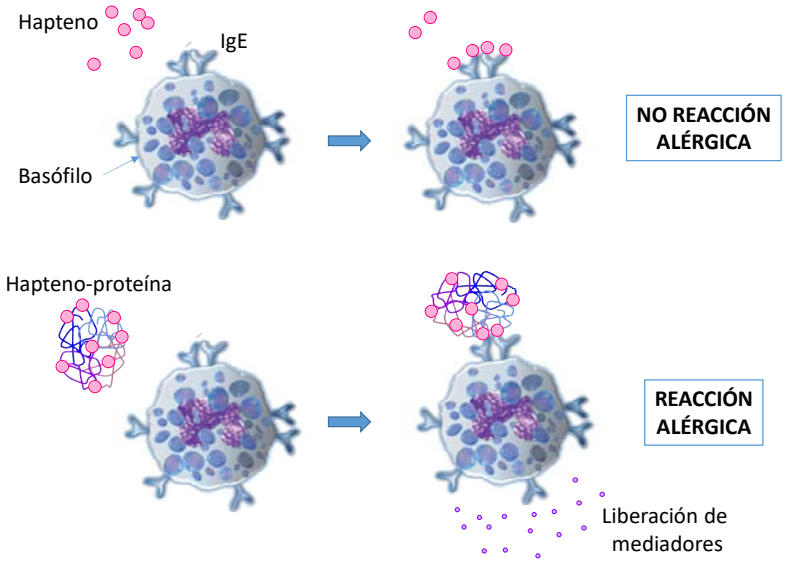

Figura R.3. Hipótesis del hapteno propuesta por Landsteiner.

Las reacciones alérgicas inmediatas a antibióticos betalactámicos son las reacciones con base inmunológica más frecuentes y pueden ser inducidas por cualquiera de las estructuras de betalactámicos disponibles. Aparecen normalmente en un intervalo de tiempo inferior a una hora tras de la administración del fármaco y están mediadas por anticuerpos IgE que reconocen específicamente estas estructuras. Dentro de los antibióticos betalactámicos, las penicilinas han sido los fármacos más estudiados y de los que se conoce bien su inmunoquímica, empleándose como modelo para estudio de las reacciones alérgicas a otros medicamentos.

Los antibióticos betalactámicos se clasifican en función de su estructura química en seis grupos: penicilinas, cefalosporinas, carbapanemas, clavamas y monobactamas (Figura R.4). Dentro de esta clasificación, las penicilinas y las cefalosporinas son los dos grupos principales.

La estructura general de todos los betalactámicos (Figura R.4) consiste en un anillo β-lactámico que, a excepción de las monobactamas, está fusionado a otro anillo: de tiazolidina en el caso de las penicilinas, de dihidrotiazina en el caso de cefalosporinas, de dihidropirrol en carbapenemas y de oxazolidina en clavamas. Cada tipo de antibiótico betalactámico presenta diferentes cadenas laterales o sustituyentes R, unidos al anillo de β-lactama (R or R^1), excepto en las clavamas, o al otro anillo (R^2, R^3) excepto en penicilinas y monobactamas. Hay una gran variedad de estructuras de cadenas laterales, que pueden ser similares o idénticas entre miembros de los diferentes grupos de betalactámicos.

Los antibióticos betalactámicos son estructuras de bajo peso molecular que actúan como haptenos en el reconocimiento por el sistema inmune, por lo que es necesario

que se unan a estructuras macromoleculares para poder inducir una respuesta inmunológica.

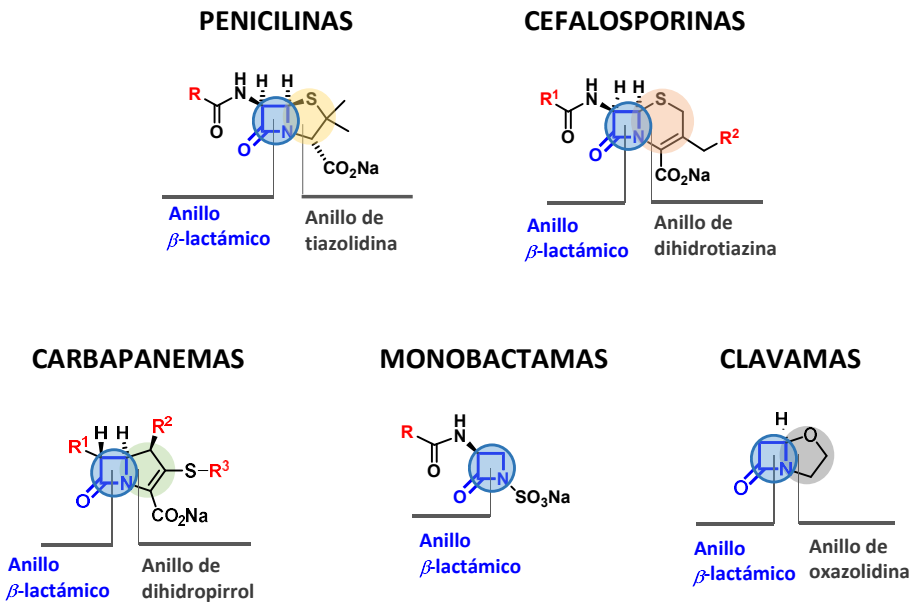

Figura R.4. Diferentes antibióticos betalactámicos con detalles de su estructura general.

Todos los antibióticos betalactámicos son químicamente reactivos sin necesidad de un proceso metabólico previo y tienen la capacidad de unirse de forma espontánea a proteínas exógenas o endógenas que pueden ser procesadas y reconocidas por el sistema inmune. Estos antibióticos se unen covalentemente a las proteínas mediante el ataque nucleofílico al grupo carbonilo en el anillo β-lactámico por un grupo amino primario de los residuos aminoacídicos de la proteína, con formación de un enlace tipo amida.

Las penicilinas son los antibióticos betalactámicos mejor estudiados y dentro de este grupo, la bencilpenicilina fue el primer hapteno del que se estudió su inmunoquímica en detalle y que tradicionalmente ha sido considerado como el hapteno modelo para el estudio de las reacciones alérgicas a fármacos. Durante muchos años, el determinante antigénico mejor conocido ha sido el bencilpeniciloil (BPO), estructura estable que se forma por la unión del grupo carbonilo resultante de la apertura nucleofílica del anillo β-lactámico con un grupo amino libre de una proteína (Figura R.5). El mismo proceso de formación del determinante BPO se ha observado con la amoxicilina (Figura R.5) y la ampicilina para la formación de sus determinantes equivalentes amoxiciloil (AXO) y ampiciloil (APO), respectivamente, y por extensión se asume que este tipo de determinante "peniciloil" se pueden generar con el resto de penicilinas. A partir de la obtención de anticuerpos frente a penicilinas empleando como inmunógeno el fármaco

conjugado a una macromolécula portadora se ha observado que tanto la naturaleza de la molécula portadora como la del hapteno pueden influir en el reconocimiento por los anticuerpos IgE específicos.

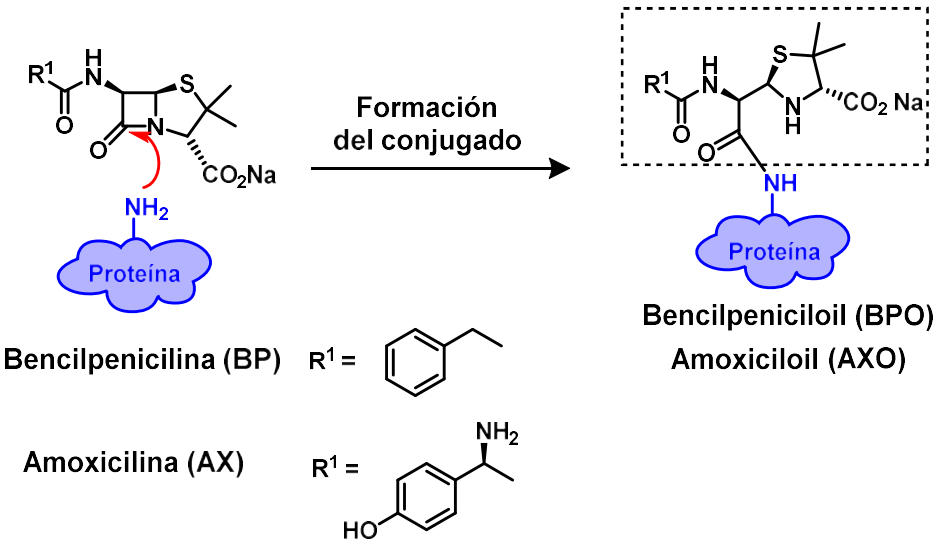

Figura R.5. Formación del determinante antigénico para amoxicilina y ácido clavulánico.

Carbapenemas y monobactamas también forman determinantes antigénicos estables tras la formación de enlace amida entre los grupos amino de las proteínas y el carbonilo del anillo β-lactámico. Sin embargo, la inestabilidad del conjugado formado por la unión covalente entre proteína y cefalosporinas o ácido clavulánico, y una reactividad química más compleja de estos fármacos, ha impedido que se conozca con exactitud la estructura del determinante antigénico responsable de las reacciones alérgicas a estos antibióticos betalactámicos.

Una aproximación general para la evaluación y el diagnóstico de sujetos que han sufrido una reacción de hipersensibilidad inmediata tras la administración de antibióticos betalactámicos se ha descrito por la Academia Europea de Alergia e Inmunología Clínica (EAACI). El algoritmo diagnóstico propuesto comprende la realización de una historia clínica plausible y de diferentes pruebas diagnósticas entre las que se incluyen las pruebas cutáneas, inmunoensayos, ensayos celulares y la administración controlada del fármaco (Figura R.6).

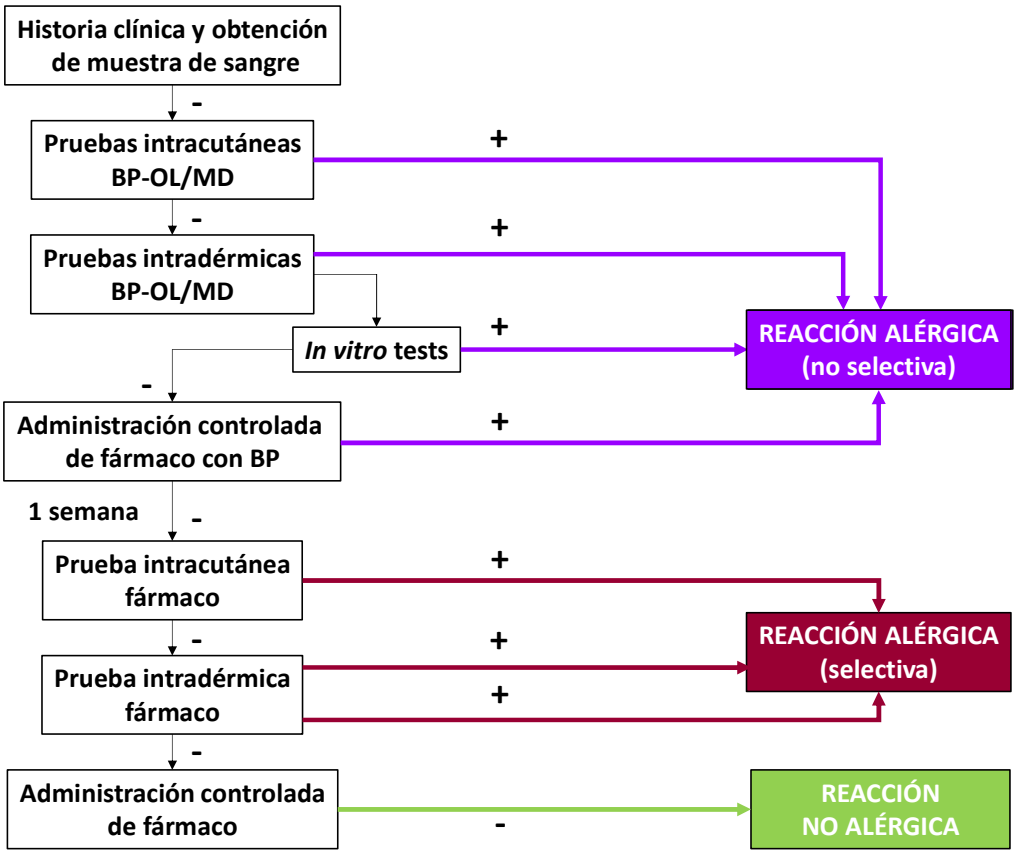

Figura R.6. Algoritmo diagnóstico para la evaluación de las reacciones alérgicas inmediatas a antibióticos betalactámicos. BP-OL: bencilpeniciloil-octalisina. MD: determinante menor (ácido bencilpeniloico).

El primer paso para realizar un diagnóstico clínico correcto es establecer una historia clínica plausible, en la que los síntomas descritos tienen que ser compatibles con este tipo de reacciones y aparecer en un intervalo de tiempo inferior a 1 hora tras la administración del fármaco.

A continuación, se realizan pruebas cutáneas, dentro de las cuales se realizan pruebas intracutáneas (o prick), y si los resultados obtenidos son negativos se realizan las pruebas intradérmicas. Las pruebas cutáneas son muy específicas (97%), sin embargo, su sensibilidad ha ido variando a lo largo del tiempo aunque sin superar el 70%.

En caso de pruebas cutáneas y pruebas *in vitro* negativas, y sólo en pacientes que no presenten ningún factor de riesgo y en los sea imprescindible obtener un diagnóstico confirmado, se realiza la administración controlada del fármaco. Estudios recientes muestran que, debido a una sensibilidad no óptima de las pruebas cutáneas e *in vitro*, más del 30% de los pacientes con reacciones alérgicas inmediatas a antibióticos betalactámicos no podrán ser diagnosticados correctamente si no se someten a una administración controlada de fármaco.

Los inmunoensayos son los métodos que se emplean en la detección de anticuerpos IgE específicos frente a betalactámicos. En estos ensayos se usa una fase sólida (sefarosa, discos de celulosa) a la que está unida una molécula portadora (poli-L-lisina, albúmina sérica humana (HSA), aminoespaciadores), a la que se conjuga el antibiótico betalactámico de interés. En las determinaciones de rutina se emplea una plataforma comercial de fluoroinmunoensayo (FEIA) ("ImmunoCAP", Phadia) que permite un análisis automatizado. La especificidad de este método está comprendida entre 83-100% y la sensibilidad entre el 0-50%. Existen estudios recientes que muestran una tendencia general a la disminución de la sensibilidad de esta técnica, posiblemente relacionada con la relevancia que están adquiriendo nuevas estructuras betalactámicos en el desarrollo de las reacciones alérgicas inmediatas. En algunos laboratorios de investigación también se realiza un radioinmunoensayo (RIA) no comercial para la determinación de anticuerpos IgE específicos conocido como prueba radioalergoabsorbente (RAST). En este método se emplean como fase sólida discos de celulosa activados con bromuro de cianógeno a los que se une una molécula portadora conjugada con el hapteno de interés. Los valores de especificidad del RAST están comprendidos entre el 68-83% y los de sensibilidad se sitúan alrededor del 43-75%. En comparación con el inmunoCAP, el RAST presenta mayor sensibilidad/especificidad, pero carece de automatización y necesita de método de detección radiactivo para el que se necesitan instalaciones especiales y personal con formación específica, no disponibles en todos los laboratorios. Con objeto de mejorar la sensibilidad de estas pruebas se están realizando estudios basados en la aplicación de la nanotecnología, fundamental para la mejora de los métodos diagnósticos en biomedicina. Así, se ha dedicado mucho esfuerzo en la incorporación de diferentes haptenos/determinantes en la construcción de sistemas nanométricos capaces de emular *in vitro* el reconocimiento que ocurre *in vivo*. En este sentido, se han utilizado estructuras dendriméricas como moléculas portadoras a las que se conjugan antibióticos betalactámicos. Además se han desarrollado diferentes métodos de anclaje a la fase sólida, incluyendo el empleo de espaciadores para aumentar la accesibilidad de los conjugados por la IgE, con un consecuente aumento de sensibilidad. Otros estudios están encaminados al empleo de nuevas fases sólidas diferentes a los tradicionales discos de celululosa como nanopartículas de sílice, zeolitas o láminas de oro.

Entre los ensayos celulares, el uso del test de activación de basófilos (BAT) está aumentando de forma progresiva en el diagnóstico de las reacciones alérgicas inmediatas. Se basa en la capacidad de los basófilos activados, tras su estimulación con el fármaco, de expresar en su superficie marcadores de activación, que pueden ser detectados mediante citometría de flujo. Este método tiene una sensibilidad del 49% y una especificidad del 93% con los antibióticos betalactámicos.

JUSTIFICACIÓN E HIPÓTESIS

La alergia a antibióticos betalactámicos constituye actualmente un problema de salud importante que necesita un diagnóstico rápido y preciso para poder instaurar una terapia antibiótica apropiada, incrementar la seguridad del paciente y reducir costes al sistema sanitario. De entre las diferentes reacciones alérgicas, las reacciones inmediatas (mediadas por IgE) a antibióticos betalactámicos constituyen las más frecuentes. El diagnóstico *in vitro* de este tipo de reacciones es objeto de estudio de esta tesis.

El hecho de poder diagnosticar correctamente la alergia a fármacos es muy importante para realizar una adecuada prescripción de medicamentos y evitar riesgos para el paciente. La primera aproximación para evaluar al paciente consiste en una historia clínica detallada, lo cual es a veces muy difícil de conseguir. La siguiente opción considera frecuentemente las pruebas cutáneas y, si son negativas, las pruebas de administración controlada. Debido al alto riesgo que supone la realización de estas pruebas *in vivo*, los métodos *in vitro* representan la alternativa ideal para el diagnóstico.

Las dos técnicas *in vitro* más empleadas consisten en inmunoensayos, basados en el reconocimiento por la IgE específica del fármaco o un metabolito unido a una fase sólida, y el BAT, basado en la cuantificación de la activación del basófilo tras su estimulación con el fármaco. Entre los inmunoensayos, el InmunoCAP es el único método comercial y está sólo disponible para algunos antibióticos betalactámicos, presentando poca sensibilidad. El RAST presenta una mayor sensibilidad pero su principal inconveniente es la necesidad del uso de un anticuerpo radioactivo. El BAT permite el diagnóstico en el 50%. Varios factores pueden influir en la falta de sensibilidad de esta técnica, entre los que se encuentra: (i) la no inclusión, en la prueba *in vitro*, del metabolito o derivado del fármaco que indujo la reacción *in vivo*; o (ii) que la molécula portadora empleada no exponga al fármaco en una conformación o número óptimo para ser reconocido por la IgE.

Sin duda, comprender el mecanismo mediante el cual la molécula del fármaco se metaboliza después de la conjugación con la proteína portadora y el conocimiento de los metabolitos exactos que interaccionan con el sistema inmune e inducen la respuesta alérgica, es clave para poder evaluar estas reacciones mediante test diagnósticos tanto *in vivo* como *in vitro*. La estructura del fármaco que permanece unida al portador se llama determinante antigénico. Los estudios dirigidos hacia la identificación de determinantes antigénicos de fármacos y los conjugados hapteno-portador resultan muy complejos y no se han abordado con éxito para prototipos importantes de fármacos, como cefaclor, cefadroxilo y ácido clavulánico. Esto implica una dificultad añadida para la realización de un diagnóstico de alergia, ya que hasta la fecha sólo

existen pruebas cutáneas, que en el caso concreto de estos fármacos no están estandarizadas, e implican un riesgo.

Con el fin de entender el mecanismo de degradación de los fármacos tras su unión con las proteínas, es necesario proponer cuales son estos mecanismos y realizar la síntesis de una serie de estructuras candidatas para su evaluación en la activación y/o reconocimiento molecular por el sistema inmune. Partimos de la base de que podemos identificar estos nuevos determinantes antigénicos y que su incorporación a los materiales diagnósticos implicaría un gran avance.

Otra causa que con probabilidad también influye en la baja sensibilidad de los métodos diagnósticos *in vitro* de alergia a fármacos, además del desconocimiento de los determinantes antigénicos implicados, es la escasa cantidad de IgE específica (femtogramos o menos) asociada a este tipo de alergias. El marcaje con fluorescencia de un anticuerpo secundario altamente específico serviría para afrontar el inconveniente de la detección con radioactividad del RAST, pudiéndose emplear en inmunoensayos convencionales. Las plataformas de microarray permiten la evaluación en paralelo de múltiples fármacos con una mínima cantidad de muestra y podrían afrontar la necesidad de gran cantidad de muestra así como la capacidad de analizar un limitado número de fármacos de los métodos actuales. El marcaje mencionado permitiría conseguir un método de detección compatible con los escáneres empleados en los microarray.

El uso de dendrones como nanoestructuras para el marcaje de anticuerpos secundarios permite aumentar el número de unidades fluorescentes en la sonda debido a su multivalencia. Un correcto diseño de estas nanoestructuras permitiría el marcaje específico del anticuerpo en regiones que no afecten al reconocimiento, así como la amplificación de la señal de detección sin incrementar las uniones inespecíficas del inmunoensayo, llegando a un compromiso óptimo entre el número de unidades fluorescentes y la emisión de fluorescencia.

Los resultados obtenidos de los estudios de identificación de determinantes antigénicos y de metodologías para la amplificación de la señal fluorescente podrían ser de importancia para el desarrollo y mejora de métodos de diagnóstico *in vitro* de alergias a antibióticos betalactámicos, con lo que se podrían conseguir avances importantes con repercusión en el sistema sanitario.

OBJETIVOS

El objetivo general de esta tesis está dirigido hacia la identificación de determinantes antigénicos y el marcaje fluorescente de anticuerpos secundarios para mejorar el

diagnóstico *in vitro* de reacciones alérgicas antibióticos betalactámicos de tipo inmediatas.

Como objetivos concretos se presentan los siguientes:

1- Síntesis y evaluación inmunológica de determinantes antigénicos potenciales de α-aminocefalosporinas mediante una aproximación de estudio SAR, utilizando RAST como inmunoensayo para evaluar el reconocimiento IgE específico.

2- Estudio de los determinantes antigénicos de ácido clavulánico mediate varias aproximaciones. (i) Estudios SAR: síntesis y evaluación inmunológica de determinantes antigénicos potenciales. (ii) Estudios de proteómica: identificación de fragmento anclado a HSA e identificación de los sitios de unión, así como identificación de proteínas séricas dianas de haptenización mediante el uso de un derivado biotinilado del ácido clavulánico.

3- Síntesis y caracterización de una serie de dendrones fluorescentes y comprobación de la validez para su anclaje quimioselectivo a anticuerpos y amplificación de la señal fluorescente.

RESULTADOS Y DISCUSIÓN

I. Estudio de los Determinantes Antigénicos de α-aminocefalosporinas

Las cefalosporinas son betalactámicos de uso creciente, no existiendo en la actualidad test con suficiente sensibilidad para detectar anticuerpos IgE específicos en pacientes con reacciones alérgicas. Para su diagnóstico *in vitro* se necesita incluir las estructuras químicas de los determinante antigénicos implicados, que aún no han sido identificados.

Los estudios estructurales de los conjugados de cefalosporinas con proteínas resultan muy complicados y nunca se han realizado con éxito. Se ha postulado como producto inicial un determinante, el cefalosporoílo (CPO), que aparece como consecuencia de la aminolisis de cefalosporinas, que posteriormente sufre fragmentaciones sucesivas en el núcleo de dihidrotiazina, durante las cuales generalmente se pierde la cadena lateral R^2. Sobre la base de esta hipótesis, y dada la inestabilidad y dificultad de aislamiento del CPO intermedio y de sus productos de degradación, en estudios previos del grupo de investigación, se abordó este estudio mediante una aproximación sintética. De modo que la relación entre la estructura química del determinante antigénico sintético y el reconocimiento molecular por IgE se determinó mediante el estudio de estructuras definidas (**I**, **II**, **III** y **IV**) mostradas en la Figura R.7 que corresponden a los determinantes propuestos de diferentes cefalosporinas. Los resultados indicaron que los determinantes antigénicos retienen el sustituyente R^1 de las cefalosporinas y alguna porción del anillo de dihidrotiazina, aunque sin incluir el átomo de azufre.

La especificidad está relacionada principalmente con la cadena lateral R^1 y la diferente funcionalización en el carbono puente refinan el reconocimiento molecular con la IgE.

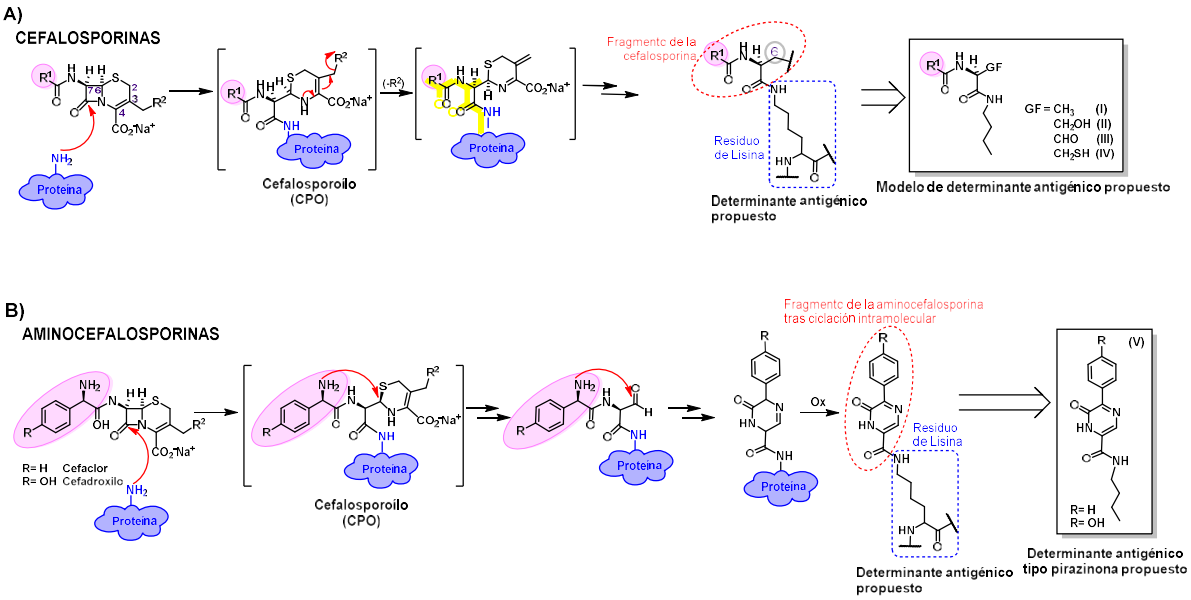

Figura R.7. Hipótesis de degradación de cefalosporinas (A) y α-aminocefalosporinas (B).

Aunque en este sentido se ha avanzado considerablemente en el conocimiento de las estructuras antigénicas de cefalosporinas, todavía no existen fases sólidas que incluyan estas moléculas ancladas adecuadamente para llevar a cabo los inmunoensayos en la clínica rutinaria. Por otro lado, otras aminocefalosporinas como el cefaclor y el cefadroxilo muestran patrones de reconocimiento diferentes, que todavía no han sido estudiados en detalle, y la evaluación clínica de un producto de degradación con un núcleo de pirazina (**V**), Figura R.7B y Figura R.8, podría ser necesaria para realizar este diagnóstico. En este trabajo, abordamos también desde una aproximación sintética el estudio del reconocimiento molecular de derivados cíclicos (pirazinonas) de cefaclor y cefadroxilo por las IgE específicas.

La estrategia sintética empleada para la síntesis de los potenciales determinantes antigénicos con estructura cíclica de cefaclor y cefadroxilo fue Ugi/Desprotección/Ciclación (UDC), cuyo esquema se muestra en la Figura R.8. En primer lugar, se llevó a cabo la reacción multicomponente de Ugi (U-4CR), en la que se emplean simultáneamente un aldehído o cetona, un isocianuro, una amina y un ácido carboxílico para dar lugar a una bisamida (aducto de Ugi). Hay que destacar que, para el diseño de las estructuras finales (**V**), los productos de partida se eligieron de tal forma que permitiese tener en el aducto de Ugi el aldehído y los grupos amino adecuadamente protegidos. En segundo lugar, la eliminación de los grupos protectores y aromatización,

dio lugar a las estructuras tipo pirazinona deseadas. El método empleado es bastante eficiente puesto que la molécula objetivo se consigue tras sólo dos pasos sintéticos y una etapa de purificación. Además, todos los productos de partida son comerciales.

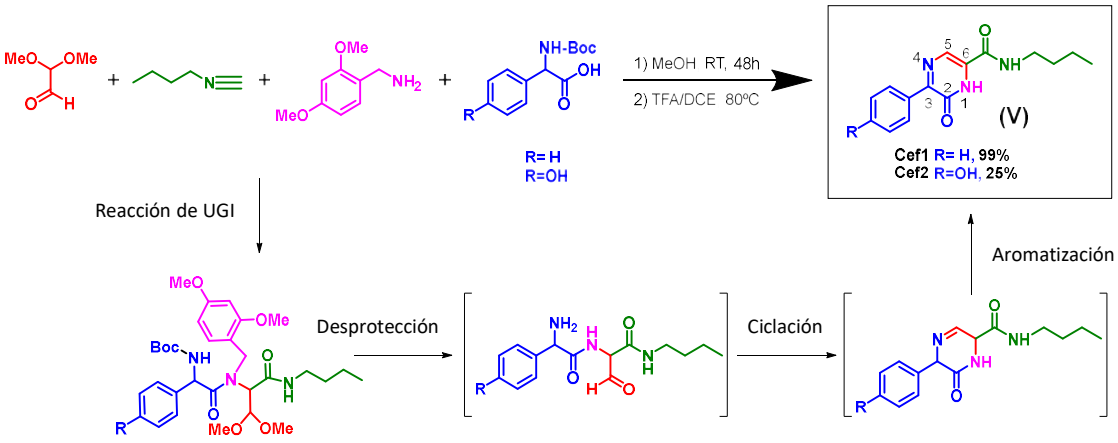

Figura R.8. Esquema sintético de las estructuras tipo pirazinona (**V**) para cefaclor y cefadroxilo, mediante la estrategia UDC.

Se evaluó el reconocimiento inmunológico de estas nuevas estructuras tipo pirazinona (**V**), junto con los determinantes sintéticos anteriormente descritos (**II**) y los conjugados monoméricos con butilamina mediante inhibición del RAST empleando suero de pacientes alérgicos a betalactamas. El ensayo consiste en una competición entre el reconocimiento de la IgE por la fase sólida (poli-L-lisina-betalactámico) *vs* los inhibidores en fase fluída. De esta manera se comparó el reconocimiento de las estructuras sintéticas perfectamente definidas (**II** y **V**) y la mezcla de compuestos resultante de la conjugación cefalosporina-butilamina.

La evaluación inmunológica de las estructuras derivadas de cefaclor (**Cef1**, **Cef3** y **Cef5**) se realizó a dos concentraciones (de 100 y 10 mM) con 8 sueros de pacientes alérgicos a cefaclor. Los resultados de inhibición de RAST se muestran en la Figura R.9.

En la mayoría de los casos, para la mayor concentración de inhibidor (100 mM), el porcentaje de inhibición obtenido para la pirazinona **Cef1** fue mayor que para la estructura **Cef3**, indicando un mayor reconocimiento de la estructura cíclica. Asimismo, importantes diferencias fueron encontradas al evaluar la positividad (cuando el porcentaje de inhibición es mayor del 50%), puesto que el 63% de los pacientes alérgicos a cefaclor reconocieron la estructura **Cef1** mientras que solo el 12% reconocieron la estructura **Cef3**. En cuanto a cefaclor-butilamina (**Cef5**), sólo en dos pacientes (casos 5 y 8) el reconocimiento fue mayor que para las estructuras sintéticas **Cef1** y **Cef3**, lo que está de acuerdo con el hecho de que cefaclor-butilamina (**Cef5**) puede contener todos

los tipos de estructuras de degradación posibles pero en una baja concentración de cada una, aumentando el uso de los nuevos determinantes sintéticos la sensibilidad del ensayo.

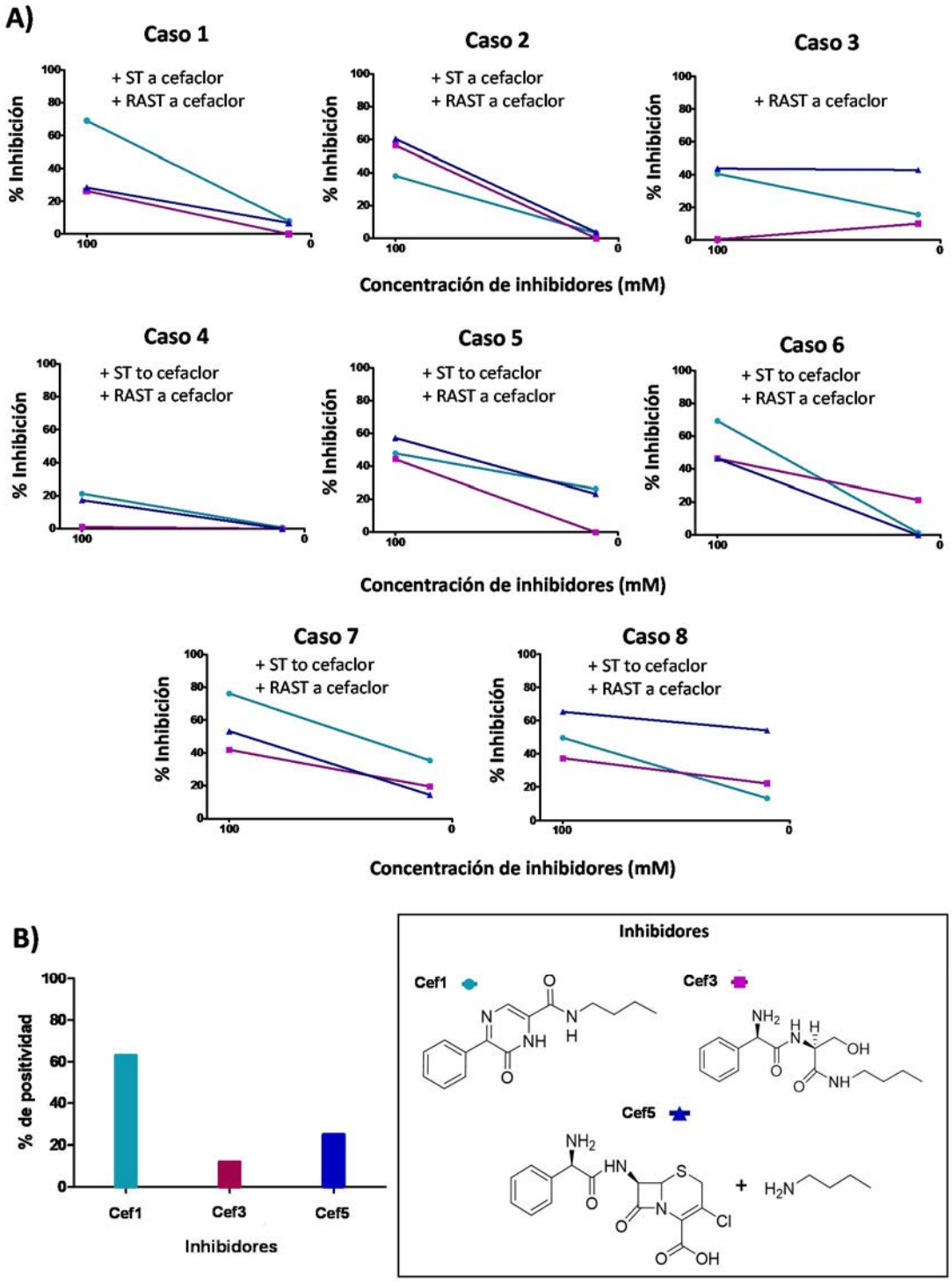

Figura R.9. Resultados de inhibición del RAST utilizando como fase sólida poli-L-lisina-cefaclor y como inhibidores estructuras derivadas de cefaclor (A) y comparación de la positividad obtenida para cada inhibidor (B).

Puesto que amoxicilina y cefadroxilo comparten la misma cadena lateral R^1, el reconocimiento de los epítopes sintéticos propuestos para cefadroxilo (**Cef2** y **Cef4**) se evaluó en nueve pacientes alérgicos a amoxicilina (Figura R.10) para estudiar la reactividad cruzada con penicilinas.

Como resultado, la mayoría de los sueros mostraron el mismo reconocimiento por la IgE específica de los pacientes de ambas estructuras **Cef2** y **Cef4** (Figura R.10A). De hecho, se observó un reconocimiento positivo (% inhibición del RAST >50%) similar para **Cef2** y **Cef4** (reactividad cruzada *in vitro*) en el 44% de los pacientes alérgicos a amoxicilina (casos 10, 12, 13 y 17). También se obtuvieron los mismos valores de positividad para **Cef2** y **Cef4** (Figura R.10B), reconociendo cada determinante antigénico derivado de cefadroxilo un 56% de los pacientes. Teniendo en cuenta que el fármaco responsible de la respuesta alérgica es amoxicilina, estos resultados pueden ser de ayuda para la elucidación del determinante antigénico implicado en la alergia a cefadroxilo, además de para el studio de la reactividad cruzada entre penicilinas y cefalosporinas.

También, hay que destacar el hecho de que los resultados de inhibición con las estructuras sintéticas concuerdan con los resultados de las pruebas *in vivo*, puesto que la inhibición fue positiva en todos los casos que presentaron skin test positivo a cefadroxilo (casos 9, 10, 11 y 13), bien con una de las estructuras (inhibición positiva con **Cef2** en caso 9 y con **Cef4** en caso 11) o con las dos (inhibición positiva con **Cef2** y **Cef4** en casos 10 y 13). Además, en tres de estos cuatro casos con inhibición del RAST y skin test a cefadroxilo positivos, los resultados de RAST directo utilizando poli-L-lisina-cefadroxilo en la fase sólida habían sido negativos, lo que confirma la aplicación potencial de las estructuras sintéticas para la mejora de la sensibilidad de los tests *in vitro* dirigidos a estudiar la reactividad cruzada amoxicilina/cefadroxilo.

El hecho de que cefadroxilo-butilamina (**Cef6**) fuese reconocido mejor que las estructuras sintéticas **Cef2** y **Cef4** en la mayoría de los casos estaría de acuerdo con el hecho de que otros determinantes antigénicos podrían estar también implicados en el desarrollo de la respuesta alérgica.

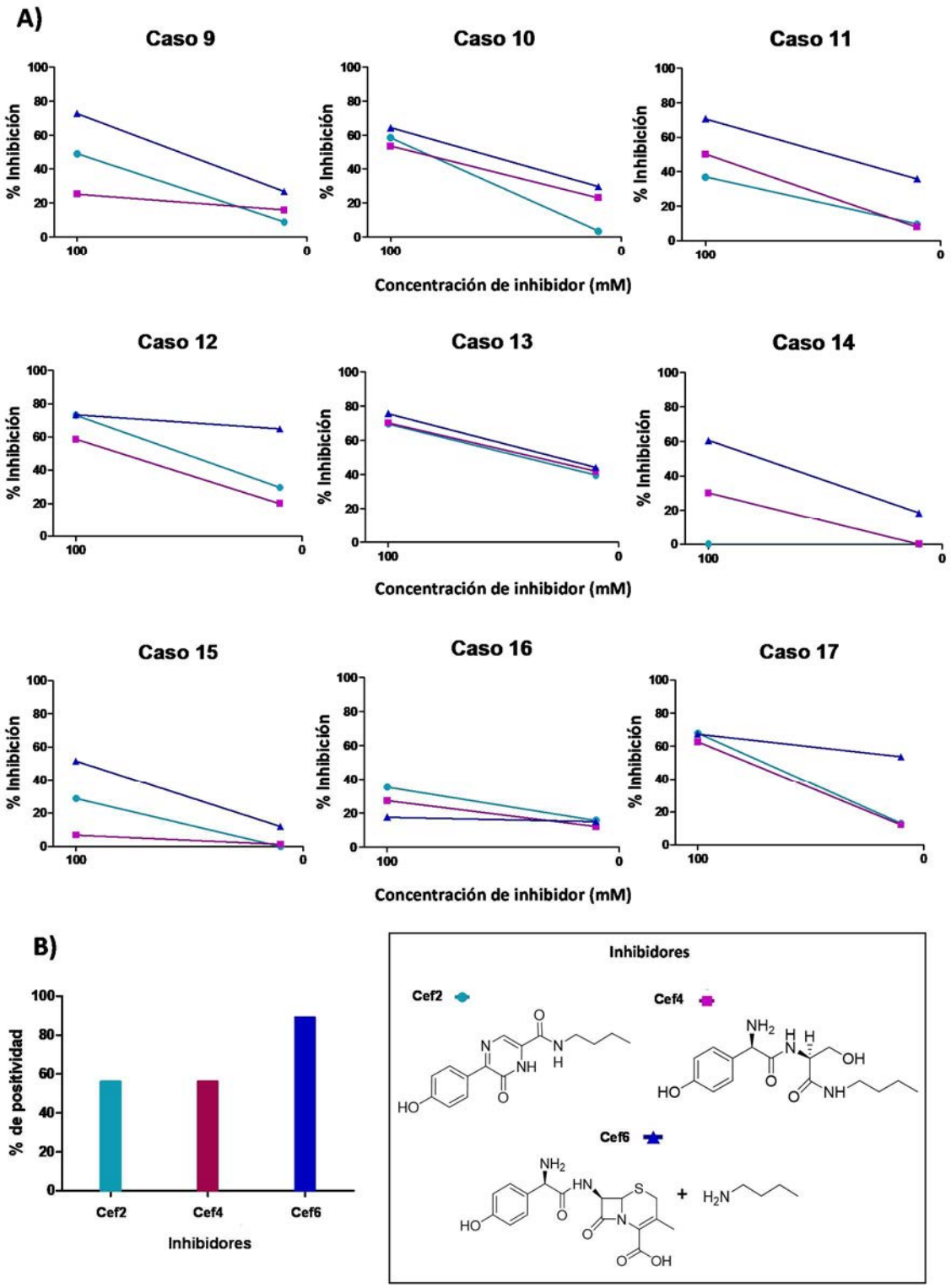

Figura R.10. Resultados de inhibición del RAST utilizando como fase sólida poli-L-lisina-amoxicilina y como inhibidores estructuras derivadas de cefadroxilo (A) y comparación de la positividad obtenida para cada inhibidor (B).

Como resumen, se han sintetizado nuevos determinantes de α-aminocefalosporinas de estructura cíclica (**Cef1** y **Cef2**) que son reconocidos por la IgE específica de pacientes

alérgicos a antibióticos betalactámicos. El anclaje de estas estructuras a fase sólida podría incrementar la sensibilidad de los inmunoensayos. Además, las estructuras sintetizadas pueden ser de uso en el diagnóstico de alergia a cefalosporinas que comparten la misma cadena lateral R^1 como cefprozilo, con la misma R^1 que cefadroxilo, o cefalexina y cefaloglicina, con la misma R^1 que cefaclor.

II. Elucidación de la Estructura de Determinantes Antigénicos del Ácido Clavulánico

Los nuevos hábitos de prescripción están modificando los patrones alérgicos de especificidad debido a la aparición de nuevos determinantes antigénicos, fenómeno que en la actualidad está ocurriendo en muchos países con la combinación amoxicilina-ácido clavulánico. El desconocimiento de la estructura del determinante antigénico del ácido clavulánico conduce a un diagnóstico incompleto cuando esta combinación está implicada en las reacciones alérgicas. Se ha descrito que el ácido clavulánico puede generar productos estables de una estructura intermedia resultante de la apertura de los anillos de β-lactama y de oxazolidina (Figura R.11), a través de un mecanismo similar a la formación de aductos con betalactamasas. Estas estructuras derivadas podrían estar implicadas en el reconocimiento molecular de la IgE en reacciones selectivas, aunque para llegar a ciertas conclusiones sería necesario profundizar con estudios que impliquen el empleo de estructuras bien definidas, lo que incluimos como hipótesis de trabajo.

Los dos determinantes antigénicos principales propuestos para ácido clavulánico, **AD-I** (compuesto 1,3-dicarbonílico) y **AD-II** (compuesto monocarbonílico), son estructuras de bajo peso molecular con sólo tres átomos de carbono. Mientras que **AD-I** puede ser reactivo frente a proteínas debido al aldehído que comprende en su estructura, la reactividad de **AD-II** es limitada. Hay que destacar que el resto de estructuras intermedias también pueden ser determinantes antigénicos responsables de la alergia a ácido clavulánico. El análisis del reconocimiento molecular por IgE específicas de estructuras sintéticas bien definidas derivadas de ácido clavulánico daría información de los grupos químicos responsables del desarrollo de la respuesta alérgica y la identificación de los determinantes antigénicos más relevantes podría ayudar a mejorar los procedimientos diagnósticos actuales.

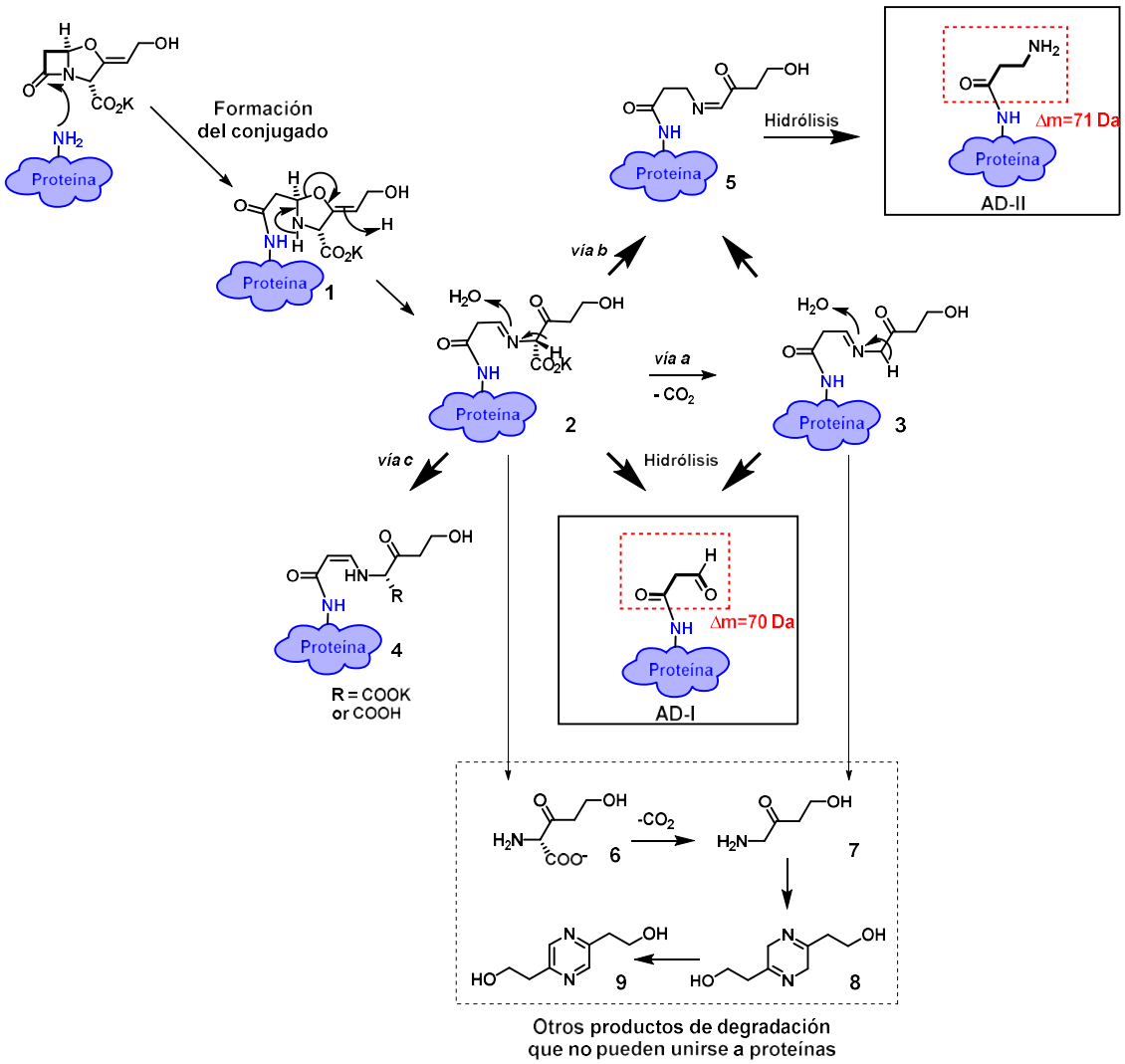

Figura R.11. Mecanismo de reacción propuesto para la unión covalente de ácido clavulánico a proteínas y diferentes vías de degradación que pueden dar lugar a diferentes posibles determinantes antigénicos.

En este trabajo, abordamos también mediante una aproximación sintética la evaluación del reconocimiento inmunológico de distintas estructuras derivadas de **AD-I** y **AD-II**.

Como primera aproximación, análogos sintéticos de **AD-I** y **AD-II** así como la molécula completa de ácido clavulánico, tanto cerrada como con el anillo β-lactámico abierto, fueron ancladas a diferentes superficies sólidas (celulosa y nanopartículas de sílice) y se sometieron a evaluación inmunológica mediante RAST utilizando sueros de pacientes alérgicos selectivos a ácido clavulánico. Los resultados no fueron satisfactorios, poniéndose de esta forma de manifiesto la dificultad para la evaluación de la inmunogenicidad de los derivados de ácido clavulánico, quizá debida a su pequeño tamaño.

Como segunda aproximación, seis análogos sintéticos, cuya estructura se representa en la Figura R.12, fueron sintetizados, purificados y caracterizados para su posterior evaluación inmunológica mediante BAT.

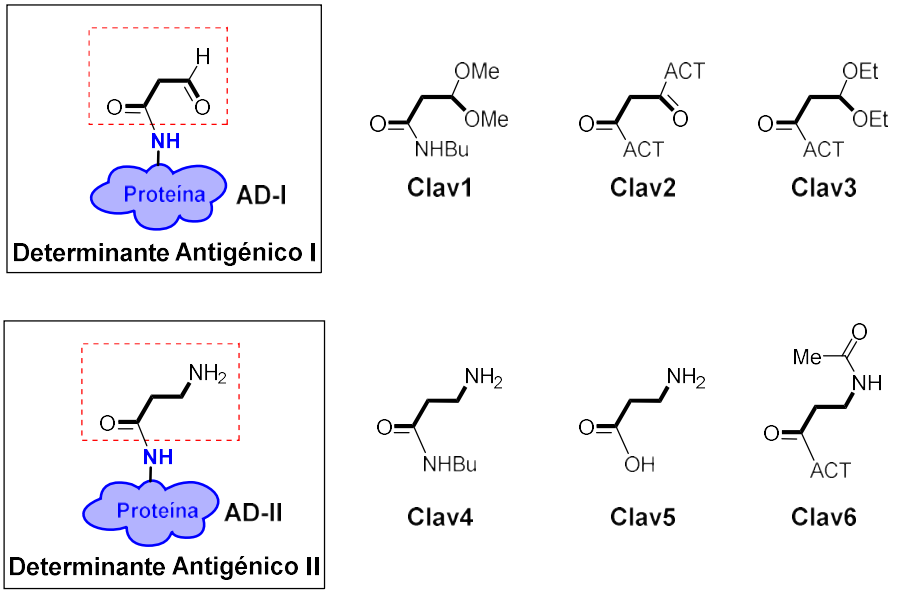

Figura R.12. Determinantes sintéticos correspondientes a **AD-I** (**Clav1**-Clav3) y **AD-II** (**Clav4**-**Clav6**).

Todos los análogos sintéticos de ácido clavulánico y el mismo ácido clavulánico fueron evaluados en 29 pacientes con alergia selectiva a ácido clavulánico y 25 controles con tolerancia confirmada a amoxicilina-ácido clavulánico. La concentración óptima para el estudio de la activación de basófilos se seleccionó tras la elaboración de curvas dosis-respuesta y resultó ser de 8 mM para ácido clavulánico, **Clav2** y **Clav3**, mientras que el resto de estructuras sintéticas no mostraron diferencia significativa entre pacientes y controles.

El mecanismo IgE mediado se confirmó mediante la inhibición de los basófilos con Wortmanina, inhibidor de unas enzimas parte del proceso de señalización, puesto que en todos los casos este tratamiento redujo notablemente el porcentaje de expresión de CD63 comparado con el ensayo sin Wortmanina.

Se observó que de los pacientes con BAT positivo a ácido clavulánico, el 75% era también positivo a **Clav2** y el 33,3% a **Clav3**. Algo más interesante, es el hecho de que en los casos con BAT negativo a ácido clavulánico, el 47.1% presentó resultados positivos con **Clav2** y el 23.5% con **Clav3** (Figura R.13A). El porcentaje de pacientes con BAT positivo aumentó notablemente cuando se combinaron los resultados obtenidos con ácidco clavulánico y **Clav2** comparado con ácido clavulánico solo pero no aumentó

al incluir también **Clav3** (Figura R.13B).

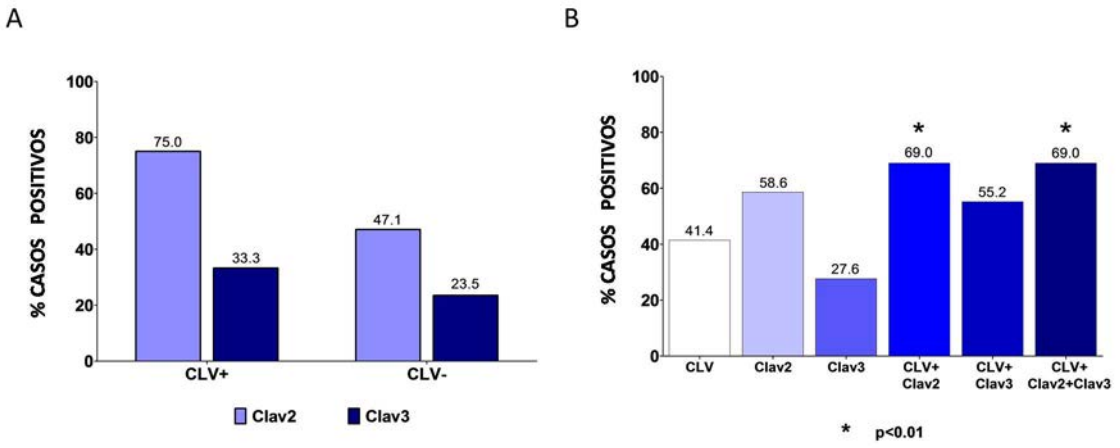

Figura R.13. Resultados de BAT positivo en pacientes alérgicos. **A**, Comparación del porcentaje de resultados de BAT positivo para **Clav2** y **Clav3** en casos de BAT positivo o negativo a ácido clavulánico. **B**, Comparación del porcentaje de positividad de BAT combinando los resultados con ácido clavulánico, **Clav2** o **Clav3**. Diferencias significativas se indicant en la gráfica (* p<0.01).

Por otro lado, puesto que la unión de antibióticos betalactámicos a proteínas juega un papel importante en el desarrollo de alergia, en primer lugar nos propusimos el estudio de la haptenización *in vitro* por ácido clavulánico, tomando la HSA como proteína modelo. El análisis mediante MALDI-TOF de los conjugados preparados (relación molar proteína/fármaco de 1:10 a 1:320) utilizando concentraciones crecientes de ácido clavulánico, tuvo como resultado un incremento en la masa de la proteína proporcional a la concentración de fármaco utilizada en la incubación.

Para posteriores estudios, elegimos el conjugado de relación molar proteína/fármaco 1:10, por ser el más próximo a las condiciones terapéuticas. Los residuos de HSA modificados se identificaron tras la digestión del conjugado con arginina C seguida del análsis por cromatografía líquida acoplada a espectrometría de masas (LC-MS/MS) de los péptidos resultantes. La molécula de ácido clavulánico completa no se encontró pero se encontraron dos residuos de lisina (lisinas 195 y 475) con un incremento de masa de 70 Da, que concuerda con la adición de un fragmento de ácido clavulánico de masa 71 y la posterior pérdida de un átomo de hidrógeno. La reactividad de estos residuos fue confirmada mediante estudios de modelización molecular, y es determinada tanto por el entorno de los residuos como por la accesibilidad del residuo. La adición de 70 Da es compatible con nuestra hipótesis de la formación de un determinante antigénico con la estructura de **AD-I** (Figura R.11) y con los resultados obtenidos con el BAT, lo que confirmaría que el determinante antigénico derivado de

AD-I que es específicamente reconocido forma parte del conjugado HSA-ácido clavulánico.

Una vez comprobada la capacidad de haptenización de ácido clavulánico, la identificación de las proteínas séricas diana de haptenización por este betalactámico podría suponer un gran avance pero la inexistencia de anticuerpos monoclonales α-ácido clavulánico hace que este estudio no sea viable. La interacción avidina-biotina es de gran afinidad y sensibilidad y permite la combinación de la modificación de proteínas con compuestos biotinilados con métodos de detección, purificación e imagen. Por ello, nos propusimos la síntesis de un derivado biotinilado de ácido clavulánico para su uso en la detección de aductos con proteínas séricas.

En primer lugar, se sintetizó un derivado biotinilado de ácido clavulánico que comprende la introducción de espaciador de tetraetilenglicol (TEG) entre ácido clavulánico y la biotina mediante un proceso sintético de dos pasos (Figura R.14) que permitió la obtención del derivado **CLV-TEG-B** con un rendimiento medio del 62%. El espaciador hidrofílico proporciona solubilidad en agua así como flexibilidad y espacio que permite a la biotina estar más accessible para su interacción con la estreptavidina y por tanto, más eficiencia en la detección.

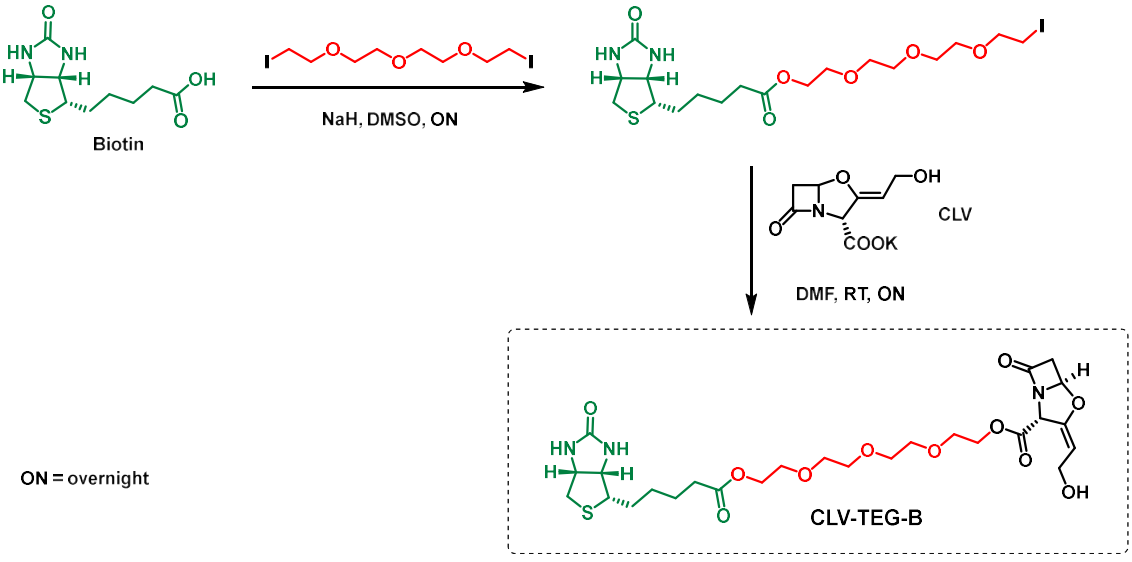

Figura R.14. Síntesis del derivado biotinilado **CLV-TEG-B**.

Tras la comprobación mediante RMN de la capacidad de reacción con nucleófilos de **CLV-TEG-B**, el siguiente paso fue el estudio de su capacidad de haptenización *in vitro* de la HSA. Se prepararon conjugados HSA-CLV-TEG-B utilizando varias relaciones molares proteína/betalactámico y tras su separación mediante SDS-PAGE se transfirieron a una

membrana de polifluoruro de vinilideno (PVDF) y se detectaron utilizando estreptavidina-peroxidasa de rábano(HRP) y reactivo de ECL (Figura R.15).

Se observó no sólo que la modificación era concentración-dependiente, sino la alta sensibilidad de la detección, puesto que incluso el conjugado preparado con una baja concentración de **CLV-TEG-B** es visible tras la detección.

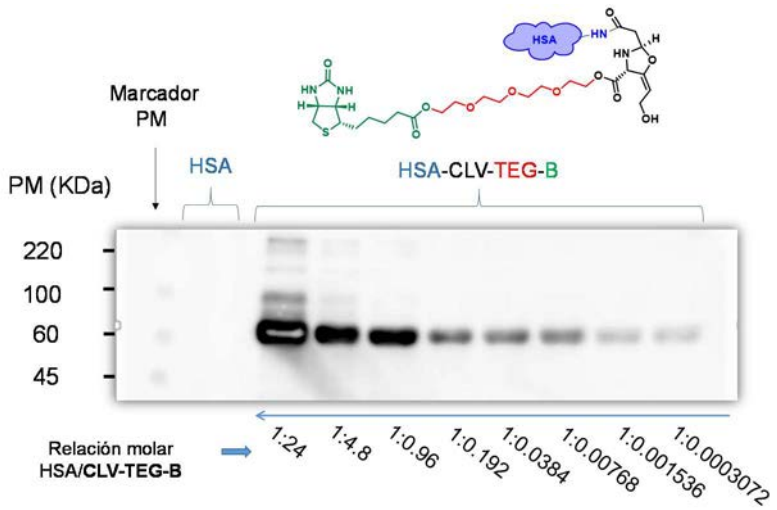

Figura R.15. Detección con estreptavidina-HRP de HSA modificada utilizando diferentes relaciones molares HSA/**CLV-TEG-B**. En cada calle, se sembraron 2 µg de conjugado.

El siguiente experimento, fue diseñado para comparar el comportamiento de haptenización de ácido clavulánico y **CLV-TEG-B** e intentar entender el mecanismo implicado. En un ensayo competitivo, se incubó HSA durante dos horas con **CLV-TEG-B** 80 mM tras la preincubación durante 16 horas con diferentes concentraciones de ácido clavulánico *per se* (de 0 a 10X) y los conjugados resultantes se purificaron mediante dodecil sulfato sódico-electroforesis en gel de poliacrilamida (SDS-PAGE), se transfirieron a una membrana de PVDF y se realizó la detección con SDS-PAGE y reactivo de ECL. Los resultados (Figura R.16) indican que la incubación de HSA en presencia de un exceso de ácido clavulánico, reduce la formación de aductos con **CLV-TEG-B**, lo que significa que ambos compuestos compiten por su unión a HSA y sugiere que pueden unirse a los mismos sitios de unión de la proteína.

Para estudiar la haptenización de proteínas séricas por **CLV-TEG-B**, suero humano fue conjugado usando dos concentraciones del derivado biotinilado y alícuotas de 4 µg de la incubación se purificaron mediante SDS-PAGE junto con un control de HSA, transferidas y detectadas con estreptavidina-HRP y reactivo de ECL (Figura R.17). La

detección de proteína total con Coomassie confirma que la diferencia de intensidad observada en las bandas en el revelado con estreptavidina-HRP es debido únicamente a la biotinilación y el hecho de que no se observe banda para el control de HSA confirma la especificidad de la detección.

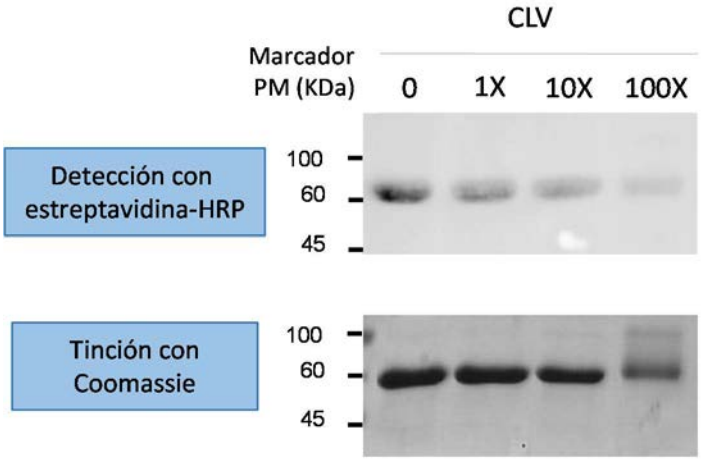

Figura R.16. Resultados de los ensayos de competición entre ácido clavulánico y **CLV-TEG-B**.

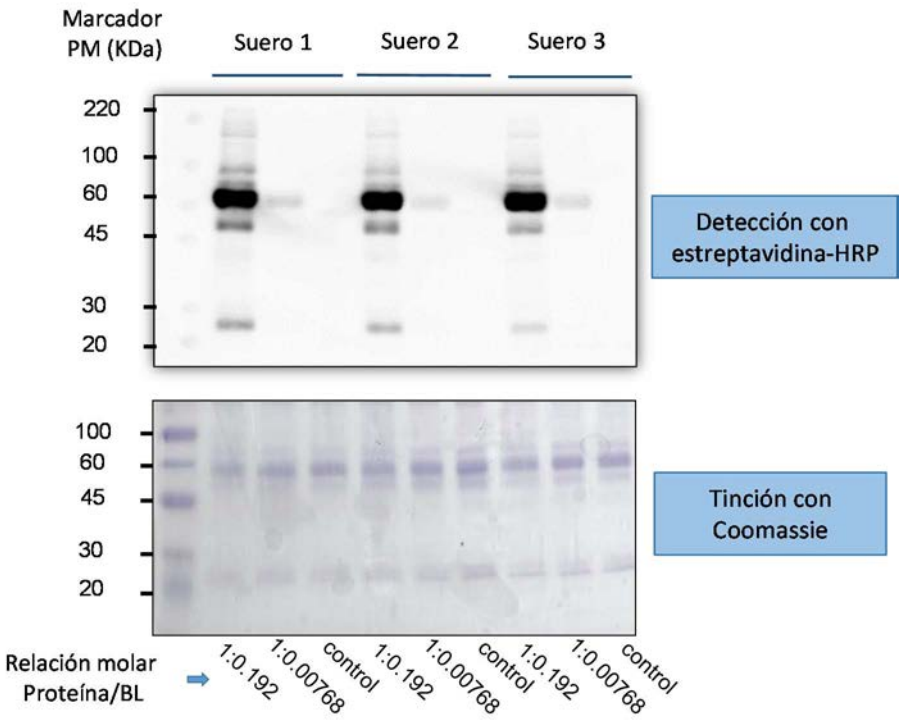

Figura R.17. Detección de proteínas séricas biotiniladas (arriba) y patron de proteínas totales con tinción de Coomassie (abajo).

Con este ensayo queda demostrado que **CLV-TEG-B** se une covalentemente a varias proteínas séricas pero para la identificación de estas proteínas se require su separación mediante 2D-SDS-PAGE y su análisis por huella peptídica. La Figura R.18 muestra el análisis mediante 2D-SDS-PAGE de un suero control y de un suero modificado con **CLV-TEG-B** a una relación molar proteína/ **CLV-TEG-B** 1:0.192 tras su transferencia y detección con estreptavidina-HRP, a la izquierda, y el patrón de proteínas totales en el suero modificado y los puntos de interés elegidos, a la derecha. Los puntos de interés señalados fueron recortados del gel, digeridos con tripsina y analizados mediante huella peptídica utilizando espectrometría de masas de desorción/ionización láser asistida por matriz-tiempo de vuelo (MALDI-TOF-TOF MS) (Tabla R.1).

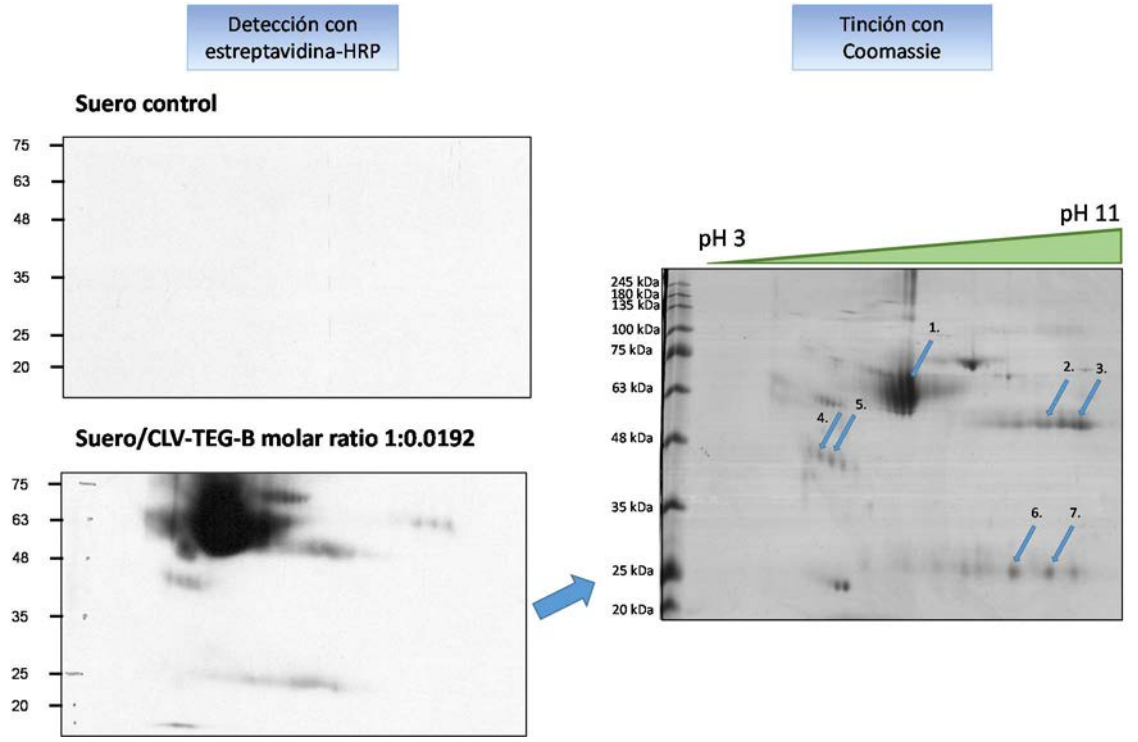

Figura R.18. Análisis de las proteínas séricas diana de haptenización por **CLV-TEG-B** mediante 2D-SDS-PAGE.

Las proteínas séricas modificadas por **CLV-TEG-B** identificadas en este experimento fueron HSA, haptoglobina y las cadenas ligeras y pesadas de las inmunoglobulinas (Ig). Aunque la inexistencia de un anticuerpo monoclonal α-ácido clavulánico impide comprobar si estas mismas proteínas son haptenizadas por ácido clavulánico *per se*, nuestra aproximación da información sobre el proceso de haptenización mediante el uso de un método de detección de alta sensibilidad.

Tabla R.1. Resultado de la identificación por huella peptídica mediante digestion tríptica y analisis por MADI-TOF-TOF de las proteínas séricas modificadas por **CLV-TEG-B**.

Spot	Número de acceso	Nombre de la proteína	Puntuación total	Puntuación límite	Peso molecular (Da)	pI	Péptidos emparejados	Cobertura (%)
1	P02768	HSA	470	56	71317	5.92	43	69
2	P01857	Ig gamma-1 chain C region human	119	56	36596	8.46	13	52
3	P01857	Ig gamma-1 chain C region human	197	56	36596	8.46	18	66
4	P00738	Haptoglobin human	128	56	45861	6.13	18	35
5	P00738	Haptoglobin human	102	56	45861	6.13	16	33
6	P01834	Ig kappa chain C region human	86	56	11773	5.58	7	76
7	P01834	Ig kappa chain C region human	66	56	11773	5.58	6	76

Para la elucidación de la estructura derivada de **CLV-TEG-B** que queda unida a la proteína tras la conjugación, como primera aproximación se incubó el péptido $^{182\text{-}195}$HSA de secuencia LDELRDEGKASSAK con un exceso molar del derivado biotinilado y tras su purificación por cromatografía de exclusión, se añalizó por MALDI-TOF tanto el péptido modificado como el péptido control sin incubar. Al analizar los resultados (Figura R.19) se observó un pico que pertenecía al péptido sin conjugar (1518.686 Da) y un pico muy bajo (2118.898 Da) correspondiente al péptido modificado con un incremento de masa de 600.2 Da.

Como segunda aproximación, para caracterizar la estructura que queda unida a la HSA completa se preparó el conjugado HSA-CLV-TEG-B 1:10 y se analizó mediante LC-MS/MS tras digestion enzimática del conjugado formado. Su análisis resultó complicado, no obteniéndose péptidos modificados cuando se utilizó el modo de fragmentación CID. Además del modo de fragmentación, la baja proporción de conjugación observada en el experimento anterior (Figura R.19) puede ser la causa de la dificultad encontrada en el análisis. Al utilizar disociación por transferencia de electrones (ETD) como modo de fragmentación, método más suave que conserva modificaciones postraduccionales, se encontró el péptido 404-430HSA, de secuencia QNALLVRYTKKVPQVSTPTLVEVSRNL, modificado con una masa de 600.22 Da, que coincide con el incremento de masa encontrado para tras el análisis por MALDI-TOF del péptido utilizado como primera aproximación.

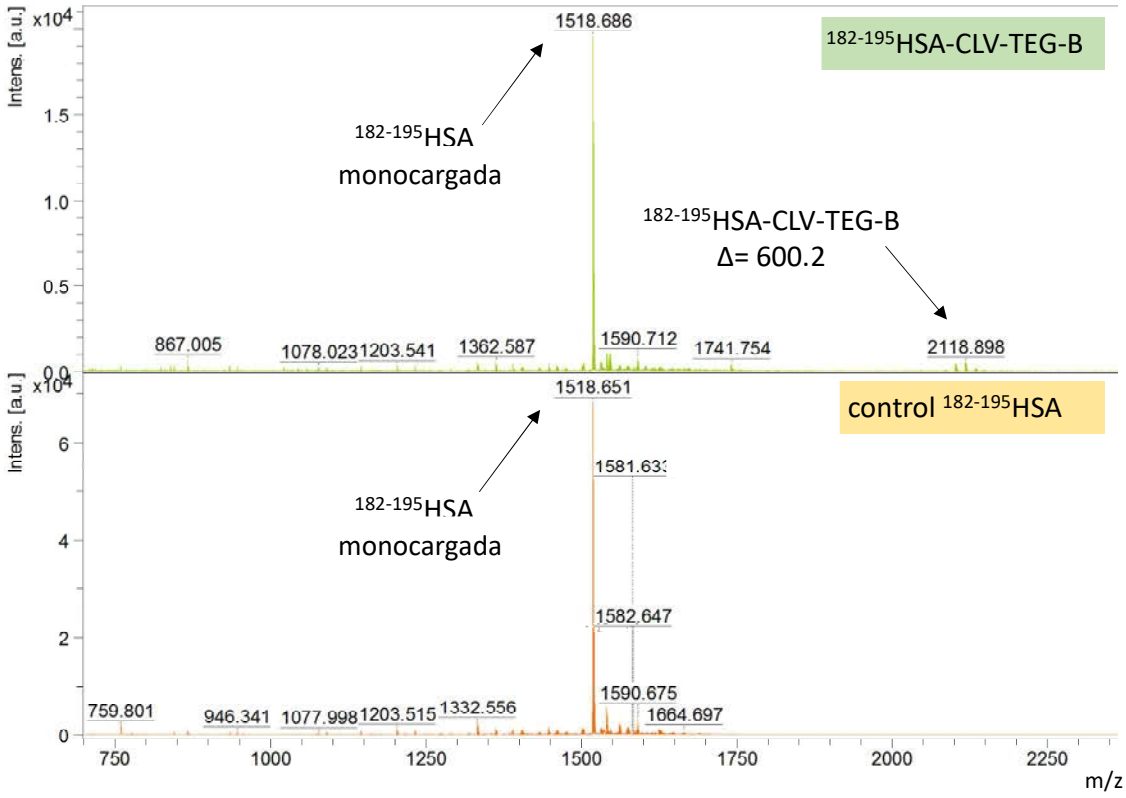

Figura R.19. MALDI-TOF MS análisis de $^{182-195}$HSA tras su conjugación con **CLV-TEG-B** (arriba) y sin conjugar (abajo).

III. Marcaje de Anticuerpos Secundarios para la Detección de IgE Específica en Alergia a Fármacos

La sensibilidad y especificidad de la detección de sIgE deben estar aseguradas en los inmunoensayos empleados el diagnóstico *in vitro* de alergia a fármacos. Para ello, se require el marcaje de los anticuerpos secundarios empleados en los ensayos con radioisótopos, luminóforos o fluorescentes. El empleo de anticuerpos marcados con radioisótopos sigue siendo necesario para la detección de sIgE en alergia a fármacos puesto que el RAST es el único ensayo disponible en muchos casos. El marcaje con fluorescescencia, puede ser una buena alternativa a los radioisótopos pero sería necesaria la amplificación de la señal para obtener la sensibilidad requerida para la detección de sIgE en alergia a fármacos.

Este capítulo está dedicado a la optimización de métodos de marcaje de anticuerpos secundarios para su utilización en los test *in vitro* empleados en el diagnóstico de alergia a fármacos. Por un lado, se ha optimizado el marcaje radiactivo de un anticuerpo α-human IgE altamente específico para su utilización en RAST caseros. Por otro lado, se ha diseñado, sintetizado y caracterizado una serie de dendrones fluorescentes con una o

varias moléculas de fluorescente y se ha probado su adecuación para el marcaje específico de anticuerpos secundarios para su futuro uso en plataformas de microarray.

Para el marcaje del anticuerpo con I^{125} en condiciones acuosas se utilizaron tubos con IodoGen como reactivo de yodación. En primer lugar, se optimizó la cantidad de NaI^{125} para la que se obtenía un mayor marcaje utilizando un anticuerpo de prueba y, una vez optimizada (250 µCi), se repitió el protocolo para marcar el anticuerpo altamente específico. La concentración y actividad por volumen finales del anticuerpo específico marcado fueron 0.15µg/mL 1.57 µCi/mL, incluso mayor que para un anticuerpo comercializado por Phadia hace años (1.06 µCi/mL).

La eficacia del marcaje se comprobó mediante la comparación de los resultados de RAST obtenidos para sueros de pacientes alérgicos a amoxicilina y controles previamente analizados utilizando diferentes anticuerpos radiactivos, obteniéndose mejores resultados con el anticuerpo marcado con nuestro protocolo optimizado (Figura R.20).

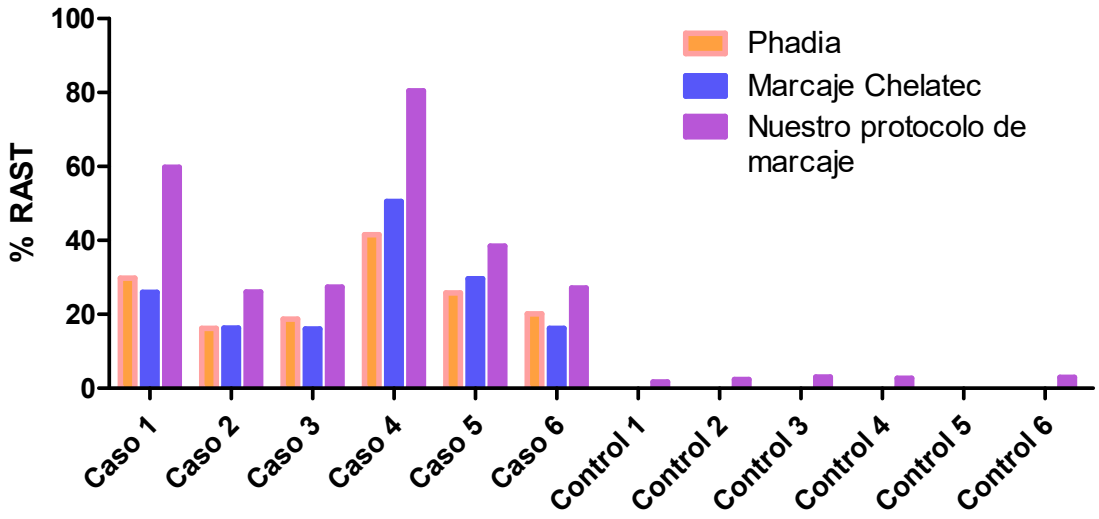

Figura R.20. Comparación de resultados de RAST obtenidos con diferentes marcajes radiactivos.

Los dendrones son moléculas monodispersas con forma de cuña que poseen varios grupos funcionales terminales y un único grupo funcional en el punto focal, por lo que pueden ser de utilidad para el marcaje selectivo de anticuerpos. Los fluoróforos tipo cianina son de los más prometedores en la región del infrarrojo cercano, ideales para imagen tanto *in vivo* como *in vitro*. Entre ellos, Cy5 parece ser el mejor, puesto que su longitud de onda de absorción superior a 600 nm reduce la interferencia por autofluorescencia de las células, si se compara con otros fluoróforos de ese espectro. Además, los escáneres de microarray presentan la posibilidad de detección de Cy5.

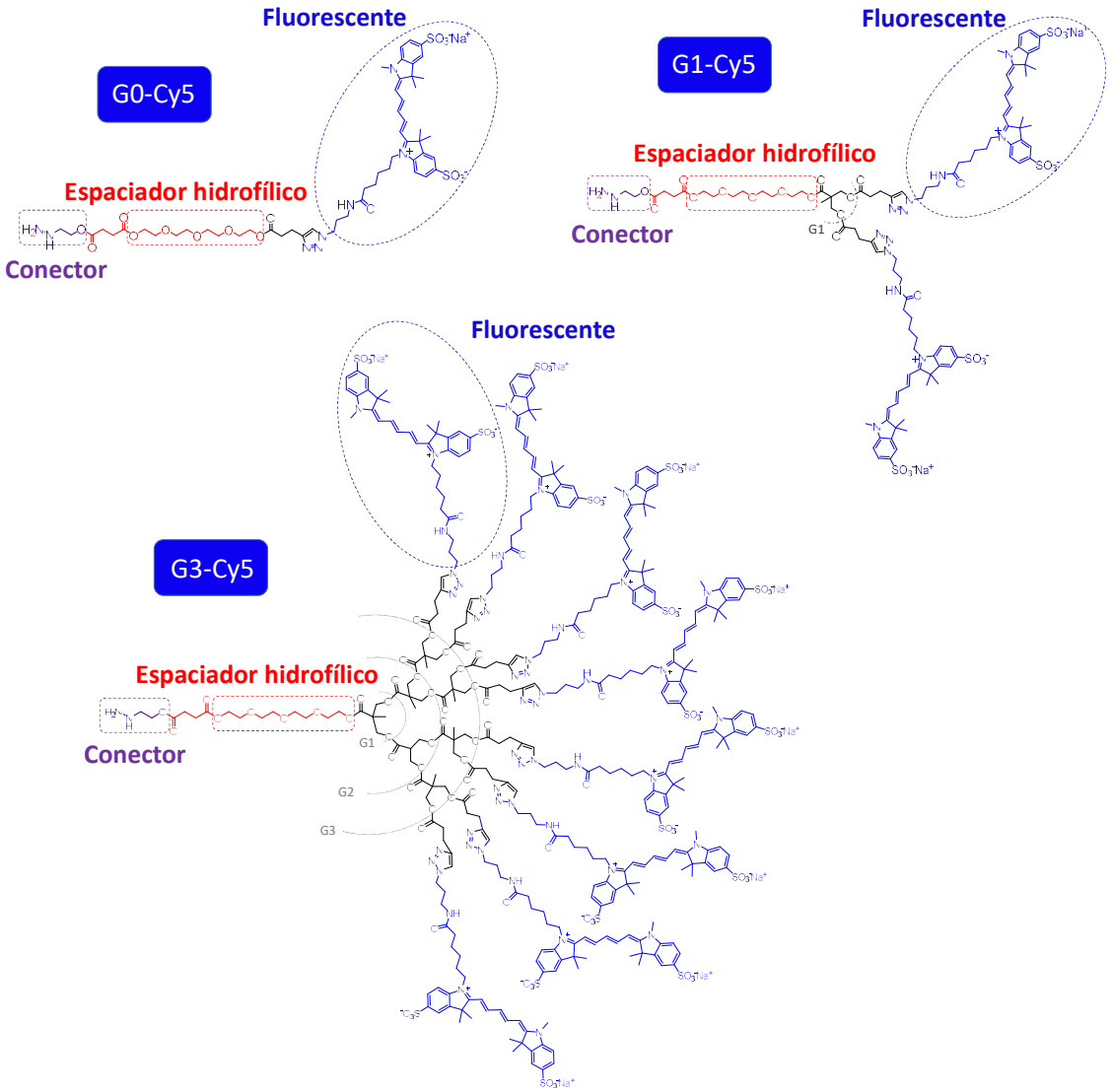

Figura R.21. Sondas mono o multivalentes con un grupo hidracina como conector para bioconjugación, un espaciador hidrofílico tipo tetraetilenglicol y una o varias unidades fluorescentes.

En este trabajo presentamos la síntesis de una serie de nuevas sondas que presentan funcionalidad hidracina en el punto focal y una o varias unidades fluorescentes en la periferia (Figura R.21). La multivalencia viene dada por la incorporación de dendrones basados en el monómero bis-MPA a la estructura.

Los dendrones **G0-Cy5**, **G1-Cy5** y **G3-Cy5** fueron sintetizados y posteriormente utilizados para la bioconjugación a un anticuerpo. En primer lugar, los precursores se diseñaron para albergar las funcionalizaciones ortogonales adecuadas: hidracina protegida en el punto focal y funcionalización alquino en la periferia para posterior funcionalización con el fluorerscente mediante química click. El esquema sintético completo se muestra en el Esquema R.1.

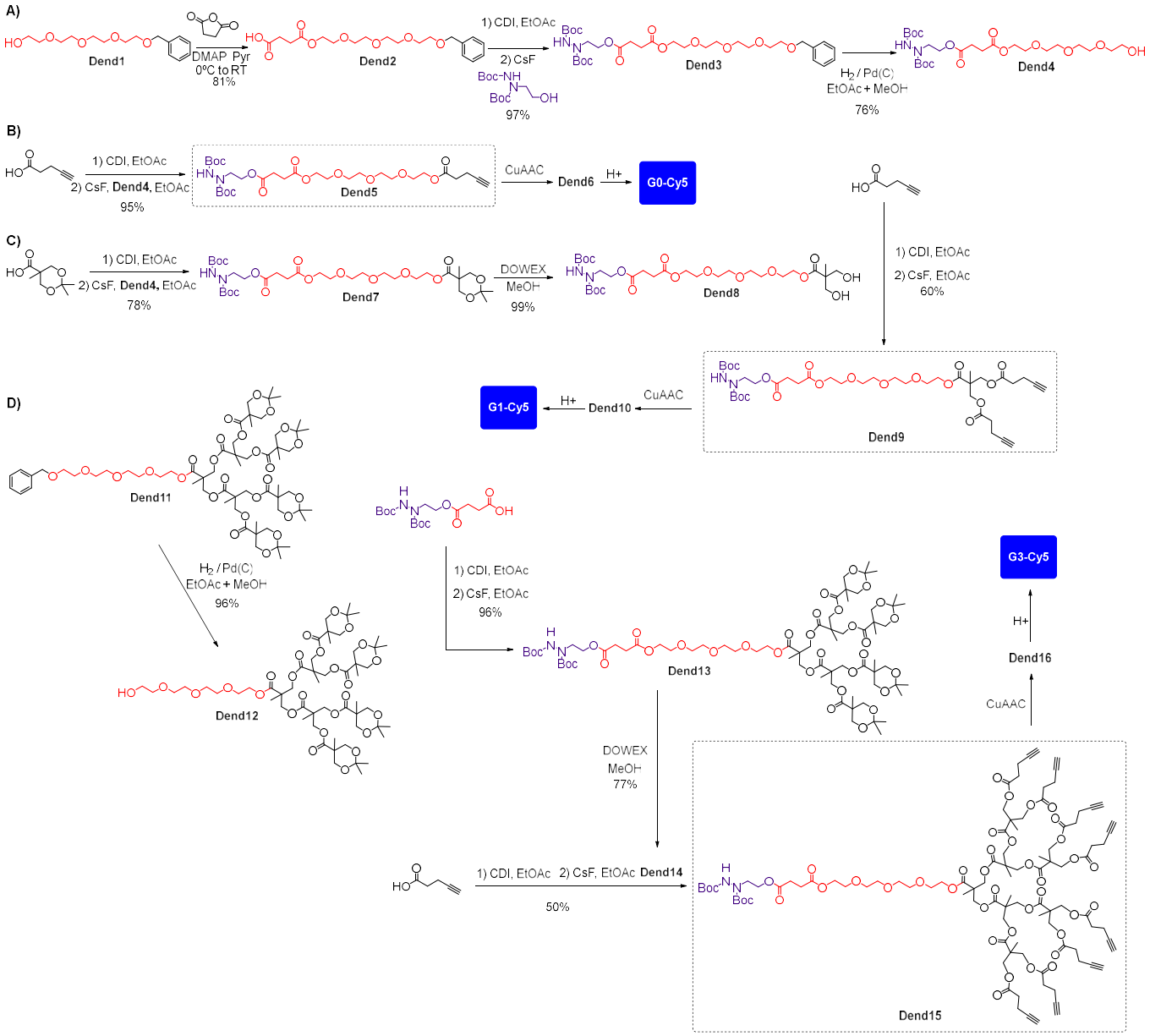

Esquema R.1. Síntesis de los dendrones fluorescentes. A) Síntesis del espaciador basada en la derivatización de una cadena de tetraetilenglicol con una molécula que contiene hidracina diprotegida con Boc. B) Síntesis de **G0-Cy5**, con una unidad fluorescente. C) Síntesis del dendrón **G1-Cy5**, con dos unidades fluorescentes. D) Síntesis del dendrón **G3-Cy5**, con ocho moléculas fluorescentes.

Las molécuas fueron caracterizadas mediante ^{1}H y ^{13}C-RMN y MALDI-TOF, y **G0-Cy5**, **G1-Cy5** y **G3-Cy5** se caracterizaron además mediante espectroscopía UV-Vis y de fluorescencia (Figura R.22).

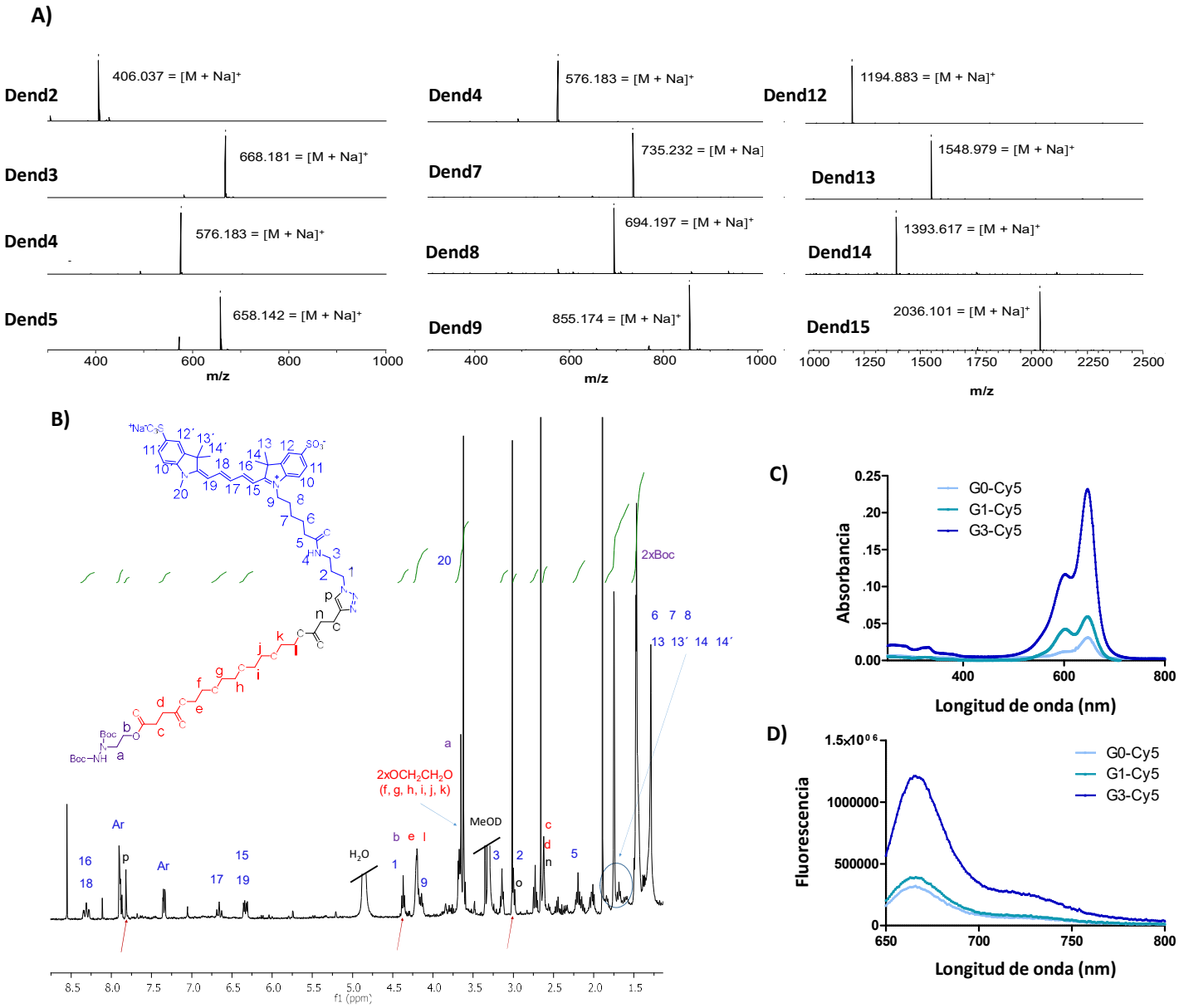

Figura R.22. Caracterización de los dendrones. A) De derecha a izquierda, monitorización mediante MALDI-TOF de la síntesis de los dendrones con funcionalización alquino en la periferia. B) Caracterización mediante ^{1}H-RMN de **G0-Cy5**. C) Espectroscopía UV-visible de los dendrones **G0-Cy5**, **G1-Cy5** and **G3-Cy5**. D) Emisión de fluorescencia de los dendrones **G0-Cy5**, **G1-Cy5** y **G3-Cy5**.

Una vez caracterizados las dendrones fluorescentes, se comprobó su utilidad como sondas para el marcaje de anticuerpos. La metodología usada para el marcaje está basada en el marcaje específico del anticuerpo a través de dos pasos Figura R.23: (i) oxidación suave con $NaIO_4$ de los 1,2-dioles del ácido siálico presente en las cadenas de carbohidratos ancladas en la región cristalizable (Fc) de las cadenas pesadas del anticuerpo; (ii) reacción selectiva del grupo hidracina presente en los dendrones (**G0-Cy5**, **G1-Cy5** y **G3-Cy5**) con los aldehídos generados mediante enlace hidrazona. Este

marcaje no afecta a la actividad del acticuerpo o a su reconocimiento ni provoca un mayor daño oxidativo. Tras el marcaje, los anticuerpos fueron purificados con sephadex G-25 y lavados adicionales usando filtros de diálisis para asegurar la eliminación del exceso de fluorescente.

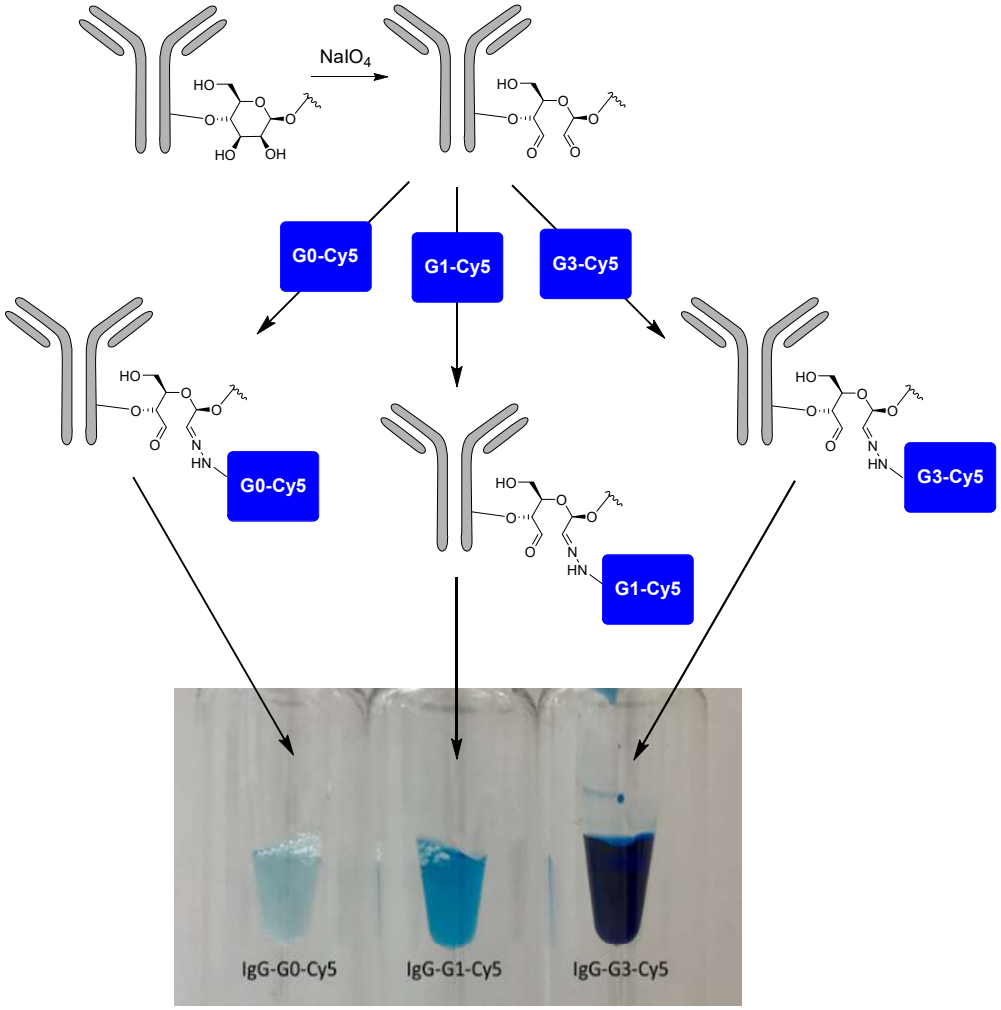

Figura R.23. Esquema del proceso empleado para el marcaje del anticuerpo. La concentración de las disoluciones del anticuerpo mostradas en la figura es de aproximadamente 8 mg/mL.

La unión covalente de las sondas fluorescentes al anticuerpo se confirmó mediante SDS-PAGE. A la derecha de la Figura R.24 se puede observar la detección fluorescente selectiva en los casos en los que el anticuerpo estaba marcado con los dendrones fluorescentes, no observándose señal para el anticuerpo sin marcar. A la izquierda de la Figura R.24, se muestra la tinción del gel con Coomassie, en la que se observa que la recuperación fue similar en los tres casos para el anticuerpo marcado tras su purificación.

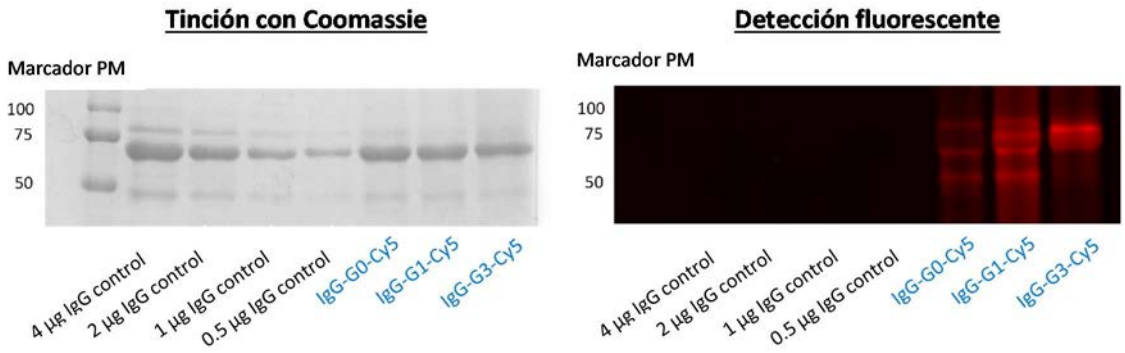

Figura R.24. Caracterización mediante SDS-PAGE del anticuerpo marcado con las sondas fluorescentes. Se cargó en el gel un marcador de peso molecular (calle 1), cuatro concentraciones decrecientes de anticuerpo sin marcar (calles 2-5) y los conjugados **IgG-G0-Cy5**, **IgG-G1-Cy5** e **IgG-G3-Cy5** (calles 6-8). Tinción con Commassie (izquierda) y detección fluorescente (derecha).

La absorbancia del anticuerpo marcado con las sondas fluorescentes presenta una banda a 646 nm cuya intensidad aumenta con el número de unidades de fluorescente. Los valores de absortividad molar (ε_{646}) fueron 49667, 274985 y 2280894 $M^{-1}\cdot cm^{-1}$ para **IgG-G0-Cy5, IgG-G1-Cy5** e **IgG-G3-Cy5**, respectivamente (Figura R.25 arriba). En el caso de **IgG-G3-Cy5** se observa una banda también a 600 nm, comportamiento previamente recogido en la literatura y debido a la formación de agregados paralelos entre moléculas de Cy5 (dímeros H) y que se reduce al añadir dodecil sulfato sódico (SDS) como se observa en la Figura R.25 abajo.

Las propiedades fluorescentes del anticuerpo marcado resultaron en una emisión fluorescencia un orden de magnitud mayor para **IgG-G1-Cy5** (ϕ= 0.25, $\varepsilon\cdot\phi$= 67891) que para **IgG-G0-Cy5** (ϕ= 0.41; $\varepsilon\cdot\phi$= 20473) como se observa en la Figura R.26 izquierda. Por el contrario, **IgG-G3-Cy5** resultó ser apenas fluorescente con un valor extremadamente bajo de rendimiento cuántico (ϕ= 0.02), lo que significaría que la mayoría de los fotones absorbidos se desactivan mediante procesos no radiativos. La caída de fluorescencia del anticuerpo marcado con respecto a la sonda fluorescente libre (**G3-Cy5**) podría ser debido a un entorno más restringido cuando se incorpora al anticuerpo, con las unidades de Cy5 probablemente más cercanas entre sí, lo que favorecería la formación de dímeros H. La adición de SDS una disolución de **IgG-G3-Cy5** tuvo como consecuencia un aumento en la fluorescencia Figura R.26 derecha, probablemente debido al desdoblamiento de la proteína en presencia del detergente. Este último argumento está en concordancia con el resultado del SDS-PAGE (en el paso de desnaturalización se utiliza SDS y β-mercaptoetanol, afectando la conformación de la proteína), en el que se detectó fluorescencia para **IgG-G3-Cy5** a pesar de apenas presentar fluorescencia en disolución acuosa.

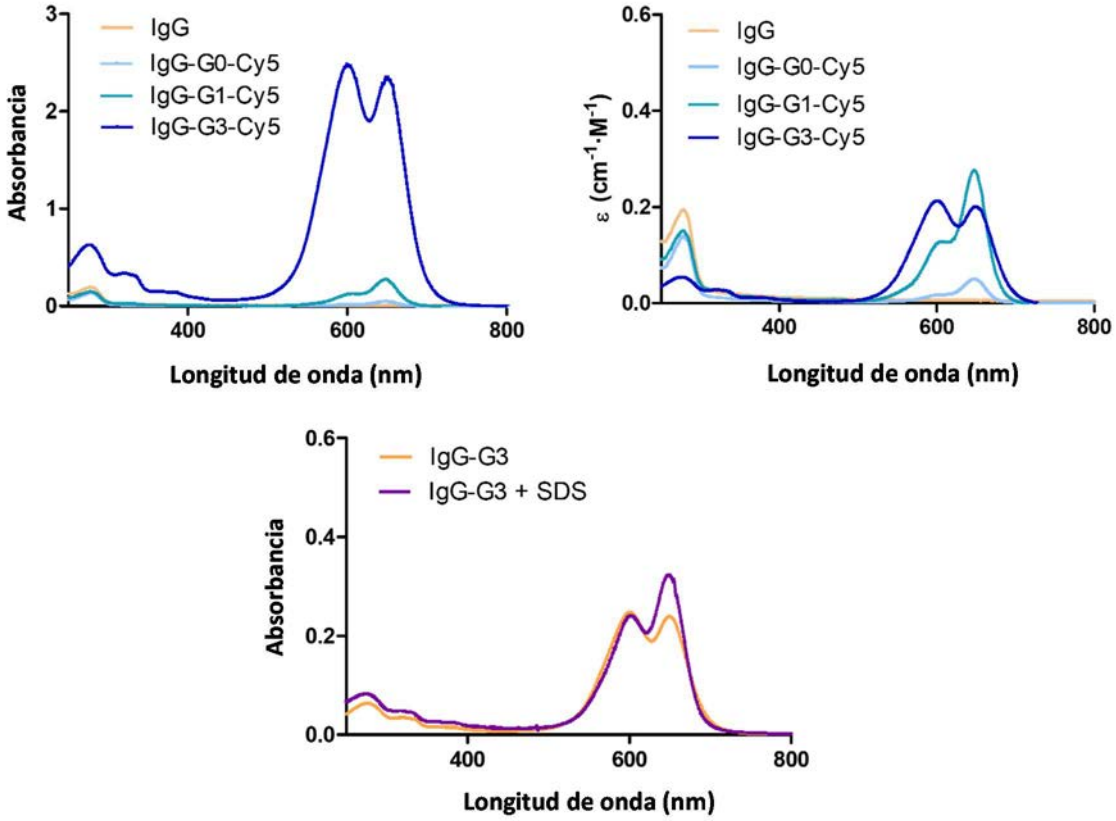

Figura R.25. Espectro de absorbancia obtenido para el anticuerpo marcado (**IgG-G0-Cy5**, **IgG-G1-Cy5**, **IgG-G3-Cy5**) (arriba izquierda). Comparación de la forma diferente del espectro para **IgG-G3-Cy5** (arriba derecha). Cambio en la absorbancia fluorescencia 90 minutos después de añadir SDS (1%) (abajo).

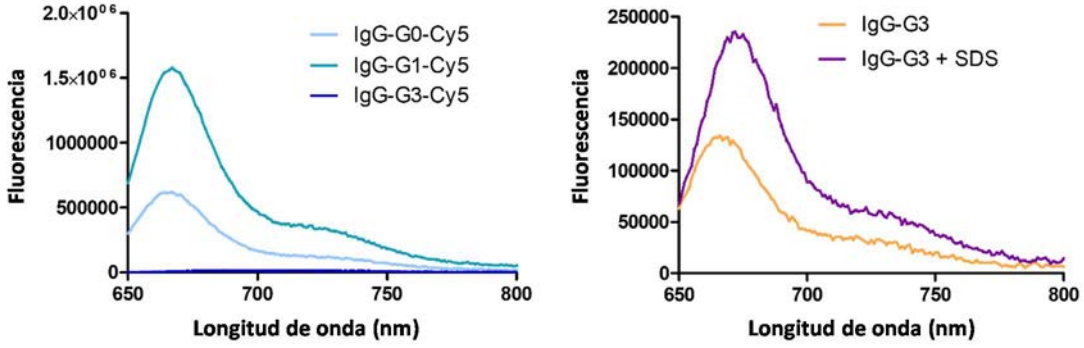

Figura R.26. Resultados de emisión de fluorescencia obtenidos para el anticuerpo marcado (**IgG-G0-Cy5**, **IgG-G1-Cy5**, **IgG-G3-Cy5**) (izquierda) y cambio en la fluorescencia 90 minutos después de añadir SDS (1%) (derecha).

De todos estos resultados se concluye que **IgG-G1-Cy5**, con dos unidades fluorescentes, es el que más amplifica la señal fluorescente y, por tanto, podría utilizarse para aumentar la sensibilidad de la detección en los inmunoensayos dirigidos al diagnóstico de alergia a fármacos. Estos resultados están en concordancia con unos estudios anteriores publicados por Gruber y Hahn que aseguraban que el número de Cy5 por molécula para el cual se obtiene una óptima fluorescencia es de dos. Sin embargo, para nuestro conocimiento, esta es la primera vez que se utilizan sondas solubles en agua con funcionalidad ortogonal para el marcaje selectivo de anticuerpos utilizando una metodología mediante la cual el sitio de unión al antígeno no se ve afectado.

CONCLUSIONES

1. De la síntesis de estructuras tipo pirazinona **V** (**Cef1** y **Cef2**), derivadas de cefaclor y cefadroxilo, y de su reconocimiento inmunológico, se deduce que este fragmento ciclado de la α-aminocefalosporina es reconocido específicamente por anticuerpos IgE de pacientes que han presentado un episodio alérgico a las correspondientes cefalosporinas o a otras penicilinas con la misma cadena lateral R^1.

La pirazinona **Cef1** parece implicar una mejora en el reconocimiento por IgE específico a cefaclor, comparada con el determinante sintético **Cef3**.

La pirazinona **Cef2** junto con el determinante sintético **Cef4** han resultado útiles para el estudio de reactividad cruzada entre penicilinas y cefalosporinas.

2. De la síntesis de estructuras bien definidas derivadas de ácido clavulánico, se concluye que su capacidad de activación de los basófilos de pacientes con alergia selectiva a este betalactámico está influenciada por su estructura química y su capacidad de unión a proteínas. **Clav2**, derivado de **AD-I**, permite aumentar el porcentaje de pacientes con BAT positivo comparado con el ácido clavulánico.

Asimismo, la estructura de 70 Da identificada, **AD-I**, que modifica los residuos de lisina 195 y 475 de la HSA *in vitro*, confirma los resultados obtenidos mediante SAR.

3. Se ha llevado a cabo el diseño y síntesis de un derivado biotinilado del ácido clavulánico (**CLV-TEG-B**) que presenta solubilidad en agua y se ha probado su capacidad de haptenización de proteínas, que es dependiente de la concentración del derivado.

Del estudio de la haptenización de proteínas séricas con **CLV-TEG-B**, se deduce que éste es una herramienta útil para la identificación de proteínas candidatas.

De hecho, HSA, haptoglobina y las cadenas pesadas y ligeras de las inmunoglubulinas han sido identificadas como potenciales dianas de haptenización por CLV.

4. Tres dendrones (**Dend5**, **Dend9**, and **Dend15**), con características ortogonales se han funcionalizado con 1, 2 u 8 unidades del fluorescente sulfo-Cy5 en su periferia, y un grupo hidrazina en el punto focal (**G0-Cy5**, **G1-Cy5** y **G3-Cy5**). De los estudios espectroscópicos se deduce que tanto absorbancia como fluorescencia aumentan con el número de unidades fluorescentes.

De la prueba de concepto que ha consistido en el uso de **G0-Cy5**, **G1-Cy5** y **G3-Cy5** como sondas fluorescentes para el marcaje de biomoléculas, se deduce que son óptimos para el marcaje selectivo de anticuerpos, utilizando α-Human IgG Fc como modelo.

La señal óptima de amplificación se ha obtenido para el anticuerpo marcado con dos unidades de sulfo-Cy5 (**IgG-G1-Cy5**), con una emission de fluorescencia un orden de magnitud mayor que **IgG-G0-Cy5**, con una única unidad fluorescente, lo que convierte al dendrón **G1-Cy5** en un valioso candidato para el marcaje de macromoléculas para aplicaciones tales como la amplificación de la señal de detección en inmunoensayos.

Por el contrario, se ha observado un enorme fenómeno de quencheo para **IgG-G3-Cy5**, que apenas es fluorescente.

BIBLIOGRAPHY

1. Bouvy, J. C., De Bruin, M. L. & Koopmanschap, M. A. (2015) Epidemiology of Adverse Drug Reactions in Europe: A Review of Recent Observational Studies, *Drug Saf.* **38**, 437-453.

2. Thong, B. Y. H. & Tan, T.-C. (2011) Epidemiology and risk factors for drug allergy, *Br J Clin Pharmacol.* **71**, 684-700.

3. Pirmohamed, M. (2014) Mechanisms of Adverse Drug Reactions in *Mann's Pharmacovigilance*.

4. Bernstein, J. A. (1995) Nonimmunologic adverse drug reactions. How to recognize and categorize some common reactions, *Postgrad Med.* **98**, 120-2, 125-6.

5. Ángela, M.-S., Nekane, B., José, A. A., Yolanda, V., Ezequiel, P.-I. & María, I. M. (2016) New Advances in the Study of IgE Drug Recognition, *Curr Pharm Des.* **22**, 1-14.

6. Doña I, B. E., Blanca-Lopez N, Torres MJ, Fernandez TD, Mayorga C, Canto G, Blanca M. (2014) Trends in Hypersensitivity Drug Reactions: More drugs, More Response Patterns, More Heterogeneity., *J Investig Allergol Clin Immunol.* **24**, 143-53.

7. Gell, P. G. H. & Coombs, R. R. A. (1963) *Clinical aspects of immunology*, Blackwell, Oxford, U.K.

8. Pichler, W. J. (2003) Delayed drug hypersensitivity reactions, *Ann Intern Med.* **139**, 683-93.

9. Lerch, M. & Pichler, W. J. (2004) The immunological and clinical spectrum of delayed drug-induced exanthems, *Curr Opin Allergy Clin Immunol.* **4**, 411-9.

10. Padial, M. A., Alvarez-Ferreira, J., Tapia, B., Blanco, R., Manas, C., Blanca, M. & Bellon, T. (2004) Acute generalized exanthematous pustulosis associated with pseudoephedrine, *Br J Dermatol.* **150**, 139-42.

11. Padilla Serrato, M. T., Arias Cruz, A., Weinmann, A., Gonzalez Diaz, S. N., Galindo Rodiguez, G. & Garcia Cobas, C. Y. (2006) Prevalence of allergy to drugs in a group of asthmatic children and adolescents of northeast of Mexico, *Rev Alerg Mex.* **53**, 179-82.

12. Demoly, P. & Hillaire-Buys, D. (2004) Classification and epidemiology of hypersensitivity drug reactions, *Immunol Allergy Clin North Am.* **24**, 345-56, v.

13. Szczeklik, A., Nizankowska-Mogilnicka, E. & Sanak, M. (2009) Hypersensitivity to aspirin and nonsteroidal anti-inflammatory drugs. 7th edition in *Middleton´s Allergy Principles & Practice* (Adkinson, N. F., Brochner, B. S., Busse, W. W., Holgate, S. T. & Lemanske, R. F., eds) pp. 1127-1243, Mosby, Philadelphia.

14. Romano, A. & Demoly, P. (2007) Recent advances in the diagnosis of drug allergy, *Curr Opin Allergy Clin Immunol.* **7**, 299-303.

15. Doña, I., Blanca-Lopez, N., Torres, M. J., Garcia-Campos, J., Garcia-Nunez, I., Gomez, F., Salas, M., Rondon, C., Canto, M. G. & Blanca, M. (2012) Drug hypersensitivity reactions: response patterns, drug involved, and temporal variations in a large series of patients, *J Investig Allergol Clin Immunol.* **22**, 363-71.

16. Blanca-Lopez, N., Andreu, I. & Torres Jaen, M. J. (2011) Hypersensitivity reactions to quinolones, *Curr Opin Allergy Clin Immunol.* **11**, 285-91.

17. Ariza A, M. C., Fernández TD, Barbero N, Martín-Serrano A, Pérez-Sala D, Sánchez-Gómez FJ, Blanca M, Torres MJ, Montañez MI (2015) Hypersensitivity Reactions to ß-Lactams: Relevance of Hapten-Protein Conjugates, *J Investig Allergol Clin Immunol.* **25**, 12-25.

18. Landsteiner, K. & Jacobs, J. (1935) Studies on the Sensitization of Animals with Simple Chemical Compounds, *J Exp Med.* **61**, 643-56.

19. Pirmohamed, M., Kitteringham, N. R. & Park, B. K. (1994) The role of active metabolites in drug toxicity, *Drug Saf.* **11**, 114-44.

20. Park, B. K., Pirmohamed, M. & Kitteringham, N. R. (1998) Role of drug disposition in drug hypersensitivity: a chemical, molecular, and clinical perspective, *Chem Res Toxicol.* **11**, 969-88.

21. Park, B. K., Coleman, J. W. & Kitteringham, N. R. (1987) Drug disposition and drug hypersensitivity, *Biochem Pharmacol.* **36**, 581-90.

22. Lee, D., Dewdney, J. M. & Edwards, R. G. (1985) The influence of hapten density on the assay of penicilloylated proteins in fluids, *J Immunol Methods.* **84**, 235-43.

23. Klaus, G. G. B. & Humphrey, J. H. (1993) The fate of antigens in *Clinical aspects of immunology* (Lachmann, P. J., Peters, D. K., Rosen, F. S. & Walport, M. J., eds) pp. 107-126, Blackwell Scientific Publications, Oxford, UK.

24. Baldo, B. A. & Pham, N. H. (1994) Structure-activity studies on drug-induced anaphylactic reactions, *Chem Res Toxicol.* **7**, 703-21.

25. Matzinger, P. (1994) Tolerance, danger, and the extended family, *Annu Rev Immunol.* **12**, 991-1045.

26. Lavergne, S. N., Wang, H., Callan, H. E., Park, B. K. & Naisbitt, D. J. (2009) "Danger" conditions increase sulfamethoxazole-protein adduct formation in human antigen-presenting cells, *J Pharmacol Exp Ther.* **331**, 372-81.

27. Pichler, W. J. (2002) Pharmacological interaction of drugs with antigen-specific immune receptors: the p-i concept, *Curr Opin Allergy Clin Immunol.* **2**, 301-5.

28. Mayorga, C., Celik, G., Rouzaire, P., Whitaker, P., Bonadonna, P., Rodrigues-Cernadas, J., Vultaggio, A., Brockow, K., Caubet, J. C., Makowska, J., Nakonechna, A., Romano, A., Montañez, M. I., Laguna, J. J., Zanoni, G., Gueant, J. L., Oude Elberink, H., Fernandez, J., Viel, S., Demoly, P., Torres, M. J. & *In vitro* tests for Drug Allergy Task Force of, E. D. I. G. (2016) *In vitro* tests for drug hypersensitivity reactions: an ENDA/EAACI Drug Allergy Interest Group position paper, *Allergy.* **71**, 1103-1134.

29. Ishizaka, K. & Ishizaka, T. (1967) Identification of gamma-E-antibodies as a carrier of reaginic activity, *J Immunol.* **99**, 1187-98.

30. Yazdanbakhsh, M., van den Biggelaar, A. & Maizels, R. M. (2001) Th2 responses without atopy: immunoregulation in chronic helminth infections and reduced allergic disease, *Trends Immunol.* **22**, 372-7.

31. Maizels, N. (2003) Yin outwits Yang at the IgE locus, *Nat Immunol.* **4**, 7-8.

32. Maizels, R. M. & Yazdanbakhsh, M. (2003) Immune regulation by helminth parasites: cellular and molecular mechanisms, *Nat Rev Immunol.* **3**, 733-44.

33. Kulczycki, A. (1987) The role of IgE in *Allergy: An international Textbook* pp. 37-47, Wiley and Sons.

34. Geha, R. S., Jabara, H. H. & Brodeur, S. R. (2003) The regulation of immunoglobulin E class-switch recombination, *Nat Rev Immunol.* **3**, 721-32.

35. King, C. L., Poindexter, R. W., Ragunathan, J., Fleisher, T. A., Ottesen, E. A. & Nutman, T. B. (1991) Frequency analysis of IgE-secreting B lymphocytes in persons with normal or elevated serum IgE levels, *J Immunol.* **146**, 1478-83.

36. Sutton, B. J. & Gould, H. J. (1993) The human IgE network, *Nature.* **366**, 421-8.

37. Smurthwaite, L. & Durham, S. R. (2002) Local IgE synthesis in allergic rhinitis and asthma, *Curr Allergy Asthma Rep.* **2**, 231-8.

38. Montañez, M. I., Ariza, A., Mayorga, C., Fernandez, T. D. & Torres, M. J. (2015) Cross-Reactivity in Betalactam Allergy: Alternative Treatments, *Curr Treat Options Allergy.* **2**, 141-154.

39. Eisen, H. N., Orris, L. & Belman, S. (1952) Elicitation of delayed allergic skin reactions with haptens; the dependence of elicitation on hapten combination with protein, *J Exp Med.* **95**, 473-87.

40. Levine, B. B. & Ovary, Z. (1961) Studies on the mechanism of the formation of the penicillin antigen. III. The N-(D-alpha-benzylpenicilloyl) group as an antigenic determinant responsible for hypersensitivity to penicillin G, *J Exp Med.* **114**, 875-904.

41. Dewdney, J. M. (1977) Immunology of the antibiotics in *The Antigens* (Sela, M., ed) pp. 114-245, Academic Press, New York.

42. Perez-Inestrosa, E., Suau, R., Montañez, M. I., Rodriguez, R., Mayorga, C., Torres, M. J. & Blanca, M. (2005) Cephalosporin chemical reactivity and its immunological implications, *Curr Opin Allergy Clin Immunol.* **5**, 323-330.

43. Montañez, M. I., Mayorga, C., Torres, M. J., Ariza, A., Blanca, M. & Perez-Inestrosa, E. (2011) Synthetic Approach to Gain Insight into Antigenic Determinants of Cephalosporins: *In Vitro* Studies of Chemical Structure−IgE Molecular Recognition Relationships, *Chem Res Toxicol.* **24**, 706-717.

44. Warbrick, E. V., Thomas, A. L., Stejskal, V. & Coleman, J. W. (1995) An analysis of beta-lactam-derived antigens on spleen cell and serum proteins by ELISA and Western blotting, *Allergy.* **50**, 910-7.

45. Adriana Ariza, D. C., Yolanda Vida, Marıa I. Montañez, Ezequiel Pérez-Inestrosa, Miguel Blanca, María José Torres, F. Javier Cañada, Dolores Pérez-Sala (2014) Study of Protein Haptenation by Amoxicillin Through the Use of a Biotinylated Antibiotic, *PLoS One.* **9**, e90891.

46. Batchelor, F. R., Dewdney, J. M. & Gazzard, D. (1965) Penicillin Allergy: The Formation of the Penicilloyl Determinant, *Nature.* **206**, 362.

47. Montañez, M. I., Najera, F. & Pérez-Inestrosa, E. (2011) NMR studies and molecular dynamic simulation of synthetic dendrimeric-antigens, *Polymers.* **3**, 1533-53.

48. de Weck, A. L. (1983) Penicillins and cephalosporins in *Allergic reactions to drugs* (de Weck, A. L. & Bundgaard, H., eds) pp. 423-482, Springer, Berlin.

49. BALDO (1999) Penicillins and cephalosporins as allergens — structural aspects of recognition and cross-reactions, *Clin Exp Allergy.* **29**, 744-749.

50. Blanca, M., Mayorga, C., Torres, M. J., Reche, M., Moya, M. C., Rodriguez, J. L., Romano, A. & Juarez, C. (2001) Clinical evaluation of Pharmacia CAP System RAST FEIA amoxicilloyl and benzylpenicilloyl in patients with penicillin allergy, *Allergy.* **56**, 862-70.

51. Montañez, M. I., Najera, F., Mayorga, C., Ruiz-Sanchez, A. J., Vida, Y., Collado, D., Blanca, M., Torres, M. J. & Perez-Inestrosa, E. (2015) Recognition of multiepitope dendrimeric antigens by human immunoglobulin E, *Nanomedicine: Nanotechnology, Biology and Medicine.* **11**, 579-588.

52. Connor, S. C., Everett, J. R., Jennings, K. R., Nicholson, J. K. & Woodnutt, G. (1994) High Resolution 1H NMR Spectroscopic Studies of the Metabolism and Excretion of Ampicillin in Rats and Amoxycillin in Rats and Man, *Journal of Pharmacy and Pharmacology.* **46**, 128-134.

53. Xiaoli Meng, C. J. E., Arun Tailor, Rosalind E. Jenkins, James C. Waddington, Paul Whitaker, Neil S. French, Dean J. Naisbitt, and B. Kevin Park (2016) Amoxicillin and Clavulanate Form Chemically and Immunologically Distinct Multiple Haptenic Structures in Patients, *Chem Res Toxicol.* **29**, 1762-1772.

54. Dewdney, J. M., Smith, H. & Wheeler, A. W. (1971) The formation of antigenic polymers in aqueous solutions of β-lactam antibodies, *Immunology.* **21**, 517-525.

55. Bundgaard, H. (1980) Pharmaceutical aspects of penicillin allergy: polymerization of penicillins and reactions with carbohydrates, *Journal of Clinical Pharmacy and Therapeutics.* **5**, 73-96.

56. Blanca, M., Mayorga, C., Perez, E., Suau, R., Juarez, C., Vega, J. M., Carmona, M. J., Perez-Estrada, M. & Garcia, J. (1992) Determination of IgE antibodies to the benzyl penicilloyl determinant. A comparison between poly-L-lysine and human serum albumin as carriers, *J Immunol Methods.* **153**, 99-105.

57. Blanca, M., Mayorga, C., Sanchez, F., Vega, J. M., Fernandez, J., Juarez, C., Suau, R. & Perez, E. (1991) Differences in serum IgE antibody activity to benzylpenicillin and amoxicillin measured by RAST in a group of penicillin allergic patients, *Allergy.* **46**, 632-8.

58. de Haan, P., de Jonge, A. J., Verbrugge, T. & Boorsma, D. M. (1985) Three epitope-specific monoclonal antibodies against the hapten penicillin, *Int Arch Allergy Appl Immunol.* **76**, 42-6.

59. Mayorga, C., Obispo, T., Jimeno, L., Blanca, M., Moscoso del Prado, J., Carreira, J., Garcia, J. J. & Juarez, C. (1995) Epitope mapping of beta-lactam antibiotics with the use of monoclonal antibodies, *Toxicology.* **97**, 225-34.

60. Nagakura, N., Souma, S., Shimizu, T. & Yanagihara, Y. (1991) Anti-ampicillin monoclonal antibodies and their cross-reactivities to various beta-lactams, *J Antimicrob Chemother.* **28**, 357-68.

61. Harle, D. G. & Baldo, B. A. (1990) Identification of penicillin allergenic determinants that bind IgE antibodies in the sera of subjects with penicillin allergy, *Mol Immunol.* **27**, 1063-71.

62. Moreno, F., Blanca, M., Mayorga, C., Terrados, S., Moya, M., Pérez, E., Suau, R., Vega, J. M., García, J., Miranda, A. & Carmona, M. J. (1995) Studies of the Specificities of IgE Antibodies Found in Sera from Subjects with Allergic Reactions to Penicillins, *Int Arch Allergy Immunol.* **108**, 74-81.

63. Ariza, A., Mayorga, C., Salas, M., Doña, I., Martín-Serrano, Á., Pérez-Inestrosa, E., Pérez-Sala, D., Guzmán, A. E., Montañez, M. I. & Torres, M. J. (2016) The influence of the carrier molecule on amoxicillin recognition by specific IgE in patients with immediate hypersensitivity reactions to betalactams, *Sci Rep.* **6**, 35113.

64. Miranda, A., Blanca, M., Vega, J. M., Moreno, F., Carmona, M. J., Garcia, J. J., Segurado, E., Justicia, J. L. & Juarez, C. (1996) Cross-reactivity between a penicillin and a cephalosporin with the same side chain, *J Allergy Clin Immunol.* **98**, 671-7.

65. Boyd, D. B., Hermann, R. B., Presti, D. E. & Marsh, M. M. (1975) Electronic structures of cephalosporins and penicillins. 4. Modeling acylation by the .beta.-lactam ring, *J Med Chem.* **18**, 408-417.

66. Boyd, D. B. & Lunn, W. H. W. (1979) Electronic structures of cephalosporins and penicillins. 9. Departure of a leaving group in cephalosporins, *J Med Chem.* **22**, 778-784.

67. Faraci, W. S. & Pratt, R. F. (1984) Elimination of a good leaving group from the 3'-position of a cephalosporin need not be concerted with .beta.-lactam ring opening: TEM-2 .beta.-lactamase-catalyzed hydrolysis of pyridine-2-azo-4'-(N',N'-dimethylaniline) cephalosporin (PADAC) and of cephaloridine, *J Am Chem Soc.* **106**, 1489-1490.

68. F. Pratt, R. & Stephen. Faraci, W. (1986) *Direct observation by 1H NMR of cephalosporoate intermediates in aqueous solution during the hydrazinolysis and β-lactamase-catalyzed hydrolysis of cephalosporins with 3′ leaving groups: Kinetics and equilibria of the 3′ elimination reaction*.

69. Sánchez-Sancho, F., Perez-Inestrosa, E., Suau, R., Montañez, M. I., Mayorga, C., Torres, M. J., Romano, A. & Blanca, M. (2003) Synthesis, characterization and immunochemical evaluation of cephalosporin antigenic determinants, *J Mol Recognit.* **16**, 148-156.

70. Antunez, C., Blanca-Lopez, N., Torres, M. J., Mayorga, C., Perez-Inestrosa, E., Montañez, M. I., Fernandez, T. & Blanca, M. (2006) Immediate allergic reactions to cephalosporins: Evaluation of cross-reactivity with a panel of penicillins and cephalosporins, *J Allergy Clin Immunol.* **117**, 404-410.

71. Romano, A., Mayorga, C., Torres, M. J., Artesani, M. C., Suau, R., Sanchez, F., Perez, E., Venuti, A. & Blanca, M. (2000) Immediate allergic reactions to cephalosporins: cross-reactivity and selective responses, *J Allergy Clin Immunol.* **106**, 1177-83.

72. de San Pedro, B. S., Mayorga, C., Torres, M. J., Florido, J. F., Quiralte, J. & Blanca, M. Boosted IgE response after anaphylaxis reaction to cefuroxime with cross-reactivity with cefotaxime, *Ann Allergy Asthma Immunol.* **89**, 101-103.

73. Novalbos, A., Sastre, J., Cuesta, J., Heras, M. D. L., Lluch-Bernal, M., Bombín, C. & Quirce, S. (2001) Lack of allergic cross-reactivity to cephalosporins among patients allergic to penicillins, *Clin Exp Allergy.* **31**, 438-443.

74. Edwards, R. G., Dewdney, J. M., Dobrzanski, R. J. & Lee, D. (1988) Immunogenicity and allergenicity studies on two beta-lactam structures, a clavam, clavulanic acid, and a carbapenem: structure-activity relationships, *Int Arch Allergy Appl Immunol.* **85**, 184-9.

75. Prescott, J. W. A., DePestel, D. D., Ellis, J. J. & E. Regal, R. (2004) Incidence of Carbapenem-Associated Allergic-Type Reactions among Patients with versus Patients without a Reported Penicillin Allergy, *Clin Infect Dis.* **38**, 1102-1107.

76. Saxon, A., Beall, G. N., Rohr, A. S. & Adelman, D. C. (1987) IMmediate hypersensitivity reactions to beta-lactam antibiotics, *Ann Intern Med.* **107**, 204-215.

77. Frumin, J. & Gallagher, J. C. (2009) Allergic Cross-Sensitivity Between Penicillin, Carbapenem, and Monobactam Antibiotics: What are the Chances?, *Ann Pharmacother.* **43**, 304-315.

78. Sodhi, M., Axtell, S. S., Callahan, J. & Shekar, R. (2004) Is it safe to use carbapenems in patients with a history of allergy to penicillin?, *Journal of Antimicrobial Chemotherapy.* **54**, 1155-1157.

79. Shimizu, T., Souma, S., Nagakura, N., Masuzawa, T., Iwamoto, Y. & Yanagiham, Y. (1992) Epitope Analysis of Aztreonam by Antiaztreonam Monoclonal Antibodies and Possible Consequences in Beta-Lactams Hypersensitivity, *Int Arch Allergy Immunol.* **98**, 392-397.

80. Torres, M. J., Ariza, A., Mayorga, C., Doña, I., Blanca-Lopez, N., Rondon, C. & Blanca, M. (2010) Clavulanic acid can be the component in amoxicillin-clavulanic acid responsible for immediate hypersensitivity reactions, *J Allergy Clin Immunol.* **125**, 502-505.e2.

81. Baggaley, K. H., Brown, A. G. & Schofield, C. J. (1997) Chemistry and biosynthesis of clavulanic acid and other clavams, *Natural Product Reports.* **14**, 309-333.

82. Martin, J., Mendez, R. & Alemany, T. (1989) Studies on clavulanic acid. Part 1. Stability of clavulanic acid in aqueous solutions of amines containing hydroxy groups, *J Chem Soc Perkin Trans 2*, 223-226.

83. Brethauer, S., Held, M. & Panke, S. (2008) Clavulanic Acid Decomposition Is Catalyzed by the Compound Itself and by Its Decomposition Products, *J Pharm Sci.* **97**, 3451-3455.

84. Finn, M. J., Harris, M. A., Hunt, E. & Zomaya, I. I. (1984) Studies on the hydrolysis of clavulanic acid, *J Chem Soc Perkin Trans 1*, 1345-1349.

85. Tremblay, L. W., Hugonnet, J.-E. & Blanchard, J. S. (2008) Structure of the Covalent Adduct Formed between Mycobacterium tuberculosis β-Lactamase and Clavulanate, *Biochemistry.* **47**, 5312-5316.

86. DiPiro, J. T., Adkinson, N. F., Jr. & Hamilton, R. G. (1993) Facilitation of penicillin haptenation to serum proteins, *Antimicrob Agents Chemother.* **37**, 1463-7.

87. Levine, B. B. (1962) N(Alpha-D-Penicilloyl) Amines as Univalent Hapten Inhibitors of Antibodydependent Allergic Reactions to Penicillin, *J Med Pharm Chem.* **91**, 1025-34.

88. Adriana Ariza, D. G., Daniel R. Abánades, Vivian de los Ríos, Giulio Vistoli, María J. Torres, Marina Carini, Giancarlo Aldini, Dolores Pérez-Sala (2012) Protein haptenation by amoxicillin: High resolution mass spectrometry analysis and identification of target proteins in serum, *J Proteomics.* **77**, 504-520.

89. Garzon, D., Ariza, A., Regazzoni, L., Clerici, R., Altomare, A., Sirtori, F. R., Carini, M., Torres, M. J., Pérez-Sala, D. & Aldini, G. (2014) Mass Spectrometric Strategies for the Identification and Characterization of Human Serum Albumin Covalently Adducted by Amoxicillin: Ex Vivo Studies, *Chem Res Toxicol.* **27**, 1566-1574.

90. Yamasaki, K., Chuang, V. T. G., Maruyama, T. & Otagiri, M. (2013) Albumin–drug interaction and its clinical implication, *Biochim Biophys Acta (BBA) - General Subjects.* **1830**, 5435-5443.

91. Carlo, B. & Enrico, D. (2002) Reversible and Covalent Binding of Drugs to Human Serum Albumin: Methodological Approaches and Physiological Relevance, *Curr Med Chem.* **9**, 1463-1481.

92. Ghuman, J., Zunszain, P. A., Petitpas, I., Bhattacharya, A. A., Otagiri, M. & Curry, S. (2005) Structural Basis of the Drug-binding Specificity of Human Serum Albumin, *J Mol Biol.* **353**, 38-52.

93. Larsen, M. T., Kuhlmann, M., Hvam, M. L. & Howard, K. A. (2016) Albumin-based drug delivery: harnessing nature to cure disease, *Molecular and Cellular Therapies.* **4**, 3.

94. Fasano, M., Curry, S., Terreno, E., Galliano, M., Fanali, G., Narciso, P., Notari, S. & Ascenzi, P. (2005) The extraordinary ligand binding properties of human serum albumin, *IUBMB Life.* **57**, 787-796.

95. Honma, K., Nakamura, M. & Ishikawa, Y. (1991) Acetylsalicylate-human serum albumin interaction as studied by NMR spectroscopy-antigenicity-producing mechanism of acetylsalicylic acid, *Mol Immunol.* **28**, 107-13.

96. Peters, T. (1996) *All about albumin: biochemistry, genetics and medical applications.*, Academic Press, San Diego and London.

97. Roche, M., Rondeau, P., Singh, N. R., Tarnus, E. & Bourdon, E. (2008) The antioxidant properties of serum albumin, *FEBS Lett.* **582**, 1783-7.

98. Lafaye, P. & Lapresle, C. (1988) Fixation of penicilloyl groups to albumin and appearance of anti-penicilloyl antibodies in penicillin-treated patients, *J Clin Invest.* **82**, 7-12.

99. Yvon, M., Anglade, P. & Wal, J. M. (1989) Binding of benzyl penicilloyl to human serum albumin. Evidence for a highly reactive region at the junction of domains 1 and 2 of the albumin molecule, *FEBS Lett.* **247**, 273-8.

100. Yvon, M., Anglade, P. & Wal, J. M. (1990) Identification of the binding sites of benzyl penicilloyl, the allergenic metabolite of penicillin, on the serum albumin molecule, *FEBS Lett.* **263**, 237-40.

101. Jenkins, R. E., Meng, X., Elliott, V. L., Kitteringham, N. R., Pirmohamed, M. & Park, B. K. (2009) Characterisation of flucloxacillin and 5-hydroxymethyl flucloxacillin haptenated HSA *in vitro* and *in vivo*, *Proteomics Clin Appl.* **3**, 720-9.

102. Whitaker, P., Meng, X., Lavergne, S. N., El-Ghaiesh, S., Monshi, M., Earnshaw, C., Peckham, D., Gooi, J., Conway, S., Pirmohamed, M., Jenkins, R. E., Naisbitt, D. J. & Park, B. K. (2011) Mass spectrometric characterization of circulating and functional antigens derived from piperacillin in patients with cystic fibrosis, *J Immunol.* **187**, 200-11.

103. Meng, X., Jenkins, R. E., Berry, N. G., Maggs, J. L., Farrell, J., Lane, C. S., Stachulski, A. V., French, N. S., Naisbitt, D. J., Pirmohamed, M. & Park, B. K. (2011) Direct evidence for the formation of diastereoisomeric benzylpenicilloyl haptens from benzylpenicillin and benzylpenicillenic acid in patients, *J Pharmacol Exp Ther.* **338**, 841-9.

104. Azoury, M. E., Fili, L., Bechara, R., Scornet, N., de Chaisemartin, L., Weaver, R. J., Claude, N., Maillere, B., Parronchi, P., Joseph, D. & Pallardy, M. (2018) Identification of T-cell epitopes from benzylpenicillin conjugated to human serum albumin and implication in penicillin allergy, *Allergy*.

105. Juan, M. G.-M., Maria, I. M., Giancarlo, A., Francisco, J. S.-G. & Dolores, P.-S. (2016) Adduct Formation and Context Factors in Drug Hypersensitivity: Insight from Proteomic Studies, *Curr Pharm Des.* **22**, 6748-6758.

106. Martin, S. F., Esser, P. R., Schmucker, S., Dietz, L., Naisbitt, D. J., Park, B. K., Vocanson, M., Nicolas, J.-F., Keller, M., Pichler, W. J., Peiser, M., Luch, A., Wanner, R., Maggi, E., Cavani, A., Rustemeyer, T., Richter, A., Thierse, H.-J. & Sallusto, F. (2010) T-cell recognition of chemicals, protein allergens and drugs: towards the development of *in vitro* assays, *Cell Mol Life Sci.* **67**, 4171-4184.

107. El-Ghaiesh, S., Monshi, M. M., Whitaker, P., Jenkins, R., Meng, X., Farrell, J., Elsheikh, A., Peckham, D., French, N., Pirmohamed, M., Park, B. K. & Naisbitt, D. J. (2012) Characterization of the Antigen Specificity of T-Cell Clones from Piperacillin-Hypersensitive Patients with Cystic Fibrosis, *J Pharmacol Exp Ther.* **341**, 597-610.

108. Magi, B., Marzocchi, B., Bini, L., Cellesi, C., Rossolini, A. & Pallini, V. (1995) Two-dimensional electrophoresis of human serum proteins modified by ampicillin during therapeutic treatment, *Electrophoresis.* **16**, 1190-2.

109. Binderup, L. & Arrigoni-Martelli, E. (1979) [14C]-D-Penicillamine: uptake and distribution in rat lymphocytes and macrophages, *Biochem Pharmacol.* **28**, 189-92.

110. O´Donnell, C. A., Foster, A. L. & Coleman, J. W. (1991) Penicillamine and penicillin can generate antigenic determinants on rat peritoneal cells *in vitro*, *Immunology.* **72**, 571-576.

111. Watanabe, H., Grimsley, G., Major, G. A. & Dawkins, R. L. (1986) Increased binding of D-penicillamine to monocytes in rheumatoid arthritis, *Clin Immunol Immunopathol.* **39**, 173-8.

112. Watanabe, H., Kelly, H. & Dawkins, R. L. (1987) Association of HLA DR1 with high D-penicillamine binding to monocytes in females, *Microbiol Immunol.* **31**, 83-8.

113. Sanchez-Gomez, F. J., Gonzalez-Morena, J. M., Vida, Y., Perez-Inestrosa, E., Blanca, M., Torres, M. J. & Perez-Sala, D. (2017) Amoxicillin haptenates intracellular proteins that can be transported in exosomes to target cells, *Allergy.* **72**, 385-396.

114. Doña, I., Torres, M. J., Montañez, M. I. & Fernández, T. D. (2017) *In Vitro* Diagnostic Testing for Antibiotic Allergy, *Allergy Asthma Immunol Res.* **9**, 288-298.

115. Xiaoli, M., Adriana, A., James, W., Kevin, P. & Dean, N. (2016) Immunological Mechanisms of Drug Hypersensitivity, *Curr Pharm Des.* **22**, 6734-6747.

116. Fernandez, T. D., Mayorga, C., Salas, M., Barrionuevo, E., Posadas, T., Ariza, A., Laguna, J. J., Moreno, E., Torres, M. J., Doña, I. & Montañez, M. I. (2017) Evolution of diagnostic approaches in betalactam hypersensitivity, *Expert Rev Clin Pharmacol.* **10**, 671-683.

117. Blanca, M., Vega, J. M., Garcia, J., Miranda, A., Carmona, M. J., Juarez, C., Terrados, S. & Fernandez, J. (1994) New aspects of allergic reactions to betalactams: crossreactions and unique specificities, *Clin Exp Allergy.* **24**, 407-15.

118. Matheu, V., Perez-Rodriguez, E., Sanchez-Machin, I., de la Torre, F. & Garcia-Robaina, J. C. (2005) Major and minor determinants are high-performance skin tests in beta-lactam allergy diagnosis, *J Allergy Clin Immunol.* **116**, 1167-8; author reply 1168-9.

119. Bousquet, P. J., Co-Minh, H. B., Arnoux, B., Daures, J. P. & Demoly, P. (2005) Importance of mixture of minor determinants and benzylpenicilloyl poly-L-lysine skin testing in the diagnosis of beta-lactam allergy, *J Allergy Clin Immunol.* **115**, 1314-6.

120. Romano, A., Bousquet-Rouanet, L., Viola, M., Gaeta, F., Demoly, P. & Bousquet, P. J. (2009) Benzylpenicillin skin testing is still important in diagnosing immediate hypersensitivity reactions to penicillins, *Allergy.* **64**, 249-53.

121. Blanca, M., Romano, A., Torres, M. J., Fernandez, J., Mayorga, C., Rodriguez, J., Demoly, P., Bousquet, P. J., Merk, H. F., Sanz, M. L., Ott, H. & Atanaskovic-Markovic, M. (2009) Update on the evaluation of hypersensitivity reactions to betalactams, *Allergy.* **64**, 183-93.

122. Torres, M. J. & Blanca, M. (2010) The complex clinical picture of beta-lactam hypersensitivity: penicillins, cephalosporins, monobactams, carbapenems, and clavams, *Med Clin North Am.* **94**, 805-20, xii.

123. Fernandez, J., Torres, M. J., Campos, J., Arribas-Poves, F. & Blanca, M. (2013) Prospective, multicenter clinical trial to validate new products for skin tests in the diagnosis of allergy to penicillin, *J Investig Allergol Clin Immunol.* **23**, 398-408.

124. Torres, M. J., Romano, A., Mayorga, C., Moya, M. C., Guzman, A. E., Reche, M., Juarez, C. & Blanca, M. (2001) Diagnostic evaluation of a large group of patients with immediate allergy to penicillins: the role of skin testing, *Allergy.* **56**, 850-6.

125. Torres, M. J., Ariza, A., Fernández, J., Moreno, E., Laguna, J. J., Montañez, M. I., Ruiz-Sanchez, A. J. & Blanca, M. (2010) Role of minor determinants of amoxicillin in the diagnosis of immediate allergic reactions to amoxicillin, *Allergy.* **65**, 590-596.

126. Weiss, M. E. & Adkinson, N. F. (1988) Immediate hypersensitivity reactions to penicillin and related antibiotics, *Clin Allergy.* **18**, 515-40.

127. Blanca, M., Vega, J. M., Garcia, J., Carmona, M. J., Terados, S., Avila, M. J., Miranda, A. & Juarez, C. (1990) Allergy to penicillin with good tolerance to other penicillins; study of the incidence in subjects allergic to beta-lactams, *Clin Exp Allergy.* **20**, 475-81.

128. Silviu-Dan, F., McPhillips, S. & Warrington, R. J. (1993) The frequency of skin test reactions to side-chain penicillin determinants, *J Allergy Clin Immunol.* **91**, 694-701.

129. Romano, A., Mayorga, C., Torres, M. J., Artesani, M. C., Suau, R., Sánchez, F., Pérez, E., Venuti, A. & Blanca, M. (2000) Immediate allergic reactions to cephalosporins: Cross-reactivity and selective responses, *J Allergy Clin Immunol*. **106**, 1177-1183.

130. Romano, A., Guéant-Rodriguez, R. M., Viola, M., Amoghly, F., Gaeta, F., Nicolas, J. P. & Guéant, J. L. (2005) Diagnosing immediate reactions to cephalosporins, *Clin Exp Allergy.* **35**, 1234-1242.

131. Torres, M. J., Montañez, M. I., Ariza, A., Salas, M., Fernandez, T. D., Barbero, N., Mayorga, C. & Blanca, M. (2016) The role of IgE recognition in allergic reactions to amoxicillin and clavulanic acid, *Clin Exp Allergy.* **46**, 264-274.

132. Sánchez-Morillas, L., Pérez-Ezquerra, P. R., Reaño-Martos, M., Laguna-Martínez, J. J., Sanz, M. L. & Martínez, L. M. (2010) Selective allergic reactions to clavulanic acid: A report of 9 cases, *J Allergy Clin Immunol.* **126**, 177-179.

133. Bousquet, P. J., Pipet, A., Bousquet-Rouanet, L. & Demoly, P. (2008) Oral challenges are needed in the diagnosis of beta-lactam hypersensitivity, *Clin Exp Allergy.* **38**, 185-90.

134. Torres, M. J., Blanca, M., Fernandez, J., Romano, A., Weck, A., Aberer, W., Brockow, K., Pichler, W. J. & Demoly, P. (2003) Diagnosis of immediate allergic reactions to beta-lactam antibiotics, *Allergy.* **58**, 961-72.

135. Garcia, J. J., Blanca, M., Moreno, F., Vega, J. M., Mayorga, C., Fernandez, J., Juarez, C., Romano, A. & de Ramon, E. (1997) Determination of IgE antibodies to the benzylpenicilloyl determinant: a comparison of the sensitivity and specificity of three radio allergo sorbent test methods, *J Clin Lab Anal.* **11**, 251-7.

136. Mayorga, C., Sanz, M. L., Gamboa, P. M., Garcia, B. E., Caballero, M. T., Garcia, J. M., Labrador, M., Lahoz, C., Longo Areso, N., Lopez Hoyos, M., Martinez Quesada, J. & Monteseirin, F. J. (2010) *In vitro* diagnosis of immediate allergic reactions to drugs: an update, *J Investig Allergol Clin Immunol.* **20**, 103-9.

137. Ebo, D. G., Leysen, J., Mayorga, C., Rozieres, A., Knol, E. F. & Terreehorst, I. (2011) The *in vitro* diagnosis of drug allergy: status and perspectives, *Allergy.* **66**, 1275-1286.

138. Montañez, M. I., Ruiz-Sanchez, A. J. & Perez-Inestrosa, E. (2010) A perspective of nanotechnology in hypersensitivity reactions including drug allergy, *Curr Opin Allergy Clin Immunol.* **10**, 297-302.

139. Mayorga, C., Perez-Inestrosa, E., Molina, N. & Montanez, M. I. (2016) Development of nanostructures in the diagnosis of drug hypersensitivity reactions, *Curr Opin Allergy Clin Immunol.* **16**, 300-7.

140. Torres, M. J., Padial, A., Mayorga, C., Fernandez, T., Sanchez-Sabate, E., Cornejo-Garcia, J. A., Antunez, C. & Blanca, M. (2004) The diagnostic interpretation of basophil activation test in immediate allergic reactions to betalactams, *Clin Exp Allergy.* **34**, 1768-75.

141. Molina, N., Martin-Serrano, A., Fernandez, T., Tesfaye, A., Najera, F., Torres, M., Mayorga, C., Vida, Y., Montañez, M. & Perez-Inestrosa, E. (2018) Dendrimeric Antigens for Drug Allergy Diagnosis: A New Approach for Basophil Activation Tests, *Molecules.* **23**, 997.

142. Salas, M., Fernández-Santamaría, R., Mayorga, C., Barrionuevo, E., Ariza, A., Posadas, T., Laguna, J. J., Montañez, M. I., Molina, N., Fernández, T. D. & Torres, M. J. (2017) Use of the Basophil Activation Test May Reduce the Need for Drug Provocation in Amoxicillin-Clavulanic Allergy, *J Allergy Clin Immunol Pract*.

143. Rose, B. G., Kamps-Holtzapple, C. & Stanker, L. H. (1995) Competitive Indirect ELISA for Ceftiofur Sodium and the Effect of Different Immunizing and Coating Antigen Conjugates, *Bioconj Chem.* **6**, 529-535.

144. Yoo, H.-S., Kim, S.-H., Kwon, H.-S., Kim, T.-B., Nam, Y.-H., Ye, Y.-M. & Park, H.-S. (2014) Immunologic Evaluation of Immediate Hypersensitivity to Cefaclor, *Yonsei Medical Journal.* **55**, 1473-1483.

145. Kim, J. E., Kim, S. H., Choi, G. S., Ye, Y. M. & Park, H. S. (2010) Detection of specific IgE antibodies to cefotiam-HSA conjugate by ELISA in a nurse with occupational anaphylaxis, *Allergy.* **65**, 791-792.

146. Himly, M., Jahn-Schmid, B., Pittertschatscher, K., Bohle, B., Grubmayr, K., Ferreira, F., Ebner, H. & Ebner, C. IgE-mediated immediate-type hypersensitivity to the pyrazolone drug propyphenazone, *J Allergy Clin Immunol.* **111**, 882-888.

147. Ruiz-Sanchez, A. J., Montanez, M. I., Mayorga, C., Torres, M. J., Kehr, N. S., Vida, Y., Collado, D., Najera, F., Cola, L. D. & Perez-Inestrosa, E. (2012) Dendrimer-Modified Solid Supports: Nanostructured Materials with Potential Drug Allergy Diagnostic Applications, *Curr Med Chem.* **19**, 4942-4954.

148. Vida, Y., Montanez, M. I., Collado, D., Najera, F., Ariza, A., Blanca, M., Torres, M. J., Mayorga, C. & Perez-Inestrosa, E. (2013) Dendrimeric antigen-silica particle composites: an innovative approach for IgE quantification, *J Mater Chem B.* **1**, 3044-3050.

149. O'Donovan, L. & De Bank, P. A. (2014) A hydrazide-anchored dendron scaffold for chemoselective ligation strategies, *Org Biomol Chem.* **12**, 7290-7296.

150. Wängler, C., Moldenhauer, G., Saffrich, R., Knapp, E. M., Beijer, B., Schnölzer, M., Wängler, B., Eisenhut, M., Haberkorn, U. & Mier, W. (2008) PAMAM Structure-Based Multifunctional

Fluorescent Conjugates for Improved Fluorescent Labelling of Biomacromolecules, *Chem Eur J.* **14**, 8116-8130.

151. Patrik Stenström, O. C. J. A. a. M. M. (2016) Fluoride-Promoted Esterification (FPE) Chemistry: A Robust Route to Bis-MPA Dendrons and Their Postfunctionalization, *Molecules.* **21**.

152. García-Gallego, S., Nyström, A. M. & Malkoch, M. (2015) Chemistry of multifunctional polymers based on bis-MPA and their cutting-edge applications, *Prog Polym Sci.* **48**, 85-110.

153. Anna Carlmark, E. M. m. a. M. M. (2013) Dendritic architectures based on bis-MPA: functional polymeric scaffolds for application-driven research, *Chem Soc Rev.* **42**.

154. Gupta, U. & Perumal, O. (2014) Chapter 15 - Dendrimers and Its Biomedical Applications A2 - Kumbar, Sangamesh G in *Natural and Synthetic Biomedical Polymers* (Laurencin, C. T. & Deng, M., eds) pp. 243-257, Elsevier, Oxford.

155. Svenson, S. & Tomalia, D. A. (2012) Dendrimers in biomedical applications—reflections on the field, *Adv Drug Deliv Rev.* **64**, 102-115.

156. Newkome, G. R., Moorefield, C. N. & Vögtle, F. (2004) Front Matter in *Dendrimers and Dendrons* pp. i-xii, Wiley-VCH Verlag GmbH & Co. KGaA.

157. Mintzer, M. A. & Grinstaff, M. W. (2011) Biomedical applications of dendrimers: a tutorial, *Chem Soc Rev.* **40**, 173-190.

158. Menjoge, A. R., Kannan, R. M. & Tomalia, D. A. (2010) Dendrimer-based drug and imaging conjugates: design considerations for nanomedical applications, *Drug Discov Today.* **15**, 171-185.

159. Sowinska, M. & Urbanczyk-Lipkowska, Z. (2014) Advances in the chemistry of dendrimers, *New J Chem.* **38**, 2168-2203.

160. Hermanson, G. (2013) Bioconjugate Techniques, 3rd Edition., Academic Press, New York.

161. Franc, G. & Kakkar, A. K. (2010) "Click" methodologies: efficient, simple and greener routes to design dendrimers, *Chem Soc Rev.* **39**, 1536-1544.

162. Walter, M. V. & Malkoch, M. (2012) Simplifying the synthesis of dendrimers: accelerated approaches, *Chem Soc Rev.* **41**, 4593-4609.

163. Antoni, P., Nystrom, D., Hawker, C. J., Hult, A. & Malkoch, M. (2007) A chemoselective approach for the accelerated synthesis of well-defined dendritic architectures, *Chem Comm*, 2249-2251.

164. Antoni, P., Robb, M. J., Campos, L., Montanez, M., Hult, A., Malmström, E., Malkoch, M. & Hawker, C. J. (2010) Pushing the Limits for Thiol−Ene and CuAAC Reactions: Synthesis of a 6th Generation Dendrimer in a Single Day, *Macromolecules.* **43**, 6625-6631.

165. Montañez, M. I., Perez-Inestrosa, E., Suau, R., Mayorga, C., Torres, M. J. & Blanca, M. (2008) Dendrimerized Cellulose as a Scaffold for Artificial Antigens with Applications in Drug Allergy Diagnosis, *Biomacromolecules.* **9**, 1461-1466.

166. Soler, M., Mesa-Antunez, P., Estevez, M. C., Ruiz-Sanchez, A. J., Otte, M. A., Sepulveda, B., Collado, D., Mayorga, C., Torres, M. J., Perez-Inestrosa, E. & Lechuga, L. M. (2015) Highly sensitive dendrimer-based nanoplasmonic biosensor for drug allergy diagnosis, *Biosens Bioelectron.* **66**, 115-123.

167. Haugland, R. P. (1995) Coupling of Monoclonal Antibodies with Fluorophores in *Monoclonal Antibody Protocols* (Davis, W. C., ed) pp. 205-221, Humana Press, Totowa, NJ.

168. Vira, S., Mekhedov, E., Humphrey, G. & Blank, P. S. (2010) Fluorescent labeled antibodies - balancing functionality and degree of labeling, *Analytical Biochemistry.* **402**, 146-150.

169. Gruber, H. J., Hahn, C. D., Kada, G., Riener, C. K., Harms, G. S., Ahrer, W., Dax, T. G. & Knaus, H.-G. (2000) Anomalous Fluorescence Enhancement of Cy3 and Cy3.5 versus Anomalous Fluorescence Loss of Cy5 and Cy7 upon Covalent Linking to IgG and Noncovalent Binding to Avidin, *Bioconj Chem.* **11**, 696-704.

170. Dougherty, C. A., Vaidyanathan, S., Orr, B. G. & Banaszak Holl, M. M. (2015) Fluorophore:Dendrimer Ratio Impacts Cellular Uptake and Intracellular Fluorescence Lifetime, *Bioconj Chem.* **26**, 304-315.

171. Manono, J., Dougherty, C. A., Jones, K., DeMuth, J., Holl, M. M. B. & DiMaggio, S. (2015) Generation 3 PAMAM dendrimer TAMRA conjugates containing precise dye/dendrimer ratios, *Materials Today Communications.* **4**, 86-92.

172. Sletten, E. M. & Bertozzi, C. R. (2009) Bioorthogonal Chemistry: Fishing for Selectivity in a Sea of Functionality, *Angewandte Chemie (International ed in English).* **48**, 6974-6998.

173. Carell, T. & Vrabel, M. (2016) Bioorthogonal Chemistry—Introduction and Overview, *Topics in Current Chemistry.* **374**, 9.

174. Freidel, C., Kaloyanova, S. & Peneva, K. (2016) Chemical tags for site-specific fluorescent labeling of biomolecules, *Amino Acids.* **48**, 1357-1372.

175. Lemieux, G. A. & Bertozzi, C. R. (1998) Chemoselective ligation reactions with proteins, oligosaccharides and cells, *Trends in Biotechnology.* **16**, 506-513.

176. Chen, X. & Wu, Y.-W. (2016) Selective chemical labeling of proteins, *Org Biomol Chem.* **14**, 5417-5439.

177. Debets, M. F., van Hest, J. C. M. & Rutjes, F. P. J. T. (2013) Bioorthogonal labelling of biomolecules: new functional handles and ligation methods, *Org Biomol Chem.* **11**, 6439-6455.

178. Hackenberger, C. P. R. & Schwarzer, D. (2008) Chemoselective Ligation and Modification Strategies for Peptides and Proteins, *Angewandte Chemie International Edition.* **47**, 10030-10074.

179. Tiefenbrunn, T. K. & Dawson, P. E. (2010) Chemoselective ligation techniques: Modern applications of time-honored chemistry, *Peptide Science.* **94**, 95-106.

180. Mix, E., Goertsches, R. & Zett, U. K. (2006) Immunoglobulins—Basic considerations, *Journal of Neurology.* **253**, v9-v17.

181. Le, H. T., Jang, J.-G., Park, J. Y., Lim, C. W. & Kim, T. W. (2013) Antibody functionalization with a dual reactive hydrazide/click crosslinker, *Analytical Biochemistry.* **435**, 68-73.

182. Makaraviciute, A. & Ramanaviciene, A. (2013) Site-directed antibody immobilization techniques for immunosensors, *Biosens Bioelectron.* **50**, 460-471.

183. O'Kennedy, R., Fitzgerald, S. & Murphy, C. (2017) Don't blame it all on antibodies – The need for exhaustive characterisation, appropriate handling, and addressing the issues that affect specificity, *TrAC Trends in Anal Chem.* **89**, 53-59.

184. Eldridge, G. M. & Weiss, G. A. (2011) Hydrazide Reactive Peptide Tags for Site-Specific Protein Labeling, *Bioconj Chem.* **22**, 2143-2153.

185. Asano, M., Doi, M., Baba, K., Taniguchi, M., Shibano, M., Tanaka, S., Sakaguchi, M., Takaoka, M., Hirata, M., Yanagihara, R., Nakahara, R., Hayashi, Y., Yamaguchi, T., Matsumura, H. & Fujita, Y. (2014) Bio-imaging of hydroxyl radicals in plant cells using the fluorescent molecular probe rhodamine B hydrazide, without any pretreatment, *J Biosci Bioeng.* **118**, 98-100.

186. Vemula, V., Ni, Z. & Fedorova, M. (2015) Fluorescence labeling of carbonylated lipids and proteins in cells using coumarin-hydrazide, *Redox Biol.* **5**, 195-204.

187. Kolb, H. C., Finn, M. G. & Sharpless, K. B. (2001) Click Chemistry: Diverse Chemical Function from a Few Good Reactions, *Angewandte Chemie International Edition.* **40**, 2004-2021.

188. Agard, N., Prescher, J. A. & Bertozzi, C. R. (2004) *A strain-promoted [3+2] azide-alkyne cycloaddition for covalent modification of blomolecules in living systems*. *J Am Chem Soc.* **126** (46) 15046–15047.

189. Nwe, K. & Brechbiel, M. W. (2009) Growing Applications of "Click Chemistry" for Bioconjugation in Contemporary Biomedical Research, *Cancer Biother Radiopharm.* **24**, 289-302.

190. Clark, P. M., Dweck, J. F., Mason, D. E., Hart, C. R., Buck, S. B., Peters, E. C., Agnew, B. J. & Hsieh-Wilson, L. C. (2008) Direct In-Gel Fluorescence Detection and Cellular Imaging of O-GlcNAc-Modified Proteins, *J Am Chem Soc.* **130**, 11576-11577.

191. Meyer, J.-P., Adumeau, P., Lewis, J. S. & Zeglis, B. M. (2016) Click Chemistry and Radiochemistry: The First 10 Years, *Bioconj Chem.* **27**, 2791-2807.

192. Kim, Y., Kim, Sung H., Tanyeri, M., Katzenellenbogen, John A. & Schroeder, Charles M. (2013) Dendrimer Probes for Enhanced Photostability and Localization in Fluorescence Imaging, *Biophysical Journal.* **104**, 1566-1575.

193. Zhu, S., Yang, Q., Antaris, A. L., Yue, J., Ma, Z., Wang, H., Huang, W., Wan, H., Wang, J., Diao, S., Zhang, B., Li, X., Zhong, Y., Yu, K., Hong, G., Luo, J., Liang, Y. & Dai, H. (2017) Molecular imaging of biological systems with a clickable dye in the broad 800- to 1,700-nm near-infrared window, *Proc Natl Acad Sci U S A.* **114**, 962-967.

194. Li, G., Xing, Y., Wang, J., Conti, P. S. & Chen, K. (2014) Near-infrared fluorescence imaging of CD13 receptor expression using a novel Cy5.5-labeled dimeric NGR peptide, *Amino Acids.* **46**, 1547-1556.

195. Zhang, X.-t., Gu, Z.-y., Liu, L., Wang, S. & Xing, G.-w. (2015) Synthesis and labeling of [small alpha]-(2,9)-trisialic acid with cyanine dyes for imaging of glycan-binding receptors on living cells, *Chem Comm.* **51**, 8606-8609.

196. Zambonino, M. A., Corzo, J. L., Muñoz, C., Requena, G., Ariza, A., Mayorga, C., Urda, A., Blanca, M. & Torres, M. J. (2014) Diagnostic evaluation of hypersensitivity reactions to beta-lactam antibiotics in a large population of children, *Pediatr Allergy Immunol.* **25**, 80-87.

197. Johansson, S. G. O., Adédoyin, J., van Hage, M., Grönneberg, R. & Nopp, A. (2013) False-positive penicillin immunoassay: An unnoticed common problem, *J Allergy Clin Immunol.* **132**, 235-237.

198. Torres, M. J. & Blanca, M. The contribution of major and minor determinants from benzylpenicillin to the diagnosis of immediate allergy to β-lactams, *J Allergy Clin Immunol.* **117**, 220-221.

199. Blanca-Lopez *et al*. (2015) Selective immediate responders to amoxicillin and clavulanic acid tolerate penicillin derivative administration after confirming the diagnosis, *Allergy.* **70**, 1013-1019.

200. Cristina Antunez, N. B.-L., Maria Jose Torres, Cristobalina Mayorga, Ezequiel Perez-Inestrosa, Maria Isabel Montañez, Tahia Fernandez, Miguel Blanca (2006) Immediate allergic reactions to cephalosporins: Evaluation of cross-reactivity with a panel of penicillins and cephalosporins, *J Allergy Clin Immunol.* **117**, 404-409.

201. Gonzalez-Morena, J. M., Montanez, M. I., Aldini, G., Sanchez-Gomez, F. J. & Perez-Sala, D. (2016) Adduct Formation and Context Factors in Drug Hypersensitivity: Insight from Proteomic Studies, *Curr Pharm Des.* **22**, 6748-6758.

202. Ariza, A., Montanez, M. I. & Perez-Sala, D. (2011) Proteomics in immunological reactions to drugs, *Curr Opin Allergy Clin Immunol.* **11**, 305-12.

203. Ariza, A., Collado, D., Vida, Y., Montañez, M. I., Pérez-Inestrosa, E., Blanca, M., Torres, M. J., Cañada, F. J. & Pérez-Sala, D. (2014) Study of protein haptenation by amoxicillin through the use of a biotinylated antibiotic, *PLoS ONE* **9**, e90891.

204. Ariza, A., Fernandez, T. D., Mayorga, C., Barbero, N., Martin-Serrano, A., Perez-Sala, D., Sanchez-Gomez, F., Blanca, M., Torres, M. J. & Montañez, M. I. (2015) Hypersensitivity reactions to Betalactams: Relevance of the hapten-protein conjugates, *J Investig Allergol Clin Immunol.* **25**, 12-25.

205. Venemalm, L. (2001) Pyrazinone conjugates as potential cephalosporin allergens, *Bioorganic & Medicinal Chemistry Letters.* **11**, 1869-1870.

206. Perez-Inestrosa *et al*. (2005) Cephalosporin chemical reactivity and its immunological implications, *Curr Opin Allergy Clin Immunol.* **5**, 323-330.

207. Baertschi, S. W., Dorman, D. E., Occolowitz, J. L., Collins, M. W., Spangle, L. A., Stephenson, G. A. & Lorenz, L. J. Isolation and Structure Elucidation of the Major Degradation Products of Cefaclor Formed Under Aqueous Acidic Conditions, *J Pharm Sci.* **86**, 526-539.

208. Dorman, D. E., Lorenz, L. J., Occolowitz, J. L., Spangle, L. A., Collins, M. W., Bashore, F. N. & Baertschi, S. W. (1997) Isolation and Structure Elucidation of the Major Degradation Products of Cefaclor in the Solid State, *J Pharm Sci.* **86**, 540-549.

209. Labenski, M. T., Fisher, A. A., Lo, H.-H., Monks, T. J. & Lau, S. S. (2009) Protein Electrophile-Binding Motifs: Lysine-Rich Proteins Are Preferential Targets of Quinones, *Drug Metab Dispos.* **37**, 1211-1218.

210. Azuaje, J., El Maatougui, A., Pérez-Rubio, J. M., Coelho, A., Fernández, F. & Sotelo, E. (2013) Multicomponent Assembly of Diverse Pyrazin-2(1H)-one Chemotypes, *J Org Chem.* **78**, 4402-4409.

211. Zhou, S. (2003) Separation and detection methods for covalent drug–protein adducts, *J Chromatogr B.* **797**, 63-90.

212. Ariza, A., Montañez, M. I. & Pérez-Sala, D. (2011) Proteomics in immunological reactions to drugs, *Curr Opin Allergy Clin Immunol.* **11**, 305-312.

213. Tailor A, W. J., Meng X, Park BK (2016) Mass Spectrometric and Functional Aspects of Drug–Protein Conjugation, *Chem Res Toxicol*. **29**(12), 1912–1935.

214. Koizumi, A., Yamano, K., Schweizer, F., Takeda, T., Kiuchi, F. & Hada, N. (2011) Synthesis of the carbohydrate moiety from the parasite Echinococcus multilocularis and their antigenicity against human sera, *Eur J Med Chem.* **46**, 1768-1778.

215. Montañez, M. I., Mayorga, C., Torres, M. J., Ariza, A., Blanca, M. & Perez-Inestrosa, E. (2011) Synthetic Approach to Gain Insight into Antigenic Determinants of Cephalosporins: *In Vitro* Studies of Chemical Structure−IgE Molecular Recognition Relationships, *Chem Res Toxicol.* **24**, 706-717.

216. Ariza, A., García-Martín, E., Salas, M., Montañez, M. I., Mayorga, C., Blanca-Lopez, N., Andreu, I., Perkins, J., Blanca, M., Agúndez, J. A. G. & Torres, M. J. (2016) Pyrazolones metabolites are relevant for identifying selective anaphylaxis to metamizole, *Sci Rep.* **6**, 23845.

217. Meng, X., Earnshaw, C. J., Tailor, A., Jenkins, R. E., Waddington, J. C., Whitaker, P., French, N. S., Naisbitt, D. J. & Park, B. K. (2016) Amoxicillin and Clavulanate Form Chemically and Immunologically Distinct Multiple Haptenic Structures in Patients, *Chem Res Toxicol.* **29**, 1762-1772.

218. Torres, M. J., Montanez, M. I., Ariza, A., Salas, M., Fernandez, T. D., Barbero, N., Mayorga, C. & Blanca, M. (2016) The role of IgE recognition in allergic reactions to amoxicillin and clavulanic acid, *Clin Exp Allergy.* **46**, 264-74.

219. Torres, M. J., Blanca, M., Fernandez, J., Romano, A., Weck, A., Aberer, W., Brockow, K., Pichler, W. J., Demoly, P., Enda & Hypersensitivity, E. I. G. o. D. (2003) Diagnosis of immediate allergic reactions to beta-lactam antibiotics, *Allergy.* **58**, 961-72.

220. Paar, J. M., Harris, N. T., Holowka, D. & Baird, B. (2002) Bivalent ligands with rigid double-stranded DNA spacers reveal structural constraints on signaling by Fc epsilon RI, *J Immunol.* **169**, 856-64.

221. Aranda, A., Mayorga, C., Ariza, A., Doña, I., Rosado, A., Blanca-Lopez, N., Andreu, I. & Torres, M. J. (2011) *In vitro* evaluation of IgE-mediated hypersensitivity reactions to quinolones, *Allergy.* **66**, 247-254.

222. Miura, K. & MacGlashan, D. W. (2000) Phosphatidylinositol-3 kinase regulates p21ras activation during IgE-mediated stimulation of human basophils, *Blood.* **96**, 2199-205.

223. Baggaley, K. H., Brown, A. G. & Schofield, C. J. (1997) Chemistry and biosynthesis of clavulanic acid and other clavams, *Nat Prod Rep.* **14**, 309-33.

224. Finn M.J., H. M. A., Hunt E. & Zomaya I.I. (1984) Studies on the hydrolysis of clavulanic acid, *J Chem Soc Perkin Trans 1.* **1**, 1345-1349.

225. Ariza, A., Garzon, D., Abánades, D. R., de los Ríos, V., Vistoli, G., Torres, M. J., Carini, M., Aldini, G. & Pérez-Sala, D. (2012) Protein haptenation by amoxicillin: High resolution mass spectrometry analysis and identification of target proteins in serum, *J Proteomics.* **77**, 504-520.

226. Meng, X., Jenkins, R. E., Berry, N. G., Maggs, J. L., Farrell, J., Lane, C. S., Stachulski, A. V., French, N. S., Naisbitt, D. J., Pirmohamed, M. & Park, B. K. (2011) Direct Evidence for the Formation of Diastereoisomeric Benzylpenicilloyl Haptens from Benzylpenicillin and Benzylpenicillenic Acid in Patients, *J Pharmacol Exp Ther.* **338**, 841-849.

227. Jenkins, R. E., Meng, X., Elliott, V. L., Kitteringham, N. R., Pirmohamed, M. & Park, B. K. (2009) Characterisation of flucloxacillin and 5-hydroxymethyl flucloxacillin haptenated HSA *in vitro* and *in vivo*, *Proteomics Clin Appl.* **3**, 720-729.

228. Whitaker, P., Meng, X., Lavergne, S. N., El-Ghaiesh, S., Monshi, M., Earnshaw, C., Peckham, D., Gooi, J., Conway, S., Pirmohamed, M., Jenkins, R. E., Naisbitt, D. J. & Park, B. K. (2011) Mass Spectrometric Characterization of Circulating and Functional Antigens Derived from Piperacillin in Patients with Cystic Fibrosis, *J Immunol.* **187**, 200-211.

229. Petrie, C. R., Adams, A. D., Stamm, M., Van Ness, J., Watanabe, S. M. & Meyer, R. B. (1991) A novel biotinylated adenylate analog derived from pyrazolo[3,4-d]pyrimidine for labeling DNA probes, *Bioconj Chem.* **2**, 441-446.

230. Li, Y., Chase, A. R., Slivka, P. F., Baggett, C. T., Zhao, T. X. & Yin, H. (2008) Design, Synthesis, and Evaluation of Biotinylated Opioid Derivatives as Novel Probes to Study Opioid Pharmacology, *Bioconj Chem.* **19**, 2585-2589.

231. Hou, X., Wei, W., Fan, Y., Zhang, J., Zhu, N., Hong, H. & Wang, C. (2017) Study on synthesis and bioactivity of biotinylated emodin, *Appl Microbiol Biotechnol.* **101**, 5259-5266.

232. Schilders, K., Eenjes, E., Edel, G., de Munck, A. B., van Kempen, M. B., Demmers, J., Wijnen, R., Tibboel, D. & Rottier, R. J. (2018) Generation of a biotinylatable Sox2 mouse model to identify Sox2 complexes *in vivo*, *Transgenic Res.* **27**, 75-85.

233. Garzón, B., Gayarre, J., Gharbi, S., Díez-Dacal, B., Sánchez-Gómez, F. J., Timms, J. F. & Pérez-Sala, D. (2010) A biotinylated analog of the anti-proliferative prostaglandin A1 allows assessment of PPAR-independent effects and identification of novel cellular targets for covalent modification, *Chem.-Biol. Interact.* **183**, 212-221.

234. Shan, K., Zhenhua, S., Jiawei, L., Wuguo, L., Qiaoling, S., Qing, Z. & Qiang, Y. (2017) Synthesis of Biotinylated 2-methoxystrypandrone and Identification of JAK2 and IKK as its Targets, *Anticancer Agents Med Chem.* **17**, 1-6.

235. Havelund, J. F., Wojdyla, K., Davies, M. J., Jensen, O. N., Moller, I. M. & Rogowska-Wrzesinska, A. (2017) A biotin enrichment strategy identifies novel carbonylated amino acids in proteins from human plasma, *J Proteomics.* **156**, 40-51.

236. Sánchez-Gómez, F. J., Gayarre, J., Avellano, M. I. & Pérez-Sala, D. (2007) Direct evidence for the covalent modification of glutathione-S-transferase P1-1 by electrophilic prostaglandins: Implications for enzyme inactivation and cell survival, *Arch Biochem Biophys.* **457**, 150-159.

237. Gayarre, J., Sánchez, D., Sánchez-Gómez, F. J., Terrón, M. C., Llorca, O. & Pérez-Sala, D. (2006) Addition of electrophilic lipids to actin alters filament structure, *Biochem Biophys Res Commun.* **349**, 1387-1393.

238. Hagan, A. K. & Zuchner, T. (2011) Lanthanide-based time-resolved luminescence immunoassays, *Anal Bioanal Chem.* **400**, 2847-2864.

239. Walker, J. M. *The Protein Protocols Handobook*.

240. Mushtaq, S., Jeon, J., Shaheen, A., Jang, B. S. & Park, S. H. (2016) Critical analysis of radioiodination techniques for micro and macro organic molecules, *J Radionanal Nucl Ch.* **309**, 859-889.

241. Wang, Z., Yue, X., Wang, Y., Qian, C., Huang, P., Lizak, M., Niu, G., Wang, F., Rong, P., Kiesewetter, D. O., Ma, Y. & Chen, X. (2014) A symmetrical fluorous dendron-cyanine dye conjugated bimodal nanoprobe for quantitative (19)F MRI and NIR fluorescence bioimaging, *Adv Healthc Mater.* **3**, 1326-1333.

242. Schneider, J. R., Carias, A. M., Bastian, A. R., Cianci, G. C., Kiser, P. F., Veazey, R. S. & Hope, T. J. (2017) Long-term direct visualization of passively transferred fluorophore-conjugated antibodies, *J Immunol Methods.* **450**, 66-72.

243. Park, J. W., Kim, Y., Lee, K.-J. & Kim, D. J. (2012) Novel Cyanine Dyes with Vinylsulfone Group for Labeling Biomolecules, *Bioconj Chem.* **23**, 350-362.

244. Pan, D., Qin, H. & Cooperman, B. S. (2009) Synthesis and functional activity of tRNAs labeled with fluorescent hydrazides in the D-loop, *RNA.* **15**, 346-354.

245. Kameyama, A., Kaneda, Y., Yamanaka, H., Yoshimine, H., Narimatsu, H. & Shinohara, Y. (2004) Detection of Oligosaccharides Labeled with Cyanine Dyes Using Matrix-Assisted Laser Desorption/Ionization Mass Spectrometry, *Anal Chem.* **76**, 4537-4542.

246. Gulati, N. M., Pitek, A. S., Steinmetz, N. F. & Stewart, P. L. (2017) Cryo-electron tomography investigation of serum albumin-camouflaged tobacco mosaic virus nanoparticles, *Nanoscale.* **9**, 3408-3415.

247. Wycisk, V., Pauli, J., Welker, P., Justies, A., Resch-Genger, U., Haag, R. & Licha, K. (2015) Glycerol-Based Contrast Agents: A Novel Series of Dendronized Pentamethine Dyes, *Bioconj Chem.* **26**, 773-781.

248. Lesniak, W. G., Mishra, M. K., Jyoti, A., Balakrishnan, B., Zhang, F., Nance, E., Romero, R., Kannan, S. & Kannan, R. M. (2013) Biodistribution of Fluorescently Labeled PAMAM Dendrimers in Neonatal Rabbits: Effect of Neuroinflammation, *Mol Pharm.* **10**, 4560-4571.

249. Ornelas, C., Lodescar, R., Durandin, A., Canary, J. W., Pennell, R., Liebes, L. F. & Weck, M. (2011) Combining Aminocyanine Dyes with Polyamide Dendrons: A Promising Strategy for Imaging in the Near-Infrared Region, *Chem Eur J..* **17**, 3619-3629.

250. Bouit, P.-A., Westlund, R., Feneyrou, P., Maury, O., Malkoch, M., Malmstrom, E. & Andraud, C. (2009) Dendron-decorated cyanine dyes for optical limiting applications in the range of telecommunication wavelengths, *New J Chem.* **33**, 964-968.

251. Feliu, N., Walter, M. V., Montañez, M. I., Kunzmann, A., Hult, A., Nyström, A., Malkoch, M. & Fadeel, B. (2012) Stability and biocompatibility of a library of polyester dendrimers in comparison to polyamidoamine dendrimers, *Biomaterials.* **33**, 1970-1981.

252. Mujumdar, R. B., Ernst, L. A., Mujumdar, S. R., Lewis, C. J. & Waggoner, A. S. (1993) Cyanine dye labeling reagents: Sulfoindocyanine succinimidyl esters, *Bioconj Chem.* **4**, 105-111.

253. García-Gallego, S., Hult, D., Olsson, J. V. & Malkoch, M. (2015) Fluoride-Promoted Esterification with Imidazolide-Activated Compounds: A Modular and Sustainable Approach to Dendrimers, *Angewandte Chemie International Edition.* **54**, 2416-2419.

254. Toseland, C. P. (2013) Fluorescent labeling and modification of proteins, *J Chem Biol.* **6**, 85-95.

255. Ogawa, M., Kosaka, N., Choyke, P. L. & Kobayashi, H. (2009) H-type Dimer Formation of Fluorophores: A Mechanism for Activatable, *in vivo* Optical Molecular Imaging, *ACS Chem Biol.* **4**, 535-546.

256. Ogawa, M., Kosaka, N., Regino, C. A. S., Mitsunaga, M., Choyke, P. L. & Kobayashi, H. (2010) High sensitivity detection of cancer *in vivo* using a dual-controlled activation fluorescent imaging probe based on H-dimer formation and pH activation, *Molecular BioSystems.* **6**, 888-893.

257. Hahn, C. D., Riener, C. K. & Gruber, H. J. (2001) Labeling of Antibodies with Cy3-, Cy3.5-, Cy5-, and Cy5.5-monofunctional Dyes at Defined Dye/Protein Ratios, *Single Molecules.* **2**, 149-149.

258. Ma, Y. M. & Hider, R. C. (2009) The selective quantification of iron by hexadentate fluorescent probes, *Bioorganic & medicinal chemistry.* **17**, 8093-101.

259. Dubowchik, G. M., Cornell, L. A., Crosswell, A. R. & Firestone, R. A. (1993) Novel polyamide inducers of HL-60 cellular differentiation, *Bioorg Med Chem Lett.* **3**, 1965-1970.

260. Brockow, K., Romano, A., Blanca, M., Ring, J., Pichler, W. & Demoly, P. (2002) General considerations for skin test procedures in the diagnosis of drug hypersensitivity, *Allergy.* **57**, 45-51.

261. Blanca-Lopez, N., Perez-Alzate, D., Ruano, F., Garcimartin, M., de la Torre, V., Mayorga, C., Somoza, M. L., Perkins, J., Blanca, M., Canto, M. G. & Torres, M. J. (2015) Selective immediate

responders to amoxicillin and clavulanic acid tolerate penicillin derivative administration after confirming the diagnosis, *Allergy.* **70**, 1013-9.

262. Moreno, F., Blanca, M., Mayorga, C., Terrados, S., Moya, M., Perez, E., Suau, R., Vega, J. M., Garcia, J., Miranda, A. & *et al*. (1995) Studies of the specificities of IgE antibodies found in sera from subjects with allergic reactions to penicillins, *Int Arch Allergy Immunol.* **108**, 74-81.

263. Edwards, R. G., Spackman, D. A. & Dewdney, J. M. (1982) Development and use of three new radioallergosorbent tests in the diagnosis of penicillin allergy, *Int Arch Allergy Appl Immunol.* **68**, 352-7.

264. Wide, L. (1969) Radioimmunoassays employing immunosorbents, *Acta Endocrinol Suppl (Copenh).* **142**, 207-21.

265. Batchelor F.R., Dewdney J.M., Weston R.D. & A.W., W. (1966) The immunogenicity of cephalosporin derivatives and their cross-reaction with penicillin, *Immunology.* **10**, 21-33.

266. Sanz, M. L., Gamboa, P. M., Antepara, I., Uasuf, C., Vila, L., Garcia-Aviles, C., Chazot, M. & De Weck, A. L. (2002) Flow cytometric basophil activation test by detection of CD63 expression in patients with immediate-type reactions to β-lactam antibiotics, *Clin Exp Allergy.* **32**, 277-86.

267. Soares da Costa, T. P., Tieu, W., Yap, M. Y., Pendini, N. R., Polyak, S. W., Sejer Pedersen, D., Morona, R., Turnidge, J. D., Wallace, J. C., Wilce, M. C. J., Booker, G. W. & Abell, A. D. (2012) Selective inhibition of Biotin Protein Ligase from Staphylococcus aureus, *J Biol Chem.* **287**, 17823-17832.

268. Tao, L., Geng, J., Chen, G., Xu, Y., Ladmiral, V., Mantovani, G. & Haddleton, D. M. (2007) Bioconjugation of biotinylated PAMAM dendrons to avidin, *Chem Comm*, 3441-3443.

269. Corona, C., Bryant, B. K. & Arterburn, J. B. (2006) Synthesis of a Biotin-Derived Alkyne for Pd-Catalyzed Coupling Reactions, *Organic Letters.* **8**, 1883-1886.

270. DeLaLuz, P. J., Golinski, M., Watt, D. S. & Vanaman, T. C. (1995) Synthesis and Use of a Biotinylated 3-Azidophenothiazine to Photolabel Both Amino- and Carboxyl-Terminal Sites in Calmodulin, *Bioconj Chem.* **6**, 558-566.

271. Iglesias-Sánchez, J. C., María, D. S., Claramunt, R. M. & Elguero, J. (2010) Molecular Recognition Studies on Naphthyridine Derivatives, *Molecules.* **15**, 1213.

272. Brown, A. G., Corbett, D. F., Goodacre, J., Harbridge, J. B., Howarth, T. T., Ponsford, R. J., Stirling, I. & King, T. J. (1984) Clavulanic acid and its derivatives. Structure elucidation of clavulanic acid and the preparation of dihydroclavulanic acid, isoclavulanic acid, esters and related oxidation products, *J Chem Soc Perkin Trans 1*, 635-650.

273. Laborde, C. M., Zubiri, I., Alonso-Orgaz, S., Mourino-Alvarez, L., Álvarez-Llamas, G. & Barderas, M. G. (2011) Aportaciones de la proteómica al laboratorio clínico, *Revista del Laboratorio Clínico.* **4**, 214-224.

274. Sugio, S., Kashima, A., Mochizuki, S., Noda, M. & Kobayashi, K. (1999) Crystal structure of human serum albumin at 2.5 A resolution, *Protein Eng.* **12**, 439-46.

275. Case, D. A., Darden, T. A., Cheatham, I., T. E., Simmerling, C. L., Wang, J., Duke, R. E., Luo, R., Walker, R. C., Zhang, W., Merz, K. M., Roberts, B. P., Hayik, S., Roitberg, A. E., Seabra, G., Swails, J. M., Kolossváry, I., Wong, K. F., Paesani, F., Vanicek, J., Wolf, R. M., Liu, J., Wu, X., Brozell, S. R., Steinbrecher, T., Gohlke, H., Cai, Q., Ye, X., Wang, J., Hsieh, M.-J., Cui, G., Roe, D. R., Mathews, D. H., Seetin, M. G., Salomon-Ferrer, R., Sagui, C., Babin, V., Luchko, T., Gusarov, S., Kovalenko, A. & Kollman, P. A. (2012) AMBER. AMBER 12 in, University of California, San Francisco.

276. Jorgensen, W. L., Chandrasekhar, J., Madura, J. D., Impey, R. W. & Klein, M. L. (1983) Comparison of simple potential functions for simulating liquid water, *J Chem Phys.* **79**, 926-935.

277. Morris, G. M., Huey, R., Lindstrom, W., Sanner, M. F., Belew, R. K., Goodsell, D. S. & Olson, A. J. (2009) AutoDock4 and AutoDockTools4: Automated docking with selective receptor flexibility, *J Comput Chem.* **30**, 2785-91.

278. Martín-Serrano Ortiz, A., Stenström, P., Mesa-Antunez, P., Andrén, O.C.J., Torres, M.J., Montañez, M.I., Michael Malkoch. (2018) Design of multivalent fluorescent dendritic probes for site-specific labeling of biomolecules, *J Polym Sci A Polym Chem.* **56**(15), 1609-1616.

279. Azuaje, J., El Maatougui, A., Pérez-Rubio, J.M., Coelho, A., Fernández, F., Sotelo, E. (2013) Multicomponent Assembly of Diverse Pyrazin-2(1H)-one Chemotypes. *J Org Chem* **78**(9), 4402-4409.

280. Brouwer, A.M. (2011) Standards for photoluminescence quantum yield measurements in solution (IUPAC Technical Report). *Pure Appl Chem*, **83**(12), 2213-2228.